Much Ado About Radicals: Mechanistic Studies in Photochemistry and $S_{RN}1$ Reactions

by

Samantha Rohe

A thesis submitted in partial fulfillment of the requirements for the

Master's degree in Chemistry

The University of Ottawa

January 2020

ABSTRACT

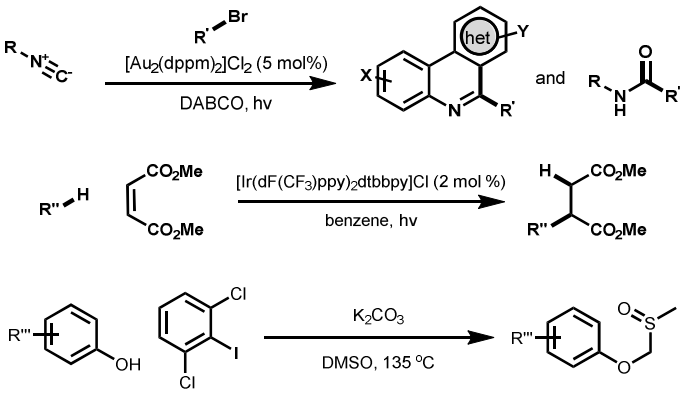

The second decade of the 21st century has witnessed a resurgence in the use of radical chemistry in both methodology and total synthesis. Many contemporary advancements can be attributed to the popularization of radical generation via photoredox catalysis, which negates the last few decades' frequent use of stoichiometric or hazardous reagents in radical reactions. With these new techniques comes advanced understanding of the underlying radical redox mechanisms as well as new and unique questions. Due to the complexity inherent in the design of successful radical reactions, it is imperative to develop thorough mechanistic understanding. Herein our group has elucidated the mechanistic behavior of three distinct radical systems. The synthesis of a variety of phenanthridines and amides has been completed via radical addition to isonitriles catalyzed by the dimeric gold photocatalyst $[Au_2(dppm)_2]Cl_2$. This catalyst has further enabled radical clock studies and has been used to determine the rate constant of primary radical addition to biphenyl isonitriles. The photoredox generation of chlorine atoms for HAT has been undertaken with the iridium polypyridyl complex $[Ir(dF(CF_3)ppy)_2(dtbbpy)]Cl$, with results supporting a tuning of HAT selectivity by solvent-chlorine complexation. Finally, mechanistic data suggest that single electron transfer from a base in DMSO catalyzes an unorthodox etherification of phenols.

To Rudy

ACKNOWLEDGEMENTS

Doing research is difficult at the best of times; it is impossible without a good advisor. I have been fortunate enough to have a great advisor. Prof. Louis Barriault guided me in a way that balanced his support and expertise with my independence and enabled me to grow farther than I ever believed I could. His patience and empathy while discussing chemistry has fostered the growth of a lab full of free-thinking scientists. I am also grateful for his advice about my career, for helping me achieve my goal of researching in Australia, and for encouraging me to pursue the CREATE diploma.

My research would not have been possible without my many support systems outside of the lab. I want to thank my parents Joanne and Peter, who always enabled me to their full ability to follow my passion for chemistry. I thank my brother Jeremy, who is an endless fountain of optimism. I also want to acknowledge the support of my friends, who have miraculously remained patient with my ramblings throughout the last few years.

The many achievements of the Barriault group exist due to our strong team collaboration and conversation. In particular I would like to thank the Photocrew, who have always been eager to discuss the complexities of photochemistry and always come up with creative solutions to the problems faced in our explorations. The majority of my research would not have been at all possible without the tireless work and creativity of Drs. Terry McCallum and Mathieu Morin. I am grateful to Terry for his guidance during my undergraduate and graduate studies, for his invaluable advice and chemistry expertise, and most of all for his friendship. I thank Mathieu for his mentorship and advice during my honors thesis, for welcoming me so warmly into the lab, and for taking the plunge to be the lab DM. I am especially grateful to Avery and Montse, who worked with me through the trials and tribulations of photochemistry; to André, Julie, Huy, and Mike for providing reprieve to research stress with political debates; to Phil, Gab, Martin, Aly and Marina

for their invaluable advice in both chemistry and life; to Daniel for teaching me how to teach and being patient throughout; to Victor, Tegan and Weldon for bearing through the last few months of my degree. I thank Professor Fabien Gagosz for helpful discussions and for many unrequited references. I am grateful to Professors Deryn Fogg, André Beauchemin, and Derek Pratt for their mentorship and advice. I also want to thank the support staff at uOttawa for their assistance, particularly: Julie Lamothe, who has smoothed over many hurdles in my path; Glenn Facey, who has helped me solve many spectroscopy problems; Sharon Curtis and the mass spectroscopy group; Dr. Wendy Pell for generously sharing her IR equipment; the staff of the science store for keeping us organized and well-stocked; the Health and Safety team for maintaining a safe environment in which to conduct my research; finally, the wonderful administrative staff at the Faculty of Science who have always eased my bureaucratic confusion. I would like to acknowledge OGS and the University of Ottawa for the funding received at the Master's level.

TABLE OF CONTENTS

TABLE OF FIGURES

TABLE OF SCHEMES

TABLE OF TABLES

GLOSSARY OF ABBREVIATIONS

AIBN	Azobisisobutyrylnitrile
BHT	3,5-di-*tert*-butyl-4-methylphenol
BO	Born-Oppenheimer
bpy	2,2’-bipyridine
CTC	charge transfer complex
DABCO	1,4-diazabicyclo[2.2.2]octane
DESO	diethyl sulfoxide
DIPA	diisopropylamine
DIPEA	diisopropylethylamine
DMSO	dimethyl sulfoxide
dppm	bis(diphenylphosphino)methane
dtbpy	4,4'-Di-tert-butyl-2,2'-dipyridyl
EPR	electron paramagnetic resonance
Equiv.	equivalents
Et	ethyl
F	fluorescence
HAT	hydrogen atom transfer
HOMO	highest occupied molecular orbital
IBX	2-iodoxybenzoic acid
IC	internal conversion
ISC	inter-system crossing
KIE	kinetic isotope effect

LFP	laser flash photolysis
LUMO	lowest occupied molecular orbital
Me	methyl
MLCT	metal-to-ligand charge transfer
NMO	4-methylmorpholine *N*-oxide
P	phosphorescence
PES	potential energy surface
PET	photoinduced electron transfer
ppy	2-phenylpyridine
PRE	persistent radical effect
PTOC	*N*-hydroxypyridine-2-thione
SCE	saturated calomel electrode
SET	single electron transfer
SOMO	singly occupied molecular orbital
TBAC	tetra-butylammonium chloride
TBADT	tetra-*N*-butylammonium decatungstate
TEA	triethylamine
TEMPO	2,2,6,6-Tetramethyl-1-piperidinyloxy
TLC	thin layer chromatography
Ts	tosyl
UV	ultraviolet
VT	vibrational transition

CHAPTER 1: INTRODUCTION

1.1 Photocatalysis for Radical Initiation

1.11 Development of Transition Metal Photoredox Catalysts and HAT

1.11a Photoredox Catalysis – a Historical Perspective

Debate surrounding climate crisis has moved far past the "inconvenient truth" polemic of 2006 and is now ubiquitous enough to cause apocalypse fatigue in households worldwide. The matter is demonstrably an existential threat and yet solutions to this looming problem are still a subject of politico-economic vitriol. In the years since Svante Arrhenius' recognition of industrial pollution's contribution to climate change in 1897, scientists have overwhelmingly accepted the reality of this crisis and the energies of the community are increasingly focused on sustainable developments.[1] It is hoped that scientists can provide the tools and set a valuable example to the groups who have thus far been reluctant to take action. A crucial motif in sustainability development is modernization of the process instrumental to scientific revolution in the first place: combustion of hydrocarbons as the dominant source of energy. Alternatives to coal and gas are as important today as they were in Ciamician's 1912 address:

> "Modern civilization is the daughter of coal, for this offers to mankind the solar energy in its most concentrated form; that is, in a form in which it has been accumulated in a long series of centuries. Modern man uses it with increasing eagerness and thoughtless prodigality for the conquest of the world and, like the mythical gold of the Rhine, coal is to-day the greatest source of

energy and wealth. The earth still holds enormous quantities of it, but coal is not inexhaustible. The problem of the future begins to interest us[.]" [2]

One has only to look out a window to wonder at the solutions offered by plant life to the "problem of the future"; Nature's energy conversion is more refined than our hydrocarbon combustion. Chemists have spent so much time borrowing intellectual property from plants that they could hardly fail to be inspired by photosynthesis and seek energy from the sun. Indeed, a tabletop replicate of photosynthesis has been a long-pursued goal to those skilled in the art.

Outside of fundamental applications such as water splitting, using alternative energy sources to raise the energy of a select group of molecules has provided a transformative paradigm in organic synthesis.[3] Many 20th century industrial forays into harnessing solar energy for organic chemistry were focused on disinfection of wastewater or breakdown of substances such as pesticides.[4] Up until the mid-2000's, efforts to build instead of destroy catalytically using photochemical energy were almost exclusively focused on heterogeneous oxidation with TiO_2, polyoxotungstate, iron or cobalt porphyrin complexes, and other polyoxometalate species.[5] Many photocatalyzed organic procedures developed prior to the 21st century relied on direct photoexcitation of the compounds themselves, which fundamentally limited applicability. Classic examples include the thermally disallowed [$8\pi_s + 8\pi_s$] photodimerizations of anthracene and styrene, isomerization of olefins such as cinnamic acid, pericyclizations, isomerizations of quinones, Norrish reactions, and others (**Scheme 1.1**).[6]

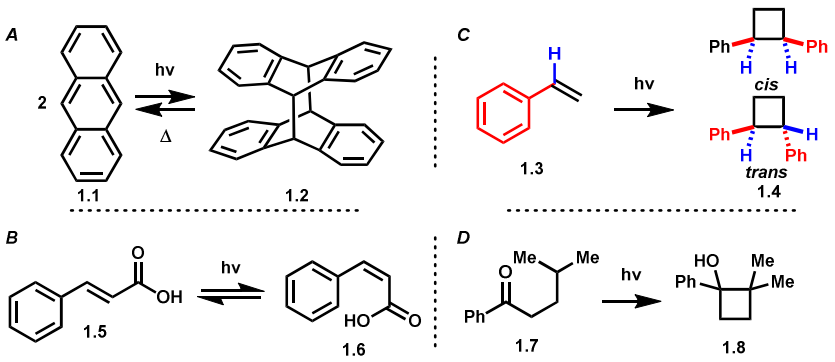

Scheme 1.1. Examples of photocatalyzed reactions involving direct irradiation of substrates. A) photodimerization of anthracene via a [$8\pi_s + 8\pi_s$] cycloaddition; B) photodimerization of stilbene via a [$4\pi_s + 4\pi_s$]; C) photoisomerization of cinnamic acid; D) One possible product of the Norrish Type II reaction.

Further expansion of photochemistry in the synthesis of organic compounds was hotly pursued throughout the nineteenth century, attempting to find homogeneous catalysts to overcome the restrictions inherent in organic molecules' excitation wavelengths. A photocatalyst capable of instigating redox flow from a light source of relatively long (and readily available) wavelength directly to a less photosensitive molecule would expand the photochemical purview to almost any substrate capable of single electron oxidation or reduction and could result in a paradigm shift of organic synthesis. Catalysts capable of fulfilling such goals were discovered as early as 1936, when both enantiomers of the first polypyridyl complex of ruthenium was synthesized and characterized.[7] The photophysical parameters of other polypyridyl complexes of ruthenium, iron, osmium, and iridium were described over the following decades; use of these complexes was however largely relegated to charge transfer to metal ions and other inorganic species, and the catalysts' applicability in organic synthesis went unexplored for many years.[8]

The first trickles that heralded the flood of research into photoredox organic chemistry with ruthenium and iridium chromophores appeared in the late 1970s with the group of Kellogg (**Scheme 1.2**).[9] The authors proposed that the ruthenium dye acted as photosensitizer for photoinduced electron transfer (PET) from the metal complex to the sulfonyl moiety, and this simple transformation sparked a flurry of similar functional group reductions and couplings with reducing agents.[10]

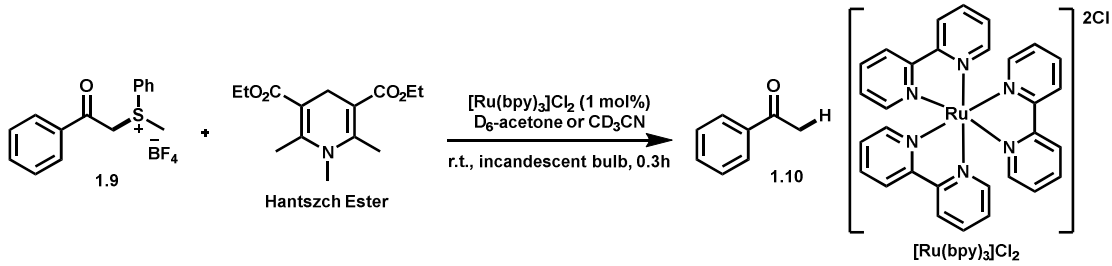

Scheme 1.2. Use of ruthenium polypyridyl complex as photocatalyst in the reductive desulfonylation of **1.9**.

The most crucial advance that these photosensitizers brought to the field was facile access to diverse radical initiation. In the 1980's, radical chemistry was fairly well-understood though research was overwhelmingly conducted using chain reaction systems like AIBN with $HSnBu_3$.[11] This set of reagents was certainly reliable for many transformations but involved heating at high temperatures for extended periods of time, generated stoichiometric quantities of tin waste, could require prefunctionalization of substrates with halogens (which is simply not possible in many cases), and was seldomly catalytic. With metal photosensitizer catalysis, whole catalogs of functional groups became available radical precursors, and the requisite redox potentials could be accurately estimated and reached with the correctly tailored polypyridyl complex.[12] Safe,

environmentally efficient, bench-stable, room temperature radical generation opened the floodgates to the 21st century's surge in photoredox catalysis methods.

The community focus was on ruthenium catalysts for the first two decades of photoredox transformations in organic synthesis, though other photosensitizing transition metal catalysts such as $[Ir(ppy)_3]^{2+}$ had been photophysically elucidated since 1984.[13] These polypyridyl complexes did not occupy center stage of organic synthesis until they captured the attention of several high-profile researchers in 2008. In under a year, three

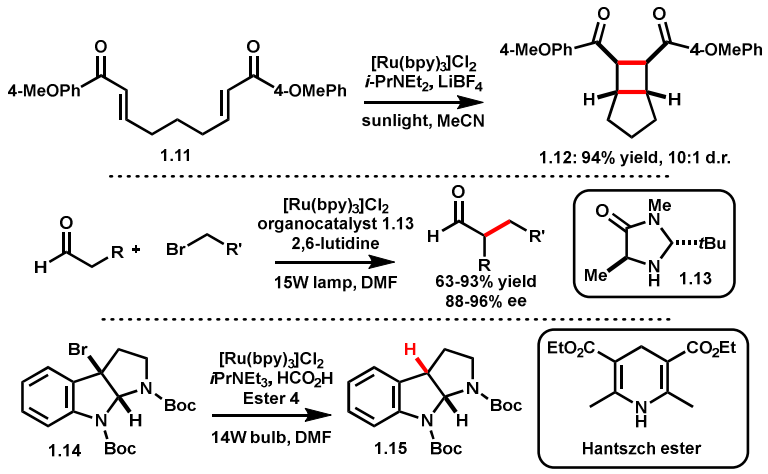

Scheme 1.3. Chemical transformations published in 2008-9 that drew attention to the potential of transition metal photosensitizers in organic synthesis.

groups independently published methodologies that catapaulted metal polypyridyl photoredox chemistry into the forefront of synthesis.[14] Though these publications are by no means the field's first introduction to photosensitized cycloadditions and homolysis of activated C-Br bonds, they did provide valuable exposure for the transformations seen in **Scheme 1.3** and propagated the sale of prominent photocatalysts by chemical supply companies. Prior to 2008, there were less than 100 total references to $[Ru(bpy)_3]^{2+}$

photocatalysis outside of inorganic chemistry journals. Now, slightly over a decade later, over 700 organic methodologies exist for $[Ru(bpy)_3]^{2+}$ catalysts alone.[15]

This literature explosion is not just the result of photochemistry's popular pundits – radical chemistry generally provides attractive complementarity to more well-established two-electron chemistry. Having this reactive complementarity is especially important in the 21st century as the rising cost of drug discovery makes ease and low cost of synthesis more relevant than ever. A reaction exemplifying this complementarity is the palladium-mediated cross-coupling: the Nobel prize-winning two-electron examples like the Heck and Suzuki couplings carry scope restrictions on alkyl halides, especially those that are sterically hindered. By contrast, palladium-mediated cross-couplings involving radical intermediates favor use of hindered alkyl halides as substrates.[16] This complementarity diversifies substrates available for synthesis in medicinal chemistry.

Radical chemistry of course contains its own set of challenges and limitations. Comparison of free radical energies – illustrated by Bond Dissociation Energy (BDE) – is significantly less understood than comparison of ions – illustrated by pKa and known to most chemists better than the backs of their own hands. In many cases, a mechanistic hypothesis is postulated by a synthetic chemist with only rough estimates at the corresponding BDE values and rate constants, whereas the two-electron chemist frequently finds that their exact substrates' acidities and Hammett plots are known in a handful of solvents and temperatures. This lack of foundational understanding can result in tenuous mechanistic proposals in the literature and is a major barrier to developments in the field.

Another limitation of contemporary radical chemistry is the tendency for most initiators to have stoichiometric requirements. This is due to the highly reactive nature of the free-radical products – free radicals often terminate instead of propagating a chain, even when chain propagation is both possible and probable based on BDEs. Studer and Curran capture this behavior eloquently: "[…] the more radicals you try to make, the faster they go away. Radicals are, in a word, impatient".[17] Examples of common stoichiometric radical initiators include metal additives such as samarium (II) iodide or manganese polycarbonyl complexes, or substrate prefunctionalization with an activating group that is then wasted (such as *N*-hydroxypyridine-2-thione [PTOC] esters, *N*-hydroxyphthalimides, and other xanthates).[18]

A downside of this high-speed radical activity is that regio- and stereoselectivity is frequently challenging – free radicals are often too "impatient" to discriminate. Some radical reactions are reversible, such as isomerization or addition to some olefin acceptors. Even when following desired reactivity free radicals often face competition between multiple termination pathways, for example in the fragmentation versus redox termination pathways available to an imidoyl radical. A successful radical methodology involves a balancing act between all these factors.

The most elegant radical methodologies would resemble the following: a substrate would accept an electron from a donor, or "lender", generating a reactive free-radical species. This free radical reacts in the desired fashion, and when product is formed, the extra electron is simply returned to the original donor in a thermodynamically favorable manner. This electron "borrowing" or "shuttling" catalysis could be similarly applied with an acceptor instead of a donor. In either case, the electron "lender" species would be

present in catalytic quantities, eliminating the waste and inconvenience present in most radical initiation methods as described above. The energy input of the system would be something precise and efficient such as photons or electric current. The key electron transfers would ideally be fast and thermodynamically favorable in all cases, minimizing formation of byproducts via alternative pathways. Notably, both electrochemistry and the photoredox chemistry explored herein can allow these criteria to be met.

1.11b Physicochemical Processes in Photochemistry

Radical chemistry has been revolutionized by the conversion of light into chemical energy, which provides facile access to synthetically valuable high-energy open-shell intermediate species that can be otherwise challenging to obtain. Because chemistry from open-shell states using light differs hugely from classical two-electron HOMO-LUMO chemistry, it is necessary to delve more deeply into the underlying physicochemical processes than for some other organic transformations. This subsection will only scratch the surface of the involved photophysics and it is suggested that the reader peruse König's *Chemical Photocatalysis* or Turro's *Modern Molecular Photochemistry of Organic Molecules* for a more comprehensive understanding.[19]

Shining light on a reaction can be interpreted as adding energy to a reaction through absorption of photons by one or more compounds, as depicted in **Scheme 1.4**.[20] The molecular structure of an absorbing compound "**X**" in the reaction medium will determine its absorption wavelength. If a photon of the appropriate wavelength hits said compound, its energy will be absorbed, promoting compound **X** to an electronically excited state **X***. This energetic excited state is often short-lived, returning to the ground state in a variety

of ways including molecular decomposition or emission of a photon, electron, or heat. In order to be an efficient photocatalyst, chromophore **X** needs to either decompose from excited state **X*** in a productive manner, or **X*** needs to be long-lived enough to transfer energy to another molecule **Y** prior to other energy loss pathways. As decomposition pathways unfortunately overwhelmingly involve destruction of the chromophore, the usual criterion for a synthetically fruitful photocatalyst is having a long-lived excited state **X***.

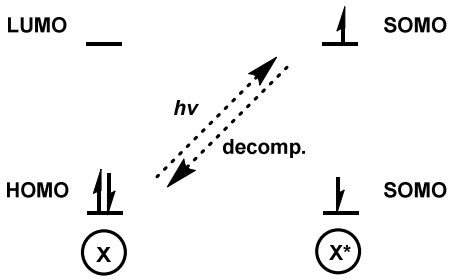

Scheme 1.4. Graphic depiction of the **X** ground state and the corresponding **X*** excited state achieved upon photoexcitation.

A deeper look at the terms “ground state” and “excited state” is required for accurate analysis of the possible permutations between them. The relative locations of electrons and nuclei in a molecule will determine the strength of bonds within that molecule and therefore the reactivity or energy of the molecule. The “ground state” of a given molecule refers to its lowest energetic configuration of electrons and nuclei at a given temperature, whereas an “excited state” refers to any one of myriads of higher-energy configurations at that temperature. To overcome computational hurdles in the modeling of molecular motion, the Born-Oppenheimer (BO) approximation is often used: it assumes that the motion of atomic nuclei and electrons in a molecule can be solved separately from each other. Each possible “solution”, or discrete energetic configuration, is a Potential Energy Surface (PES) which corresponds to molecular conformation.

For most electronic transitions between vibrational levels, the transition itself is instantaneous relative to the time required for nuclear motion. Because of this, it is said that an excited-state vibrational level must be instantaneously compatible with the nuclear coordinate and momentum of the ground-state vibrational level. This assumption that molecular coordinates will not change when undergoing electronic transition has been termed the Franck-Condon principle. This principle states that a molecule will only undergo vibronic transition if there is significant overlap between vibrational wave functions, in other words if two vibrational wavefunctions have near-identical nuclear coordinates and momenta. A molecule in a Franck-Condon state therefore changes configuration following, but not during, a vibronic transition between states.

The molecular PES is not just a visualization of the pathway between ground and excited state configurations – it also provides insight as to the varied degradation pathways available to an excited state. These degradation pathways are important to the photochemist because of their implications in photocatalyst design. The photophysical processes of a chromophore are described in the simplified Jablonski diagram of chromophore **S** in **Scheme 1.5**, in which the BO approximation allows representation of each electronic state as a single discrete energy.

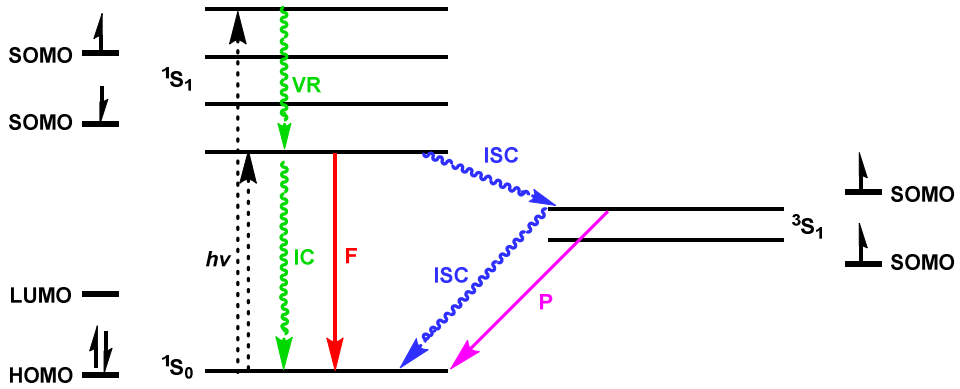

Scheme 1.5. Jablonski diagram of photophysical transitioning processes.

In this Jablonski diagram, the singlet states $^1S_0$ and $^1S_1$ are grouped into the left column and the triplet state $^3S_1$ is shown in the right column. Spin multiplicity is depicted in HOMO, LUMO, and SOMO on the outer edges of the diagram as being either closed- or open-shell, singlet (spin paired) or triplet (spin unpaired) state. A molecule can transition through vibrational states in either radiative or non-radiative processes. The three radiative transitions involve absorption or emission of a photon and are represented in **Scheme 1.5** with straight arrows. The initial transition from ground state to excited state is radiative through absorption of a photon of sufficient energy to reach a vibrational level within singlet excited state $^1S_1$. This excited state can then undergo radiative decay by spin-allowed emission of a photon from $^1S_1$, resulting in Fluorescence (**F**) of the molecule and depicted in red in **Scheme 1.5**. The triplet excited state $^3S_1$ can decay through a similar spin-forbidden radiative process involving emission of a photon, termed Phosphorescence (**P**, depicted in pink). As spin-flip and loss of energy must occur in order to transition between $^3S_1$ to $^1S_0$, the Phosphorescence (**P**) process is of lower energy than Fluorescence (and is correspondingly redshifted).

Three non-radiative processes, depicted in **Scheme 1.5** with wavy arrows, can occur from an excited vibrational state. A molecule can undergo Vibrational Relaxation, moving from a higher to lower vibrational level within state $^1S_1$ (**VR**, depicted in green). The molecule can also relax from excited state $^1S_1$ to ground state $^1S_0$ through a process called Internal Conversion (**IC**), depicted in green, that manifests as dispersion of heat and requires collision between the excited molecule and a neighboring molecule. The third type of non-radiative process involves transition to a state with different spin multiplicity,

depicted in blue and termed Inter-System Crossing (**ISC**). Transitioning from singlet excited state $^{1}S_1$ to triplet excited state $^{3}S_1$ is one example of ISC and must precede any phosphorescence. ISC is also required in the non-radiative process of vibrational relaxation from $^{3}S_1$ to $^{1}S_0$. As all decay processes from the triplet excited state involve ISC, a longer time period is required before the vibrational wavefunctions between excited and ground state have significant enough overlap to transition. This creates a long-lived triplet excited state $^{3}S_1$.

This theory relates to photocatalyst and reaction design in several ways. Since ISC is not necessary for relaxation from singlet excited state $^{1}S_1$ to singlet ground state $^{1}S_0$, the singlet excited state tends to be too short-lived to engage in bimolecular energy transfer processes. Conversely, as the decay of triplet excited state $^{3}S_1$ requires ISC and this is a more difficult process, the triplet catalyst excited state usually has the longest excited-state lifetime and is the state from which most bimolecular reactions occur.

All catalyst excited state quenching rates must be carefully considered in catalyst design. Experimental determination of these rates will not be discussed to full depth in this manuscript; readers wanting more information should refer to the texts mentioned *vide supra*. However, it should be noted that the Stern-Volmer equation is a straightforward and reliable tool used to determine the rate constant of a photocatalyst's excited-state quenching with a substrate (Eqns 1.1 and 1.2).

Eqn 1.1. $$\frac{F_0}{F} = 1 + K_{sv}[Q]$$

Where F_0 and F are fluorescence intensities observed in the absence and presence of different concentrations of quencher substrate, [Q] is quencher substrate concentration, and K_{sv} is the Stern-Volmer quenching constant.

Eqn 1.2. $$K_{sv} = k_q \cdot \tau_0$$

Where k_q is the bimolecular quenching rate constant and τ_0 is the excited state lifetime in the absence of quencher.

1.11c Contemporary Transition Metal Photoredox Catalysts and their Uses

When translating the theory described above into rational reaction design, one must consider the possible bimolecular transitional pathways as well as the unimolecular.[20] Further simplifying the Jablonski diagram of chromophore **S** seen in **Scheme 1.5** and adding a quencher molecule **X** produces a schematic such as the one in **Scheme 1.6A**. A bimolecular reaction provides more pathways for excited state quenching including triplet-triplet energy transfer, depicted in **Scheme 1.6B**, and transfer of electrons.

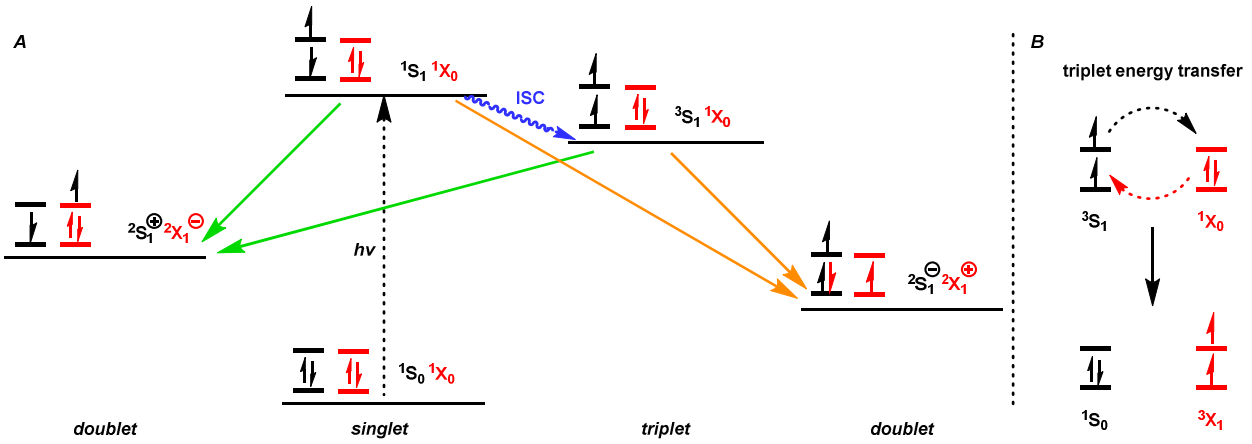

Scheme 1.6. Bimolecular Jablonski diagrams. A) Bimolecular Jablonski diagram with photosensitizer **S** and quencher **X**; B) depiction of triplet-triplet Dexter energy transfer, another excited state quenching process.

The electron transfer depicted in **Scheme 1.6A** is fundamental to photoredox catalysis. After a chromophore **S** absorbs a photon and transitions to the singlet excited state, it may quench by electron transfer from its SOMO to the SOMO of **X** or by accepting an electron from the HOMO of **X** into its SOMO. Both cases create an ion pair. Equally, electron transfer may happen after ISC to triplet excited state $^{3}\mathbf{S}_{1}$. The likelihood of excited state catalyst being either reduced or oxidized in this manner depends on the relative energies of the catalyst excited state and the substrate ground state orbitals. These energies may be represented by catalyst redox potentials. The resulting ion pairs contain high-energy open-shell species that can be harnessed for chemical reactions.

In the advent of the 21st century's explosion of interest in transition metal photocatalysis, a plethora of ruthenium and iridium polypyridyl complexes have been synthesized.[21] General ligand-related trends have been observed: as expected, the oxidative power of the complex tends to increase with ligands that pull electron density away from the metal center, and the reductive power of the complex tends to be proportional to the electron density on the ligands. There exists an abundance of reviews expounding upon the various redox potentials of these catalysts and their tunability.[20]

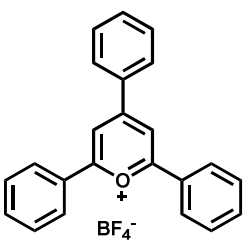

1.16: 2,4,6-triphenylpyrylium tetrafluoroborate

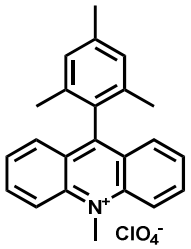

1.17: 9-mesityl-10-methyl-acridinium perchlorate

Scheme 1.7. Structures of two highly oxidizing organocatalysts TPT and Mes-Acr.

It is important to note that photochemistry in organic synthesis is not strictly limited to metal polypyridyl complexes – in fact organic photoredox catalysts have recently garnered similar levels of infamy to their transition metal counterparts.[22] These organocatalysts, such as the highly oxidizing triphenylpyrilium (TPT) and mesityl methylacridinium salts (Mes-Acr, **Scheme 1.7**), are occasionally able to perform energy transfer from the singlet excited state, and offer a wider variety of redox potentials than metal polypyridyl complexes.

Photocatalysis's main added value to substrate synthesis is found in its facile generation of free radicals. Free radicals not only provide complementarity to two-electron pathways as mentioned *vide supra* but carry many synergistic benefits. Most radical transformations don't require time- and resource-intensive protection and deprotection of alcohols. Other important functionalities such as carbonyls will be functionally inert towards most free radicals. The high energy and speed of reactivity of the free radical lends itself well to the development of radical cascades, allowing syntheses to be designed with atom-economical expedient "zipping together" of a molecule in a single step. Furthermore, interconversion between radical and ionic mechanisms is facile through redox manipulation (also possible using photocatalysts).

1.11d Bond Dissociation Energy and Hydrogen Atom Transfer

The formation of covalent bonds is by necessity thermodynamically favorable, in other words the energy of the formed bond is lower than the energies of the two molecular components used to form the bond.[23] In order to break this bond, energy must therefore be added to it. One way of illustrating this energy is by breaking the covalent bond homolytically: in such a manner as to leave each fragment with one of the two electrons that made up the bond. This energy change associated with the homolytic cleavage of a bond at a specified temperature is termed Bond Dissociation Energy (BDE) and is fundamental to reaction design and outcome prediction in radical chemistry.

Bond Dissociation Energy is also termed Bond Dissociation Enthalphy, as it refers directly to the energy of a free radical (in kcal/mol or kJ/mol) and can be used to determine whether a bond-breaking or -forming reaction is thermodynamically favorable or highly reversible. Strong covalent bonds have high BDEs (i.e. BDE >100 kcal/mol). Factors affecting BDE are similar to the factors affecting pKa: stabilization via hyperconjugation and resonance contribute to a lower BDE and a more stable set of radicals. Free radicals with low parent BDE therefore become easier to form and may be less reactive, while free radicals with high parent BDE are challenging to form but extremely reactive.[24]

A radical “quenching”, or a return to a spin-paired system from a spin-unpaired system, is generally so thermodynamically favorable that the principles of “thermodynamic vs kinetic” stability require revision in a radical context. Free radicals quench so quickly relative to their ionic counterparts that most radical species exist in extremely low concentrations in a reaction mixture, making radical-radical homocouplings statistically

rare. If a desired coupling partner is also present in low concentrations, a meeting of free-radical and coupling partner also becomes statistically unlikely. Instead a Hydrogen Atom Transfer (HAT) from a molecule of solvent to the free radical becomes significantly more likely due to kinetics, even if this HAT is not the most thermodynamically favorable reaction available. Furthermore, radical stability does not preclude persistence of the radical. A stable free radical is one in which unpaired spin is stabilized thermodynamically (e.g. by hyperconjugation). A persistent free radical has a long lifetime due to kinetics: it may or may not be hyperconjugatively stabilized but is sterically prevented from reacting.

A prime example of a persistent radical is the TEMPO free-radical (BDE_{O-H} = 69 kcal/mol) compared to other nitroxyl radicals (BDE_{O-H} = 70-90 kcal/mol) as depicted in **Scheme 1.8A**.[25] Persistence is also the reason for the discovery of the first free radical by Gomberg in 1900. Its utility is further shown in the decomposition of phenylazotriphenyl methane in benzene in the sixties by Perkins: the only products that formed from the reaction were from either disproportionation or the heterocoupling of intermediates.[26] No homocoupled products were formed. At the time, this reaction was surprisingly selective considering that radicals were frequently perceived as being “uncontrollable”. This selectivity arises due to steric hindrance of the persistent triphenylmethyl radical – preventing it from dimerizing and slowing its reaction with other species.

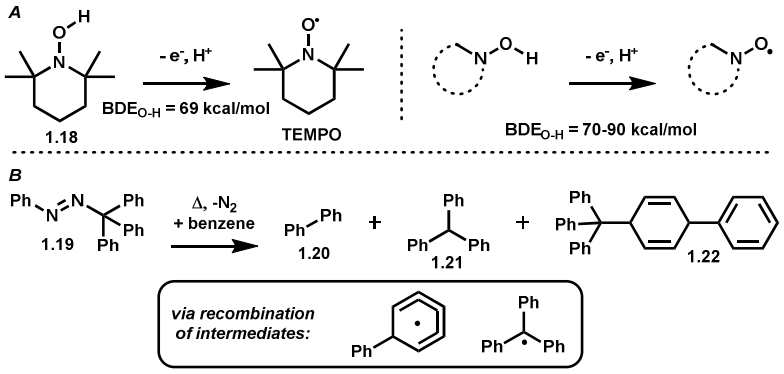

Scheme 1.8. Stable and persistent radicals. A) Stability and persistence of TEMPO due to steric hindrance compared to other nitroxyl radicals; B) Thermal decomposition of phenylazotriphenylmethane reveals products formed from reaction of persistent radicals.

BDE is fundamental to developing understanding of radical mechanisms, especially when considering a mechanism involving HAT which is simply the transfer of a hydrogen atom (one proton and one electron) from one molecule to another. Due to both the importance and prevalence of HAT, there is fortunately a vast and growing body of literature containing X-H BDEs and relevant kinetics. A beautifully organized and highly comprehensive table of BDEs can be found in Lange's Handbook of Chemistry.[27] The sheer volume of prior art simplifies outcome prediction for reactions involving HAT. For example, one may predict that a captodative H in one area of a molecule is more likely to be abstracted by a free radical partner than a completely aliphatic H in another area of the molecule, and that a hydroxy H on the molecule will be left totally untouched regardless. This informs the chemist that a captodative radical intermediate is likely to be formed following HAT and that alcohol protecting groups are not required – which allows the reactant in question to be designed elegantly and efficiently.

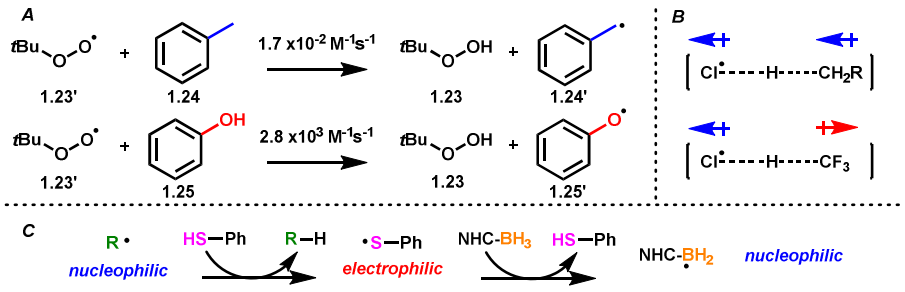

Scheme 1.9. Radical kinetics**.** A) Rate constant comparison between toluene (BDE_{tol} = 89.8 kcal/mol) and phenol (BDE_{phenol} = 88.0 kcal/mol) HAT by *tert*-butyl peroxyl radical; B) depiction of polar and non-polar HAT transition states; C) an example of HAT polarity reversal catalysis.

The kinetics of a HAT reaction can also be roughly predicted by comparison of BDEs. For many reactions involving HAT from a substrate to R●, the rate constants are directly proportional to the reaction energy, and reaction energy – approximated by differences in BDEs from different substrates – can inform rate constants.[28] However, bond strength is not the only factor in determining substrate HAT kinetics. H-bonding ability and polarity can play large roles, for example in the observed trend of HAT to peroxides being orders of magnitude faster from an O-H bond than from a C-H bond of the same strength (**Scheme 1.9A**). It is also seen to be advantageous in many cases to have an electronic "alignment" between a radical and HAT substrate, meaning that one partner is more "nucleophilic" (or electron-rich) and the other partner is more "electrophilic" (or electron-poor).[29] Aligning two reacting partners to create an electronic push-pull effect facilitates the formation of a polar transition state, which lowers transition state energy and results in a faster reaction (**Scheme 1.9B**). In cases where reactions are sluggish due to

electronic misalignment of reactive partners, strategies such as the polarity-reversal catalysis seen in **Scheme 1.9C** can be employed.

Even one initiated in the chemistry of radicals can easily become overwhelmed by the sheer number of interwoven factors to consider in a radical reaction. A chemist can be reassured by the tendency for solvent to play insignificant roles in radical reactions yet end up performing a radical reaction where the identity of the solvent is crucial. A researcher could be found confidently adding water to their radical reaction, safe in their knowledge that the BDE of water is 119 kcal/mol – comfortably far outside of competitive reactivity with the aliphatic ketone they are trying to oxidize. A month later this same researcher may sweat over reports of the reduction of carbonyls by samarium diiodide-mediated HAT from water.[30] Those wishing to step onto the Radical Rollercoaster are in for quite the ride.

1.12 Radical Redox Flow with Gold and Iridium

1.12a Discovery of Gold Photoredox Catalysts and their Properties

Around 2013, the Barriault research group began to believe that perhaps Ciamician's "mythical gold of the Rhine" was not coal, but in fact gold itself.[2a] The first work elucidating gold's potential as a photosensitizing catalyst appeared late in the 20th century, wherein the dimeric bisphosphine complex **1.26** was described by Che and colleagues (**Scheme 1.10**).[31] This complex caught the attention of the Barriault group researchers due to its unique mechanism of photochemical energy transfer; unlike the metal-to-ligand charge transfer (MLCT) from the ruthenium and iridium polypyridyl complexes that had become ubiquitous in 21st century photocatalysis, the $[Au_2(dppm)_2]Cl_2$ catalyst is thought to

operate *via* inner-sphere electron transfer.[32] This unique charge transfer mechanism is perhaps the reason why this photocatalyst can reduce unactivated bromoalkane bonds (E_{red} ≥ -1.90 V *vs*. SCE) even though the process is thermodynamically uphill based on the catalyst's oxidative potential (E_{ox}^* = -1.63 V *vs*. SCE). Most other ruthenium and iridium polypyridyl complexes only allow access to weaker (more easily reducible) bonds, and as such any bromoalkanes requiring homolysis must be activated by tethering to a highly electron-withdrawing group. The $[Au_2(dppm)_2]Cl_2$ catalyst thus provides researchers with easy access to high-energy free radicals in solution from cheap, readily available starting materials and under mild conditions.

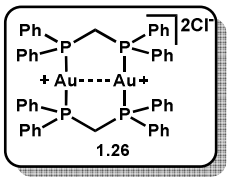

Scheme 1.10. Dimeric gold bis(diphenylphosphino)methane dichloride complex.

1.12b Photophysical Properties of Dimeric Gold Photoredox Catalyst

Having been studied by our group for almost a decade, the mechanism of action of the dimeric gold photocatalyst is now reasonably well understood. The catalyst absorbs light most strongly in the UVB range (λ_{abs} = 295 nm) with an absorption tail in the UVA (λ_{abs} = 365 nm), and following absorption is promoted to a triplet excited state as seen in **Scheme 1.11**. This excited state precipitates formation of a Au-Au bond which does not exist in the ground state, and it is thought that the formation of this bond frees a coordination site on one of the two gold centers where substrates can bind. This coordination site could be

occupied with bromoalkane substrates, forming an exciplex which would then undergo inner-sphere electron transfer.

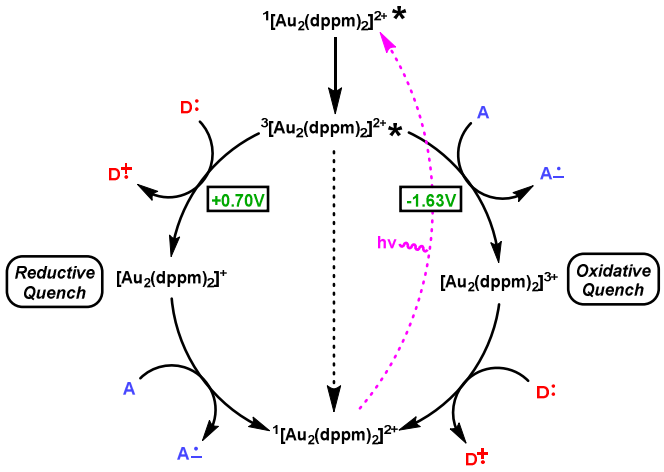

Scheme 1.11. Depiction of photoexcitation of dimeric gold photoredox catalyst $[Au_2(dppm)_2]Cl_2$ and its oxidative and reductive quenching cycles.

This dimeric photoredox catalyst provides further synthetic versatility in its two quenching cycles. The triplet excited-state of the catalyst (E_{red}^* = 0.70 V *vs.* SCE) can access the reductive quenching cycle depicted in **Scheme 1.11** by SET from a donor molecule, usually trialkylamine bases such as *N,N*-diisopropylamine (DIPEA, k_q = 2.7 x 10^7 $M^{-1}s^{-1}$). This reductive quench creates a Au^{1+}-Au^0 species that can easily reduce bromine-carbon bonds to return to its neutral ground state.[32,33] The resulting carbon-centered radical can then undergo a variety of transformations before termination. Alternatively, the excited-state catalyst can also access an oxidative quenching cycle where it quenches first with a bromoalkane species such as *n*-BuBr (k_q = 2.9 x 10^6 $M^{-1}s^{-1}$), generating bromide, a carbon-centered radical which may undergo further radical reactions, and a highly reducible Au^{1+}-Au^{2+} species. To return to the catalyst's neutral

ground state, it can accept an electron from either a donor molecule (mainly a trialkylamine base) or from a carbon-centered radical to generate a carbocation (*hopefully*, from a radical downstream from some useful chemistry). As the quenching rates for both bromoalkanes and trialkylamines are separated by roughly a degree of magnitude, redox cycles can be tuned by varying the concentration of each species.

The Barriault group has spent a productive half-decade elucidating the various chemical manipulations made possible by the dimeric gold catalyst $[Au_2(dppm)_2]Cl_2$. The group of Hashmi has also contributed several important methodological advancements with this catalyst.[34]

1.12c Iridium Polypyridyl Catalysis

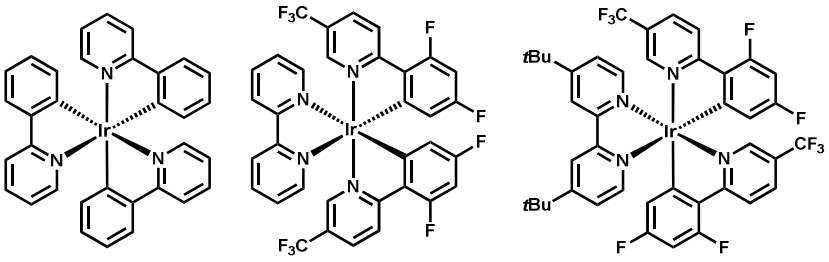

	$Ir(ppy)_3$	$Ir(dF(CF_3)ppy)_2(bpy)$	$Ir(dF(CF_3)ppy)_2(dtbbpy)$
Max absorption (λ_{max})	375 nm	405 nm	380 nm
Ox. potential Ir(III)* / Ir(II)	0.31 V	0.97 V	1.21 V
Red. potential Ir(III)* / Ir(IV)	-1.73 V	-0.97 V	-0.89 V
Excited state lifetime (τ)	1900 ns	2280 ns	2300 ns
Triplet energy (E_T)	55.2 kcal/mol	60.4 kcal/mol	60.1 kcal/mol

Scheme 1.12. The physicochemical parameters (maximum absorption, excited state reduction potential, excited state oxidation potential, lifetime, and triplet energy) for three synthetically useful iridium polypyridyl photocatalysts.[35]

Shortly following the explosion of the first $[Ru(bpy)_3]^{2+}$ photocatalysts in organic synthesis, attention turned to polypyridyl complexes of iridium such as $[Ir(ppy)_3]^{2+}$. Like its

ruthenium counterparts, the polypyridyl complexes function in photochemical reactions via Metal-to-Ligand Charge Transfer (MLCT), which allows potential access to both oxidative and reductive quenching cycles. Overall, iridium catalysts are more highly reducing than their ruthenium counterparts, though in both cases the redox potentials are highly tunable with ligand variation.[20,35] Some useful examples and their physicochemical parameters are portrayed in **Scheme 1.12**.

1.12d Generation of Halogen Atoms for HAT

Halogen radicals (or halogen *atoms*, which is the more accurate nomenclature for open-shell halogen species) are valuable initiators for HAT due to their reactivity: spanning from the "sheer insanity" of F▪ to the relatively tame Br▪ and the almost unreactive I▪. In particular the chlorine and bromine atoms stand out from this family due to their moderate place on the scale of reactivity: in HAT reactions, the chlorine atom (BDE_{Cl-H} = 103 kcal/mol) is able to access the most unactivated C-H alkyl bonds, and the bromine atom (BDE_{Br-H} = 88 kcal/mol) can access C-H bonds with low stabilization (e.g. tertiary alkyl C-H bonds). Facile and mild access to halogen atoms in solution could present a valuable methodology for diverse functionalization of feedstock hydrocarbons in industry, or for late-stage C-H activation in total synthesis.

Currently there exist few methods to generate chlorine or bromine atoms in solution, and those that do are not catalytic or easily controllable. For the past century, the most common method has been through photolysis of Cl_2 or Br_2 in solution.[36] Recently, some forays into catalytic generation of chlorine atoms have been made in conjunction with dual nickel/iridium and organic photoredox catalysis.[37]

1.2 A Basic Toolkit for Mechanistic Elucidation in Radical Chemistry

The breakneck speed of many free-radical reactions makes mechanistic considerations integral to successful reaction design – though unfortunately also makes radical mechanisms incredibly difficult to study. Fast reaction rates can make it prohibitive to observe a reaction in real time with Electron Paramagnetic Resonance (EPR) spectroscopy, unless there happens to be a persistent radical involved. In many reactions multiple types of radical species are present in solution at any given moment, which may result in complex mixtures of products that are difficult to identify. Presence or absence of a radical propagation chain can also be vital to determine. To probe these questions and manage the high rates, many mechanistic devices in the radical toolkit involve indirect detection.

A prominent example of this includes the various radical trapping experiments.[38] Persistent radicals such as triphenylmethyl, TEMPO, or even O_2 can undergo radical termination by combining with any free radicals that are generated in solution (so long as the two species' have a matched electronic alignment). Similar trapping experiments can be undertaken by adding terminal olefins to the reaction medium – with appropriate electronic alignment of the olefin and radical species, an addition reaction can occur. In both cases, the resultant radical-trap or olefin adducts can be isolated and used as evidence for the existence of the free radical species in question. A third and immensely popular method is employing "radical clocks" as probes: reactions such as cyclizations, ring-openings, or rearrangements that have known radical rate constants (**Scheme 1.13**). These clocks can be used to support the existence of free radicals in a reaction, and to

estimate the rate constant of the reaction by comparing it to the ratio of the various products of the radical clock.

These radical clocks can also be employed in the determination of the absolute rate of a radial reaction. Pseudo first-order reaction conditions can be created by using such a large excess of one reagent in a bimolecular reaction that that reagent's concentration is effectively constant. The rate constant for a bimolecular reaction (Eqn 1.3) can then be simplified to that of a unimolecular reaction (Eqn 1.4) and the dependence of the rate on the concentration of the remaining reagent can be evaluated.

Eqn 1.3 $$v = k\,[A]^x[B]^y$$

Eqn 1.4 $$v = k\,[A]^x$$

Where *v* is the reaction speed, *k* is the rate constant of the reaction at a set temperature, *x* and *y* are the partial orders of reaction for each component, and A and B are the concentrations of the reagents in the bimolecular reaction.

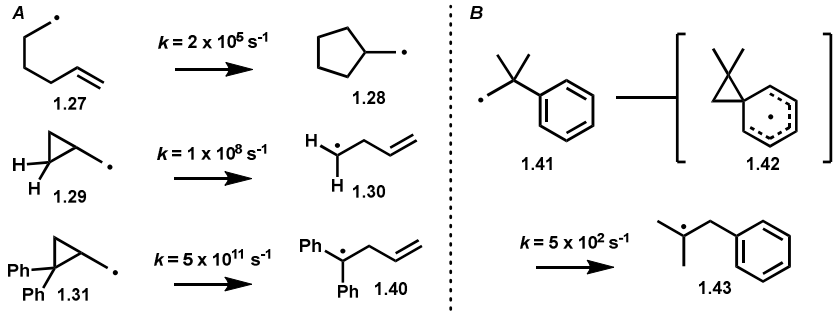

Scheme 1.13. Useful radical kinetic experiments. A) Cyclization and ring-opening radical clocks; B) neophyl rearrangement radical clock.[39]

Another invaluable mechanistic probe is the Kinetic Isotope Effect (KIE). This effect represents a change in reaction rate inversely proportional to the mass of the moving atom(s) and can be observed when replacing abundant atomic isotopes in a molecule with heavier isotopes. The effect relies on a large difference between relative zero-point energies of the ground state isotopes and their relative energies at the transition state. The KIE can be found by dividing the reaction rate constant of the lighter isotope by the rate constant of the heavier isotope. Estimates of these rates can be obtained using ratios of isotopic composition in the products. The simplest (and most widely employed) example of this is the replacement of protium with deuterium. Though both ionic and radical reactions can exhibit isotope effects, these effects tend to be significantly more pronounced in radical reactions. Thus, a large KIE can provide evidence to support a radical reaction mechanism. The KIE can further be used to support existence of radical chain propagation.

1.3 References

1. Arrhenius, S., On the Influence of Carbonic Acid in the Air upon the Temperature of the Earth. *Pubs. Astr. Soc. Pacific* **1897,** *9*, 14.
2. a) Ciamician, G., THE PHOTOCHEMISTRY OF THE FUTURE. *Science* **1912,** *36*, 385; b) Albini, A.; Fagnoni, M., 1908: Giacomo Ciamician and the Concept of Green Chemistry. *ChemSusChem* **2008,** *1*, 63-66.
3. This goal has been pursued since the advent of the field of photochemistry in the 1900s, and we are still in hot pursuit today. a) Graetzel, M., Artificial photosynthesis: water cleavage into hydrogen and oxygen by visible light. *Acc. Chem. Res.* **1981,** *14*, 376-384; b) Meyer, T. J., Chemical approaches to artificial photosynthesis. *Acc. Chem. Res.* **1989,** *22*, 163-170; c) Ni, M.; Leung, M. K. H.; Leung, D. Y. C.; Sumathy, K., A review and recent developments in photocatalytic water-splitting using TiO2 for hydrogen production. *Ren. Sus. En. Rev.* **2007,** *11*, 401-425; d) Fajrina, N.; Acar, C.; Dincer, I.; Naterer, G. F., Review of photocatalytic water-splitting methods for sustainable hydrogen production. *Int. J. Energ. Res.* **2016,** *40*, 1449-1473; e) Tahir, M., A critical review in strategies to improve photocatalytic water splitting towards hydrogen production. *Int. J. Hydrog. En.* **2019,** *44*, 540-577; f) Hisatomi, T.; Domen, K., Reaction systems for solar hydrogen production via water splitting with particulate semiconductor photocatalysts. *Nat. Catal.* **2019,** *2*, 387-399; Important to note it is not the only attempt by chemists to mimic photosynthesis: g) Imahori, H., Porphyrin–fullerene linked systems as artificial photosynthetic mimics. *Org. Biomol. Chem.* **2004,** *2*, 1425-1433; Fukuzumi, S., Bioinspired Electron-Transfer Systems and Applications. *Bull. J. Chem. Soc.* **2006,** *79*, 177-195.

4. a) Malati, M. A., The Photocatalysed Removal of Pollutants from Water. *Environ. Tech.* **1995,** *16*, 1093-1099; b) Devipriya, S.; Yesodharan, S., Photocatalytic degradation of pesticide contaminants in water. *Sol. En. Mater. Sol. Cell* **2005,** *86*, 309-348; c) Chatterjee, D.; Dasgupta, S., Visible light induced photocatalytic degradation of organic pollutants. *J. Photoch. Photobio. C* **2005,** *6*, 186-205; d) Dalrymple, O. K.; Yeh, D. H.; Trotz, M. A., Removing pharmaceuticals and endocrine-disrupting compounds from wastewater by photocatalysis. *J. Chem. Tech. Biotech.* **2007,** *82*, 121-134; e) Malato, S.; Fernández-Ibáñez, P.; Maldonado, M. I.; Blanco, J.; Gernjak, W., Decontamination and disinfection of water by solar photocatalysis: Recent overview and trends. *Cat. Today* **2009,** *147*, 1-59.
5. For some notable examples of TiO_2 in organic synthesis: a) Kitano, M.; Matsuoka, M.; Ueshima, M.; Anpo, M., Recent developments in titanium oxide-based photocatalysts. *Appl. Cat. A***2007,** *325*, 1-14; b) Hernández-Alonso, M. D.; Fresno, F.; Suárez, S.; Coronado, J. M., Development of alternative photocatalysts to TiO2: Challenges and opportunities. *En. Environ. Sci.* **2009,** *2*, 1231-1257; c) Augugliaro, V.; Caronna, T.; Di Paola, A.; Marcì, G.; Pagliaro, M.; Palmisano, G.; Palmisano, L., TiO2-Based Photocatalysis for Organic Synthesis. In *Environmentally Benign Photocatalysts: Applications of Titanium Oxide-based Materials*, Anpo, M.; Kamat, P. V., Eds. Springer New York: New York, NY, **2010**; pp 623-645; d) Ma, D.; Liu, A.; Li, S.; Lu, C.; Chen, C., TiO2 photocatalysis for C–C bond formation. *Cat. Sci. Tech.* **2018,** *8*, 2030-2045; General reviews including polyoxometalate, cobalt and iron porphyrin complexes in photocatalytic organic synthesis up until 2009: e) Texier, I.; Giannotti, C.; Malato, S.; Richter, C.; Ouazzani, J.; Delaire, J., Potential applications of solar reactions

photocatalysed by the decatungstate anion. *J. Chim. Phys.* **1999,** *96*, 430-436; f) Palmisano, G.; Augugliaro, V.; Pagliaro, M.; Palmisano, L., Photocatalysis: a promising route for 21st century organic chemistry. *Chem. Comm.* **2007**, 3425-3437; g) Fagnoni, M.; Dondi, D.; Ravelli, D.; Albini, A., Photocatalysis for the Formation of the C–C Bond. *Chem. Rev.* **2007,** *107*, 2725-2756; h) Protti, S.; Ravelli, D.; Fagnoni, M.; Albini, A., Solar light-driven photocatalyzed alkylations. Chemistry on the window ledge. *Chem. Comm.* **2009**, 7351-7353;

6. Roth, H. D., The Beginnings of Organic Photochemistry. *Angew. Chem. Int. Ed.* **1989,** *28*, 1193-1207; Norrish Type I Reaction; Norrish Type II Reaction. In *Comprehensive Organic Name Reactions and Reagents*; pp 2062-2071.
7. Burstall, F. H., 34. Optical activity dependent on co-ordinated bivalent ruthenium. *J. Chem. Soc. Res.* **1936**, 173-175.
8. a) Dwyer, F. P. J.; Gyarfas, F. C., The chemistry of ruthenium. Part VII. The oxidation of d and l tris 2:2′ dipyridyl ruthenium II iodide. *J. Roy. Soc. N.S.W.* **1949,** *83*, 177-180; For examples of the first applications of $Ru(bpy)_3^{2+}$ in inorganic chemistry, see: b) Natarajan, P.; Endicott, J. F., Direct observation of the dibromide radical anion oxidation of tris(bipyridyl)ruthenium(II). Evidence for a triplet-to-triplet energy transfer mechanism in the photosensitized redox decomposition of cobalt(III) substrates. *J. Phys. Chem.* **1973,** *77*, 971-972; c) Creutz, C.; Sutin, N., Electron-transfer reactions of excited states: direct evidence for reduction of the charge-transfer excited state of tris(2,2'-bipyridine)ruthenium(II). *J. Am. Chem. Soc.* **1976,** *98*, 6384-6385; First direct evidence of quenching with an organic agent: d) Michael-Grätzel, M. M., 530 nm-Laser Photolysis Studies of the Photo Reduction of Tris (2,2-bipyridine)-ruthenium(II) by

Organic Donors. *Berichte der Bunsengesellschaft für physikalische Chemie* **1977,** *81*, 504-507.

9. a) Hedstrand, D. M.; Kruizinga, W. H.; Kellogg, R. M., Light induced and dye accelerated reductions of phenacyl onium salts by 1,4-dihydropyridines. *Tet. Lett.* **1978,** *19*, 1255-1258; b) van Bergen T. J., Hedstrand D. M., Kruizinga W. H., Kellogg R. M.; Chemistry of dihydropyridines. 9. Hydride transfer from 1,4-dihydropyridines to sp^3-hybridized carbon in sulfonium salts and activated halides. Studies with NAD(P)H model. *J. Org. Chem.* **1979**, *44*, 4953.
10. Teplý, F. Photoredox Catalysis by $[Ru(bpy)_3]^{2+}$ to Trigger Transformations of Organic Molecules. Organic Synthesis Using Visible-Light Photocatalysis and its 20th Century Roots. *Collect. Czech. Chem. Commun*. **2011**, *76*, 859–917.
11. Tin hydride as initiator
12. Tailoring of photoredox catalysts to expand to all f'nal groups
13. King, K. A., Finlayson, M. F., Spellane, P. J., Watts, R. J.; Luminescence spectroscopy and oxidative quenching of orthometallated complexes of iridium(III). *Sci. Pap. Phys. Chem. Res.* **1984**, *78*, 97-106.
14. a) Ischay, M. A.; Anzovino, M. E.; Du, J.; Yoon, T. P., Efficient Visible Light Photocatalysis of [2+2] Enone Cycloadditions. *J. Am. Chem. Soc.* **2008,** *130*, 12886-12887; b) Nicewicz, D. A.; MacMillan, D. W. C., Merging Photoredox Catalysis with Organocatalysis: The Direct Asymmetric Alkylation of Aldehydes. *Science* **2008,** *322*, 77; c) Narayanam, J. M. R.; Tucker, J. W.; Stephenson, C. R. J., Electron-Transfer Photoredox Catalysis: Development of a Tin-Free Reductive Dehalogenation Reaction. *J. Am. Chem. Soc.* **2009,** *131*, 8756-8757; d) Du, J.; Yoon, T. P., Crossed

Intermolecular [2+2] Cycloadditions of Acyclic Enones via Visible Light Photocatalysis. *J. Am. Chem. Soc.* **2009,** *131*, 14604-14605; e) Nagib, D. A.; Scott, M. E.; MacMillan, D. W. C., Enantioselective α-Trifluoromethylation of Aldehydes via Photoredox Organocatalysis. *J. Am. Chem. Soc.* **2009,** *131*, 10875-10877.

15. Literature searches were conducted in CAS Scifinder for the terms “Ru(bpy)3” and “Ru(bipy)3” prior to and post-2008. The results were then filtered by exclusion of journals for known inorganic content, e.g. with “inorganic” or “organometallic” in the title.
16. a) Liu, Q.; Dong, X.; Li, J.; Xiao, J.; Dong, Y.; Liu, H., Recent Advances on Palladium Radical Involved Reactions. *ACS Catal.* **2015,** *5*, 6111-6137; b) Kaga, A.; Chiba, S., Engaging Radicals in Transition Metal-Catalyzed Cross-Coupling with Alkyl Electrophiles: Recent Advances. *ACS Catal.* **2017,** *7*, 4697-4706; c) Parasram, M.; Gevorgyan, V., Visible light-induced transition metal-catalyzed transformations: beyond conventional photosensitizers. *Chem. Soc. Rev.* **2017,** *46*, 6227-6240; d) Chuentragool, P.; Kurandina, D.; Gevorgyan, V., Catalysis with Palladium Complexes Photoexcited by Visible Light. *Angew. Chem. Int. Ed.* **2019,** *58*, 11586-11598.
17. Studer, A.; Curran, D. P., Catalysis of Radical Reactions: A Radical Chemistry Perspective. *Angew. Chem. Int. Ed.* **2016,** *55*, 58-102.
18. Initiation of radical reactions is too broad a topic to be cited comprehensively. Included here are selected reviews and book chapters: a) Baguley, P. A.; Walton, J. C., Flight from the Tyranny of Tin: The Quest for Practical Radical Sources Free from Metal Encumbrances. *Angew. Chem. Int. Ed.* **1998,** *37*, 3072-3082; b) Ollivier, C.; Renaud, P., Organoboranes as a Source of Radicals. *Chem. Rev.* **2001,** *101*, 3415-3434; c)

Gilbert, B. C.; Parsons, A. F., The use of free radical initiators bearing metal–metal, metal–hydrogen and non-metal–hydrogen bonds in synthesis. *J. Chem. Soc. Perk. T. 2* **2002,** (3), 367-387; d) Myers, T. N. (**2002**). Initiators, Free-Radical. In *Encyclopedia of Polymer Science and Technology*, (Ed.); e) Denisov, E. T., Denisova, T. G. and Pokidova, T. S. (**2005**). Compounds with Weak C-C, N-N, C-N, and N-O Bonds. In *Handbook of Free Radical Initiators* (Ed. E. T. Denisov, T. G. Denisova and T. S. Pokidova); f) Braun, D., Origins and Development of Initiation of Free Radical Polymerization Processes. *Int. J. Polym. Sci.* **2009,** *2009*, 1-10; g) Lalevée, J. and Fouassier, J. P. (**2012**). Overview of Radical Initiation. In *Encyclopedia of Radicals in Chemistry, Biology and Materials* (Ed. C. Chatgilialoglu; A. Studer)

19. a) Bernard, D.; 3: Photophysics of Photocatalysts. *Chemical Photocatalysis*. (Ed. König, B.) De Gruyter **2013**, 19-44. b) Turro, N. J.; Ramamurthy, V.; Scaiano, J. C., *Modern Molecular Photochemistry of Organic Molecules*. University Science Books **2010**.

20. This section is an agglomeration of a large body of literature that is too numerous and interrelated to be cited comprehensively or individually. A set of important and modern reviews and books include: a) Zeitler, K., Photoredox Catalysis with Visible Light. *Angew. Chem. Int. Ed.* **2009,** *48*, 9785-9789; b) Xuan, J.; Xiao, W.-J., Visible-Light Photoredox Catalysis. *Angew. Chem. Int. Ed.* **2012,** *51*, 6828-6838; c) Tucker, J. W.; Stephenson, C. R. J., Shining Light on Photoredox Catalysis: Theory and Synthetic Applications. *J. Org. Chem.* **2012,** *77*, 1617-1622; d) Teplý, F.; 7: Visible light photoredox catalysis with $[Ru(bpy)_3]^{2+}$: General principles and the twentieth century roots. *Chemical Photocatalysis*. (Ed. König, B.) De Gruyter **2013**, 111-138; e) Yoon,

T. P., Visible Light Photocatalysis: The Development of Photocatalytic Radical Ion Cycloadditions. *ACS Catal.* **2013,** *3*, 895-902; f) Prier, C. K.; Rankic, D. A.; MacMillan, D. W. C., Visible Light Photoredox Catalysis with Transition Metal Complexes: Applications in Organic Synthesis. *Chem. Rev.* **2013,** *113*, 5322-5363; g) Shaw, M. H.; Twilton, J.; MacMillan, D. W. C., Photoredox Catalysis in Organic Chemistry. *J. Org. Chem.* **2016,** *81*, 6898-6926; McAtee, R. C.; h) Corrigan, N.; Shanmugam, S.; Xu, J.; Boyer, C., Photocatalysis in organic and polymer synthesis. *Chem. Soc. Rev.* **2016,** *45*, 6165-6212; i) Xie, J.; Jin, H.; Hashmi, A. S. K., The recent achievements of redox-neutral radical C–C cross-coupling enabled by visible-light. *Chem. Soc. Rev.* **2017,** *46*, 5193-5203; j) McClain, E. J.; Stephenson, C. R. J., Illuminating Photoredox Catalysis. *Trends in Chemistry* **2019,** *1*, 111-125.

21. For compendiums of Ir (II) and Ru (II) photocatalysts, see: a) DiRocco, D.; Electrochemical Series of Photocatalysts and Common Organic Compounds Reference Sheet, **2014**, Merck (visible here); b) Corrigan, N.; Shanmugam, S.; Xu, J.; Boyer, C., Photocatalysis in organic and polymer synthesis. *Chem. Soc. Rev.* **2016,** *45*, 6165-6212.
22. Organic photoredox catalysis: Romero, N. A.; Nicewicz, D. A., Organic Photoredox Catalysis. *Chem. Rev.* **2016,** *116*, 10075-10166.
23. Stauffer, E.; Dolan, J. A.; Newman, R. (**2008**) Chapter 3 - Review of Basic Organic Chemistry. In *Fire Debris Analysis* (Eds. Stauffer, E.; Dolan, J. A.; Newman, R.) Academic Press: Burlington; pp 49-83.
24. a) Chapter 1 Introduction to free radicals. In *Laboratory Techniques in Biochemistry and Molecular Biology* (**1991**) (Eds. Rice-Evans, C. A.; Diplock, A. T.; Symons, M. C.

R.) Elsevier pp 1-18; b) Zipse, H. (**2006**) Radical Stability—A Theoretical Perspective. In *Radicals in Synthesis I* (Ed. Gansäuer, A.) Springer Berlin Heidelberg: Berlin, Heidelberg, 2006 pp 163-189.

25. a) Studer, A., The Persistent Radical Effect in Organic Synthesis. *Chem. Eur. J.* **2001,** *7*, 1159-1164; b) Smith, M. B.; March, J. (**2006**) Carbocations, Carbanions, Free Radicals, Carbenes, and Nitrenes. In *March's Advanced Organic Chemistry*. John Wiley & Sons, pp 234-295; c) Galli, C. (**2008**) Nitroxyl Radicals. In *The Chemistry of Hydroxylamines, Oximes and Hydroxamic Acids* (Eds. Patai, S.; Rappoport, Z; Liebman, J. F.) pp 705-750; d) Leifert, D.; Studer, A., The Persistent Radical Effect in Organic Synthesis. *Angew. Chem. Int. Ed.* **2019,** *Article ASAP*. See also ref. 25.
26. a) Gomberg, M. *J. Am. Chem. Soc.* **1900**, *22*, 757-771. b) Hey, D. H.; Perkins, M. J.; William, G. H., Mechanisms of free-radical aromatic substitution. *Tet. Lett.* **1963,** *4*, 445-452.
27. Dean, J. A. (**1999**) Properties of Atoms, Radicals, and Bonds in *Handbook of Chemistry*. (Eds. Dean, J. A; Lange, N. A.) McGraw-Hill pp 4.41-4.53.
28. a) Mayer, J. M., Understanding Hydrogen Atom Transfer: From Bond Strengths to Marcus Theory. *Acc. Chem. Res.* **2011,** *44*, 36-46; b) Sherburn, M. S. (**2012**) Basic Concepts on Radical Chain Reactions. In *Encyclopedia of Radicals in Chemistry, Biology and Materials*. (Eds. Studer, A.; Chatgilialoglu, C.) John Wiley and Sons; c) Capaldo, L.; Ravelli, D., Hydrogen Atom Transfer (HAT): A Versatile Strategy for Substrate Activation in Photocatalyzed Organic Synthesis. *Eur. J. Org. Chem.* **2017,** *2017*, 2056-2071

29. a) Tedder, J. M., Which Factors Determine the Reactivity and Regioselectivity of Free Radical Substitution and Addition Reactions? *Angew. Chem. Int. Ed.* **1982,** *21*, 401-410; b) P. Roberts, B., Polarity-reversal catalysis of hydrogen-atom abstraction reactions: concepts and applications in organic chemistry. *Chem. Soc. Rev.* **1999,** *28*, 25-35; c) Pan, X.; Lacôte, E.; Lalevée, J.; Curran, D. P., Polarity Reversal Catalysis in Radical Reductions of Halides by N-Heterocyclic Carbene Boranes. *J. Am. Chem. Soc.* **2012,** *134*, 5669-5674.

30. Chciuk, T. V.; Flowers, R. A., Proton-Coupled Electron Transfer in the Reduction of Arenes by SmI_2–Water Complexes. *J. Am. Chem. Soc.* **2015,** *137*, 11526-11531.

31. Che, C.-M.; Kwong, H.-L.; Yam, V. W.-W.; Cho, K.-C., Spectroscopic properties and redox chemistry of the phosphorescent excited state of $[Au_2(dppm)_2]^{2+}$ [dppm = bis(diphenylphosphino)methane]. *J. Chem. Soc. Chem. Comm..* **1989**, 885-886; b) Che, C.-M.; Kwong, H.-L.; Poon, C.-K.; Yam, V. W.-W., Spectroscopy and redox properties of the luminescent excited state of [Au2(dppm)2]2+(dppm = Ph2PCH2PPh2). *J. Chem. Soc. Dalt. Trans.* **1990**, 3215-3219.

32. McTiernan, C. D.; Morin, M.; McCallum, T.; Scaiano, J. C.; Barriault, L., Polynuclear gold(i) complexes in photoredox catalysis: understanding their reactivity through characterization and kinetic analysis. *Cat. Sci. Tech.* **2016,** *6*, 201-207.

33. a) McCallum, T.; Rohe, S.; Barriault, L., Thieme Chemistry Journals Awardees – Where Are They Now? What's Golden: Recent Advances in Organic Transformations Using Photoredox Gold Catalysis. *Synlett* **2017,** *28*, 289-305; b) Zidan, M.; Rohe, S.; McCallum, T.; Barriault, L., Recent advances in mono and binuclear gold photoredox catalysis. *Cat. Sci. Tech.* **2018,** *8*, 6019-6028.

34. a) Revol, G.; McCallum, T.; Morin, M.; Gagosz, F.; Barriault, L., Photoredox Transformations with Dimeric Gold Complexes. *Angew. Chem. Int. Ed.* **2013,** *52*, 13342-13345; b) McCallum, T.; Slavko, E.; Morin, M.; Barriault, L., Light-Mediated Deoxygenation of Alcohols with a Dimeric Gold Catalyst. *Eur. J. Org. Chem.* **2015,** *2015*, 81-85; c) Xie, J.; Shi, S.; Zhang, T.; Mehrkens, N.; Rudolph, M.; Hashmi, A. S. K., A Highly Efficient Gold-Catalyzed Photoredox α-C(sp3)□H Alkynylation of Tertiary Aliphatic Amines with Sunlight. *Angew. Chem. Int. Ed.* **2015,** *54*, 6046-6050; d) Kaldas, S. J.; Cannillo, A.; McCallum, T.; Barriault, L., Indole Functionalization via Photoredox Gold Catalysis. *Org. Lett.* **2015,** *17*, 2864-2866; e) McTiernan, C. D.; Morin, M.; McCallum, T.; Scaiano, J. C.; Barriault, L., Polynuclear gold(i) complexes in photoredox catalysis: understanding their reactivity through characterization and kinetic analysis. *Cat. Sci. Tech.* **2016,** *6*, 201-207; f) Xie, J.; Zhang, T.; Chen, F.; Mehrkens, N.; Rominger, F.; Rudolph, M.; Hashmi, A. S. K., Gold-Catalyzed Highly Selective Photoredox C(sp2)–H Difluoroalkylation and Perfluoroalkylation of Hydrazones. *Angew. Chem. Int. Ed.* **2016,** *55*, 2934-2938; g) McCallum, T.; Barriault, L., Direct alkylation of heteroarenes with unactivated bromoalkanes using photoredox gold catalysis. *Chem. Sci.* **2016,** *7*, 4754-4758; h) Xie, J.; Li, J.; Weingand, V.; Rudolph, M.; Hashmi, A. S. K., Intermolecular Photocatalyzed Heck-like Coupling of Unactivated Alkyl Bromides by a Dinuclear Gold Complex. *Chem. Eur. J.* **2016,** *22*, 12646-12650; i) Tran, H.; McCallum, T.; Morin, M.; Barriault, L., Homocoupling of Iodoarenes and Bromoalkanes Using Photoredox Gold Catalysis: A Light Enabled Au(III) Reductive Elimination. *Org. Lett.* **2016,** *18*, 4308-4311; l) Zidan, M.; McCallum, T.; Thai-Savard, L.; Barriault, L., Photoredox meets gold Lewis acid catalysis in the

alkylative semipinacol rearrangement: a photocatalyst with a dark side. *Org. Chem. Front.* **2017,** *4*, 2092-2096; m) McCallum, T.; Pitre, S. P.; Morin, M.; Scaiano, J. C.; Barriault, L., The photochemical alkylation and reduction of heteroarenes. *Chem. Sci.* **2017,** *8*, 7412-7418; n) Rohe, S.; McCallum, T.; Morris, A. O.; Barriault, L., Transformations of Isonitriles with Bromoalkanes Using Photoredox Gold Catalysis. *J. Org. Chem.* **2018,** *83*, 10015-10024; o) Zhao, Y.; Jin, J.; Chan, P. W. H., Gold Catalyzed Photoredox C1-Alkynylation of N-Alkyl-1,2,3,4-tetrahydroisoquinolines by 1-Bromoalkynes with UVA LED Light. *Adv. Synth. Catal.* **2019,** *361*, 1313-1321; p) Zhang, L.; Si, X.; Yang, Y.; Witzel, S.; Sekine, K.; Rudolph, M.; Rominger, F.; Hashmi, A. S. K., Reductive C–C Coupling by Desulfurizing Gold-Catalyzed Photoreactions. *ACS Catal.* **2019,** *9*, 6118-6123; q) Zidan, M.; Morris, A. O.; McCallum, T.; Barriault, L., The Alkylation and Reduction of Heteroarenes with Alcohols Using Photoredox Catalyzed Hydrogen Atom Transfer via Chlorine Atom Generation. *Eur. J. Org. Chem.* **2019,** *in press*.

35. a) Teegardin, K.; Day, J. I.; Chan, J.; Weaver, J., Advances in Photocatalysis: A Microreview of Visible Light Mediated Ruthenium and Iridium Catalyzed Organic Transformations. *Org. Proc. Res. Dev.* **2016,** *20*, 1156-1163; see also refs. 20 and 21.

36. a) Russell, G. A.; Brown, H. C., The Liquid Phase Photochlorination and Sulfuryl Chloride Chlorination of Branchedchain Hydrocarbons; the Effect of Structure on the Relative Reactivities of Tertiary Hydrogen in Free Radical Chlorinations1,2. *J. Am. Chem. Soc.* **1955,** *77*, 4031-4035; b) Russell, G. A.; Haffley, P. G., Photochlorination of 2,4-Dimethylpentane, 2,2,4-Trimethylpentane, and 2,2,4,4-Tetramethylpentane1. *J. Org. Chem.* **1966,** *31*, 1869-1871; c) Clayden, J.; Greeves, N.; Warren, S. (**2012**)

Ch. 39: Radical Reactions. In *Organic Chemistry*. Second Edition ed.; Oxford University Press: Oxford, New York; p 1019.

37. a) Shields, B. J.; Doyle, A. G., Direct C(sp3)–H Cross Coupling Enabled by Catalytic Generation of Chlorine Radicals. *J. Am. Chem. Soc.* **2016,** *138*, 12719-12722; b) Heitz, D. R.; Tellis, J. C.; Molander, G. A., Photochemical Nickel-Catalyzed C–H Arylation: Synthetic Scope and Mechanistic Investigations. *J. Am. Chem. Soc.* **2016,** *138*, 12715-12718; c) Nielsen, M. K.; Shields, B. J.; Liu, J.; Williams, M. J.; Zacuto, M. J.; Doyle, A. G., Mild, Redox-Neutral Formylation of Aryl Chlorides through the Photocatalytic Generation of Chlorine Radicals. *Angew. Chem. Int. Ed.* **2017,** *56*, 7191-7194; d) Nielsen, M. K.; Shields, B. J.; Liu, J.; Williams, M. J.; Zacuto, M. J.; Doyle, A. G., Mild, Redox-Neutral Formylation of Aryl Chlorides through the Photocatalytic Generation of Chlorine Radicals. *Angew. Chem. Int. Ed.* **2017,** *129*, 7297-7300; e) Ackerman, L. K. G.; Martinez Alvarado, J. I.; Doyle, A. G., Direct C–C Bond Formation from Alkanes Using Ni-Photoredox Catalysis. *J. Am. Chem. Soc.* **2018,** *140*, 14059-14063; f) Deng, H.-P.; Zhou, Q.; Wu, J., Microtubing-Reactor-Assisted Aliphatic C–H Functionalization with HCl as a Hydrogen-Atom-Transfer Catalyst Precursor in Conjunction with an Organic Photoredox Catalyst. *Angew. Chem. Int. Ed.* **2018,** *57*, 12661-12665.

38. a) Newcomb, M., Competition Methods and Scales for Alkyl Radical Reaction Kinetics. *Tetrahedron* **1993,** *49*, 1151-1176; b) Newcomb, M. (**2012**) Radical Kinetics and Clocks. In *Encyclopedia of Radicals in Chemistry, Biology and Materials*. (Eds Chatgilialoglu, C. and Studer, A.) See also refs. 25b and 36c.

39. Newcomb, M.; Johnson, C. C.; Manek, M. B.; Varick, T. R., Picosecond radical kinetics. Ring openings of phenyl-substituted cyclopropylcarbinyl radicals. *J. Am. Chem. Soc.* **1992,** *114*, 10915-10921.

CHAPTER 2: GOLD PHOTOREDOX CATALYZED ALKYLATION OF ISONITRILES WITH BROMOALKANES

Rohe, S., McCallum, T., Morris, A. O., Barriault, L. Transformations of Isonitriles with Bromoalkanes Using Photoredox Gold Catalysis. *J. Org. Chem.* **2018**, 83, 10015-10024.

S. Rohe thanks T. McCallum and A. O. Morris for their contributions. Conceived by T. McCallum, optimization completed by S. Rohe. Substrate scope completed by S. Rohe (molecules colored in blue) and A. O. Morris. Cyclization studies completed by S. Rohe (Table 2.4) and absolute rate of radical addition to isonitrile completed by T. McCallum (Scheme 2.3). Progress towards synthesis of sarpagine alkaloids completed by S. Rohe.

2.1 Abstract

Isonitriles are masked carbenes, able to react with both electrophiles and nucleophiles from the same carbon atom. These isosteres of carbon monoxide are underappreciated functional groups, proving invaluable in multicomponent reactions and as free radical acceptors. Isonitriles also exhibit particular tunability when used as radical acceptors, bestowing options to continue radical propagation, undergo β-fragmentation, or to be reduced or oxidized depending on ambient conditions. With synergistic use of the gold photosensitizing catalyst $[Au_2(dppm)_2]Cl_2$ developed in our lab as radical initiator, we conceptualized a reaction applying isonitriles as radical acceptors to produce 6-substituted phenanthridine scaffolds and α-alkylated amides. With careful tuning, we favored propagation from the addition product or oxidation while altogether avoiding the competitive pathways of β-fragmentation and reduction. Furthermore, as the dimeric gold

catalyst $[Au_2(dppm)_2]Cl_2$ allows generation of radicals from simple bromoalkanes and 365nm light, we used bromoalkanes as alternatives to existing radical clocks and probe the rate of primary radical addition. Herein, we describe the photocatalytic generation of alkyl radicals from unactivated bromoalkanes as part of an efficient cross-coupling strategy for the diversification of isonitriles using a dimeric gold(I) photoredox catalyst.

2.2 Introduction

Inspired by the complexity found in the light-harvesting biomolecules in Nature, chemists have developed photoexcitable complexes for use in organic transformations that equip us with complementary alternatives to two-electron processes.[1] These photoredox catalysts have allowed for modern variants of classical radical chemistry, unlocking mild and efficient methodology for the construction of new C-C, C-O, and C-N bonds. These processes are advantageous to classical methods of radical generation by circumventing the use of radical initiators, poor atom economy, harsh reagents and conditions.[2] The construction of heterocyclic scaffolds through multicomponent radical coupling reactions and cascade cyclizations has been instrumental in the expedient synthesis of complex and medicinally relevant structures.[3] The use of isonitrile moieties has been important for the diversification of such structures and has enabled the synthesis of many heteroarene scaffolds.

Work from Shono and Saegusa showed that radical intermediates can add to isonitriles to form an imidoyl radical intermediate **2.1** (**Scheme 2.1**).[4] The latter can undergo two competitive pathways, addition to an acceptor (*path A*) to provide compound **2.2** or a β-fragmentation to give the corresponding nitrile **2.3** (*path B*). The imidoyl radical

can also be oxidized to the cation or reduced to the anion, allowing entry to ionic chemical pathways. Each of these pathways from the radical intermediate can be favored or disfavored by careful curation of reaction conditions, including by variation of the oxidative or reductive quenching pathways of the dimeric gold photocatalyst. This immense capacity for variation makes addition of carbon centered radical types to isonitriles a rich medium for methodological advancements.[5]

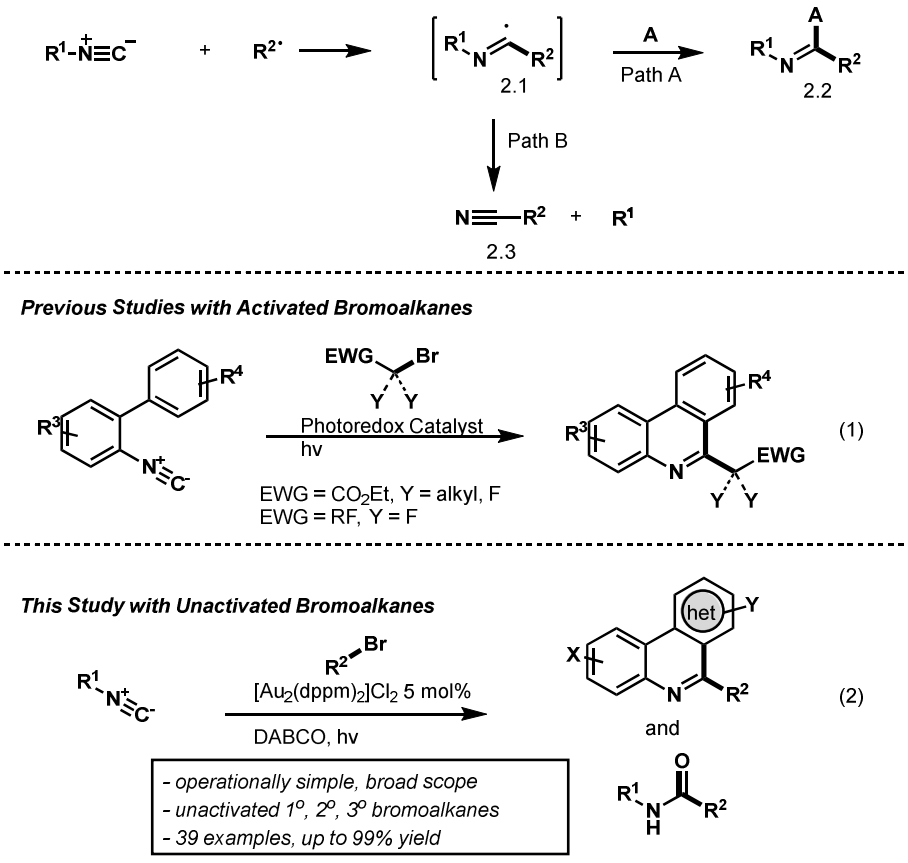

Scheme 2.1. Phenanthridine and amide synthesis as examples of isonitrile functionalization using photoredox catalysis.

Facile generation of radicals from bromoalkanes for use in intermolecular transformations has been limited to activated molecules, such as perfluorinated or highly

electron-deficient substrates. Particularly, unactivated alkyl radical genesis has been an area where little mild and broadly applicable methodology exists for isonitrile functionalization.[6] These processes typically employ stoichiometric initiators/oxidants or use the parent alkane as solvent; this reagent-intensive methodology is limiting in scope. Recently, a variety of photoredox catalyzed reaction modes have been developed to circumvent the described limitations (**Scheme 2.1**, eq. 1).[7] Although the use of common photocatalysts like Ru and Ir-based polypyridyl complexes has given mild and high yielding protocols, these complexes are limited by the redox potentials inherent to each photocatalyst. With this in mind, we hypothesized that several practical coupling strategies for *path A* (selective isonitrile alkylation) of broader applicability could be conceived using photoredox catalysis and simple bromoalkanes (**Scheme 2.1**, eq. 2). To that effect, a dimeric gold(I) photocatalyst, $[Au_2(dppm)_2]Cl_2$ is described for the mild generation of a broad scope of alkyl radicals for the functionalization of isonitriles.

Based on our group's previous studies, we envisioned that a redox-neutral isonitrile functionalization protocol employing a photoredox dimeric gold catalyst as reductant and oxidant would mitigate the need for stoichiometric additives and harsh conditions.[8] This strategy generates alkyl radicals derived from readily available bromoalkanes **2.4** (≈ –2.0 V *vs.* SCE)[9] through an inner-sphere oxidative quenching mechanism with photoexcited $[Au_2(dppm)_2]Cl_2$ ($E_{1/2}^{M+/M^*}$ –1.63 V *vs.* SCE) (**Scheme 2.2**).

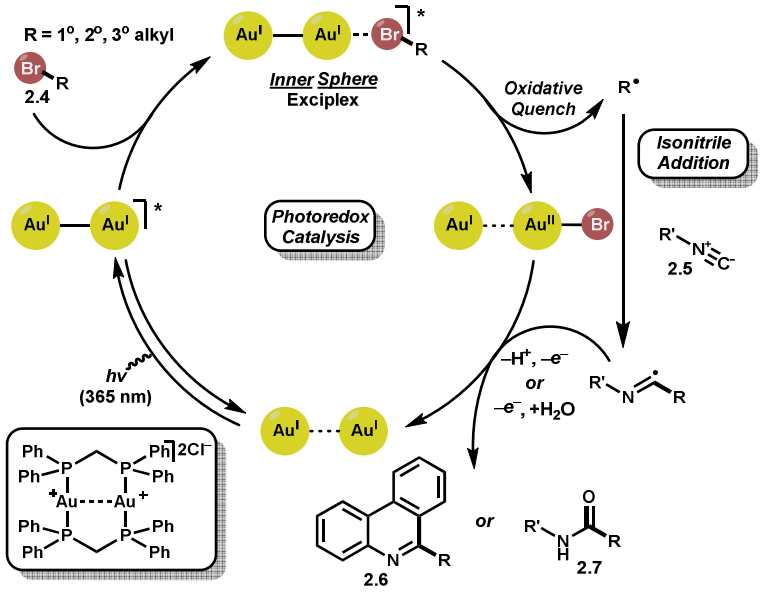

Scheme 2.2. Proposed oxidative quenching mechanism of gold-catalyzed photoredox.

Any ensuing alkyl radicals would then add to isonitriles **2.5**, forming a sp^2 hybridized radical that would proceed to react through one of two pathways: 1) cyclization upon a pendant arene to generate a cyclohexadienyl radical, followed by oxidation by $[Au_2(dppm)_2]^{3+}$ to complete the catalytic cycle and produce the phenanthridine products **2.6**; 2) the imidoyl radical formed subsequent to isonitrile addition could be directly oxidized by $[Au_2(dppm)_2]^{3+}$ and be trapped with water, hydrolyzing to create amide products **2.7**. Binuclear Au(I) phosphine complexes such as $[Au_2(dppm)_2]Cl_2$ have little aurophilic interaction in the ground state but upon excitation, an Au-Au interaction is forged.[10] An open coordination site is made available where haloalkanes may bind, leading to inner sphere C-X bond activation which can occur through photoinduced electron transfer of the exciplex.[11]

It is essential to note that both redox quenching pathways available to the dimeric gold photocatalyst may be employed in this reaction, and that modulation between these

oxidative or reductive pathways affords an extra dimension of control to tune radical generation. A reductive quenching mechanism is also possible, wherein a gold atom in $[Au_2(dppm)_2]Cl_2$ ($E_{1/2}^{M/M-}$ –1.70 V *vs*. SCE) is first reduced by a trialkylamine base and subsequently reduces the bromoalkene. Quenching rates of excited-state catalyst with trialkylamine bases such as DABCO and DIPEA (K_q = 1.97 ± 0.54 × 10^8 and 2.7 × 10^7 M^{-1} s^{-1} respectively) are also known to be many times faster than excited-state quenching with primary bromoalkanes such as *n*-butyl bromide (K_q = 2.9 × 10^6 M^{-1} s^{-1}).[11,12] Changes to the relative concentrations of photocatalyst and bromoalkane or trialkylamine base can act as a pseudo mechanistic switch.

2.3 Results and Discussion

To verify our hypothesis, we first examined the generation of phenanthridines **2.6** via UVA irradiation (365 nm) of bromocyclohexane **2.9** and isonitrile **2.8** in the presence of $[Au_2(dppm)_2]Cl_2$ (5.0 mol %) and Na_2CO_3 (3 equivalents) (**Table 2.1**). Further optimizations established that reactions carried out at 0.1 M in degassed acetronitrile gave **2.10** along with **2.10'** (R = H) in 74% and 7% yield, respectively (entry 1). The addition of a sub-stoichiometric quantity of DABCO proved to be beneficial to the reaction, yielding **2.10** in 87% yield (82% isolated yield, entry 2). As shown in a previous study, this reagent may act as a resuscitator or repair agent of the $[Au^{I}\text{-}Au^{II}]^{3+}$ intermediate if the oxidation of another reaction intermediate becomes unfavourable.[12] Alternatively, the amine base could promote a reductive quenching process of excited state photocatalyst (k_q^{DABCO} = 1.97 x 10^8 $M^{-1}s^{-1}$), leading to a complex $[Au^{I}\text{-}Au^{0}]^{1+}$ which can reduce bromoalkane **2.9** to generate the corresponding alkyl radical.[11] Interestingly, the phenanthridine by-product **2.10'** (R = H) was not observed when using DABCO.

Decreasing the catalyst loading to 2.5 and 1.0 mol% gave similar results of 85% and 82% yields, respectively, showing the efficiency of the transformation (entries 3 and 4). Furthermore, the gram-scale reaction gave the desired product in 66% yield (entry 5), demonstrating the robustness of the process. Finally, light irradiation and photocatalyst were shown to be vital to the success of the reaction (entries 6, 7).

Table 2.1. Optimization of the reaction conditions.[a]

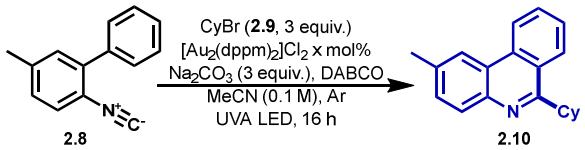

Entry	$[Au_2(dppm)_2]Cl_2$ (mol %)	DABCO (mol%)	Yield (%)
1	5.0	---	74
2	5.0	20	87 (82)
3	2.5	20	85
4	1.0	20	82
5	1.0	20	66[b]
6	---	20	s.m.
7	5.0	20	s.m.[c,d]

[a] Procedure: 5a (0.2 mmol), CyBr 4a, (3 equiv.), $[Au_2(dppm)_2]Cl_2$ (x mol%), Na_2CO_3 (3 equiv.), DABCO (20 mol%), MeCN, Ar degas, irradiation with UVA LEDs for 16 hours. Yields determined by ^1H NMR analysis using an internal standard mesitylene (isolated yield). [b] 1.0 gram (5.2 mmol, c = 0.5 M) scale of 5a irradiated for 36 hours using 3 UVA

LEDs. [c] In absence of irradiation, 36 hours. [d] In absence of irradiation and heating to 80 °C, 36 hours.

Following the optimization, the addition of various bromoalkanes to aryl isonitriles was explored (**Table 2.2**). Primary bromoalkane coupling partners **2.11-2.16** proceeded in moderate to excellent yields (33-83%), with notable success when using the glucose derivative **2.16** highlighting the potential of this methodology for application in the synthesis of structurally complex compounds. Light-enabled addition of protected bromoalcohols **2.14** and **2.15** gave the desired phenanthridines in 83% and 33% yields, respectively. In the cases where full conversion was not obtained, the mass balance was fulfilled with starting material. Compounds **2.17-2.24** containing 2° and 3° bromoalkanes fared significantly better, affording phenanthridine products **2.8** in good to excellent yields (64-99%). Notably, five of the substrates exhibited comparable yields when using a catalyst loading of 1.0 mol%.

Table 2.2. Bromoalkane scope in phenanthridine synthesis.

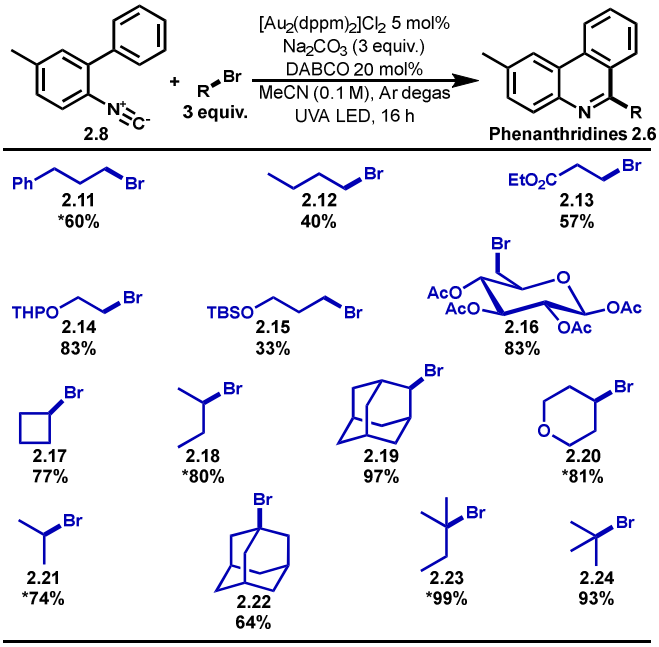

[a] Reaction performed with 1 mol% catalyst loading

As outlined in **Table 2.3**, the generality of the isonitrile biaryl coupling partner under the optimized reaction conditions was examined. It was hypothesized initially that electron-withdrawing functional groups might stabilize the isonitrile as well as the imidoyl radical intermediate, allowing for a scope broadening. Unfortunately, the synthesis of electronically diverse biphenyl isonitrile reagents proved to be prohibitively challenging. Upon examination of the synthesizable substrates, it was noted that the electronic nature of the substituents on the biphenyl isonitrile right-hand ring did not have much influence on the outcome of the reaction with little correlation between the yield and electronic properties. For instance, both compounds **2.26** and **2.30** (R = CF_3, R = OMe) were furnished in 67% and 65% yields, respectively. Irradiation of a pyrrole-substituted isonitrile using the standard conditions gave the heterocycle **2.28** in 64% yield. However,

photodegradation of the materials was observed when substituents R' ≠ H or Me, or heterocycles on the left-hand ring, except for with one substrate which gave the desired product **2.25** in 63% yield. Aside from the initial biphenyl isonitrile starting material, a double cyclization was attempted on *p*-methoxyphenylisonitrile **2.32**. The resulting quinoline **2.35** and quinoxaline **2.36** resulting from dual cyclization with 5-bromopentyne **2.33** and 4-bromobutyronitrile **2.34** were obtained in moderate isolated yields of 40% and 30%, respectively.

Table 2.3. Isonitrile scope using bromocyclohexane.

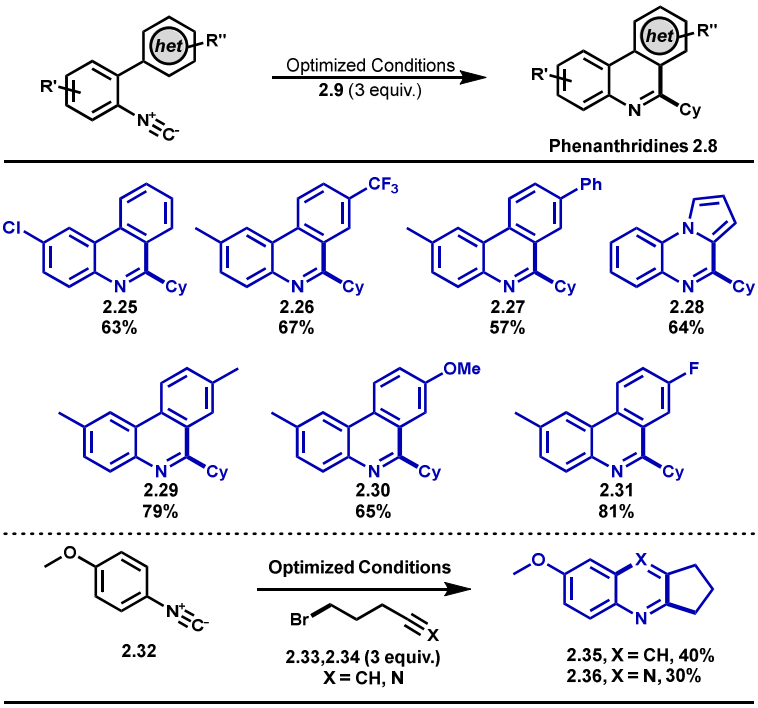

The most important contribution of this work is the elaboration of a safe and simplified radical clock kinetic tool. This technique is designed to streamline rate estimations for radical methodologies and relies on use of radicals that undergo unimolecular radical ring-opening and closing reactions prior to bimolecular reaction. These radical clocks are

prized in organic reaction kinetic studies as they do not require specialized detection equipment such as EPR and can be conveniently analyzed by NMR of a crude mixture. Here, we cast off tin hydride as initiator and instead use the $[Au_2(dppm)_2]Cl_2$ catalyst alongside bromoalkane substrates to provide an estimate of the rate of addition of primary alkyl radicals to isonitriles. Known literature rate constants of ring-opening and ring-closing of the radical intermediates allow a preliminary estimate of the magnitude as well as a precise determination of rate under pseudo first-order conditions as demonstrated in **Table 2.4**. This radical clock method is milder than most alternatives and thus is pertinent in almost any methodology involving addition of primary radicals to acceptor molecules.

Rates of radical addition can be estimated by comparing the ratios of cyclized and uncyclized products with the known rate constant for cyclization, as seen in **Table 2.4**. The use of bromomethylcyclopropane **2.38** afforded exclusively ring-opened product **2.37** (n = 1) in 53% yield (entry 1). The use of (bromomethyl)cyclobutane **2.39** afforded a 50:50 mixture of ring-opened and -closed products **2.36** (n = 2) and **2.37** (n = 2) in 64% yield (entry 2). These results are in accordance with expectations given that the rate of ring-opening is slower for cyclobutylmethyl radicals than cyclopropylmethyl radicals. Conversely, ring-closing radical cyclization reactions were attempted in entries 3-6. These substrates allow comparison of a putative radical intermediate by evaluating direct addition to the isonitrile substrate versus the *exo-trig* cyclization prior to isonitrile addition. Bromoalkane **2.40** resulted in exclusive formation of **2.37** in 33% yield as the *4-exo-trig* cyclization is not favoured whereas bromoalkane **2.41** gave **2.36** (n = 3) as the sole product in 52% yield, favouring the *5-exo-trig* cyclization prior the addition to **2.8** (entry 4). Interestingly, a 48:52 ratio of **2.36** (n = 4) and **2.37** (n = 4) was observed with

bromoalkene **2.42**, indicating that addition of the primary radical and the *6-exo-trig* cyclization take place at similar rates (entry 5). Finally, reaction with substrate **2.43** gave **2.37** in 64% yield as the sole product (entry 6). As the rate constants for these equilibria between ring-closed and ring-opened alkyl radicals are known, this experiment showcases a superior approach radical clock protocols.

Table 2.4. Ring-opening and forming reactions of known radical clock bromoalkanes.

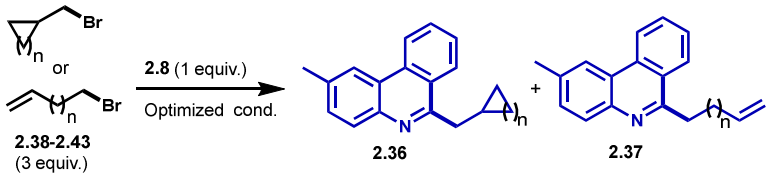

Entry	RBr	n =	Yield (%)	Ratio 2.36:2.37	Reaction rate constant at 20 °C (s^{-1}) [13]
1	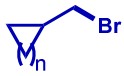	1, **2.38**	53	0:100	9.4 E 7
2		2, **2.39**	64	50:50	5.0 E 3
3		2, **2.40**	33	0:100	1
4		3, **2.41**	52	100:0	1.8 E 5
5		4, **2.42**	53	48:52	5 E 3
6		5, **2.43**	64	0:100	7 E 2

Using this same radical clock methodology, the absolute rate of 1° radical addition to isonitrile **2.8** was determined using a kinetic study with (bromomethyl)cyclobutane **2.39** as shown in **Scheme 2.3**. In this experiment, the ratio of ring-closed product **2.44** versus the rearranged ring-opened product **2.45** was compared under increasing concentration of **2.8**. It was found that the absolute rate of addition of primary alkyl radicals to **2.8** was

2.17 ± 0.25 x 10^4 $M^{-1}s^{-1}$. The results show a linear correlation under pseudo-first order conditions, indicative of a free radical addition process.[14] Using the binuclear gold(I) photocatalyst and bromoalkanes with known rearrangement rate constants offer an attractive alternative to standard photochemical radical clocking experiments using the pyridine-2-thione-N-oxycarbonyl (PTOC) ester method.[15]

Scheme 2.3. Kinetic study of the absolute rate of primary radical addition to isocyanide **2.8**, ratio of products **2.44** / **2.45** vs. [**2.8**] (M).

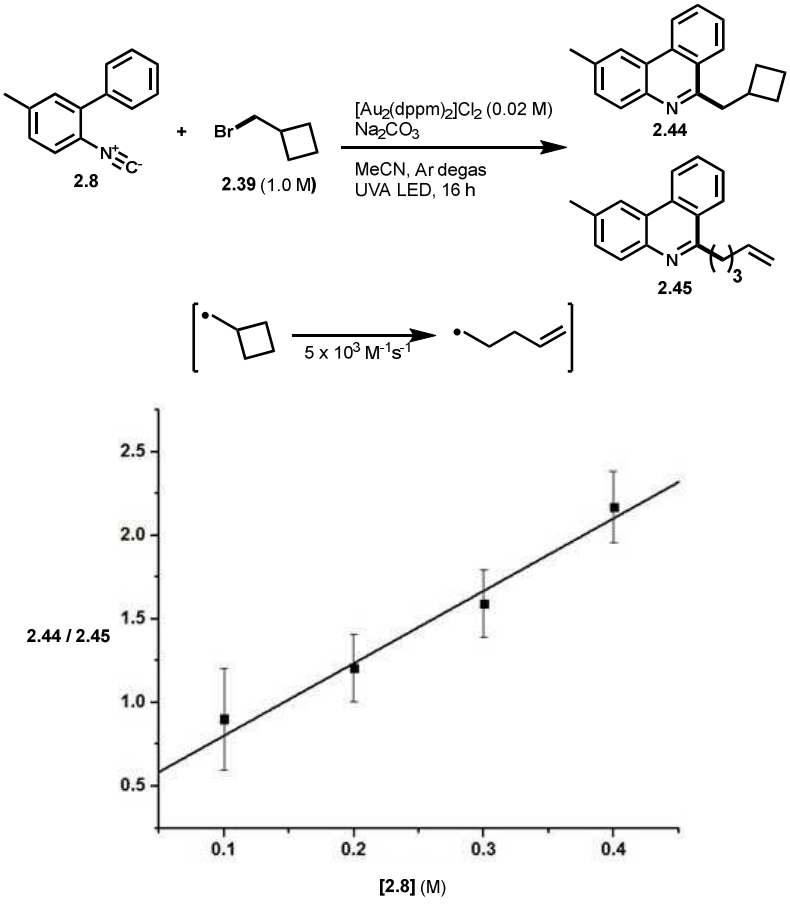

Finally, the prospects of applying the developed methodology for alkyl radical addition to isonitriles for the synthesis of amides were evaluated. The formation of the amides **2.7** may proceed through oxidation of the imidoyl radical intermediate to the corresponding

carbocation (**Table 2.5B**). When considering that the reaction may proceed through an oxidative quenching cycle, the role of DABCO remains elusive though can be speculated upon. While phenanthridine synthesis reached full conversion of substrate with 20 mol% of DABCO additive, amide formation became sluggish with the same quantity of DABCO and only obtained full conversion with 1 equivalent. Considering that the trialkylamine base and bromoalkane are close to equimolar in the amide synthesis and that excited-state catalyst quenching is slightly faster with DABCO, it seems reasonable to propose that amide formation primarily progresses *via* the gold reductive quenching cycle as presented in **Scheme 2.4**. This alternative mechanism would therefore begin with a photoinduced electron transfer from the amine to the excited-state gold catalyst creating its reduced state [Au^{I}-Au^{0}]. The gold catalyst then becomes highly reducing and undergoes SET to bromoalkanes **2.4**, completing the gold catalytic cycle and generating an alkyl radical intermediate. Addition of this alkyl radical to an isonitrile then follows, and the resulting imidoyl radical can be oxidized by either catalyst turnover or SET to the amine radical cation.[16] The generated nitrilium ion can then hydrolyze in the expected fashion to generate the final products.

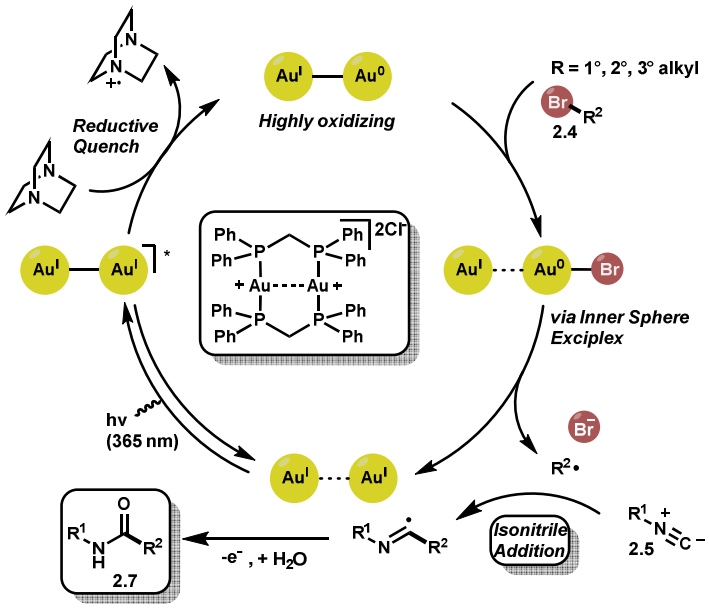

Scheme 2.4. Proposed reductive quenching mechanism of gold photoredox catalyst.

There are few examples using isonitriles for the synthesis of amides and, to the best of our knowledge, this would be the first photochemical and alkyl radical mediated amide synthesis using isonitriles **2.5** as seen in **Table 2.5A**.[17] Employing the standard conditions described above with 1 equivalent DABCO, the addition of electrophilic radicals to *tert*-butyl isonitrile gave the desired amides **2.46-249** in yields ranging from 22% to 99%. During the establishment of the reaction scope, we noted that the reaction yields were improved significantly with the addition of a small quantity of water (21 equiv). Interestingly, β-fragmentation alkyl nitrile products were not observed.

Full conversion was also observed with 2,6-dimethylphenyl isonitrile leading to the corresponding amides **2.50-2.53** in 57-64% yields while 4-methoxylphenyl isonitrile and bromide **2.9** produced amide **2.54** in 31% yield. One can recognize that photodegradation of products and rearrangement of putative radical intermediates via Path B are likely to

occur, though products of the fragmentation were not directly observed. Photochemical rearrangement of isonitrile to nitrile was observed in several cases.[19]

Table 2.5. Bromoalkane and isonitrile scope in amide synthesis.

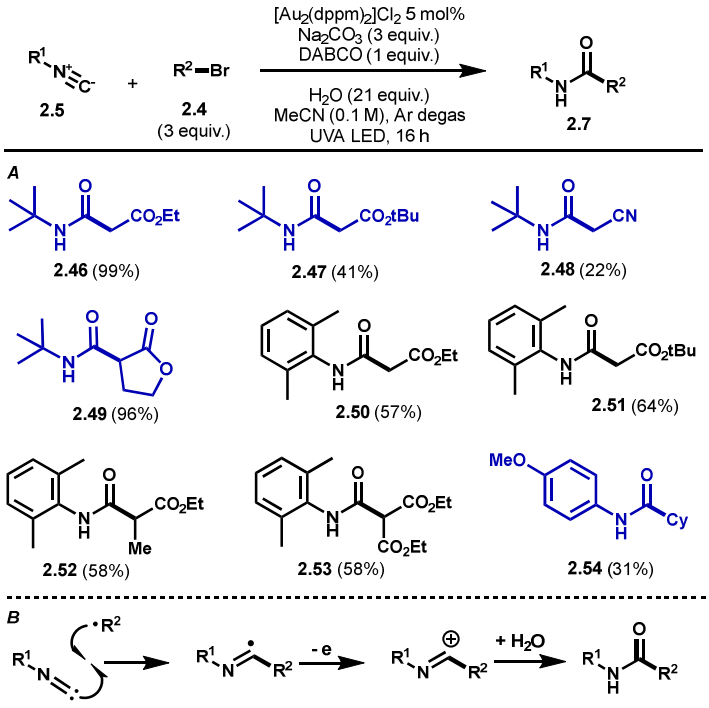

2.4 Further Information

The breadth of success of this methodology led us to consider its use in the synthesis of indole-containing natural products. Though indoles have been the target of similar radical methodologies such as the Fukuyama indole synthesis (**Scheme 2.5A**), the inherent restrictions associated with Fukuyama conditions have constrained its utility in total synthesis.[20] We envisioned application of our methodology in the synthesis of the cores of complex bioactive molecules such as alstonerine or talcarpine depicted in **Scheme 2.5B**.[21] Our knowledge of the rate of addition of radicals to isonitriles would allow us to curate conditions favoring addition of a β-keto radical from precursor **2.56** to aryl

isonitrile **2.55**, creating an intermediate imidoyl radical **a** (**Scheme 2.5C, D**). This radical would then perform a 5-*exo* cyclization to form the indole core seen in intermediate **b**, hopefully undergoing a second cyclization onto the Michael acceptor in **2.55** to form the Sarpagine indole alkaloid core in a one-pot process (**Scheme 2.5D**, intermediate **c**).

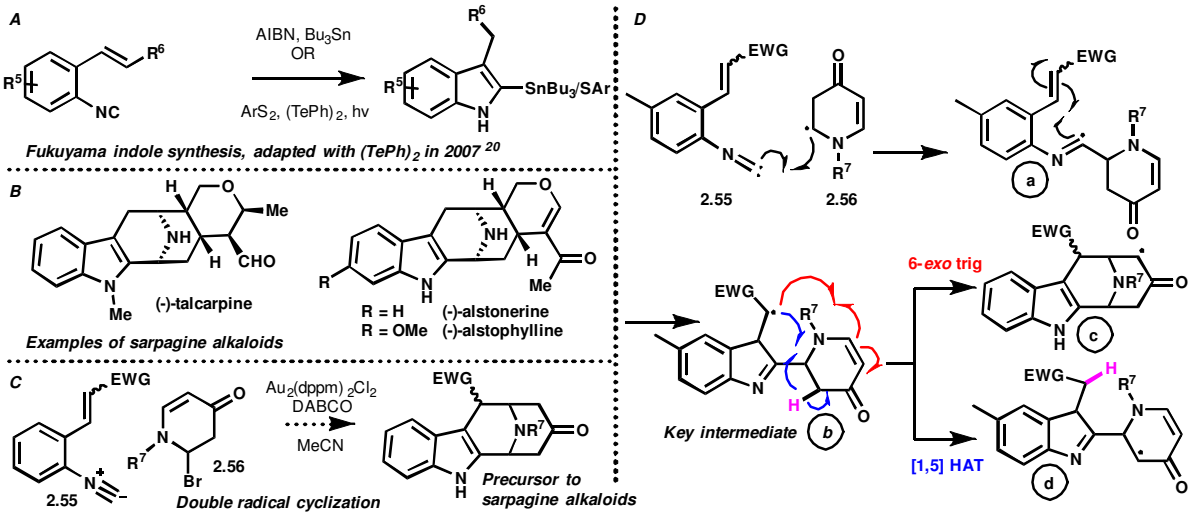

Scheme 2.5. Origin of radical synthesis of sarpagine alkaloids. A) precedent for indole synthesis via radical addition to isonitrile; B) examples of indole alkaloid natural products containing substitutions at the 2- and 3-position; C) envisioned application of this methodology in total synthesis; D) proposed mechanism of key step.

Model substrate **2.56** served to probe the efficacy of the addition to the isonitrile compared to that of the subsequent cyclizations. Imidoyl radical intermediate **a** (**Scheme 2.5D**) is susceptible to five possible pathways, including 6-*endo*- and 5-*exo*-*trig* ring formation, β-fragmentation leading to an unstable phenyl radical, or reduction or oxidation to anion or cation respectively. The proposed ring-closure reactions are lucrative and may be prohibitively challenging to the synthesis: firstly, the initial cyclizations following intermediate **a** are reversible and an electron-withdrawing group (EWG) may be

necessary to favor formation of the indole product via 5-*exo* as opposed to 6-*endo* cyclization. Consequently, key radical intermediate **b** would be electron-poor, the opposite electronic alignment needed to undergo further 6-*exo* cyclization onto the enamine to create intermediate **c**. Furthermore, the 6-*exo* cyclization itself is difficult to control as it can be highly reversible and competes against possible HAT leading to intermediate **d**.

We began our investigation by synthesizing precursor **2.55** and model substrate **2.56** via pathways depicted in **Scheme 2.6**. The olefin isonitrile acceptors were synthesized using a 3-step process beginning with a Heck reaction between ethyl acrylate or styrene and commercially available iodoaniline **2.57**.[22] The yields for isolated intermediates **2.58a** and **b** were somewhat unreliable, with the lowest obtained yields reported here (52% and 45% yields respectively, both >99% trans olefin). The electron-rich P(*o*-tolyl)$_3$ ligand proved necessary as the reaction failed completely with Pd(PPh$_3$)$_4$, though an extensive ligand screen was not conducted. The subsequent steps to generate the isonitriles **2.55a** and **b** were performed in sequence without column chromatography of the intermediate amide in good yields over two steps, 40% and 50% respectively. While purification of this intermediate was minimal, removing all traces of acetic formic anhydride and other acidic impurities was integral to the success of the subsequent dehydration step.

It was also possible to perform the synthesis in a different order, with generation of the formamide from the parent aniline first, followed by a Heck coupling and the final dehydration to form the isonitrile. This pathway was attempted to circumvent purification issues with **2.58b**, which was consistently a messy reaction with many unidentified by-products. Though the formamide was easier to purify following the Heck reaction, it

suffered from slow decomposition at room temperature. Because of this, the reverse-order pathway with Heck coupling after formamide generation was not used for batching. Attempts to perform the Heck coupling with a bromoaniline as opposed to iodoaniline **2.57** resulted in a mixture of *cis* and *trans* products. While it is not necessary for the material to be stereochemically pure for the subsequent radical cyclization, the *trans*-selective reaction using the iodoaniline allowed ease of purification.

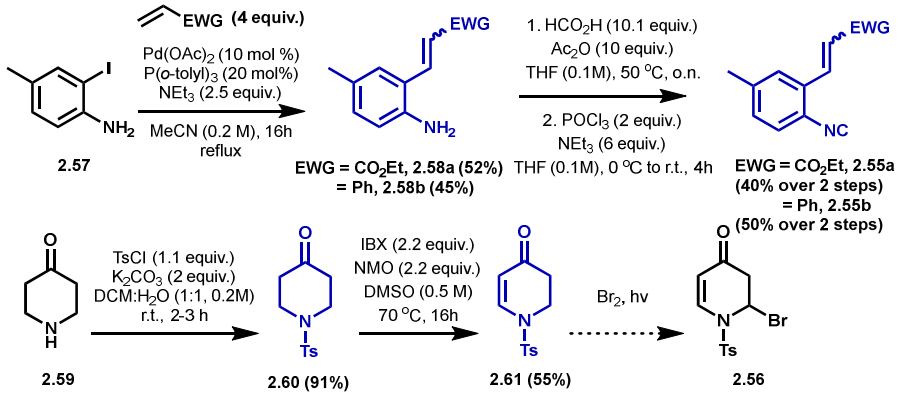

Scheme 2.6. Synthesis of starting materials for indole synthesis.

In order to determine the prevalence of cyclization issues as early as possible, we attempted to synthesize **2.56** starting from 4-piperidone **2.59** commercially available as hydrated HCl salt. We suspected that any halogen installed on **2.56** would be highly susceptible to hydrolysis or elimination, though we hoped to mitigate this with use of an electron-withdrawing protecting group such as toluenesulfonyl (Ts, 91%) or benzenesulfonyl or storage of the amine as ammonium salt. Carbonyl-based protecting groups were deemed to be incompatible on substrate **2.60** in the subsequent reaction conditions as any hydrocarbon moieties may be susceptible to HAT. The ensuing oxidation of the protected piperidone proved difficult, and after attempting many variants

on the Saegusa-Ito reaction, O_2 oxidation, and bromination-elimination, it was found that a modified Nicolaou oxidation with IBX was optimal (55% yield).[23]

While the synthesis of **2.56** was ongoing, optimization of the radical Fukuyama-like indole synthesis was conducted to verify reliability of the first cyclization under known conditions (**Table 2.6**). It was suspected that the ester-containing substrate **2.55a** (EWG = CO_2Et) would be unable to turn over the oxidatively quenched gold cycle (Scheme 2) as it is not a suitable reducing agent, even though its ability to stabilize the radical product would likely make it a good acceptor for the first cyclization step. Substrate **2.55b** (EWG = Ph) would likely be a better reducing agent to resuscitate an Au^{II} species and would still provide stabilization to radical intermediate **b** (**Scheme 2.5D**). An alternative approach to optimization of this reaction would be to incite the reductive quenching cycle with stoichiometric trialkylamine base, which negates the requirement for a substrate capable of performing single electron reduction to complete a gold catalytic cycle.

With these strategies and restrictions in mind, we commenced optimization on **2.55a** as it would be an excellent acceptor for the 5-*exo* trig cyclization step following radical addition to the isonitrile (**Table 2.6**). Stoichiometric DABCO and DIPEA (entries 1 and 2) in conjunction with optimized conditions from our phenanthridine synthesis methodology afforded full conversion but only a complex mixture of products was observed by NMR. Complete removal of a trialkylamine base (entry 3) resulted only in some degradation of starting material with no perceivable product, indicating that some additive may be necessary for the success of the reaction. The optimization was continued with substrate **2.55b** which was purported to be compatible with both reductive and oxidative quenching cycles. Blank experiments were performed without the bromoalkane radical precursor

(entry 4) and without both radical precursor, trialkylamine base, and photosensitizing catalyst (entry 5). The degradation resulting from removal of radical precursor suggested that energy transfer from the catalyst may be catalyzing substrate degradation. Furthermore, running the reaction without bromoalkane, catalyst, or additive (entry 5) revealed the substrate's inherent sensitivity to UV light, with isomerization of the double bond from 100% *trans* to 62:38 *trans:cis*. This isomerization was not possible to quantify by NMR in cases where degradation occurred due to the mass of overlapping peaks. Removing the additive entirely resulted in a complex mixture with trace product (entry 6). Aliquots were taken from a reaction run in standard conditions after 10 minutes, 2h, and 8h of irradiation (entries 7-9). Trace product was not observed until 8h had passed, though degradation was visible at 2h. The completely *trans* starting material isomerized to 62:38 *trans:cis* after only 10 minutes of irradiation and gave a mixture of 48:52 *trans:cis* at 8h. As non-quantitative aliquots were used in the time study it is not possible to determine whether the change in ratio is due to the system equilibration or if one isomer degrades faster than the other.

A set of conditions known to generate radicals at 410 nm was employed (entry 10), and an activated substrate was employed (entry 11), to no avail.[24] Changes to solvent (entry 12) or concentration (entry 13) had no positive effect on desired yield. Exposing **2.55b** to trialkylamine bases such as DABCO and DIPEA mostly resulted in complex mixtures, with only trace yields of **2.62** produced with 0.2 equiv. DIPEA (entries 14-16). Bases such as DIPA, TEA, and tributylamine were also used and resulted in complex mixtures with trace product; these entries are not included for brevity.

Table 2.6. Preliminary trials for photoredox-catalyzed indole synthesis.

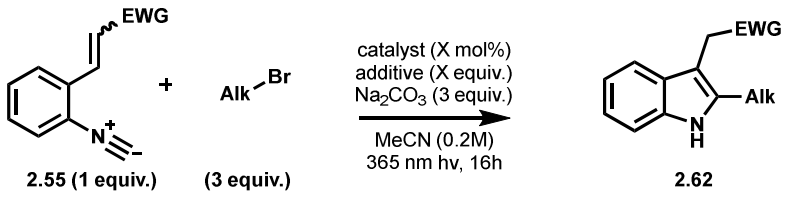

2.55 (1 equiv.) **(3 equiv.)** **2.62**

Entry	EWG	Alk-Br	Catalyst (mol %)	Additive (equiv.)	Conversion[a]	Yield[a]
1	CO_2Et	bromocyclohexane	$[Au_2(dppm)_2]Cl_2$ (5)	DABCO (1)	>90%	complex mixture, trace bp[b]
2	CO_2Et	bromocyclohexane	$[Au_2(dppm)_2]Cl_2$ (5)	DIPEA (1)	100	complex mixture
3	CO_2Et	bromocyclohexane	$[Au_2(dppm)_2]Cl_2$ (5)	none	40	degrad.
4	Ph	none	$[Au_2(dppm)_2]Cl_2$ (5)	DABCO (1)	<10	some degrad.
5	Ph	none	None	none	19	39% cis olefin
6	Ph	bromocyclohexane	$[Au_2(dppm)_2]Cl_2$ (5)	none	100	complex mixture
7[c]	Ph	bromocyclohexane	$[Au_2(dppm)_2]Cl_2$ (5)	DABCO (0.2)	62:38 trans:cis	0
8[d]	Ph	bromocyclohexane	$[Au_2(dppm)_2]Cl_2$ (5)	DABCO (0.2)	56:44 trans:cis	degrad.
9[e]	Ph	bromocyclohexane	$[Au_2(dppm)_2]Cl_2$ (5)	DABCO (0.2)	48:52 trans:cis	trace
10[f]	Ph	Iodocyclohexane	*fac*-$Ir(ppy)_3$ (1)	NBu_3 (2)	100	trace

11	Ph	Ethyl bromoacetate	$[Au_2(dppm)_2]Cl_2$ (5)	DABCO (0.2)	100	trace
12	Ph	bromocyclohexane	$[Au_2(dppm)_2]Cl_2$ (5)	DABCO (0.2), H_2O (0.05 mL)	100	trace
13 [g]	Ph	bromocyclohexane	$[Au_2(dppm)_2]Cl_2$ (5)	DABCO (0.2)	100	trace
14	Ph	bromocyclohexane	$[Au_2(dppm)_2]Cl_2$ (5)	DABCO (1)	>90%	complex mixture
15	Ph	bromocyclohexane	$[Au_2(dppm)_2]Cl_2$ (5)	DABCO (0.2)	76	complex mixture
16	Ph	bromocyclohexane	$[Au_2(dppm)_2]Cl_2$ (5)	DIPEA (0.2)	>95	trace

[a] Yield determined by NMR standard comparison to mesitylene peaks. [b] bp: byproduct containing ester CH_2 peak at 4.76 ppm. [c] Aliquot taken after 10 minutes of irradiation. [d] Aliquot taken after 2h of irradiation. [e] Aliquot taken after 8h of irradiation. [f] Irradiated with 410nm hv LED, 1.2 equiv. iodocyclohexane, 0 equiv. Na_2CO_3. [g] Run in 0.5M MeCN.

The Fukuyama aldol reaction and most other successful radical indole syntheses are based on thermal as opposed to photochemical initiation, with a few exceptions utilizing visible light to homolyze diphenyltellurides (>400 nm light).[25] Considering this and the evidence of decomposition of the isonitrile substrate under our methodology's conditions (**Table 2.6**), it is possible that the photoactive **2.55** is simply incompatible with a methodology involving high-energy 365 nm light. Evidence suggests that the indole final product may also absorb light in the UVB, UVC and even early UVA and may degrade as soon as it is formed under our conditions.[26] For these reasons, we believe that the dimeric

gold catalyst $[Au_2(dppm)_2]Cl_2$ may be ill-suited for total synthesis of indole-containing alkaloid scaffolds.

2.5 Conclusions

In summary, we demonstrated that our group's gold photosensitizer $[Au_2(dppm)_2]Cl_2$ augments the functional diversity of phenanthridine scaffolds and amides by coupling alkyl and aryl isonitriles with cheap readily available bromoalkanes. This binuclear Au(I) complex proved to be an exceptionally efficient and tunable photocatalyst in this transformation, likely accessing both reductive and oxidative quenching cycles simply by changing relative concentrations of substrate and additive. The reaction was shown to be robust and broad in scope with respect to both coupling partners and successfully mitigated undesired reactivities like imidoyl radical β-fragmentation. Moreover, this methodology describes a valuable contribution to radical kinetic studies that is complementary to those with PTOC esters and is readily applicable in laboratories lacking specialty knowledge and equipment. Due to the high tunability of this reaction between two mechanistically distinct photoredox cycles and knowledge of the rate of primary radical addition to isonitriles, it is believed this reaction may prove valuable in late-stage natural product synthesis on scaffolds inert towards UVA.

2.6 Experimental Procedures

General information. All reactions were performed under argon atmosphere Pyrex glassware equipped with a magnetic stir bar, capped with a septum, unless otherwise indicated. All commercial reagents were used without further purification, unless otherwise noted. Reactions were monitored by thin layer chromatography (TLC) analysis.

TLC plates were viewed under UV light and stained with potassium permanganate or p-anisaldehyde staining solution. Yields refer to products isolated after purification, unless otherwise stated. Proton nuclear magnetic resonance spectra were recorded on a Bruker AMX 400 MHz. NMR samples were dissolved in chloroform-d (unless specified otherwise) and chemical shifts are reported in ppm referenced to residual non-deuterated solvent. Data are reported as follows: chemical shift, multiplicity, coupling, integration. Carbon nuclear magnetic resonance spectra were recorded on the same Bruker instrument at 101 MHz. Assignments of ^{13}C signals were made by DEPT-135 experiments. IR spectra were recorded with an Agilent Technologies Cary 630 FTIR Spectrometer equipped with a diamond ATR module. HRMS were obtained on a Kratos Analytical Concept EI-Magnetic Sector instrument (University of Ottawa Mass Spectrum Centre). Isocyanide starting materials were synthesized according to Chatani's procedure.[19]

General procedure for the preparation of alkylated heteroarenes (GP1). To an 8 mL pyrex screw-top reaction vessel was added isonitrile **5** (0.20 mmol, 1.00 equiv), bromoalkane **4** (0.60 mmol, 3.00 equiv), sodium carbonate (0.60 mmol, 3.00 equiv), DABCO (0.04 mmol, 0.20 equiv), $[Au_2(dppm)_2]Cl_2$ (0.01 mmol, 0.05 equiv), and MeCN (2.00 mL, 0.10 M). The reaction vessel was degassed by sparging under argon for 10 minutes, sealed with parafilm and irradiated under an UVA (365 nm) LED at a distance of 1 cm for 16 hours. *Bromoalkanes with boiling points below 100˚C (e.g. 2-bromobutane) were added after sparging the mixture. The resulting mixture was filtered over a short cotton plug, concentrated *in vacuo*, and purified by silica gel chromatography, where relevant fractions were combined, concentrated and characterized by proton and carbon NMR (400 and 101 MHz, respectively), HRMS, and IR unless previously characterized.

General Procedure for the kinetic study (GP2). Reactions were prepared from stock solutions of aryl isonitrile **2.8** (1.0 M), $[Au_2(dppm)_2]Cl_2$ (0.2 M) in MeCN, (bromomethyl)-cyclobutane (neat) and solid Na_2CO_3. In a given run, 5 samples were prepared using the stock solutions of 2a (100-500 µL, 0.1-0.5 M), $[Au_2(dppm)_2]Cl_2$ (100 µL, 0.02 M each), Na_2CO_3 (10.6-53.0 mg, 0.1-0.5 M) and reactions were degassed lightly with argon for 5 minutes. A degassed solution of (bromomethyl)cyclobutane **2.39** (113 µL, 1.0 M each) was then added and each solution was added the remaining MeCN to make a 1 mL volume (687µL, 587 µL, 487 µL, 387 µL, 287 µL, respectively). The reactions were then irradiated for 16 hours with a UVA LED. The resulting mixtures were then subjected to the work-up portion of GP1. After irradiation, the ^{1}H NMR of crude products showed the same ratios as the ^{1}H NMR that had been purified by flash chromatography. The crude mixture could then be analyzed by ^{1}H NMR reliably for product ratios.

General Procedure for the preparation of amides (GP3). To an 8 mL pyrex screw-top reaction vessel was added isocyanide (0.20 mmol, 1.00 equiv), bromoalkane (0.60 mmol, 3.00 equiv), sodium carbonate (0.60 mmol, 3.00 equiv), DABCO (0.2 mmol, 1 equiv), $[Au_2(dppm)_2]Cl_2$ (0.01 mmol, 0.05 equiv), water (80µL, 21 equiv), and MeCN (2.00 mL, 0.10 M). The reaction vessel was degassed by sparging under argon for 10 minutes, sealed with parafilm and irradiated under an UVA (365 nm) LED at a distance of 1 cm for 16 hours. *Bromoalkanes with boiling points below 100°C (e.g. 2-bromobutane) were added after sparging the mixture. The resulting mixture was diluted with DCM and washed sequentially with 1N HCl, saturated sodium bicarbonate, and brine. The organic phase was dried with Na_2SO_4, filtered, concentrated *in vacuo*, and purified by silica gel chromatography on base-neutralized silica, where relevant fractions were combined,

concentrated and characterized by proton and carbon NMR (400 and 101 MHz, respectively), HRMS, and IR unless previously characterized.

General procedure for preparation of styryl isonitriles 2.55 (GP4) [20c]

To a flame-dried round-bottom flask with stir bar under argon was added 2-iodoaniline **2.57** (2g, 9.13 mmol, 1 equiv.), olefin coupling partner (36.52 mmol, 1 equiv.), NEt_3 (3.17 mL, 22.8 mmol, 2.5 equiv.), and acetonitrile (45mL, 0.2M). The mixture was sparged with argon through a needle for 15 minutes then $Pd(OAc)_2$ (0.205g, 0.91 mmol, 10 mol %) and P(*o*-tolyl)$_3$ (0.56g, 1.83 mmol, 20 mol%) were added and stirring commenced. The reaction was refluxed overnight (16 hours) and was cooled to r.t. following confirmation of complete conversion by TLC. Water was added and the mixture was extracted 3x with EtOAc. The organic phases were combined and washed with water and brine, then dried with $MgSO_4$. The solids were removed by filtration and solvent was removed under reduce pressure to afford a crude residue that was purified by column chromatography (0-20% EtOAc in hexanes) to afford styryl anilines **2.58**.

To an open-air round-bottom flask was added acetic anhydride (2.61 mL, 27.59 mmol, 10 equiv.) and formic acid (1.15 mL, 30.35 mmol, 10.1 equiv.). Stirring was commenced and the mixture was heated at 50 ^oC for 2 hours. A separate open-air round-bottom flask was prepared containing styryl aniline **2.58** (2.76 mmol, 1 equiv.) and THF (5 mL, 0.5M). The second flask was cooled to 0 ^oC in an ice bath while stirring, and the total quantity of the first flask was added over 2h to the second flask via syringe pump. The reaction was allowed to warm to room temperature and stirred overnight. Following confirmation of full conversion of starting material by TLC, the crude reaction mixture was

diluted with water. The mixture was extracted 3x with EtOAc, then the organic phases were combined and dried with $MgSO_4$. Solids were removed by filtration and solvent was removed under reduced pressure. 3 mL of toluene was added and removed under reduced pressure 3x to remove any residual traces of acetic formic anhydride from the crude. This crude brown oil was then used in the next step without further purification.

To a flame-dried round-bottom flask under argon with a stir bar was added the crude oil from the previous step (2.76 mmol, 1 equiv.), NEt_3 (2.3 mL, 16.55 mmol, 6 equiv.), and THF (5 mL, 0.5 M). The reaction was cooled to 0 ^oC in an ice bath and $POCl_3$ (0.52 mL, 5.52 mmol, 2 equiv.) was added dropwise over 10 mins. The mixture was stirred for 2-4h at 0 ^oC or until confirmation of full conversion by TLC. The reaction was quenched by slow addition of $NaHCO_3$ (sat.) at 0 ^oC. Once bubbling ceased, the mixture was extracted 3x with DCM, the organic phases were combined, washed with water and brine, and dried with $MgSO_4$. Solids were removed by filtration and solvent was removed under reduced pressure. The resulting crude oil was purified by column chromatography (0-5% diethyl ether, inhibitor-free, in hexanes) to obtain pure styryl isonitriles **2.55**.

Typical procedure for preparation of tosylated piperidinones (TP1)[27]

To a flame-dried round-bottom flask under argon with a stir bar was added 4-piperidone hydrochloride monohydrate (4g, 26 mmol, 1 equiv.), K_2CO_3 (7.2g, 52 mmol, 2 equiv.), and DCM:H_2O (1:1, 130 mL, 0.2 M). Stirring was commenced and toluenesulfonyl chloride (5.4 g, 1.1 equiv.) was added dropwise at r.t. The reaction was allowed to stir until observed complete by TLC (2-3 h). The reaction was quenched with water and diluted with DCM. The organic layer was washed successively with HCl and brine, dried

with $MgSO_4$, filtered, and solvent was removed using rotary evaporation to afford the crude product. The crude product was pure enough to use in subsequent reactions without further purification.

Typical procedure for preparation of α,β-unsaturated piperidinones (TP2)[23]

To a flame-dried round-bottom flask under argon with a stir bar was added IBX (4.8 g, 17.4 mmol, 2.2 equiv.), NMO (2.0 g, 17.4 mmol, 2.2 equiv.) and DMSO (15 mL, 0.5 M). The mixture was stirred until dissolution of all reagents was observed (about 15 minutes). Upon dissolution, a solution of piperidone (2g, 7.8 mmol, 1 equiv.) in DMSO (1.6 mL, 5 M) was added dropwise to the stirred mixture. A reflux condenser was fitted to the flask and the reaction was heated to 50 °C overnight. Upon full conversion of starting material by TLC, the reaction was cooled to r.t., diluted with sat. $NaHCO_3$ and diethyl ether and extracted 3x with diethyl ether. The combined organic extracts were washed successively with sat. $NaHCO_3$, water, and brine. The organic layer was then dried with $MgSO_4$, filtered, and the solvent removed by rotary evaporation. Further purification by silica gel chromatography afforded the final product.

2.7 Characterization Data

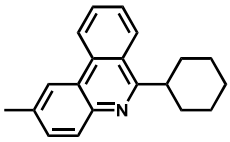

6-Cyclohexyl-2-methylphenanthridine (2.10)

Synthesized according to GP1. Purification by silica gel chromatography with a gradient of 0 – 10% EtOAc in hexanes gave the product as 48.1 mg of yellow oil (83%),

characterized according to NMR comparison.[19] ^{1}H NMR (400 MHz, $CDCl_3$): δ = 8.65 (d, *J* = 8.0 Hz, 1H), 8.37-8.26 (m, 2H), 8.02 (d, *J* = 8.3 Hz, 1H), 7.80 (t, *J* = 7.2 Hz, 1H), 7.68 (t, *J* = 7.1 Hz, 1H), 7.53 (dd, *J* = 8.2, 1.6 Hz, 1H), 3.73-3.46 (m, 1H), 2.62 (s, 3H), 2.14-1.75 (m, 7H), 1.60 (s, 2H), 1.50-1.39 (m, 1 H) ppm; ^{13}C NMR (101 MHz, $CDCl_3$): δ = 164.2 (C), 142.1 (C), 135.8 (C), 132.8 (C), 130.0 (CH), 129.6 (CH), 126.8 (CH), 125.5 (CH), 124.7 (C), 123.1 (C), 122.5 (2 X CH), 121.4 (CH), 41.9 (CH), 32.3 (2 X CH_2), 26.9 (2 X CH_2), 26.3 (CH_2), 21.9 (CH_3) ppm.

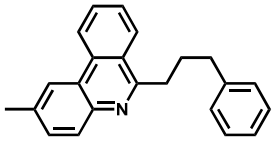

2-Methyl-6-(3-phenylpropyl)phenanthridine (2.63)

Synthesized according to GP1. Purification by silica gel chromatography with a gradient of 0 – 10% EtOAc in hexanes gave the product as 37.4 mg of yellow oil (60%). IR (neat NaCl) 3025, 2920, 2856, 1584, 1497, 1453, 825 cm^{-1}. ^{1}H NMR (400 MHz, $CDCl_3$) δ = 8.60 (dd, *J* = 8.4, 1.2 Hz, 1H), 8.30 (t, *J* = 1.3 Hz, 1H), 8.09 (dd, *J* = 8.3, 1.2 Hz, 1H), 8.01 (d, *J* = 8.3 Hz, 1H), 7.77 (ddd, *J* = 8.3, 7.0, 1.3 Hz, 1H), 7.61 (ddd, *J* = 8.3, 7.0, 1.2 Hz, 1H), 7.53 (dd, *J* = 8.3, 1.9 Hz, 1H), 7.36-7.20 (m, 4H), 7.24-7.14 (m, 1H), 3.47-3.33 (m, 2H), 2.85 (t, *J* = 7.7 Hz, 2H), 2.60 (s, 3H), 2.34-2.20 (m, 2H). ^{13}C NMR (101 MHz, $CDCl_3$) δ = 160.8 (C), 142.2 (C), 142.0 (C), 136.1 (C), 132.7 (C), 130.3 (CH), 130.1 (CH), 129.3 (CH), 128.6 (2 X CH), 128.4 (2 X CH), 127.1 (CH), 126.2 (CH), 125.9 (CH), 125.3 (C), 123.5 (C), 122.5 (CH), 121.6 (CH), 36.0 (CH_2), 35.6 (CH_2), 30.9 (CH_2), 21.9 (CH_3). HRMS (EI) *m/z*: [M^+]calc'd for $C_{23}H_{21}N$ 311.1674, found 311.1648.

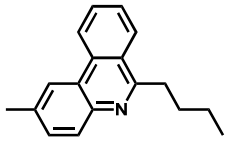

6-Butyl-2-methylphenanthridine (2.64)

Synthesized according to GP1. Purification by silica gel chromatography with a gradient of 0 – 10% EtOAc in hexanes gave the product as 20.0 mg of yellow oil (40%), characterized according to NMR comparison.[19] ^{1}H NMR (400 MHz, $CDCl_3$): δ = 8.61 (dt, J = 8.3, 0.8 Hz, 1H), 8.30 (s, 1H), 8.22 (dt, J = 8.1, 1.0 Hz, 1H), 7.99 (d, J = 8.3 Hz, 1H), 7.78 (ddd, J = 8.3, 7.0, 1.3 Hz, 1H), 7.65 (ddd, J = 8.2, 7.0, 1.2 Hz, 1H), 7.51 (dd, J = 8.3, 1.9 Hz, 1H), 3.38-3.29 (m, 2H), 2.59 (s, 3H), 1.95-1.82 (m, 2H), 1.53 (dt, J = 14.8, 7.4 Hz, 2H), 0.99 (t, J = 7.4 Hz, 3H) ppm; ^{13}C NMR (101 MHz, $CDCl_3$): δ = 161.5 (C), 142.1 (C), 136.0 (C), 132.8 (C), 130.3 (CH), 130.0 (CH), 129.3 (CH), 127.0 (CH), 126.3 (CH), 125.3 (C), 123.5 (C), 122.5 (CH), 121.6 (CH), 36.2 (CH_2), 31.8 (CH_2), 23.2 (CH_2), 21.9 (CH_3), 14.1 (CH_3) ppm.

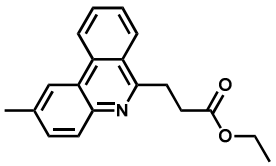

Ethyl 3-(2-methylphenanthridin-6-yl)propanoate (2.65)

Synthesized according to GP1. Purification by silica gel chromatography with a gradient of 0 – 20% EtOAc in hexanes gave the product as 33.6 mg of yellow oil (57%). IR (neat NaCl) 2983, 2916, 1732, 1498, 1174 cm^{-1}. ^{1}H NMR (400 MHz, $CDCl_3$) δ = 8.63-8.56 (m, 1H), 8.32-8.20 (m, 2H), 7.96 (d, J = 8.3 Hz, 1H), 7.79 (ddd, J = 8.3, 7.1, 1.3 Hz,

1H), 7.66 (ddd, *J* = 8.2, 7.0, 1.2 Hz, 1H), 7.54-7.46 (m, 1H), 4.17 (q, *J* = 7.1 Hz, 2H), 3.68 (t, *J* = 7.4 Hz, 2H), 3.08-3.00 (m, 2H), 2.59 (s, 3H), 1.25 (t, *J* = 7.1 Hz, 3H). ^{13}C NMR (101 MHz, $CDCl_3$) δ = 173.6 (C), 158.1 (C), 136.3 (C), 132.5 (C), 130.2 (CH), 129.4 (CH), 129.3 (CH), 127.2 (CH), 125.7 (CH), 125.3 (C), 123.5 (2 X C), 122.4 (CH), 121.6 (CH), 60.4 (CH_2), 32.0 (CH_2), 29.9 (CH_2), 21.9 (CH_3), 14.3 (CH_3). HRMS (EI) *m/z*: [M^+] calc'd for $C_{19}H_{19}NO_2$ 293.1416, found 293.1411.

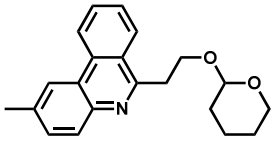

2-Methyl-6-(2-((tetrahydro-2H-pyran-2-yl)oxy)ethyl)-phenanthridine (2.66)

Synthesized according to GP1. Purification by silica gel chromatography with a gradient of 0 – 10% EtOAc in hexanes gave the product as 53.4 mg of yellow oil (83%). IR (neat,): 2942, 2869, 1119, 1032 cm^{-1}. ^{1}H NMR (400 MHz, $CDCl_3$): δ = 8.58 (dt, *J* = 8.3, 0.6 Hz, 1H), 8.34-8.26 (m, 2H), 7.99 (d, *J* = 8.3 Hz, 1H), 7.78 (ddd, *J* = 8.3, 7.0, 1.3 Hz, 1H), 7.64 (ddd, *J* = 8.3, 7.0, 1.2 Hz, 1H), 7.50 (dd, *J* = 8.3, 1.8 Hz, 1H), 4.67 (dd, *J* = 4.4, 2.9 Hz, 1H), 4.34 (ddd, *J* = 9.8, 7.8, 6.8 Hz, 1H), 4.15-3.96 (m, 2H), 3.79 (ddd, *J* = 11.1, 8.2, 3.2 Hz, 1H), 3.67 (t, *J* = 7.1 Hz, 2H), 3.50-3.40 (m, 1H), 2.59 (s, 3H), 1.83-1.60 (m, 2H), 1.60-1.36 (m, 2H), 1.24 (t, *J* = 7.2 Hz, 1H). ^{13}C NMR (101 MHz, $CDCl_3$) δ = 158.3 (C), 136.2 (2 X C), 132.6 (C), 130.3 (CH), 130.1 (CH), 129.4 (CH), 127.1 (CH), 126.5 (CH), 125.8 (C), 123.5 (C), 122.3 (CH), 121.6 (CH), 99.0 (CH), 66.7 (CH_2), 62.3 (CH_2), 36.1 (CH_2), 30.7 (CH_2), 25.5 (CH_2), 21.9 (CH_3), 19.5 (CH_2). HRMS (EI) *m/z*: [M^+] calc'd for $C_{21}H_{23}NO_2$ 321.1729, found 321.1731.

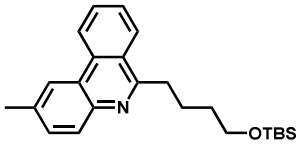

6-(4-((tert-Butyldimethylsilyl)oxy)butyl)-2-methylphenanthridine (2.67)

Synthesized according to GP1. Purification by silica gel chromatography with a gradient of 0 – 10% EtOAc in hexanes gave the product as 24.1 mg of yellow oil (33%). IR (neat NaCl) 2955, 2930, 2856, 1102 cm^{-1}. ^{1}H NMR (400 MHz, $CDCl_3$) δ = 8.65-8.58 (m, 1H), 8.35-8.28 (m, 2H), 8.03 (d, *J* = 8.2 Hz, 1H), 7.85-7.76 (m, 1H), 7.66 (ddd, *J* = 8.2, 7.0, 1.2 Hz, 1H), 7.56-7.48 (m, 1H), 3.81 (t, *J* = 6.1 Hz, 2H), 3.50-3.40 (m, 2H), 2.60 (s, 3H), 2.20-2.07 (m, 2H), 0.92 (s, 9H), 0.07 (s, 6H). ^{13}C NMR (101 MHz, $CDCl_3$) δ = 161.1 (C), 158.5 (C), 132.8 (C), 130.4 (CH), 127.2 (CH), 127.0 (CH), 126.6 (C), 125.3 (C), 123.6 (C), 122.4 (2 X CH), 121.6 (2 X CH), 62.9 (2 X CH_2), 32.5 (CH_2), 26.0 (3 X CH_3), 21.9 (CH_3), 18.4 (C), -5.3 (2 X CH_3). HRMS (EI) *m/z*: [M^+] calc'd for $C_{24}H_{33}NOSi$ 379.2331, found 379.2320.

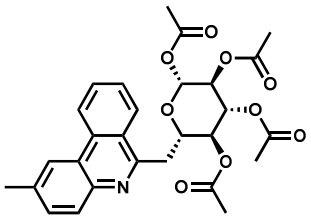

(2S,3R,4S,5R,6R)-6-((2-Methylphenanthridin-6-yl)methyl)-tetrahydro-2H-pyran-2,3,4,5-tetrayl tetraacetate (2.68)

Synthesized according to GP1. Purification by silica gel chromatography with a 30% EtOAc, 5% AcOH in hexanes gave the product as 86.9 mg of yellow oil (83%). IR (neat

NaCl) 2922, 1754, 1367, 1214, 1076, 1036 cm^{-1}. ^1H NMR (400 MHz, $CDCl_3$) δ = 8.62 (d, *J* = 8.2 Hz, 1H), 8.32 (s, 1H), 8.17 (d, *J* = 8.0 Hz, 1H), 8.02 (d, *J* = 8.2 Hz, 1H), 7.82 (ddd, *J* = 8.0, 7.1, 1.0 Hz, 1H), 7.67 (ddd, *J* = 8.0, 7.1, 1.0 Hz, 1H), 7.55 (dd, *J* = 8.4, 1.6 Hz, 1H), 5.79 (d, *J* = 8.2 Hz, 1H), 5.33-5.13 (m, 3H), 4.63 (ddd, *J* = 9.6, 6.8, 4.6 Hz, 1H), 3.69 (dd, *J* = 15.1, 6.9 Hz, 1H), 3.53 (dd, *J* = 15.3, 4.7 Hz, 1H), 2.62 (s, 3H), 2.03 (s, 3H), 2.01 (s, 6H) 1.78 (s, 3H). ^{13}C NMR (101 MHz, $CDCl_3$) δ = 170.1 (C), 169.8 (C), 169.3 (C), 168.7 (C), 155.4 (C), 141.8 (C), 136.5 (C), 132.6 (C), 130.4 (CH), 130.1 (CH), 129.6 (CH), 127.1 (CH), 126.1 (CH), 125.6 (C), 123.5 (C), 122.3 (CH), 121.5 (CH), 91.8 (CH), 73.2 (CH), 73.1 (CH), 72.0 (CH), 70.7 (CH), 37.7 (CH_2), 21.9 (CH_3), 20.7 (CH_3), 20.6 (CH_3), 20.6 (CH_3), 20.5 (CH_3). HRMS (ESI-MS) *m/z*: [M^+ Na+] calc'd for $C_{28}H_{29}NO_9Na$ 546.1740, found 546.1771.

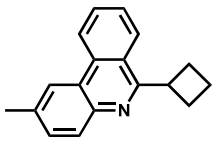

6-Cyclobutyl-2-methylphenanthridine (2.69)

Synthesized according to GP1. Purification by silica gel chromatography with a gradient of 0 – 10% EtOAc in hexanes gave the product as 38.3 mg of yellow (77%), characterized according to NMR comparison.[28] ^1H NMR (400 MHz, $CDCl_3$): δ = 8.59 (ddt, *J* = 8.2, 1.1, 0.5 Hz, 1H), 8.32-8.26 (m, 1H), 8.13-8.03 (m, 2H), 7.76 (ddd, *J* = 8.3, 7.0, 1.3 Hz, 1H), 7.62 (ddd, *J* = 8.2, 7.0, 1.2 Hz, 1H), 7.56-7.48 (m, 1H), 4.45-4.31 (m, 1H), 2.83-2.67 (m, 2H), 2.60 (s, 3H), 2.56-2.45 (m, 2H), 2.29-2.12 (m, 1H), 2.06-1.90 (m, 1H) ppm; ^{13}C NMR (101 MHz, $CDCl_3$): δ = 162.1 (C), 142.0 (C), 136.0 (C), 132.7 (C), 130.1

(CH), 129.9 (CH), 129.6 (CH), 126.9 (CH), 126.1 (CH), 124.9 (C), 123.4 (C), 122.4 (CH), 121.6 (CH), 53.4 (CH_2), 39.8 (CH), 27.3 (CH_2), 21.9 (CH_3), 18.5 (CH_2) ppm.

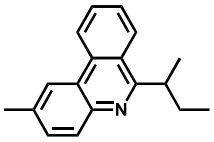

6-(sec-Butyl)-2-methylphenanthridine (2.70)

Synthesized according to GP1. Purification by silica gel chromatography with a gradient of 0 – 10% EtOAc in hexanes gave the product as 39.8 mg of yellow oil (80%), characterized according to NMR comparison.[19] ^{1}H NMR (400 MHz, $CDCl_3$): δ = 8.63 (dt, *J* = 8.2, 0.6 Hz, 1H), 8.32-8.30 (m, 1H), 8.29 (ddt, *J* = 8.3, 1.3, 0.5 Hz, 1H), 8.02 (d, *J* = 8.3 Hz, 1H), 7.78 (ddd, *J* = 8.3, 7.0, 1.3 Hz, 1H), 7.65 (ddd, *J* = 8.3, 7.0, 1.2 Hz, 1H), 7.52 (ddd, *J* = 8.3, 2.0, 0.5 Hz, 1H), 3.73 (sex, *J* = 6.8 Hz, 1H), 2.60 (s, 3H), 2.21-2.07 (m, 1H), 1.80 (dt, *J* = 13.5, 7.2 Hz, 1H), 1.47 (d, *J* = 6.8 Hz, 3H), 0.97 (t, *J* = 7.4 Hz, 3H) ppm; ^{13}C NMR (101 MHz, $CDCl_3$): δ = 164.4 (C), 142.2 (C), 135.8 (C), 132.8 (C), 130.1 (CH), 129.7 (2 X CH), 126.9 (CH), 125.6 (CH), 125.3 (C), 123.1 (C), 122.5 (CH), 121.5 (CH), 38.3 (CH), 29.2 (CH_2), 21.9 (CH_3), 19.8 (CH_3), 12.5 (CH_3) ppm.

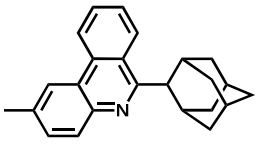

6-(Adamantan-2-yl)-2-methylphenanthridine (2.71)

Synthesized according to GP1. Purification by silica gel chromatography with a gradient of 0 – 10% EtOAc in hexanes gave the product as 60.8 mg of yellow oil (97%).

IR (neat NaCl) 2904, 2850 cm^{-1}. ^1H NMR (400 MHz, $CDCl_3$): δ = 8.61 (dd, *J* = 8.3, 1.2 Hz, 1H), 8.30 (dd, *J* = 1.8, 0.9 Hz, 1H), 8.17-8.09 (m, 1H), 8.05 (d, *J* = 8.2 Hz, 1H), 7.74 (ddd, *J* = 8.2, 7.0, 1.3 Hz, 1H), 7.61 (ddd, *J* = 8.2, 7.0, 1.3 Hz, 1H), 7.51 (dd, *J* = 8.3, 2.0 Hz, 1H), 3.96 (s, 1H), 2.70-2.61 (m, 2H), 2.61 (s, 3H), 2.53-2.46 (m, 2H), 2.20-1.99 (m, 4H), 1.93 (p, *J* = 3.1 Hz, 1H), 1.84 (d, *J* = 3.2 Hz, 2H), 1.63 (dt, *J* = 13.9, 2.0 Hz, 2H). ^{13}C NMR (101 MHz, $CDCl_3$): δ = 162.9 (C), 141.8 (C), 135.8 (C), 132.8 (C), 130.0 (CH), 129.9 (CH), 129.4 (CH), 126.7 (CH), 126.1 (CH), 125.0 (C), 123.0 (C), 122.6 (CH), 121.4 (CH), 47.6 (CH), 40.2 (2 X CH_2), 38.2 (CH_2), 32.8 (2 X CH), 32.7 (2 X CH_2), 28.6 (CH), 28.1 (CH), 22.0 (CH_3). HRMS (EI) *m/z*: [M^+ -H] calc'd for $C_{24}H_{25}N$ 326.1909, found 326.1910.

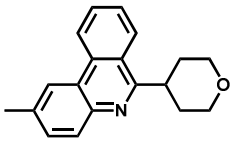

2-Methyl-6-(tetrahydro-2H-pyran-4-yl)phenanthridine (2.72)

Synthesized according to GP1. Purification by silica gel chromatography with a gradient of 0 – 10% EtOAc in hexanes gave the product as 44.9 mg of yellow oil (81%). IR (neat NaCl,): 2951, 2837, 1132 cm^{-1}. ^1H NMR (400 MHz, $CDCl_3$): δ = 8.64 (dd, *J* = 8.2, 1.1 Hz, 1H), 8.30 (t, *J* = 1.2 Hz, 1H), 8.26 (d, *J* = 8.2 Hz, 1H), 8.01 (d, *J* = 8.3 Hz, 1H), 7.79 (ddd, *J* = 8.2, 6.9, 1.2 Hz, 1H), 7.66 (ddd, *J* = 8.2, 6.9, 1.2 Hz, 1H), 7.52 (dd, *J* = 8.3, 1.9 Hz, 1H), 4.18 (ddd, *J* = 11.4, 4.5, 1.9 Hz, 2H), 3.82 (tt, *J* = 11.4, 3.6 Hz, 1H), 3.71 (td, *J* = 11.9, 2.0 Hz, 2H), 2.60 (s, 3H), 2.32 (dtd, *J* = 13.6, 11.8, 4.3 Hz, 2H), 1.94 (ddt, *J* = 13.5, 3.8, 2.1 Hz, 2H). ^{13}C NMR (101 MHz, $CDCl_3$): δ = 161.9 (C), 142.1 (C), 136.2 (C), 132.9 (C), 130.2 CH), 129.9 (CH), 129.8 (CH), 127.0 (CH), 125.2 (CH), 124.5 (C), 123.2

(C), 122.8 (CH), 121.5 (CH), 68.3 (2 X CH_2), 39.1 (CH), 32.0 (2 X CH_2), 22.0 (CH_3). HRMS (EI) *m/z*: [M^+ -C_3H_6O] calc'd for $C_{16}H_{13}N$ 219.1048, found 219.1033.

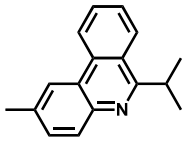

6-Isopropyl-2-methylphenanthridine (2.73)

Synthesized according to GP1. Purification by silica gel chromatography with a gradient of 0 – 10% EtOAc in hexanes gave the product as 34.7 mg of yellow oil (74%). IR (neat NaCl,): 2965, 2926, 2869, 1582, 1497 cm^{-1}. ^1H NMR (400 MHz, $CDCl_3$): δ = 8.62 (ddt, *J* = 8.3, 1.3, 0.6 Hz, 1H), 8.33-8.25 (m, 2H), 8.03 (d, *J* = 8.3 Hz, 1H), 7.77 (ddd, *J* = 8.3, 7.0, 1.3 Hz, 1H), 7.65 (ddd, *J* = 8.2, 7.0, 1.2 Hz, 1H), 7.52 (ddd, *J* = 8.3, 1.9, 0.6 Hz, 1H), 4.05-3.89 (m, 1H), 2.60 (s, 3H), 1.51 (d, *J* = 6.8 Hz, 6H). ^{13}C NMR (101 MHz, $CDCl_3$): δ = 164.8 (C), 142.1 (C), 135.9 (C), 132.8 (C), 130.1 (CH), 129.7 (2 X CH), 126.9 (CH), 125.7 (CH), 124.8 (C), 123.2 (C), 122.6 (CH), 121.5 (CH), 31.4 (CH), 22.0 (2 X CH_3), 21.9 (CH_3). HRMS (EI) *m/z*: [M^+] calc'd for $C_{17}H_{17}N$ 235.1361, found 235.1358.

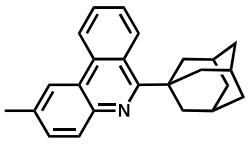

6-(Adamantan-1-yl)-2-methylphenanthridine (2.74)

Synthesized according to GP1. Purification by silica gel chromatography with a gradient of 0 – 10% EtOAc in hexanes gave the product as 46.0 mg of yellow oil (70%), characterized according to NMR comparison.[28] ^1H NMR (400 MHz, $CDCl_3$): δ = 8.83 (dd,

J = 8.5, 1.2 Hz, 1H), 8.66 (dd, *J* = 8.4, 1.3 Hz, 1H), 8.28 (t, *J* = 1.3 Hz, 1H), 8.00 (d, *J* = 8.3 Hz, 1H), 7.73 (ddd, *J* = 8.2, 6.9, 1.2 Hz, 1H), 7.60 (ddd, *J* = 8.4, 6.9, 1.4 Hz, 1H), 7.54-7.47 (m, 1H), 2.60 (s, 3H), 2.48 (d, *J* = 2.9 Hz, 6H), 2.22 (p, *J* = 3.1 Hz, 3H), 1.90 (qt, *J* = 12.1, 3.1 Hz, 6H). ^{13}C NMR (101 MHz, $CDCl_3$): δ = 165.0 (C), 141.5 (C), 136.2 (C), 133.9 (C), 130.0 (CH), 130.0 (CH), 129.0 (CH), 127.9 (CH), 125.5 (CH), 124.5 (C), 123.1 (CH), 123.1 (C), 121.3 (CH), 42.1 (3 X CH_2), 37.3 (3 X CH_2), 29.3 (3 X CH), 22.0 (CH_3).

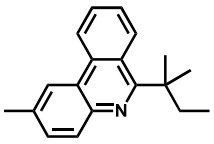

2-Methyl-6-(tert-pentyl)phenanthridine (2.75)

Synthesized according to GP1. Purification by silica gel chromatography with a gradient of 0 – 10% EtOAc in hexanes gave the product as 52.1 mg of yellow oil (99%), characterized according to NMR comparison.[29] ^{1}H NMR (400 MHz, $CDCl_3$): δ = 8.63 (dddd, *J* = 21.8, 8.5, 1.4, 0.7 Hz, 2H), 8.30 (tt, *J* = 1.5, 0.7 Hz, 1H), 8.02 (d, *J* = 8.3 Hz, 1H), 7.74 (ddd, *J* = 8.3, 6.9, 1.3 Hz, 1H), 7.60 (ddd, *J* = 8.4, 7.0, 1.4 Hz, 1H), 7.51 (ddd, *J* = 8.3, 1.9, 0.6 Hz, 1H), 2.61 (s, 3H), 2.21 (q, *J* = 7.5 Hz, 2H), 1.69 (s, 6H), 0.74 (t, *J* = 7.5 Hz, 3H) ppm; ^{13}C NMR (101 MHz, $CDCl_3$): δ = 164.7 (C), 141.3 (C), 136.1 (C), 133.6 (C), 130.1 (CH), 130.0 (CH), 129.0 (CH), 127.6 (CH), 125.8 (CH), 124.9 (C), 123.1 (C), 122.9 (CH), 121.2 (CH), 43.9 (C), 35.5 (CH_2), 29.2 (2 X CH_3), 22.0 (CH_3), 9.5 (CH_3) ppm.

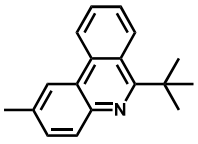

6-(tert-Butyl)-2-methylphenanthridine (2.76)

Synthesized according to GP1. Purification by silica gel chromatography with a gradient of 0 – 10% EtOAc in hexanes gave the product as 46.4 mg of yellow oil (93%), characterized according to NMR comparison.[28] ^{1}H NMR (400 MHz, $CDCl_3$): δ = 8.63 (dddd, *J* = 21.2, 8.5, 1.3, 0.6 Hz, 2H), 8.29 (dq, *J* = 2.0, 0.7 Hz, 1H), 8.01 (d, *J* = 8.3 Hz, 1H), 7.74 (ddd, *J* = 8.3, 7.0, 1.3 Hz, 1H), 7.61 (ddd, *J* = 8.4, 7.0, 1.4 Hz, 1H), 7.51 (ddd, *J* = 8.4, 1.9, 0.6 Hz, 1H), 2.65-2.56 (m, 3H), 1.73 (s, 9H) ppm; ^{13}C NMR (101 MHz, $CDCl_3$): δ = 165.6 (C), 141.3 (C), 136.1 (C), 133.8 (C), 130.0 (CH), 130.0 (CH), 129.0 (CH), 128.2 (CH), 125.8 (CH), 124.4 (C), 123.2 (C), 122.9 (CH), 121.3 (CH), 40.1 (C), 31.2 (3 X CH_3), 22.0 (CH_3) ppm.

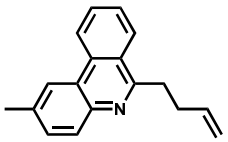

2-Methyl-6-(but-3-en-1-yl)phenanthridine (2.77)

Synthesized according to GP1. Purification by silica gel chromatography with a gradient of 0 – 10% EtOAc in hexanes gave the product as 17.3 mg of yellow oil (44%). IR (neat NaCl) 3080, 2919, 2856, 1584, 1498, 911 cm^{-1}. ^{1}H NMR (400 MHz, $CDCl_3$): δ = 8.61 (dd, *J* = 8.4, 1.2 Hz, 1H), 8.33-8.27 (m, 1H), 8.21 (dd, *J* = 8.3, 1.2 Hz, 1H), 8.01 (d, *J* = 8.3 Hz, 1H), 7.79 (ddd, *J* = 8.3, 7.0, 1.3 Hz, 1H), 7.66 (ddd, *J* = 8.3, 7.0, 1.2 Hz, 1H), 7.52 (dd, *J* = 8.3, 1.9 Hz, 1H), 6.03 (ddt, *J* = 16.8, 10.2, 6.6 Hz, 1H), 5.14 (dq, *J* = 17.1, 1.7 Hz, 1H), 5.02 (dq, *J* = 10.2, 1.4 Hz, 1H), 3.48-3.39 (m, 2H), 2.69 (dtt, *J* = 7.9, 6.6, 1.4 Hz, 2H), 2.60 (s, 3H). ^{13}C NMR (101 MHz, $CDCl_3$): δ = 160.3 (C), 141.9 (C), 138.1 (CH),

136.2 (C), 132.7 (C), 130.3 (CH), 130.2 (CH), 129.3 (CH), 127.2 (CH), 126.2 (CH), 125.3 (C), 123.4(C), 122.5 (CH), 121.6 (CH), 115.1 (CH_2), 35.3 (CH_2), 33.2 (CH_2), 21.9 (CH_3). HRMS (EI) *m/z*: [M^+ -C_2H_3] calc'd for $C_{16}H_{14}N$ 220.1126, found 220.1124.

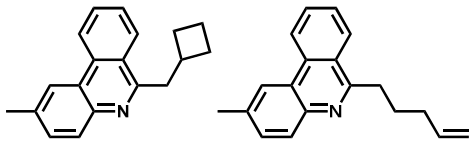

6-(Cyclobutylmethyl)-2-methylphenanthridine (2.44) and

2-methyl-6-(pent-4-en-1-yl)phenanthridine (2.45)

Synthesized according to GP1. Use bromomethyl cyclobutane **2.39.** Purification by silica gel chromatography with a gradient of 0 – 10% EtOAc in hexanes gave the product as 42.1 mg of yellow oil (64%, 50:50 mix of **2.44** and **2.45**). IR (neat NaCl) 3070, 2931, 2861, 1583, 1498 cm^{-1}. For **2.44**: ^1H NMR (400 MHz, $CDCl_3$): δ = 8.60 (ddd, *J* = 8.3, 4.7, 1.1 Hz, 1H), 8.29 (s, 1H), 8.21 (ddd, *J* = 7.9, 6.3, 1.2 Hz, 1H), 8.01 (dd, *J* = 8.3, 4.8 Hz, 1H), 7.78 (dddd, *J* = 8.3, 7.0, 2.7, 1.3 Hz, 1H), 7.64 (tdd, *J* = 7.0, 3.1, 1.2 Hz, 1H), 7.51 (dt, *J* = 8.3, 2.0 Hz, 1H), 3.10-2.88 (m, 2H), 2.59 (s, 3H), 2.20-1.78 (m, 7H). ^{13}C NMR (101 MHz, $CDCl_3$): δ = 161.0 (C), 160.0 (C), 142.0 (C), 136.0 (C), 132.7 (CH), 130.2 (CH), 129.3 (CH), 127.0 (CH), 126.2 (CH), 125.6 (C), 123.4 (C), 122.4 (CH), 121.5 (CH), 42.6 (CH_2), 36.1 (CH), 34.0 (3 X CH_2), 18.6(CH_3). For **2.45**: ^1H NMR (400 MHz, $CDCl_3$): δ = 8.60 (ddd, *J* = 8.3, 4.7, 1.1 Hz, 1H), 8.29 (s, 1H), 8.21 (ddd, *J* = 7.9, 6.3, 1.2 Hz, 1H), 8.01 (dd, *J* = 8.3, 4.8 Hz, 1H), 7.78 (dddd, *J* = 8.3, 7.0, 2.7, 1.3 Hz, 1H), 7.64 (tdd, *J* = 7.0, 3.1, 1.2 Hz, 1H), 7.51 (dt, *J* = 8.3, 2.0 Hz, 1H), 5.91 (ddt, *J* = 16.9, 10.2, 6.7 Hz, 1H), 5.08 (dq, *J* = 17.1, 1.7 Hz, 1H), 5.01 (ddd, *J* = 10.2, 2.2, 1.1 Hz, 1H), 3.45 (d, *J* = 7.4 Hz, 2H), 3.39-

3.30 (m, 2H), 2.59 (d, J = 1.8 Hz, 3H), 2.28 (q, J = 7.3 Hz, 2H). ^{13}C NMR (101 MHz, CDCl3): δ = 161.0 (C), 142.0 (C), 138.4 (CH), 136.1 (C), 132.8 (C), 130.0 (CH), 129.36 (C), 129.2 (C), 127.1 (CH), 126.5 (CH), 125.6 (C), 123.4 (C), 122.5 (CH), 121.6 (CH), 115.1 (CH_2), 36.1 (CH_3), 35.6 (CH_2), 28.5 (CH_2), 21.8 (CH_3). HRMS (EI) m/z: [M^+] calc'd for $C_{19}H_{19}N$ 261.1517, found 261.1526.

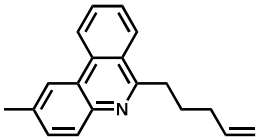

2-Methyl-6-(pent-4-en-1-yl)phenanthridine (2.45)

Synthesized according to GP1. Purification by silica gel chromatography with a gradient of 0 – 10% EtOAc in hexanes gave the product as 17.5 mg of yellow oil (33%). IR (neat NaCl) 3075, 2923, 2856, 1591, 1501, 911 cm^{-1}. ^{1}H NMR (400 MHz, CDCl3): δ = 8.68 – 8.55 (m, 1H), 8.30 (t, J = 1.4 Hz, 1H), 8.20 (dt, J = 8.1, 1.0 Hz, 1H), 7.99 (d, J = 8.3 Hz, 1H), 7.79 (ddd, J = 8.3, 7.0, 1.3 Hz, 1H), 7.65 (ddd, J = 8.2, 7.0, 1.2 Hz, 1H), 7.52 (dd, J = 8.4, 1.9 Hz, 1H), 5.91 (ddt, J = 16.9, 10.1, 6.7 Hz, 1H), 5.07 (dq, J = 17.1, 1.7 Hz, 1H), 5.00 (ddt, J = 10.2, 2.2, 1.2 Hz, 1H), 3.41 – 3.30 (m, 2H), 2.60 (s, 3H), 2.33 – 2.20 (m, 3H), 2.02 (tt, J = 8.4, 6.4 Hz, 2H); ^{13}C NMR (101 MHz, $CDCl_3$): δ = 160.9 (C), 141.9 (C), 138.3 (CH), 135.9 (C), 132.6 (C), 130.1 (CH), 129.9 (C), 129.2 (C), 127.0 (CH), 126.1 (CH), 125.2 (C), 123.3 (C), 122.3 (CH), 121.4 (CH), 114.9 (CH_2), 35.5 (CH_2), 33.8 (CH_2), 28.5 (CH_2), 21.8 (CH_3) ppm. HRMS (EI) m/z: [M^+] calc'd for $C_{19}H_{19}N$ 261.1517, found 261.1521.

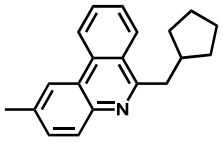

6-(Cyclopentylmethyl)-2-methylphenanthridine (2.78)

Synthesized according to GP1. Purification by silica gel chromatography with a gradient of 0 – 10% EtOAc in hexanes gave the product as 28.6 mg of yellow oil (52%), characterized according to NMR comparison.[19] ^{1}H NMR (400 MHz, CDCl3): δ = 8.64-8.57 (m, 1H), 8.33-8.21 (m, 2H), 8.00 (d, *J* = 8.3 Hz, 1H), 7.78 (ddd, *J* = 8.3, 7.0, 1.3 Hz, 1H), 7.64 (ddd, *J* = 8.2, 7.0, 1.2 Hz, 1H), 7.51 (ddd, *J* = 8.2, 1.9, 0.6 Hz, 1H), 3.35 (d, *J* = 7.4 Hz, 2H), 2.59 (s, 3H), 2.51 (tt, *J* = 8.6, 7.2 Hz, 1H), 1.81-1.53 (m, 3H), 1.59-1.20 (m, 4H), 0.91-0.78 (m, 1H) ppm; ^{13}C NMR (400 MHz, $CDCl_3$): δ = 160.9 (C), 142.1 (C), 135.9 (C), 132.7 (C), 130.2 (CH), 130.0 (CH), 129.4 (CH), 126.9 (CH), 126.5 (CH), 125.6 (C), 123.4 (C), 122.4 (CH), 121.5 (CH), 41.8 (CH_2), 40.4 (CH), 32.7 (CH_2), 25.0 (CH_2), 21.9 (CH_3).

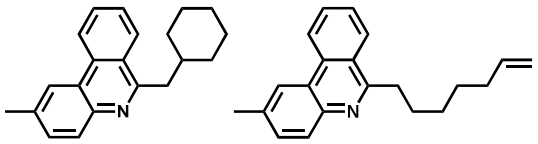

6-(Cyclohexylmethyl)-2-methylphenanthridine (2.79) and 2-methyl-6-(hept-6-en-1-yl)phenanthridine (2.80)

Synthesized according to GP1. Purification by silica gel chromatography with a gradient of 0 – 10% EtOAc in hexanes gave the product as 30.7 mg of yellow oil (53%, 48:52 mix of **2.79** and **2.80**). IR (neat NaCl) 2924, 2852, 1584, 1498 cm^{-1}. For **2.79**: ^{1}H NMR (400 MHz, $CDCl_3$): δ = 8.61 (d, *J* = 8.3 Hz, 1H), 8.30 (d, *J* = 1.7 Hz, 1H), 8.21 (ddd,

J = 7.8, 6.1, 1.2 Hz, 1H), 8.01 (t, *J* = 8.2 Hz, 1H), 7.79 (ddt, *J* = 8.2, 6.9, 1.1 Hz, 1H), 7.65 (ddd, *J* = 8.2, 7.0, 1.2 Hz, 1H), 7.52 (dd, *J* = 8.3, 1.9 Hz, 1H), 3.22 (d, *J* = 7.2 Hz, 2H), 2.59 (s, 3H), 2.07 (tdd, *J* = 6.8, 5.4, 1.4 Hz, 1H), 1.97-1.85 (m, 2H), 1.72 (m, 2H), 1.59-1.43 (m, 2H), 1.22-1.11 (m, 4H). ^{13}C NMR (101 MHz, $CDCl_3$): δ = 160.5 (C), 136.1 (2 X C), 132.8 (C), 130.3 (CH), 130.1 (CH), 129.3 (CH), 127.1 (CH), 126.6 (CH), 125.8 (C), 123.5 (C), 122.5 (CH), 121.6 (CH), 43.6 (CH_2), 38.8 (CH), 33.7 (2 X CH_2), 29.5 (3 X CH_2), 21.9 (CH_3). For **2.80**: ^{1}H NMR (400 MHz, $CDCl_3$): δ = 8.61 (d, *J* = 8.3 Hz, 1H), 8.30 (d, *J* = 1.7 Hz, 1H), 8.21 (ddd, *J* = 7.8, 6.1, 1.2 Hz, 1H), 8.01 (t, *J* = 8.2 Hz, 1H), 7.79 (ddt, *J* = 8.2, 6.9, 1.1 Hz, 1H), 7.65 (ddd, *J* = 8.2, 7.0, 1.2 Hz, 1H), 7.52 (dd, *J* = 8.3, 1.9 Hz, 1H), 5.81 (ddt, *J* = 16.9, 10.2, 6.7 Hz, 1H), 5.04-4.88 (m, 2H), 3.38-3.29 (m, 2H), 2.59 (s, 3H), 2.07 (tdd, *J* = 6.8, 5.4, 1.4 Hz, 2H), 1.70-1.58 (m, 2H), 1.22-1.11 (m, 4H). ^{13}C NMR (101 MHz, $CDCl_3$) δ = 161.3 (C), 139.1 (CH), 136.1 (2 X C), 132.7 (C), 130.1 (CH), 130.1 (CH), 129.3 (CH), 127.0 (CH), 126.3 (CH), 125.3 (C), 123.4 (C), 122.4 (CH), 121.5 (CH), 114.3 (CH_2), 36.3 (CH_2), 33.7 (CH_2), 28.8 (CH_2), 26.5 (CH_2), 26.4 (CH_2), 21.9 (CH_3). HRMS (EI) m/z: [M^+] calc'd for $C_{21}H_{23}N$ 289.1830, found 289.1819.

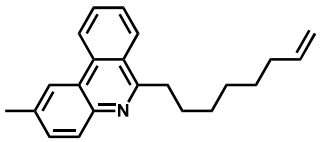

2-Methyl-6-(oct-7-en-1-yl)phenanthridine (2.81)

Synthesized according to GP1. Purification by silica gel chromatography with a gradient of 0 – 10% EtOAc in hexanes gave the product as 38.8 mg of yellow oil (64%). IR (neat NaCl) 3072, 2926, 2855, 1584, 1498 cm^{-1}. ^{1}H NMR (400 MHz, $CDCl_3$): δ = 8.60 (dd, *J* = 8.3, 1.1 Hz, 1H), 8.32-8.17 (m, 2H), 8.00 (d, *J* = 8.3 Hz, 1H), 7.78 (ddd, *J* = 8.3,

7.0, 1.3 Hz, 1H), 7.65 (ddd, *J* = 8.2, 6.9, 1.2 Hz, 1H), 7.51 (dd, *J* = 8.3, 1.9 Hz, 1H), 5.80 (ddt, *J* = 16.9, 10.2, 6.7 Hz, 1H), 4.98 (dd, *J* = 17.1, 1.8 Hz, 1H), 4.91 (ddt, *J* = 10.2, 2.4, 1.3 Hz, 1H), 3.43-3.29 (m, 2H), 2.59 (s, 3H), 2.03 (dtt, *J* = 7.0, 3.3, 1.8 Hz, 2H), 1.96-1.84 (m, 2H), 1.58-1.43 (m, 2H), 1.40 (p, *J* = 3.7 Hz, 4H) ppm; ^{13}C NMR (101 MHz, $CDCl_3$): δ = 161.4 (C), 142.0 (C), 139.1 (CH), 136.1 (C), 132.8 (C), 130.3 (CH), 130.1 (CH), 129.3 (CH), 127.1 (CH), 126.3 (CH), 125.3 (CH), 123.5 (C), 122.5 (C), 121.6 (CH), 114.2 (CH_2), 36.4 (CH_2), 33.8 (CH_2), 29.8 (CH_2), 29.6 (CH_2), 29.1 (CH_2), 28.9 (CH_2), 21.9 (CH_3) ppm; HRMS (EI) *m/z*: [M^+] calc'd for $C_{22}H_{25}N$ 303.1987, found 303.1974.

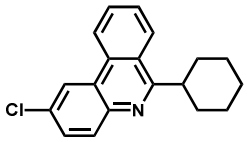

2-Chloro-6-cyclohexylphenanthridine (2.25)

Synthesized according to GP1. Purification by silica gel chromatography with a gradient of 0 – 10% EtOAc in hexanes gave the product as 37.3 mg of yellow oil (63%), characterized according to NMR comparison.[30] ^{1}H NMR (400 MHz, $CDCl_3$): δ = 8.51 (dt, J = 8.1, 0.7 Hz, 1H), 8.44 (d, J = 2.2 Hz, 1H), 8.28 (dt, J = 8.3, 0.6 Hz, 1H), 8.03 (d, J = 8.7 Hz, 1H), 7.78 (ddd, J = 8.3, 7.0, 1.3 Hz, 1H), 7.68 (ddd, J = 8.2, 7.0, 1.3 Hz, 1H), 7.60 (dd, J = 8.7, 2.3 Hz, 1H), 3.57 (tt, J = 11.4, 3.3 Hz, 1H), 2.11-1.78 (m, 8H), 1.55 (qt, J = 11.7, 3.0 Hz, 2H), 1.41 (qt, J = 12.9, 3.4 Hz, 1H) ppm; ^{13}C NMR (101 MHz, $CDCl_3$): δ = 165.6 (C), 142.3 (C), 132.0 (C), 131.9 (C), 131.4 (CH), 130.2 (CH), 128.8 (CH), 127.7 (CH), 125.7 (CH), 124.8 (C), 124.4 (C), 122.6 (CH), 121.5 (CH), 42.0 (CH), 32.3 (2 X CH_2), 26.8 (2 X CH_2), 26.3 (CH_2) ppm.

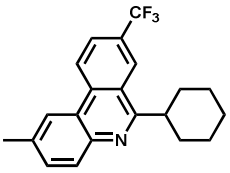

6-Cyclohexyl-2-methyl-8-(trifluoromethyl)phenanthridine (2.26)

Synthesized according to GP1. Purification by silica gel chromatography with a gradient of 0 – 10% EtOAc in hexanes gave the product as 46.1 mg of yellow oil (67%), characterized according to NMR comparison.[31] ^{1}H NMR (400 MHz, $CDCl_3$): δ = 8.69 (d, *J* = 8.7 Hz, 1H), 8.51 (s, 1H), 8.28 (t, *J* = 1.2 Hz, 1H), 8.03 (d, *J* = 8.3 Hz, 1H), 7.95 (dd, *J* = 8.7, 1.8 Hz, 1H), 7.57 (dd, *J* = 8.3, 1.8 Hz, 1H), 3.56 (tt, *J* = 11.2, 3.3 Hz, 1H), 2.60 (s, 3H), 2.08-1.79 (m, 7H), 1.58 (qt, *J* = 12.8, 3.3 Hz, 2H), 1.43 (ddt, *J* = 16.4, 12.8, 6.2 Hz, 1H) ppm; ^{13}C NMR (101 MHz, $CDCl_3$): δ = 164.1 (C), 142.9 (C), 136.6 (2 X C), 135.0 (2 X C), 131.3 (CH), 129.9 (CH), 128.7 (q, *J* = 32.6 Hz, C), 125.5 (q, *J* = 3.7 Hz, CH), 123.6 (CH), 123.1 (q, *J* = 187.9 Hz, CF_3) 122.9 (q, *J* = 4.1 Hz, CH), 121.8 (CH), 41.9 (CH), 32.4 (2 X CH_2), 26.8 (2 X CH_2), 26.3 (CH_2), 21.9 (CH_3) ppm.

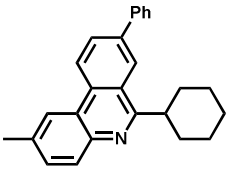

6-Cyclohexyl-2-methyl-8-phenylphenanthridine (2.27)

Synthesized according to GP1. Purification by silica gel chromatography with a gradient of 0 – 10% EtOAc in hexanes gave the product as 40.1 mg of yellow oil (57%), characterized according to NMR comparison.[30] ^{1}H NMR (400 MHz, $CDCl_3$): δ = 8.67 (d, J = 8.6 Hz, 1H), 8.44 (d, J = 1.8 Hz, 1H), 8.31 (t, J = 1.3 Hz, 1H), 8.06-7.97 (m, 2H), 7.78-

7.72 (m, 2H), 7.59-7.48 (m, 3H), 7.44 (tt, J = 7.3, 1.2 Hz, 1H), 3.66 (tt, J = 11.1, 3.4 Hz, 1H), 2.61 (s, 3H), 2.16-2.06 (m, 2H), 2.03-1.88 (m, 4H), 1.90-1.79 (m, 1H), 1.65-1.52 (m, 2H), 1.44 (qt, *J* = 12.9, 3.3 Hz, 1H) ppm; ^{13}C NMR (101 MHz, $CDCl_3$): δ = 164.4 (C), 142.2 (C), 140.9 (C), 139.8 (C), 136.0 (C), 131.9 (C), 130.1 (CH), 129.7 (CH), 129.1 (2 x CH), 129.0 (CH), 127.7 (CH), 127.5 (2 X CH), 125.1 (C), 123.7 (CH), 123.2 (CH), 123.0 (C), 121.5 (CH), 42.0 (CH), 32.4 (2 X CH_2), 26.9 (2 X CH_2), 26.4 (CH_2), 21.9 (CH_3) ppm.

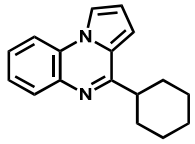

4-Cyclohexylpyrrolo[1,2-a]quinoxaline (2.28)

Synthesized according to GP1. Purification by silica gel chromatography with a gradient of 0 – 10% EtOAc in hexanes gave the product as 32.0 mg of yellow oil (64%), characterized according to NMR comparison.[7g] ^{1}H NMR (400 MHz, $CDCl_3$): δ = 7.92 (dd, J = 7.7, 1.8 Hz, 1H), 7.87 (dd, J = 2.8, 1.3 Hz, 1H), 7.79 (dd, J = 7.8, 1.7 Hz, 1H), 7.41 (ddd, J = 15.1, 7.3, 1.7 Hz, 2H), 6.91 (dd, J = 4.0, 1.3 Hz, 1H), 6.81 (dd, J = 4.0, 2.7 Hz, 1H), 3.11 (tt, J = 11.8, 3.3 Hz, 1H), 2.07-1.73 (m, 7H), 1.55-1.35 (m, 3H) ppm; ^{13}C NMR (101 MHz, $CDCl_3$): δ = 161.1 (C), 136.2 (C), 129.7 (CH), 127.2 (C), 126.7 (CH), 125.6 (C), 124.9 (CH), 113.9 (CH), 113.5 (CH), 113.2 (CH), 105.7 (CH), 43.6 (CH), 31.3 (2 X CH_2), 26.6 (2 X CH_2), 26.1 (CH_2) ppm.

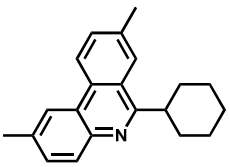

6-Cyclohexyl-2,8-dimethylphenanthridine (2.29)

Synthesized according to GP1. Purification by silica gel chromatography with a gradient of 0 – 10% EtOAc in hexanes gave the product as 37.8 mg of yellow oil (65%), characterized according to NMR comparison.[30] ^{1}H NMR (400 MHz, $CDCl_3$): δ = 8.50 (d, *J* = 8.4 Hz, 1H), 8.26 (dd, *J* = 1.6, 1.0 Hz, 1H), 8.05-8.02 (m, 1H), 8.00 (d, *J* = 8.2 Hz, 1H), 7.59 (dd, *J* = 8.3, 1.7 Hz, 1H), 7.47 (dd, *J* = 8.3, 1.9 Hz, 1H), 3.57 (tt, *J* = 11.2, 3.3 Hz, 1H), 2.59 (d, *J* = 6.7 Hz, 6H), 2.11-2.00 (m, 2H), 2.05-1.85 (m, 4H), 1.90-1.79 (m, 1H), 1.66-1.49 (m, 2H), 1.44 (ddt, *J* = 16.1, 12.7, 6.2 Hz, 1H) ppm; ^{13}C NMR (101 MHz, $CDCl_3$): δ = 164.0 (C), 141.9 (C), 136.7 (C), 135.7 (C), 131.4 (CH), 130.7 (C), 129.6 (CH), 125.0 (CH), 124.9 (C), 123.2 (C), 122.5 (CH), 121.3 (2 X CH), 41.8 (CH), 32.3 (2 X CH_2), 26.9 (2 X CH_2), 26.4 (CH_2), 22.0 (CH_3), 21.9 (CH_3) ppm.

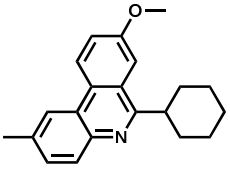

6-Cyclohexyl-8-methoxy-2-methylphenanthridine (2.30)

Synthesized according to GP1. Purification by silica gel chromatography with a gradient of 0 – 10% EtOAc in hexanes gave the product as 48.4 mg of yellow oil (79%) characterized according to NMR comparison.[30] ^{1}H NMR (400 MHz, $CDCl_3$): δ = 8.57-8.50 (m, 1H), 8.24-8.18 (m, 1H), 7.97 (d, *J* = 8.3 Hz, 1H), 7.60 (d, *J* = 2.6 Hz, 1H), 7.48-7.37 (m, 2H), 3.99 (s, 3H), 3.53-3.42 (m, 1H), 2.60-2.55 (m, 3H), 2.10-2.00 (m, 3H), 2.00-1.76 (m, 5H), 1.62-1.33 (m, 2H) ppm; ^{13}C NMR (101 MHz, $CDCl_3$): δ = 163.4 (C), 158.4 (C), 144.7 (C), 141.4 (C), 135.9 (C), 129.6 (CH), 129.1 (CH), 127.1 (C), 124.2 (CH), 123.2

(C), 121.0 (CH), 119.5 (CH), 106.6 (CH), 55.5 (CH_3), 42.1 (CH), 32.2 (2 X CH_2), 26.9 (2 X CH_2), 26.3 (CH_2), 21.9 (CH_3) ppm.

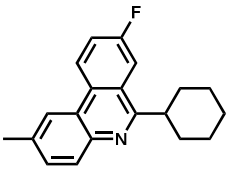

6-Cyclohexyl-8-fluoro-2-methylphenanthridine (2.31)

Synthesized according to GP1. Purification by silica gel chromatography with a gradient of 0 – 10% EtOAc in hexanes gave the product as 47.6 mg of yellow oil (81%), characterized according to NMR comparison.[31] ^{1}H NMR (400 MHz, $CDCl_3$): δ = 8.58 (dd, *J* = 9.1, 5.5 Hz, 1H), 8.21 (t, *J* = 1.3 Hz, 1H), 8.01 (d, *J* = 8.4 Hz, 1H), 7.87 (dd, *J* = 10.4, 2.6 Hz, 1H), 7.55-7.45 (m, 2H), 3.42 (tt, *J* = 11.4, 3.3 Hz, 1H), 2.58 (s, 3H), 2.08-1.85 (m, 6H), 1.83 (dddd, *J* = 10.5, 5.1, 3.2, 1.6 Hz, 1H), 1.58 (dt, *J* = 13.2, 3.6 Hz, 1H), 1.52 (dt, *J* = 11.3, 2.8 Hz, 1H), 1.43 (tt, *J* = 12.8, 3.3 Hz, 1H) ppm; ^{13}C NMR (101 MHz, $CDCl_3$): δ = 164.0 (C), 141.9 (C), 136.7 (C), 135.7 (C), 131.4 (CH), 130.7 (C), 129.6 (CH), 125.0 (CH), 124.9 (C), 123.2 (C), 122.5 (CH), 121.3 (CH), 41.8 (CH), 32.3 (2 X CH_2), 26.9 (2 X CH_2), 26.4 (CH_2), 22.0 (CH), 21.9 (CH_3) ppm.

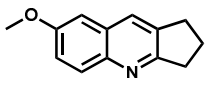

7-Methoxy-2,3-dihydro-1H-cyclopenta[b]quinoline (2.35)

Synthesized according to GP1. Purification by silica gel chromatography with a gradient of 0 – 10% EtOAc in hexanes gave the product as 21.8 mg of yellow oil (55%),

characterized according to NMR comparison.[32] ^{1}H NMR (400 MHz, $CDCl_3$): δ = 7.89 (d, *J* = 9.1 Hz, 1H), 7.78 (s, 1H), 7.29-7.22 (m, 1H), 7.00 (d, *J* = 2.8 Hz, 1H), 3.90 (s, 3H), 3.08 (dt, *J* = 22.3, 7.5 Hz, 4H), 2.18 (p, *J* = 7.5 Hz, 2H) ppm; ^{13}C NMR (101 MHz, $CDCl_3$): δ = 165.3 (C), 157.0 (C), 143.4 (C), 135.8 (C), 129.8 (CH), 129.2 (CH), 128.2 (C), 120.4 (CH), 105.5 (CH), 55.4 (CH_3), 34.2 (CH_2), 30.5 (CH_2), 23.6 (CH_2) ppm.

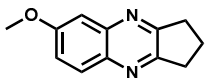

6-Methoxy-2,3-dihydro-1H-cyclopenta[b]quinoxaline (2.36)

Synthesized according to GP1. Purification by silica gel chromatography with a gradient of 0 – 10% EtOAc in hexanes gave the product as 12.0 mg of yellow oil (30%), characterized according to NMR comparison.[5d] ^{1}H NMR (400 MHz, $CDCl_3$): δ = 7.86 (dd, *J* = 8.4, 1.1 Hz, 1H), 7.30 (d, *J* = 8.4 Hz, 2H), 3.92 (s, 3H), 3.15 (td, *J* = 7.7, 1.9 Hz, 4H), 2.27 (p, *J* = 7.6 Hz, 2H) ppm; ^{13}C NMR (101 MHz, $CDCl_3$): δ = 160.5 (C), 159.9 (C), 157.9 (C), 143.0 (C), 137.4 (C), 129.6 (CH), 121.3 (CH), 107.0 (CH), 55.7 (CH_3), 32.4 (CH_2), 32.1 (CH_2), 21.3 (CH_2) ppm.

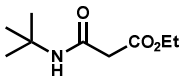

Ethyl 3-(tert-butylamino)-3-oxopropanoate (2.46)

Synthesized according to GP3. Purification by silica gel chromatography with a gradient of 0 – 20% EtOAc in hexanes gave the product as 37.2 mg of yellow oil (99%), characterized according to NMR comparison.[33] ^{1}H NMR (400 MHz, $CDCl_3$): δ = 6.87 (s,

1H), 4.16 (q, *J* = 7.1 Hz, 2H), 3.19 (s, 2H), 2.01 (d, *J* = 0.6 Hz, 1H), 1.33 (d, *J* = 0.6 Hz, 9H), 1.26 (td, *J* = 7.2, 0.6 Hz, 3H) ppm; ^{13}C NMR (101 MHz, $CDCl_3$): δ = 169.8 (C), 163.8 (C), 61.3 (CH_2), 51.2 (CH_2), 42.1 (C), 28.5 (3 X CH_3), 13.9 (CH_3) ppm.

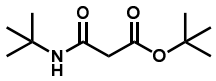

tert-Butyl 3-(tert-butylamino)-3-oxopropanoate (2.47)

Synthesized according to GP3. Purification by silica gel chromatography with a gradient of 0 – 20% EtOAc in hexanes gave the product as 17.7 mg of yellow oil (41%), characterized according to NMR comparison.[34] ^{1}H NMR (400 MHz, $CDCl_3$): δ = 6.87 (s, 1H), 3.10 (s, 2H), 1.44 (s, 9H), 1.33 (s, 9H) ppm; ^{13}C NMR (101 MHz, $CDCl_3$): δ = 169.0 (C), 164.4 (C), 82.11 (C), 51.1 (C), 43.4 (CH_2), 28.6 (3 X CH_3), 27.9 (3 X CH_3) ppm.

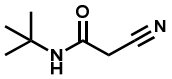

N-(tert-butyl)-2-cyanoacetamide (2.48)

Synthesized according to GP3. Purification by silica gel chromatography with a gradient of 0 – 20% EtOAc in hexanes gave the product as 6.2 mg of yellow oil (22%), characterized according to NMR comparison.[35] ^{1}H NMR (400 MHz, $CDCl_3$): δ = 5.83 (s, 1H), 3.27 (s, 2H), 1.36 (s, 9H) ppm; ^{13}C NMR (101 MHz, $CDCl_3$): δ = 159.7 (C), 115.1 (C), 52.6 (C), 28.5 (3 X CH_3), 26.7 (CH_2) ppm.

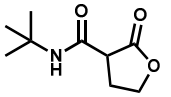

N-(tert-butyl)-2-oxotetrahydrofuran-3-carboxamide (2.49)

Synthesized according to GP3. Purification by silica gel chromatography with a gradient of 0 – 20% EtOAc in hexanes gave the product as 35.6 mg of yellow oil (96%), characterized according to NMR comparison.[36] ^{1}H NMR (400 MHz, $CDCl_3$): δ = 6.74 (s, 1H), 4.40 (td, *J* = 8.8, 4.6 Hz, 1H), 4.28 (dt, *J* = 9.0, 7.8 Hz, 1H), 3.32 (dd, *J* = 9.8, 8.6 Hz, 1H), 2.72 (dtd, *J* = 13.3, 8.6, 8.0 Hz, 1H), 2.45 (dddd, *J* = 13.3, 9.8, 7.7, 4.6 Hz, 1H), 1.35 (s, 9H) ppm; ^{13}C NMR (101 MHz, $CDCl_3$): δ = 175.9 (C), 163.7 (C), 67.4 (CH_2), 51.6 (C), 45.5 (CH), 28.5 (3 X CH_3), 24.4 (CH_2). ppm.

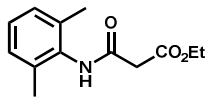

Ethyl 3-((2,6-dimethylphenyl)amino)-3-oxopropanoate (2.50)

Synthesized according to GP3. Purification by silica gel chromatography with a gradient of 0 – 10% EtOAc in hexanes gave the product as 26.9 mg of clear oil (57%). IR (neat NaCl) 3072, 2926, 2855 1584 1498 cm^{-1}. ^{1}H NMR (400 MHz, $CDCl_3$): δ = 8.52 (s, 1H), 7.19 – 6.99 (m, 3H), 4.25 (q, *J* = 7.1 Hz, 2H), 3.50 (s, 2H), 2.22 (s, 6H), 1.32 (t, *J* = 7.1 Hz, 3H). ^{13}C NMR (101 MHz, $CDCl_3$): δ = 169.8 (C), 163.2 (C), 135.1 (2 X C), 133.4 (C), 128.1 (2 X CH), 127.3 (CH), 61.7 (CH_2), 41.0 (CH_2), 18.3 (2 X CH_3), 14.0 (CH_3). HRMS (ESI) *m/z*: [M^+ Na^+] calc'd for $C_{13}H_{17}NO_3Na$ 258.1106, found 258.1115.

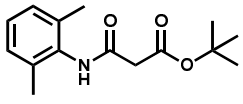

tert-Butyl 3-((2,6-dimethylphenyl)amino)-3-oxopropanoate (2.51)

Synthesized according to GP3. Purification by silica gel chromatography on with a gradient of 0 – 25% EtOAc in hexanes (1% Et_3N) gave the product as 33.5 mg of clear oil (64%). IR (neat NaCl) 3241, 2977, 2931, 1733, 1651, 1143 cm^{-1}. ^1H NMR (400 MHz, $CDCl_3$): δ = 8.52 (s, 1H), 7.13 – 7.00 (m, 3H), 3.41 (s, 2H), 2.22 (s, 6H), 1.50 (s, 9H). ^{13}C NMR (101 MHz, $CDCl_3$): δ = 169.1 (C), 163.6 (C), 135.1 (C), 133.6 (C), 128.1 (2 X CH), 127.2 (CH), 82.8 (C), 42.4 (CH_2), 27.9 (3 X CH_3), 18.3 (2 X CH_3). HRMS (ESI) *m/z*: [M^+] calc'd for $C_{15}H_{21}NO_3$ 263.1521, found 263.1506.

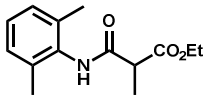

Ethyl (S)-3-((2,6-dimethylphenyl)amino)-2-methyl-3-oxopropanoate (2.52)

Synthesized according to GP3. Purification by silica gel chromatography with a gradient of 0 – 25% EtOAc in hexanes (1% Et_3N) gave the product as 29.1 mg of clear oil (58%). IR (neat NaCl) 3237, 2983, 1737, 1646, 1203, 1179 cm^{-1}. ^1H NMR (400 MHz, $CDCl_3$): δ = 7.91 (s, 1H), 7.06 (q, *J* = 5.3 Hz, 3H), 4.25 (q, *J* = 7.1 Hz, 2H), 3.48 (q, *J* = 7.3 Hz, 1H), 2.20 (s, 6H), 1.58 (d, *J* = 7.3 Hz, 3H), 1.31 (t, *J* = 7.1 Hz, 3H). ^{13}C NMR (101 MHz, $CDCl_3$): δ = 172.8 (C), 167.2 (C), 133.3 (2 X CH), 127.2 (CH), 61.7 (CH_2), 47.1 (CH), 18.2 (2 X CH_3), 15.8 (CH_3), 14.0 (CH_3) ppm. HRMS (ESI) *m/z*: [M^+] calc'd for $C_{14}H_{19}NO_3$ 249.1365, found 249.1345.

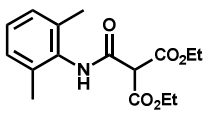

Diethyl 2-((2,6-dimethylphenyl)carbamoyl)malonate (2.53)

Synthesized according to GP3. Purification by silica gel chromatography on with a gradient of 0 – 25% EtOAc in hexanes (1% Et_3N) gave the product as 35.8 mg of clear oil (58%). IR (neat NaCl) 3231, 2980, 2923, 2209, 1721, 1620, 1239 cm^{-1}. ^1H NMR (400 MHz, $CDCl_3$): δ = 9.70 (s, 1H), 7.18 – 7.10 (m, 3H), 4.30 (q, *J* = 7.2 Hz, 4H), 2.26 (s, 6H), 1.29 (td, *J* = 7.1, 1.1 Hz, 9H). ^{13}C NMR (101 MHz, $CDCl_3$): δ = 165.5 (C), 162.2 (2 X C), 161.5 (C), 154.2 (C), 136.8 (C), 134.6 (C), 129.1 (CH), 128.3 (2 X CH), 91.1 (CH), 62.4 (2 X CH_2), 18.2 (CH_3), 17.9 (CH_3), 13.7 (2 X CH_3). HRMS (ESI) *m/z*: [M^+ –CO_2Et] calc'd for $C_{13}H_{16}NO_3$ 234.1130, found 234.1099.

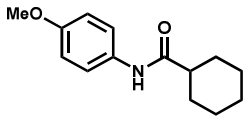

N-(4-methoxyphenyl)cyclohexanecarboxamide (2.54).

Synthesized according to GP3. Purification by silica gel chromatography with a gradient of 0 – 20% EtOAc in hexanes gave the product as 14.5 mg of yellow oil (31%), characterized according to NMR comparison.[37] ^1H NMR (400 MHz, $CDCl_3$): δ = 7.44 – 7.35 (m, 2H), 7.11 – 7.06 (m, 1H), 6.87 – 6.78 (m, 2H), 3.76 (s, 3H), 2.18 (tt, *J* = 11.7, 3.5 Hz, 1H), 1.97 – 1.88 (m, 2H), 1.87 – 1.77 (m, 2H), 1.51 (qd, *J* = 12.1, 3.2 Hz, 2H), 1.36 – 1.15 (m, 4H) ppm; ^{13}C NMR (101 MHz, $CDCl_3$): δ = 174.0 (C), 156.1 (C), 131.1 (C), 121.5 (2 X CH), 114.0 (2 X CH), 55.4 (CH_3), 46.3 (CH), 29.6 (2 X CH_2), 25.6 (2 X CH_2) ppm.

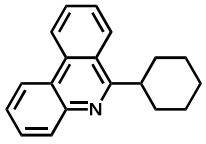

6-cyclohexylphenanthridine (2.10)

Synthesized according to GP2. Purification by silica gel chromatography with a gradient of 0 – 10% EtOAc in hexanes gave the product as 17.3 mg of yellow oil (33%), characterized according to NMR comparison.[38] ^{1}H NMR (400 MHz, $CDCl_3$): δ = 8.63 (dd, *J* = 8.3, 1.2 Hz, 1H), 8.52 (dd, *J* = 8.2, 1.4 Hz, 1H), 8.30 (dd, *J* = 8.4, 1.2 Hz, 1H), 8.14 (dd, *J* = 8.1, 1.3 Hz, 1H), 7.79 (ddd, *J* = 8.3, 7.0, 1.3 Hz, 1H), 7.68 (dddd, *J* = 10.0, 8.3, 7.0, 1.3 Hz, 2H), 7.59 (ddd, *J* = 8.3, 7.0, 1.4 Hz, 1H), 3.61 (tt, *J* = 11.2, 3.3 Hz, 1H), 2.14 – 2.03 (m, 2H), 1.99 (d, *J* = 3.3 Hz, 1H), 2.00 – 1.87 (m, 3H), 1.84 (dddd, *J* = 12.6, 5.2, 3.1, 1.5 Hz, 1H), 1.57 (dtd, *J* = 16.9, 13.5, 12.8, 4.2 Hz, 2H), 1.43 (qt, *J* = 12.9, 3.3 Hz, 1H) ppm; ^{13}C NMR (101 MHz, $CDCl_3$): δ = 165.1 (C), 143.8 (C), 132.9 (C), 129.8 (CH), 129.8 (CH), 128.3 (CH), 126.9 (CH), 126.0(CH), 125.5 (CH), 124.6 (C), 123.2 (C), 122.5 (CH), 121.7 (CH), 41.9 (CH), 32.2 (2 X CH_2), 26.8 (2 X CH_2), 26.2 (CH_2) ppm.

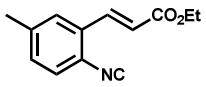

(E)-3-(2-isocyano-5-methylphenyl)acrylate (2.55a)

Synthesized according to GP4. Purification by silica gel chromatography with a gradient of 0 – 10% EtOAc in hexanes gave the product as an of off-white solid (40%) over two steps. Characterized according to NMR comparison.[39] ^{1}H NMR (400 MHz, $CDCl_3$): δ = 7.92 (dd, *J* = 16.1, 0.5 Hz, 1H), 7.30 (d, *J* = 8.1 Hz, 1H), 7.20 – 7.14 (m, 1H), 6.50 (d, *J* = 16.1 Hz, 1H), 4.27 (q, *J* = 7.1 Hz, 2H), 2.38 (d, *J* = 0.8 Hz, 3H), 1.33 (t, *J* = 7.1 Hz, 3H); ^{13}C NMR (101 MHz, $CDCl_3$): δ = 166.1 (C), 140.0 (C), 137.8 (CH), 131.4 (CH), 130.6 (C), 127.5 (CH), 127.4 (CH), 122.2 (CH), 60.9 (CH_2), 21.4 (CH_2), 14.3 (CH_2).

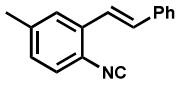

(E)-1-isocyano-4-methyl-2-styrylbenzene (2.55b)

Synthesized according to GP4. Purification by silica gel chromatography with a gradient of 0 – 10% EtOAc in hexanes gave the product as an of off-white solid (50%) over two steps. ^{1}H NMR (400 MHz, $CDCl_3$): δ = 7.59 – 7.53 (m, 2H), 7.52 (t, *J* = 1.2 Hz, 1H), 7.41 – 7.34 (m, 3H), 7.33 – 7.25 (m, 2H), 7.17 (d, *J* = 16.3 Hz, 1H), 7.08 – 7.03 (m, 1H), 2.39 (s, 3H); ^{13}C NMR (101 MHz, $CDCl_3$): δ = 139.6 (C), 136.5 (C), 133.4 (C), 132.3 (CH), 128.9 (CH), 128.8 (2 X CH), 128.5 (CH), 127.1 (CH), 127.0 (2 X CH), 125.9 (CH), 122.4 (CH), 21.5 (CH_3).

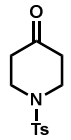

1-tosylpiperidin-4-one (2.60)

Synthesized according to TP1. Recrystallization of product in DCM gave pure product as an of off-white solid (91%). Characterized according to NMR comparison.[40] ^{1}H NMR (400 MHz, $CDCl_3$): δ = 7.70 – 7.59 (m, 2H), 7.44 – 7.26 (m, 2H), 3.36 (t, *J* = 6.3 Hz, 4H), 2.51 (t, *J* = 6.3 Hz, 4H), 2.42 (s, 3H); ^{13}C NMR (101 MHz, $CDCl_3$): δ = 205.6 (C), 144.1 (C), 133.4 (C), 129.9 (2 X CH), 127.6 (2 X CH), 45.9 (2 X CH_2), 40.7 (2 X CH_2), 21.6 (CH_3).

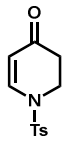

1-tosyl-2,3-dihydropyridin-4(1H)-one (2.61)

Synthesized according to TP2. Purification by silica gel chromatography with a gradient of 0 – 20% EtOAc in hexanes gave the product as an of off-white solid (55%). Characterized according to NMR comparison.[41] ^{1}H NMR (400 MHz, $CDCl_3$): δ = 7.73 – 7.62 (m, 3H), 7.39 – 7.32 (m, 2H), 5.35 (d, *J* = 8.3 Hz, 1H), 3.76 – 3.66 (m, 2H), 2.54 – 2.47 (m, 2H), 2.44 (s, 3H); ^{13}C NMR (101 MHz, $CDCl_3$): δ = 191.7 (C), 145.4 (C), 143.5 (CH), 133.8 (C), 130.4 (2 X CH), 127.3 (2 X CH), 108.2 (CH), 43.9 (CH_2), 35.5 (CH_2), 21.7 (CH_3).

2.8 References

1. (a) Ciamician, G. The Photochemistry of the Future. *Science* **1912**, *36*, 385. (b) Balzani, V.; Credi, A.; Venturi, M., Photochemical Conversion of Solar Energy. *ChemSusChem* **2008**, *1*, 26-58.
2. (a) Prier, C. K.; Rankic, D. A.; MacMillan, D. W. C., Visible Light Photoredox Catalysis with Transition Metal Complexes: Applications in Organic Synthesis. *Chem. Rev.* **2013**, *113*, 5322-5363. (b) Fagnoni, M.; Dondi, D.; Ravelli, D.; Albini, A., Photocatalysis for the Formation of the C–C Bond. *Chem. Rev.* **2007**, *107*, 2725-2756. (c) Narayanam, J. M. R.; Stephenson, C. R. J., Visible light photoredox catalysis: applications in organic synthesis. *Chem. Soc. Rev.* **2011**, *40*, 102-113. (d) Schultz, D. M.; Yoon, T. P., Solar Synthesis: Prospects in Visible Light Photocatalysis. *Science* **2014**, *343,* 12391761-12391768. (e) Romero, N. A.; Nicewicz, D. A., Organic Photoredox Catalysis. *Chem. Rev.* **2016**, *116*, 10075-10166.
3. Barton, D. H. R.; Beaton, J. M.; Geller, L. E.; Pechet, M. M., A New Photochemical Reaction1. *J. Am. Chem. Soc.* **1961**, *83*, 4076-4083.
4. (a) Shono, T.; Kimura, M.; Ito, Y.; Nishida, K.; Oda, R., Studies of Isocyanide. II. The Reaction of Isocyanide with Some Radical Sources. *Bull. Chem. Soc. Jpn.* **1964**, *37,* 635-637. (b) Ito, Y.; Inubushi, Y.; Saegusa, T., 1-(N-alkyliminoformyl)azole — a reagent of trans-formimidoylation. *Tetrahedron Lett.* **1974,** *15,* 1283-1286.
5. (a) Curran, D. P.; Liu, H., 4 + 1 Radical annulations with isonitriles: a simple route to cyclopenta-fused quinolines. *J. Am. Chem. Soc.* **1991**, *113,* 2127-2132. (b) Curran, D. P.; Liu, H., New 4 + 1 radical annulations. A formal total synthesis of (.+-.)-camptothecin. *J. Am. Chem. Soc.* **1992**, *114*, 5863-5864. (c) Ryu, I.; Sonoda, N.;

Curran, D. P., Tandem Radical Reactions of Carbon Monoxide, Isonitriles, and Other Reagent Equivalents of the Geminal Radical Acceptor/Radical Precursor Synthon. *Chem. Rev.* **1996**, *96,* 177-194. (d) Camaggi, C. M.; Leardini, R.; Nanni, D.; Zanardi, G., Radical annulations with nitriles: Novel cascade reactions of cyano-substituted alkyl and sulfanyl radicals with isonitriles. *Tetrahedron* **1998**, *54,* 5587-5598.

6. For recent reviews, see: (a) Zhang, B.; Studer, A., Recent advances in the synthesis of nitrogen heterocycles via radical cascade reactions using isonitriles as radical acceptors. *Chem. Soc. Rev.* **2015**, *44,* 3505-3521 and references therein. (b) Lei, J.; Huang, J.; Zhu, Q., Recent progress in imidoyl radical-involved reactions. *Org. Biomol. Chem.* **2016**, *14,* 2593-2602. (c) Giustiniano, M.; Basso, A.; Mercalli, V.; Massarotti, A.; Novellino, E.; Tron, G. C.; Zhu, J., To each his own: isonitriles for all flavors. Functionalized isocyanides as valuable tools in organic synthesis. *Chem. Soc. Rev.* **2017**, *46*, 1295-1357.

7. (a) Sun, X.; Yu, S., Visible-Light-Promoted and Photoredox-Catalyzed Radical Addition to Triple Bonds. *Synlett* **2016,** *27*, 2659-2675. (b) Jiang, H.; Cheng, Y.; Wang, R.; Zheng, M.; Zhang, Y.; Yu, S., Synthesis of 6-Alkylated Phenanthridine Derivatives Using Photoredox Neutral Somophilic Isocyanide Insertion. *Angew. Chem. Int. Ed.* **2013,** *52,* 13289-13292. (c) Xiao, T.; Li, L.; Lin, G.; Wang, Q.; Zhang, P.; Mao, Z.-w.; Zhou, L., Synthesis of 6-substituted phenanthridines by metal-free, visible-light induced aerobic oxidative cyclization of 2-isocyanobiphenyls with hydrazines. *Green Chemistry* **2014,** *16*, 2418-2421. (d) Zhang, Z.; Tang, X.; Dolbier, W. R., Photoredox-Catalyzed Tandem Insertion/Cyclization Reactions of Difluoromethyl and 1,1-Difluoroalkyl Radicals with Biphenyl Isocyanides. *Org. Lett.* **2015**, *17*, 4401-4403. (e)

Jin, Y.; Yang, H.; Fu, H., Thiophenol-Catalyzed Visible-Light Photoredox Decarboxylative Couplings of N-(Acetoxy)phthalimides. *Org. Lett.* **2016,** *18*, 6400-6403. (f) Zhou, H.; Deng, X. Z.; Zhang, A. H.; Tan, R. X., Visible-light-promoted synthesis of phenanthridines via an intermolecular isocyanide insertion reaction. *Org. Biomol. Chem.* **2016,** *14*, 10407-10414. (g) He, Z.; Bae, M.; Wu, J.; Jamison, T. F., Synthesis of Highly Functionalized Polycyclic Quinoxaline Derivatives Using Visible-Light Photoredox Catalysis. *Angew. Chem. Int. Ed.* **2014,** *53*, 14451-14455. (h) Yuan, Y.-C.; Liu, H.-L.; Hu, X.-B.; Wei, Y.; Shi, M., Visible-Light-Induced Trifluoromethylation of Isonitrile-Substituted Methylenecyclopropanes: Facile Access to 6-(Trifluoromethyl)-7,8-Dihydrobenzo[k]phenanthridine Derivatives. *Chem. Eur. J.* **2016**, *22*, 13059-13063. (i) Zhou, X.; Wang, P.; Zhang, L.; Chen, P.; Ma, M.; Song, N.; Ren, S.; Li, M., Transition-Metal-Free Synthesis of C-Glycosylated Phenanthridines via K_2S2O_8-Mediated Oxidative Radical Decarboxylation of Uronic Acids. *J. Org. Chem.***2018,** *83*, 588-603.

8. (a) Kaldas, S. J.; Cannillo, A.; McCallum, T.; Barriault, L., Indole Functionalization via Photoredox Gold Catalysis. *Org. Lett.* **2015**, *17*, 2864-2866. (b) McCallum, T.; Barriault, L., Direct alkylation of heteroarenes with unactivated bromoalkanes using photoredox gold catalysis. *Chem. Sci.* **2016,** *7*, 4754-4758. (c) Tran, H.; McCallum, T.; Morin, M.; Barriault, L., Homocoupling of Iodoarenes and Bromoalkanes Using Photoredox Gold Catalysis: A Light Enabled Au(III) Reductive Elimination. *Org. Lett.* **2016,** *18,* 4308-4311. (d) McCallum, T.; Rohe, S.; Barriault, L., Thieme Chemistry Journals Awardees – Where Are They Now? What's Golden: Recent Advances in

Organic Transformations Using Photoredox Gold Catalysis. *Synlett* **2017,** *28*, 289-305 and references cited therein.

9. (a) Rondinini, S.; Mussini, P. R.; Muttini, P.; Sello, G., Silver as a powerful electrocatalyst for organic halide reduction: the critical role of molecular structure. *Electrochim. Acta* **2001**, *46,* 3245-3258. (b) Roth, H. G.; Romero, N. A.; Nicewicz, D. A., Experimental and Calculated Electrochemical Potentials of Common Organic Molecules for Applications to Single-Electron Redox Chemistry. *Synlett* **2016**, *27,* 714-723.
10. Ma, C.; Chan, C. T.-L.; To, W.-P.; Kwok, W.-M.; Che, C.-M., Deciphering Photoluminescence Dynamics and Reactivity of the Luminescent Metal–Metal-Bonded Excited State of a Binuclear Gold(I) Phosphine Complex Containing Open Coordination Sites. *Chem. Eur. J.* **2015,** *21*, 13888-13893.
11. McTiernan, C. D.; Morin, M.; McCallum, T.; Scaiano, J. C.; Barriault, L., Polynuclear gold(I) complexes in photoredox catalysis: understanding their reactivity through characterization and kinetic analysis. *Cat. Sci. Tech.* **2016**, *6*, 201-207.
12. Zidan, M.; McCallum, T.; Thai-Savard, L.; Barriault, L., Photoredox meets gold Lewis acid catalysis in the alkylative semipinacol rearrangement: a photocatalyst with a dark side. *Org. Chem. Front.* **2017,** *4,* 2092-2096.
13. a) Griller, D.; Ingold, K. U. Free-Radical Clocks. *Acc. Chem. Res.* **1980**, *13*, 317-323; b) Giese, B.; Kopping, B.; Göbel, T.; Dickhaut, J.; Thoma, G.; Kulicke, K.; Trach, F. (**2004**). Radical Cyclization Reactions. In Organic Reactions, (Ed.); c) Beckwith, A. L. J.; Scheisser, C. H. *Tetrahedron* **1985**, *41*, 3925-3941.

14. This cannot rule out the formation of unfunctionalized phenanthridine byproduct that may undergo Minisci type reaction, leading to the desired product. Phenanthridine was subjected to the optimized reaction conditions, where 33% of the cyclohexane functionalized product **2.10** was found, see supporting information.
15. (a) Newcomb, M., Competition Methods and Scales for Alkyl Radical Reaction Kinetics. *Tetrahedron* **1993**, *49*, 1151-1176. (b) M. Newcomb in Chatgilialoglu, C.; Studer, A., Encyclopedia of radicals in chemistry, biology, and materials. **2014**.
16. Ismaili, H., Pitre, S. P., Scaiano, J. C., Active Participation of Amine-Derived Radicals in Photoredox Catalysis as Exemplified by a Reductive Cyclization. *Cat. Sci. Tech.* **2013**, *3*, 935-937.
17. (a) Yavari, I.; Bayat, M. J.; Ghazanfarpour-Darjani, M., Synthesis of N-alkyl-N′-aryl-piperazines via copper-catalyzed C–N bond formation. *Tetrahedron Lett.* **2014,** *55*, 5595-5596. (b) Rafique, J.; Saba, S.; Franco Marcelo, S.; Bettanin, L.; Schneider Alex, R.; Silva Lais, T.; Braga Antonio, L., Direct, Metal-free C(sp2)–H Chalcogenation of Indoles and Imidazopyridines with Dichalcogenides Catalysed by KIO_3. *Chem. Eur. J.* **2018,** *24*, 4173-4180. (c) Liu, J.-Q.; Shen, X.; Liu, Z.; Wang, X.-S., Copper-catalyzed synthesis of arylcarboxamides from aldehydes and isocyanides: the isocyano group as an N1 synthon. *Org. Biomol. Chem.* **2017,** *15*, 6314-6317. (d) Gu, Z.-Y.; Li, J.-H.; Wang, S.-Y.; Ji, S.-J., Cobalt(II)-catalyzed bis-isocyanide insertion reactions with sulfonyl azides via nitrene radicals: chemoselective synthesis of sulfonylamidyl amide and 3-imine indole derivatives. *Chem. Comm.* **2017,** *53*, 11173-11176. (e) Lu, F.; Chen, Z.; Li, Z.; Wang, X.; Peng, X.; Li, C.; Fang, L.; Liu, D.; Gao, M.; Lei, A., Palladium/Copper-Catalyzed Oxidative Coupling of Arylboronic Acids with

Isocyanides: Selective Routes to Amides and Diaryl Ketones. *Org. Lett.* **2017,** *19*, 3954-3957. (f) Khalaj, M.; Taherkhani, M.; Mousavi-Safavi, S. M.; Akbari, J., Synthesis of Benzamide Derivatives by the Reaction of Arenes and Isocyanides through a C–H Bond Activation Strategy. *Synlett* **2018,** *29*, 94-98. (g) Zhang, X.; Liu, Z.; Gao, Y.; Li, F.; Tian, Y.; Li, C.; Jia, X.; Li, J., Selective Oxidative Coupling Reaction of Isocyanides Using Peroxide as Switchable Alkylating and Alkoxylating Reagent. *Adv. Synth. Catal.* **2017,** *360*, 272-277. (h) Malacarne, M.; Protti, S.; Fagnoni, M., A Visible-Light-Driven, Metal-free Route to Aromatic Amides via Radical Arylation of Isonitriles. *Adv. Synth. Catal.* **2017,** *359*, 3826-3830.

18. Rüchardt, C.; Meier, M.; Haaf, K.; Pakusch, J.; Wolber Erwin, K. A.; Müller, B., The Isocyanide–Cyanide Rearrangement; Mechanism and Preparative Applications. *Angew. Chem. Int. Ed.* **2003**, *42*, 893-901.
19. Tobisu, M.; Koh, K.; Furukawa, T.; Chatani, N., Modular Synthesis of Phenanthridine Derivatives by Oxidative Cyclization of 2-Isocyanobiphenyls with Organoboron Reagents. *Angew. Chem. Int. Ed.* **2012,** *51*,11363-11366.
20. Distinct methodological examples include: a) Tokuyama, H.; Yamashita, T.; Reding, M. T.; Kaburagi, Y.; Fukuyama, T., Radical Cyclization of 2-Alkenylthioanilides: A Novel Synthesis of 2,3-Disubstituted Indoles. *J. Am. Chem. Soc.* **1999,** *121*, 3791-3792; b) Mitamura, T.; Iwata, K.; Ogawa, A., Photoinduced Intramolecular Cyclization of o-Ethenylaryl Isocyanides with Organic Disulfides Mediated by Diphenyl Ditelluride. *J. Org. Chem.* **2011,** *76*, 3880-3887. For reviews and key examples of radical indole syntheses applied to total synthesis, see: c) Tokuyama, H.; Fukuyama, T., Indole synthesis by radical cyclization of o-alkenylphenyl isocyanides and its application to

the total synthesis of natural products. *Chem. Rec.* **2002,** *2*, 37-45; d) Kaburagi, Y.; Tokuyama, H.; Fukuyama, T., Total Synthesis of (–)-Strychnine. *J. Am. Chem. Soc.* **2004,** *126*, 10246-10247; e) Lei, J.; Huang, J.; Zhu, Q., Recent progress in imidoyl radical-involved reactions. *Org. Biomol. Chem.* **2016,** *14*, 2593-2602; f) Giustiniano, M.; Basso, A.; Mercalli, V.; Massarotti, A.; Novellino, E.; Tron, G. C.; Zhu, J., To each his own: isonitriles for all flavors. Functionalized isocyanides as valuable tools in organic synthesis. *Chem. Soc. Rev.* **2017,** *46*, 1295-1357.

21. a) Liao, X.; Zhou, H.; Yu, J.; Cook, J. M., An Improved Total Synthesis of (+)-Macroline and Alstonerine as Well as the Formal Total Synthesis of (–)-Talcarpine and (–)-Anhydromacrosalhine–methine. *J. Org. Chem.* **2006,** *71*, 8884-8890 (and references therein); b) Miller, K. A.; Martin, S. F., Concise, Enantioselective Total Synthesis of (–)-Alstonerine. *Org. Lett.* **2007,** *9*, 1113-1116 (and references therein).

22. Evoniuk, C. J.; Ly, M.; Alabugin, I. V., Coupling cyclizations with fragmentations for the preparation of heteroaromatics: quinolines from o-alkenyl arylisocyanides and boronic acids. *Chem. Comm.* **2015,** *51*, 12831-12834.

23. Reaction conditions modified from: a) Nicolaou, K. C.; Zhong, Y. L.; Baran, P. S., A New Method for the One-Step Synthesis of α,β-Unsaturated Carbonyl Systems from Saturated Alcohols and Carbonyl Compounds. *J. Am. Chem. Soc.* **2000,** *122*, 7596-7597; b) Nicolaou, K. C.; Montagnon, T.; Baran, P. S., Modulation of the Reactivity Profile of IBX by Ligand Complexation: Ambient Temperature Dehydrogenation of Aldehydes and Ketones to α,β-Unsaturated Carbonyl Compounds. *Angew. Chem. Int. Ed.* **2002,** *41*, 993-996.

24. Nguyen, J. D.; D'Amato, E. M.; Narayanam, J. M. R.; Stephenson, C. R. J., Engaging unactivated alkyl, alkenyl and aryl iodides in visible-light-mediated free radical reactions. *Nat. Chem.* **2012,** *4*, 854.

25. The two exceptions employ light specifically >400nm: a) Makhmutov, A. R., Single-Pot Synthesis of Alkyl-Substituted Quinolines and Indoles via Photoinduced Oxidation of Primary Alcohols. *Rus. J. Gen. Chem.* **2018,** *88*, 892-897 (and see ref. 20b). For other radical indole syntheses, see: b) Zhang, B.; Studer, A., 2-Trifluoromethylated Indoles via Radical Trifluoromethylation of Isonitriles. *Org. Lett.* **2014,** *16*, 1216-1219; c) Bode, M. L.; Gravestock, D.; Rousseau, A. L., Synthesis, Reactions and Uses of Isocyanides in Organic Synthesis. An Update. *Organic Preparations and Procedures International* **2016,** *48*, 89-221; d) Gribble, G. W (**2016**). Fukuyama Indole Synthesis (Ch. 49, pp 405-408) and Miscellaneous Radical-Promoted Indole Syntheses (Ch. 52, pp 414-423) in Indole Ring Synthesis: From Natural Products to Drug Discovery (Ed.); e) Vidyasagar, A.; Shi, J.; Kreitmeier, P.; Reiser, O., Bromo- or Methoxy-Group-Promoted Umpolung Electron Transfer Enabled, Visible-Light-Mediated Synthesis of 2-Substituted Indole-3-glyoxylates. *Org. Lett.* **2018,** *20*, 6984-6989; see also refs. 6b and 17g.

26. a) Ward, F. W., The Absorption Spectra of some Indole Derivatives. *Biochem. J.* **1923,** *17*, 891-897; b) Sharma, N.; Jain, S. K.; Rastogi, R. C., Solvatochromic study of excited state dipole moments of some biologically active indoles and tryptamines. *Spectrochim. Acta A.* **2007,** *66*, 171-176; c) Rani, G. N.; Ayachit, N. H., Excited state electric dipole moment of 5-hydroxy indole and 5-hydroxy indole 3-acetic acid through solvatochromic shifts. *J. Electron. Spectrosc.* **2010,** *182*, 1-3; d) Meng, X.;

Harricharran, T.; Juszczak, L. J., A spectroscopic survey of substituted indoles reveals consequences of a stabilized 1Lb transition. *Photochem. Photobiol.* **2013,** *89*, 40-50.

27. Moustafa, M. M. A. R.; Pagenkopf, B. L., Synthesis of 5-Azaindoles via a Cycloaddition Reaction between Nitriles and Donor–Acceptor Cyclopropanes. *Organic Letters* **2010,** *12*, 3168-3171.
28. Yao, Q.; Zhou, X.; Zhang, X.; Wang, C.; Wang, P.; Li, M., Convenient synthesis of 6-alkyl phenanthridines and 1-alkyl isoquinolines via silver-catalyzed oxidative radical decarboxylation. *Org. Biomol. Chem.* **2017**, *15*, 957-971.
29. Lu, S.; Gong, Y.; Zhou, D., Transition Metal-Free Oxidative Radical Decarboxylation/Cyclization for the Construction of 6-Alkyl/Aryl Phenanthridines. *J. Org. Chem.* **2015**, *80*, 9336-9341.
30. Li, Z.; Fan, F.; Yang, J.; Liu, Z.-Q., A Free Radical Cascade Cyclization of Isocyanides with Simple Alkanes and Alcohols. *Org. Lett.* **2014,** *16*, 3396-3399.
31. Zhu, Z.-Q.; Wang, T.-T.; Bai, P.; Huang, Z.-Z., A cascade alkylarylation reaction of 2-isocyanobiphenyls with simple alkanes for 6-alkyl phenanthridines via dual C(sp3)-H/C(sp2)-H functionalizations. *Org. Biomol. Chem.* **2014,** *12*, 5839-5842.
32. Anand, N.; Chanda, T.; Koley, S.; Chowdhury, S.; Singh, M. S., $CuSO_4$-d-glucose, an inexpensive and eco-efficient catalytic system: direct access to diverse quinolines through modified Friedlander approach involving SNAr/reduction/annulation cascade in one pot. *RSC Advances* **2015,** *5*, 7654-7660.
33. Elothmani, D.; Do, Q. T.; Simonet, J.; Le Guillanton, G., Anodic oxidation of di-tert-butyl disulfide: a facile method for the preparation of N-tert-butylamides. *J. Chem. Soc., Chem. Commun.* **1993**, 715-717.

34. Lamm, B; Holmstrom, A. A Halogen Exchange Reaction in a Diazonium Compound, *Acta Chem. Scand.* **1971**, *1*, 351-352.

35. Ben Cheikh, A.; Chuche, J.; Manisse, N.; Pommelet, J. C.; Netsch, K. P.; Lorencak, P.; Wentrup, C., Synthesis of alpha-cyano carbonyl compounds by flash vacuum thermolysis of (alkylamino)methylene derivatives of Meldrum's acid. Evidence for facile 1,3-shifts of alkylamino and alkylthio groups in imidoylketene intermediates. *J. Org. Chem.* **1991,** *56*, 970-975.

36. Hayamizu, K.; Terayama, N.; Hashizume, D.; Dodo, K.; Sodeoka, M., ChemInform Abstract: Unique Features of Chiral Palladium Enolates Derived from β-Ketoamide: Structure and Catalytic Asymmetric Michael and Fluorination Reactions. *Tetrahedron* **2015**, *71*, 6594-6601.

37. Chow Shiao, Y.; Stevens Marc, Y.; Åkerbladh, L.; Bergman, S.; Odell Luke, R., Mild and Low-Pressure *fac*-Ir(ppy)$_3$-Mediated Radical Aminocarbonylation of Unactivated Alkyl Iodides through Visible-Light Photoredox Catalysis. *Chem. Eur. J.* **2016**, *22*, 9155-9161.

38. Klauck Felix, J. R.; James Michael, J.; Glorius, F., Deaminative Strategy for the Visible-Light Mediated Generation of Alkyl Radicals. *Angew. Chem. Int. Ed.* **2017**, *56*, 12336-12339.

39. Heckman, L. M.; He, Z.; Jamison, T. F., Synthesis of Highly Substituted 2-Arylindoles via Copper-Catalyzed Coupling of Isocyanides and Arylboronic Acids. *Organic Letters* **2018,** *20*, 3263-3267.

40. Ambler, B. R.; Peddi, S.; Altman, R. A., Ligand-Controlled Regioselective Copper-Catalyzed Trifluoromethylation To Generate (Trifluoromethyl)allenes. *Organic Letters* **2015,** *17*, 2506-2509.

41. Némethová, I.; Bilka, S.; Šebesta, R., Enantioselective copper-catalyzed conjugate additions of in situ generated organozirconium reagents to N-heterocyclic Michael acceptors. *Journal of Organometallic Chemistry* **2018,** *856*, 100-108.

CHAPTER 3: IRIDIUM PHOTOREDOX-GENERATED CHLORINE AS HYDROGEN ATOM TRANSFER AGENT

Rohe, S., Morris, A. O., McCallum, T., L. Barriault. Hydrogen Atom Transfer Reactions Via Photoredox Catalyzed Chlorine Atom Generation. *Angew. Chem. Int. Ed*. **2018**, 57, 15664-15669.

S. Rohe thanks T. McCallum and A. O. Morris for their contributions. Conceived by T. McCallum, optimization completed by S. Rohe and A. O. Morris. Scope completed by S. Rohe (molecules in blue) and A. O. Morris. Solvent selectivity trials and Stern-Volmer experiments completed by S. Rohe, A. O. Morris and T. McCallum. Isotope labelling experiments conducted by S. Rohe (alkane and aldehyde) and A. O. Morris (ether). Polarity reversal experiments conducted by S. Rohe.

3.1 Abstract

The selective functionalization of chemically inert C-H bonds remains to be fully realized in achieving organic transformations that are redox-neutral, waste-limiting, and atom-economical, though radical chemistry has contributed to many key advancements in this field. Comprehensive access to C-H bonds of all reactivities could change the chemical industry by promulgating industrial use of currently useless shale gas byproducts, such as methane or ethane, as feedstocks. Capitalizing on this opportunity would not only provide crucial financial incentive to capture and recycle these pollutants but could drastically lower the cost of the derived chemicals. The challenge associated with access to these pollutants rests in their high energies of activation, illustrated by their

C-H BDEs of >100 kcal/mol. These BDEs are accessible using other high-energy transformations such as hydrogen atom transfer (HAT) from halogen atoms like chlorine, and though possible, in many cases this is just relaying the difficulty baton to a different chemical species. Oxidation of chloride ions to chlorine atoms is a notoriously energy-intensive redox process which has thus far prohibited its use in industry. We herein propose a mild, controlled, and catalytic generation of chlorine atoms from highly stable HCl allowing unprecedented access to a broad scope of HAT. The discovery of the photoredox mediated generation of chlorine atoms with Ir-based polypyridyl complex, $[Ir(dF(CF_3)ppy)_2(dtbbpy)]Cl$, under blue LED irradiation is reported.

3.2 Introduction

Chlorine atoms have traditionally been accessed by photolysis or thermolysis processes of chlorine in the gas phase.[1] The requirement for such conditions has rendered methodological and technological advancements limited to chlorination of saturated hydrocarbons because many functional groups are unstable to the conditions or the high reactivity of the generated chlorine atom. Despite these challenges, exploration of the reactivity and selectivity of various halogen atoms has still taken place, though unfortunately mostly within these limitations. A mild and catalytic generation of chlorine atoms would represent a breakthrough into new chemical space and enable studies towards new organic transformations.

Much progress has been made towards understanding the highly reactive chlorine intermediate in comparison to its more selective bromine counterpart with respect to alkane halogenation reactions, as seen in **Scheme 3.1a**.[2] Though radical reactions have

often exhibited a lack of sensitivity to solvent effects other than viscosity, it has been demonstrated that stabilization of chlorine atoms occurs via solvent complexation by aromatic molecules such as benzene and pyridine. Formation of either a π-complex with aromatic or Lewis basic solvents or a σ-complex with acceptors such as carbon disulfide can attenuate the highly reactive chlorine atom, influencing its selectivity in HAT processes (**Scheme 3.1b**). Formation of these complexes not only allows tuning of chlorine's selectivity between primary, secondary and tertiary aliphatic C-H bond abstraction, but provides evidence for the catalytic formation of chlorine atoms in solution. Selectivity tuning of halogen atom HAT is fundamentally restricted due to its use of thermodynamic criteria to instill stability, as opposed to stabilization of a transition state or other reactive intermediate. This unfortunately means that selectivity will always only increase towards

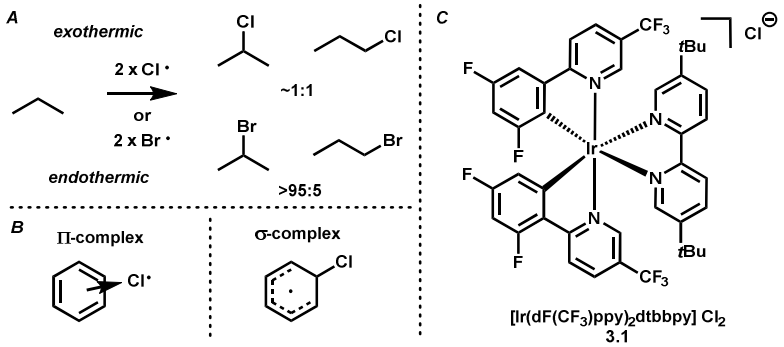

Scheme 3.1. Behavior of halogen radicals. A) Inherent selectivities of reactive halogen atoms; B) types of complexation attenuating reactivity of chlorine; C) photosensitizing iridium polypyridyl complex employed in this methodology.

more stable C-H bonds, in other words selectivity increases towards tertiary over primary C-H bonds. Other HAT methodologies employing metals or non-halogen radicals as

initiators will almost overwhelmingly also produce the most stable radical, i.e. that with the lowest BDE (**Table 3.1**).[3] The radical revolution sought by both academia and industry is a methodology allowing preferential HAT of the most sterically accessible and thermodynamically unstable position, the primary unactivated C-H bond. Though this may perhaps be accomplished using an unusually energetic yet sterically hindered catalyst such as tetra-*n*-butylammonium decatungstate (TBADT), it presently depicts a major deficiency of the field.[4]

Table 3.1. Comparison of key H-X and H-R Bond Dissociation Energies.[5]

Halogen-H bonds (*D*, kcal/mol)			
H-I 71	H-Br 88	H-Cl 103	H-F 136
R-H bonds (*D*, kcal/mol)			
O-H 110-111	S-H 82	Ge-H <65	Si-H 71
P-H 82	NH_2C-H 95	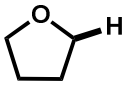 92	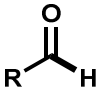 87
C-H (1°) 98-105	C-H (2°) 92-101	C-H (3°) 91-96	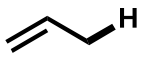 85

Alkyl radical initiation is no longer limited to the heyday's explosive and toxic reagents (tributylstannanes, azobisisobutyronitrile (AIBN), triethylborane, peroxides).[6] Transition metal and organic dye based photocatalysts enable the use of lower-energy wavelengths that circumvent degradation pathways associated with direct excitation of organic

substrates.[7] Highly reactive excited state complexes trigger reductive or oxidative quenching processes that allow access to highly reactive organic intermediates seldom accessed through other methods. Frequently, this involves a combination of photoredox HAT dual catalysis with cocatalyst additives such as thiols, quinuclidines, amides, sulfonamides, and phosphates.[8] At the time of publication of this manuscript, few examples of photoredox processes catalytically generating chlorine atoms existed.[9] Recently, advances in Ir^{III}/Ni^{0} dual photoredox HAT catalysis have enabled the cross-coupling of alkanes (as solvent) with haloarenes through a proposed halogen atom (Br or Cl) intermediate (**Scheme 3.2b**).[10] Herein we report the photoredox mediated catalytic generation of chlorine atoms and their subsequent hydrogen atom transfer (HAT) reactions with a variety of substrates.

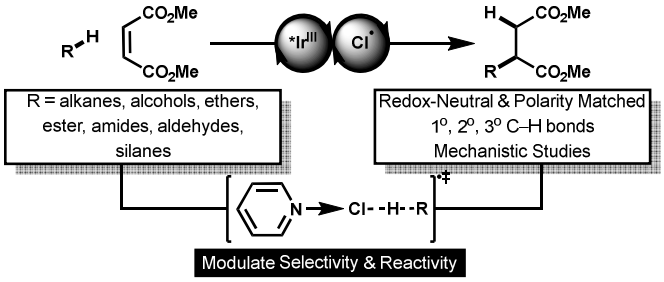

Scheme 3.2. Cl atom-mediated transformations in organic synthesis.

3.3 Results and Discussion

Table 3.2: Optimization of conditions.[a]

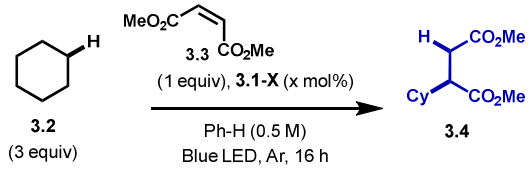

Entry	X	[mol%]	TBAC [mol%]	Conv. [%]	Yield [%]
1	PF_6	2	10	100	80
2	PF_6	2	5	100	84
3	PF_6	1	20	100	84
4	PF_6	1	---	20[b]	0
5	Cl	1	5	100	89
6	Cl	1	---	100	84
7	**Cl**	**2**	**---**	**100**	**86(68)**
8	Cl	2	---	0[c]	0
9	Cl	2	---	0[d]	0
10	---	---	20	0	0

[a] See Experimental Section, reactions run between 60 and 80°C. **3.3** = dimethyl maleate; **3.5** = dimethyl fumarate. Yields outside of brackets are done by NMR comparison to an internal standard (trimethylphenylsilane). [b] **3.3** (80%) as 1.73:1 *Z*:*E* (**3.3**:**3.5**). [c] Reaction run at room temperature. [d] In absence of irradiation.

A preliminary screening of reaction conditions identified $[Ir(dF(CF_3)ppy)_2(dtbbpy)]PF_6$ (**3.1-PF$_6$**, 2 mol%) with tetrabutylammonium chloride (TBAC) (10 mol%), cyclohexane (**3.2**, 3 equiv), and dimethyl maleate (**3.3**, 1 equiv) in benzene (0.5 M) under 465 nm LED

irradiation as conditions leading to **3.4** in 80% yield (**Table 3.2**, entry 1). Expanding upon this exciting result, it was found that lowering the amount of TBAC or photocatalyst were not detrimental to the yield of the reaction (entries 2, 3, and 5). No product was observed in the absence of a chloride source; however, some conversion of the dimethyl maleate radical acceptor was observed. The major byproduct observed was isomerization to the corresponding fumarate (1.73:1 **3.3**:**3.5**) (entry 4). The isomerization process was not observed in the absence of photocatalyst which could be consistent with background energy transfer mechanisms (entry 10). Finally, we considered combining the chromophore and the chloride source together by simply running the reaction with the $[Ir(dF(CF_3)ppy)_2(dtbbpy)]Cl$ (**3.1-Cl**) catalyst, as this was a significantly more convenient source of chloride ion.[11] To our delight, 1 mol% of **3.1-Cl** led to product in 84% yield (entry 6). A slight increase in yield was observed when using 2 mol% of the photocatalyst, giving product in 86% yield (68% isolated, entry 7). This loading was used for all further examples to ensure reactivity in challenging cases. Finally, control experiments reveled that photocatalyst, light irradiation, and heat were necessary for the transformation to proceed (entries 8-10).

Following determination of optimal conditions for this transformation, an investigation of the alkane coupling partner tolerance was performed (**Table 3.3**). Cyclopentane, cyclooctane, and adamantane **3.5-3.7** underwent the coupling with **3.3** in 69%, 53%, and 61% (62:38 H_A:H_B) yields, respectively. *Cis*-decalin reacted quantitatively though unfortunately provided an inseparable mixture of isomers, whereas the *trans*-decalin completely resisted any type of reaction under our conditions. Alkane selectivity proved difficult to identify when using asymmetrical or more complex alkanes, and though use of

substrates such as dimethylcyclohexane and 2-methylpentane resulted in full conversion of the acceptor substrate, the products were an inseparable and indistinguishable mix of isomers. This was expected considering the tendency of the chlorine atom to react almost indiscriminately with tertiary, secondary and primary alkane C-H bonds. These same substrates were attempted using various solvents and dilutions that were hypothesized to change chlorine's selectivity, however, changes in selectivity were inconsistently visible by NMR. These selectivity experiments may answer questions valuable to the future of chlorine HAT in academia and industry, and it is suggested that future experiments utilize quantitative GC-MS to determine product isomer ratios.

Use of cyclopentanol and isobutanol for HAT resulted in in 33 and 69% respective product yields, giving cyclized lactone products **3.8** and **3.9**. Ethers proved to be effective substrates in this transformation. Simple, ubiquitous substrates such as THF and pyran (**3.11-3.12**) underwent efficient couplings at the highly hydridic α-position in yields ranging from 55% to 70%. Methoxycyclopentane **3.13** afforded 59% total yield of the corresponding products, isolated separately as a 3:1 ratio of the products deriving from HAT at the 3° and 1° positions. Interestingly, ketone **3.10** gave product in 63% yield, selecting for the relatively nucleophilic C-H bond or hydridic position as opposed to the relatively electrophilic α-keto C-H bond. Notably, a variety of silanes **3.18-3.22** underwent efficient coupling in 55-81% yields; this provides a useful method of functional handle installation at unactivated positions. Amine **3.23** also produced product at the least stabilized but most sterically accessible position in 49% yield, though it is possible that this product was formed *via* direct amine quenching of catalyst excited state. Acyclic and cyclic amides **3.14-3.16** furnished the desired product in some of the best yields ranging

74-96%. Finally, a variety of maleates and fumarates **3.24-3.28** underwent coupling with cyclohexane in good-to-excellent yields ranging 58-87%.

Table 3.3. Selected substrate scope.

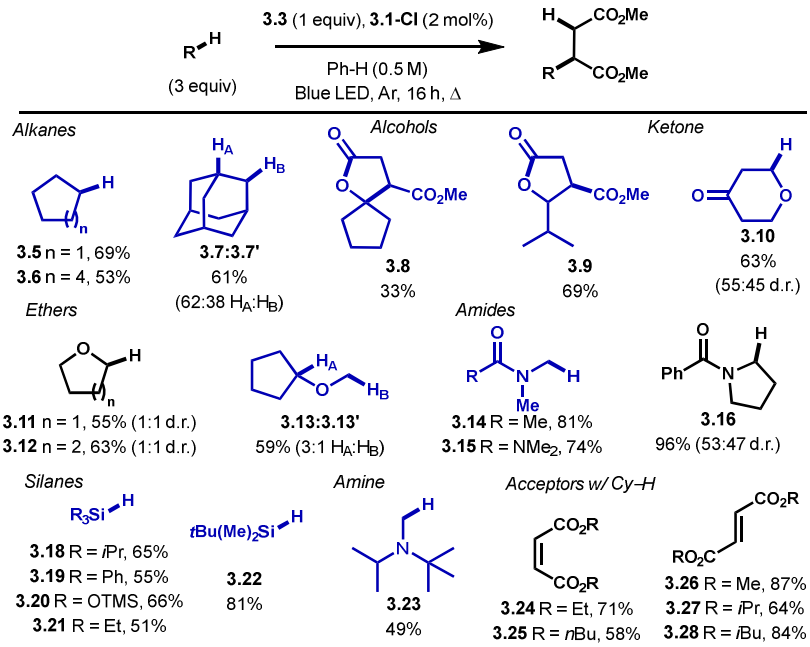

Several substrates of note afforded interesting preliminary results that were not explored to their full potential. Due to the unusually low Ge-H BDE (77 kcal/mol), it was believed that tributylgermanium hydride would be an excellent candidate for this methodology though it would contend with reduced succinate as a prominent byproduct.[5] The reaction exhibited successful product formation by crude NMR (57%), though upon isolation it was evident that the product was inseparably contaminated with a tributylgermanium-derived byproduct. Another potential substrate family with conspicuously accessible BDE is the phosphine oxides' P-H (~82 kcal/mol). Preliminary studies conducted with diphenylphosphine oxide and diethylphosphite also proved fruitful by crude NMR, though both products degraded following purification attempts. These

results are unique from other HAT methodologies and are worth pursuit in future research while keeping in mind their inherent stability idiosyncrasies.

We noticed that benzylic and allylic C-H bonds on substrates such as toluene, mesitylene, 3-methylcyclohexene, and limonene (and the >10 allylic substrates that were attempted) were totally ineffective in this transformation under the reported conditions. These failures were startling initially as the BDEs for benzylic and allylic C-H bonds are reported to be 85-90 kcal/mol, which should be readily accessible by our catalytic system. We first suspected that the resulting carbon-centered radicals were so stable that they reacted only sluggishly, resulting in poor yields. However, this idea was refuted by our highly successful aldehyde scope ($BDE_{\text{aldehyde C-H}}$ ~ 86). It is possible that the intermediate benzylic and allylic radicals may possess the incorrect "philicity" for success within our system for two reasons.[12] Firstly, the HAT from the electron-deficient chlorine is most successful with hydridic C-H bonds which allow formation of a polar transition state. Benzylic and allylic C-H bonds are unfortunately less hydridic due to delocalization. Furthermore, the resulting carbon-centered radicals are poorly electronically aligned for addition to a Michael acceptor in the classic Giese reaction. We theorized that this problem may be solved by use of a "polarity reversal" perfluorinated solvent such as HFIP or TFE, or alternatively with more electron-rich olefin acceptor such as methyl vinyl ether.[13] If an electron-rich acceptor partner is employed, it may be prudent to lower concentration or lower reaction catalyst loading, as the reaction may become more dependent on chain propagation. Preliminary results of these studies (**Table 3.4**) indicate that HFIP may allow success with allylic but not benzylic substrates.

Table 3.4. Success of allylic and benzylic HAT in various solvents.

Entry	Solvent	Allylic substrate	Conversion [a] (%)	Product (%)	3.29 (%)
1	Benzene	cyclohexene	27	<5	22
2	DMSO	4-methyl-cyclohexene	100	52	0
3	HFIP	cyclohexene	75	54	0
4	HFIP:benzene (1:1)	cyclohexene	>95	75	0
5	HFIP	toluene	72	0	10
6	HFIP:benzene (1:1)	toluene	65	0	<5

[a] Conversion and yields obtained by NMR yield with trimethylphenylsilane as internal standard.

Following scope elucidation, mechanistic studies were conceived to develop an understanding of the underlying pathways and the prevalence of chain propagation. The sheer variety of substrates employed for HAT as well as the highly variable scope results made us suspect differential involvement of chain propagation for each family of substrates. Isotope labelling experiments were performed with alkane, ether, and aldehyde substrates to assess where deuterium incorporation may occur (**Table 3.5**). Filling of any gaps in these studies is a worthwhile pursuit for future research due to the

Table 3.5. Isotope labelling studies.

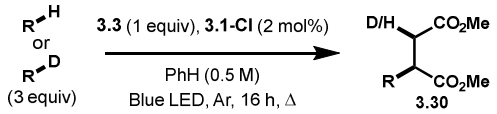

Entry	R-H/D	BDE[5] (kcal/mol)	H_2O [equiv]	D_2O [mol%]	Yield [%]	3.30:d-3.30	ratio [H/D]
1	**3.2** C_6H_{12}	96	---	10	60	85:15	---
2	**d_{12}-3.2**	---	10	---	78	95:5	---
3	**3.2:d_{12}-3.2** (1:1)	---	---	---	63	82:18	4.5
4	**3.11** THF	92	---	10	65[a,b]	0:100	---
5	**d_8-3.11**	---	10	---	72[a,c]	100:0	---
6	**3.11**:**d_8-3.11** (1:1)	---	---	---	58[a]	75:25	3.0
7	**3.31** PhCHO	87	---	10	82	60:40	---
8	**d-3.31** PhCDO	---	---	---	85	72:28	---
9	**3.31:d-3.31** (1:1)	---	---	---	49	86:14	6.1

[a] Isolated yields. All diastereomers in a 1:1 ratio. [b] Diastereomer 1 (less polar, 1:1 d.r. with respect to D incorporation); Diastereomer 2 (more polar, 1:1 d.r. with respect to D incorporation). Diastereomers assigned by ^{1}H NMR analysis. [c] 55:45 d.r.

impact of chain propagation on methodologies involving short-lived high-energy radical species such as chlorine.

Isotope studies produced complicated results except for the ether example (**Table 3.5**). It is important to note that for each of these reactions the solvent was not pre-dried and so likely contains traces of water. It is also possible that HAT could occur from the solvent, though this is unlikely as it is thermodynamically uphill in most cases ($BDE_{benzene}$ = 103 kcal/mol). Cyclohexane **3.2** (96 kcal/mol) should be the substrate with the most endothermic chain propagation as it has the highest energy R-H bond. Despite this high barrier, the reaction using cyclohexane as substrate with D_2O (10 equiv.) produced product **d-3.30** with only 15% deuterium scrambling, indicating that the final radical was most likely not totally reduced to the anion by the iridium catalyst. We propose that chain propagation contributes to the catalytic cycle with alkane substrates because the protonated product is overwhelmingly produced via HAT from cyclohexane. Factors contributing to this pathway could be firstly successful electronic alignment of the electrophilic α-ester radical with the hydridic cyclohexane C-H bonds, and secondly the speed of reduction of α-ester radical from the catalyst. The same experiment repeated with **d-3.2** and water (10 equiv.) resulted in 95% protonated product, which could be due to an overvaluation of chain propagation in entry 1 or to a kinetic isotope effect drastically slowing the chain. To determine the magnitude of any isotope effect, the reaction was conducted using 1:1 **3.2** and **d-3.2** without water additive resulting in a 63% yield of 82:18 (**3.30:D-3.30**) and ratio = 4.5 (entry 3). This large difference in rate between HAT on protonated and deuterated substrates may be the justification for the disparities of results in entries 1 and 2.

THF **3.11** in the presence of D_2O (10 equiv) gave solely the deuterium incorporated **d-3.30** without the observation of any scrambling in 65% yield (Entry 4). This result is indicative of 1) the radical intermediate formed after coupling with **3.3** must then be reduced as opposed to undergoing chain reaction with a THF equivalent, 2) the product is not in equilibrium with any other intermediates, and 3) ether substrates proceed *via* a closed cycle mechanism. The opposite experiment was performed using **d_8-3.11** in the presence of water (10 equiv) and gave the expected H-incorporated product in 72% yield, further validating the hypothesis (Entry 5). Furthermore, a competition experiment using a 1:1 mixture of **3.11**:**d_8-3.11** gave a 3:1 mixture of products derived from the addition favouring the **3.11** (ratio = 3, Entry 6).

Finally, aldehyde **3.31** afforded a scrambling of products in 82% yield (60:40 **3.30:d-3.30**, entry 7) when D_2O was used as an additive. Unfortunately, due to the difficulty of synthesizing **d-3.31**, the full range of competition experiments was not completed. Despite this difficulty some key results were obtained. Deuterated aldehyde **d-3.31** was submitted to the regular conditions with no additive and provided a scrambled product (72:28 **3.30:d-3.30**, entry 8). Since the only sources of hydrogen in this reaction would be a) benzene C-H via HAT and b) trace water via an ionic mechanism, this reaction implies that earlier chain transfer results may be overestimated. As HAT from benzene is highly unlikely due to the thermodynamic barrier, it is more likely that the final radical is simply reduced to make the anion which reacts with trace water or HCl. HAT from benzene solvent was substantiated by running the reaction with C_6D_6 as solvent and no deuteration of the final product was observed, however, the reaction was slowed (52% product yield, 7% RSM), indicating a non-innocent role of solvent. In the example with **d-3.31** (entry 8),

as deuterium is still incorporated into the final product, it is evident that some chain propagation occurs, though likely less than insinuated by the results in **Table 3.4**. Finally, the competition experiment was performed with 1:1 **3.31:d-3.31** giving 86:14 **3.30:d-3.30** and a ratio of 6.1 (entry 9).

After establishment that the reaction pathway likely proceeds through a mix of closed and open cycles, we decided to explore the extent of the unusual selectivities we had obtained from reacting substrate **3.13** (**Table 3.6**). First, the **3.1-Cl** and **3.1-Br** catalyst counterions were evaluated for differences in selectivity at various concentrations in benzene (Entries 1-5). The reactions proceeded in 54-66% yields with **3.1-Br** being slightly more selective at low concentrations (4.8 vs 4.4, Br:Cl). Overall, the **3.1-Cl** catalyst was more robust towards low concentrations, affording a 5.4 selectivity at low concentration and 1 mol% catalyst loading (**3.1-Br** gave little conversion at 1 mol%). To our surprise, almost no change to the yield and selectivity of the transformation was observed when varying the electronics and sterics of the arene-based solvent (Entries 6-10). Arene rings containing functional groups such as Me, OAc, CO_2Me, C(O)Me, and CF_3 afforded yields and selectivity that ranged 40-70% and 3.9-4.4 respectively (**3.1-Cl** 2 mol%, 0.5 M); these results were like those of benzene. This similarity was unexpected given the body of literature that propose the π-complexation of chlorine atoms.[2,14] Using **3.13** as the solvent similarly gave the product in 82% yield with a selectivity of 4.1 (Entry 11). It is probable that little complexation of chlorine atoms is evident considering these benzene-based solvents or that a background chain reaction may be at play. The high temperature of our reaction (~80 ^{0}C) may also significantly lower the observed selectivity despite any complexation effects. Pleasingly, when switching to pyridine (an efficient

complex forming solvent), the selectivity soared to 9.1 (Entry 12). This may be due to pyridine's ability to attenuate chlorine based on Lewis basicity, forming a σ-complex, as opposed to π-complexation. Further, the selectivity of **3.1-Br** was found to be lower than **3.1-Cl**, 7.7, which demonstrates that a chlorine atom can be rendered more stable towards HAT than the bromine atom (Entry 13). Lowering the concentration, the selectivity was improved to 10.0 with **3.1-Cl**, besting **3.1-Br** (Entries 14-16).

Table 3.6. Solvent effects on the HAT reactions of **3.1-Cl** and **3.1-Br** with **3.2**.

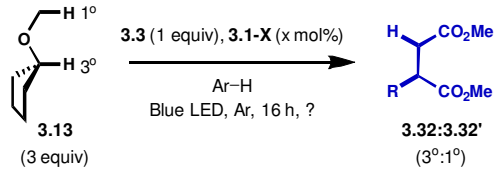

Entry	Ar-H	[M]	X	[mol%]	[%][(a)]	3°/1°
1	PhH	0.5	Cl	2	66	3.6
2	PhH	0.5	Br	2	62	4.2
3	PhH	0.05	Cl	2	64	4.4
4	PhH	0.05	Br	2	60	4.8
5	PhH	0.05	Cl	1	54	5.4
6	PhMe	0.5	Cl	2	70	3.9
7	PhOAc	0.5	Cl	2	48	4.4
8	$PhCO_2Me$	0.5	Cl	2	40	4.0

9	PhC(O)Me	0.5	Cl	2	64	4.0
10	$PhCF_3$	0.5	Cl	2	57	4.1
11	**3.13**	0.5	Cl	2	82	4.1
12	Pyr	0.5	Cl	2	72	9.1
13	Pyr	0.5	Br	2	22	7.7
14	**Pyr**	**0.05**	**Cl**	**2**	**64**	**10.0**
15	Pyr	0.05	Br	2	16	8.5
16	Pyr	0.05	Cl	1	72	9.5
17[b]	CS_2	0.5	Cl	2	35	6.4

[a] Isolated yields where ratio of **3.32** and **3.32'** were determined by ^{1}H NMR analysis. [b] Recovered 12% starting material.

Other electron-rich-, styryl-, and enone-based alkenes were examined as radical acceptors in this transformation, however, either low conversion or decomposition was observed (see SI). We hypothesize that triplet-triplet energy transfer processes may have been responsible for this lack of desired product formation.

After obtaining several mechanistic data, a product forming pathway may be proposed (**Figure 3.1**). Upon excitation of catalyst **3.1**, reductive quenching of chloride may occur (**3.1***, $E_{1/2}^{M^*/M^-}$ = +1.21 V *vs* SCE; TBAC, $E_{1/2}^{red}$ = +2.03 V *vs* SCE),[10b, 11] despite large uphill thermodynamic requirements, giving chlorine atom and Ir^{II} (**3.1-A**). This

interaction may be facilitated by the heat (required for the transformation to proceed) and the proximity of the chloride ion. Stern-Volmer fluorescence quenching experiments found this process to be feasible when considering kinetics (**3.1-PF6**, $k_q^{TBAC} = 1.1 \pm 0.1 \times 10^6$ $M^{-1}s^{-1}$; **3.1-Cl**, $k_q^{TBAC} = 8.2 \pm 0.9 \times 10^5$ $M^{-1}s^{-1}$). Several alkene types may undergo background activation through triplet-triplet energy transfer processes and was elegantly demonstrated in Hong's recent study (**3.1-PF6**, $k_q^{cyclohexenone} = 3.2 \times 10^8$ $M^{-1}s^{-1}$).[15] Quenching of **3.3** was found to be slower than chloride in our study (**3.1-PF6**, $k_q^{2a} = 6.3 \pm 0.7 \times 10^5$ $M^{-1}s^{-1}$; **3.1-Cl**, $k_q^{2a} = 7.0 \pm 1.6 \times 10^5$ $M^{-1}s^{-1}$) and may explain why maleates and fumarates are tolerated under the described conditions. Upon generation of the electrophilic chlorine atom, complexation to a solvent such as pyridine may take place (**Pyr-Cl**), where the chlorine atom can undergo HAT with a variety of substrates, giving nucleophilic alkyl radical **I**.[14] This radical can add efficiently to an activated alkene, giving intermediate **II**. This intermediate then likely undergoes single-electron transfer (SET) with **3.1-A** (**II**, $E_{1/2}^{red} = -0.6$ V *vs* SCE; **3.1-A**, $E_{1/2}^{M/M-} = -1.37$ V *vs* SCE),[8o, 9, 11, 16, 17] regenerating **3.1** and furnishing the desired product. It should be noted that substrates such as aldehydes are known to undergo chain reaction processes and this transformation is likely no exception.[18]

Figure 3.1. Proposed mechanism.

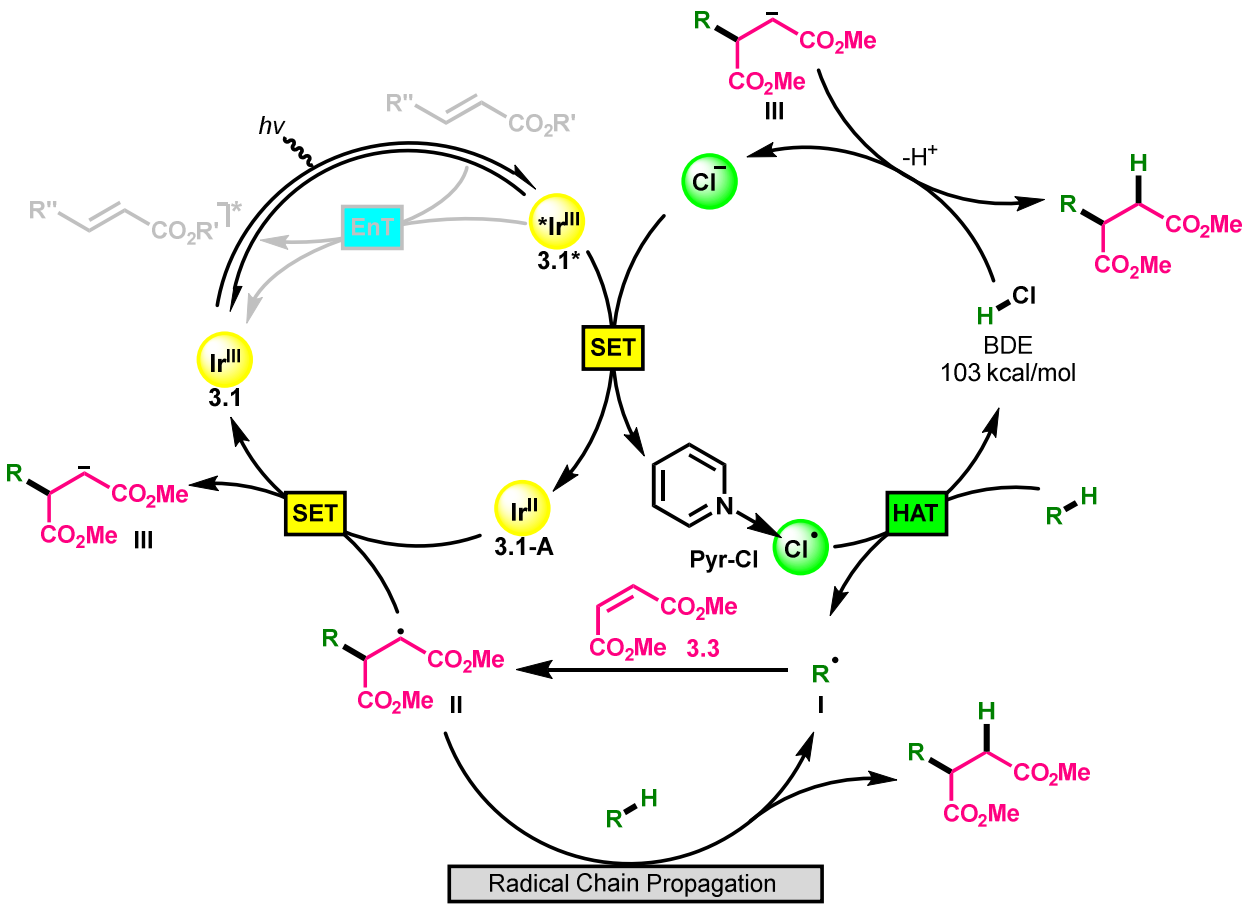

3.4 Conclusions

In summary, chlorine atoms have been formed from chloride ions using photoredox mediated activation. The chlorine atoms engaged with a variety of hydridic C-H bonds including alkanes, alcohols, ethers, amides, and silanes, for the redox-neutral Giese-type addition of alkyl radicals to activated alkenes. Substrates that were not well-aligned electronically for the transformation, i.e. substrates that had only poorly hydridic C-H bonds, were shown to be ineffective unless a polarity-reversal strategy was employed. Mechanistic studies indicated that the catalytic cycle could be closed or open depending on the HAT substrate. Results were obtained demonstrating how chlorine atoms could be

attenuated by aromatic solvents such as pyridine, resulting in HAT more selective than that with bromine atoms. Finally, it was found that the substrate scope was restricted by background energy transfer pathways forming triplet-state olefin by-products. These results challenge the currently accepted information about chlorine atoms and future studies evaluating these highly reactive intermediates in the context of synthesis will be reported in due course.

3.5 Further Information

3.5.1 Optimization

Table 3.7. Full Optimization of Reaction Conditions.

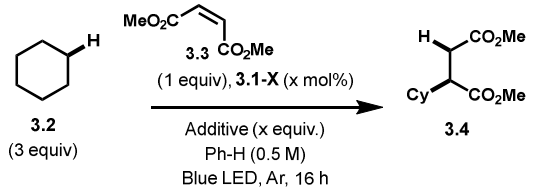

Entry	3.1-X [mol%]	Additive [mol%]	3.2 [equiv.]	Solvent [M]	t [h]	%Conv 3.3	%Yield 3.4
1	PF_6 [2]	TBACl [10]	3	PhH [0.5]	16	100	80
2	PF_6 [2]	TBACl [5]	3	PhH [0.5]	16	100	84
3	PF_6 [1]	TBACl [20]	3	PhH [0.5]	16	100	84
4	PF_6 [1]	---	3	PhH [0.5]	16	20	0
5	Cl [1]	TBACl [5]	3	PhH [0.5]	16	100	89
6	Cl [1]	---	3	PhH [0.5]	16	100	84

Entry	3.1-X [mol%]	Additive [mol%]	3.2 [equiv.]	Solvent [M]	t [h]	%Conv 3.3	%Yield 3.4
7	Cl [2]	---	3	PhH [0.5]	16	100	86(68)
8[a]	Cl [2]	---	3	PhH [0.5]	16	0	0
9[b]	Cl [2]	---	3	PhH [0.5]	16	0	0
10	---	TBACl [20]	3	PhH [0.5]	16	0	0
11	PF_6 [2]	TBACl [0.2]	10	$PhCF_3$ [0.1]	48	90	40
12	PF_6 [2]	TBACl [200]	10	$PhCF_3$ [0.1]	48	94	47
13	PF_6 [2]	TBACl [20]	10	DCE [0.1]	48	94	10
14	PF_6 [2]	TBACl [20]	10	DMSO [0.1]	48	100	61
15	PF_6 [2]	TBACl [20]	10	MeOH [0.1]	48	100	42
16	PF_6 [2]	TBACl [20]	10	MeCN [0.1]	48	48	10
17	PF_6 [2]	TBACl [20]	10	DMF [0.1]	48	100	49
18	PF_6 [2]	TBACl [20]	10	$(CH_3)_2CO$	48	70	65
19	PF_6 [2]	TBACl [20]	10	PhH [0.1]	48	100	60
20	PF_6 [2]	TBACl [20]	10	PhH [0.2]	48	100	82
21	PF_6 [2]	TBACl [20]	10	PhH [0.5]	48	100	82
22	PF_6 [2]	TBACl [20]	10	PhH [0.033]	48	100	84
23	PF_6 [2]	TBACl [20]	10	PhH [0.5]	24	100	93
24	PF_6 [2]	TBACl [20]	10	PhH [0.1]	4	65	65
25	PF_6 [2]	TBACl [20]	10	PhH [0.1]	8	85	85

Entry	3.1-X [mol%]	Additive [mol%]	3.2 [equiv.]	Solvent [M]	t [h]	%Conv 3.3	%Yield 3.4
26	PF_6 [2]	TBACl [10]	10	PhH [0.5]	16	100	95
27	PF_6 [2]	TBACl [5]	10	PhH [0.5]	16	100	94
28	PF_6 [2]	TBACl [5]	5	PhH [0.5]	16	100	84
29	PF_6 [2]	TBACl [5]	3	PhH [0.5]	16	100	86
30	PF_6 [2]	TBACl [10]	3	PhH [0.5]	16	100	80
31	PF_6 [2]	NaCl [20]	10	PhH [0.5]	16	6	0
32	PF_6 [2]	KCl [20]	10	PhH [0.5]	16	4	0

[a] Reaction vessel was placed 1.5 cm from LED light source and cooled to room temperature using a fan. [b] Reaction vessel was coated in aluminum foil and heated to 80ºC.

3.5.2 Isotope Labelling Competition Experiments

For the kinetic isotope experiments the reaction mixture was prepared in the usual way with a 1:1 mixture of d_n-alkane:alkane as the alkylating agent. Isotope ratio data was obtained by analyzing the ratio between deuterated and protonated products at complete conversion following isolation (^{1}H NMR spectrum below).

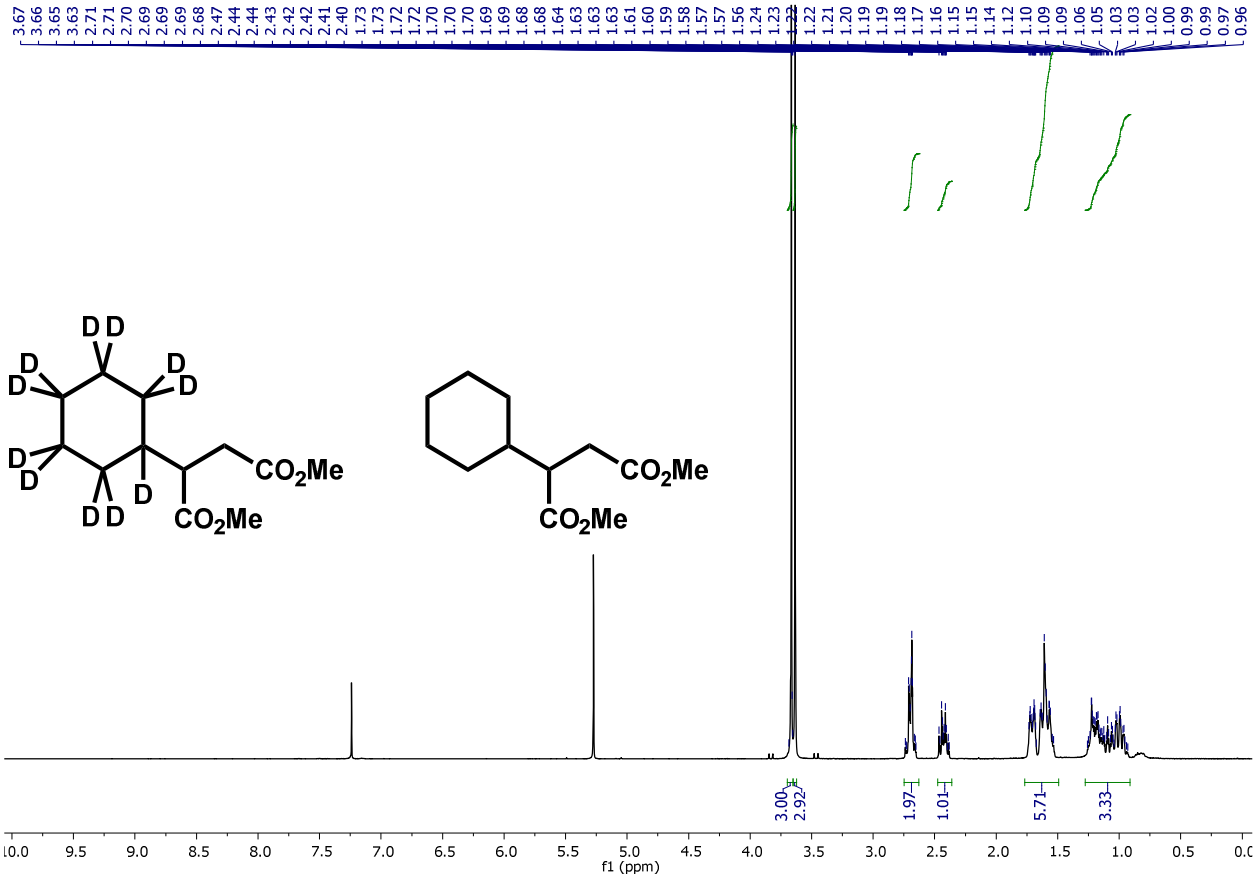

Figure 3.2. ^{1}H NMR spectrum for the isotope labelling study with cyclohexane as substrate. Analysis of the product distribution yields a 18:82 ratio for the addition of cyclohexane-*d*12:cyclohexane to dimethyl maleate giving a ratio of 4.5.

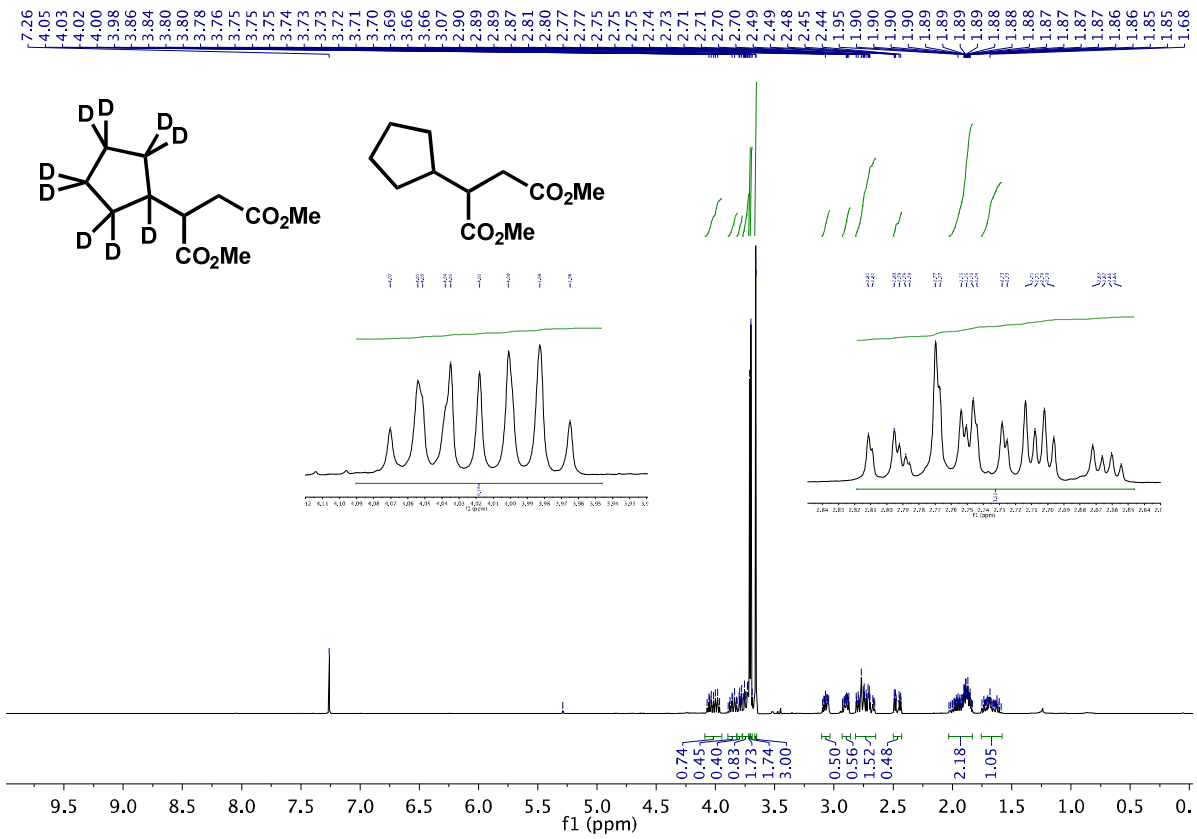

Figure 3.3. ^{1}H NMR spectrum for the isotope labelling study with THF as substrate (1:1 d.r.). Analysis of the product distribution yields a 25:75 ratio for the addition of THF-*d*8:THF to dimethyl maleate giving a ratio of 3.00.

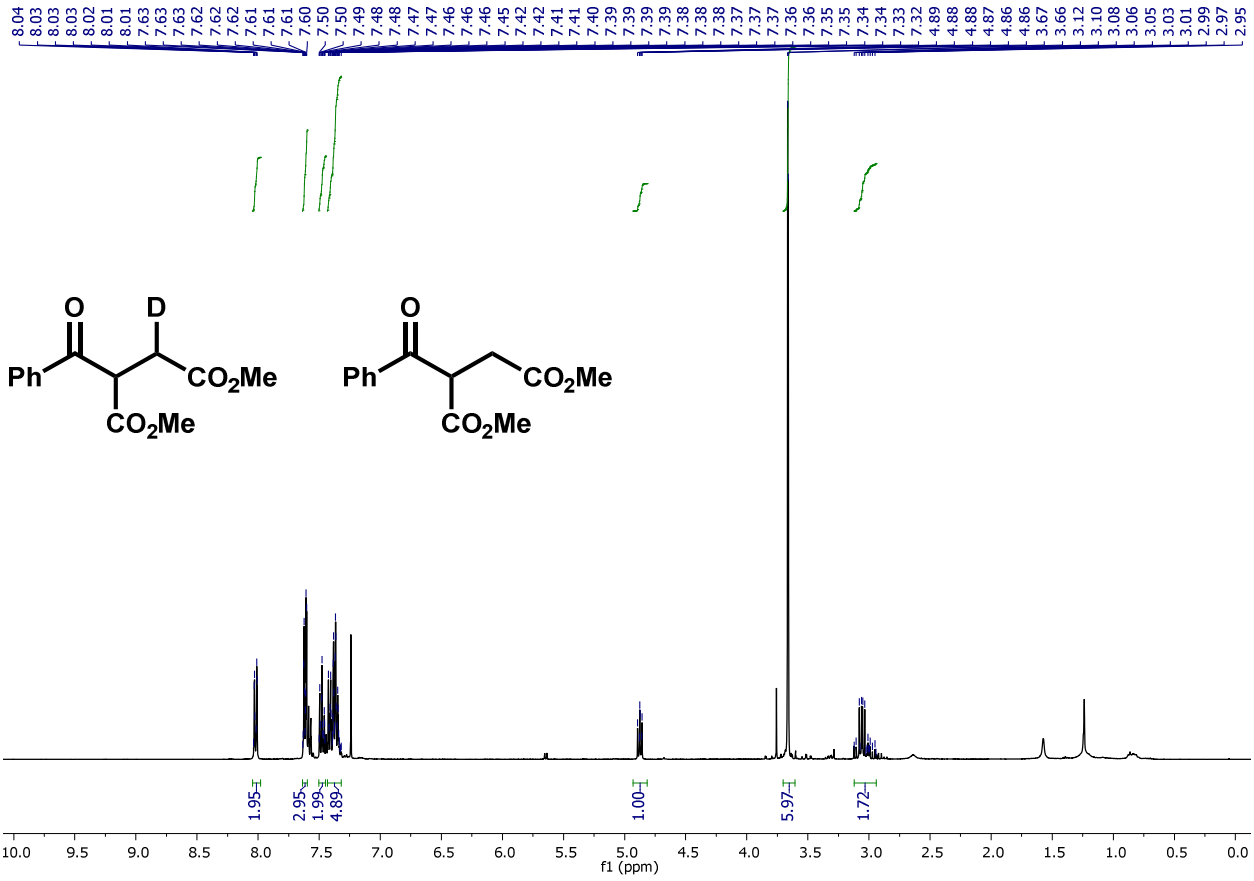

Figure 3.4. Crude ^{1}H NMR spectrum for the isotope labelling study with benzaldehyde as substrate. NMR contains a 42:58 mixture of product:starting material. Analysis of the product distribution yields a 14:86 ratio for the addition of benzaldehyde-*d*:benzaldehyde to dimethyl maleate giving a ratio of 6.14.

3.5.3 Unsuccessful Radical Acceptors

Radical acceptors that polymerized, isomerized, dimerized, or decomposed due to competitive triplet-triplet energy transfer from the excited-state catalyst include: ethyl acrylate, methyl methacrylate, phenyl vinyl sulfone, fumaronitrile, N-phenylsuccinimide, trans-stilbene, 2-cyclohexen-1-one, 2-methyl-2-cyclopenten-1-one, 3-methyl-2-

cyclopenten-1-one, 4-cyclopentene-1,3-dione, 2(5H)-furanone, maleic anhydride, and diisopropyl azodicarboxylate. Small optimizations were attempted on each of these substrates with no success.

3.5.4 Solvent Effect Experiments

All reactions used in the solvent effect experiments were prepared in the same manner as GP2. Following the reaction, all mixtures were purified by flash column chromatography (15:85 EtOAc:Hex) and all fractions containing the product of primary or tertiary addition of methoxycyclopentane **3.13** to dimethyl maleate **3.3** were combined, concentrated *in vacuo*, and total yield recorded. The ratio of 3º:1º additions were elucidated by comparison of the integration of ^{1}H NMR peaks belonging to each product.

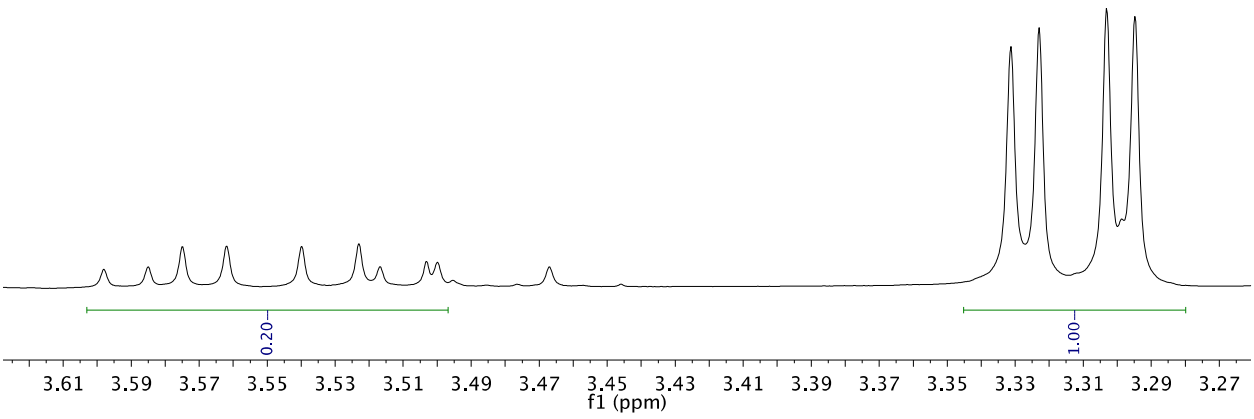

Figure 3.5. Example region and integrations used to calculate the tertiary:primary ratio of addition.

The above example spectrum shows the multiplet belonging to the primary addition product centered at 3.55 ppm (2H) and the doublet of doublets at 3.32 ppm belonging to the tertiary addition product (1H) giving a 3º:1º ratio of 10:1 (see product characterizations **3.32** and **3.32'**).

3.5.5 Stern-Volmer Analysis

The collection of emission spectra for the fluorescence quenching measurements for **3.1-Cl** and **3.1-PF6** were carried out in a Photon Technology International (PTI) spectrofluorimeter at room temperature in Ar atmosphere using 1 × 1 cm^2 quartz cuvettes. Samples of **3.1-Cl** and **3.1-PF6** were prepared with a final absorbance of 0.01 at 400 nm, the wavelength employed for excitation, in MeCN, degassed in Ar. Dimethyl maleate and the solution of TBACl (2.0 M in MeCN) quenchers were degassed with Ar prior to use.

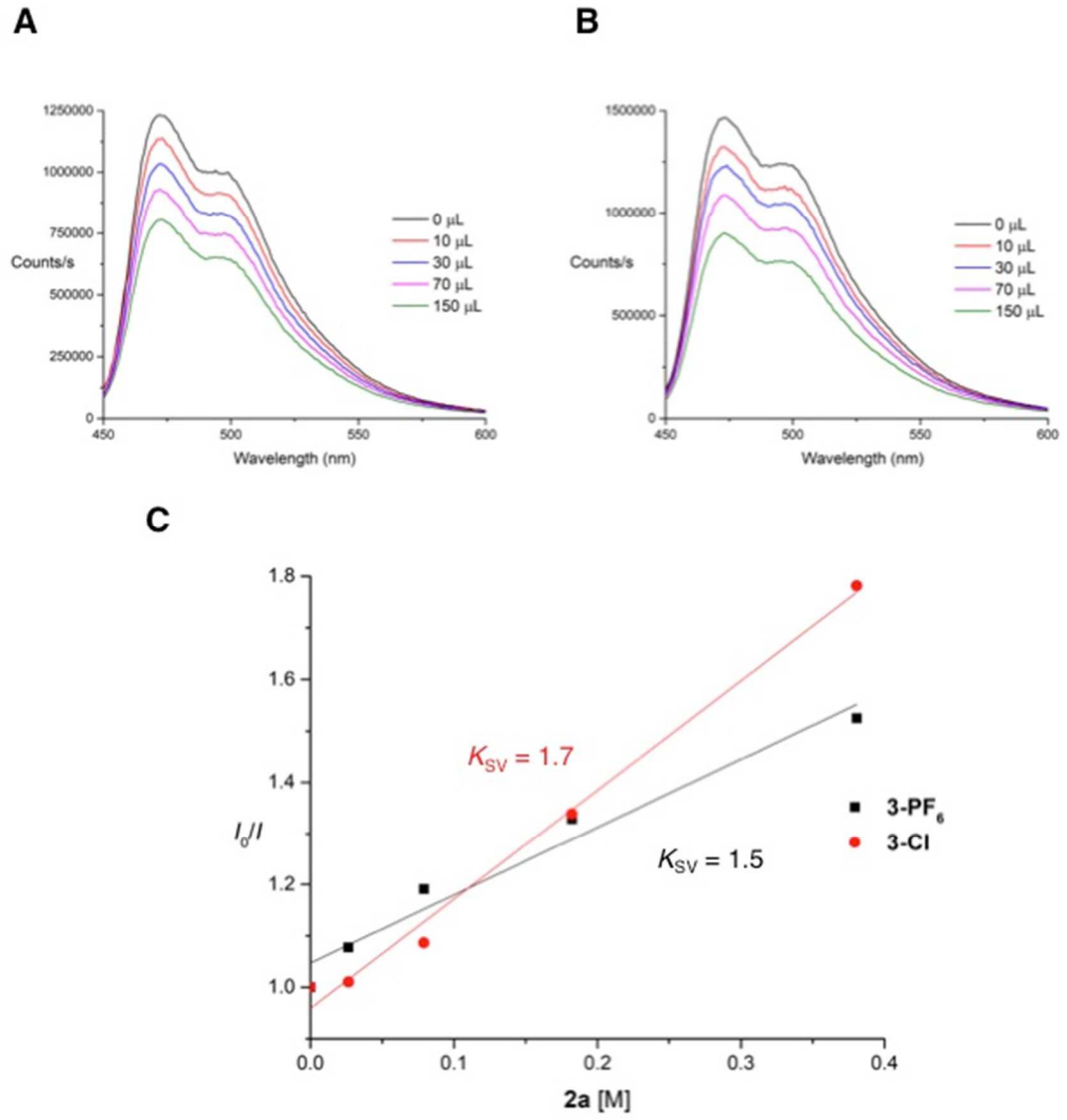

Figure 3.6. Data for the steady state quenching studies of 3.1-PF6 and 3.1-Cl by dimethyl maleate. **(A)** Quenching of 3.1-PF6 emission, **(B)** Quenching of 3.1-Cl emission, and **(C)** corresponding Stern-Volmer plots.

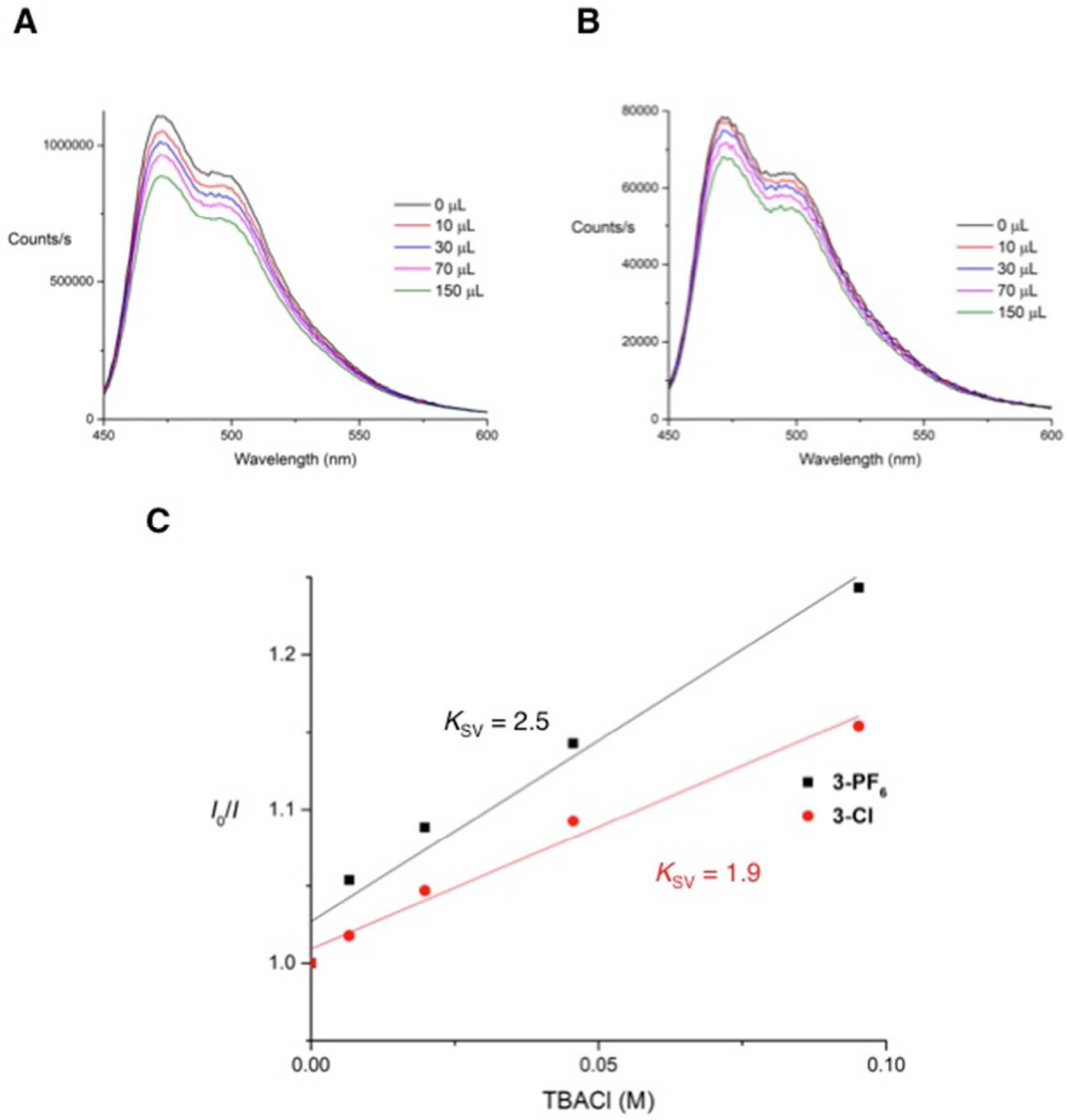

Figure 3.7. Data for the steady state quenching studies of 3.1-PF6 and 3.1-Cl by tetrabutylammonium chloride. **(A)** Quenching of 3.1-PF6 emission, **(B)** Quenching of 3.1-Cl emission, and **(C)** corresponding Stern-Volmer plots.

3.6 Experimental Procedures

3.6.1 General Information

All reactions were performed in Pyrex glassware equipped with a magnetic stir bar, capped with a septum, unless otherwise indicated. All commercial reagents were used without further purification, unless otherwise noted. Reactions were monitored by thin layer chromatography (TLC) analysis. TLC plates were viewed under UV light and stained with potassium permanganate or p-anisaldehyde staining solution. Yields refer to products isolated after purification, unless otherwise stated. Proton nuclear magnetic resonance (^{1}H NMR) spectra were recorded on a Bruker AMX 400 MHz. NMR samples were dissolved in chloroform-d (unless specified otherwise) and chemical shifts are reported in ppm referenced to residual non-deuterated solvent. Carbon nuclear magnetic resonance (^{13}C NMR) spectra were recorded on the same Bruker instrument (101 MHz). IR spectra were recorded with an Agilent Technologies Cary 630 FTIR Spectrometer equipped with a diamond ATR module. HRMS were obtained on a Kratos Analytical Concept instrument (University of Ottawa Mass Spectrum Centre).

Note: The complete Supporting Information for this methodology is available online at https://onlinelibrary.wiley.com/doi/abs/10.1002/anie.201810187. Included in this thesis are the spectral data for compounds *synthesized by S. Rohe only*.

3.6.2 General Procedures

General Procedure 1 (GP1) - *Preparation of Photocatalysts.*

Ir dimers [(dF(CF_3)ppy)$_2$-Ir-μ-Cl]$_2$ and [(dF(CF_3)ppy)$_2$-Ir-μ-Br]$_2$ were synthesized according to literature[19] with modification of aqueous extraction of the filtrate using EtOAc until the aqueous phase was not yellow, resulting in the recuperation of a large amount of the title compound.

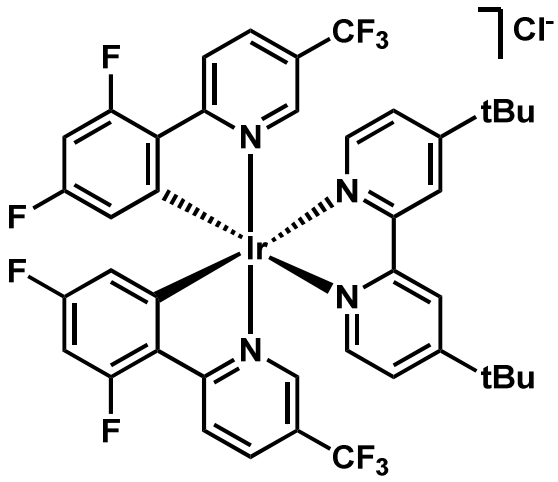

[Ir(dF(CF_3)ppy)$_2$(dtbbpy)]Cl (3.1-Cl)

To a flame-dried round-bottomed flask equipped with a magnetic stir bar under Ar atmosphere was added [(dF(CF_3)ppy)$_2$-Ir-μ-Cl]$_2$ (1.0 equiv), dtbbpy (2.2 equiv), and 2-methoxyethanol (0.02 M) and refluxed while stirring for overnight. The reaction was cooled to room temperature and was extracted with EtOAc and concentrated by rotovap. The resulting solid was dissolved in a minimum of hot dichloromethane, where immediate dilution with hexane resulted in a fine precipitate that was filtered by vacuum filtration, further dried *in vacuo*, giving the title complex in 58% yield as a yellow solid.

IR (neat, cm^{-1}): 2962 (w), 2870 (w), 1600 (s), 1575 (s), 1488 (m), 1442 (m), 1414 (m), 1384 (m), 1327 (vs), 1295 (s), 1134 (s), 1107 (vs), 1088 (vs), 1049 (m), 1020 (m), 990 (s), 919 (w), 897 (w), 846 (s), 831 (s), 721 (s); ^{1}H NMR (400 MHz, $CDCl_3$) δ = 9.79 (d, *J* = 1.7 Hz, 2H), 8.49 (dd, *J* = 8.8, 3.2 Hz, 2H), 8.06 (dd, *J* = 8.8, 2.0 Hz, 2H), 7.84–7.80 (m, 2H), 7.57 (dd, *J* = 5.9, 1.9 Hz, 2H), 7.40 (s, 2H), 6.63 (ddd, *J* = 12.4, 8.9, 2.3 Hz, 2H), 5.63 (dd, *J* = 8.0, 2.3 Hz, 2H), 1.59 (s, 18H) ppm; HRMS (ESI): m/z calc'd for $C_{42}H_{34}N_4F_{10}Ir$ [M^+-Cl^-] 977.2253, found 977.2269.

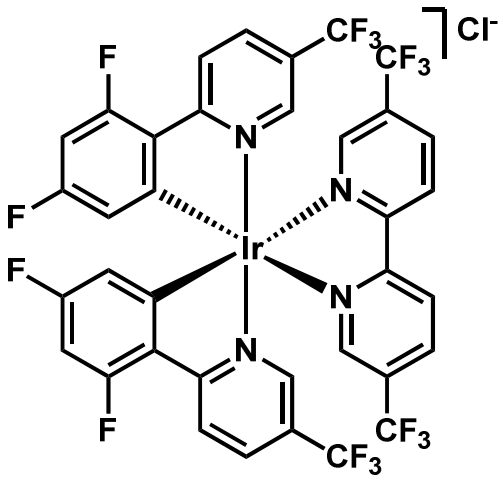

[Ir(dF(CF_3)ppy)$_2$(5,5'-dCF_3bpy)]Cl

Synthesized following the same protocol as 3.1-Cl with 5,5'-dCF_3bpy. After extraction, the resulting solid was dissolved in a minimum of acetone, loaded onto a silica column, and purified by flash chromatography. Initial compound elution between 0-25% acetone:DCM gave a complex that was not the competent photoredox catalyst. Further elution (20% MeOH:DCM) gave a yellow solid after concentration by rotovap. The solid was dissolved in a minimum of hot acetone, where immediate dilution with hexane resulted in a fine

precipitate that was filtered by vacuum filtration, further dried *in vacuo*, giving the title complex in 78% yield as a yellow solid.

IR (neat, cm^{-1}): 2996 (w), 1602 (m), 1578 (m), 1493 (w), 1439 (w), 1384 (w), 1327 (vs), 1298 (s), 1141 (s), 1112 (s), 1091 (s), 1050 (m), 993 (s), 833 (m), 721 (m), 687 (m); ^1H NMR (400 MHz, DMSO-d_6) δ = 9.32 (d, J = 8.7 Hz, 2H), 8.93 (d, J = 8.2 Hz, 2H), 8.46 (s, 4H), 8.11 (s, 2H), 7.73 (s, 2H), 7.18–7.07 (m, 2H), 5.78 (dd, J = 8.5, 2.4 Hz, 2H) ppm; HRMS (ESI): m/z calc'd for $C_{36}H_{16}N_4F_{16}Ir$ $[M^+-Cl^-]$ 1001.0749, found 1001.0771.

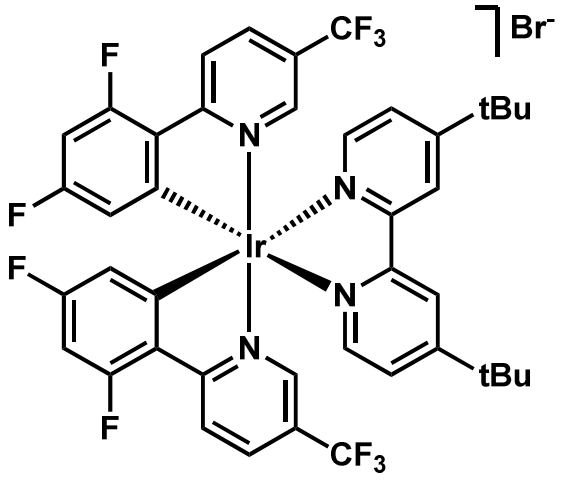

[Ir(dF(CF_3)ppy)$_2$(dtbbpy)]Br (3.1-Br)

Synthesized following the same protocol as 3.1-Cl with [(dF(CF_3)ppy)$_2$-Ir-μ-Br]$_2$. The resulting solid after extraction was dissolved in a minimum of hot acetone, where immediate dilution with hexane resulted in a fine precipitate that was filtered by vacuum filtration, further dried *in vacuo*, giving the title complex in 44% yield as a yellow solid.

IR (neat, cm^{-1}): 2967 (w), 2868 (w), 1600 (s), 1575 (m), 1488 (m), 1438 (w), 1488 (w), 1415 (w), 1385 (w), 1328 (vs), 1297 (s), 1250 (m), 1168 (m), 1130 (s), 1108 (vs), 1089 (s), 1049 (m), 1020 (m), 992 (s), 848 (s), 832 (s), 722 (s); ^1H NMR (400 MHz, $CDCl_3$) δ = 9.61 (d, *J* = 1.9 Hz, 2H), 8.49 (dd, *J* = 8.8, 3.2 Hz, 2H), 8.06 (dd, *J* = 8.8, 2.1 Hz, 2H), 7.84 (d, *J* = 5.8 Hz, 2H), 7.59 (dd, *J* = 5.9, 1.9 Hz, 2H), 7.40 (s, 2H), 6.64 (ddd, *J* = 12.4, 8.9, 2.3 Hz, 2H), 5.63 (dd, *J* = 8.0, 2.3 Hz, 2H), 1.59 (s, 18H) ppm; HRMS (ESI): m/z calc'd for $C_{42}H_{34}N_4F_{10}Ir$ [M^+-Br^-] 977.2253, found 977.2247.

General Procedure 2 (GP2) - *Synthesis of Products.*

To an 8 mL screw-topped Pyrex reaction vessel equipped with a stir bar was added [Ir(dF(CF_3)ppy)$_2$(dtbbpy)]Cl (0.004 mmol, 2 mol%), maleate/fumarate acceptor (0.2 mmol, 1 equiv), alkylating agent (0.6 mmol, 3.0 equiv), and benzene (0.4 mL, 0.5 M). The solution was degassed by sparging under argon for 5 minutes, sealed with parafilm, and irradiated with a Blue LED (465 nm) at a distance of 1 mm for 16 hours. Upon completion, the solution was concentrated by rotovap and the crude residue was further purified by column chromatography (0-100% EtOAc:Hex or 0-20% MeOH:DCM), where relevant fractions were combined, concentrated and characterized by proton and carbon NMR (400 and 101 MHz, respectively), HR-MS, and IR.

3.7 Characterization Data

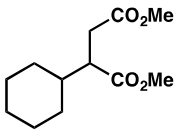

dimethyl 2-cyclohexylsuccinate (3.4)

Synthesized according to GP2 and isolated as clear oil from dimethyl maleate and fumarate in 68% and 74% yield, respectively, characterized according to NMR comparison.[20]

^{1}H NMR (400 MHz, $CDCl_3$): δ = 3.67 (s, 3H), 3.64 (s, 3H), 2.76–2.65 (m, 2H), 2.44 (dt, *J* = 13.1, 8.9 Hz, 1H), 1.77–1.68 (m, 2H), 1.68–1.53 (m, 4H), 1.28–1.14 (m, 2H), 1.14–0.93 (m, 3H) ppm; ^{13}C NMR (101 MHz, $CDCl_3$): δ = 175.1 (C), 173.1 (C), 51.8 (CH_3), 51.7 (CH_3), 47.1 (CH), 40.1 (CH), 33.4 (CH_2), 30.7 (CH_2), 30.3 (CH_2), 26.4 (2 X CH_2), 26.2 (CH_2) ppm.

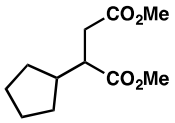

dimethyl 2-cyclopentylsuccinate (3.33)

Synthesized according to GP2 and isolated as a clear oil in 69% yield.

IR (neat, cm^{-1}): 2951 (m), 2870 (w), 1732 (vs), 1436 (m), 1350 (m), 1258 (m), 1193 (s), 1159 (vs), 1004 (m), 847 (w); ^{1}H NMR (400 MHz, $CDCl_3$): δ = 3.68 (s, 3H), 3.65 (s, 3H), 2.74 (dd, *J* = 15.8, 10.7 Hz, 1H), 2.70–2.63 (m, 1H), 2.49 (dd, *J* = 16.0, 3.3 Hz, 1H), 2.01–1.89 (m, 1H), 1.81–1.71 (m, 1H), 1.70–1.57 (m, 3H), 1.57–1.46 (m, 2H), 1.32–1.22 (m, 1H), 1.22–1.10 (m, 1H) ppm; ^{13}C NMR (101 MHz, $CDCl_3$): δ = 175.5 (C), 172.8 (C), 51.9 (CH_3), 51.7 (CH_3), 46.3 (CH), 42.5 (CH), 35.5 (CH_2), 30.6 (CH_2), 30.5 (CH_2), 25.1 (CH_2), 25.0 (CH_2) ppm; HRMS (EI): m/z calc'd for $C_9H_{15}O_2$ [M^+-$C_2H_3O_2$] 155.1072, found 155.1057.

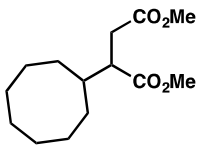

dimethyl 2-cyclooctylsuccinate (3.34)

Synthesized according to GP2 and isolated as a clear oil in 53% yield.

IR (neat, cm^{-1}): 2921 (m), 2853 (w), 1736 (vs), 1437 (w), 1344 (w), 1259 (w), 1163 (s), 10023 (w), 1003 (w); ^1H NMR (400 MHz, $CDCl_3$): δ = 3.67 (s, 3H), 3.65 (s, 3H), 2.81–2.68 (m, 2H), 2.40 (dd, *J* = 15.6, 2.6 Hz, 1H), 1.96–1.86 (m, 1H), 1.71–1.27 (m, 14H) ppm; ^{13}C NMR (101 MHz, $CDCl_3$): δ = 175.2 (C), 173.2 (C), 51.9 (CH_3), 51.8 (CH_3), 48.1 (CH), 39.2 (CH), 33.0 (CH_2), 31.1 (CH_2), 29.8 (CH_2), 26.7 (CH_2), 26.6 (CH_2), 26.6 (CH_2), 26.0 (CH_2), 25.9 (CH_2) ppm; HRMS (EI): m/z calc'd for $C_{13}H_{21}O_3$ [M^+-CH_3O] 225.1491, found 225.1487.

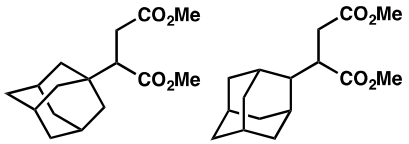

dimethyl 2-(adamantan-2-yl)succinate and dimethyl 2-(adamantan-1-yl)succinate (3.35:3.35', 62:38)

Synthesized according to GP2, isolated as a clear oil in 61% yield, and characterized by NMR comparison.[21]

IR (neat, cm^{-1}): 2905 (w), 2850 (s), 1735(s), 1437 (m), 1162 (s), 846 (m);

3.35: ^1H NMR (400 MHz, $CDCl_3$): δ = 3.66 (s, 3H), 3.62 (s, 3H), 2.72 (dd, *J* = 17.1, 12.3 Hz, 1H), 2.51–2.34 (m, 2H), 2.09–1.34 (m, 15H) ppm; ^{13}C NMR (101 MHz, $CDCl_3$): δ = 174.3 (C), 173.4 (C), 52.3 (CH), 51.8 (CH_3), 51.6 (CH_3), 42.9 (CH), 38.7 (CH_2), 38.0 (CH_2), 36.7 (2 X CH_2), 34.4 (C), 31.3 (CH_2), 31.0 (CH_2), 30.8 (CH), 29.0 (CH), 27.6 (CH_2) ppm;

3.35': ^1H NMR (400 MHz, $CDCl_3$): δ = 3.66 (s, 3H), 3.63 (s, 3H), 3.17–3.03 (m, 1H), 2.64–2.52 (m, 2H), 2.51–2.34 (m, 1H), 2.09–1.34 (m, 14H); ^{13}C NMR (101 MHz, $CDCl_3$): δ = 176.1 (C), 172.8 (C), 52.3 (2 X CH), 51.8 (CH_3), 51.3 (CH_3), 46.6 (CH), 40.0 (2 X CH_2),

38.8 (CH_2), 34.9 (CH_2), 31.6 (CH_2), 28.5 (3 X CH), 27.8 (CH_2) ppm; HRMS (EI): m/z calc'd for $C_{16}H_{24}O_4$ [M^+] 280.1675, found 280.1673.

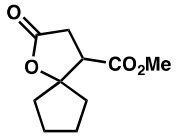

methyl 2-oxo-1-oxaspiro[4.4]nonane-4-carboxylate (3.9)

Synthesized according to GP2 and isolated as a clear oil in 33% yield.

IR (neat, cm^{-1}): 2957 (w), 2879 (w), (1778 (vs), 1736 (vs), 1437 (w), 1360 (w), 1343 (w), 1238 (m), 1167 (m), 985 (m), 928 (w); ^1H NMR (400 MHz, $CDCl_3$): δ = 3.75 (s, 3H), 3.36 (t, J = 8.4 Hz, 1H), 3.00 (dd, J = 17.7, 8.2 Hz, 1H), 2.72 (dd, J = 17.7, 8.6 Hz, 1H), 2.09–1.92 (m, 2H), 1.90–1.79 (m, 3H), 1.79–1.67 (m, 2H), 1.66–1.58 (m, 1H) ppm; ^{13}C NMR (101 MHz, $CDCl_3$): δ = 174.3 (C), 170.9 (C), 94.9 (C), 52.5 (CH_3), 48.1 (CH), 39.0 (CH_2), 34.7 (CH_2), 32.8 (CH_2), 23.9 (CH_2), 23.4 (CH_2) ppm; HRMS (EI): m/z calc'd for $C_{10}H_{14}O_4$ [M^+] 198.0892, found 198.0886.

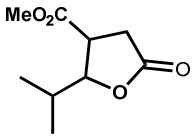

methyl 2-isopropyl-5-oxotetrahydrofuran-3-carboxylate (3.10)

Synthesized according to GP2 and isolated as an inseparable mixture of two diastereoisomers. Isolated yellow oil in 69% yield, characterized by NMR comparison.[22]

Major diasteroisomer: ^1H NMR (400 MHz, $CDCl_3$): δ = 4.42 (dd, J = 6.7, 6.1 Hz, 1H), 3.74 (s, 3H), 3.10 (ddd, J = 10.0, 8.0, 6.7 Hz, 1H), 2.95 – 2.68 (m, 2H), 1.98 – 1.83 (m, 1H), 0.97 (t, J = 6.8 Hz, 6H) ppm; ^{13}C NMR (101 MHz, $CDCl_3$): δ = 174.4 (C), 172.2 (C), 86.5 (CH), 52.7 (CH_3), 42.8 (CH_2), 32.6 (CH), 32.5 (CH), 17.2 (2 X CH_3) ppm.

Minor diastereoisomer: ^{1}H NMR (400 MHz, $CDCl_3$): δ = 3.99 – 3.86 (m, 2H), 3.71 (s, 3H), 2.95 – 2.68 (m, 2H), 2.35 (dd, *J* = 16.5, 7.3 Hz, 1H), 0.97 (t, *J* = 6.8 Hz, 6H) ppm; ^{13}C NMR (101 MHz, $CDCl_3$): δ = 174.4 (C), 172.2 (C), 86.5 (CH), 52.1 (CH_3), 47.1 (CH_2), 29.5 (CH), 24.1 (CH), 17.7 (2 X CH_3) ppm.

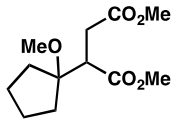

dimethyl 2-(1-methoxycyclopentyl)succinate (3.32)

Synthesized according to GP2 and isolated as a clear oil in 44% yield.

IR (neat, cm^{-1}): 2957 (w), 2874 (w), 2829 (w), 1731 (vs), 1436 (m), 1193 (m), 1160 (vs), 1066 (s), 976 (w), 899 (w), 849 (w); ^{1}H NMR (400 MHz, $CDCl_3$): δ = 3.70 (s, 3H), 3.66 (s, 3H), 3.32 (dd, *J* = 11.3, 3.3 Hz, 1H), 3.13 (s, 3H), 2.84 (dd, *J* = 17.2, 11.3 Hz, 1H), 2.62 (dd, *J* = 17.2, 3.3 Hz, 1H), 1.92–1.84 (m, 1H), 1.78–1.59 (m, 5H), 1.56–1.49 (m, 2H) ppm; ^{13}C NMR (101 MHz, $CDCl_3$): δ = 173.9 (C), 173.2 (C), 87.0 (C), 52.0 (CH_3), 51.9 (CH_3), 49.5 (CH_3), 45.5 (CH), 33.5 (CH_2), 33.2 (CH_2), 32.6 (CH_2), 23.8 (CH_2), 23.4 (CH_2) ppm; HRMS (ESI): m/z calc'd for $C_{12}H_{20}O_5Na$ [M^+] 267.1208, found 267.1221.

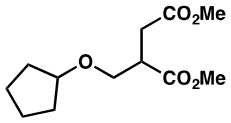

dimethyl 2-((cyclopentyloxy)methyl)succinate (3.32')

Synthesized according to GP2 and isolated as a clear oil in 15% yield.

IR (neat, cm^{-1}): 2957 (w), 2874 (w), 2829 (w), 1731 (vs), 1436 (m), 1193 (m), 1160 (vs), 1066 (s), 976 (w), 899 (w), 849 (w); ^{1}H NMR (400 MHz, $CDCl_3$): δ = 3.87–3.81 (m, 1H), 3.70 (s, 3H), 3.68 (s, 3H), 3.62–3.51 (m, 2H), 3.09 (ddt, *J* = 8.4, 6.8, 5.4 Hz, 1H), 2.78 (dd, *J* = 16.8, 8.4 Hz, 1H), 2.58 (dd, *J* = 16.8, 5.5 Hz, 1H), 1.72–1.58 (m, 6H), 1.53–1.45

(m, 2H) ppm; ^{13}C NMR (101 MHz, $CDCl_3$): δ = 173.5 (C), 172.7 (C), 81.8 (CH), 68.3 (CH_2), 52.1 (CH_3), 51.9 (CH_3), 42.3 (CH), 33.2 (CH_2), 32.3 (CH_2), 32.2 (CH_2), 23.6 (CH_2), 23.6 (CH_2) ppm; HRMS (ESI): m/z calc'd for $C_{12}H_{20}O_5Na$ [M^+] 267.1208, found 267.1213.

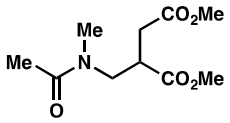

dimethyl 2-((*N*-methylacetamido)methyl)succinate (3.37)

Synthesized according to GP2 and isolated as a pale-yellow oil in 86% yield and characterized as a 70:30 mixture of rotamers.

IR (neat, cm^{-1}): 2955 (w), 2854 (w), 1731 (vs), 1634 (s), 1438 (m), 1408 (m), 1369 (m), 1266 (m), 1202 (s), 1167 (s), 1013 (m), 889 (w), 839 (w);

Major Rotamer: ^{1}H NMR (400 MHz, $CDCl_3$): δ = 3.67 (s, 3H), 3.64 (s, 3H), 3.66–3.39 (m, 2H), 3.20–3.08 (m, 1H), 2.97 (s, 3H), 2.70 (dd, *J* = 16.0, 10.0 Hz 1H), 2.48 (dd, *J* = 18.0, 6.0 Hz, 1H), 2.03 (s, 3H) ppm; ^{13}C NMR (101 MHz, $CDCl_3$): δ = 173.6 (C), 172.2 (C), 171.3 (C), 52.3 (CH_3), 51.9 (CH_3), 49.1 (CH_2), 40.0 (CH), 37.0 (CH_3), 33.6 (CH_2), 21.9 (CH_3) ppm;

Minor Rotamer: ^{1}H NMR (400 MHz, $CDCl_3$): δ = 3.69 (s, 3H), 3.67 (s, 3H), 3.66–3.39 (m, 2H), 3.20–3.08 (m, 1H), 2.87 (s, 3H), 2.69 (dd, *J* = 16.0, 8.0 Hz, 1H), 2.44 (dd, *J* = 16.0, 4.0 Hz, 1H), 2.06 (s, 3H) ppm; ^{13}C NMR (101 MHz, $CDCl_3$): δ = 173.4 (C), 171.5 (C), 170.8 (C), 52.5 (CH_3), 52.2 (CH_3), 51.8 (CH_2), 40.5 (CH), 37.0 (CH_3), 33.4 (CH_2), 21.2 (CH_3) ppm; HRMS (EI): m/z calc'd for $C_8H_{14}NO_4$ [M^+-C_2H_3O] 188.0923, found 188.0950.

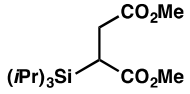

dimethyl 2-(triisopropylsilyl)succinate (3.38)

Synthesized according to GP2 and isolated as a clear oil in 65% yield.

IR (neat, cm^{-1}): 2947 (m), 2869 (m), 1742 (s), 1720 (vs), 1464 (m), 1435 (m), 1203 (s), 1152 (vs), 882 (s), 670 (m); ^1H NMR (400 MHz, $CDCl_3$): δ = 3.66 (s, 3H), 3.64 (s, 3H), 3.03 (dd, *J* = 17.2, 12.5 Hz, 1H), 2.75 (dd, *J* = 12.6, 2.4 Hz, 1H), 2.39 (dd, *J* = 17.2, 2.4 Hz, 1H), 1.21–1.13 (m, 3H), 1.11 (d, *J* = 6.6 Hz, 9H), 1.05 (d, *J* = 6.9 Hz, 9H) ppm; ^{13}C NMR (101 MHz, $CDCl_3$): δ = 175.9 (C), 173.8 (C), 51.9 (CH_3), 51.4 (CH_3), 31.8 (CH_2), 28.1 (CH), 18.6 (3 X CH_3), 18.5 (3 X CH_3), 11.5 (3 X CH) ppm; HRMS (EI): m/z calc'd for $C_{12}H_{23}O_4Si$ [M^+-C_3H_7] 259.1366, found 259.1384.

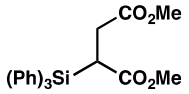

dimethyl 2-(triphenylsilyl)succinate (3.39)

Synthesized according to GP2, isolated as a clear oil in 55% yield, and characterized by NMR comparison.[10]

^1H NMR (400 MHz, $CDCl_3$): δ = 7.63–7.56 (m, 6H), 7.48–7.36 (m, 9H), 3.63 (s, 3H), 3.53–3.44 (m, 1H), 3.32 (s, 3H), 3.02 (dd, *J* = 17.6, 12.2 Hz, 1H), 2.51 (dd, *J* = 17.5, 2.9 Hz, 1H) ppm; ^{13}C NMR (101 MHz, CDCl3): δ = 174.7 (C), 173.4 (C), 136.2 (6 X CH), 132.0 (3 X C), 130.2 (3 X CH), 128.1 (6 X CH), 52.0 (CH_3), 51.4 (CH_3), 32.8 (CH_2), 31.2 (CH) ppm.

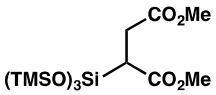

dimethyl 2-(1,1,1,5,5,5-hexamethyl-3-((trimethylsilyl)oxy)trisiloxan-3-yl)succinate (3.40)

Synthesized according to GP2 and isolated as a clear oil in 66% yield.

IR (neat, cm^{-1}): 2957 (w), 1732 (m), 1436 (w), 1251 (m), 1155 (m), 1056 (vs), 836 (vs), 754 (s), 689 (w); ^1H NMR (400 MHz, $CDCl_3$): δ = 3.67 (s, 3H), 3.65 (s, 3H), 2.85 (dd, *J* = 17.3, 11.8 Hz, 1H), 2.51–2.36 (m, 2H), 0.11 (s, 27H) ppm; ^{13}C NMR (101 MHz, $CDCl_3$): δ = 173.9 (C), 173.7 (C), 52.0 (CH_3), 51.6 (CH_3), 31.8 (CH), 31.2 (CH_2), 1.7 (9 X CH_3) ppm; HRMS (EI): m/z calc'd for $C_{15}H_{36}O_7Si_4$ [M^+] 440.1538, found 440.1544.

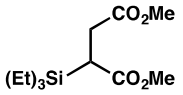

dimethyl 2-(triethylsilyl)succinate (3.41)

Synthesized according to GP2, isolated as a clear oil in 51% yield, and characterized by NMR comparison.[10]

^1H NMR (400 MHz, $CDCl_3$): δ = 3.64 (s, 3H), 3.63 (s, 3H), 2.87 (dd, *J* = 17.2, 12.2 Hz, 1H), 2.56 (dd, *J* = 12.2, 3.0 Hz, 1H), 2.31 (dd, *J* = 17.2, 3.0 Hz, 1H), 0.93 (t, *J* = 7.9 Hz, 9H), 0.59 (qd, *J* = 7.9, 3.6 Hz, 6H) ppm; ^{13}C NMR (101 MHz, $CDCl_3$): δ = 175.3 (C), 173.5 (C), 52.1 (CH_3), 51.3 (CH_3), 31.2 (CH_2), 29.7 (CH), 7.1 (3 X CH_3), 2.5 (3 X CH_2) ppm.

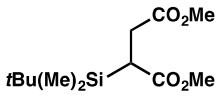

dimethyl 2-(*tert*-butyldimethylsilyl)succinate (3.42)

Synthesized according to GP2 and isolated as a clear oil in 81% yield.

IR (neat, cm^{-1}): 2953 (w), 2930 (w), 2858 (w), 1742 (s), 1720 (vs), 1435 (m), 1229 (m), 1202 (s), 1151 (vs), 841 (s), 825 (s), 775 (m); ^1H NMR (400 MHz, $CDCl_3$): δ = 3.66 (s, 3H), 3.65 (s, 3H), 2.91 (dd, *J* = 17.3, 12.3 Hz, 1H), 2.58 (dd, *J* = 12.3, 3.0 Hz, 1H), 2.40 (dd, *J* = 17.3, 2.9 Hz, 1H), 0.92 (s, 9H), 0.06 (s, 3H), 0.01 (s, 3H) ppm; ^{13}C NMR (101 MHz, $CDCl_3$): δ = 175.7 (C), 173.6 (C), 52.0 (CH_3), 51.4 (CH_3), 32.4 (CH_2), 30.2 (CH),

26.7 (3 X CH_3), 17.7 (C), -6.5 (CH_3), -6.6 (CH_3) ppm; HRMS (EI): m/z calc'd for $C_{11}H_{21}O_3Si$ [M^+-CH_3O] 229.1260, found 229.1287.

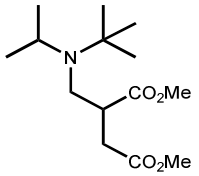

dimethyl 2-((tert-butyl(isopropyl)amino)methyl)succinate (3.43)

Synthesized according to GP2 and isolated as a light yellow oil in 49% yield. ^1H NMR (400 MHz, $CDCl_3$): δ = 3.66 (s, 3H), 3.64 (s, 3H), 3.24 (hept, *J* = 6.7 Hz, 1H), 2.96 (dddd, *J* = 10.4, 9.4, 6.5, 3.9 Hz, 1H), 2.86 (dd, *J* = 14.4, 6.5 Hz, 1H), 2.77 (dd, *J* = 16.8, 3.9 Hz, 1H), 2.51 (ddd, *J* = 14.4, 12.8, 9.9 Hz, 2H), 1.04 (s, 9H), 1.03 – 0.86 (m, 6H) ppm; ^{13}C NMR (101 MHz, $CDCl_3$): δ = 175.3 (C), 173.2 (C), 55.9 (C), 51.6 (2 X CH_3), 51.6 (CH) 46.6 (CH), 44.7 (CH_2), 44.3 (2 X CH_3), 33.8 (CH_2), 28.6 (3 X CH_3) ppm; HRMS (EI): m/z calc'd for $C_{14}H_{28}NO_4$ [M^+ + H^+] 274.2010, found 274.2008.

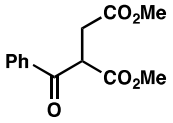

dimethyl 2-benzoylsuccinate (3.44)

Synthesized according to GP2, isolated as a yellow oil in 63% yield, and characterized by NMR comparison.[11]

^1H NMR (400 MHz, $CDCl_3$): δ = 8.07–8.01 (m, 2H), 7.64–7.57 (m, 1H), 7.53–7.47 (m, 2H), 4.89 (dd, *J* = 7.7, 6.7 Hz, 1H), 3.69 (s, 3H), 3.68 (s, 3H), 3.15–3.00 (m, 2H) ppm; ^{13}C NMR (101 MHz, $CDCl_3$): δ = 194.2 (C), 171.9 (C), 169.3 (C), 135.9 (C), 133.9 (CH), 129.0 (2 X CH), 128.9 (2 X CH), 53.0 (CH_3), 52.3 (CH_3), 49.4 (CH), 33.2 (CH_2) ppm.

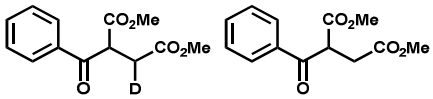

dimethyl 2-benzoylsuccinate-3-d (3.44' containing 3.44)

Synthesized according to GP2, isolated as a yellow oil as an inseparable mixture of 3.44 and 3.44' in 85% yield.

^{1}H NMR (400 MHz, $CDCl_3$): δ = 8.07 – 7.95 (m, 2H), 7.64 – 7.55 (m, 1H), 7.52 – 7.42 (m, 2H), 4.93 – 4.81 (m, 1H), 3.66 (d, *J* = 2.3 Hz, 6H), 3.12 – 2.94 (m, 2H) ppm; ^{13}C NMR (101 MHz, $CDCl_3$): δ = 194.0 (C), 171.7 (C), 169.2 (C), 135.8 (C), 133.8 (CH), 128.8 (4 X CH), 52.9(CH_3), 52.1 (CH_3), 49.3 (CH), 33.1 (t, CD) ppm. HRMS (ESI): m/z calc'd for $C_{13}H_3DO_5Na$ [M^+] 274.0796, found 274.0760.

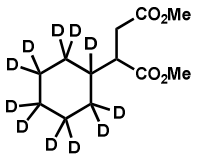

Dimethyl 2-(cyclohexyl-d11)succinate (3.45)

Synthesized according to GP2, isolated as a yellow oil in 78% yield.

^{1}H NMR (400 MHz, $CDCl_3$): δ = 3.66 (s, 3H), 3.63 (s, 3H), 2.74 – 2.64 (m, 2H), 2.47 – 2.36 (m, 1H) ppm; ^{13}C NMR (101 MHz, $CDCl_3$): δ = 175.0 (C), 173.0 (C), 51.7 (CH_3), 51.6 (CH_3), 46.9 (CH), 39.0 (m, 2 X CD_2), 29.16 (m, 2 X CD_2), 24.9 (m, CD_2) 33.2 (CH_2) ppm; HRMS (ESI): m/z calc'd for $C_{12}H_9D_{11}O_4Na$ [M^+] 262.1950, found 262.1940.

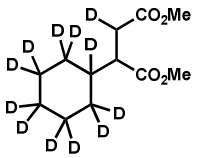

dimethyl 2-(cyclohexyl-d11)succinate-3-d (3.45')

Synthesized according to GP2, isolated as a yellow oil as an inseparable mixture of (3.45 and 3.45') in 63% yield.

^{1}H NMR (400 MHz, $CDCl_3$): δ = 3.66 (s, 3H), 3.63 (s, 3H), 2.74 – 2.64 (m, 2H), 2.47 – 2.36 (m, 1H) ppm; ^{13}C NMR (101 MHz, $CDCl_3$): δ = 175.0 (C), 173.0 (C), 51.7 (CH_3), 51.6 (CH_3), 46.9 (CH), 39.0 (m, 2 X CD_2), 29.16 (m, 2 X CD_2), 24.9 (m, CD_2) 33.2 (CH_2) ppm; HRMS (EI): m/z calc'd for $C_{12}H_8D_{12}O_4Na$ [M^+] 262.1955, found 262.1950.

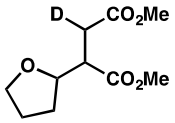

dimethyl 2-(tetrahydrofuran-2-yl)-succinate-3-*d* (d-3.47:d-3.47', 1:1 d.r.)

Synthesized according to GP2, isolated diastereomers separately as clear oils in 65% yield (1:1 d.r. with respect to THF) and characterized as two separate 1:1 mixtures of diastereomers (with respect to D).

IR (neat, cm^{-1}): 2953 (w), 2876 (w), 1732 (vs), 1436 (m), 1250 (m), 1200 (s), 1167 (s), 1067 (s), 1018 (m); Diastereomer 1 (d-4aga, less polar): ^{1}H NMR (400 MHz, $CDCl_3$): δ = 4.03–3.96 (m, 1H), 3.80 (dt, *J* = 8.4, 6.7 Hz, 1H), 3.75–3.69 (m, 4H), 3.66 (s, 3H), 2.94–2.87 (m, 1H), 2.76 (dt, *J* = 9.7, 2.5 Hz, 0.52H, diastereomer), 2.68 (quint, *J* = 2.4 Hz, 0.47H, diastereomer), 1.98 (ddt, *J* = 11.7, 8.5, 6.2 Hz, 1H), 1.93–1.81 (m, 2H), 1.77–1.66 (m, 1H) ppm; ^{13}C NMR (101 MHz, $CDCl_3$): δ = 173.5 (C), 172.8 (C), 78.8 (CH, diastereomers), 68.2 (CH_2), 52.2 (CH_3), 51.9 (CH_3), 46.7 (CH, diastereomers), 33.0 (t, *J* = x.x Hz, CHD), 29.8 (CH_2), 25.7 (CH_2) ppm; Diastereomer 2 (d-4aga', more polar): ^{1}H NMR (400 MHz, $CDCl_3$): δ = 4.05 (q, *J* = 7.0 Hz, 1H), 3.85 (dt, *J* = 8.3, 6.7 Hz, 1H), 3.77–3.69 (m, 4H), 3.66 (s, 3H), 3.07 (td, *J* = 6.5, 3.0 Hz, 1H), 2.74 (dt, *J* = 12.0, 4.0 Hz, 0.4H, diastereomer), 2.45 (dt, *J* = 4.5, 2.3 Hz, 0.60H, diastereomer), 1.99–1.82 (m, 3H), 1.70–

1.58 (m, 1H) ppm; ^{13}C NMR (101 MHz, $CDCl_3$): δ = 173.4 (C), 172.4 (C), 79.0 (CH), 68.5 (CH_2), 52.2 (CH_3), 52.0 (CH_3), 46.1 (CH, diastereomers), 32.3 (t, *J* = 19.7 Hz, CHD), 28.8 (CH_2), 25.8 (CH_2) ppm;

HRMS (EI): m/z calc'd for $C_9H_{21}DO_4$ [M^+-CH_3O] 186.0877, found 186.08743.

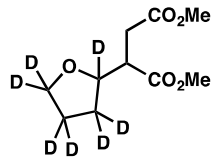

dimethyl 2-(tetrahydrofuran-2-yl-*d*$_7$)succinate (d$_7$-3.45:d$_7$-3.45', 55:45 d.r.)

Synthesized according to GP2 and isolated as a clear oil in 72% yield.

IR (neat, cm^{-1}): 2996 (w), 2954 (w), 2239 (w), 2102 (w), 1731 (vs), 1437 (m), 1345 (m), 1265 (m), 1233 (m), 1192 (s), 1161 (vs), 1104 (m), 1041 (s), 880 (w), 849 (m), 753 (w), 688 (w); ^{1}H NMR (400 MHz, $CDCl_3$): δ = 3.70 (s, 3H, minor diastereomer), 3.69 (s, 3H, major diastereomer), 3.65 (s, 3H), 3.06 (dd, *J* = 10.1, 4.5 Hz, 0.45H, minor diastereomer), 2.89 (dd, *J* = 9.3, 4.7 Hz, 0.55H, major diastereomer), 2.81–2.42 (m, 2H) ppm; Major diastereomer: ^{13}C NMR (101 MHz, $CDCl_3$): δ = 173.5 (C), 172.8 (C), 52.1 (CH_3), 51.9 (CH_3), 46.6 (CH), 32.6 (CH_2) ppm; Minor diastereomer: ^{13}C NMR (101 MHz, $CDCl_3$): δ = 173.4 (C), 172.4 (C), 52.1 (CH_3), 52.0 (CH_3), 46.0 (CH), 32.6 (CH_2) ppm; HRMS (EI): m/z calc'd for $C_9H_6D_7O_4$ [M^+-CH_3O] 192.1253, found 192.1272.

3.8 References

1. a) G. A. Russell, H. C. Brown, The Liquid Phase Photochlorination and Sulfuryl Chloride Chlorination of Branchedchain Hydrocarbons; the Effect of Structure on the Relative Reactivities of Tertiary Hydrogen in Free Radical Chlorinations. *J. Am. Chem.*

Soc. **1955**, *77*, 4031; b) J. S. Pilgrim, A. McIlroy, C. A. Taatjes, Kinetics of Cl Atom Reactions with Methane, Ethane, and Propane from 292 to 800 K. *J. Phys. Chem. A* **1997**, *101*, 1873.

2. a) H. O. Pritchard, J. B. Pyke, A. F. Trotman-Dickenson, The Study of Chlorine Atom Reactions in the Gas Phase. *J. Am. Chem. Soc*. **1955**, *77*, 2629; b) G. A. Russell, Solvent Effects in the Reactions of Free Radicals and Atoms. *J. Am. Chem. Soc*. **1957**, *79*, 2977; c) G. A. Russell, Solvent Effects in the Reactions of Free Radicals and Atoms. II. Effects of Solvents on the Position of Attack of Chlorine Atoms upon 2,3-Dimethylbutane, Isobutane and 2-Deuterio-2-methylpropane. *J. Am. Chem. Soc*. **1958**, *80*, 4987; d) C. Walling, M. F. Mayahi, Some Solvent and Structural Effects in Free Radical Chlorination. *J. Am. Chem. Soc*. **1959**, *81*, 1485; e) E. Tschuikow-Roux, J. Niedzielski, F. Faraji, Competitive photochlorination and kinetic isotope effects for hydrogen/deuterium abstraction from the methyl group in C_2H_6, C_2D_6, CH_3CHCl_2, CD_3CHCl_2, CH_3CCl_3, and CD_3CCl_3. *Can. J. Chem*. **1985**, *63*, 1093; f) S. Forgeteg, T. Berces, Laser flash photolysis study of chlorine atom/simple arene π-complexes in carbon tetrachloride and acetonitrile. *J. Photochem. Photobiol. A: Chem*. **1993**, *73*, 187; g) J. E. Chateauneuf, Kinetic Evidence for Chlorine Atom Complexes in "Noncomplexing" Solvents *J. Org. Chem*. **1999**, *64*, 1054; For overview on BDEs and reaction enthalpy of aliphatic halogenation: h) *Advanced Organic Chemistry: Reactions, Mechanisms and Structure, 6th Ed.* (Eds.: M. B. Smith, J. March), Wiley-VCH, Weinheim, **2006**.

3. a) Salamone, M.; Bietti, M., Tuning Reactivity and Selectivity in Hydrogen Atom Transfer from Aliphatic C–H Bonds to Alkoxyl Radicals: Role of Structural and Medium

Effects. *Accounts of Chemical Research* **2015,** *48*, 2895-2903; b) Capaldo, L.; Ravelli, D., Hydrogen Atom Transfer (HAT): A Versatile Strategy for Substrate Activation in Photocatalyzed Organic Synthesis. *European Journal of Organic Chemistry* **2017,** *2017*, 2056-2071; c) Milan, M.; Salamone, M.; Costas, M.; Bietti, M., The Quest for Selectivity in Hydrogen Atom Transfer Based Aliphatic C–H Bond Oxygenation. *Accounts of Chemical Research* **2018,** *51*, 1984-1995.

4. a) Tzirakis, M. D.; Lykakis, I. N.; Orfanopoulos, M., Decatungstate as an efficient photocatalyst in organic chemistry. *Chemical Society Reviews* **2009,** *38*, 2609-2621; b) Ravelli, D.; Fagnoni, M.; Fukuyama, T.; Nishikawa, T.; Ryu, I., Site-Selective C–H Functionalization by Decatungstate Anion Photocatalysis: Synergistic Control by Polar and Steric Effects Expands the Reaction Scope. *ACS Catalysis* **2018,** *8*, 701-713.
5. Becerra, R.; Walsh, R. (**1998**) Thermochemistry In *The Chemistry of Organic Silicon Compounds* (Eds Rappoport, Z.; Apeloig, Y.) John Wiley & Sons pp 153-180; b) Dean, J. A. (**1999**) Properties of Atoms, Radicals, and Bonds in *Handbook of Chemistry*. (Eds. Dean, J. A; Lange, N. A.) McGraw-Hill pp 4.41-4.53
6. For recent reviews, see: a) J. M. R. Narayanam, C. R. J. Stephenson, Visible light photoredox catalysis: applications in organic synthesis. *Chem. Soc. Rev*. **2011**, *40*, 102; b) J. Xuan, W.-J. Xiao, Visible-Light Photoredox Catalysis. *Angew. Chem. Int. Ed*. **2012**, *51*, 6828; c) C. K. Prier, D. A. Rankic, D. W. C. MacMillan, Visible Light Photoredox Catalysis with Transition Metal Complexes: Applications in Organic Synthesis. *Chem. Rev*. **2013**, *113*, 5322; d) D. Ravelli, S. Protti, M. Fagnoni, Carbon–Carbon Bond Forming Reactions via Photogenerated Intermediates. *Chem. Rev*. **2016**, *116*, 9850; e) K. L. Skubi, T. R. Blum, T. P. Yoon, Dual Catalysis Strategies in

Photochemical Synthesis. *Chem. Rev*. **2016**, *116*, 10035; f) N. A. Romero, D. A. Nicewicz, Organic Photoredox Catalysis. *Chem. Rev*. **2016**, *116*, 10075; g) M. Silvi, P. Melchiorre, Enhancing the potential of enantioselective organocatalysis with light. *Nature* **2018**, *554*, 41; For classic radical methodology: h) *Radicals in Organic Synthesis* (Eds.: P. Renaud, M. P. Sibi), Wiley-VCH, Weinheim, **2001**; i) *Encyclopedia of Radicals in Chemistry, Biology and Materials, Vols. 1 and 2* (Eds.: C. Chatgilialoglu, A. Studer), Wiley, Chichester, **2012**.

7. V. Balzani, A. Credi, M. Venturi, Photochemical Conversion of Solar Energy. *ChemSusChem* **2008**, *1*, 26.
8. For reviews, see: a) S. Protti, M. Fagnoni, D. Ravelli, Photocatalytic C□H Activation by Hydrogen-Atom Transfer in Synthesis. *ChemCatChem* **2015**, *7*, 1516; b) L. Capaldo, D. Ravelli, Hydrogen Atom Transfer (HAT): A Versatile Strategy for Substrate Activation in Photocatalyzed Organic Synthesis. *Eur. J. Org. Chem*. **2017**, 2056; For selected examples, see: c) J. D. Cuthbertson, D. W. C. MacMillan, The direct arylation of allylic sp^3 C–H bonds via organic and photoredox catalysis. *Nature* **2015**, *519*, 74; d) J. L. Jeffrey, J. A. Terrett, D. W C. MacMillan, O–H hydrogen bonding promotes H-atom transfer from α C–H bonds for C-alkylation of alcohols. *Science* **2015**, *349*, 1532; e) M. H. Shaw, V. W. Shurtleff, J. A. Terrett, J. D. Cuthbertson, D. W. C. MacMillan, Native functionality in triple catalytic cross-coupling: sp^3 C–H bonds as latent nucleophiles. *Science* **2016**, *352*, 1304; f) G. J. Choi, Q. Zhu, D. C. Miller, C. J. Gu, R. R. Knowles, Catalytic alkylation of remote C–H bonds enabled by proton-coupled electron transfer. *Nature* **2016**, *539*, 268; g) J. C. K. Chu, T. Rovis, Amide-directed photoredox-catalysed C–C bond formation at unactivated sp^3 C–H bonds.

Nature, **2016**, *539*, 272; h) D.-F. Chen, J. C. K. Chu, T. Rovis, Directed γ-C(sp^3)–H Alkylation of Carboxylic Acid Derivatives through Visible Light Photoredox Catalysis. *J. Am. Chem. Soc*. **2017**, *139*, 14897; i) K. A. Margrey, W. L. Czaplyski, D. A. Nicewicz, E. J. Alexanian, "A General Strategy for Aliphatic C–H Functionalization Enabled by Organic Photoredox Catalysis. *J. Am. Chem. Soc*. **2018**, *140*, 4213; j) H. Tanaka, K. Sakai, A. Kawamura, K. Oisaki, M. Kanai, Sulfonamides as new hydrogen atom transfer (HAT) catalysts for photoredox allylic and benzylic C–H arylations. *Chem. Commun*. **2018**, *54*, 3215; k) J. Twilton, M. Christensen, D. A. DiRocco, R. T. Ruck, I. W. Davies, D. W. C. Macmillan, Selective Hydrogen Atom Abstraction through Induced Bond Polarization: Direct α-Arylation of Alcohols through Photoredox, HAT, and Nickel Catalysis. *Angew. Chem. Int. Ed*. **2018**, *57*, 5369; l) I. A. Perry, T. F. Brewer, P. J. Sarver, D. M. Schultz, D. A. DiRocco, D. W. C. MacMillan, Direct arylation of strong aliphatic C–H bonds. *Nature* **2018**, *560*, 70; For catalyst mediated HAT, see: m) M. Okada, T. Fukuyama, K. Yamada, I. Ryu, D. Ravelli, M. Fagnoni, Sunlight photocatalyzed regioselective β-alkylation and acylation of cyclopentanones. *Chem. Sci*. **2014**, *5*, 2893; n) X.-Q. Hu, J.-R. Chen, W.-J. Xiao, Controllable Remote C-H Bond Functionalization by Visible-Light Photocatalysis. *Angew. Chem. Int. Ed.* **2017**, *56*, 1960; o) X.-Z. Fan, J.-W. Rong, H.-L. Wu, Q. Zhou, H.-P. Deng, J. D. Tan, C.-W. Xue, L.-Z. Wu, H.-R. Tao, J. Wu, Eosin Y as a Direct Hydrogen-Atom Transfer Photocatalyst for the Functionalization of C-H Bonds. *Angew. Chem. Int. Ed*. **2018**, *57*, 8514; p) A. Hu, J.-J. Guo, H. Pan, Z. Zuo, Selective functionalization of methane, ethane, and higher alkanes by cerium photocatalysis. *Science* **2018**, *361*, 668.

9. a) J. Kiwi, M. Gratzel, Oxidation of chloride to chlorine in aqueous solution via redox catalysis. *Chem. Phys. Lett*. **1981**, *78*, 241; b) S. A. M. Wehlin, L. Troian-Gautier, G. Li, G. J. Meyer, C hloride Oxidation by Ruthenium Excited-States in Solution. *J. Am. Chem. Soc*. **2017**, *139*, 12903; c) L. Troian-Gautier, M. D. Turlington, S. A. M. Whelin, A. B. Maurer, M. D. Brady, W. B. Swords, G. J. Meyer, Halide Photoredox Chemistry. *Chem. Rev.* **2019**, *119*, 4628; c) photoredox generation of chlorine atom was reported *during* preparation of this manuscript: H.-P. Deng, Q. Zhou, J. Wu, Microtubing-Reactor-Assisted Aliphatic C-H Functionalization with HCl as a Hydrogen-Atom-Transfer Catalyst Precursor in Conjunction with an Organic Photoredox Catalyst. *Angew. Chem. Int. Ed*. **2018**, *57*, 12661; d) post publication of this manuscript: M. Zidan, A. O. Morris, T. McCallum, L. Barriault, The Alkylation and Reduction of Heteroarenes with Alcohols Using Photoredox Catalyzed Hydrogen Atom Transfer via Chlorine Atom Generation. *Eur. J. Org. Chem.* **2019**, *in press.*
10. a) D. R. Heitz, J. C. Tellis, G. A. Molander, Photochemical Nickel-Catalyzed C–H Arylation: Synthetic Scope and Mechanistic Investigations. *J. Am. Chem. Soc*. **2016**, *138*, 12715; b) B. J. Shields, A. G. Doyle, Practical Ni-Catalyzed Aryl–Alkyl Cross-Coupling of Secondary Redox-Active Esters. *J. Am. Chem. Soc*. **2016**, *138*, 12719; M. K. Nielsen, B. J. Shields, J. Liu, M. J. Williams, M. J. Zacuto, A. G. Doyle, Mild, Redox-Neutral Formylation of Aryl Chlorides through the Photocatalytic Generation of Chlorine Radicals. *Angew. Chem. Int. Ed.* **2017**, *56*, 7191.
11. M. S. Lowry, J. I. Goldsmith, J. D. Slinker, R. Rohl, R. A. Pascal Jr., G. G. Malliaras, S. Bernhard, Single-Layer Electroluminescent Devices and Photoinduced Hydrogen Production from an Ionic Iridium(III) Complex. *Chem. Mater*. **2005**, *17*, 5712.

12. De Vleeschouwer, F.; Van Speybroeck, V.; Waroquier, M.; Geerlings, P.; De Proft, F., Electrophilicity and Nucleophilicity Index for Radicals. *Organic Letters* **2007,** *9*, 2721-2724.
13. a) Salamone, M.; Bietti, M., Tuning Reactivity and Selectivity in Hydrogen Atom Transfer from Aliphatic C–H Bonds to Alkoxyl Radicals: Role of Structural and Medium Effects. *Accounts of Chemical Research* **2015,** *48*, 2895-2903; b) Salamone, M.; Mangiacapra, L.; Bietti, M., Kinetic Solvent Effects on the Reactions of the Cumyloxyl Radical with Tertiary Amides. Control over the Hydrogen Atom Transfer Reactivity and Selectivity through Solvent Polarity and Hydrogen Bonding. *The Journal of Organic Chemistry* **2015,** *80*, 1149-1154; c) Dantignana, V.; Milan, M.; Cussó, O.; Company, A.; Bietti, M.; Costas, M., Chemoselective Aliphatic C–H Bond Oxidation Enabled by Polarity Reversal. *ACS Central Science* **2017,** *3*, 1350-1358.
14. R. Breslow, M. Brandl, J. Hunger, N. Turro, K. Cassidy, K. Krogh-Jespersen, J. D. Westbrook, Pyridine complexes of chlorine atoms. *J. Am. Chem. Soc*. **1987**, *109*, 7204.
15. G. S. Lee, S. H. Hong, Formal Giese addition of C(sp3)–H nucleophiles enabled by visible light mediated Ni catalysis of triplet enone diradicals. *Chem. Sci*. **2018**, *9*, 5810.
16. N. Bortolamei, A. A. Isse, A. Gennaro, Estimation of standard reduction potentials of alkyl radicals involved in atom transfer radical polymerization. *Electrochim. Acta* **2010**, *55*, 8312.
17. For examples of silanes, see: a) R. Zhou, Y. Y. Goh, H. Liu, H. Tao, L. Li, J. Wu, Visible-Light-Mediated Metal-Free Hydrosilylation of Alkenes through Selective Hydrogen Atom Transfer for Si-H Activation. *Angew. Chem. Int. Ed.* **2017**, *56*, 16621;

b) H. Qrareya, D. Dondi, D. Ravelli, M. Fagnoni, Decatungstate-Photocatalyzed Si–H/C–H Activation in Silyl Hydrides: Hydrosilylation of Electron-Poor Alkenes. *ChemCatChem* **2015**, *7*, 3350; for examples of alkanes, see: c) P. S. Skell, H. N. Baxter, J. M. Tanko, V. Chebolu, Chlorine atom/benzene system. 1. The role of 6-chlorocyclohexadienyl radical. *J. Am. Chem. Soc.* **1986**, *108*, 6300; d) S. M. Aschmann, R. Atkinson, Rate constants for the gas-phase reactions of alkanes with Cl atoms at 296 ± 2 K. *Int. J. Chem. Kinet.* **1995**, *27*, 613.

18. J. Jiang, R. Ramozzi, S. Moteki, A. Usui, K. Maruoka, K. Morokuma, Mechanism of Metal-Free C–H Activation of Branched Aldehydes and Acylation of Alkenes Using Hypervalent Iodine Compound: A Theoretical Study. *J. Org. Chem*. **2015**, *80*, 9264.
19. M. S. Lowry, J. I. Goldsmith, J. D. Slinker, R. Rohl, R. A. Pascal Jr., G. G. Malliaras, S.Bernhard, Single-Layer Electroluminescent Devices and Photoinduced Hydrogen Production from an Ionic Iridium(III) Complex. *Chem. Mater.* **2005**, *17*, 5712.
20. S. Sumino, I. Ryu, Hydroalkylation of Alkenes Using Alkyl Iodides and Hantzsch Ester under Palladium/Light System. *Org. Lett.* **2016**, *18*, 52.
21. K. Fukunishi, I. Tabushi, Regioselective Radical Addition of Adamantanes to Dimethyl Maleate. *Synthesis* **1988**, 826.
22. Hünig, S.; Schäfer, M., Trimethylsilylcyanid als Umpolungsreagens, XX. Zur Regioselektivität der Addition von Carbonyl-;Verbindungen an umgepolte α,β-ungesättigte Aldehyde. *Chemische Berichte* **1993,** *126*, 177-189.

CHAPTER 4: SYNTHESIS OF METHYLSULFINYLMETHYL ETHERS VIA SINGLE ELECTRON TRANSFER FROM DIMSYL POTASSIUM

Rohe, S., Révol, G., Marmin, T., Barriault, D., Barriault, L. Single Electron Transfer from Dimsyl Anion in the Alkylation of Phenols. *J. Org. Chem.* **2020,** *ASAP.*

S. Rohe thanks G. Révol, T. Marmin, and D. Barriault for their contributions. Project conceived by G. Révol and T. Marmin, optimization conducted by D. Barriault and S. Rohe. Background, scope, and mechanistic studies completed by S. Rohe.

4.1 Abstract

Aryl ethers are an important class of organic molecules. In particular, biaryl ether motifs which are found in many biologically active molecules including natural products, pharmaceutical and agrochemical products.[1] Most synthetic methods for the preparation of biaryl ethers are based on the formation of C-O bond through a classic Ullman type coupling reaction using copper (I) or palladium (II) complexes.[2] Alternatively, nucleophilic S_NAr reactions represent an attractive and complementary method for the direct coupling of phenols and aryl halides.[3] As such, we attempted the formation of biaryl **4.4** using phenol **4.1** and 2,6-dichloroiodobenzene **4.2** in DMSO (**Scheme 4.1 A**). Surprisingly, the desired biaryl **4.4** was not isolated but a single byproduct **4.3** was consistently formed. The identification of this byproduct revealed the addition of DMSO to the phenolic-OH moiety as opposed to the expected arene. Though this result did not advance our immediate goals, we realized this S_NAr "failure" could represent an interesting method to install methylsulfinylmethyl ether units in a one-step process via a unique mechanism.

4.2 Introduction

A cursory survey of the literature reveals that aryl methylsulfinylmethyl ethers are present in many bioactive compounds and also serve as synthetic handles for the installation of various other functional groups.[4] In these examples, the addition of methylsulfinylmethyl ethers to phenols is mainly conducted via a patented two-step process which involves the formation of a methylthiomethyl ether (MTM) followed by oxidation into the corresponding sulfoxide (**Scheme 4.1B**).[5] Although the first step is generally reliable, the second step could be susceptible to overoxidation of the sulfide and will restrict functional group tolerance in the scope.

Preliminary discussions of the alkylation mechanism raised further interest in this transformation. It was found that ample mechanistic precedent exists for the involvement of DMSO in radical reactions, sometimes as a redox agent,[6] and other times as a source of C1 and other alkyl groups in synthesis.[7] Moreover, there is evidence that dimsyl anion can act as a single electron reducing agent (**Scheme 4.1C**).[6c]

Scheme 4.1. Unexpected alkylation of DMSO.

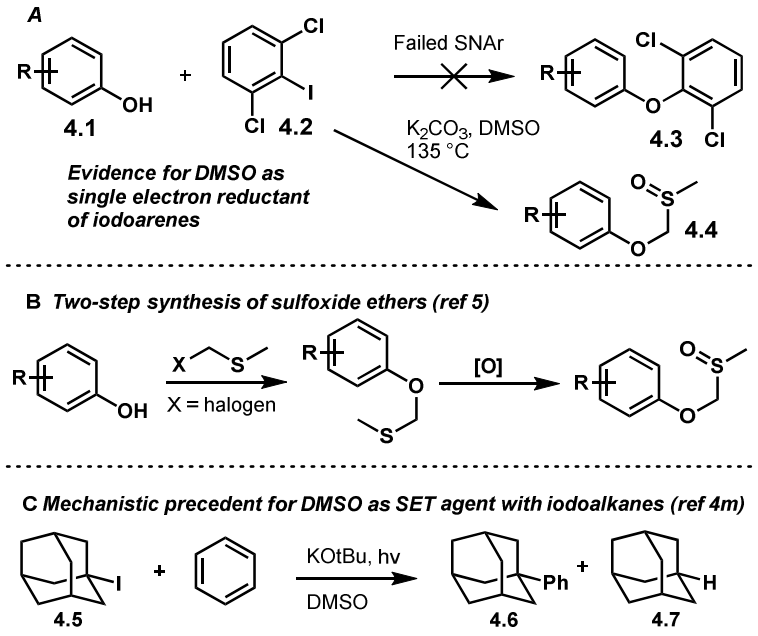

4.3 Results and Discussion

Optimization of the reaction conditions began by first determining the role of the base counterion (**Table 4.1**, entries 1-3). Changing from potassium to sodium proved to counterproductive as only starting materials were recovered (entries 1 and 2). Use of cesium as a counterion, however, led to moderate success (entry 3). Although this trend does not follow the solubility of these carbonate bases in DMSO, one can suggest that the counterion might influence the outcome of electron transfer radical reactions.[8] Lowering base loading resulted in decreased yields (entry 4).

Secondly, it was observed that lowering the temperature below 130˚C resulted in a sharp decrease in yield, with no product formed at room temperature (entry 5). When lowering or reducing to zero the equivalents of iodoarene **4.2**, the reaction suffered from reduced yields or failure (entries 6 and 7). Furthermore, performing the reaction at higher concentration in DMSO (entries 8 and 9) proved to be detrimental. Attempts to run

reactions in DMSO with various cosolvents resulted in recovery of starting material and prohibitively low yields (<15%) (see Supporting Information for complete optimization tables).

Table 4.1. Optimization of DMSO alkylation reaction.

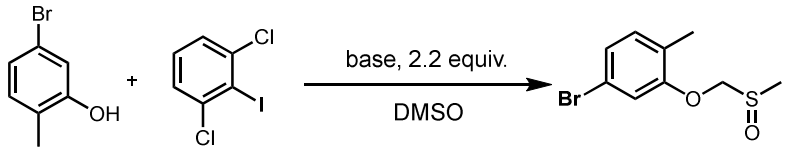

4.8 1 equiv. **4.2** 1.5 equiv. **4.9**

Entry	Base	Conc (M)	Temp (°C)	Time (h)	Yield (%)[a]
1	K_2CO_3	0.1	135	16	**96** (70)[b]
2	Na_2CO_3	0.1	135	16	0
3	Cs_2CO_3	0.1	135	16	54
4[c]	K_2CO_3	0.1	135	16	79
5	K_2CO_3	0.1	22	16	0
6[d]	K_2CO_3	0.1	135	16	67
7[e]	K_2CO_3	0.1	135	16	0
8	K_2CO_3	0.5	135	16	26
9	K_2CO_3	0.05	135	16	84

[a] Yields determined by NMR internal standard using trimethyl(phenyl)silane; [b] Isolated yield in brackets; [c] 1.1 equivalents of base; [d] 1.1 equivalents of **4.2**; [e] Reaction performed without **4.2**.

Following determination of the optimal conditions, the generality of the reaction was examined. Overall, scope yields varied widely from poor to good (25-75%). The reaction was not contingent on substrate electronics, obtaining good yields with electronically opposite substrates **4.13** and **4.14** (59% and 45% yields respectively). Interestingly, the reaction was very amenable to some steric hindrance, such as the hindrance exhibited in

ortho-substituted phenols **4.10**, **4.12**, and **4.27** (70%, 53% and 75% yields), though the presence of extremely large groups such as the 2-adamantyl-4-methylphenol **4.20** led to reductions in yield (33%).

All reactions went to completion except when phenol **4.15** was used, which resulted in isolation of 5% of the phenol starting material. In every case no major byproduct was observed and iodoarene was completely decomposed, except for a few substrates where traces of S_NAr product **4.4** were detected *via* GC-MS. Notably, iodophenols **4.11** and **4.21** afforded good yields (62% and 53%), showing that all aryl-I bonds are resilient towards the reaction conditions aside from the required haloarene **4.2**. The conditions were also tolerant of functionally important substrates 2-propenylphenol **4.26** (43%), which exhibited minimal thermal *cis-trans* isomerization (starting material 72:28 *E:Z*, see SI), and 2-hydroxyphenylacetylene **4.24** (51%), where the alkyne remained intact throughout the transformation. The thioether substrate **4.28** (75%) demonstrates the utility of the transformation as the thioether moiety remained intact under the reaction conditions. Existing methods to alkylate phenols with sulfoxides could oxidize any thioethers, thiols, or sulfoxides present.[5] Finally, the reaction is amenable to large molecules of biological relevance such as estrone **4.29** (25%) and α-tocopherol **4.30** (29%).

Scheme 4.2. Substrate scope.[a]

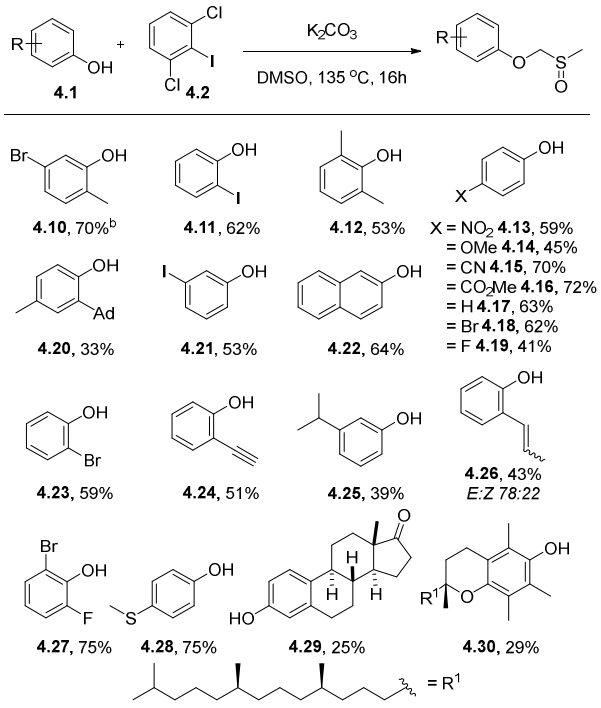

[a] Reaction conditions: **4.1** (0.3 mmol), **4.2** (0.45 mmol), K_2CO_3 (0.66 mmol), DMSO (3 mL), 135 °C, 16h. * Reaction run on 2g scale, yield = 60%.

A few sulfoxides other than DMSO were examined as solvents to expand the sulfoxide scope (see SI). Though methylsulfinylmethyl ether product from these reactions was observed by NMR and GC-MS, the product was inseparable from the parent sulfoxide. Attempts to run reactions in sulfoxide with various cosolvents resulted in a halting of the reaction or prohibitively low yields (<15%). Unusual results were observed when diethyl sulfoxide (DESO) was employed as the solvent, forming complex mixtures of products in which a black tarry polymer dominated. This may be due to faster single electron transfer from electron-rich sulfoxides such as DESO.[9]

We then delved into mechanistic elucidation by considering many possibilities. Firstly, the role of the iodoarene was probed (**Scheme 4.3**). The 2,6-dichloroiodobenzene **4.2**

proved necessary to the transformation, as attempts to substitute it with 2-chloroiodobenzene and iodobenzene did not produce any product and simply resulted in decomposition of the phenol (eq. 4.1). Use of benzoyl peroxide as a surrogate source of phenyl radical resulted in low yields (<15%). We then considered that the iodine on **4.2** may be oxidizing DMSO and attempted to use other sources of iodine in the reaction. Use of N-iodosuccinimide (NIS) and molecular iodine, in place of the iodoarene, also resulted in decomposition of the phenol or inseparable mixtures of products respectively.

Scheme 4.3. Additional mechanistic studies.

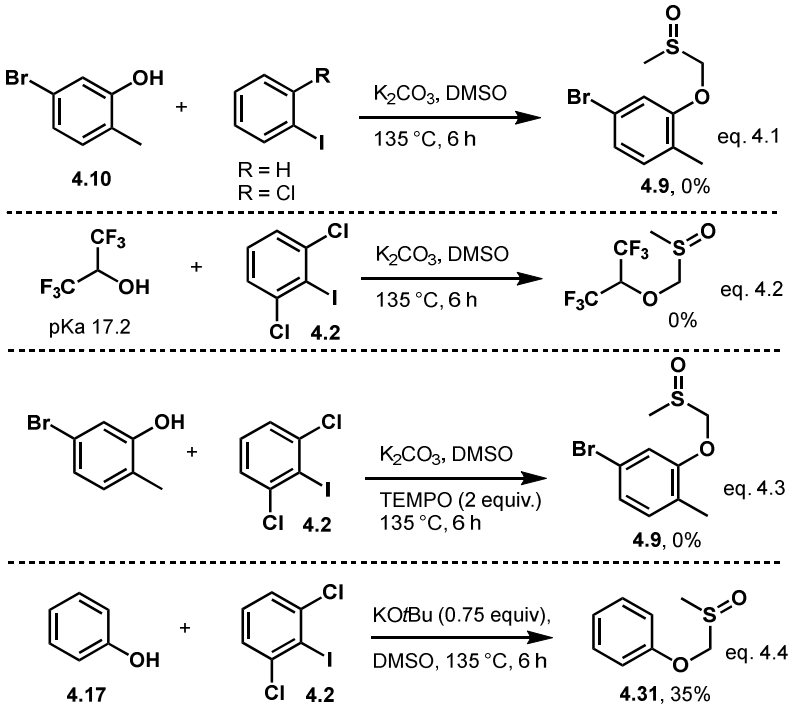

An ionic mechanism involving α-oxidation of the sulfoxide with a halogen followed by S_N2 substitution was then considered. Intermediacy of an alkoxide was probed by using aliphatic alcohol HFIP in place of phenol, as the pKa's in DMSO are similar (pka_{phenol} = 18, pKa_{HFIP} = 17.2) (eq. 4.2).[10] However, no product was observed. The use of nucleophiles such as anilines, thiophenols, and cyclopentanol afforded only

decomposition or recovery of starting material, indicating that the mechanism is not simply bimolecular substitution on iodomethyl methyl sulfoxide. A putative benzyne intermediate, generated via an ionic pathway, was then probed using trapping experiments. Trihalogenated arenes such as **4.2** can form benzyne relatively slowly,[11] however, studies of similar substrates indicate that the aryl radical can be formed more rapidly.[12] Our attempts to trap a benzyne intermediate with furan or 1,3-cyclohexadiene resulted in complex mixtures containing no Diels-Alder adduct. However, these experiments do not completely rule out involvement of phenoxide or diradical benzyne intermediates.

A radical mechanism was then considered. Addition of 2 equivalents of TEMPO or BHT to the standard conditions resulted in exclusive formation of insoluble polymer containing only traces of product, which suggests mechanistic involvement of radicals (eq. 4.3). Peñéñory and co-workers suggested that dimsyl anion can function as a single electron reductant in the presence of KO*t*Bu and can form complexes that facilitate charge transfer to iodoalkanes, with electron transfer occurring from dimsyl anion rather than potassium *tert*-butoxide.[8c, 12] One can suppose that dimsyl potassium generated in the presence of K_2CO_3 may function similarly. Attempts to reproduce the results of Peñéñory in our system by replacing the carbonate base with 0.75 equivalents of KO*t*Bu resulted in 35% yield of desired product (eq. 4.4). However, it is important to note that using 2 equivalents of KO*t*Bu or KH led to the recovery of the starting material. These results suggest that the presence of the phenolic O-H bond is essential for the reaction to proceed.

Involvement of an aryl radical offers rationale for the requirement of **4.2** as additive. Per-halogenated arenes, especially iodoarenes vicinally *bis*-substituted with other halogens such as chlorine, can undergo dissociative electron transfer, forming iodide and

a corresponding high-energy aryl radical.[13] Indeed, 2,2',6,6'-tetrachloro-1,1'-biphenyl, the dimer of this putative aryl radical, was detected in trace quantities in all scope reactions (see Supporting Information). Attempts to quantitatively trap aryl radical intermediates with benzonitrile or styrene as acceptors have thus far resulted in degradation.[14]

Consideration of a radical mechanism imparts an explanation for some unusual scope results. As steric hindrance tends to decrease nucleophilicity of a compound, yet several sterically encumbered examples in the scope provide excellent yields (**4.12**, 53% yield and **4.27**, 75% yield), nucleophilic substitution is not indicated as a major mechanistic factor. However, *bis-ortho* substitution of phenols can stabilize the associated O-centered radical, increasing its persistence to the point where it may be able to react with a nucleophilic species.[15] Our attempts to trap such a phenoxyl radical with 2-allylphenol have unfortunately met with failure due to the substrate's slow cyclization.[16]

Finally, isotope labelling studies were conducted to probe DMSO's involvement in the reaction (**Scheme 4.4**). As all positions alpha to the sulfoxide are enolizable and will therefore exchange with any water present, it was not feasible to determine accurate ratios.[17] However, when the reaction was run in DMSO-d6, the product contained 95% deuterium incorporation at both alpha-sulfoxide positions. The yield (**d-4.9**, 62%) is comparable to the same reaction run in protiated DMSO (**4.9**, 70%), indicating that the presence of deuterium had minimal impact on yield. Likewise, when the reaction was run in a 1:1 mixture of DMSO:DMSO-d6, the alpha-sulfoxide CH_3 was 32% deuterated and the alpha-oxo CH's were 10 and 24% deuterated. A small reduction in yield (52% compared to 70% in DMSO) was observed, though no additional byproducts were identified, and all starting materials were consumed. Due to the elevated concentration of

acidic protons in the mixed solvent, it seems that H-D exchange may be so prevalent as to obfuscate meaningful results in the second trial.

Scheme 4.4. Isotope labelling studies.[a]

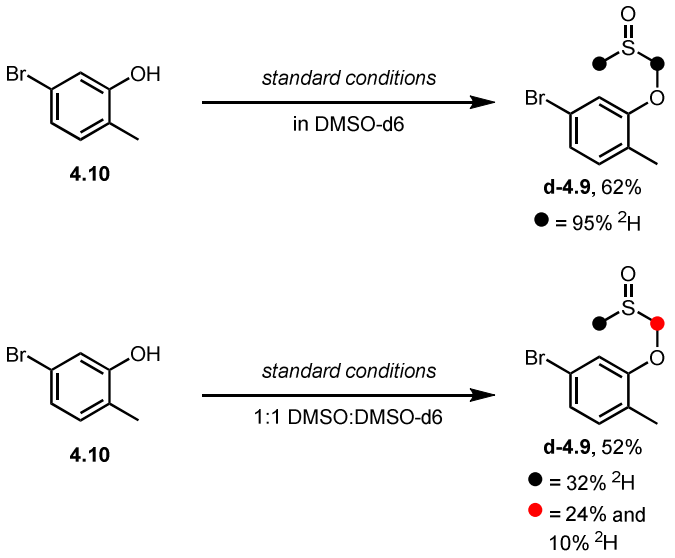

[a] Ratios of H:D determined by comparison of ^{1}H NMR integrals between aromatic or aliphatic C-H bonds and alpha-sulfoxide C-H bonds. See Supporting Information.

Based on precedent and the above mechanistic studies, the following mechanism is proposed (**Scheme 4.5**). The mixture of K_2CO_3 and DMSO produces a low concentration of dimsyl potassium at 135°C. We propose that this dimsyl anion can inject a single electron into the weak carbon-iodine bond of **4.2** under these conditions [BDE(iodobenzene) = 64], generating the dichloroaryl radical **i**, a DMSO radical, and iodide.[18] The aryl radical (BDE ≈ 103 kcal/mol) is then able to perform H-atom transfer (HAT) on the phenol (BDE ≈ 86),[19,20] generating a more stable radical species **ii** and 1,3-dichlorobenzene. The resulting oxygen-centered radical **ii** reacts with dimsyl anion via **Path A**, creating a powerfully reducing radical ion **iii** that becomes oxidized by molecular

oxygen or can propagate a chain cycle by SET to iodoarene **4.2**.[22] Alternatively, the phenol radical **ii** could recombine with the DMSO radical anion generated during an initiating SET event as seen in **Path B**. As the dimsyl anion is likely present in higher concentrations than the DMSO radical, **Path A** is proposed to be the dominant pathway. This mechanistic proposal involves reactions of species present in relatively low concentrations, which contextualizes the long reaction time and non-quantitative yields. These results do not completely eliminate the possibility that the iodoarene **4.2** may be oxidizing DMSO, making iodomethyl methyl sulfoxide which then undergoes nucleophilic substitution with a phenolate. If this pathway is present, we suspect that it is minor based on available evidence. Finally, we submitted a pure sample of 1,3-dichlorobenzene to the reaction conditions in the absence of phenol and observed complete decomposition of the compound.

Scheme 4.5. Proposed mechanism.

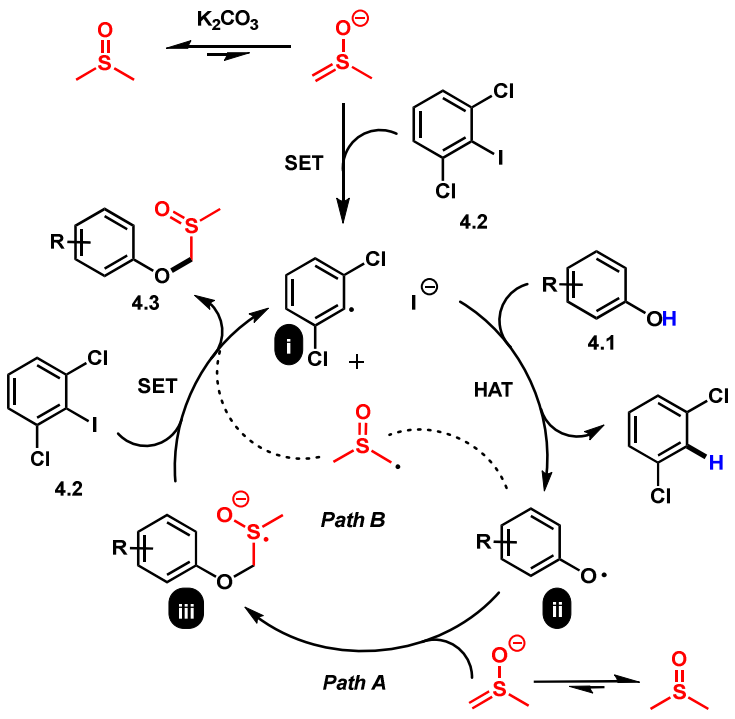

4.4 Conclusions

In summary, the examination of a curious byproduct of S_NAr has led to a serendipitous streamlining of methylsulfinylmethyl ether synthesis. Submitting this unusual transformation to mechanistic studies suggests the role of DMSO as not only solvent but also possibly single electron reducing agent in the presence of base. Investigations into the capacity of DMSO as a radical reducing agent are currently under investigation by our group.

4.5 Further Information

4.51 Optimization

Table 4.2. Full optimization of the reaction conditions.

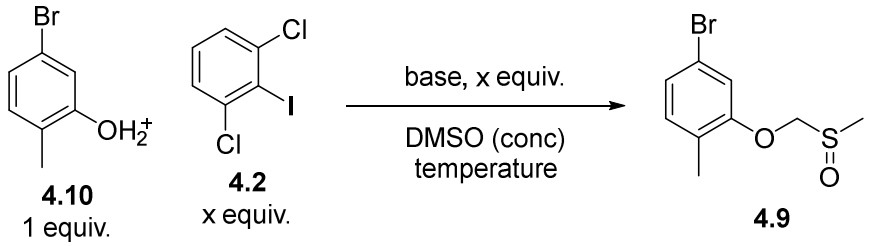

Entry	Iodoarene (equiv)	DMSO conc. (M)	Base (equiv)	Temp (°C)	t (h)	conversion of sm	% yield
1	2 (1.1)	0.1	K_2CO_3 (2.2)	135	16	92	67 (58[i])
2	2 (1.1)	0.1	K_2CO_3 (2.2)	160	16	100	54
3	2 (1.1)	0.1	K_2CO_3 (2.2)	110	16	100	37
4	2 (1.1)	0.1	K_2CO_3 (2.2)	70	16	38	<5
5	2 (1.1)	0.1	K_2CO_3 (2.2)	135	66	100	57
6	2 (1.1)	0.1	K_2CO_3 (2.2)	r.t.	32	100	0

Entry	Iodoarene (equiv)	DMSO conc. (M)	Base (equiv)	Temp (°C)	t (h)	conversion of sm	% yield
7	2 (1.1)	0.1	none	135	16	degradation	0
8	2 (1.1)	0.1	Na_2CO_3 (2.2)	135	16	100	trace
9	2 (1.1)	0.1	Cs_2CO_3 (2.2)	135	16	100	54
10	2 (1.1)	0.1	Cs_2CO_3 (2.2)	70	16	70	32
11	2 (1.1)	0.1	K_2CO_3 (1.1)	135	16	100	79
12	2 (1.1)	0.1	K_2CO_3 (3.3)	135	16	>95%	31
13	2 (1.1)	0.1	K_2CO_3 (0.5)	135	16	Recovered 80% phenol	0
14	2 (1.5)	0.1	K_2CO_3 (2.2)	135	16	100	96 (70[i])
15	2 (0.5)	0.1	K_2CO_3 (2.2)	135	16	>95	32
16	none	0.1	K_2CO_3 (2.2)	135	16	94	0

Entry	Iodoarene (equiv)	DMSO conc. (M)	Base (equiv)	Temp (°C)	t (h)	conversion of sm	% yield
17	1-chloro-2-iodobenzene (1.5)	0.1	K_2CO_3 (2.2)	135	16	Degradation of phenol, recovered arene	0
18	Iodobenzene (1.5)	0.1	K_2CO_3 (2.2)	135	16	Degradation of phenol, recovered haloarene	0
19	Trichlorobenzene (1.5)	0.1	K_2CO_3 (2.2)	135	16	Degradation of phenol, recovered haloarene	0
20	2 (1.5)	0.5	K_2CO_3 (2.2)	135	16	100	26
21	2 (1.5)	0.2	K_2CO_3 (2.2)	135	16	100	0
22	2 (1.5)	0.05	K_2CO_3 (2.2)	135	16	100	84
23	2 (1.5)	0.025	K_2CO_3 (2.2)	135	16	100	62
24	2 (1.1)	0.1	K_2CO_3 (2.2)	135	6	84	30
25	2 (1.5)	0.1	KO*t*Bu (3)	135	16	decomposition	6

Entry	Iodoarene (equiv)	DMSO conc. (M)	Base (equiv)	Temp (°C)	t (h)	conversion of sm	% yield
26	2 (1.5)	0.1	KO*t*Bu (0.75)	135	16	100	35
27[a]	2 (1.5)	0.1	K_2CO_3 (2.2)	135	16	degradation	0
28[b]	2 (1.5)	0.1	K_2CO_3 (2.2)	135	16	100	64
29[c]	2 (1.5)	0.1	K_2CO_3 (2.2)	135	16	100	44
30[d]	2 (1.5)	0.1	K_2CO_3 (2.2)	135	16	100	79
31[e]	2 (1.5)	0.1	K_2CO_3 (2.2)	135	16	100	60
32[f]	2 (1.5)	0.1	K_2CO_3 (2.2)	r.t.	16	Recovered 22% phenol, 88% haloarene	0
33[g]	2 (1.5)	0.1	K_2CO_3 (2.2)	r.t.	16	Recovered 25% phenol	0
34[h]	2 (1.5)	0.1	K_2CO_3 (1.1)	135	16	Recovered 11% BHT	trace

All yields are by comparison to an NMR standard (phenyltrimethylsilane) unless otherwise noted. [i] = isolated yield. [a] reaction run with 2 equivalents of TEMPO. [b] solvent

50:50 toluene:DMSO. [c] reaction degassed and run under Ar atmosphere. [d] reaction run on 0.5g of phenol. [e] reaction run on 1g of phenol. [f] reaction run at r.t. irradiated under blue LED for 16h WITHOUT degassing solvent. [g] reaction run at r.t. irradiated under blue LED for 16h with DEGASSED solvent under Ar. [h] reaction run with 2 equivalents of BHT.

4.52. 2,2',6,6'-tetrachloro-1,1'-biphenyl Byproduct

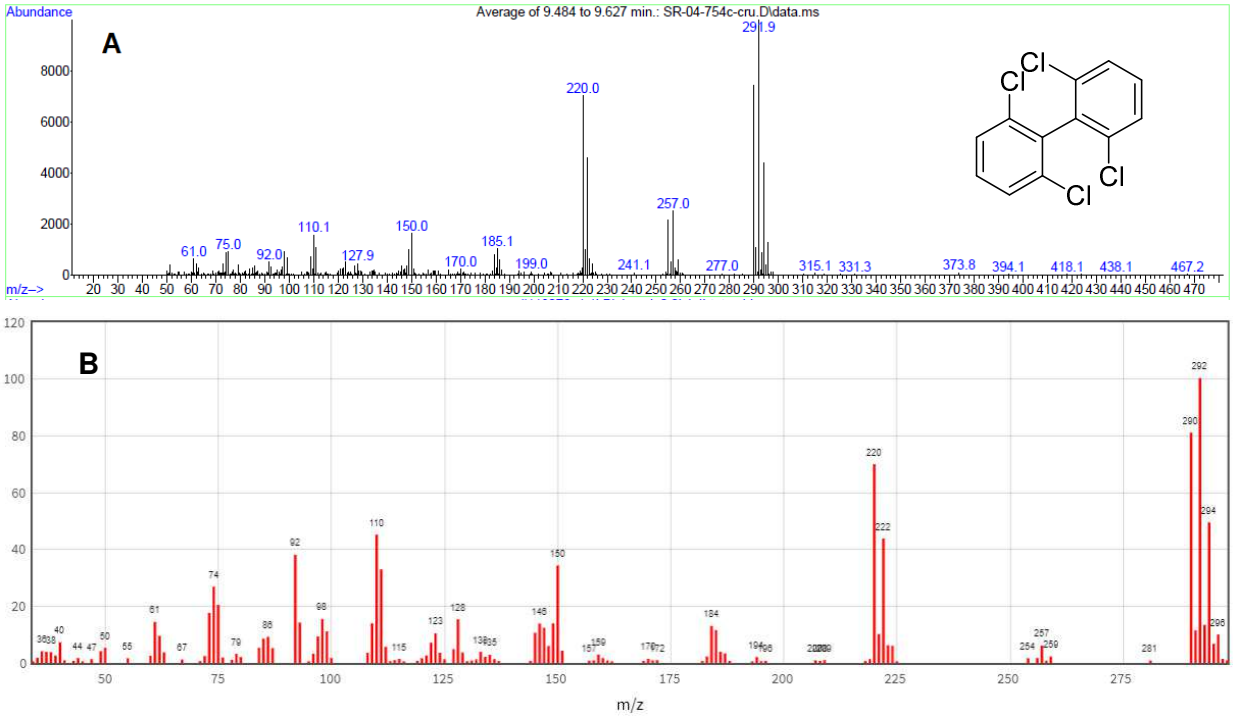

Figure 4.1. 2,2',6,6'-tetrachloro-1,1'-biphenyl Byproduct. A) Fragmentation pattern for byproduct observed in most of the scope reactions. B) NIST Mass Spectral Database Webbook EI mass spectrum for 2,2',6,6'-tetrachloro-1,1'-biphenyl. Online record can be found at https://webbook.nist.gov/cgi/inchi/InChI%3D1S/C12H6Cl4/c13-7-3-1-4-8(14)11(7)12-9(15)5-2-6-10(12)16/h1-6H.

4.53. Solvent Screen for Sulfoxide Scope

Table 4.3. Optimization attempts for sulfoxide scope.

Cosolvent (vol, mL)	**Sulfoxide (vol, mL)**	**Yield (%)[a]**
None	Phenyl methyl sulfoxide (3)	<15 [b]
Benzene (1.5)	Dimethyl sulfoxide (1.5)	65
Benzene (1.5)	Phenyl methyl sulfoxide (1.5)	<15
Toluene (1.5)	Phenyl methyl sulfoxide (1.5)	Trace
o-xylene (1.5)	Phenyl methyl sulfoxide (1.5)	Trace
Mesitylene (1.5)	Phenyl methyl sulfoxide (1.5)	Trace
None	Diethyl sulfoxide (3)	Complex mixture
Benzene (1.5)	Diethyl sulfoxide (1.5)	Trace

[a] NMR Yield with phenyltrimethylsilane. [b] Product inseparable from phenyl methyl sulfoxide starting material by flash chromatography.

4.54. Unsuccessful Substrates

Other Nucleophiles:

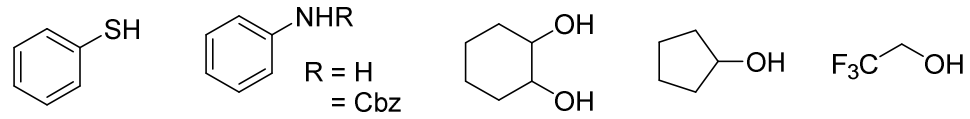

Phenols:

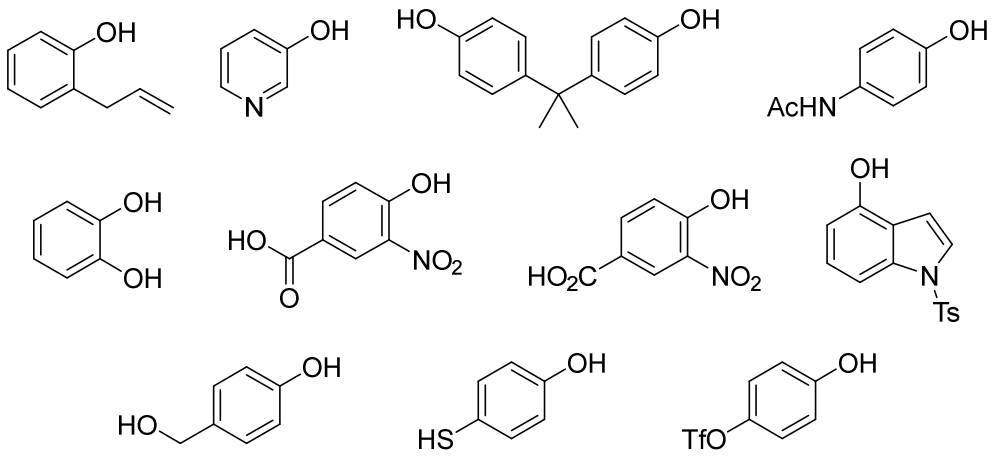

Figure 4.2. Substrates attempted under standard reaction conditions that resulted in <15% of product or recovery/degradation of starting material.

4.55. Isomerization of 2-propenylphenol Under Standard Conditions

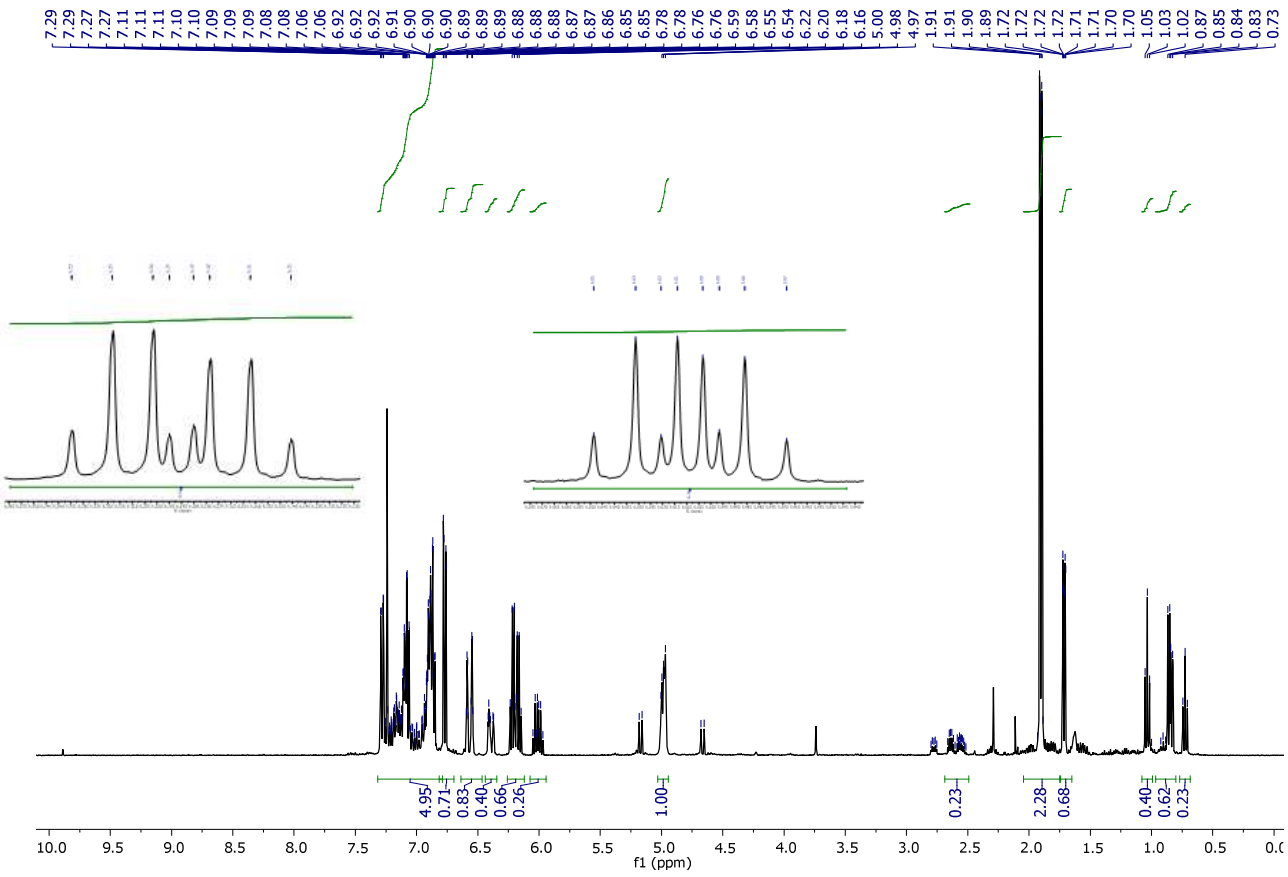

Figure 4.3. ^{1}H NMR spectrum of starting material **4.26**.

The insert regions within the above spectrum detail the peaks used to calculate ratio of *E:Z* olefins in the parent phenol substrate. These peaks represent the same proton in the *E* and *Z* configurations (left and right respectively). Raw integration of each region was expressed as a percentage of the total giving a ratio of 72:28 *E:Z*.

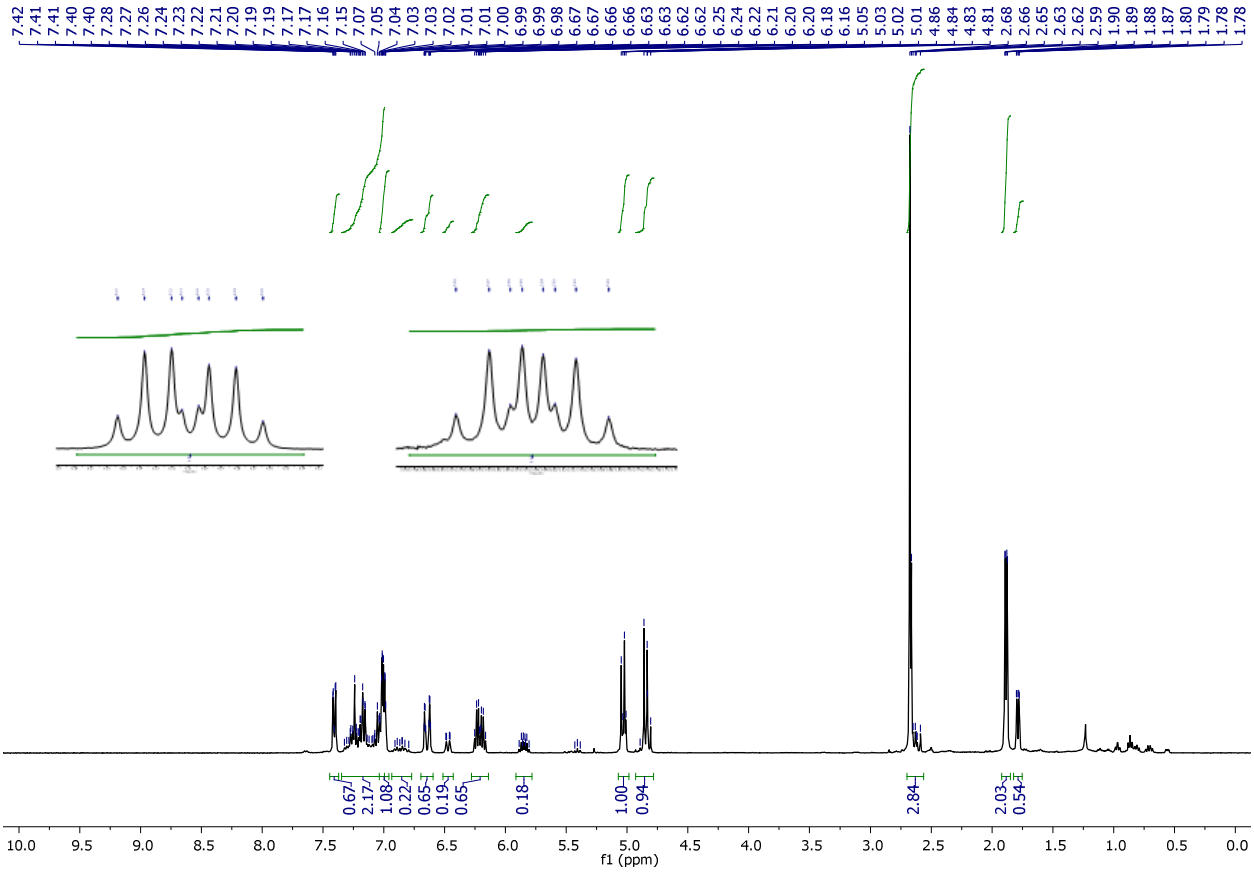

Figure 4.4. ^{1}H NMR spectrum of product **4.46**.

The insert regions within the above spectrum detail the peaks used to calculate ratio of *E:Z* olefins in the alkylated phenol product **4.46**. These peaks represent the same proton in the *E* and *Z* configurations (left and right respectively). Raw integration of each region was expressed as a percentage of the total giving a ratio of 78:22 *E:Z*.

4.56. Isotope Labelling Competition Experiments

Deuterium-labeling experiments were performed as per GP1 with either pure DMSO-d6 or a 1:1 mixture of DMSO:DMSO-d6 as solvent. Isotopic ratio data was obtained by analyzing the ratio between deuterated and proteated products following isolation of product (see ^{1}H NMR spectrum below). Most notably, it was observed that the deuterium

incorporation in the reaction with 1:1 DMSO:DMSO-d6 was asymmetrical with respect to the α-sulfoxide positions (10% and 24% deuterium incorporation at the etheric position, and 48% deuterium incorporation at the terminal position). This data suggests that any ratios obtained with this method will be unreliable due to facile deuterium-protium exchange at the α-sulfoxide positions.

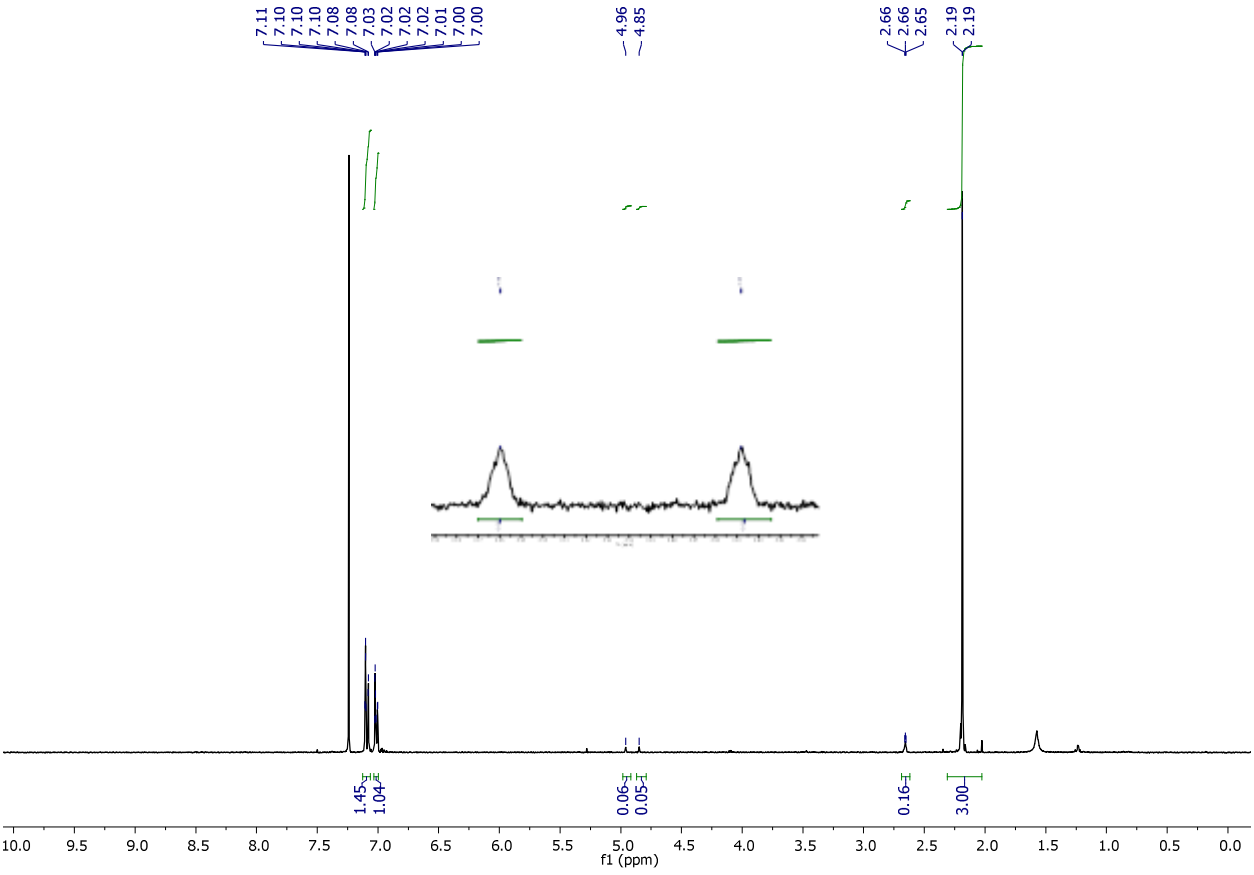

Figure 4.5. ^{1}H NMR spectrum of product **d-4.9.**

The insert region within the above spectrum details two peaks used to calculate ratio of etheric α-sulfoxide deuterium incorporation in product **d-4.9**. The singlet at 2.66 ppm was also used to calculate terminal α-sulfoxide deuterium incorporation. Solvent used for this experiment was 100% DMSO-d6.

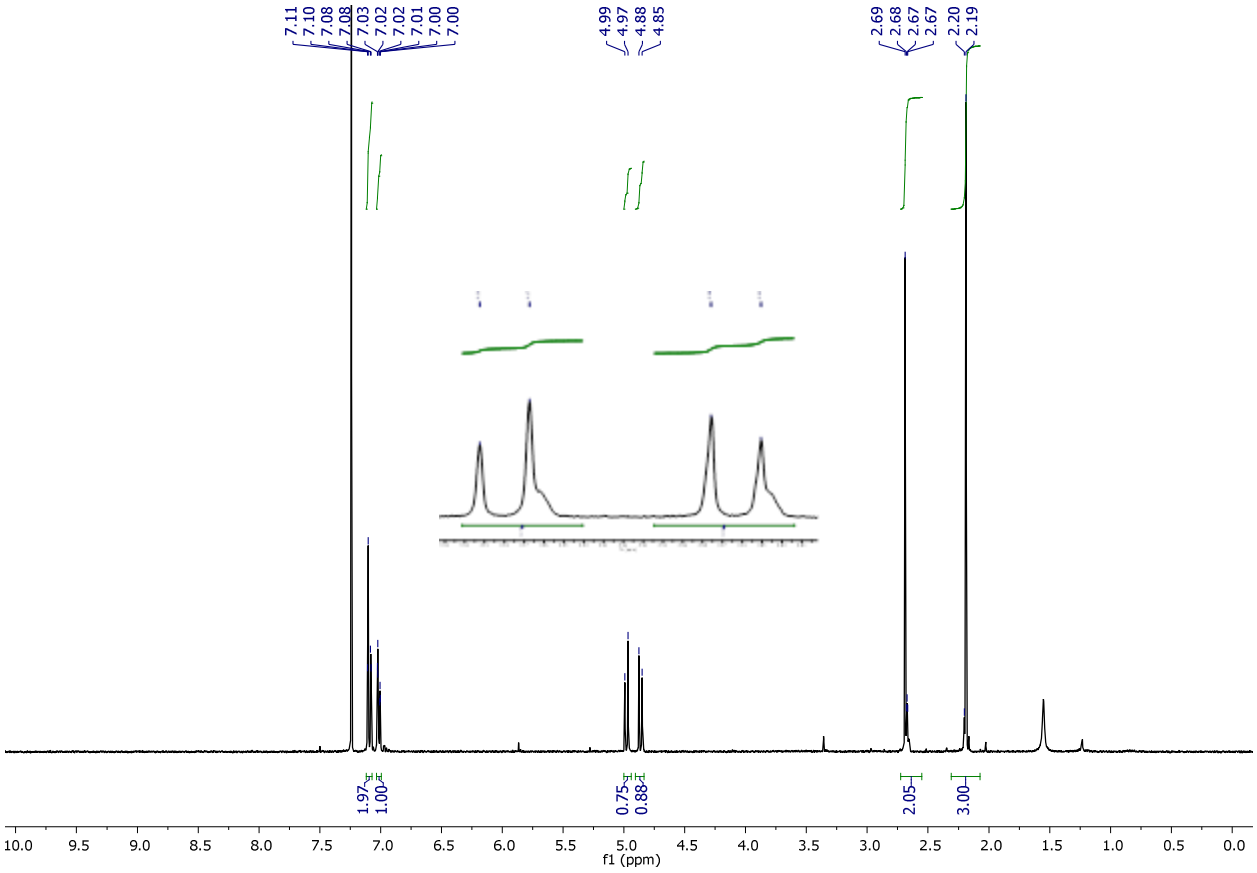

Figure 4.6. ^{1}H NMR spectrum of mixed deuterated product **4.9** and **d-4.9.**

The insert region within the above spectrum details two peaks used to calculate ratio of etheric α-sulfoxide deuterium incorporation in product **d-4.9**. The large singlet at 2.66 ppm was also used to calculate terminal α-sulfoxide deuterium incorporation. Solvent used for this experiment was 1:1 DMSO:DMSO-d6.

4.6 Experimental Procedures

General Information. All reactions were performed in Pyrex glassware equipped with a magnetic stir bar, capped with a septum, unless otherwise indicated. All commercial reagents were obtained from Sigma Aldrich, Alfa Aesar or Combi Blocks and used without further purification, unless otherwise noted. Reactions were monitored by thin layer chromatography (TLC) analysis. TLC plates were viewed under UV light and stained with potassium permanganate or p-anisaldehyde staining solution. Yields refer to products isolated after purification, unless otherwise stated. Proton nuclear magnetic resonance (^{1}H NMR) spectra were recorded on a Bruker AMX 400 MHz, Bruker Avance 500, or a Bruker Avance III HD 600 MHz instrument. Carbon nuclear magnetic resonance (^{13}C NMR) spectra were recorded on the same Bruker instruments (101, 126, and 151 MHz respectively). Fluorine nuclear magnetic resonance (^{19}F NMR) spectra were recorded on a Bruker Avance 377 MHz instrument. NMR samples were dissolved in chloroform-d (unless specified otherwise) and chemical shifts are reported in ppm referenced to residual non-deuterated solvent. IR spectra were recorded with an Agilent Technologies Cary 630 FTIR Spectrometer equipped with a diamond ATR module. GC-MS (EI) were obtained on an Agilent 5975 series MSD instrument (University of Ottawa Centre for Catalysis Research and Innovation High-Throughput Experimentation Core Facility). HRMS were obtained on a Kratos Analytical Concept instrument (EI) and a Micromass Q-TOF I instrument (ESI) at the University of Ottawa Mass Spectrum Centre.

General Procedure: methylsulfinyl methyl etherification of phenols (Table 4.1, Scheme 4.2). To an open-air round-bottom flask equipped with a stir bar was added K_2CO_3 (0.66 mmol, 2.2 eq.), 2,6-dichloroiodobenzene (0.45 mmol, 1.5 eq.), and phenol

substrate (0.3 mmol, 1 eq.). DMSO (0.1M, 3mL) was added and the flask was fitted with a Vigreux column OR a reflux condenser open at the top to ambient atmosphere. The reaction was stirred at 135 ^{o}C for 16 hours. Upon completion, the reaction was cooled to room temperature and diluted with water (20 mL) and ethyl acetate (10 mL). The layers were separated and the aqueous phase was extracted a further 2x with 10 mL ethyl acetate. The organic layers were combined and washed successively with water (10 mL) and brine (10 mL). The organic layer was dried, filtered, and concentrated under reduced pressure to afford the crude brown oil product. The crude residue was purified *via* silica gel chromatography to afford the final product (solvent system: gradient of 5 – 80% ethyl acetate in hexanes).

4.7 Characterization Data

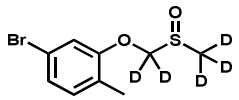

4-bromo-1-methyl-2-(((methyl-d3)sulfinyl)methoxy-d2)benzene (d-4.9). From 5-bromo-2-methylphenol (56 mg, 0.3 mmol) and DMSO-d6 as solvent (3 mL, 0.1M), product was obtained as an amorphous off-white solid (in DMSO-d6: 49 mg, 0.19 mmol, 62% yield; in 1:1 DMSO:DMSO-d6: 42 mg, 0.16 mmol, 52% yield). IR (neat, cm^{-1}): 3060, 2964, 2919, 2916, 2844, 2280, 1582; ^{1}H NMR (400 MHz, Chloroform-*d*) δ = 7.12 – 7.06 (m, 2H), 7.03 – 7.00 (m, 1H), 4.96 (s, 1H), 4.85 (s, 1H), 2.66 (t, *J* = 1.9 Hz, 3H), 2.19 (d, *J* = 0.7 Hz, 3H); ^{13}C NMR (101 MHz, $CDCl_3$) δ = 156.2 (C), 132.3 (CH), 126.4 (C), 125.7 (CH), 119.6 (C), 116.3 (CH), 83.9 (CD_2), 34.9 (CD_3), 15.9 (CH_3); HRMS (ESI): m/z [M + Na, ^{79}Br]$^{+}$ calc'd for $C_9H_6D_5BrO_2SNa$, 289.9875; found, 289.9887.

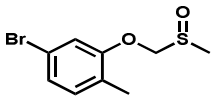

4-bromo-1-methyl-2-((methylsulfinyl)methoxy)benzene (4.9). From 5-bromo-2-methylphenol (56 mg, 0.3 mmol; or 0.5g, 2.67 mmol; or 1g, 5.35 mmol), **4.9** was obtained as an amorphous pale red solid (56 mg scale: 49 mg, 0.19 mmol, 70% yield; 0.5 g scale: 0.55 g, 2.1 mmol, 79% yield; 1 g scale: 0.84 g, 3.2 mmol, 60% yield). IR (neat, cm^{-1}): 3062, 2922, 2914, 2089, 1582; ^{1}H NMR (400 MHz, $CDCl_3$) δ = 7.12 – 7.07 (m, 2H), 7.01 (dt, *J* = 7.8, 0.7 Hz, 1H), 4.98 (d, *J* = 10.0 Hz, 1H), 4.86 (d, *J* = 10.0 Hz, 1H), 2.69 (s, 3H), 2.19 (d, *J* = 0.7 Hz, 3H); ^{13}C NMR (126 MHz, $CDCl_3$) δ = 156.2 (C), 132.3 (CH), 126.4 (C), 125.8 (CH), 119.6 (C), 116.3 (CH), 84.4 (CH_2), 35.8 (CH_3), 15.9 (CH_3); HRMS (ESI): m/z [M + Na, ^{81}Br]$^{+}$ calc'd for $C_9H_{11}BrO_2SNa$, 286.9540; found, 286.9556.

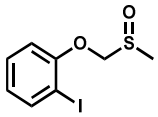

1-iodo-2-((methylsulfinyl)methoxy)benzene (4.32). From 2-iodophenol (**4.11**, 89 mg, 0.3 mmol) **4.32** was obtained as an amorphous pale yellow solid (55 mg, 0.19 mmol, 62% yield). IR (neat, cm^{-1}): 3055, 2995, 2915, 2909, 1582, 1034; ^{1}H NMR (400 MHz, $CDCl_3$) δ = 7.77 (dd, *J* = 7.8, 1.6 Hz, 1H), 7.33 (ddd, *J* = 8.2, 7.4, 1.6 Hz, 1H), 7.06 (dd, *J* = 8.2, 1.4 Hz, 1H), 6.82 (ddd, *J* = 7.8, 7.4, 1.3 Hz, 1H), 5.07 (d, *J* = 10.0 Hz, 1H), 4.89 (d, *J* = 10.0 Hz, 1H), 2.78 (s, 3H); ^{13}C NMR (101 MHz, $CDCl_3$) δ = 156.3 (C), 139.9 (CH), 129.9 (CH), 124.9 (CH), 114.4 (CH), 86.6 (C), 84.5 (CH_2), 36.3 (CH_3); HRMS (ESI): m/z [M + Na]$^{+}$ calc'd for $C_8H_9IO_2SNa$, 318.9260; found, 318.9264.

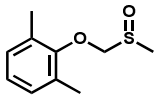

1,3-dimethyl-2-((methylsulfinyl)methoxy)benzene (4.33). From 2,6-dimethylphenol (**4.12**, 37 mg, 0.3 mmol) **4.33** was obtained as an amorphous colorless solid (32 mg, 0.16 mmol, 53% yield). IR (neat, cm^{-1}): 3040, 2998, 2919, 2852, 1031; ^{1}H NMR (400 MHz, $CDCl_3$) δ = 7.04 – 6.99 (m, 2H), 6.99 – 6.94 (m, 1H), 4.76 (d, *J* = 9.5 Hz, 1H), 4.71 (d, *J* = 9.5 Hz, 1H), 2.71 (s, 3H), 2.29 (d, *J* = 0.7 Hz, 6H); ^{13}C NMR (101 MHz, $CDCl_3$) δ = 155.1 (C), 130.1 (2 X C), 129.3 (2 X CH), 125.1 (CH), 88.3 (CH_2), 35.9 (CH_3), 16.7 (2 X CH_3); HRMS (ESI): m/z $[M + Na]^+$ calc'd for $C_{10}H_{14}O_2SNa$, 221.0612; found, 221.0604.

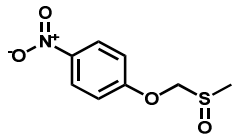

1-((methylsulfinyl)methoxy)-4-nitrobenzene (4.34). From 4-nitrophenol (**4.13**, 42 mg, 0.3 mmol) **4.34** was obtained as an amorphous deep yellow solid (38 mg, 0.18 mmol, 59% yield). Characterized by NMR comparison.[5c] ^{1}H NMR (400 MHz, $CDCl_3$) δ = 8.31 – 8.13 (m, 2H), 7.18 – 7.10 (m, 2H), 5.04 (d, *J* = 2.0 Hz, 2H), 2.71 (s, 3H); ^{13}C NMR (101 MHz, $CDCl_3$) δ = 162.2 (C), 143.1 (C), 126.0 (2 X CH), 115.7 (2 X CH), 83.7 (CH_2), 35.5 (CH_3).

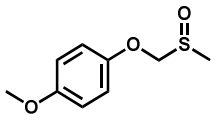

1-methoxy-4-((methylsulfinyl)methoxy)benzene (4.35). From 4-methoxyphenol (**4.14**, 37 mg, 0.3 mmol) **4.35** was obtained as an amorphous pale yellow solid (27 mg, 0.14 mmol, 45% yield). Characterized by NMR comparison.[5c] ^{1}H NMR (400 MHz, $CDCl_3$) δ = 7.06 – 6.90 (m, 2H), 6.90 – 6.73 (m, 2H), 4.96 (dd, *J* = 10.2, 3.2 Hz, 1H), 4.86 – 4.75 (dd, *J* = 10.2, 1.6 Hz, 1H), 3.84 – 3.67 (m, 3H), 2.66 (d, *J* = 3.0 Hz, 3H); ^{13}C NMR (101 MHz,

$CDCl_3$) δ = 155.5 (C), 151.6 (C), 117.0 (2 X CH), 114.9 (2 X CH), 85.5 (CH_2), 55.7 (CH_3), 35.6 (CH_3).

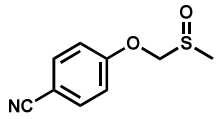

4-((methylsulfinyl)methoxy)benzonitrile (4.36). From 4-cyanophenol (**4.15**, 36 mg, 0.3 mmol) **4.36** was obtained as an amorphous colorless solid (41 mg, 0.21 mmol, 70% yield). IR (neat, cm^{-1}): 3068, 3009, 3003, 2918, 2852, 2221, 1594; ^1H NMR (400 MHz, $CDCl_3$) δ = 7.66 – 7.59 (m, 2H), 7.18 – 7.10 (m, 2H), 4.99 (d, *J* = 0.9 Hz, 2H), 2.70 (s, 3H); ^{13}C NMR (101 MHz, $CDCl_3$) δ = 160.6 (C), 134.2 (2 X CH), 118.5 (C), 116.3 (2 X CH), 106.5 (C), 83.6 (CH_2), 35.4 (CH_3); HRMS (ESI): m/z $[M + Na]^+$ calc'd for $C_9H_9NO_2SNa$, 218.0268; found, 218.0252.

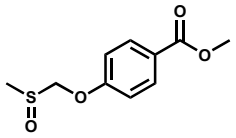

methyl 4-((methylsulfinyl)methoxy)benzoate (4.37). From methyl 4-hydroxybenzoate (**4.16**, 47 mg, 0.3 mmol) **4.37** was obtained as an amorphous pale yellow solid (49 mg, 0.22 mmol, 72% yield). Characterized by NMR comparison.[5c] ^1H NMR (400 MHz, $CDCl_3$) δ = 8.11 – 7.95 (m, 2H), 7.14 – 6.96 (m, 2H), 5.04 (d, *J* = 10.2 Hz, 1H), 4.93 (d, *J* = 10.2 Hz, 1H), 3.88 (s, 3H), 2.70 (s, 3H); ^{13}C NMR (101 MHz, $CDCl_3$) δ = 166.3 (C), 160.9 (C), 131.8 (2 X CH), 124.9 (C), 115.0 (2 X CH), 83.6 (CH_2), 52.1 (CH_3), 35.7 (CH_3).

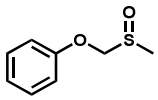

((methylsulfinyl)methoxy)benzene (4.32). From phenol (**4.17**, 28 mg, 0.3 mmol) **4.32** was obtained as a yellow oil (32 mg, 0.19 mmol, 63% yield). Characterized by NMR comparison.[20] ^{1}H NMR (400 MHz, $CDCl_3$) δ = 7.33 – 7.26 (m, 2H), 7.07 – 6.98 (m, 3H), 5.00 (d, *J* = 10.1 Hz, 1H), 4.84 (d, *J* = 10.1 Hz, 1H), 2.65 (s, 3H); ^{13}C NMR (101 MHz, $CDCl_3$) δ = 157.4 (C), 129.8 (2 X CH_2), 123.0 (CH), 115.6 (2 X CH), 84.4 (CH_2), 35.8 (CH_3).

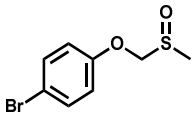

1-bromo-4-((methylsulfinyl)methoxy)benzene (4.38). From 4-bromophenol (**4.18**, 52 mg, 0.3 mmol) **4.38** was obtained as an amorphous pale yellow solid (46 mg, 0.19 mmol, 62% yield). Characterized by NMR comparison.[5c] ^{1}H NMR (400 MHz, $CDCl_3$) δ = 7.45 – 7.35 (m, 2H), 7.00 – 6.86 (m, 2H), 4.94 (d, *J* = 10.3 Hz, 1H), 4.85 (d, *J* = 10.3 Hz, 1H), 2.65 (s, 3H); ^{13}C NMR (101 MHz, $CDCl_3$) δ = 156.7 (C), 132.7 (2 X CH), 117.5 (2 X CH), 115.5 (C), 84.4 (CH_2), 35.6 (CH_3).

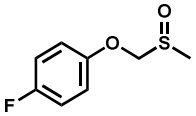

1-fluoro-4-((methylsulfinyl)methoxy)benzene (4.39). From 4-fluorophenol (**4.19**, 34 mg, 0.3 mmol) **4.39** was obtained as an amorphous off-white solid (23 mg, 0.12 mmol, 41% yield). **IR** (neat, cm^{-1}): 3051, 2960, 2932, 2910, 2835, 1503; ^{1}H NMR (400 MHz, $CDCl_3$) δ = 7.03 – 6.93 (m, 4H), 4.93 (d, *J* = 10.3 Hz, 1H), 4.84 (d, *J* = 10.4 Hz, 1H), 2.65 (s, 3H); ^{13}C NMR (101 MHz, $CDCl_3$) δ = 158.5 (d, *J* = 242.4 Hz, C), 153.7 (d, *J* = 6.0 Hz, C) 117.2 (d, *J* = 8.1 Hz, 2 X CH), 116.2 (d, *J* = 23.2 Hz), 85.1 (CH_2), 35.4 (CH_3); ^{19}F NMR

(377 MHz, $CDCl_3$) δ = -120.52; HRMS (ESI): m/z $[M + Na]^+$ calc'd for $C_8H_9FO_2SNa$, 211.0205; found, 211.0215.

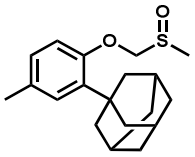

1-(5-methyl-2-((methylsulfinyl)methoxy)phenyl)adamantane (4.40). From 2-(adamantan-1-yl)-4-methylphenol (**4.20**, 73 mg, 0.3 mmol) **4.40** was obtained as an amorphous yellow solid (32 mg, 0.10 mmol, 33% yield). IR (neat, cm^{-1}): 3058, 2994, 2903, 2846, 1583, 1045; ^1H NMR (600 MHz, $CDCl_3$) δ = 7.07 – 7.01 (m, 1H), 6.98 (ddd, *J* = 8.3, 2.2, 0.8 Hz, 1H), 6.90 (d, *J* = 8.2 Hz, 1H), 5.01 (d, *J* = 9.8 Hz, 1H), 4.86 (d, *J* = 9.8 Hz, 1H), 2.72 (s, 3H), 2.28 (s, 3H), 2.10 – 2.01 (m, 9H), 1.80 – 1.68 (m, 6H); ^{13}C NMR (151 MHz, $CDCl_3$) δ = 154.7 (C), 138.7 (C), 132.1 (C), 127.9 (CH), 127.3 (CH), 114.2 (CH), 85.1 (CH_2), 40.9 (3 X CH_2), 37.0 (3 X CH_2), 36.9 (C), 36.0 (CH_3), 29.0 (3 X CH), 20.9 (CH_3); HRMS (ESI): m/z $[M + Na]^+$ calc'd for $C_{19}H_{26}O_2SNa$, 341.1551; found, 341.1542.

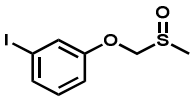

1-iodo-3-((methylsulfinyl)methoxy)benzene (4.41). From 3-iodophenol (**4.21**, 66 mg, 0.3 mmol) **4.41** was obtained as an amorphous off-white solid (31 mg, 0.16 mmol, 53% yield). **IR** (neat, cm^{-1}): 3055, 2992, 2915, 2909, 1582, 1034; ^1H NMR (600 MHz, $CDCl_3$) δ = 7.44 – 7.35 (m, 2H), 7.07 – 6.97 (m, 2H), 4.96 (d, *J* = 10.2 Hz, 1H), 4.85 (d, *J* = 10.2 Hz, 1H), 2.68 (s, 3H); ^{13}C NMR (151 MHz, $CDCl_3$) δ = 157.9 (C), 132.3 (CH), 131.1 (CH), 125.0 (CH), 115.0 (CH), 94.3 (C), 84.0 (CH_2), 35.7 (CH_3); HRMS (ESI): m/z $[M + Na]^+$ calc'd for $C_8H_9IO_2SNa$, 318.9266; found, 318.9261.

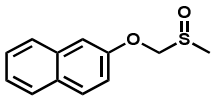

2-((methylsulfinyl)methoxy)naphthalene (4.42). From naphthalen-1-ol (**4.22**, 43 mg, 0.3 mmol) **4.42** was obtained as an amorphous yellow solid (42 mg, 0.19 mmol, 64% yield). Characterized by NMR comparison.[5c] ^{1}H NMR (400 MHz, $CDCl_3$) δ = 7.76 (dd, *J* = 12.3, 8.4 Hz, 3H), 7.47 (ddd, *J* = 8.2, 6.8, 1.3 Hz, 1H), 7.39 (ddd, *J* = 8.1, 6.9, 1.3 Hz, 1H), 7.34 (d, *J* = 2.6 Hz, 1H), 7.21 (dd, *J* = 9.0, 2.6 Hz, 1H), 5.16 (d, *J* = 10.1 Hz, 1H), 4.96 (d, *J* = 10.1 Hz, 1H), 2.72 (s, 3H); ^{13}C NMR (101 MHz, $CDCl_3$) δ = 155.2 (C), 134.1 (C), 130.1 (CH), 129.9 (C), 127.7 (CH), 127.1 (CH), 126.9 (CH), 124.8 (CH), 118.1 (CH), 109.0 (CH), 84.1 (CH_2), 35.9 (CH).

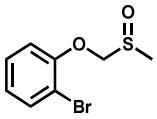

1-bromo-2-((methylsulfinyl)methoxy)benzene (4.43). From 2-bromophenol (**4.23**, 52 mg, 0.3 mmol) **4.43** was obtained as an amorphous colorless solid (44 mg, 0.18 mmol, 59% yield). Characterized by NMR comparison.[5c] ^{1}H NMR (400 MHz, $CDCl_3$) δ = 7.54 (dd, *J* = 7.9, 1.6 Hz, 1H), 7.29 (ddd, *J* = 8.2, 7.4, 1.6 Hz, 1H), 7.15 (dd, *J* = 8.3, 1.4 Hz, 1H), 6.95 (ddd, *J* = 7.9, 7.4, 1.4 Hz, 1H), 5.07 (d, *J* = 10.1 Hz, 1H), 4.90 (d, *J* = 10.1 Hz, 1H), 2.76 (s, 3H); ^{13}C NMR (101 MHz, $CDCl_3$) δ = 154.1 (C), 133.8 (CH), 128.9 (CH), 124.5 (CH), 115.9 (CH), 112.9 (C), 84.7 (CH_2), 36.0 (CH_3).

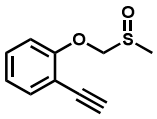

1-ethynyl-2-((methylsulfinyl)methoxy)benzene (4.44). From 2-ethynylphenol (**4.24**, 35 mg, 0.3 mmol) **4.44** was obtained as an amorphous pale yellow solid (30 mg, 0.15 mmol,

51% yield). IR (neat, cm^{-1}): 3286, 3061, 2993, 2916, 2850, 2100, 1584, 1574; ^1H NMR (400 MHz, $CDCl_3$) δ = 7.24 (t, *J* = 7.9 Hz, 1H), 7.16 (dt, *J* = 7.6, 1.3 Hz, 1H), 7.12 (dd, *J* = 2.7, 1.4 Hz, 1H), 7.02 (ddd, *J* = 8.3, 2.7, 1.1 Hz, 1H), 4.97 (d, *J* = 10.2 Hz, 1H), 4.85 (d, *J* = 10.2 Hz, 1H), 3.07 (s, 1H), 2.65 (s, 3H); ^{13}C NMR (101 MHz, $CDCl_3$) δ = 157.2 (C), 129.8 (CH), 126.9 (CH), 123.7 (C), 118.9 (CH), 116.5 (CH), 84.1 (CH_2), 82.8 (C), 78.0 (CH), 35.7 (CH_3); HRMS (ESI): m/z $[M + Na]^+$ calc'd for $C_{10}H_{10}O_2SNa$, 217.0294; found, 217.0299.

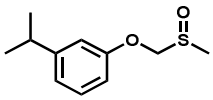

1-isopropyl-3-((methylsulfinyl)methoxy)benzene (4.45). From 3-isopropylphenol (**4.25**, 41 mg, 0.3 mmol) **4.45** was obtained as a yellow oil (25 mg, 0.12 mmol, 39% yield). IR (neat, cm^{-1}): 3031, 2957, 2924, 1589, 1585; ^1H NMR (400 MHz, $CDCl_3$) δ = 7.21 (t, *J* = 7.9 Hz, 1H), 6.91 (ddt, *J* = 7.7, 1.5, 0.7 Hz, 1H), 6.88 (dd, *J* = 2.6, 1.7 Hz, 1H), 6.82 (ddd, *J* = 8.2, 2.7, 0.9 Hz, 1H), 5.02 (d, *J* = 10.0 Hz, 1H), 4.82 (d, *J* = 10.0 Hz, 1H), 2.86 (hept, *J* = 6.9 Hz, 1H), 2.66 (s, 3H), 1.21 (d, *J* = 7.0 Hz, 6H); ^{13}C NMR (101 MHz, $CDCl_3$) δ = 157.5 (C), 151.2 (C), 129.6 (CH), 121.2 (CH), 113.9 (CH), 112.4 (CH), 84.2 (CH_2), 35.8 (CH_3), 34.1 (CH), 23.9 (2 X CH_3); HRMS (ESI): m/z $[M + Na]^+$ calc'd for $C_{11}H_{16}O_2SNa$, 235.0764; found, 235.0769.

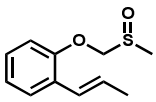

1-((methylsulfinyl)methoxy)-2-(prop-1-en-1-yl)benzene (4.46). From 3-(prop-1-en-1-yl)phenol (**4.26**, 40 mg, 0.3 mmol, 72:28 *E*:*Z*) **4.46** was obtained as an amorphous pale yellow solid (27 mg, 0.13 mmol, 43% yield, 78:22 *E*:*Z*). IR (neat, cm^{-1}): 3030, 2941, 2923,

2853, 1972, 1685, 1599, 1048; ^{1}H NMR (trans isomer) (400 MHz, $CDCl_3$) δ = 7.41 (dd, *J* = 7.9, 1.7 Hz, 1H), 7.32 – 7.09 (m, 1H), 7.10 – 6.95 (m, 2H), 6.64 (dq, *J* = 15.8, 1.8 Hz, 1H), 6.21 (dq, *J* = 15.9, 6.6 Hz, 1H), 5.03 (dd, *J* = 10.0, 5.4 Hz, 1H), 4.83 (dd, *J* = 11.9, 10.0 Hz, 1H), 2.59 (s, 3H), 1.89 (dd, *J* = 6.6, 1.8 Hz, 3H); ^{13}C NMR (trans isomer) (101 MHz, $CDCl_3$) δ = 154.0 (C), 130.7 (C), 128.0 (CH), 127.8 (CH), 126.8 (CH), 124.7 (CH), 123.3 (CH), 114.1 (CH), 85.1 (CH_2), 41.0 (CH_3), 18.9 (CH_3); ^{1}H NMR (cis isomer) (400 MHz, $CDCl_3$) δ = 7.32 – 7.09 (m, 2H), 7.10 – 6.95 (m, 2H), 6.47 (dd, *J* = 11.5, 2.0 Hz, 1H), 5.85 (dq, *J* = 11.6, 7.1 Hz, 1H), 5.03 (dd, *J* = 10.0, 5.4 Hz, 1H), 4.83 (dd, *J* = 11.9, 10.0 Hz, 1H), 2.68 (s, 3H), 1.79 (dd, *J* = 7.1, 1.8 Hz, 3H); ^{13}C NMR (cis isomer) (101 MHz, $CDCl_3$) δ = 154.0 (C), 130.7 (C), 128.2 (CH), 128.1 (CH), 128.1 (CH), 124.5 (CH), 122.7 (CH), 114.2 (CH), 85.0 (CH_2), 35.9 (CH_3), 14.6 (CH_3); HRMS (ESI): m/z $[M + Na]^+$ calc'd for $C_{11}H_{14}O_2SNa$, 233.0607; found, 233.0612.

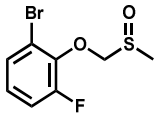

1-bromo-3-fluoro-2-((methylsulfinyl)methoxy)benzene (4.47). From 2-bromo-6-fluorophenol (**4.27**, 57 mg, 0.3 mmol) **4.47** was obtained as an amorphous colorless solid (60 mg, 0.23 mmol, 75% yield). IR (neat, cm^{-1}): 3059, 3030, 2939, 2920, 2848, 1603, 1585, 1043; ^{1}H NMR (400 MHz, $CDCl_3$) δ = 7.46 (dd, *J* = 8.8, 6.0 Hz, 1H), 6.92 (dd, *J* = 9.7, 2.7 Hz, 1H), 6.67 (ddd, *J* = 8.8, 7.7, 2.7 Hz, 1H), 4.99 (d, *J* = 10.3 Hz, 1H), 4.92 (d, *J* = 10.3 Hz, 1H), 2.73 (s, 3H); ^{13}C NMR (101 MHz, $CDCl_3$) δ = 162.4 (d, *J* = 250.5 Hz, C), 154.8 (d, *J* = 10.1 Hz, C), 134.1 (d, *J* = 9.1 Hz, CH), 111.3 (d, *J* = 22.2 Hz, CH), 107.0 (d, *J* = 4.0 Hz, C), 104.2 (d, *J* = 23.7 Hz, CH), 84.5 (CH_2), 35.7 (CH_3); ^{19}F NMR (377 MHz,

$CDCl_3$) δ = -110.3 ppm; HRMS (ESI): m/z [M + Na, ^{81}Br]$^+$ calc'd for $C_8H_8BrFO_2SNa$, 290.9291; found, 290.9290.

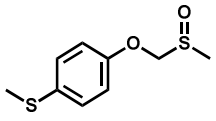

methyl(4-((methylsulfinyl)methoxy)phenyl)sulfane (4.48). From 4-(methylthio)phenol (**4.28**, 42 mg, 0.3 mmol) **4.48** was obtained as an amorphous colorless solid (49 mg, 0.23 mmol, 75% yield). IR (neat, cm^{-1}): 3057, 3002, 2981, 2919, 1592, 1585; ^1H NMR (400 MHz, $CDCl_3$) δ = 7.28 – 7.17 (m, 2H), 7.04 – 6.91 (m, 2H), 4.98 (d, *J* = 10.2 Hz, 1H), 4.84 (d, *J* = 10.2 Hz, 1H), 2.66 (d, *J* = 1.8 Hz, 3H), 2.44 (s, 3H); ^{13}C NMR (101 MHz, $CDCl_3$) δ = 155.7 (C), 132.2 (C), 129.4 (2 X CH), 116.3 (2 X CH), 84.5 (CH_2), 35.7 (CH_3), 17.3 (CH_3); HRMS (ESI): m/z [M + Na]$^+$ calc'd for $C_9H_{12}O_2S_2Na$, 239.0171; found, 239.0176.

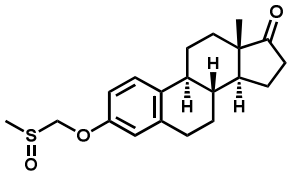

3-((methylsulfinyl)methoxy)-estrone (4.49). From estrone (**4.29**, 81 mg, 0.3 mmol) **4.49** was obtained as an amorphous colorless solid (26 mg, 0.08 mmol, 25% yield). IR (neat, cm^{-1}): 3030, 2923, 2863, 1734, 1606, 1496; ^1H NMR (400 MHz, $CDCl_3$) δ = 7.21 (dd, *J* = 8.6, 1.1 Hz, 1H), 6.81 (dd, *J* = 8.6, 2.9 Hz, 1H), 6.76 (dd, *J* = 2.9, 1.2 Hz, 1H), 5.00 (d, *J* = 10.1 Hz, 1H), 4.81 (dd, *J* = 10.1, 1.5 Hz, 1H), 2.88 (dd, *J* = 8.8, 4.1 Hz, 2H), 2.66 (s, 3H), 2.53 – 2.43 (m, 1H), 2.37 (ddt, *J* = 9.0, 3.9, 1.8 Hz, 1H), 2.31 – 2.03 (m, 2H), 2.07 – 1.86 (m, 3H), 1.68 – 1.34 (m, 6H), 0.88 (s, 3H); ^{13}C NMR (101 MHz, $CDCl_3$) δ = 155.4 (C), 138.4 (C), 134.6 (C), 126.7 (CH), 115.6 (CH), 113.0 (CH), 84.3 (CH_2), 50.4 (CH), 48.0 (C), 44.0 (CH), 38.2 (CH), 35.8 (CH_2), 35.8 (CH_3), 31.6 (CH_2), 29.6 (CH_2), 26.4 (CH_2),

25.9 (CH_2), 21.6 (CH_2), 13.8 (CH_3), -18.1 (C); HRMS (ESI): m/z $[M + Na]^+$ calc'd for $C_{20}H_{26}O_3SNa$, 369.1495; found, 369.1500.

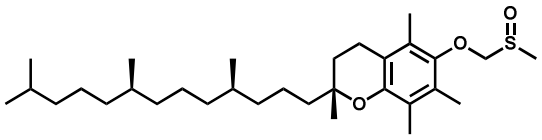

(2R)-2,5,7,8-tetramethyl-6-((methylsulfinyl)methoxy)-2-((4R,8R)-4,8,12-trimethyltridecyl)chromane (4.50). From α-tocopherol (**4.30**, 130 mg, 0.3 mmol) **4.50** was obtained as a viscous dark brown oil (44 mg, 0.09 mmol, 29% yield). IR (neat, cm^{-1}): 2952, 2922, 2895, 2844, 1457; ^1H NMR (400 MHz, $CDCl_3$) δ = 4.67 (d, *J* = 9.4 Hz, 1H), 4.61 (d, *J* = 9.3 Hz, 1H), 2.70 (s, 3H), 2.55 (t, *J* = 6.8 Hz, 2H), 2.16 (s, 3H), 2.13 (s, 3H), 2.06 (s, 3H), 1.78 (dp, *J* = 19.7, 6.9 Hz, 2H), 1.58 – 1.44 (m, 2H), 1.43 – 0.95 (m, 17H), 0.83 (dd, *J* = 9.7, 6.5 Hz, 16H); ^{13}C NMR (101 MHz, $CDCl_3$) δ = 148.7 (C), 147.7 (C), 127.0 (C), 125.2 (C), 123.5 (C), 117.9 (C), 89.3 (CH_2), 75.1 (C), 40.0 (CH_2), 39.4 (CH_2), 37.6-37.3 (m, 4 X CH_2), 35.9 (CH_3), 32.8 (CH), 32.7 (CH), 31.2 (CH_2), 28.0 (CH), 24.8 (CH_2), 24.4 (CH_2), 23.9 (2 X CH_3), 22.7 (CH_3), 21.0 (CH_2), 20.7 (CH_2), 19.8-19.6 (m, 2 X CH_3), 13.2 (CH_3), 12.3 (CH_3), 11.8 (CH_3); HRMS (ESI): m/z $[M + Na]^+$ calc'd for $C_{31}H_{54}O_3SNa$, 529.3691; found, 529.3688.

4.8 References

1. Frlan, R.; Kikelj, D. Recent Progress in Diaryl Ether Synthesis. *Synthesis* **2006**, *14*, 2271-2885.

2. For recent reviews on the synthesis of biaryl ethers using Pd(0) or Cu(I), see: a) Monnier, F.; Taillefer, M. Catalytic C-C, C-N, and C-O Ullmann-Type Coupling Reactions. *Angew. Chem. Int. Ed.* **2009,** *48*, 6954-6971; b) Enthaler, S.; Company, A. Palladium-catalysed hydroxylation and alkoxylation. *Chem. Soc. Rev.* **2011,** *40*, 4912-4924; c) ; Pitsinos, E. M.; Vidali, V. P.; Couladouros, E. A. Diaryl Ether Formation in the Synthesis of Natural Products. *Eur. J. Org. Chem* **2011,** *7*, 1207-1222; d) Sambiagio, C; Marsden S. P.; Blacker, A. J.; McGowan, P. C. Copper catalysed Ullmann type chemistry: from mechanistic aspects to modern development. *Chem. Soc. Rev.* **2013,** *43*, 3525-3550.

3. For recent reviews on the synthesis of biaryl ethers using S_NAr and other substitution reactions, see: a) Olofsson, B. Arylation with Diaryliodonium Salts. In *Hypervalent Iodine Chemistry;* Wirth, T., Ed.; Springer: Cham, 2015; Vol. 373, pp. 135-166 b) Pant, P. L.; Shankarling, G. S. Recent advances in synthetic methodologies for transition metal-free Ullmann condensation reactions. *New J. Chem.* **2018**, *42*, 13212-13224; For selected examples, see; c) Li, F.; Wang, Q.; Ding, Z.; Tao, F. Microwave-Assisted Synthesis of Diaryl Ethers without Catalyst. *Org. Lett.* **2003,** *5*, 2169-2171; d) Lindstedt, E.; Ghosh, R.; Olofsson, B. Metal-Free Synthesis of Aryl Ethers in Water. *Org. Lett.* **2013**, *15*, 6070-6073; e) Huang, L. Z.; Han, P.; Li, Y. Q.; Xu, Y. M.; Zhang, T.; Du, Z. T. A Facile and Efficient Synthesis of Diaryl Amines or Ethers under Microwave Irradiation at Presence of KF/Al_2O_3 without Solvent and Their Anti-Fungal Biological Activities against Six Phytopathogens. *Int. J. Mol. Sci.* **2013**, *14*, 18850-18860; f) Yuyang,

D.; Lipschutz, M. I.; Tilley, T. D. Regioselective, Transition Metal-Free C–O Coupling Reactions Involving Aryne Intermediates. *Org. Lett.* **2016**, *18*, 1530−1533; g) Wang, D.-Y.; Yang, Z.-K.; Wang, C.; Zhang, A.; Uchiyama, M. From Anilines to Aryl Ethers: A Facile, Efficient, and Versatile Synthetic Method Employing Mild Conditions. *Angew. Chem. Int. Ed.* **2018**, *57*, 3641-3645.

4. a) Monkovi ć , I.; Brown, M.; Luke, G. M.; Standridge, R. T.; Willner, D.; Crosswell, A. R.; Algieri, A.; Buyniski, J. P.; Crenshaw, R. R.; Juby, P. F. Potential non-dopaminergic gastrointestinal prokinetic agents in the series of substituted benzamides. *Eur. J. Med. Chem.* **1989,** *24*, 233-239. For selected examples of methylsulfinylmethyl ether used as functional handle or protecting group, see: b) Okada, Y.; Wang, J.; Yamamoto, T.; Yokoi, T.; Mu, Y. Amino Acids and Peptides. L. Development of a Novel Nπ-Protecting Group for Histidine, N π -2-Adamantyloxymethylhistidine, and Its Application to peptide Synthesis. *Chem. Pharm. Bull.* **1997,** *45*, 452-456; c) Ringom, R.; Benneche, T.; Colapietro, M.; Pieretti, A.; Ramondo, F.; Møller, J.; Senning, A.; Yao, X.-K.; Wang, H.-G.; Tuchagues, J. P.; Ögren, M. Synthesis and Nucleophilic Substitution Reactions of Mono alpha-Fluoro Ethers. *Acta Chem. Scand.* **1999,** *53*, 41-47; d) Adachi, M.; Hashimoto, H.; Sakakibara, R.; Imazu, T.; Nishikawa, T. A New Deprotection Procedure of MTM Ether. *Synlett* **2014,** *25*, 2498-2502; e) Geng, Y.; Liang, A.; Gao, X.; Niu, C.; Li, J.; Zou, D.; Wu, Y.; Wu, Y. CuI-Catalyzed Fluorodesulfurization for the Synthesis of Monofluoromethyl Aryl Ethers. *J. Org. Chem.* **2017,** *82*, 8604-8610.

5. For examples of synthesis of methylsulfinylmethyl ethers, see: a) Dahnke, K. R.; Gajewski, R. P.; Jones, C. D.; Linebarger, J. H.; Lu, J.; Ma, T.; Nagpal, S.; Simard, T. P.; Yee, Y. K.; Bunel, E. E.; Stites, R. E. Phenyl-Thiophene Type Vitamin D Receptor

Modulators. WO03101978 (A1), 2003/12/11/, **2003**; b) Burdi, D. F.; Tanaka, D.; Fujiwara, H. Tricyclic Guanidine Derivative. US2016083400 (A1), 2016/03/24/, **2016**; c) Wu, Y.; Geng, Y.; Niu, C.; Liang, E.; Liu, J.; Meng, Q.; Li, J.; Zou, D.; Wu, Y. Synthesis method of monofluoromethoxyl or monofluoro-deuterated methoxyl compound. CN106083539 (A), 2016/11/09/, **2016**; d) Riesinger, S.; Lazarova, T.; Ribovskaia, Z. Nitric Oxide Donors. WO2017223182 (A1), 2017/12/28/, **2017**.

6. a) Pichette Drapeau, M.; Tlili, A.; Zaid, Y.; Toummini, D.; Ouazzani Chahdi, F.; Sotiropoulos, J.-M.; Ollevier, T.; Taillefer, M. Transition-Metal-Free Synthesis of Biarylmethanes from Aryl Iodides and Benzylic Ketones. *Chem. Eur. J.* **2018,** *24*, 17449-17453; b) Wu, Y.; Huang, Z.; Luo, Y.; Liu, D.; Deng, Y.; Yi, H.; Lee, J.-F.; Pao, C.-W.; Chen, J.-L.; Lei, A. X-ray Absorption and Electron Paramagnetic Resonance Guided Discovery of the Cu-Catalyzed Synthesis of Multiaryl-Substituted Furans from Aryl Styrene and Ketones Using DMSO as the Oxidant. *Org. Lett.* **2017,** *19*, 2330-2333.

7. a) Jones-Mensah, E.; Karki, M.; Magolan, J. Dimethyl Sulfoxide as a Synthon in Organic Chemistry. *Synthesis* **2016,** *48*, 1421-1436; b) Garza-Sanchez, R. A.; Patra, T.; Tlahuext-Aca, A.; Strieth-Kalthoff, F.; Glorius, F. DMSO as a Switchable Alkylating Agent in Heteroarene C–H Functionalization. *Chem. Eur. J.* **2018,** *24*, 10064-10068; c) Zhang, J.; Cheng, S.; Cai, Z.; Liu, P.; Sun, P. Radical Addition Cascade Cyclization of 1,6-Enynes with DMSO To Access Methylsulfonylated and Carbonylated Benzofurans under Transition-Metal-Free Conditions. *J. Org. Chem.* **2018,** *83*, 9344-9352; d) Shu, W.-M.; He, J.-X.; Zhang, X.-F.; Wang, S.; Wu, A.-X. TFA-Mediated DMSO-Participant Sequential Oxidation/1,3-Dipolar Cycloaddition Cascade of Pyridinium Ylides for the Assembly of Indolizines. *J. Org. Chem.* **2019,** *84*, 2962-2968.

8. a) Barham, J. P.; Coulthard, G.; Emery, K. J.; Doni, E.; Cumine, F.; Nocera, G.; John, M. P.; Berlouis, L. E. A.; McGuire, T.; Tuttle, T.; Murphy, J. A. KOtBu: A Privileged Reagent for Electron Transfer Reactions? *J. Am. Chem. Soc.* **2016,** *138*, 7402-7410; b) Barham, J. P.; Dalton, S. E.; Allison, M.; Nocera, G.; Young, A.; John, M. P.; McGuire, T.; Campos, S.; Tuttle, T.; Murphy, J. A. Dual Roles for Potassium Hydride in Haloarene Reduction: CSNAr and Single Electron Transfer Reduction via Organic Electron Donors Formed in Benzene. *J. Am. Chem. Soc.* **2018,** *140*, 11510-11518.

9. Rossi, R. A.; Palacios, S. M. Photostimulated reactions of alkanethiolate ions with haloarenes. Electron transfer vs. fragmentation of the radical anion intermediate. *J. Org. Chem.* **1981,** *46*, 5300-5304.

10. a) Christ, P.; Lindsay, A. G.; Vormittag, S. S.; Neudörfl, J.-M.; Berkessel, A.; O'Donoghue, A. C. pKa Values of Chiral Brønsted Acid Catalysts: Phosphoric Acids/Amides, Sulfonyl/Sulfuryl Imides, and Perfluorinated TADDOLs (TEFDDOLs). *Chem. Eur. J.* **2011,** *17*, 8524-8528; b) Huffman, L. M.; Casitas, A.; Font, M.; Canta, M.; Costas, M.; Ribas, X.; Stahl, S. S. Observation and Mechanistic Study of Facile C□O Bond Formation between a Well-Defined Aryl–Copper(III) Complex and Oxygen Nucleophiles. *Chem. Eur. J.* **2011,** *17*, 10643-10650.

11. Bunnett, J. F. Base-catalyzed halogen dance, and other reactions of aryl halides. *Acc. Chem. Res.* **1972,** *5*, 139-147.

12. a) Argüello, J. E.; Peñéñory, A. B.; Rossi, R. A. Quantum Yields of the Initiation Step and Chain Propagation Turnovers in SRN1 Reactions: Photostimulated Reaction of 1-Iodo-2-methyl-2-phenyl Propane with Carbanions in DMSO. *J. Org. Chem.* **2000,** *65*, 7175-7182; b) Pichette Drapeau, M.; Fabre, I.; Grimaud, L.; Ciofini, I.; Ollevier, T.; Taillefer, M. Transition-Metal-Free α-Arylation of Enolizable Aryl Ketones and Mechanistic

Evidence for a Radical Process. *Angew. Chem. Int. Ed.* **2015,** *54*, 10587-10591; c) Caminos, D. A.; Puiatti, M.; Bardagí, J. I.; Peñéñory, A. B. Anions involved in the initiation of the thermally induced SRN1 reaction for α-arylation of ketones. *RSC Adv.* **2017,** *7*, 31148-31157.

13. a) Bunnett, J. F.; Wamser, C. C. Radical Abstraction of Iodine from Aryl Iodides1. *J. Am. Chem. Soc.* **1966,** *88*, 5534-5537; b) Bunnett, J. F.; Wamser, C. C. Radical-induced deiodination of aryl iodides in alkaline methanol. *J. Am. Chem. Soc.* **1967,** *89*, 6712-6718; c) Bunnett, J. F.; Victor, R. R. Base-induced dehalogenation of aryl halides in tert-butyl alcohol-dimethyl sulfoxide and similar solvent mixtures. *J. Am. Chem. Soc.* **1968,** *90*, 810-811; d) Bunnett, J. F.; Kim, J. K. Evidence for a radical mechanism of aromatic "nucleophilic" substitution. *J. Am. Chem. Soc.* **1970**, *92*, 7463-7464; e) Bunnett, J. F.; Kim, J. K. Alkali metal promoted aromatic "nucleophilic" substitution. *J. Am. Chem. Soc.* **1970,** *92*, 7464-7466; f) Soria-Castro, S. M.; Caminos, D. A.; Peñéñory, A. B. An expedient route to heterocycles through α-arylation of ketones and arylamides by microwave induced thermal SRN1 reactions. *RSC Adv.* **2014,** *4*, 17490-17497.

14. These species may also be formed by the decomposition of DMSO at high temperature. See: Wang, Z.; Richter, S. M.; Gates, B. D.; Grieme, T. A. Safety Concerns in a Pharmaceutical Manufacturing Process Using Dimethyl Sulfoxide (DMSO) as a Solvent. *Org. Proc. Res. Dev.* **2012,** *16*, 1994-2000.

15. Altwicker, E. R. The Chemistry of Stable Phenoxy Radicals. *Chem. Rev*. **1967**, 67, 475-531.

16. Miranda, M. A.; Tormos, R. Photochemistry of o-allylphenol. Identification of the minor products and new mechanistic proposals. *J. Org. Chem.* **1993**, 58, 3304-3307.

17. Control experiments showed a H-D exchange between DMSO/D_2O (1:1) under the reaction conditions.

18. Dean, J. A.; Lange, N. A. (**1992**) Section 4: Properties of Atoms, Radicals and Bonds. In *Lange's handbook of chemistry*, pp 4.41-4.53. McGraw-Hill, New York.

19. Luo, Y.-R., *Handbook of Bond Dissociation Energies in Organic Compounds*. CRC Press 2002.

20. a) Rajan, S.; Muralimohan, K. Aromatic SRN1 reactions stimulated by sunlight - phenylation of dimsyl anion. *Tet. Lett.* **1978,** *19*, 483-486; b) Alonso, R. A.; Rossi, R. A. On the reactivity of dimsyl anion with aryl radicals. *Tet. Lett.* **1985,** *26*, 5763-5764; c) Bunnett, J. F. Radical-chain, electron-transfer dehalogenation reactions. *Acc. Chem. Res.* **1992,** *25*, 2-9; d) Rossi, R. A.; Pierini, A. B.; Peñéñory, A. B. Nucleophilic Substitution Reactions by Electron Transfer. *Chem. Rev.* **2003,** *103*, 71-168.

21. Although 1,3-dichlorobenzene is a byproduct of this transformation, the latter was not observed nor isolated from any crude reaction mixtures. Control experiments showed that pure 1,3-dichlorobenzene rapidly degrades under the reaction conditions (K_2CO_3 (2 equivalents) in DMSO at 135^{o}C in an open-air flask).

22. Tsuchihashi, G.; Ogura, K. Neue Sulfoxydderivate und Verfahren zu ihrer Herstellug. DE2130923 (C3), 1973/10/04/, **1973.**

CONCLUSION

In summary, the importance of a diverse mechanistic toolbox in radical chemistry is not to be underestimated. As radical chemistry – particularly that generated by photoredox catalysis – becomes more pervasive in syntheses of complex bioactive products, there is a higher imperative for profound understanding of all concomitant factors in a radical reaction. Our group has undertaken mechanistic investigation of three organic radical transformations herein and has obtained results that challenge the conventional. The dimeric gold photocatalyst $[Au_2(dppm)_2]Cl_2$ has been shown to easily generate alkyl radicals from bromoalkanes by accessing both its oxidative and reductive quenching cycles, generating phenanthridines and amide products. The utility of this catalyst has been extended to include kinetic "clock" studies, wherein the rate constant for addition of a primary radical to a biphenyl isonitrile was established. The polypyridyl iridium complex $[Ir(dF(CF_3)ppy)_2(dtbbpy)]Cl$ catalytically generated chlorine atoms in solution, which were able to access totally unactivated C^{sp3}–H bonds for HAT. Mechanistic data from this methodology illustrate the crucial role factors such as solvent, substrate polarity, competitive energy transfer pathways, and reaction kinetics can have on radical reactions. Finally, the etherification of phenols in DMSO with base was revealed to have a unique radical mechanism. Previous art and new experimental evidence indicate that single electron transfer from dimsyl potassium into C^{sp2}–I bonds is possible under precise conditions. A variety of mechanistic tools have been shown to shine light on the "black box" at the center of many radical reactions.

NMR SPECTRA

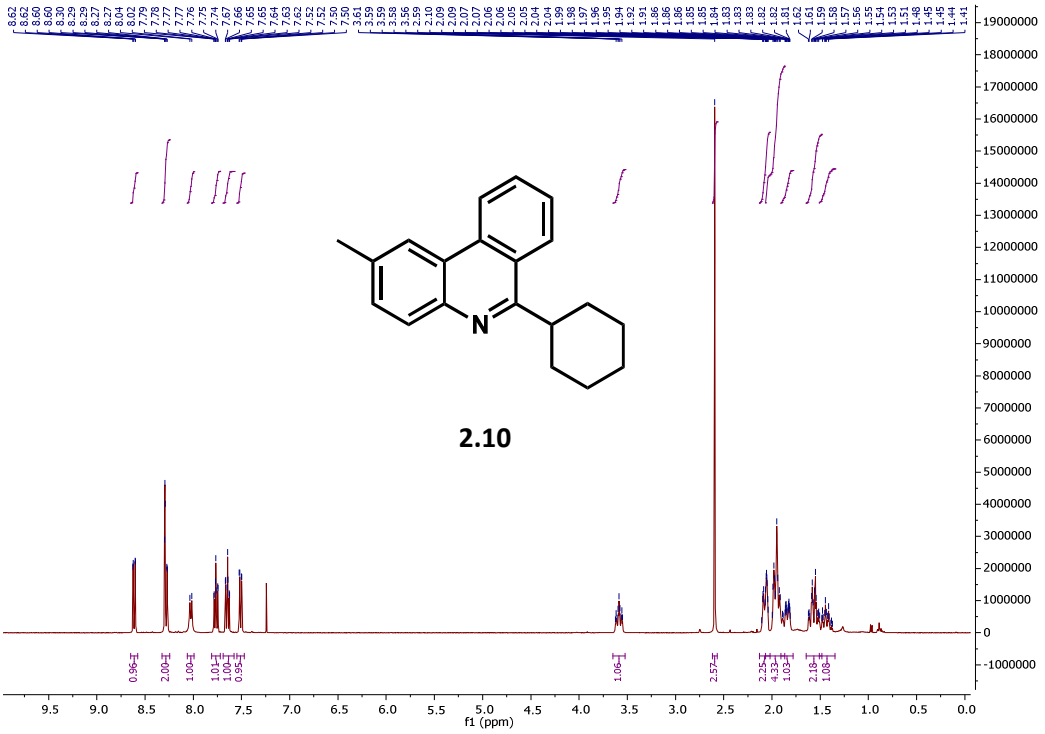

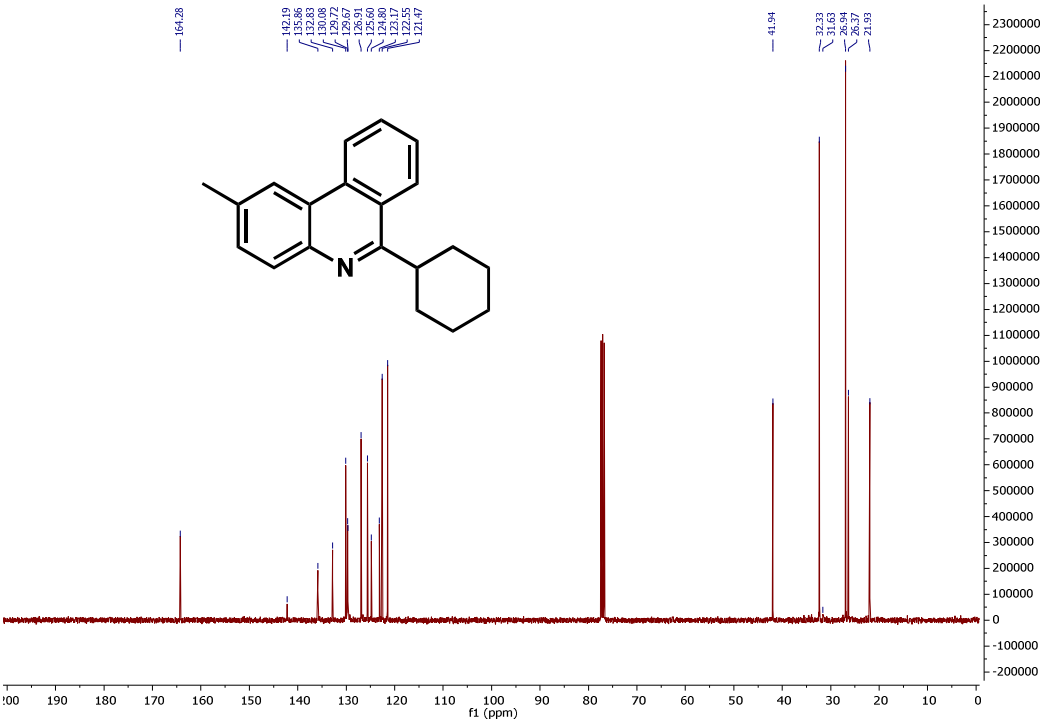

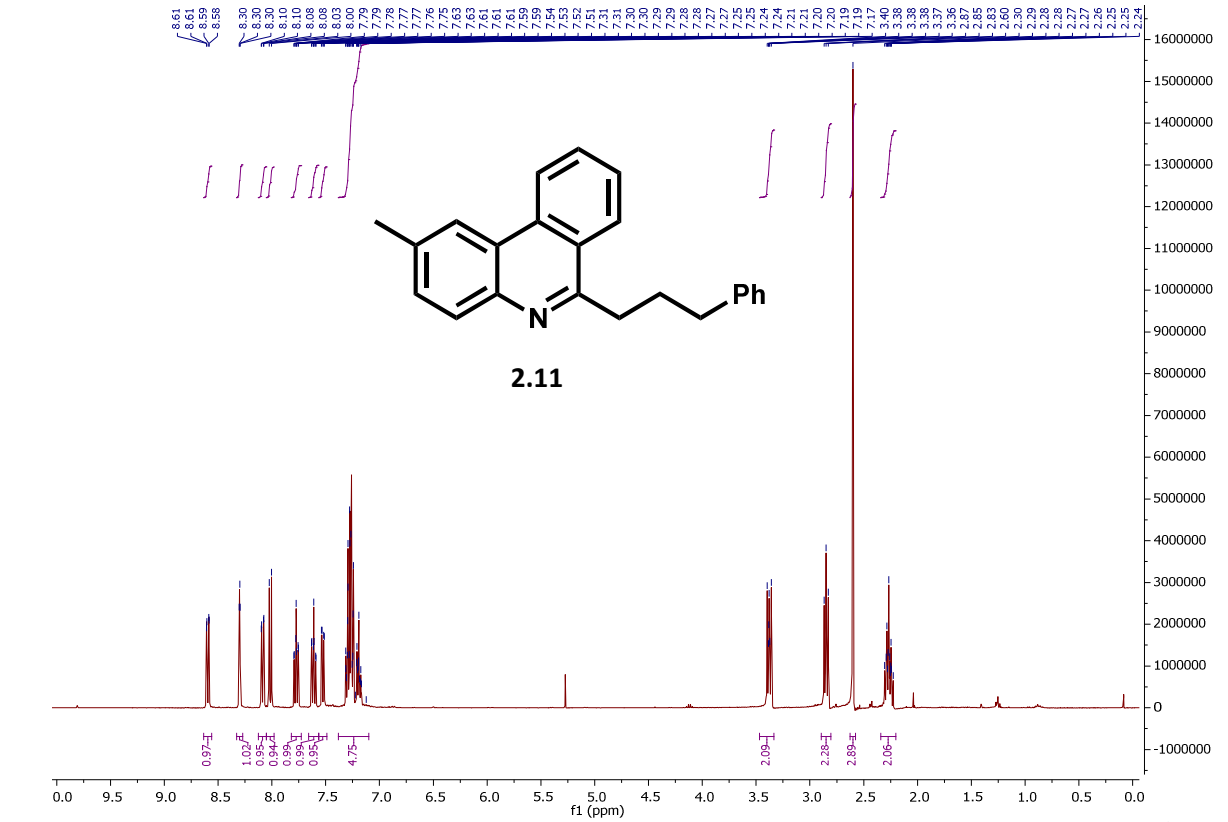

2.11

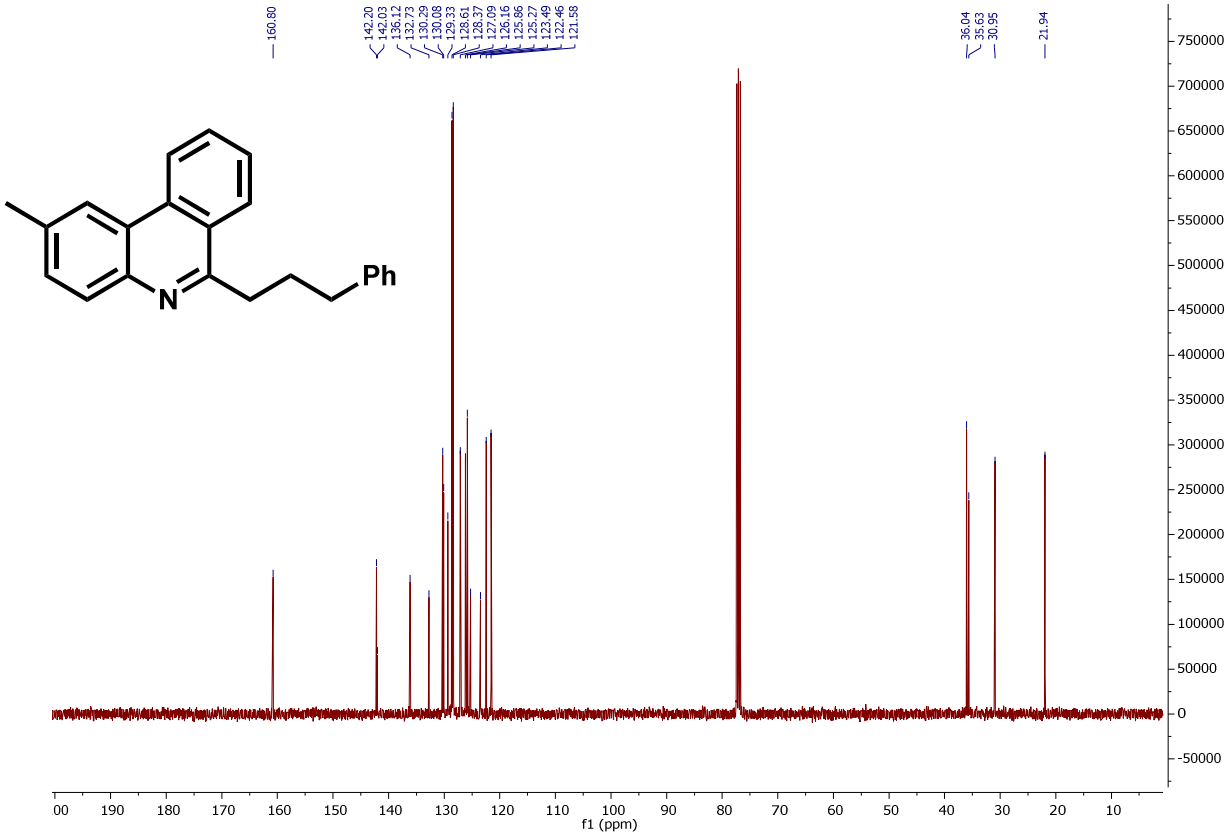

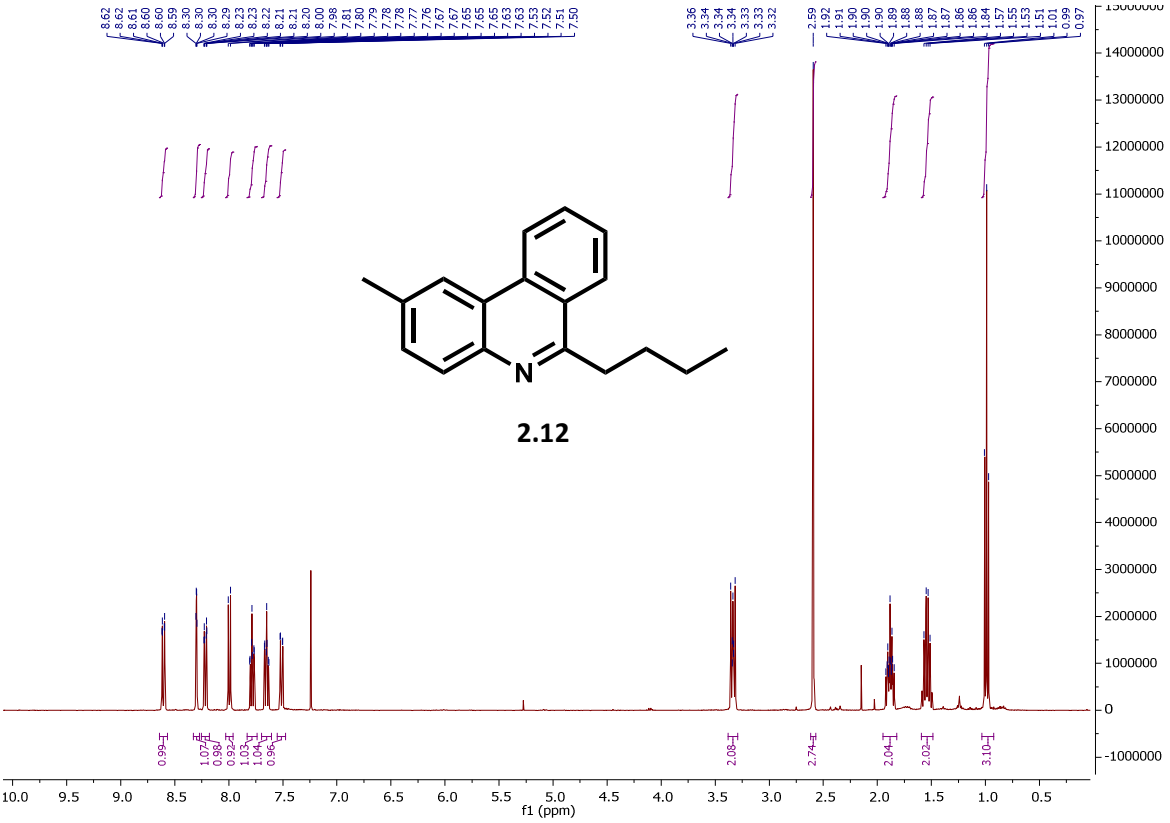

2.12

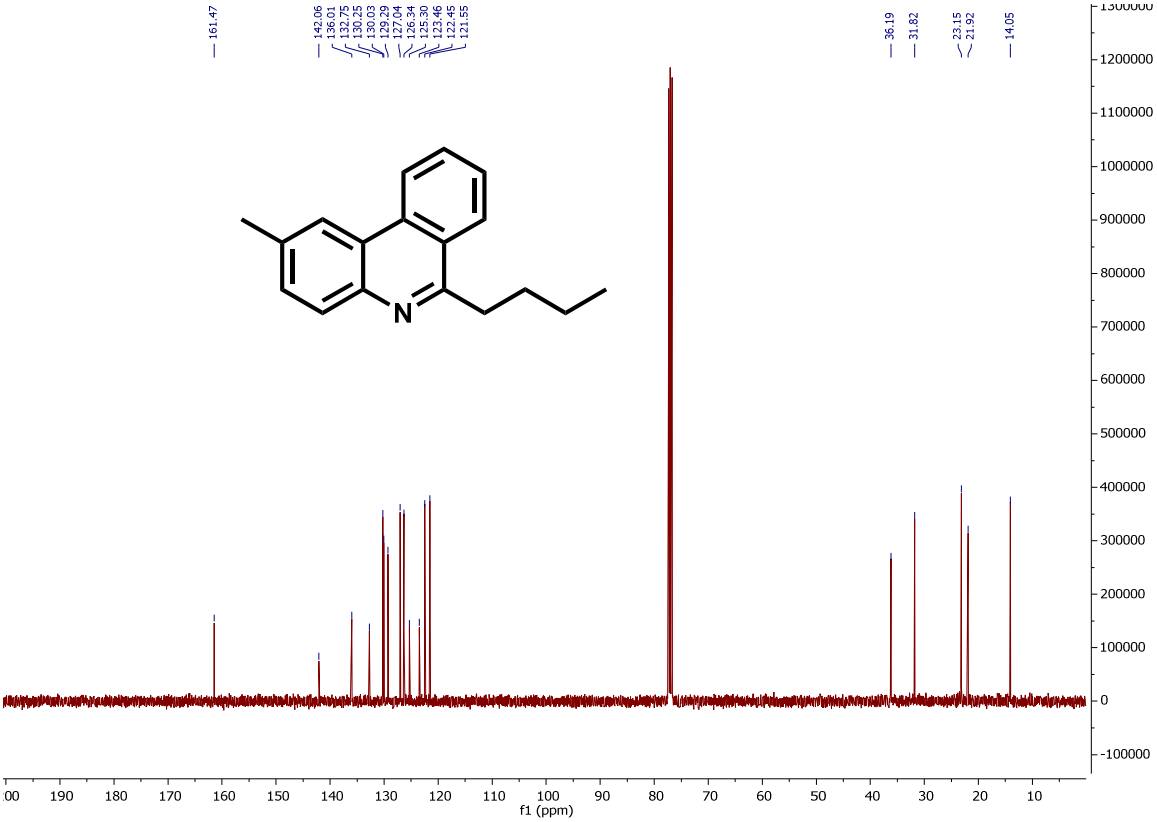

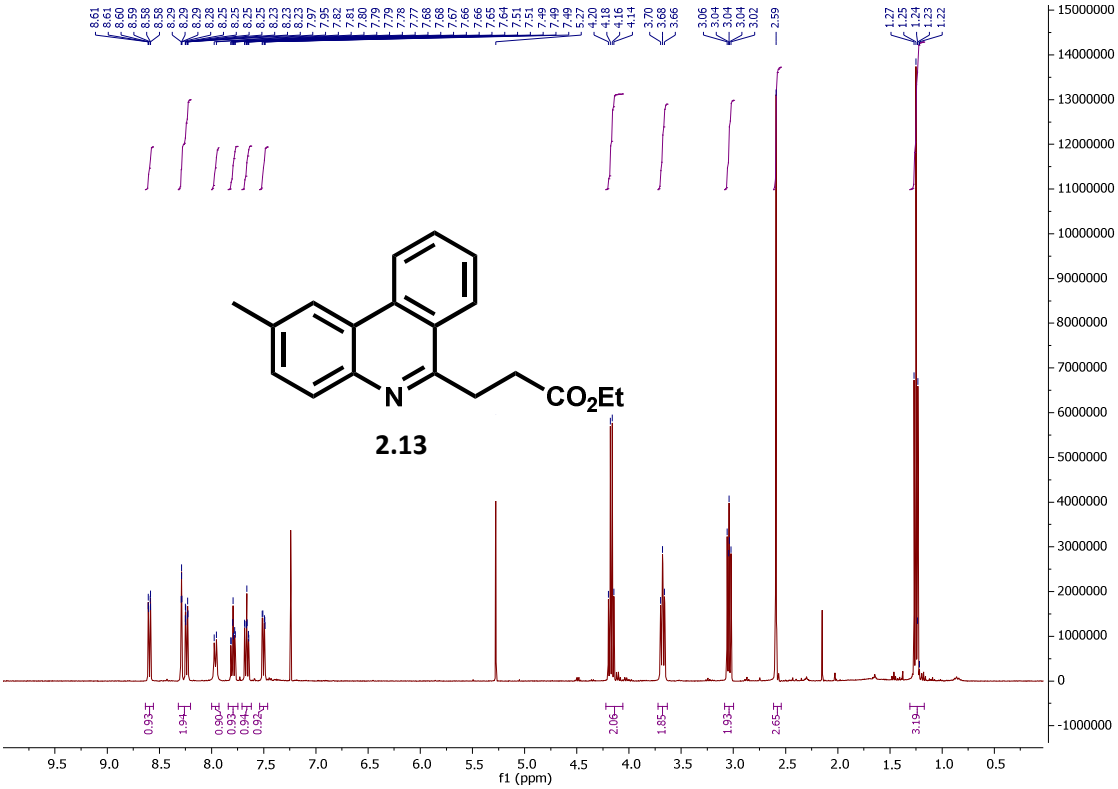
8.61
8.61
8.60
8.59
8.58
8.58
8.29
8.29
8.29
8.28
8.25
8.25
8.25
8.23
8.23
7.97
7.95
7.82
7.81
7.80
7.79
7.79
7.78
7.77
7.68
7.67
7.66
7.66
7.65
7.64
7.51
7.51
7.49
7.49
7.49
7.27
4.20
4.18
4.16
4.14
3.70
3.68
3.66
3.06
3.04
3.04
3.04
3.02
2.59
1.27
1.25
1.24
1.23
1.22
N
CO2Et
2.13
0.93
1.94
0.90
0.93
0.94
0.92
2.06
1.85
1.93
2.65
3.19
f1 (ppm)

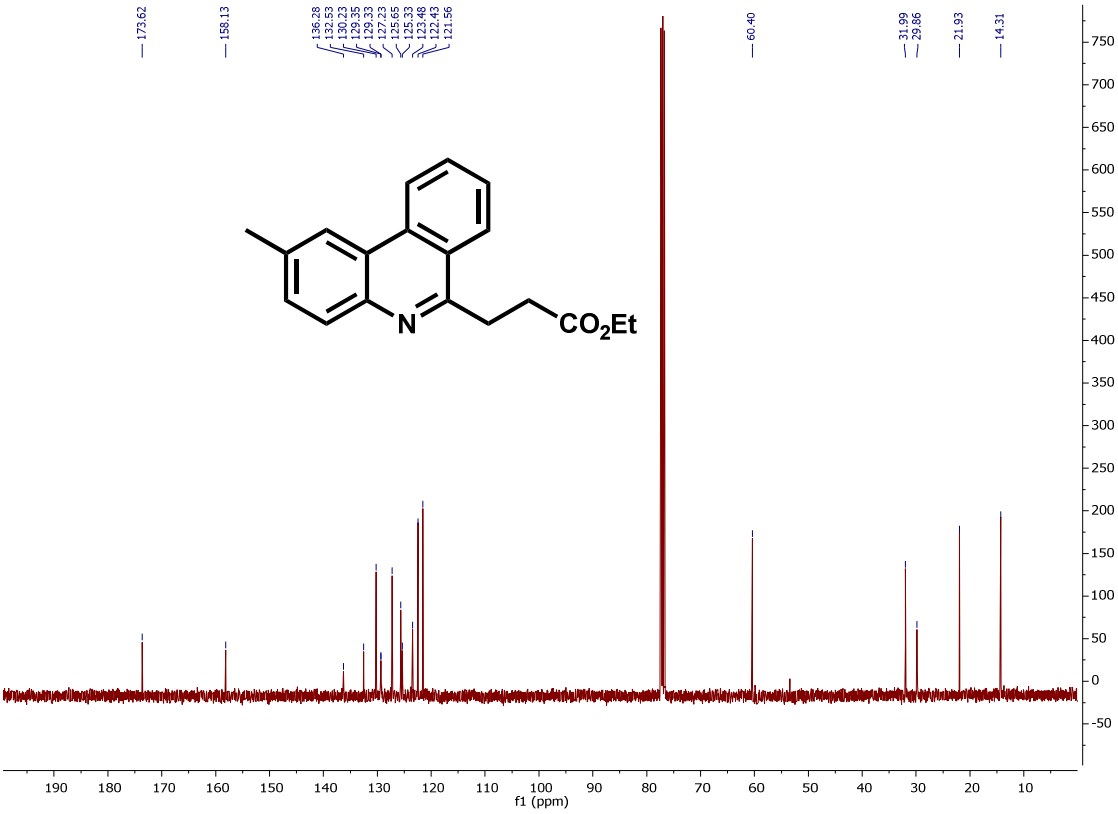
173.62
158.13
136.28
132.23
130.23
129.35
129.33
127.23
125.65
125.33
123.48
122.43
121.56
60.40
31.99
29.86
21.93
14.31
N
CO2Et
f1 (ppm)

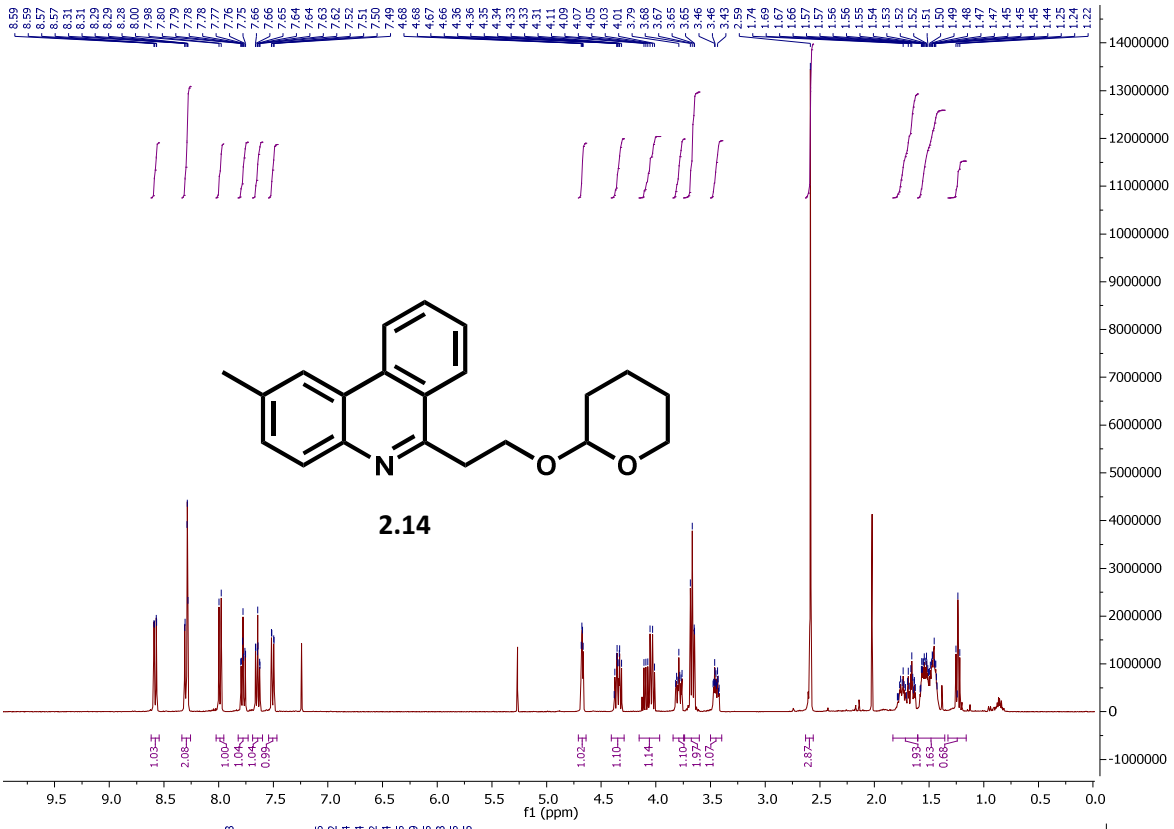

2.14

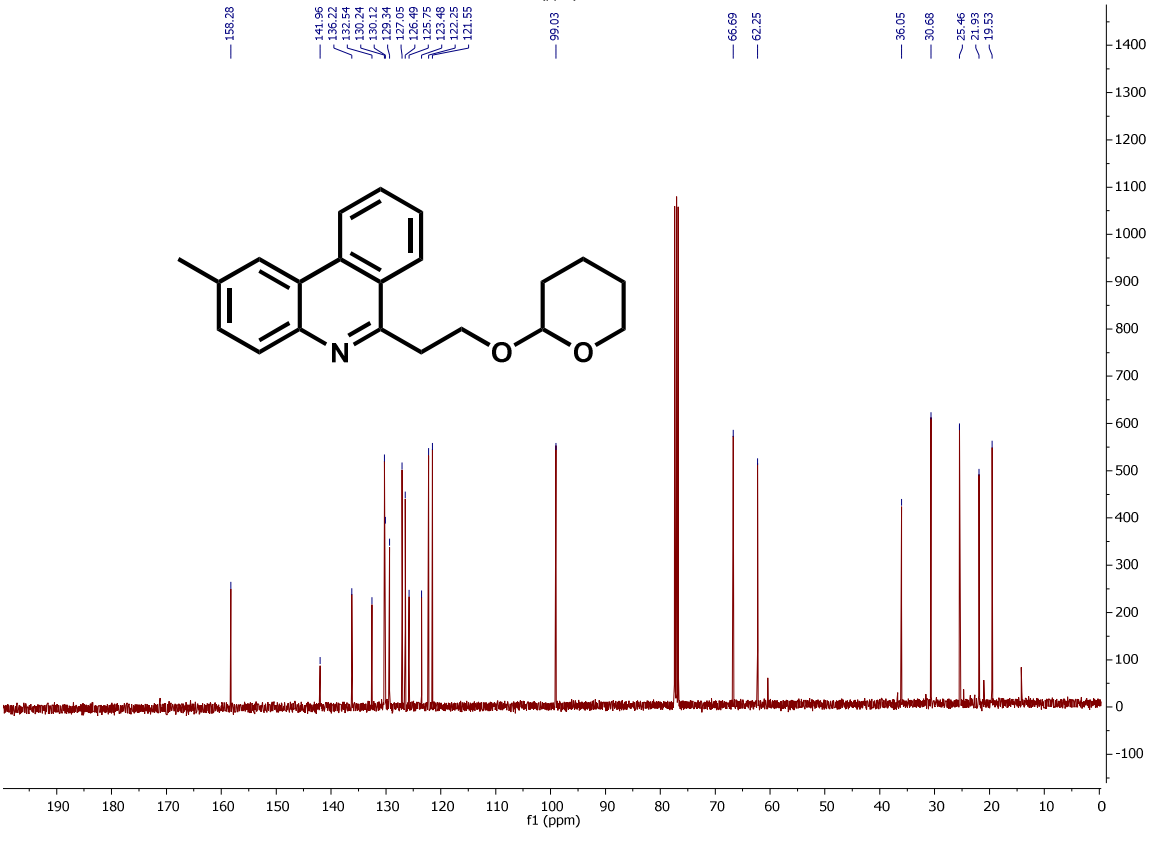

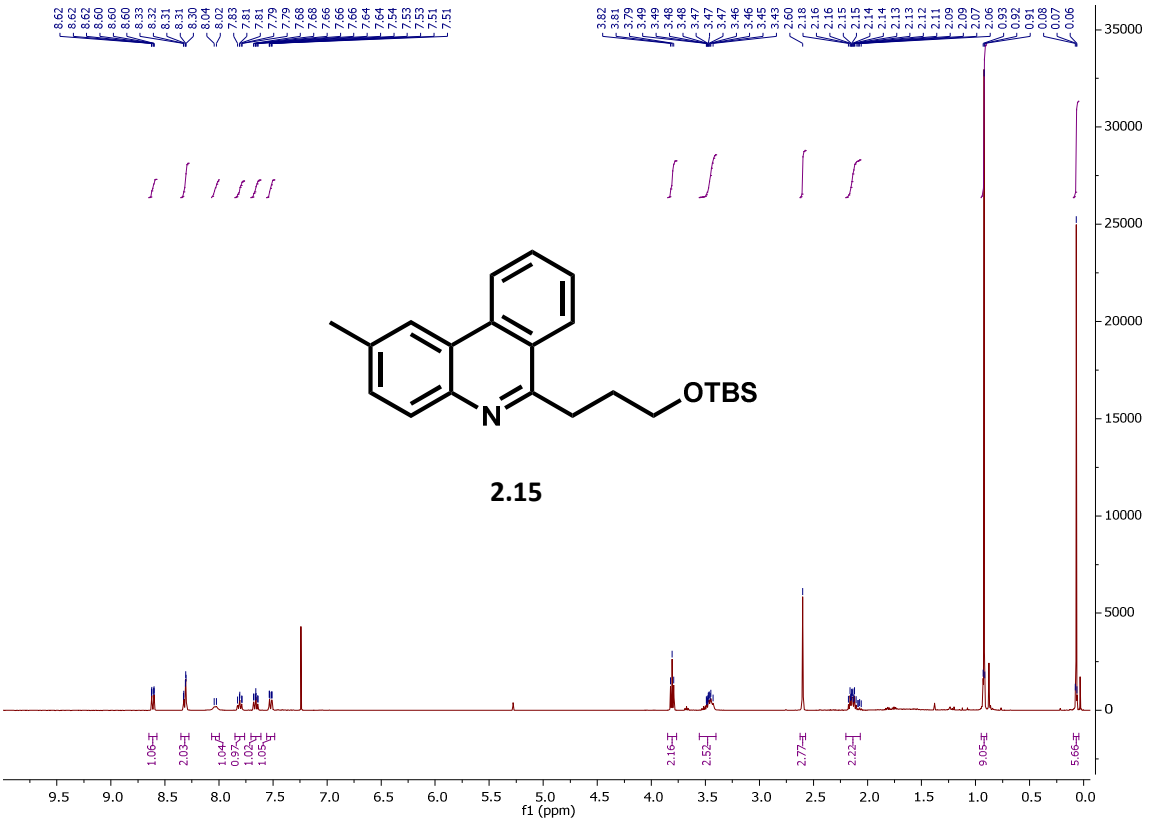

2.15

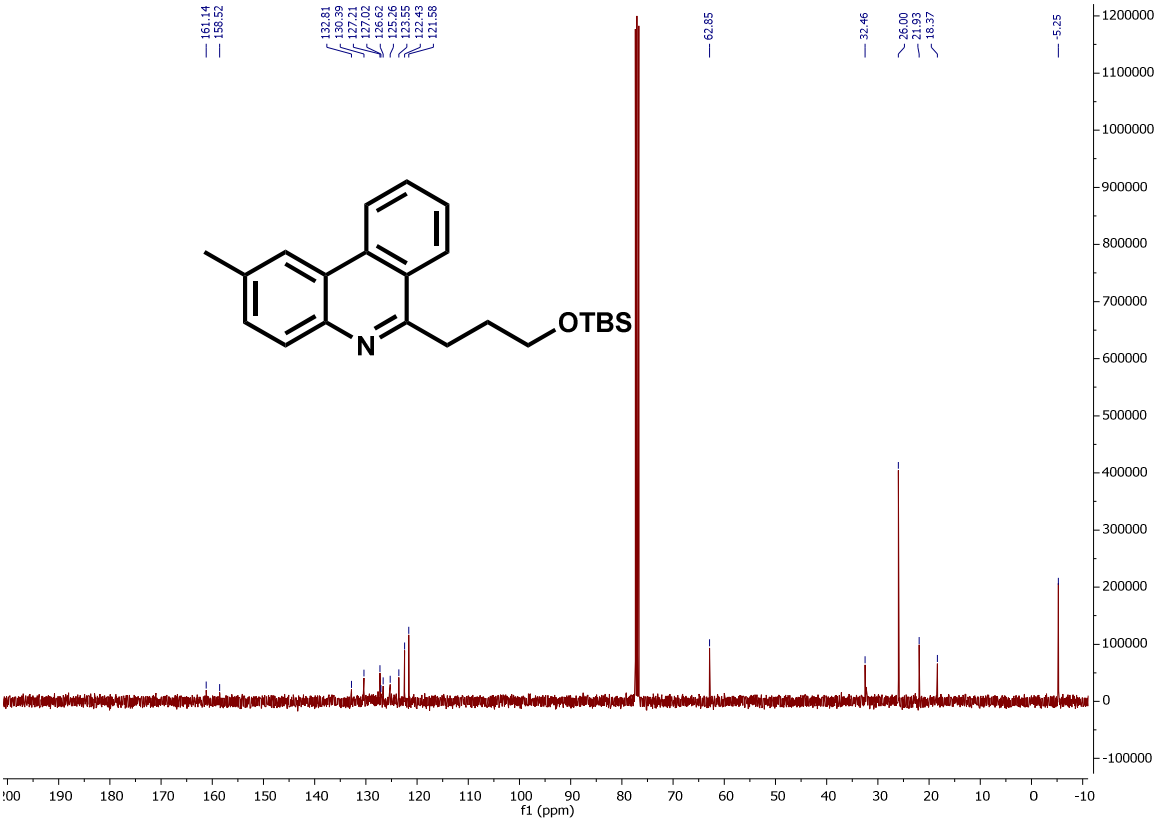

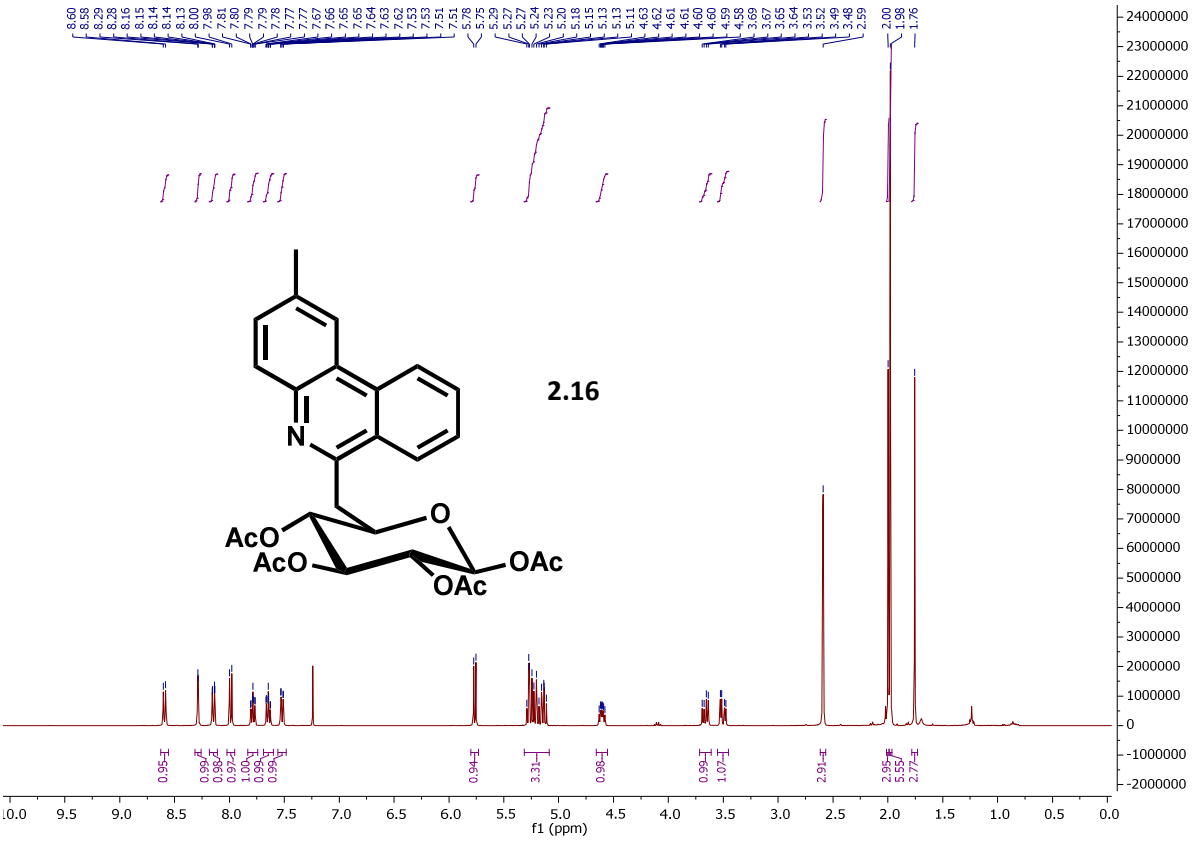
2.16
AcO
AcO
OAc
OAc
O
N
f1 (ppm)

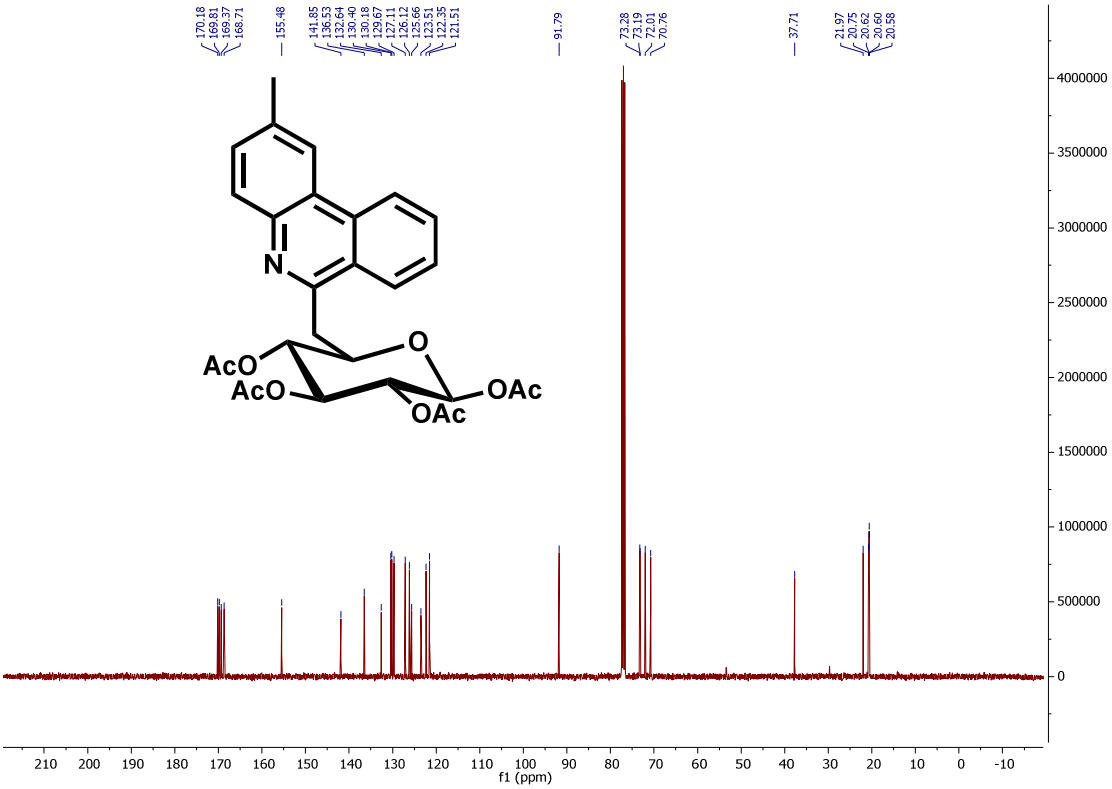
AcO
AcO
OAc
OAc
O
N
f1 (ppm)

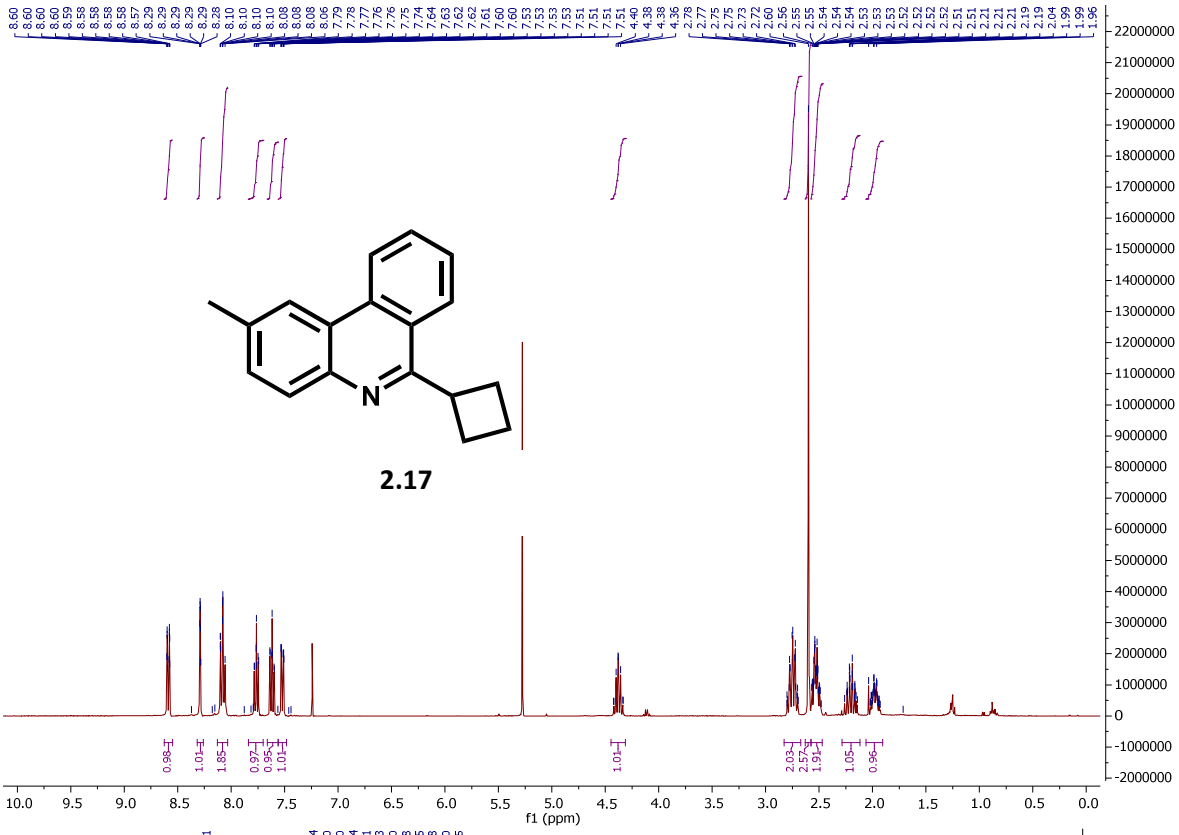
N
2.17
f1 (ppm)

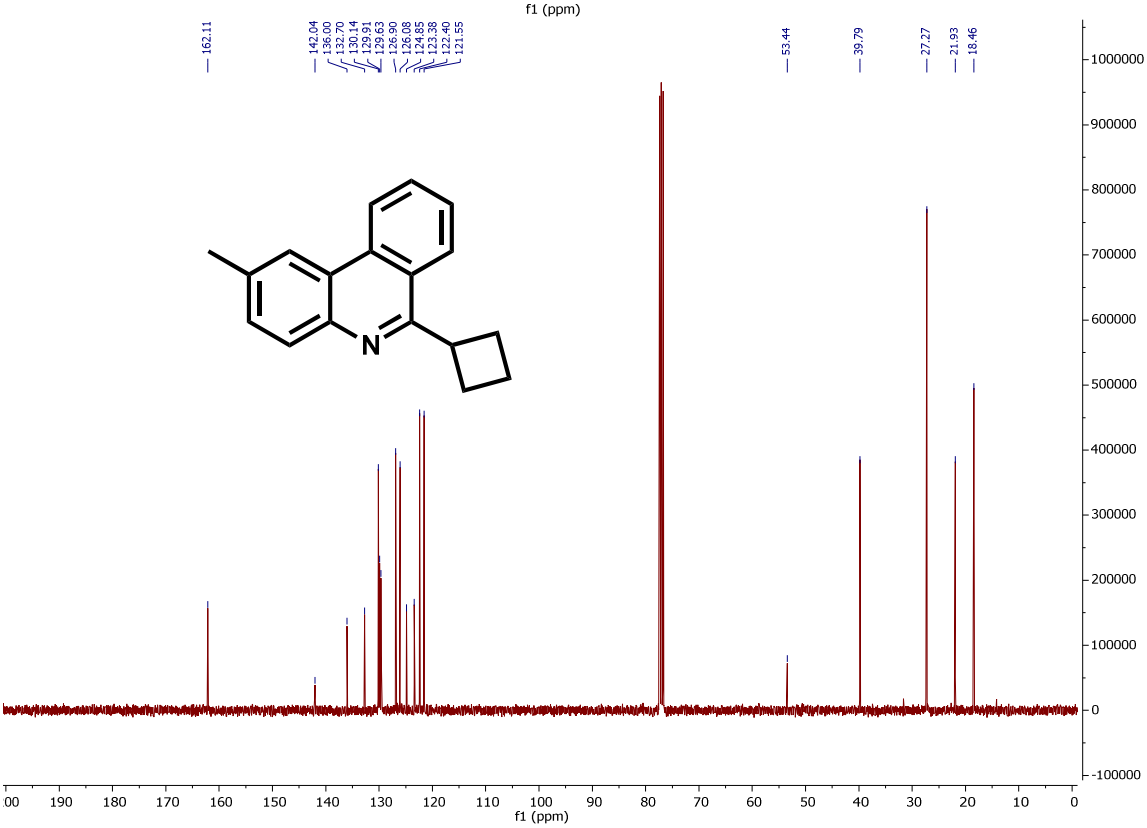
N
f1 (ppm)

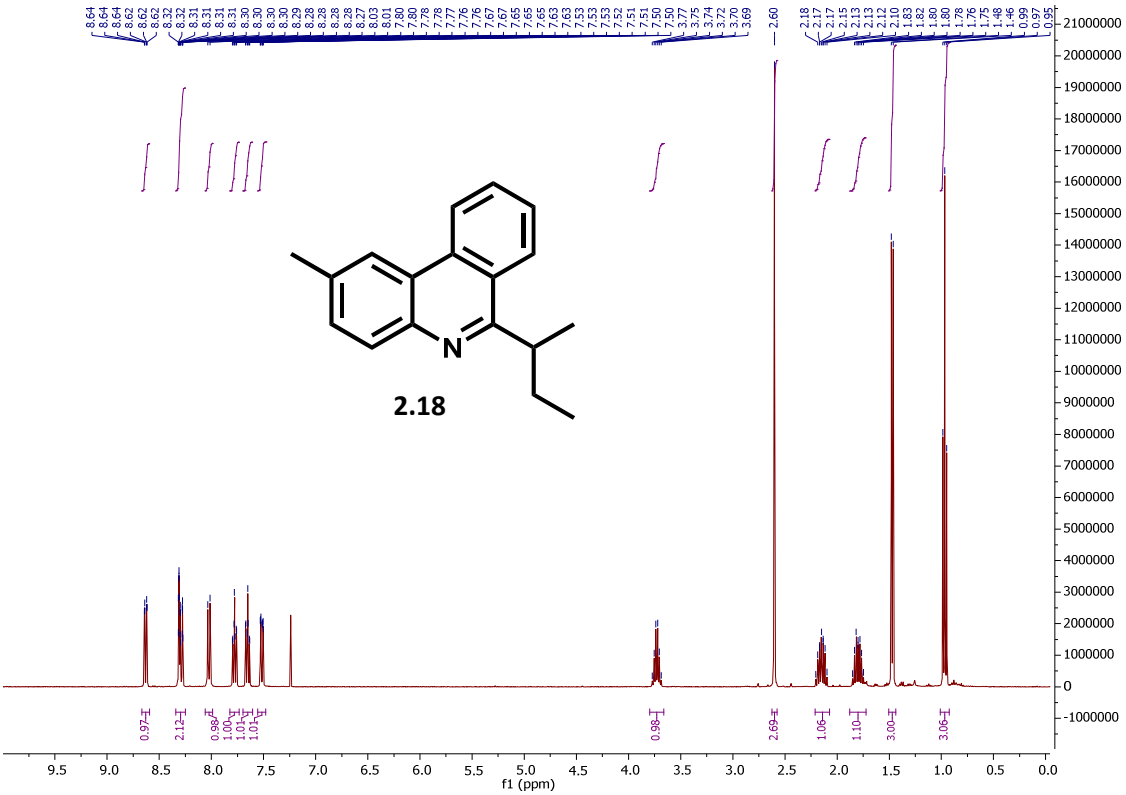
2.18
f1 (ppm)

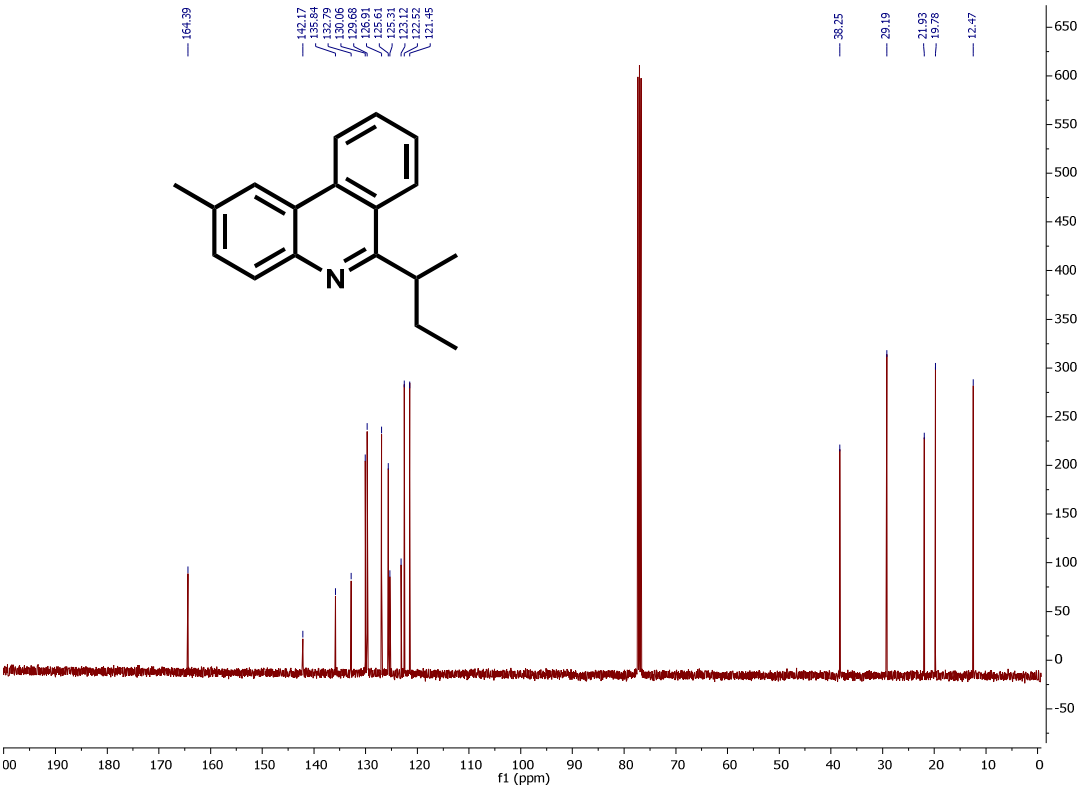
f1 (ppm)

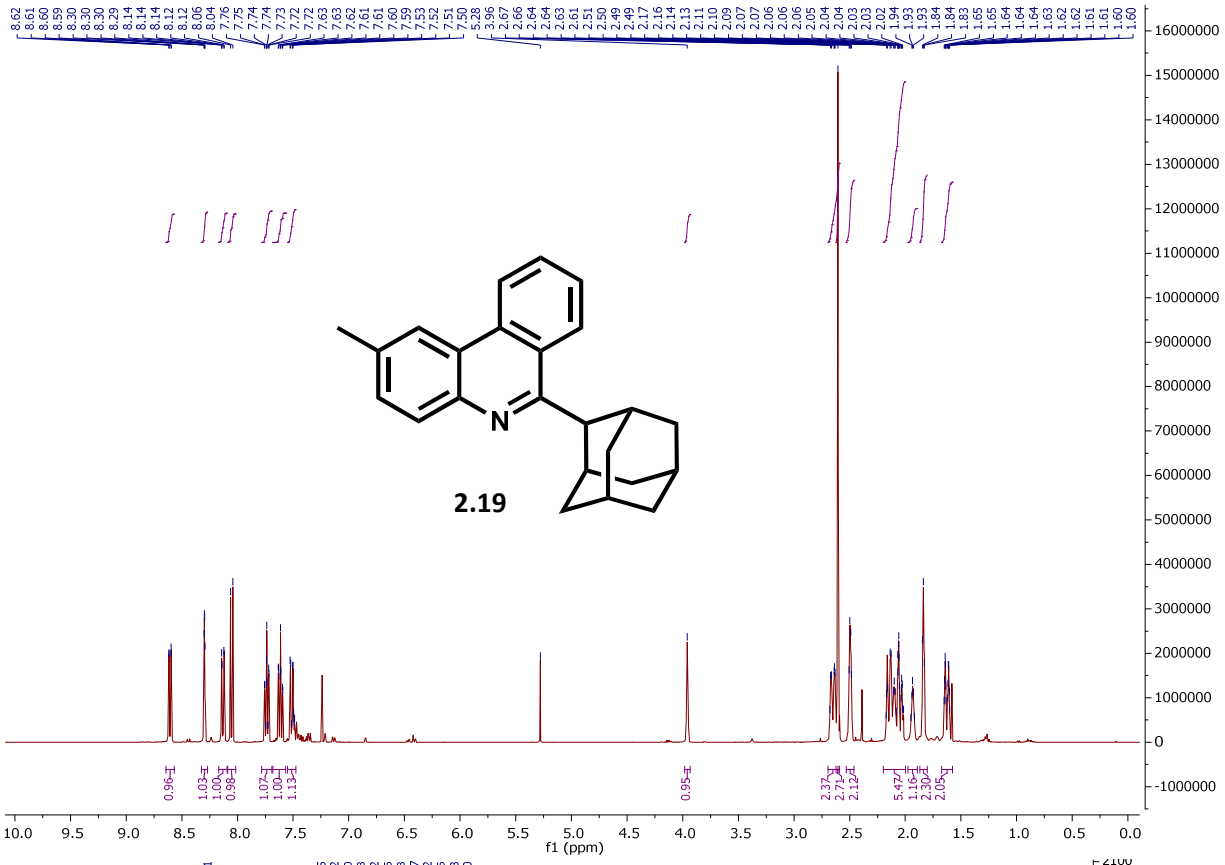
N
2.19
f1 (ppm)

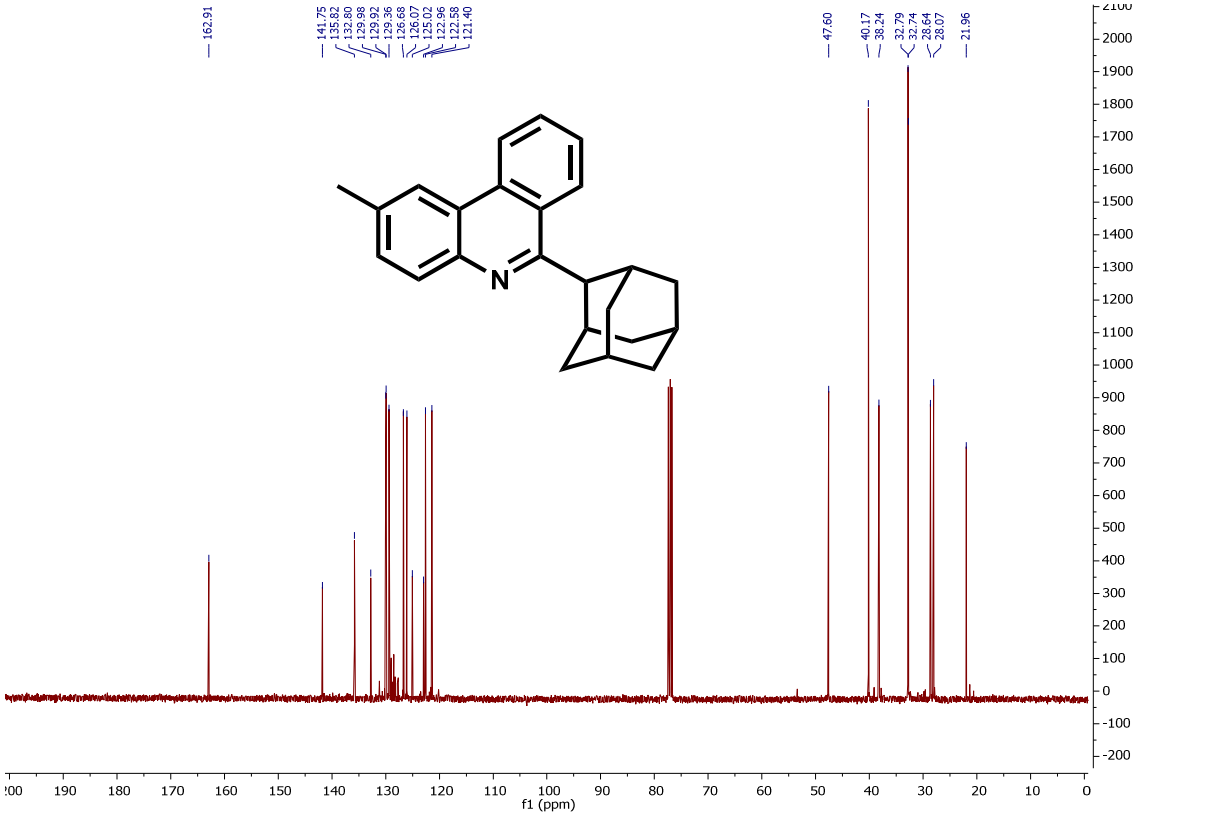
N
f1 (ppm)

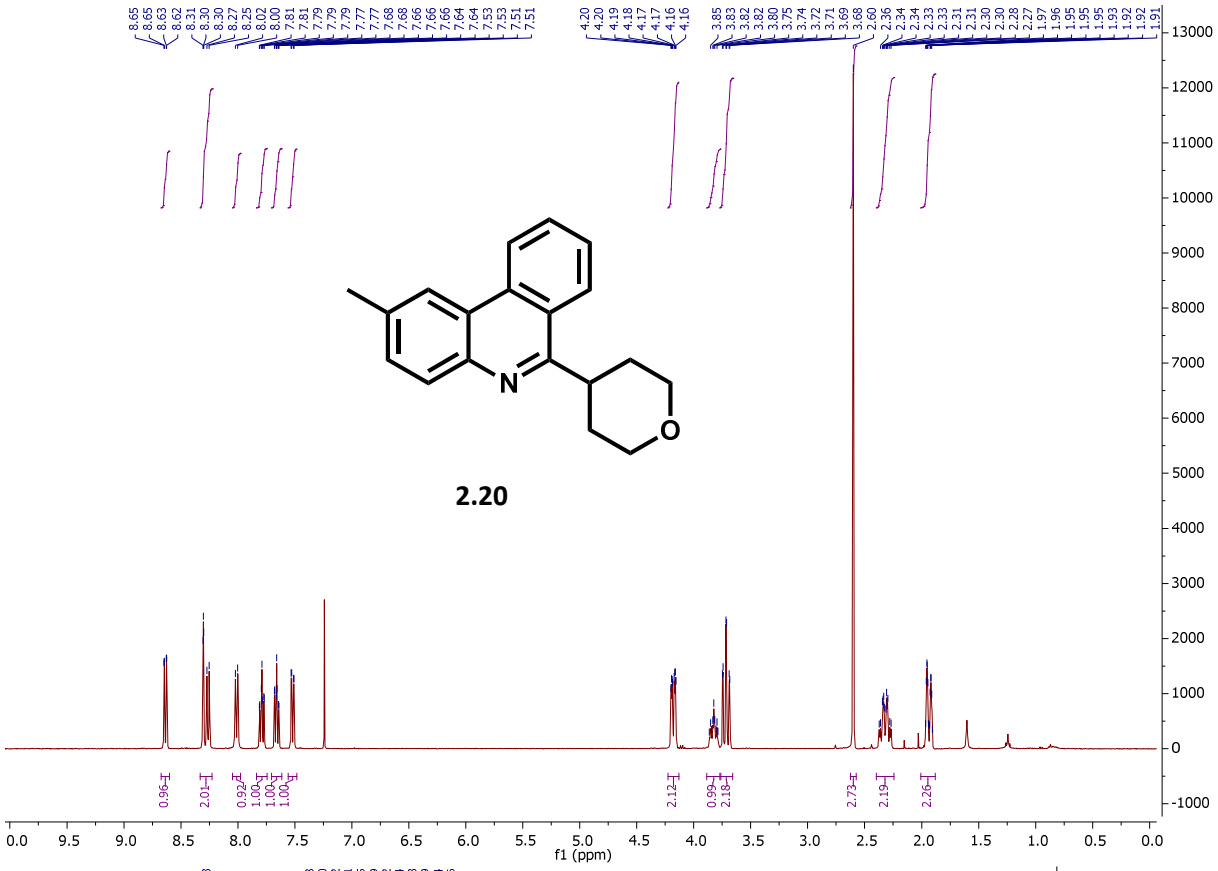
8.65
8.65
8.63
8.62
8.31
8.30
8.30
8.27
8.25
8.02
8.00
7.81
7.81
7.79
7.79
7.79
7.77
7.77
7.68
7.68
7.66
7.66
7.66
7.64
7.64
7.53
7.53
7.51
7.51
7.51
4.20
4.20
4.19
4.18
4.17
4.17
4.16
4.16
4.16
3.85
3.83
3.82
3.82
3.80
3.75
3.74
3.72
3.71
3.69
3.68
2.60
2.36
2.34
2.34
2.33
2.33
2.31
2.31
2.30
2.30
2.28
2.27
1.97
1.96
1.95
1.95
1.95
1.93
1.92
1.92
1.91
N
O
2.20
0.96
2.01
0.92
1.00
1.00
1.00
2.12
0.99
2.18
2.73
2.19
2.26
f1 (ppm)

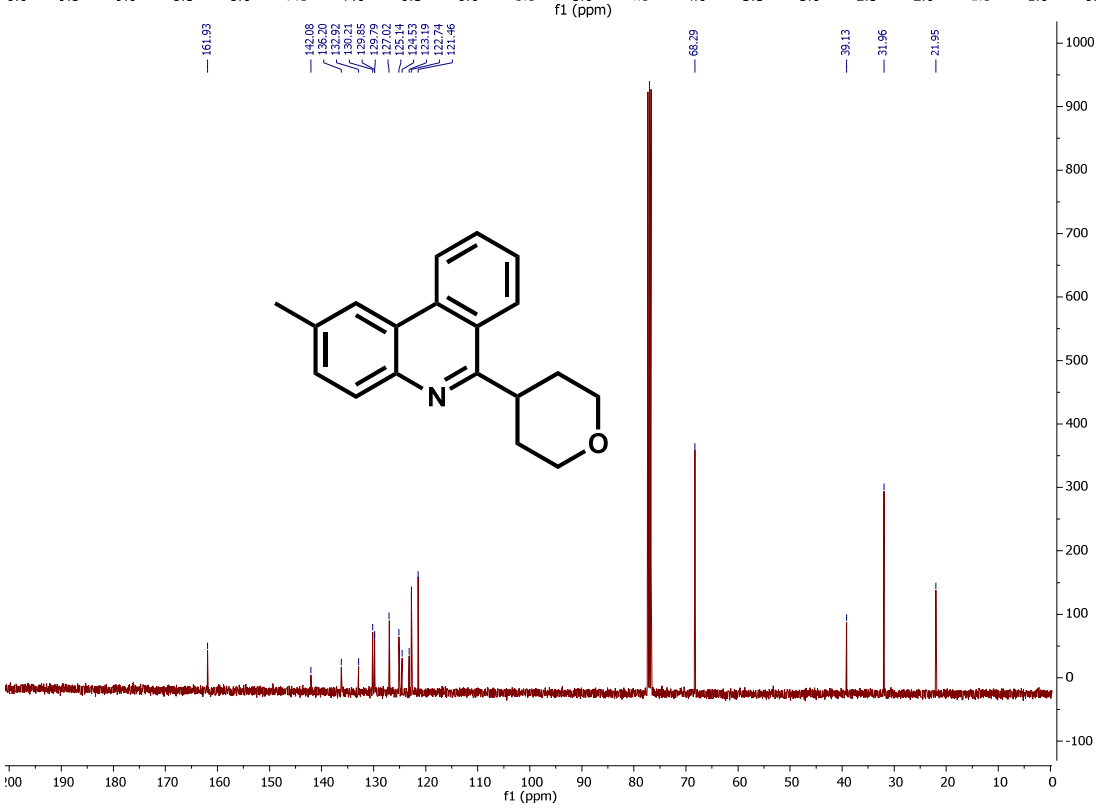
161.93
142.08
136.20
132.92
130.21
129.85
129.79
127.02
125.14
124.53
123.19
122.74
121.46
68.29
39.13
31.96
21.95
N
O
f1 (ppm)

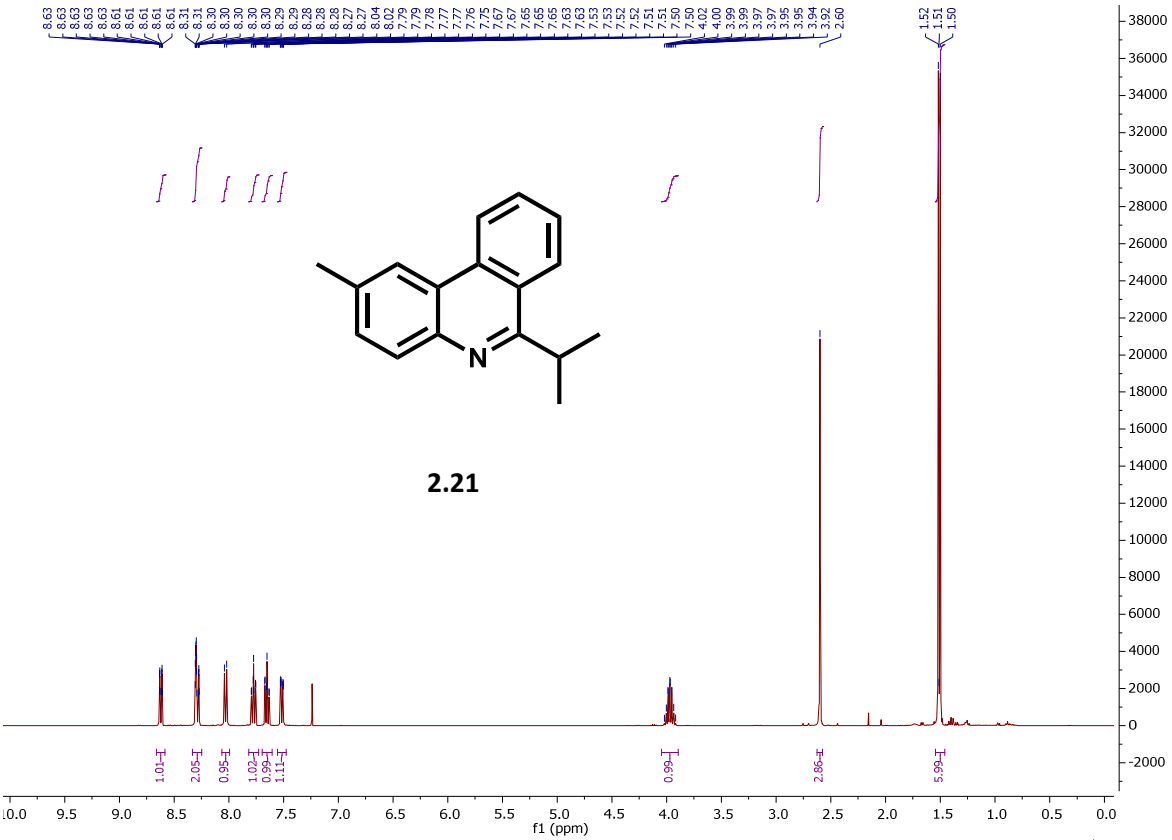
8.63 8.63 8.63 8.63 8.61 8.61 8.61 8.61 8.61 8.31 8.31 8.30 8.30 8.30 8.30 8.30 8.29 8.29 8.28 8.28 8.28 8.27 8.27 8.04 8.02 7.79 7.79 7.78 7.77 7.77 7.76 7.75 7.67 7.67 7.65 7.65 7.65 7.63 7.63 7.53 7.53 7.52 7.52 7.51 7.51 7.50 7.50 4.02 4.00 3.99 3.99 3.97 3.97 3.95 3.95 3.94 3.92 2.60
1.52 1.51 1.50
N
1.01 2.05 0.95 1.02 0.99 1.11 0.99 2.86 5.99
f1 (ppm)

2.21

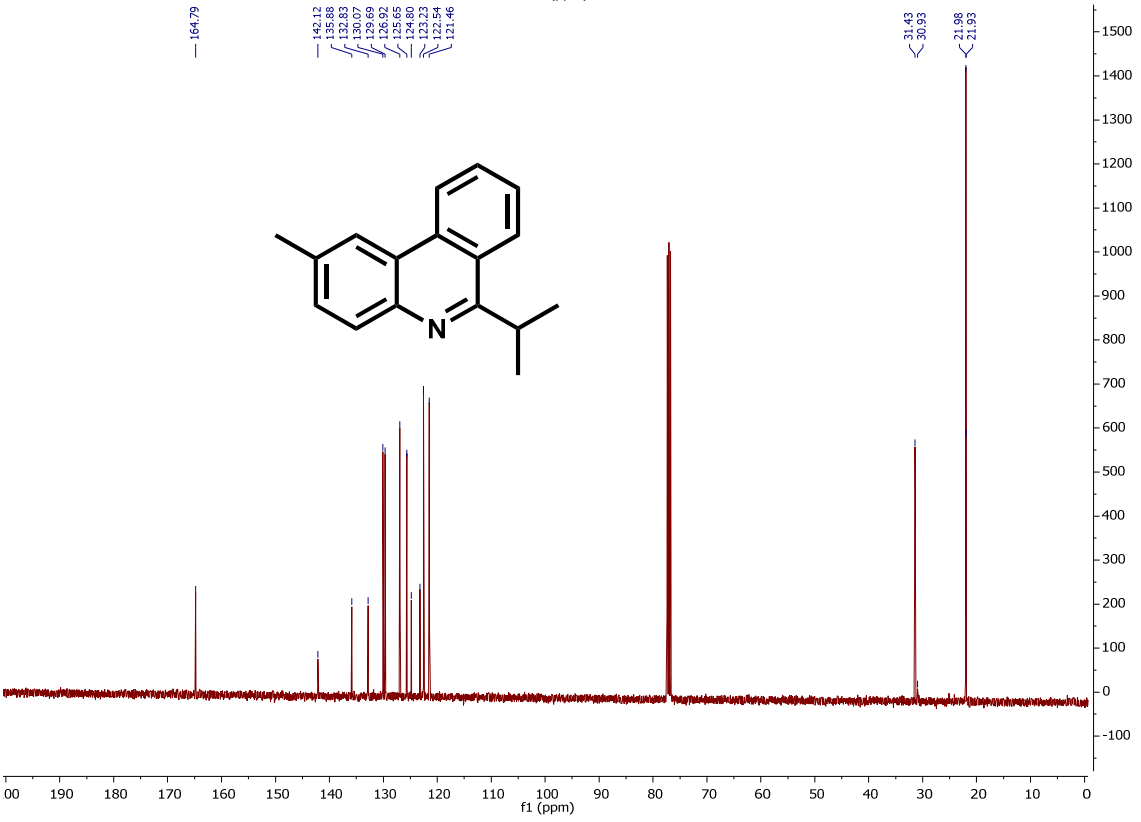
164.79
142.12 135.88 132.83 130.07 129.69 126.92 125.65 124.80 123.23 122.54 121.46
31.43 30.93
21.98 21.93
N
f1 (ppm)

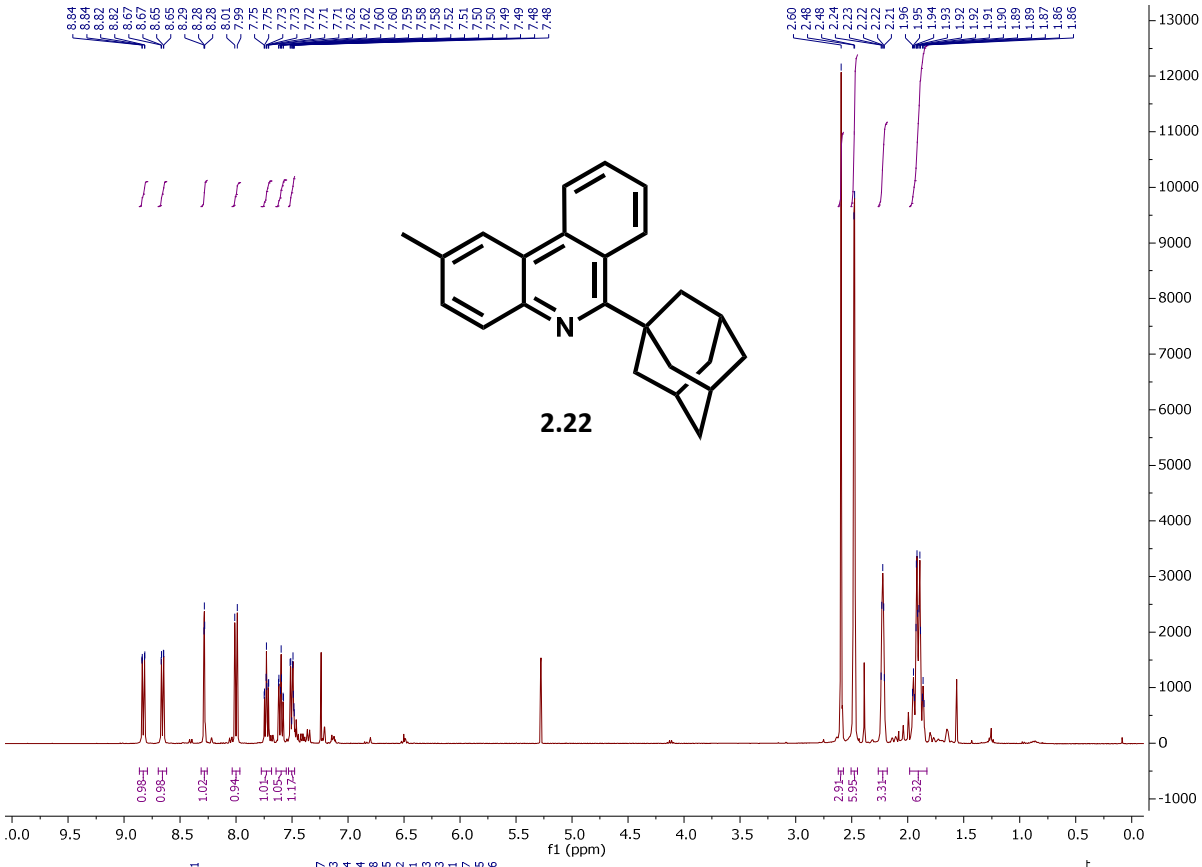
8.84
8.84
8.82
8.82
8.67
8.67
8.65
8.65
8.29
8.28
8.28
8.01
7.99
7.75
7.75
7.73
7.73
7.72
7.71
7.71
7.62
7.62
7.60
7.60
7.59
7.58
7.58
7.52
7.51
7.50
7.50
7.49
7.49
7.48
7.48
2.60
2.48
2.48
2.24
2.23
2.22
2.22
2.21
1.96
1.95
1.94
1.93
1.92
1.92
1.91
1.90
1.89
1.89
1.87
1.86
1.86
N
2.22
0.98
0.98
1.02
0.94
1.01
1.05
1.17
2.91
5.95
3.31
6.32
f1 (ppm)

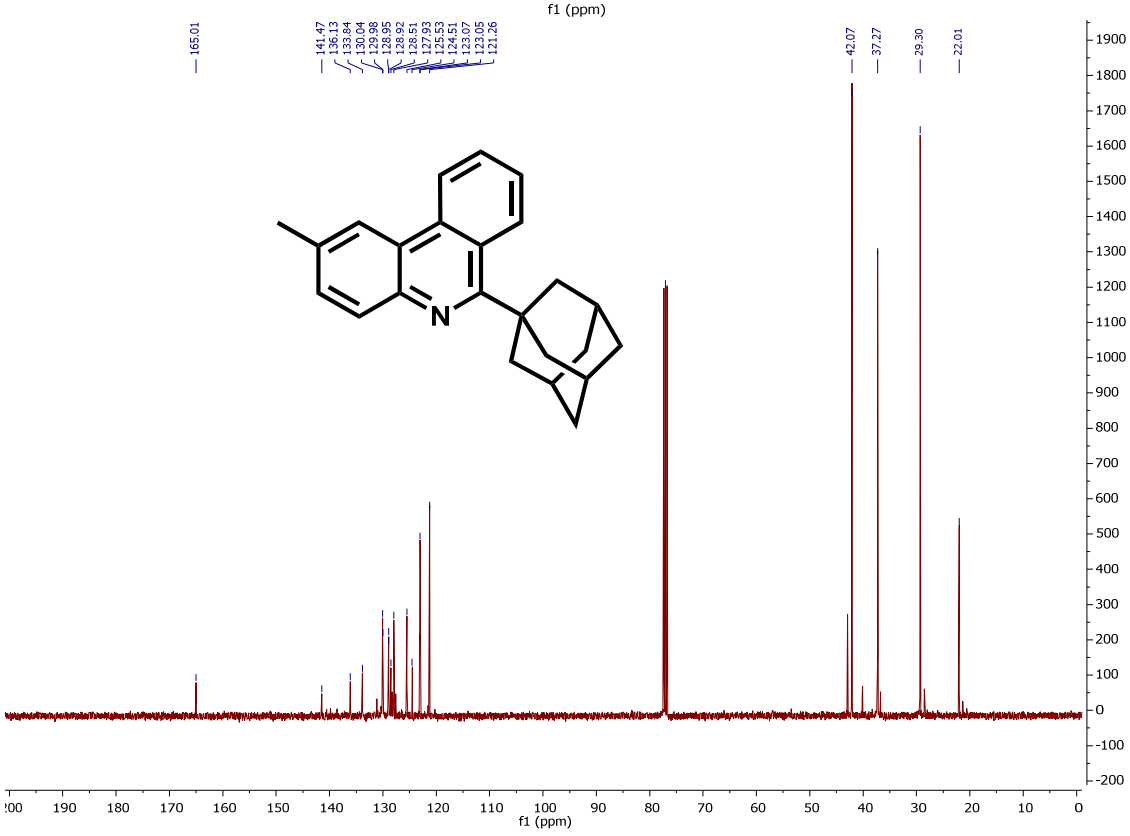
165.01
141.47
136.13
133.84
130.04
129.98
129.95
128.92
128.51
127.93
125.53
124.51
123.07
123.05
121.26
42.07
37.27
29.30
22.01
N
f1 (ppm)

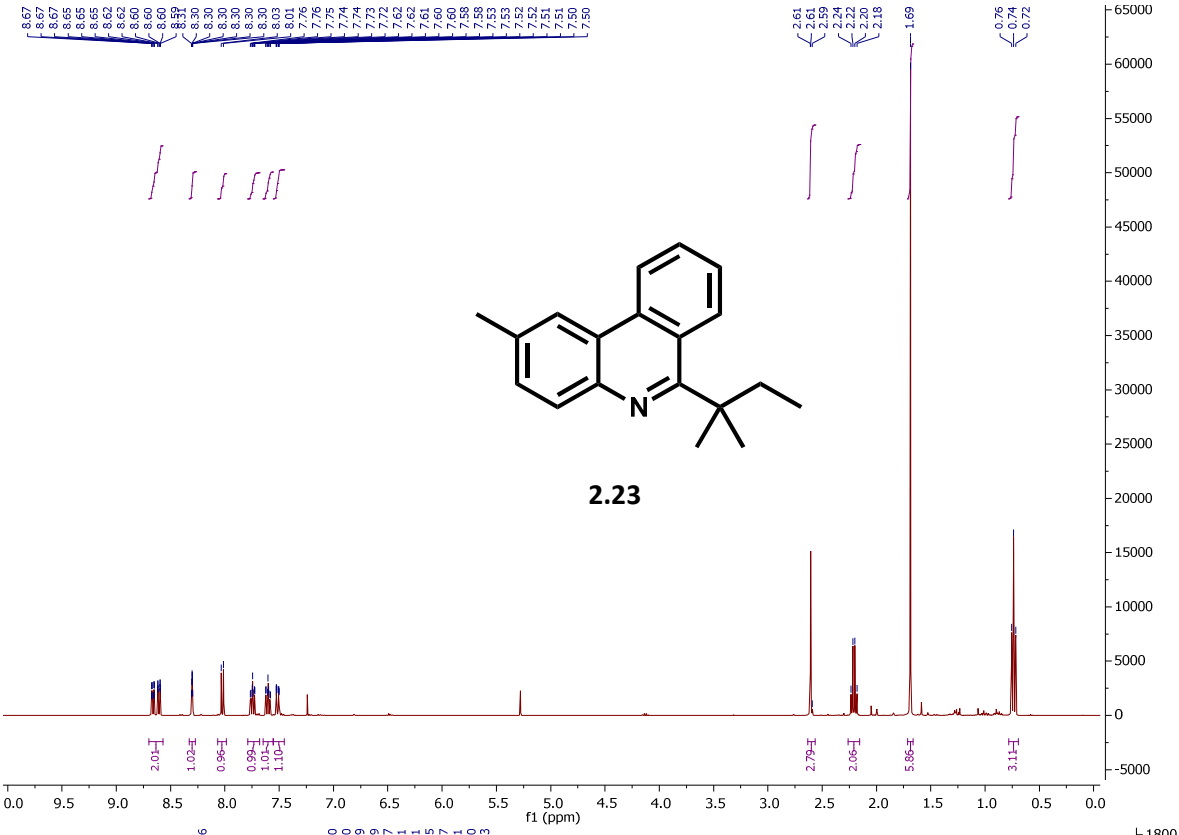
8.67 8.67 8.67 8.65 8.65 8.62 8.62 8.60 8.60 8.60 8.60 8.31 8.30 8.30 8.30 8.30 8.30 8.30 8.03 8.01 7.76 7.76 7.75 7.74 7.74 7.73 7.72 7.62 7.62 7.61 7.60 7.60 7.58 7.58 7.53 7.53 7.52 7.52 7.51 7.51 7.50 7.50
2.61 2.61 2.59 2.24 2.22 2.20 2.18 1.69 0.76 0.74 0.72
N
2.23
2.01 1.02 0.96 0.99 1.01 1.10 2.79 2.06 5.86 3.11
f1 (ppm)

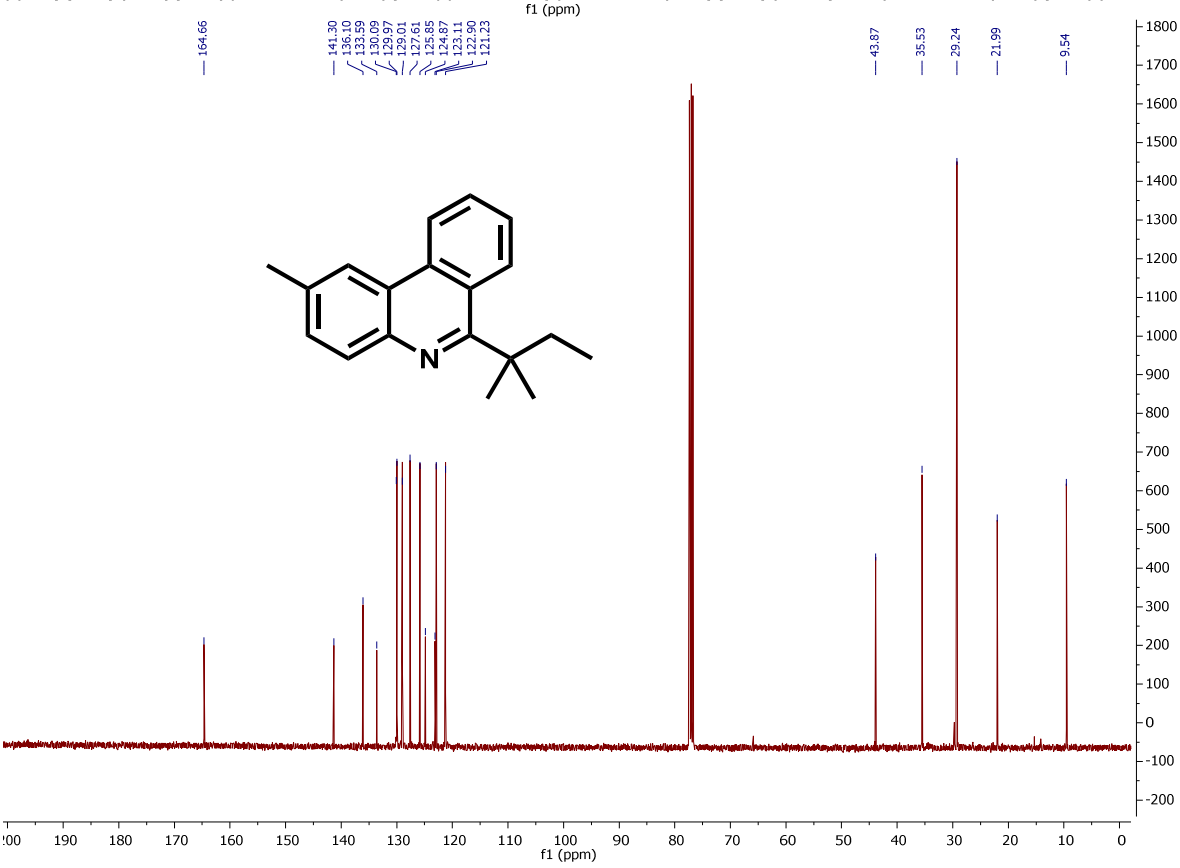
164.66
141.30 136.10 133.59 130.09 129.97 129.01 127.61 125.85 124.87 123.11 122.90 121.23
43.87 35.53 29.24 21.99 9.54
N
f1 (ppm)

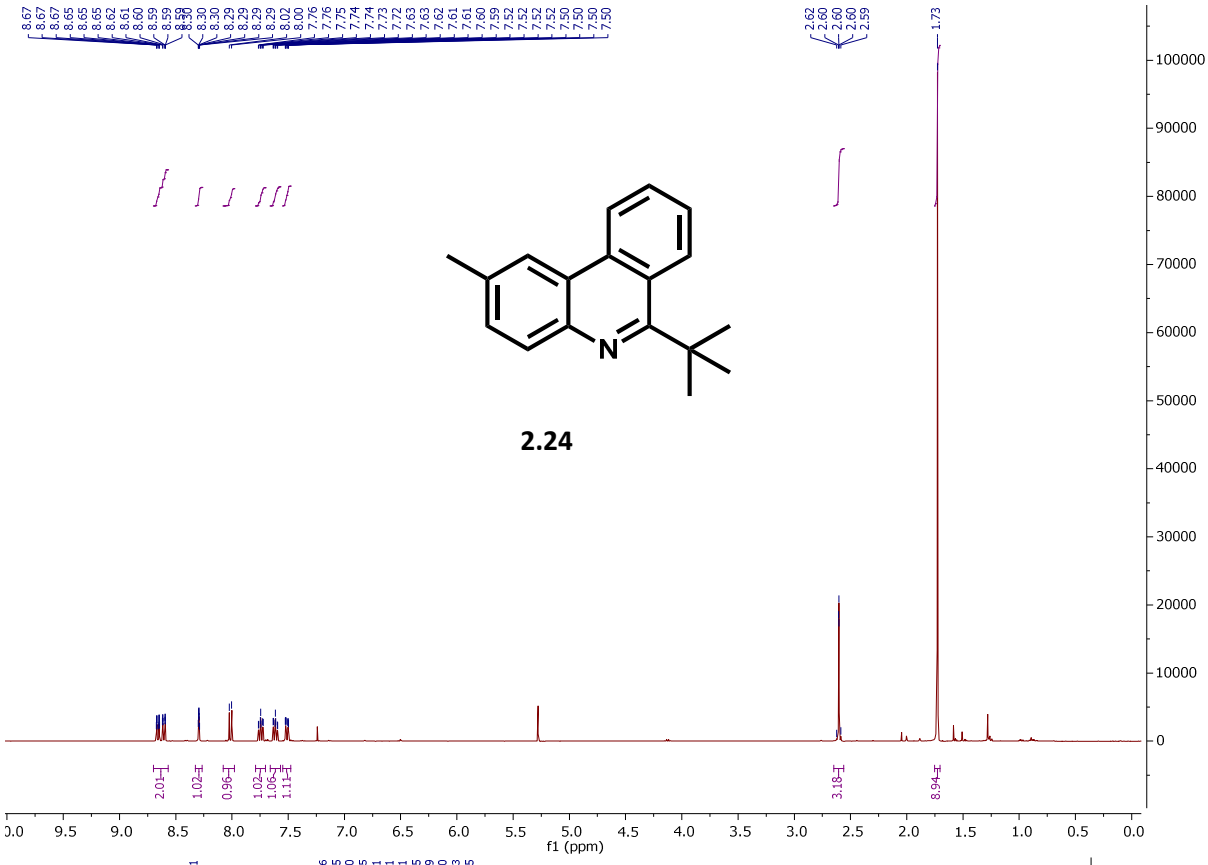
8.67
8.67
8.67
8.65
8.65
8.62
8.61
8.60
8.59
8.59
8.58
8.30
8.30
8.29
8.29
8.29
8.29
8.29
8.02
8.00
7.76
7.76
7.75
7.74
7.74
7.73
7.72
7.63
7.63
7.62
7.61
7.61
7.60
7.59
7.52
7.52
7.52
7.50
7.50
7.50
7.50
2.62
2.60
2.60
2.60
2.59
1.73
2.01
1.02
0.96
1.02
1.06
1.11
3.18
8.94
f1 (ppm)

2.24

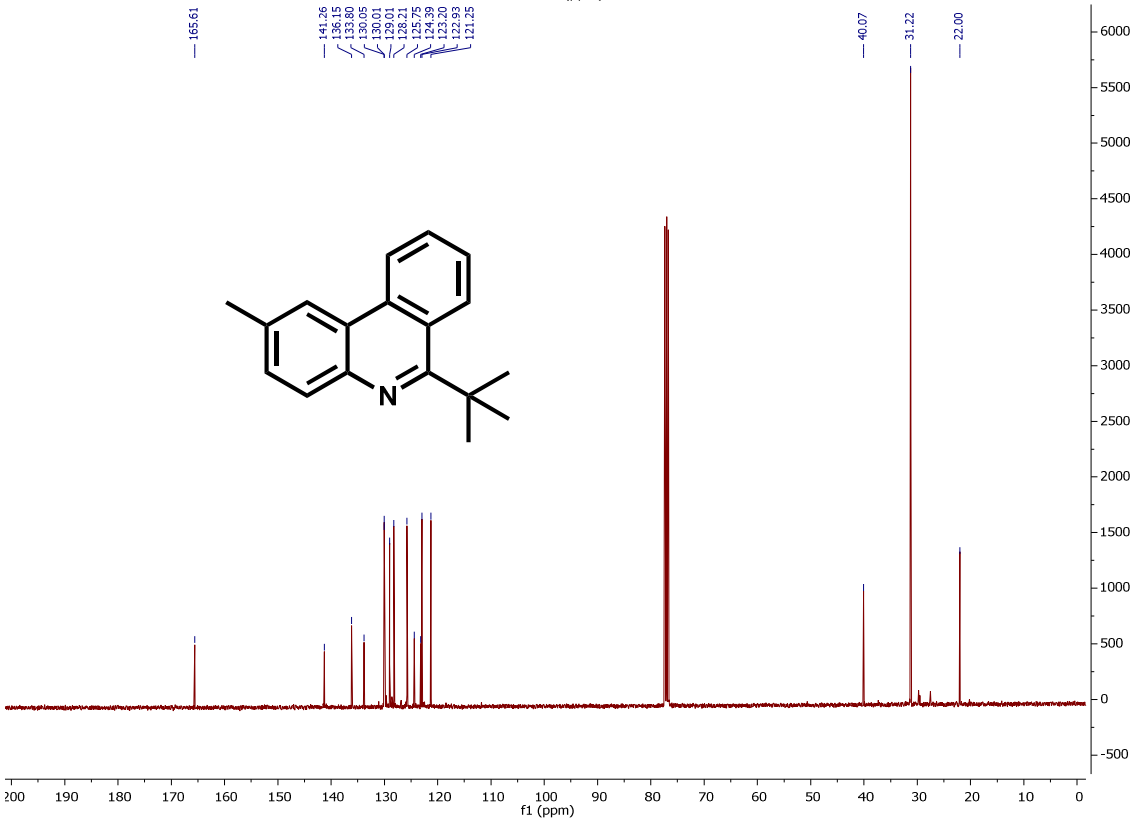
165.61
141.26
136.15
133.80
130.05
130.01
129.01
128.21
125.75
124.39
123.20
122.93
121.25
40.07
31.22
22.00
f1 (ppm)

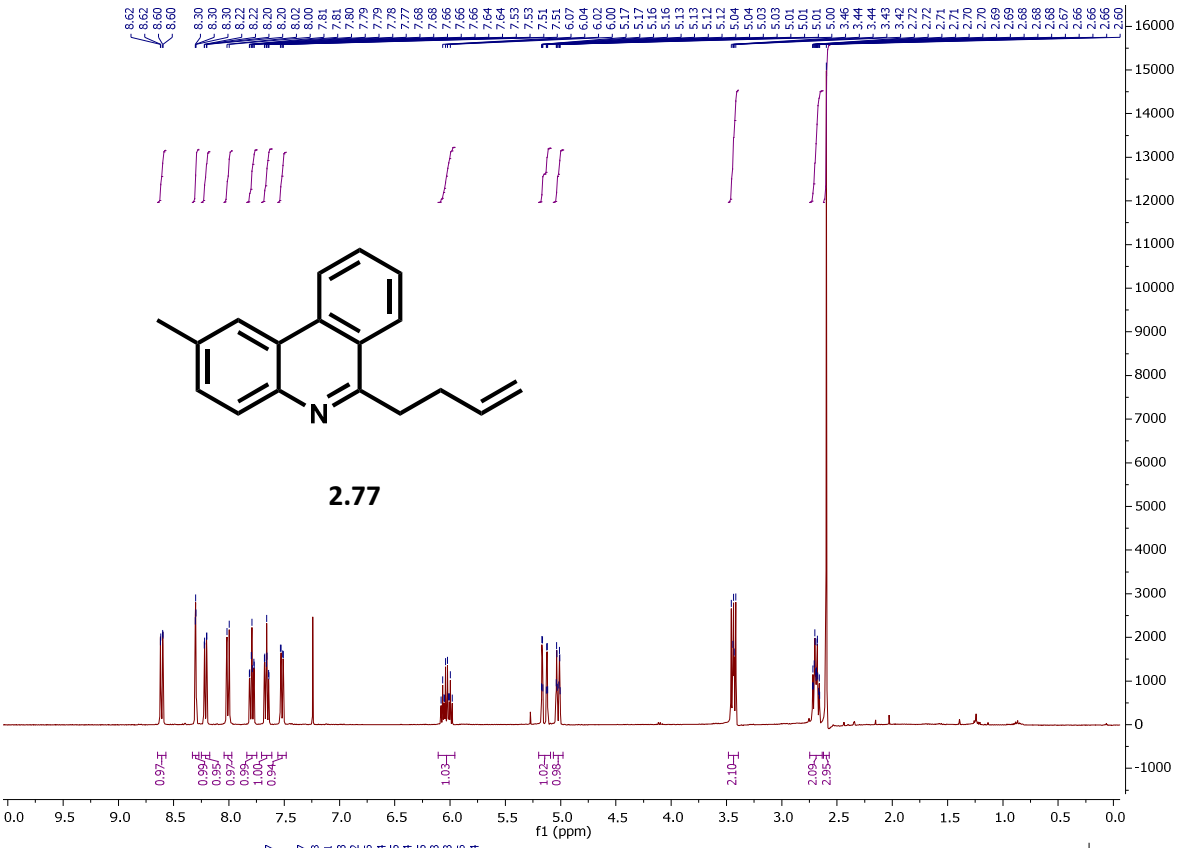
N
2.77
f1 (ppm)

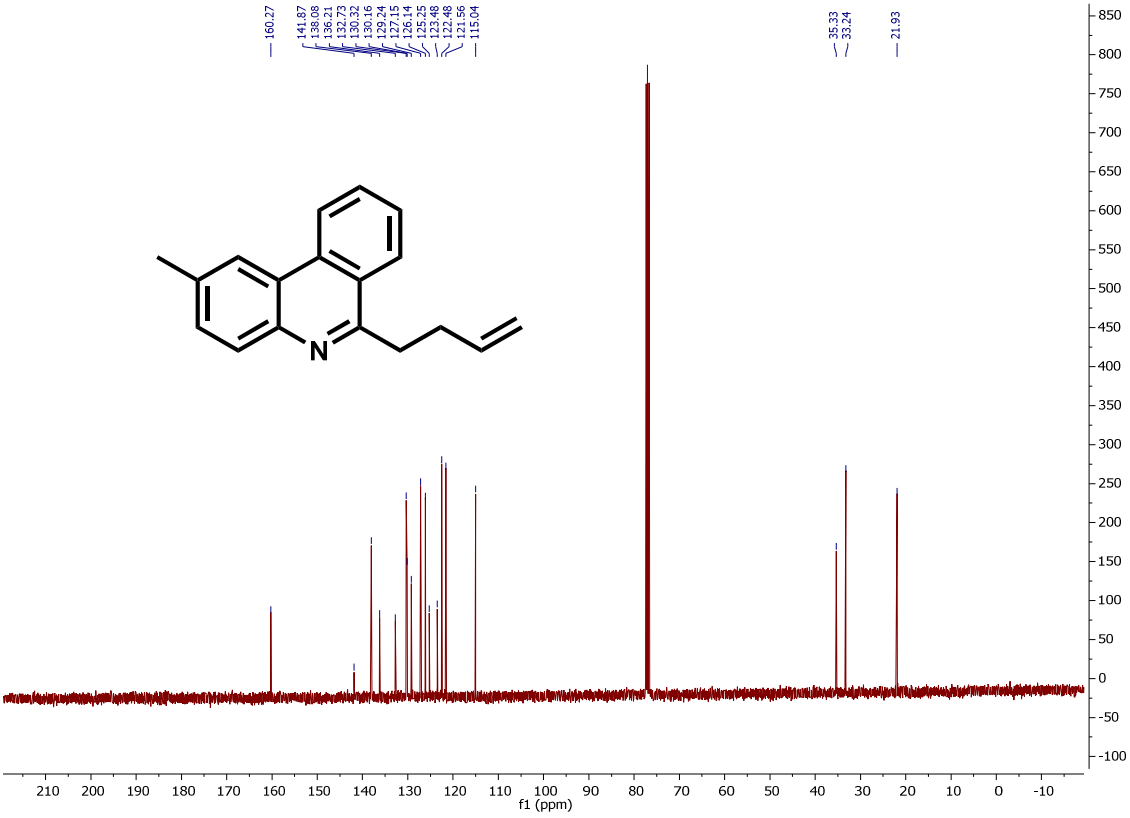
N
f1 (ppm)

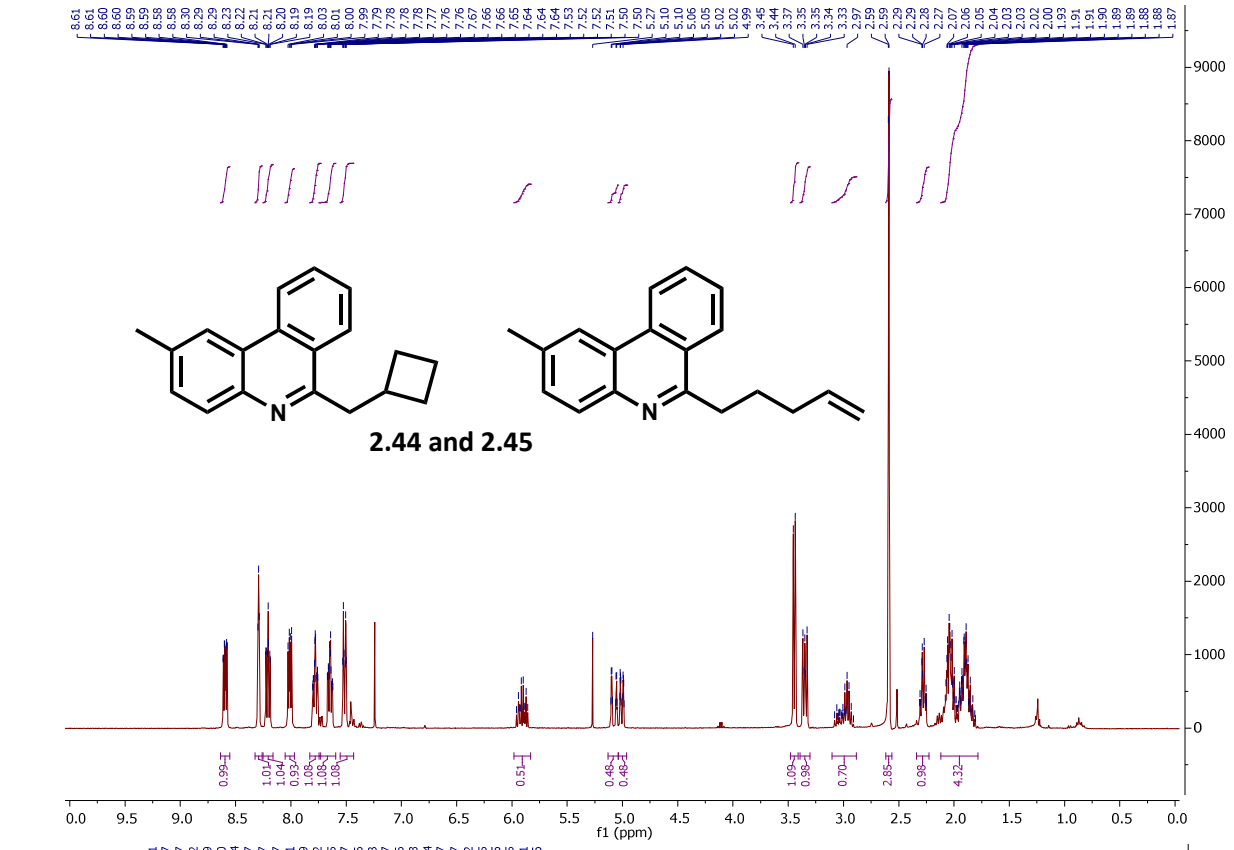
2.44 and 2.45
f1 (ppm)

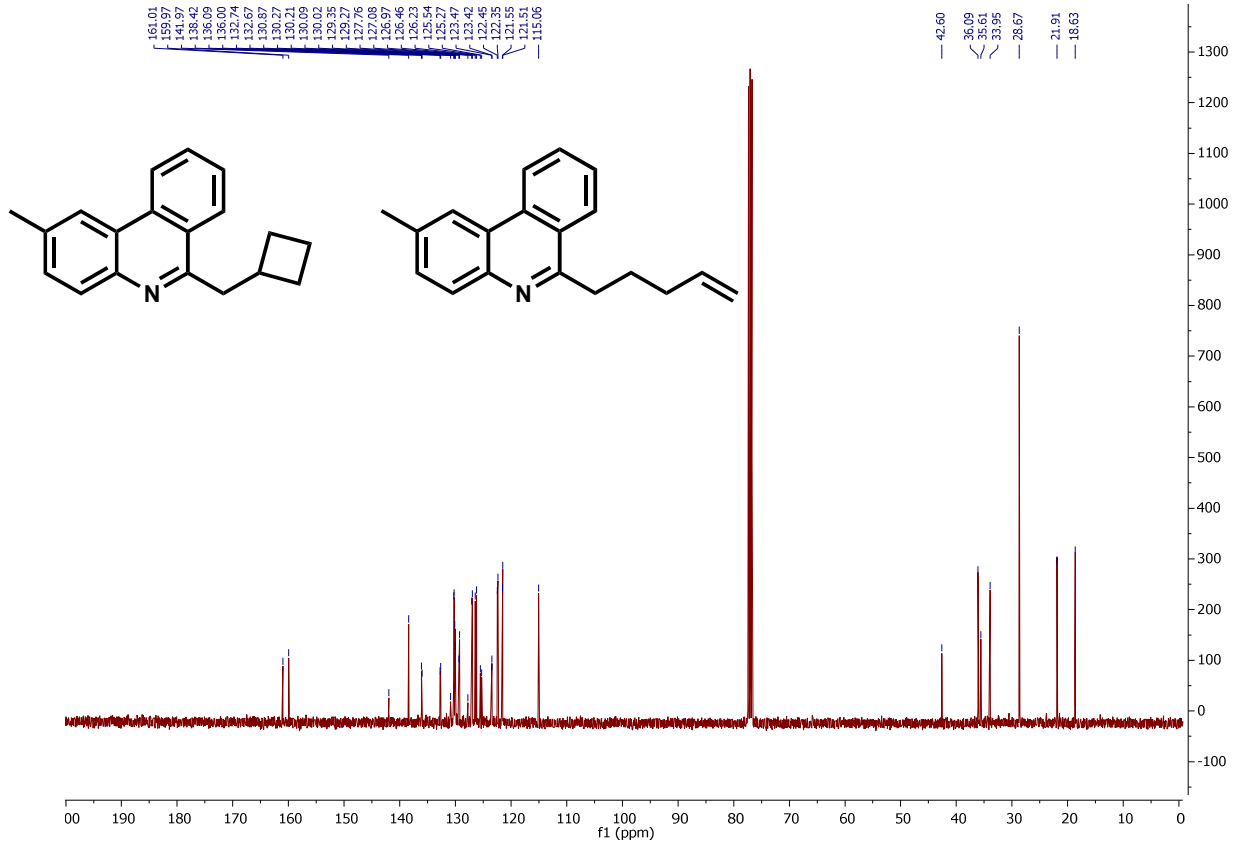
f1 (ppm)

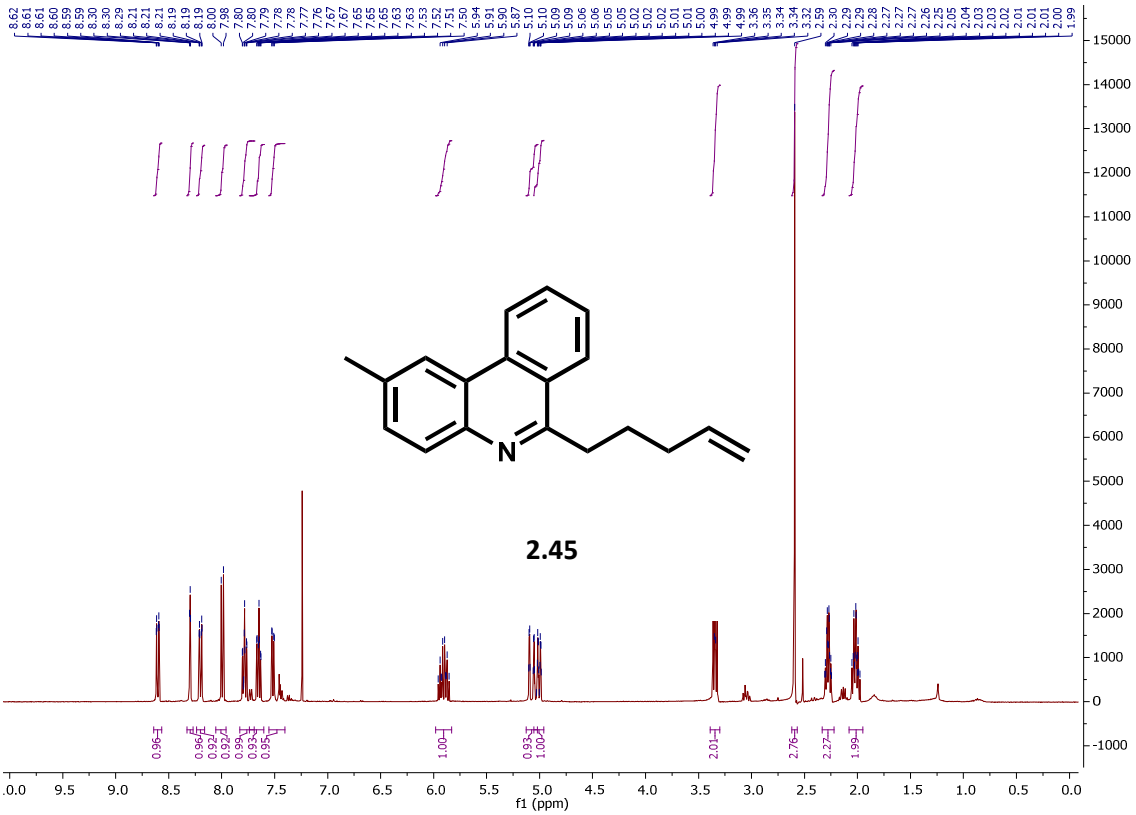
N
2.45
f1 (ppm)

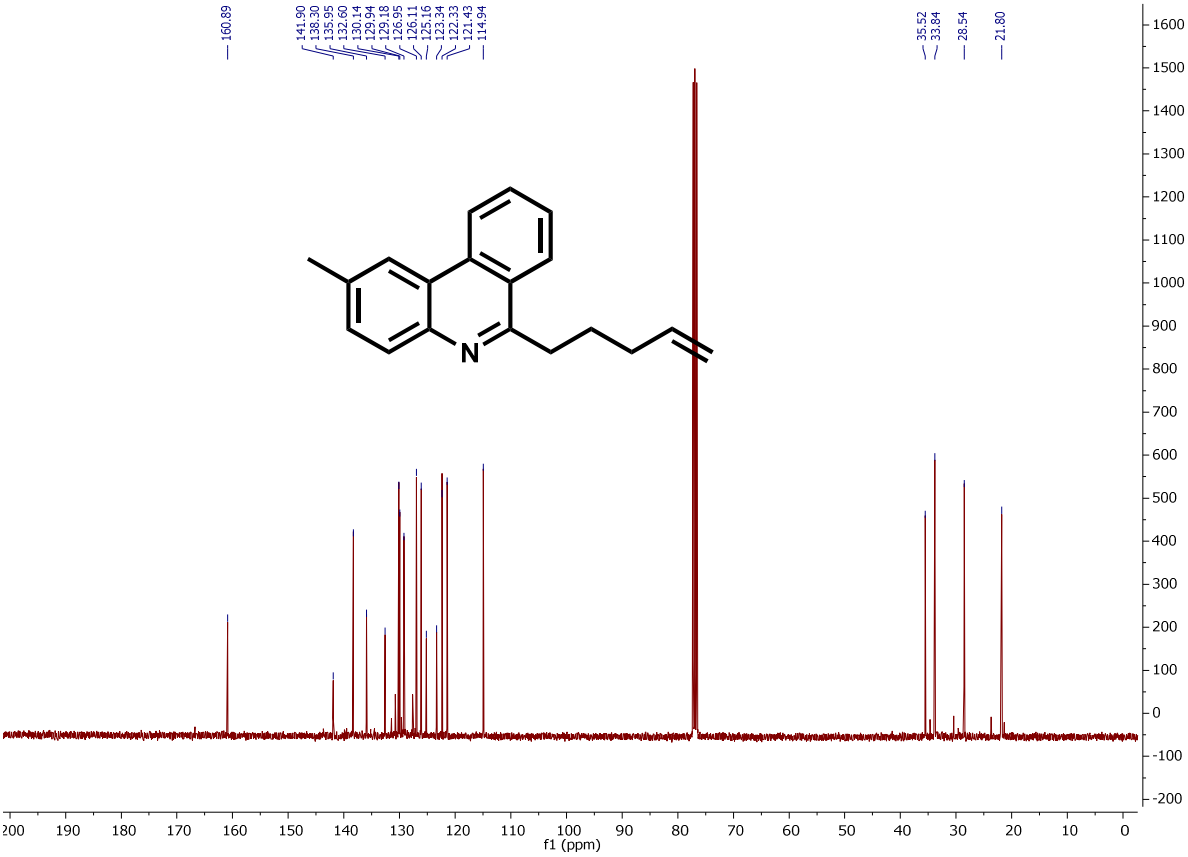
N
f1 (ppm)

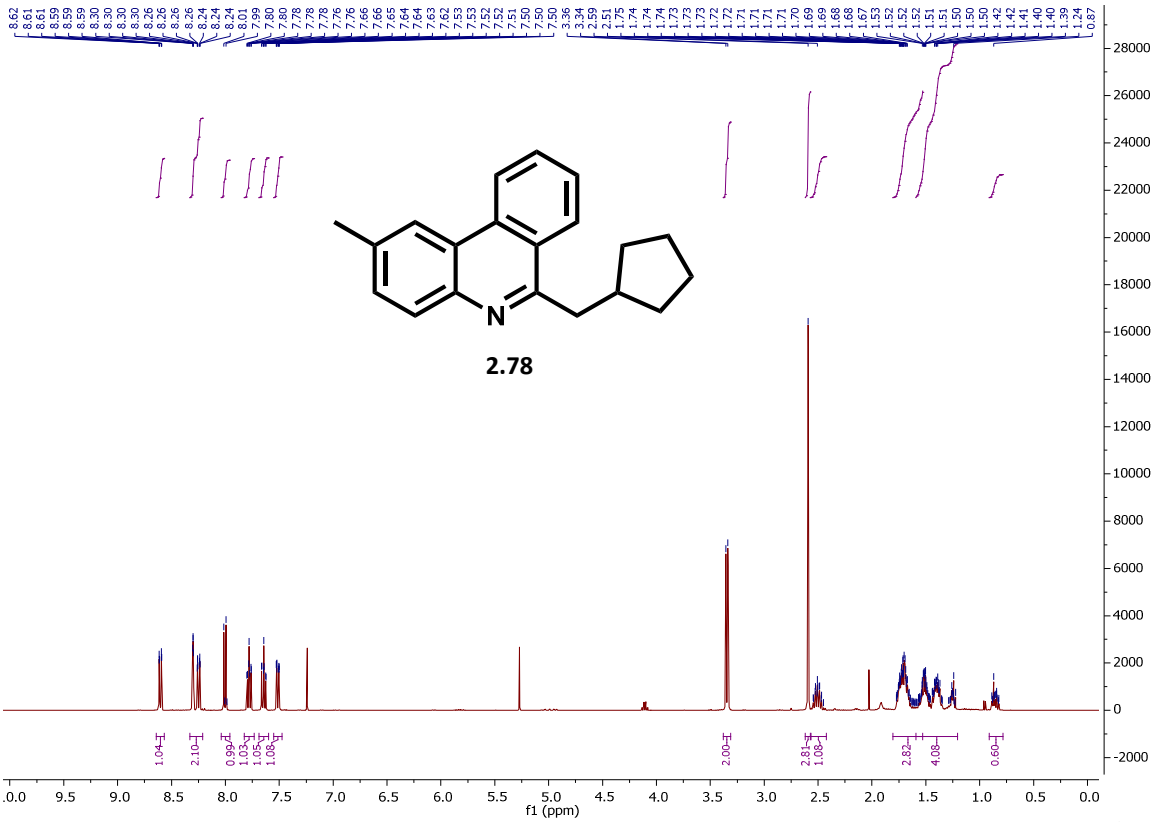

2.78

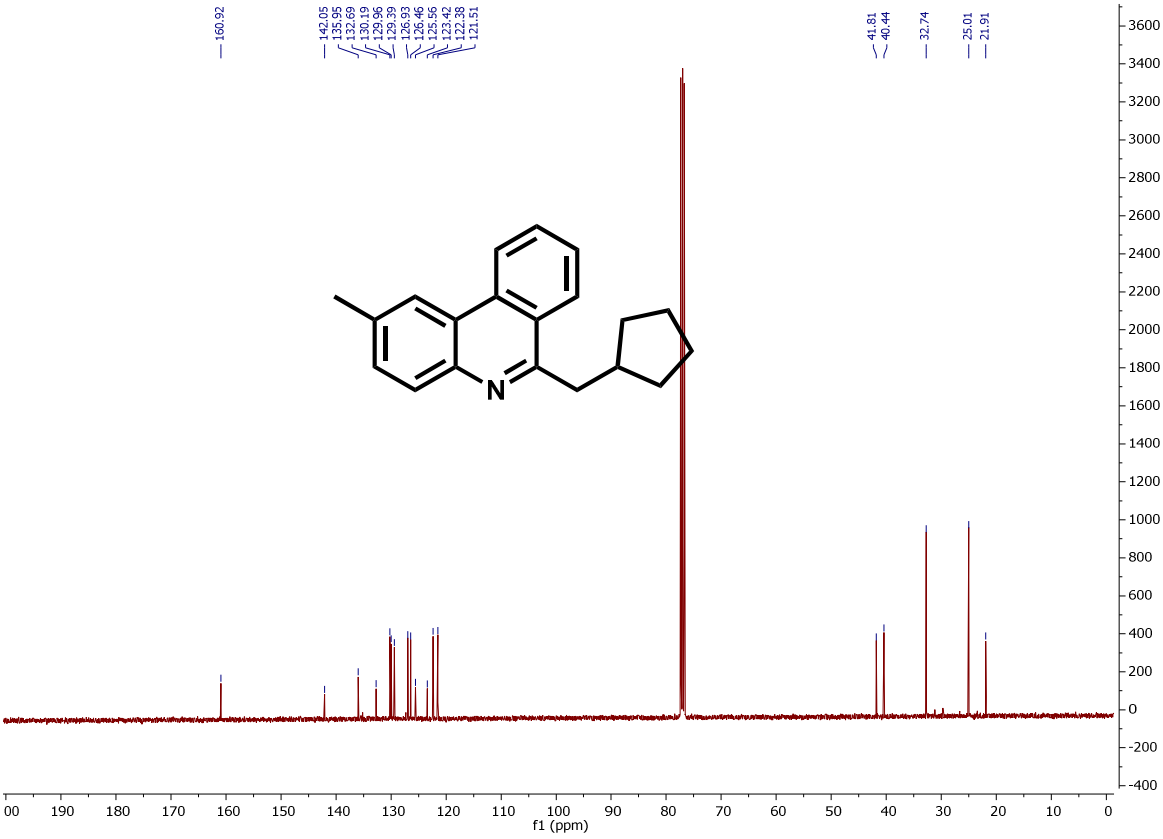

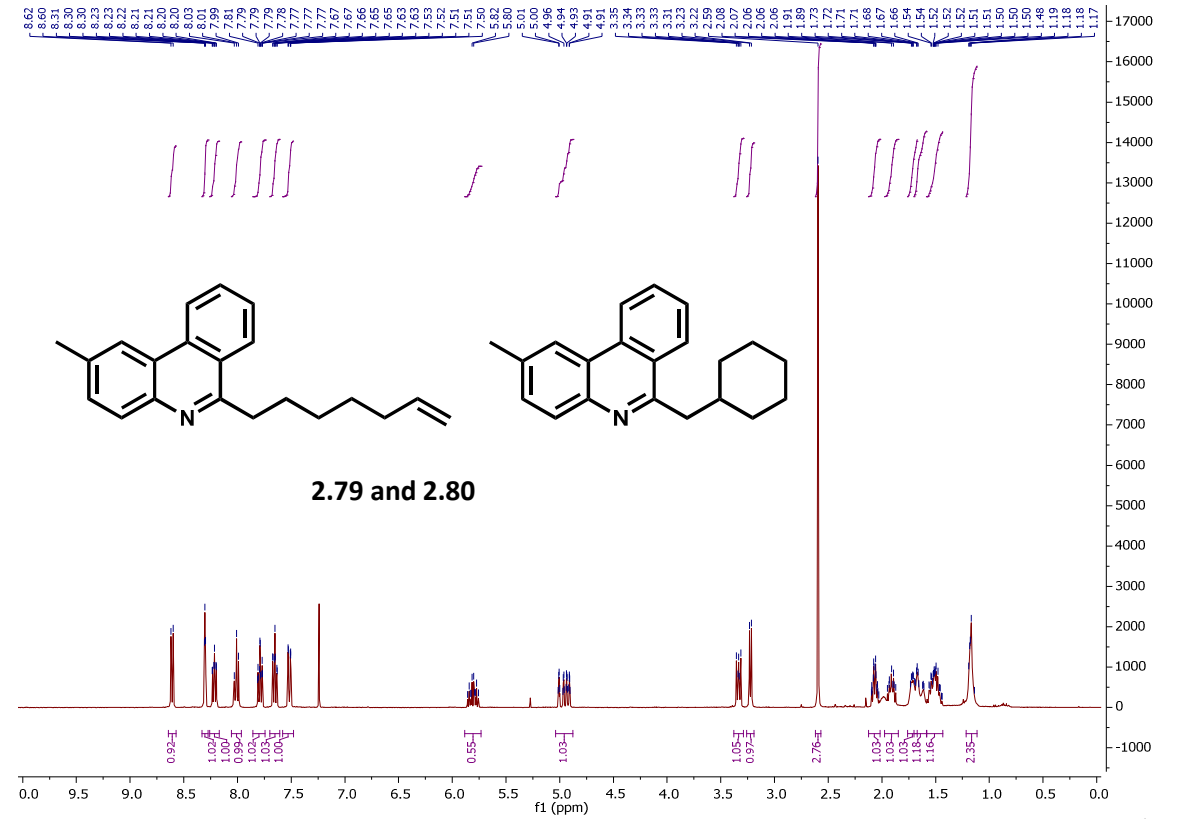
2.79 and 2.80
f1 (ppm)

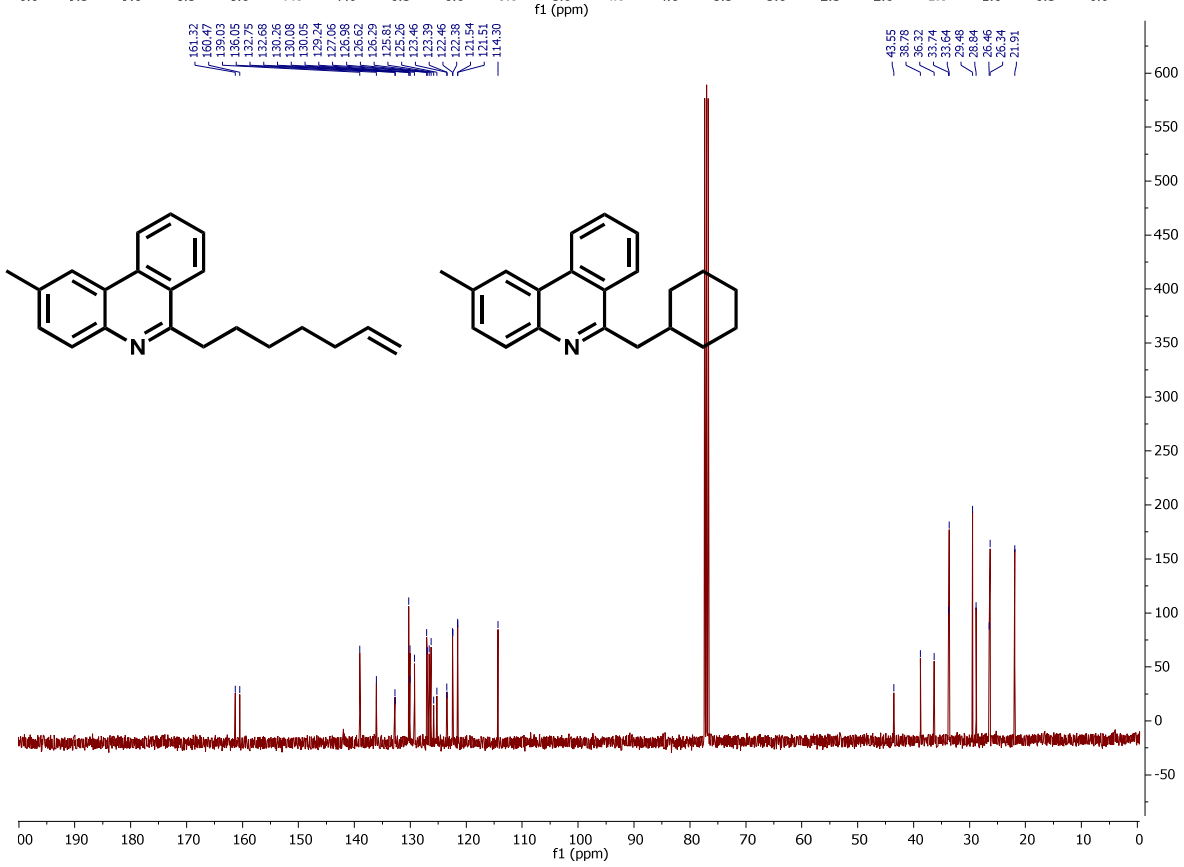
f1 (ppm)

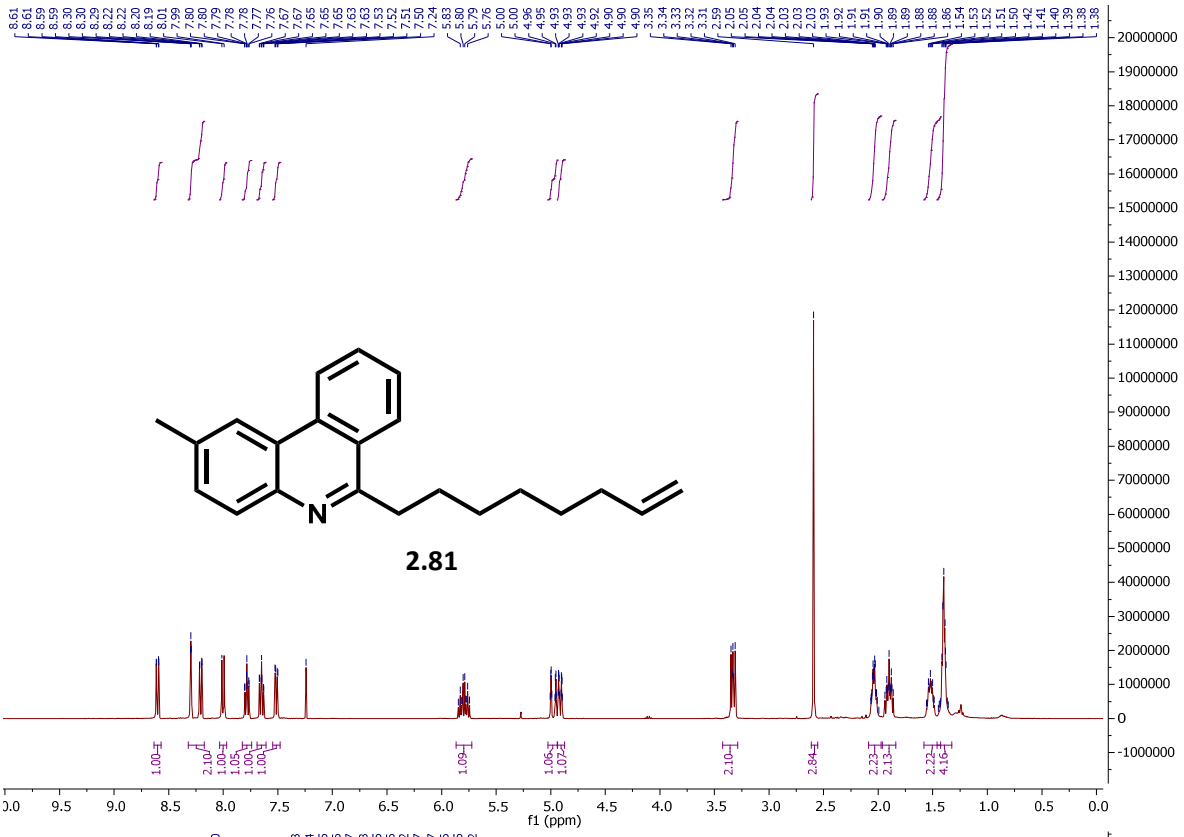
N
2.81
f1 (ppm)

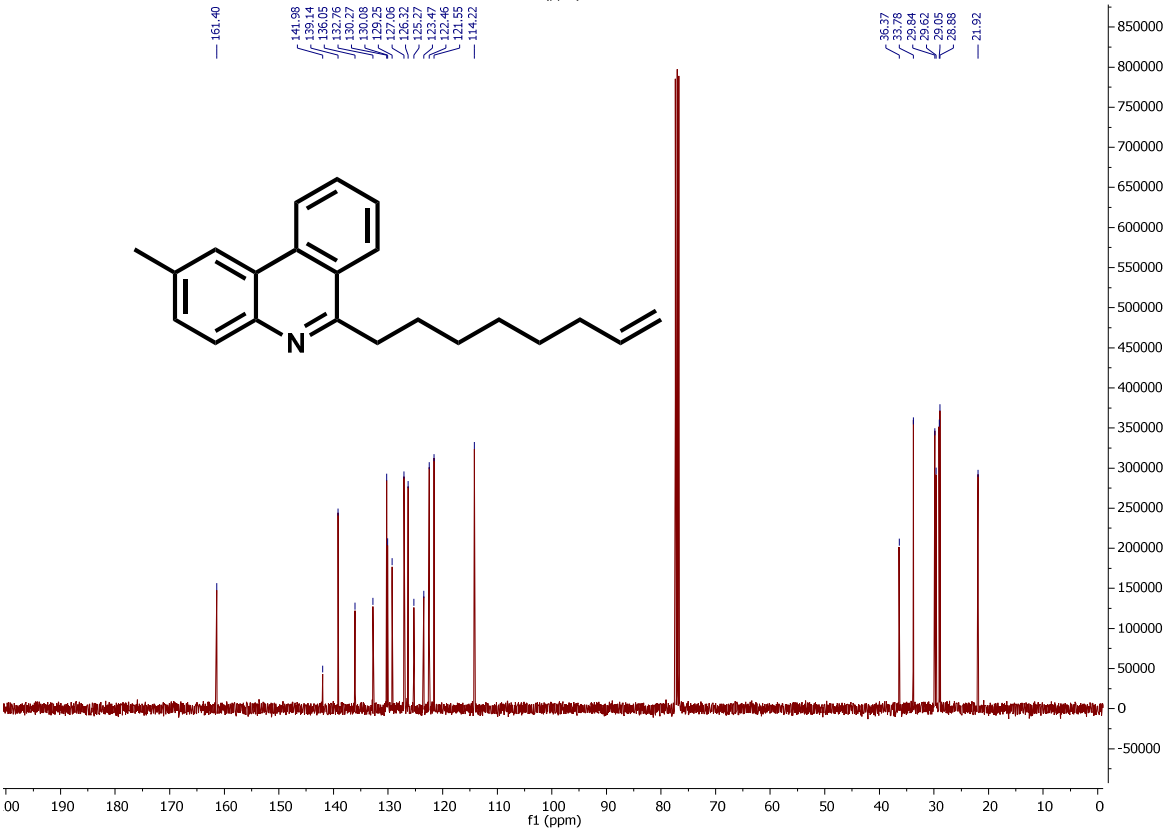
N
f1 (ppm)

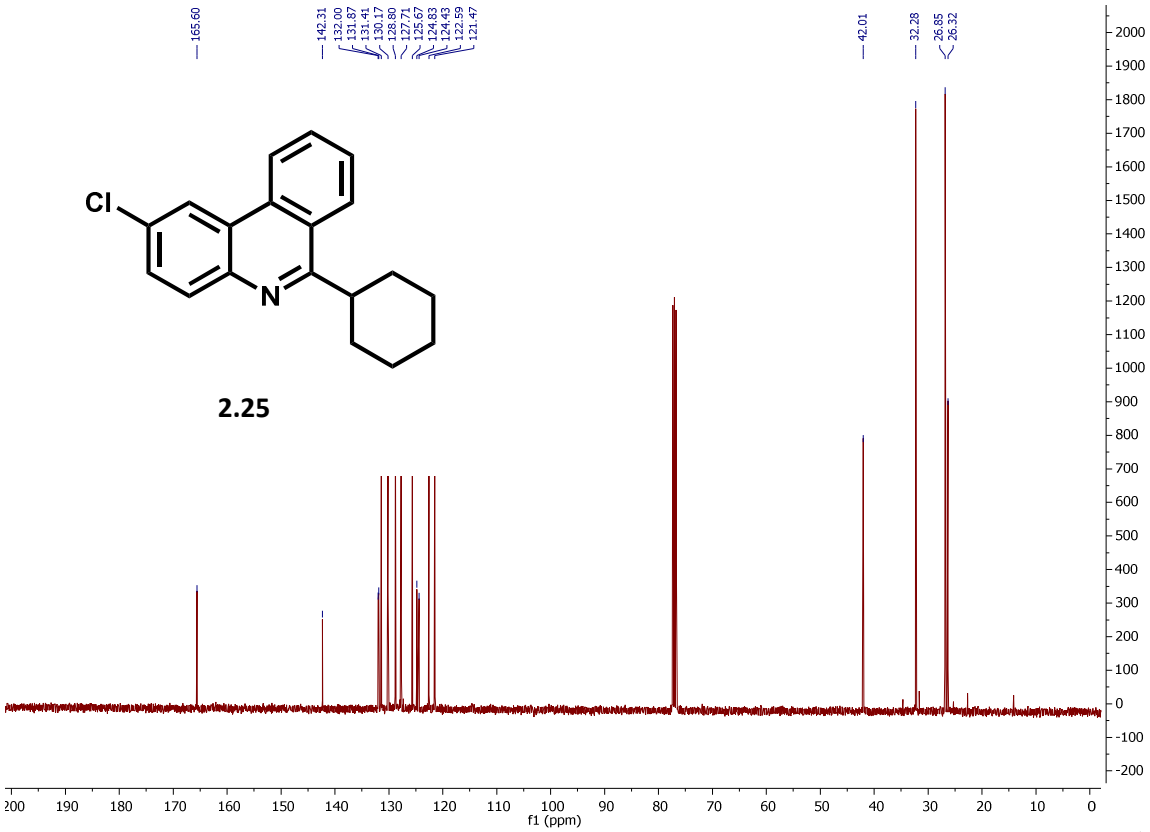
165.60
142.31
132.00
131.87
131.41
130.17
128.80
127.71
125.67
124.83
124.43
122.59
121.47
42.01
32.28
26.85
26.32
Cl
N
f1 (ppm)

2.25

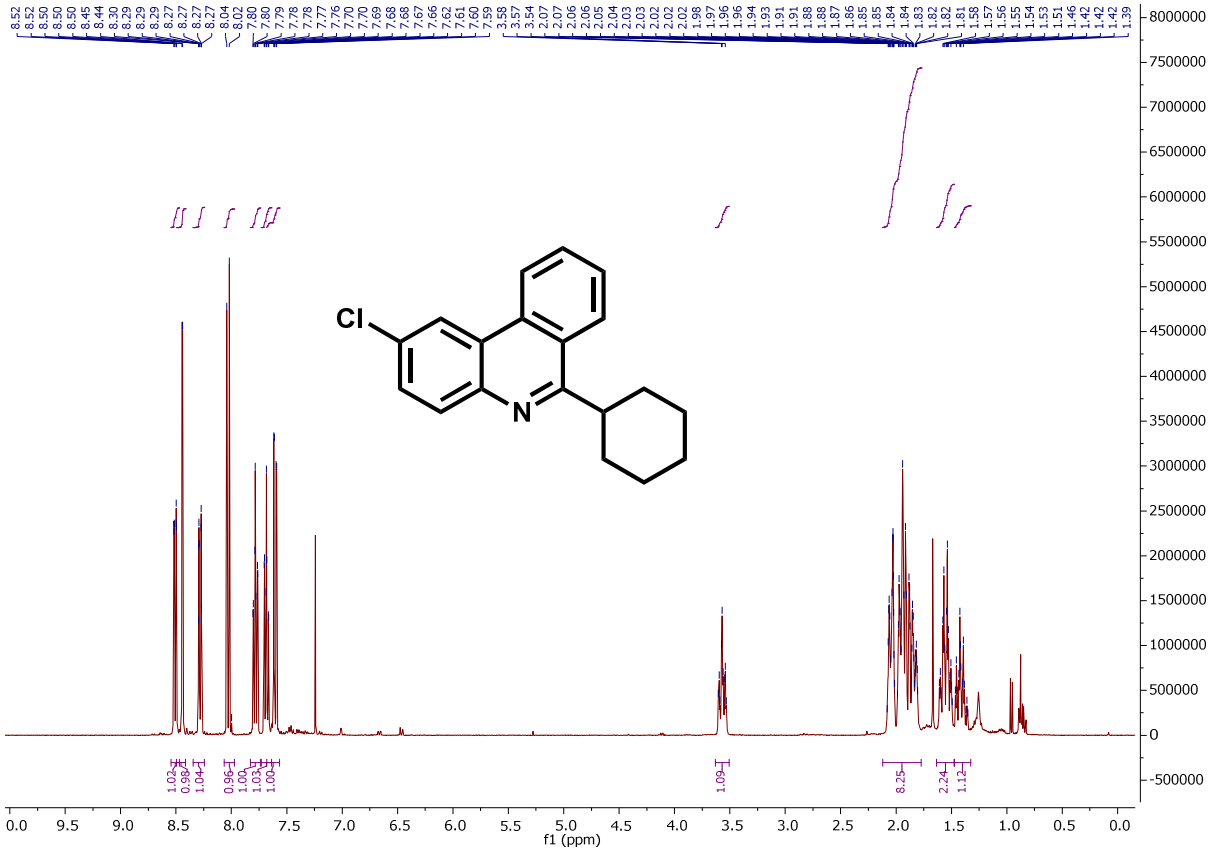
Cl
N
1.02
0.98
1.04
0.96
1.00
1.03
1.00
1.09
8.25
2.24
1.12
f1 (ppm)

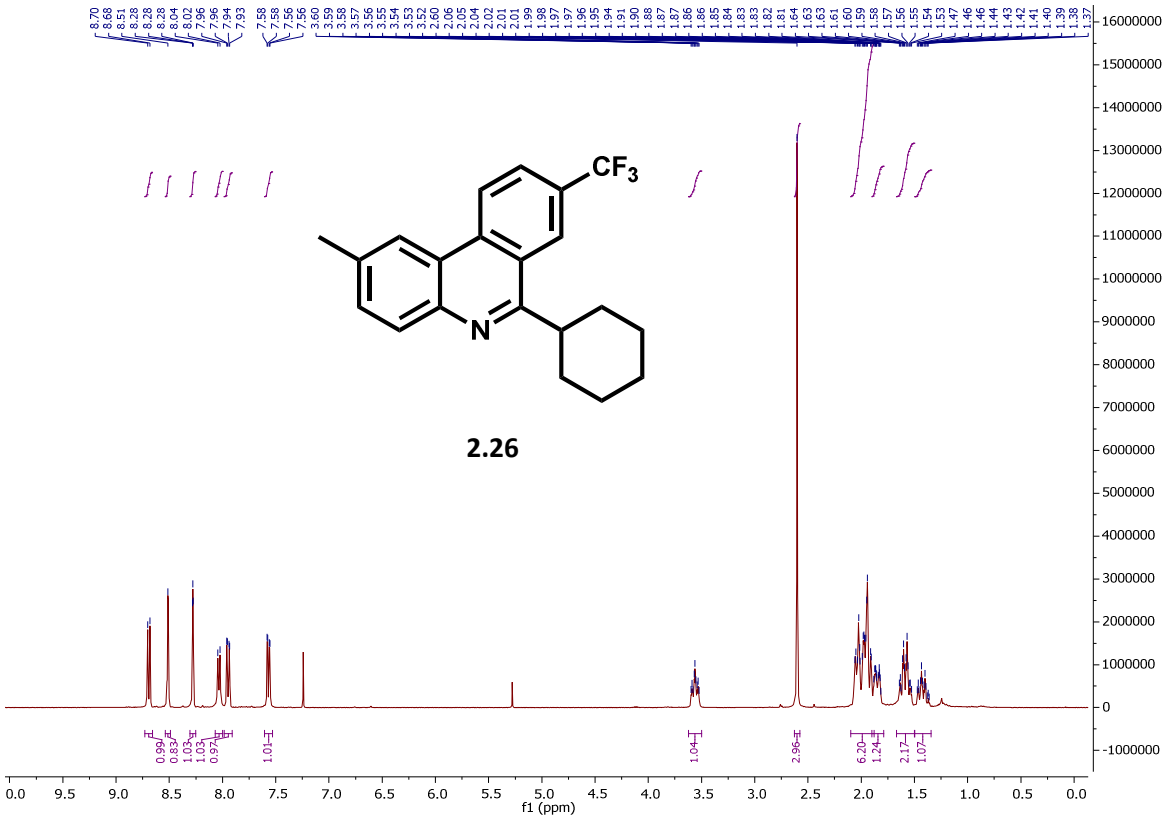

2.26

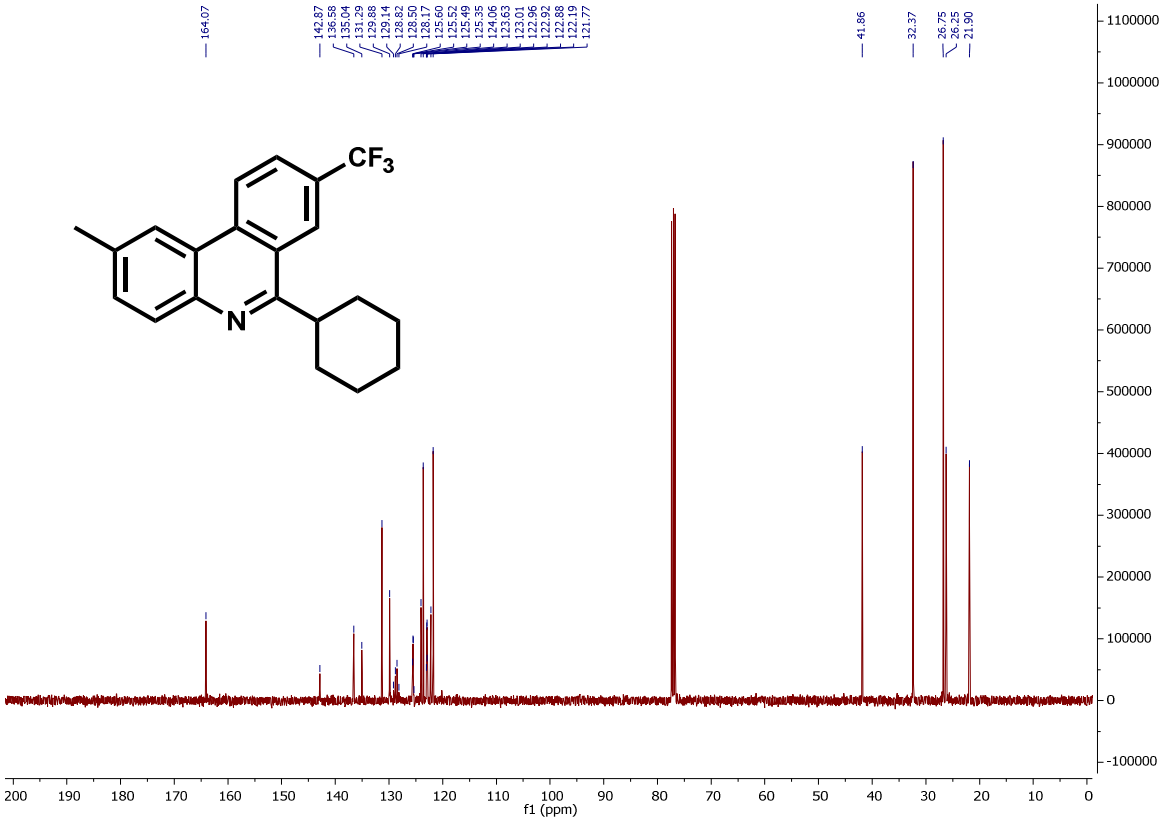

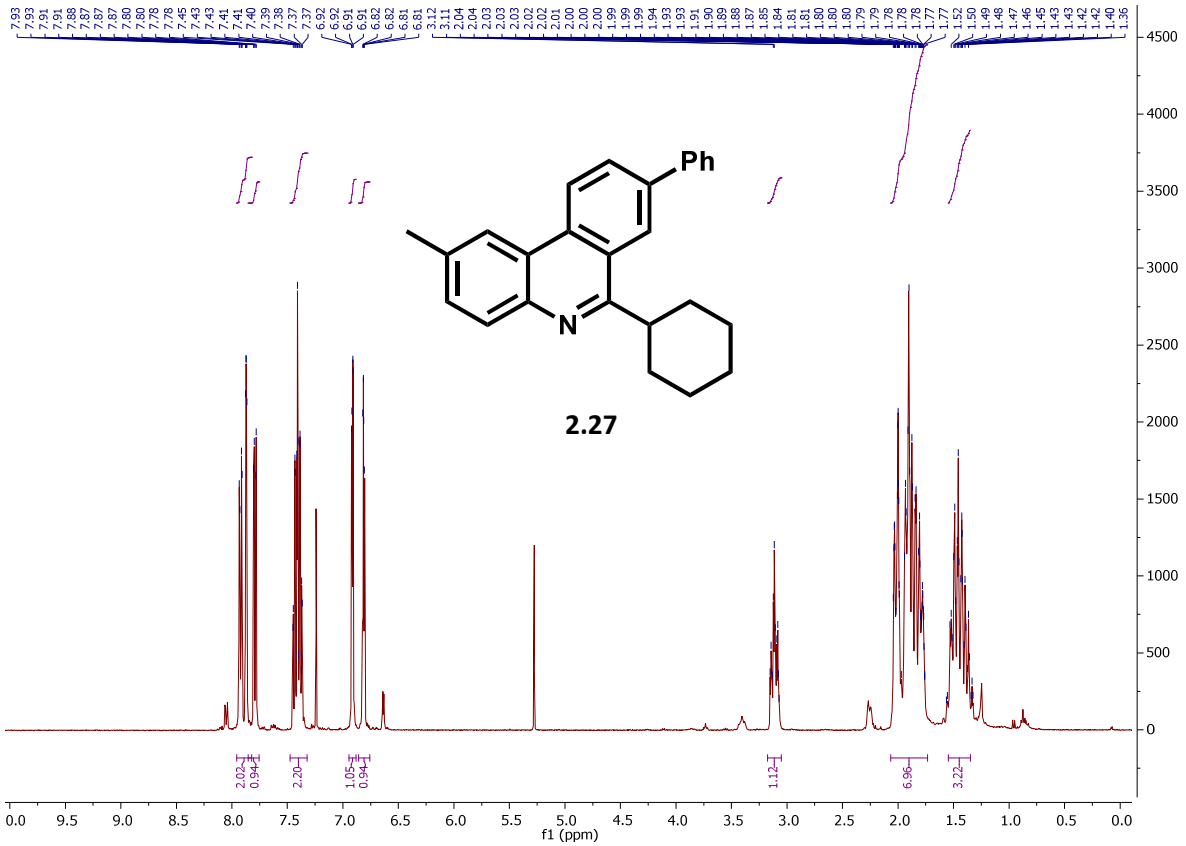
Ph
N
2.27
f1 (ppm)

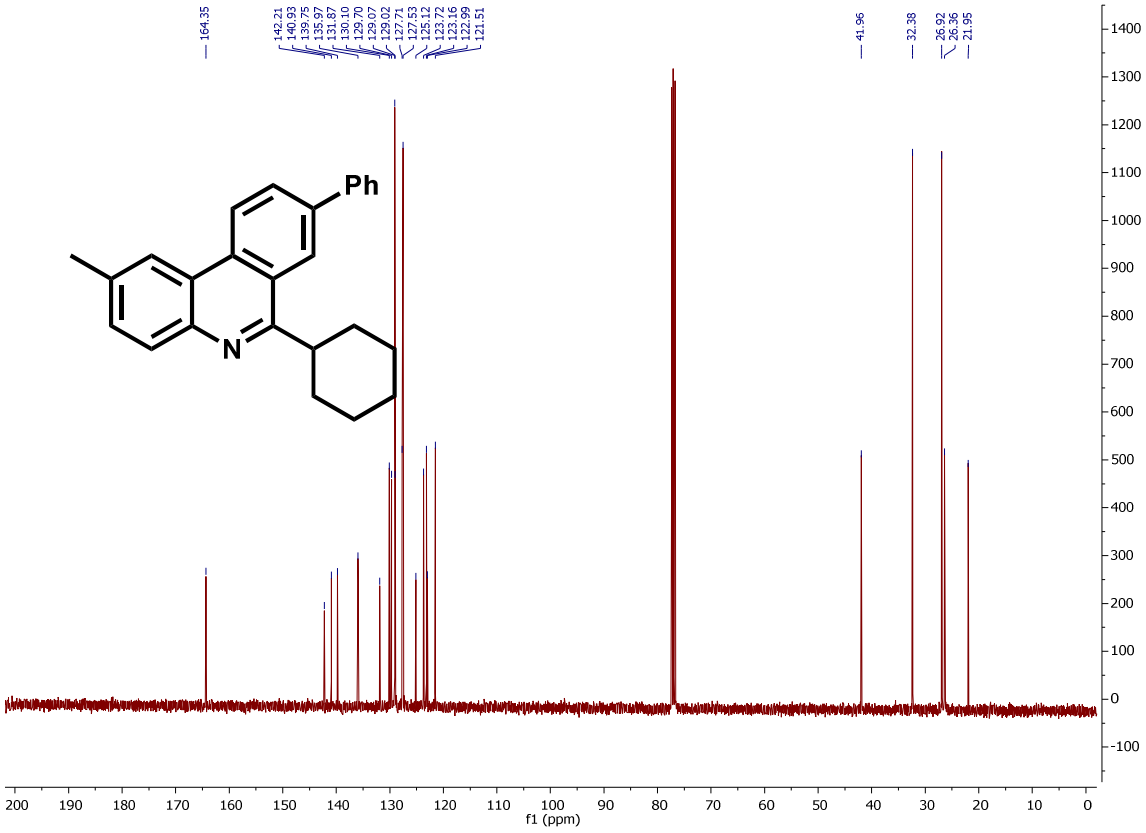
Ph
N
f1 (ppm)

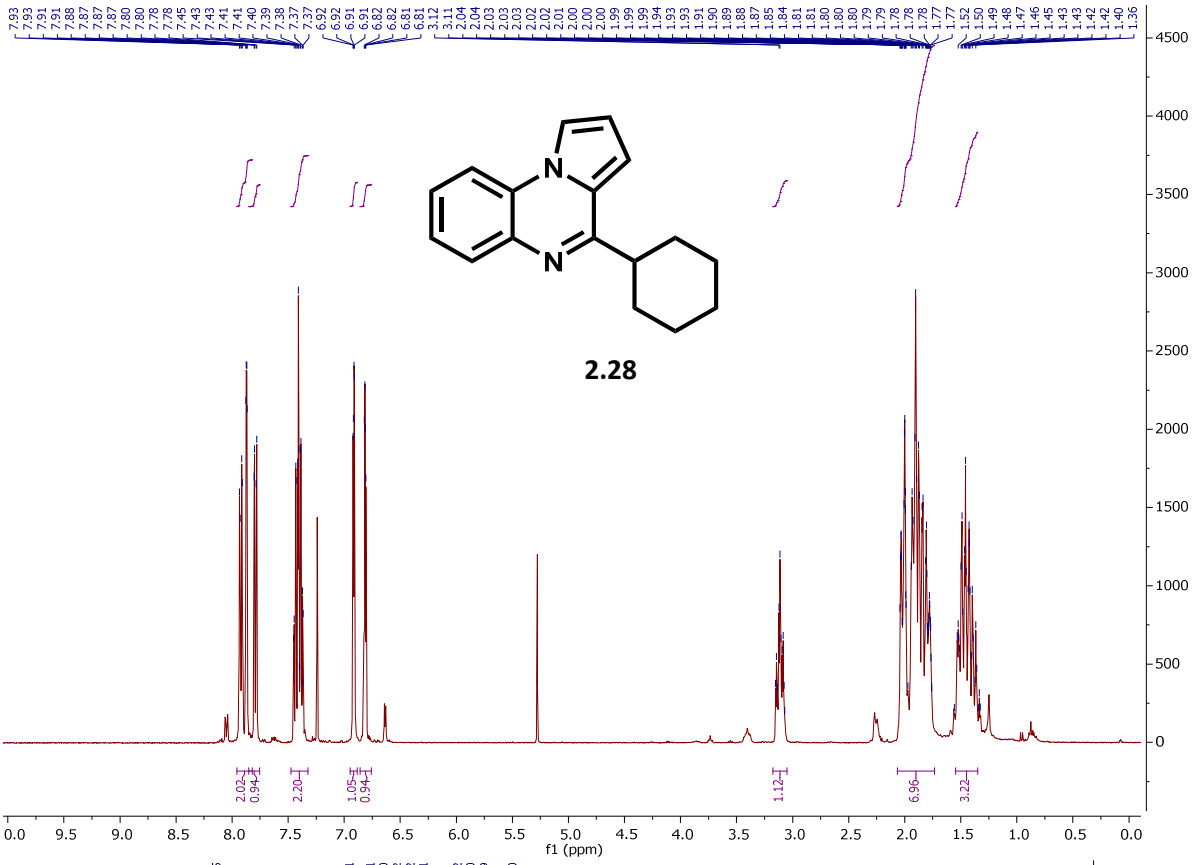
7.93 7.93 7.91 7.91 7.88 7.87 7.87 7.87 7.80 7.80 7.78 7.78 7.45 7.43 7.43 7.41 7.41 7.40 7.39 7.38 7.37 7.37 6.92 6.92 6.91 6.91 6.82 6.82 6.81 6.81 3.12 3.11 2.04 2.04 2.03 2.03 2.02 2.02 2.01 2.00 2.00 2.00 1.99 1.99 1.99 1.94 1.93 1.93 1.91 1.90 1.89 1.88 1.87 1.85 1.84 1.81 1.81 1.80 1.80 1.80 1.79 1.79 1.78 1.78 1.78 1.77 1.77 1.52 1.50 1.49 1.48 1.47 1.46 1.45 1.43 1.43 1.42 1.42 1.40 1.36
2.28
2.02 0.94 2.20 1.05 0.94 1.12 6.96 3.22
f1 (ppm)

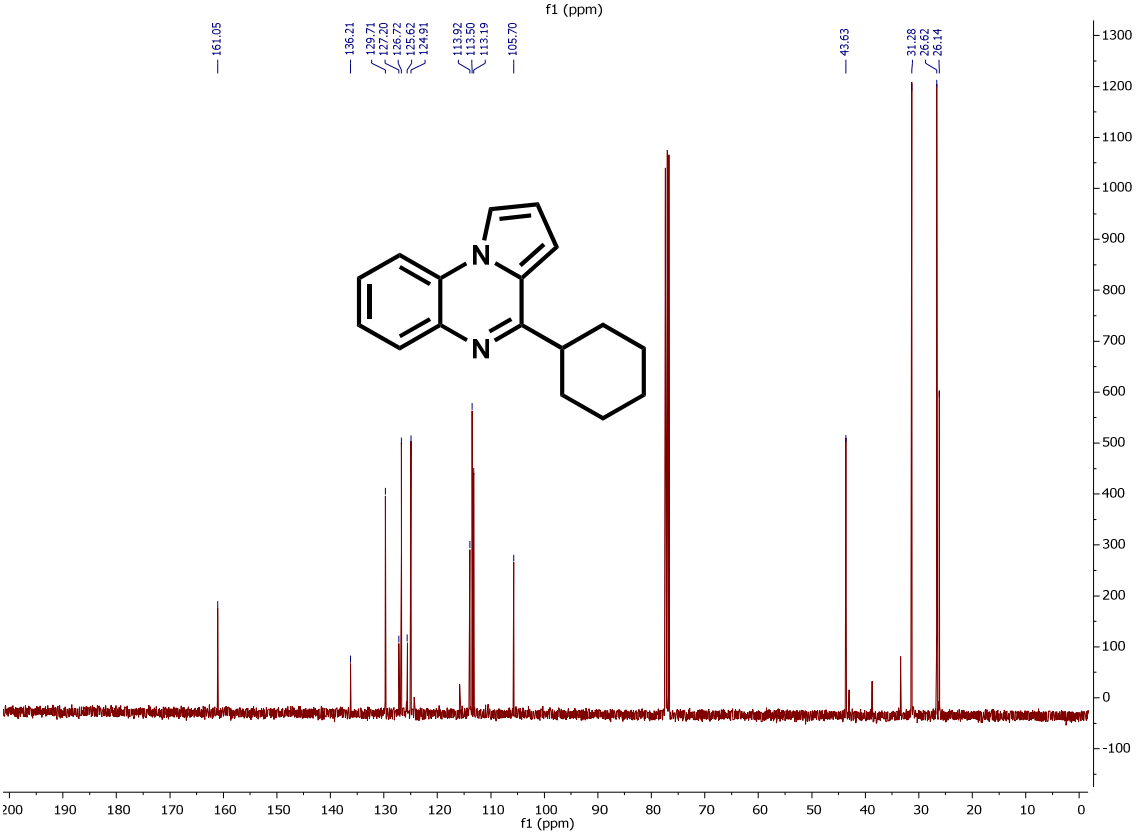
161.05 136.21 129.71 127.20 126.72 125.62 124.91 113.92 113.50 113.19 105.70 43.63 31.28 26.62 26.14
f1 (ppm)

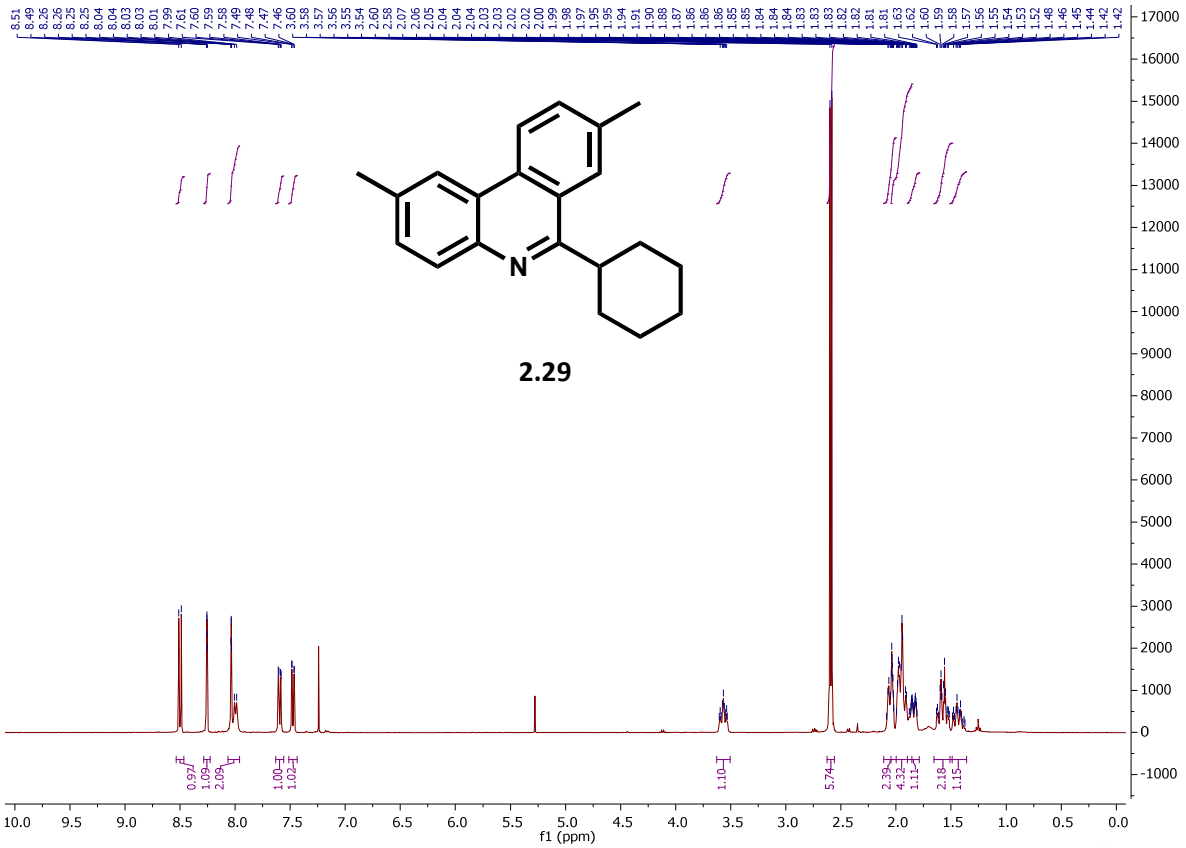
N
2.29
f1 (ppm)

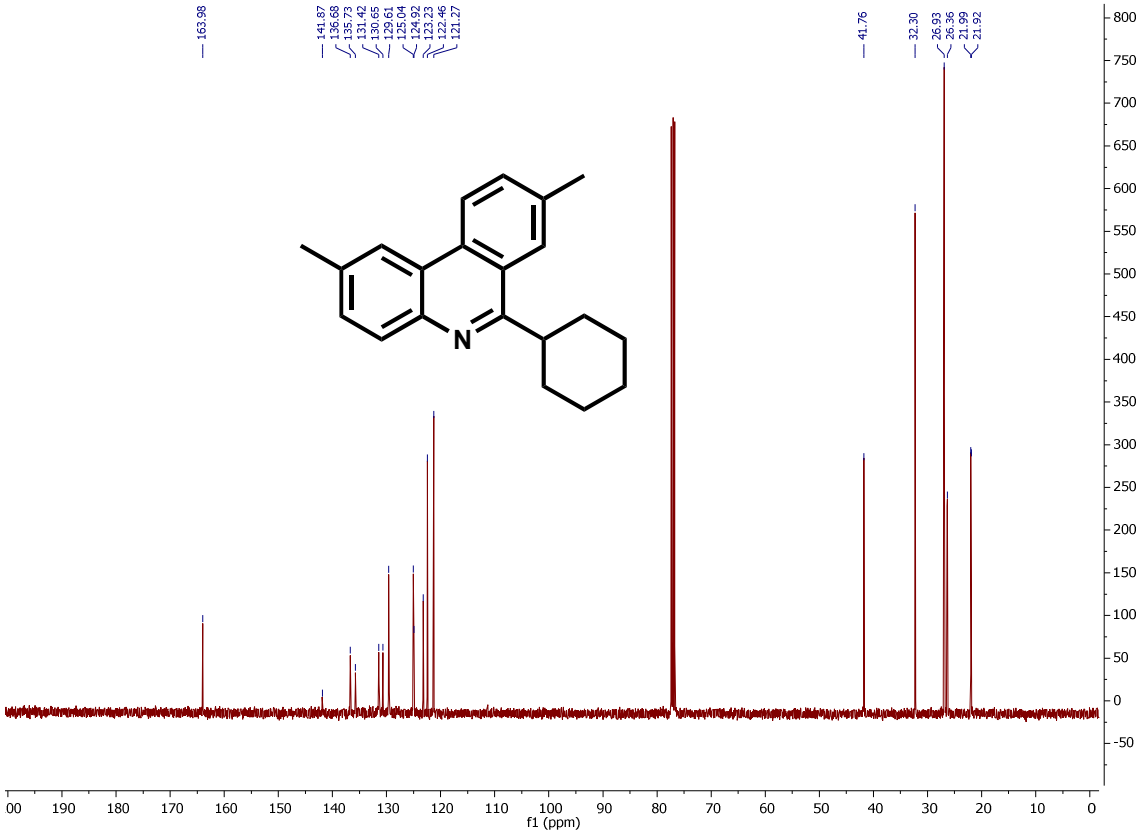
N
f1 (ppm)

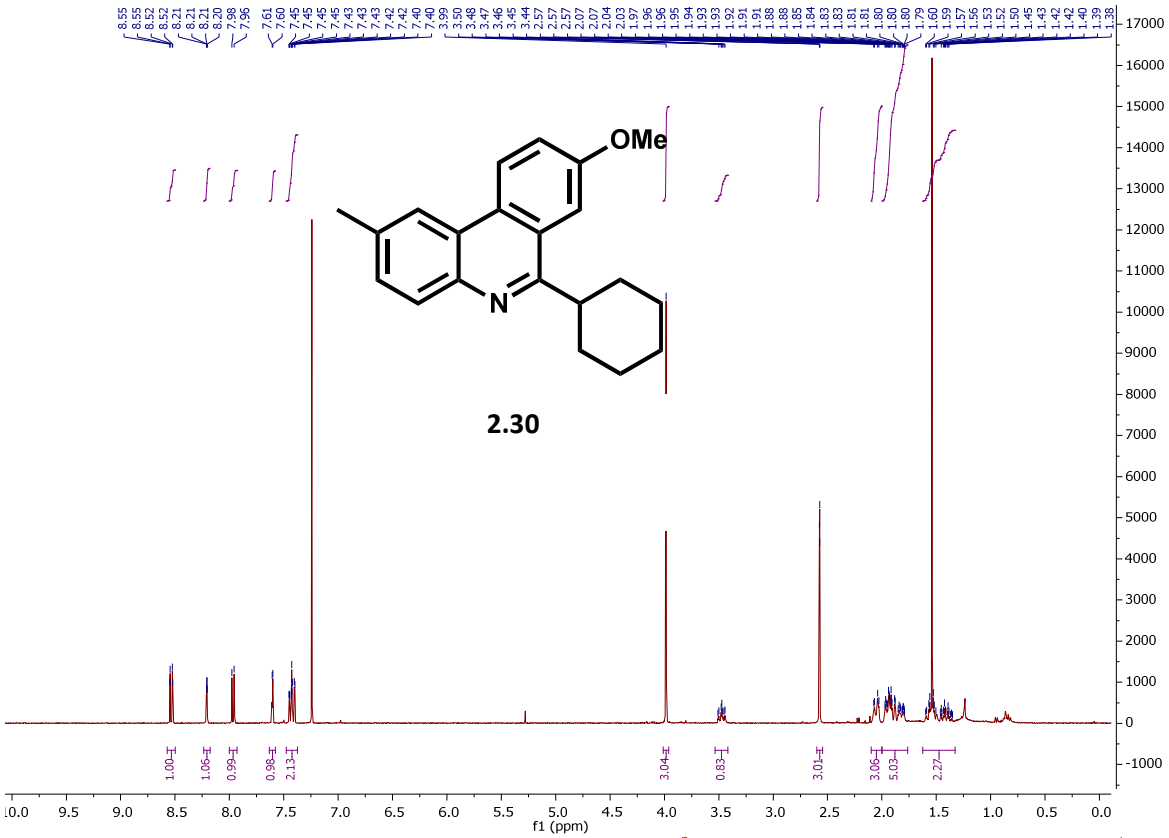
OMe
N
2.30
f1 (ppm)

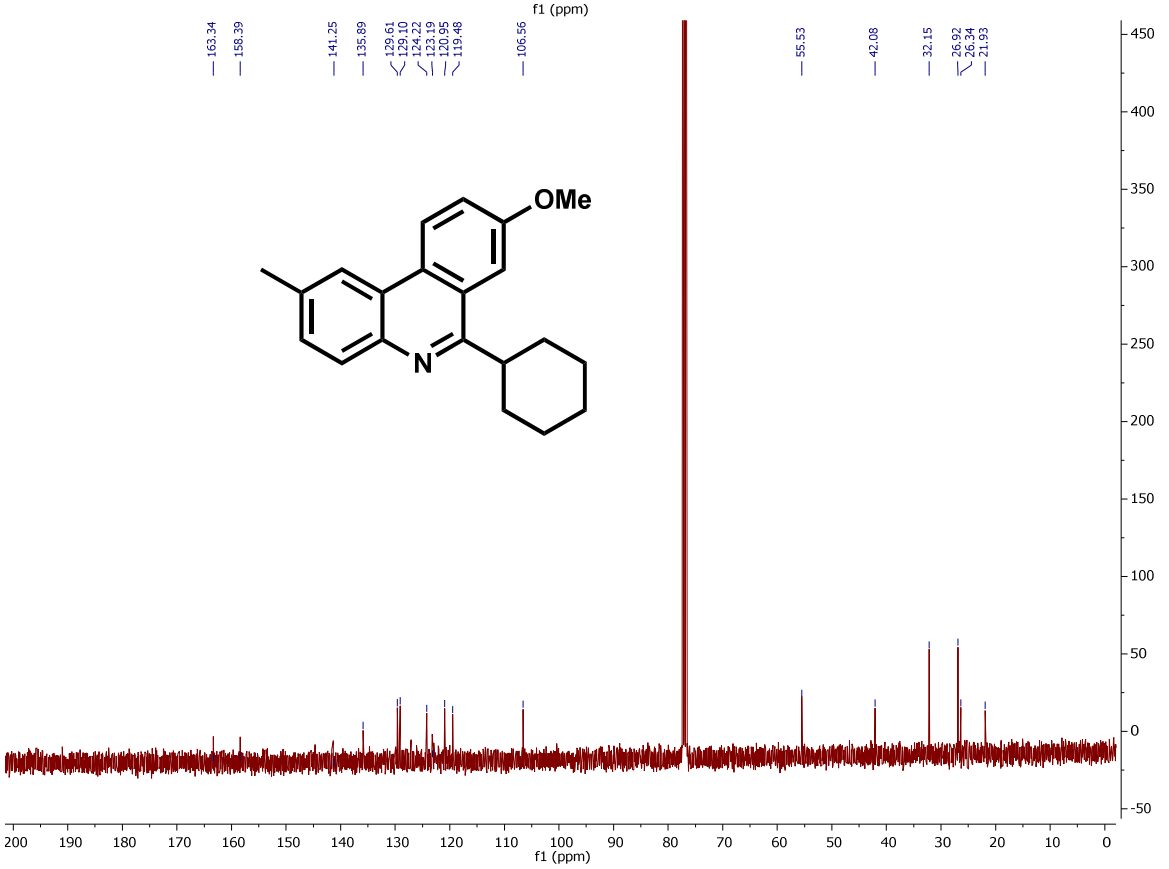
OMe
N
f1 (ppm)

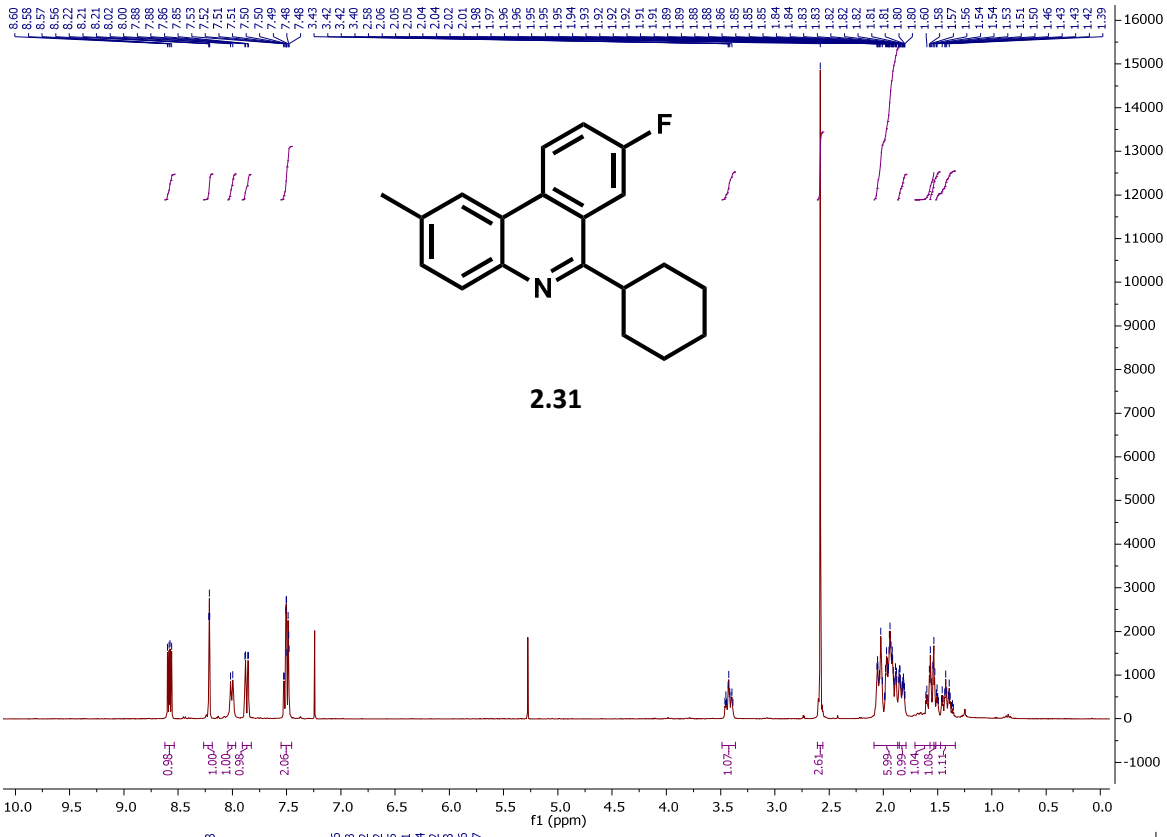

2.31

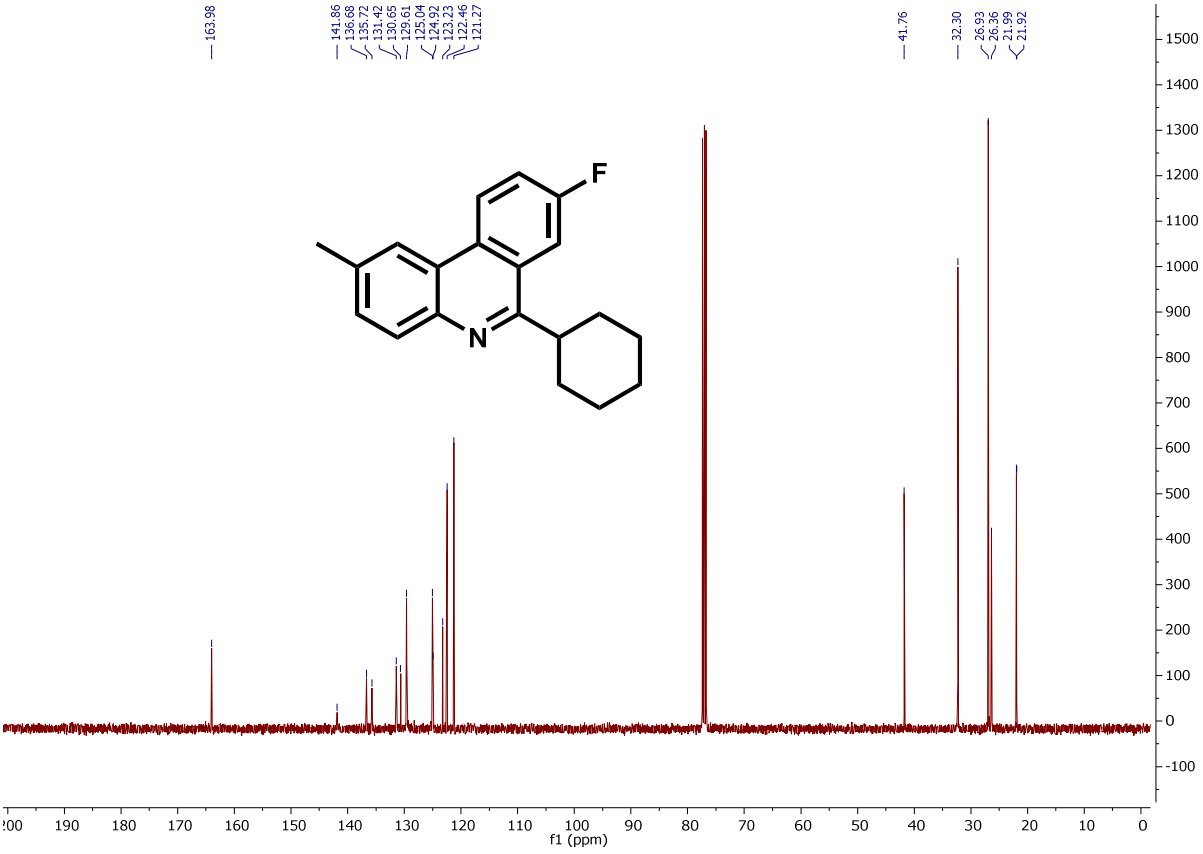

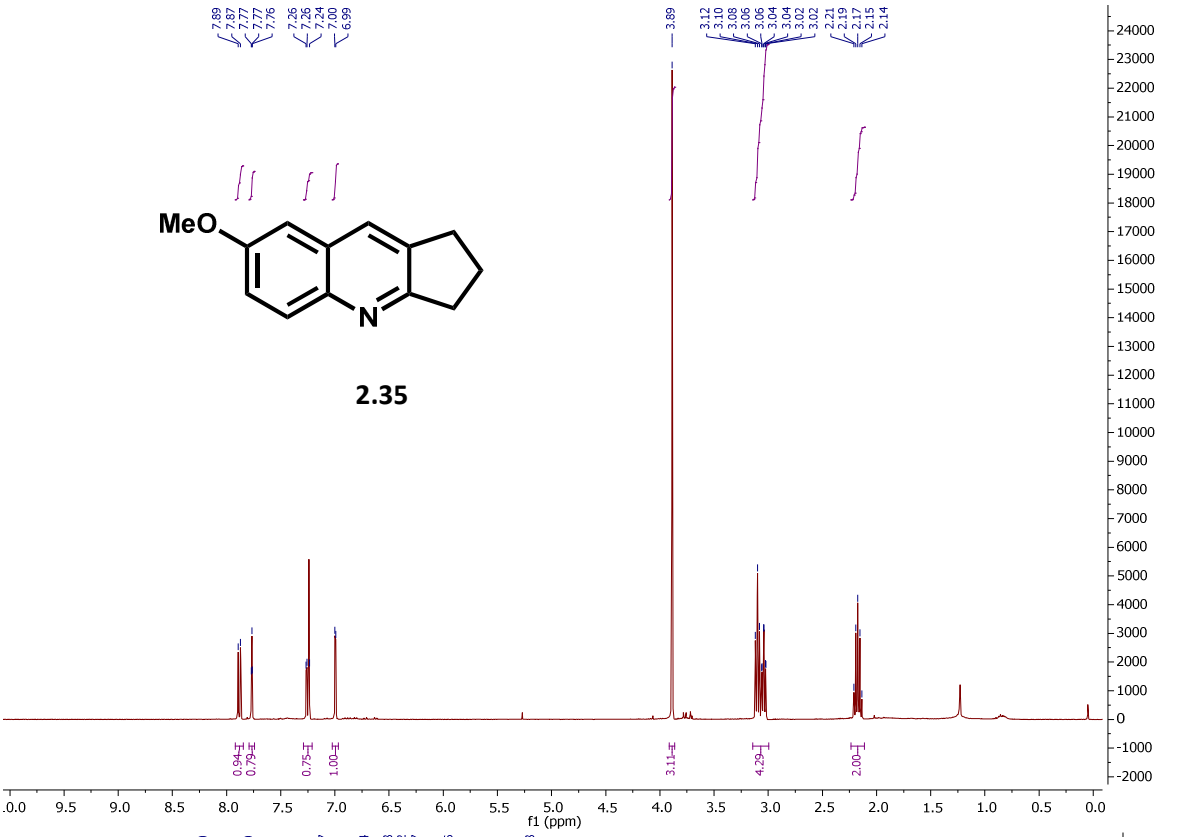
7.89
7.87
7.77
7.77
7.76
7.26
7.26
7.24
7.00
6.99
3.89
3.12
3.10
3.08
3.06
3.06
3.04
3.04
3.02
3.02
2.21
2.19
2.17
2.15
2.14
MeO
N
0.94
0.79
0.75
1.00
3.11
4.29
2.00
f1 (ppm)

2.35

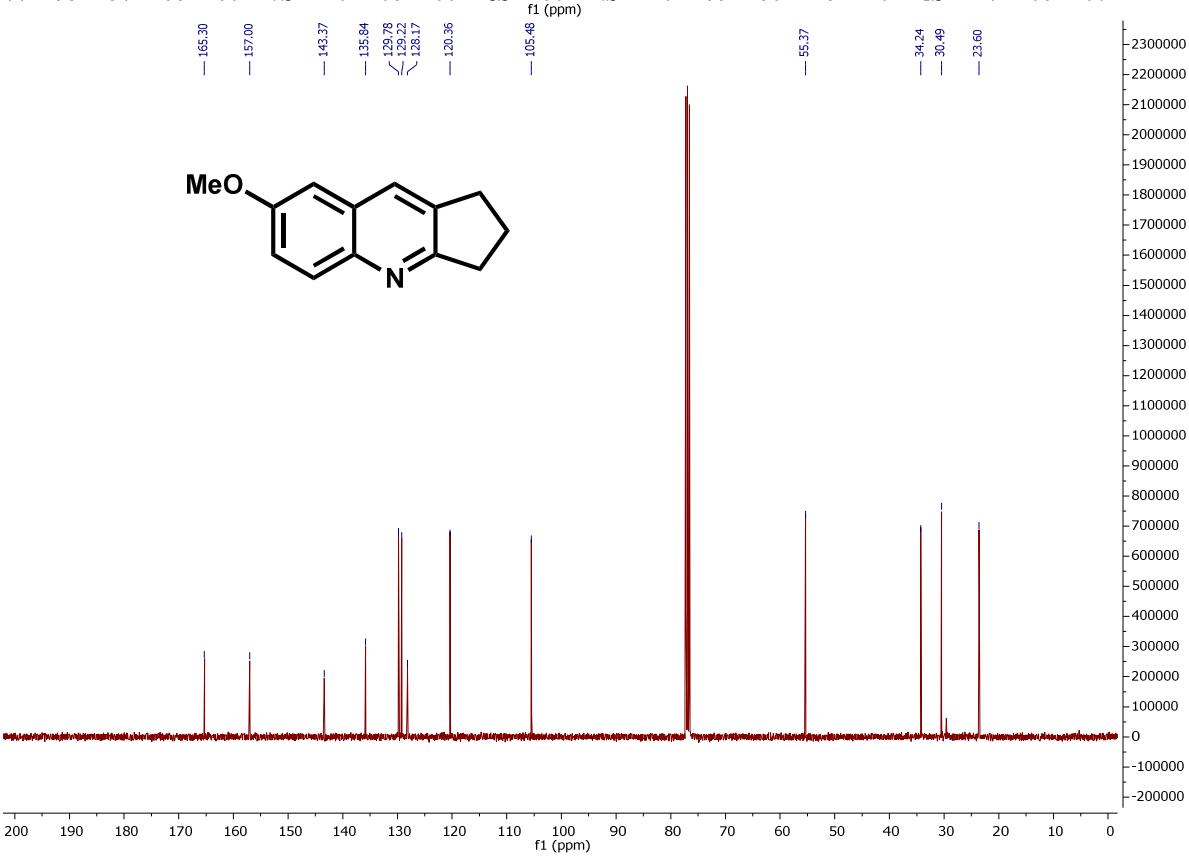
165.30
157.00
143.37
135.84
129.78
129.22
128.17
120.36
105.48
55.37
34.24
30.49
23.60
MeO
N
f1 (ppm)

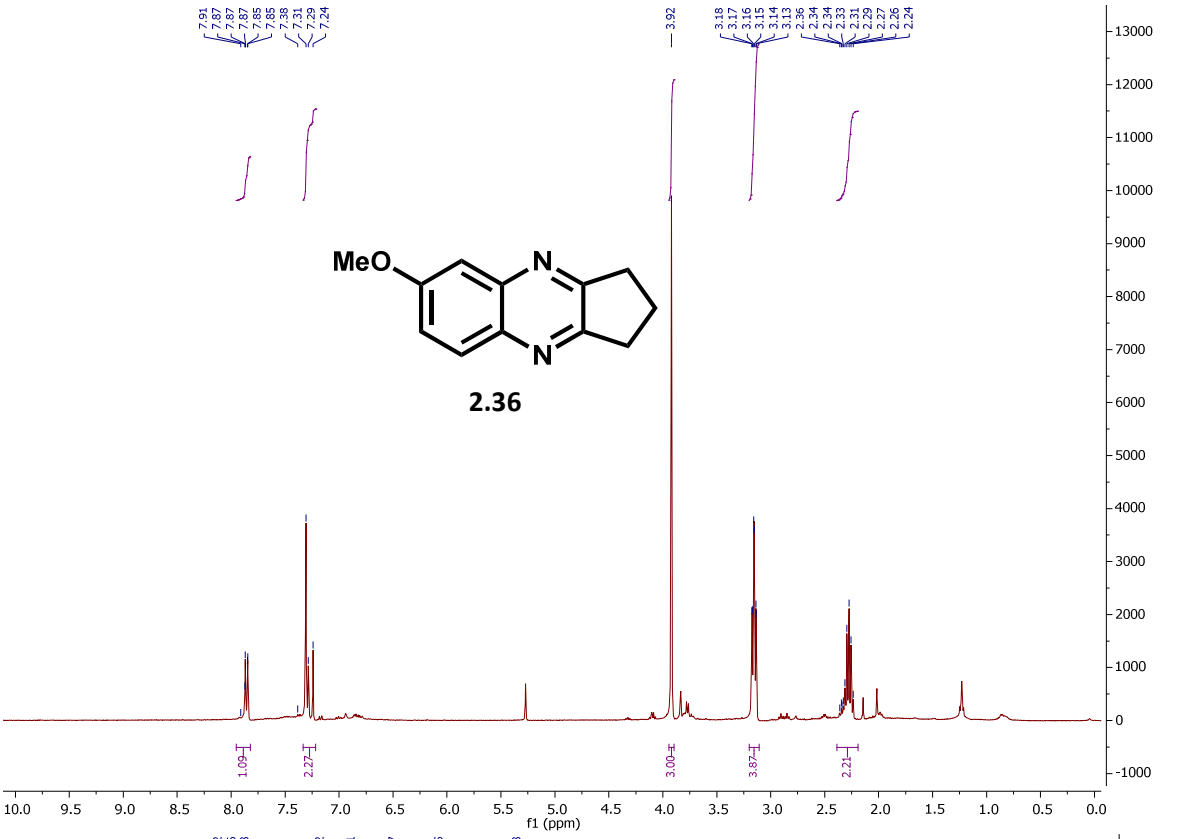
7.91
7.87
7.87
7.87
7.85
7.85
7.38
7.31
7.29
7.24
3.92
3.18
3.17
3.16
3.15
3.14
3.13
2.36
2.34
2.34
2.33
2.31
2.29
2.27
2.26
2.24
MeO
N
N
2.36
1.09
2.27
3.00
3.87
2.21
f1 (ppm)

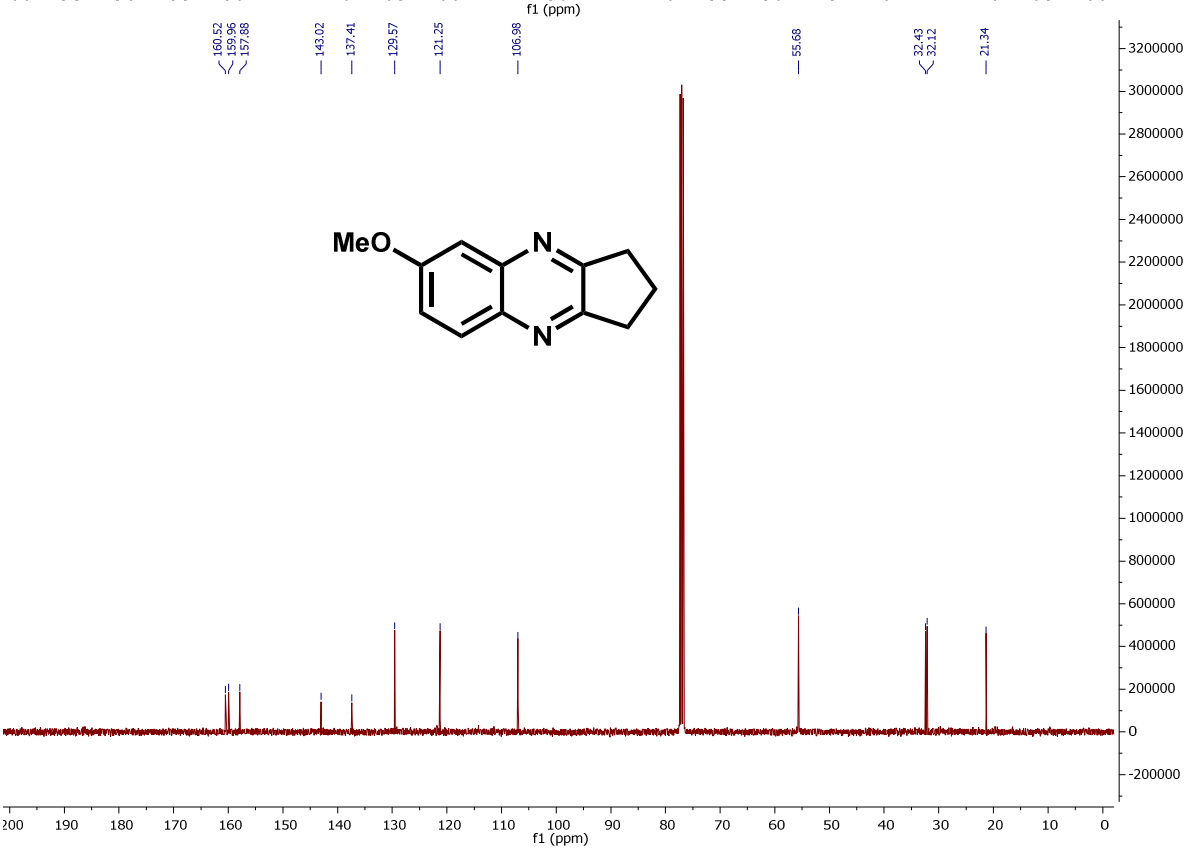
160.52
159.96
157.88
143.02
137.41
129.57
121.25
106.98
55.68
32.43
32.12
21.34
MeO
N
N
f1 (ppm)

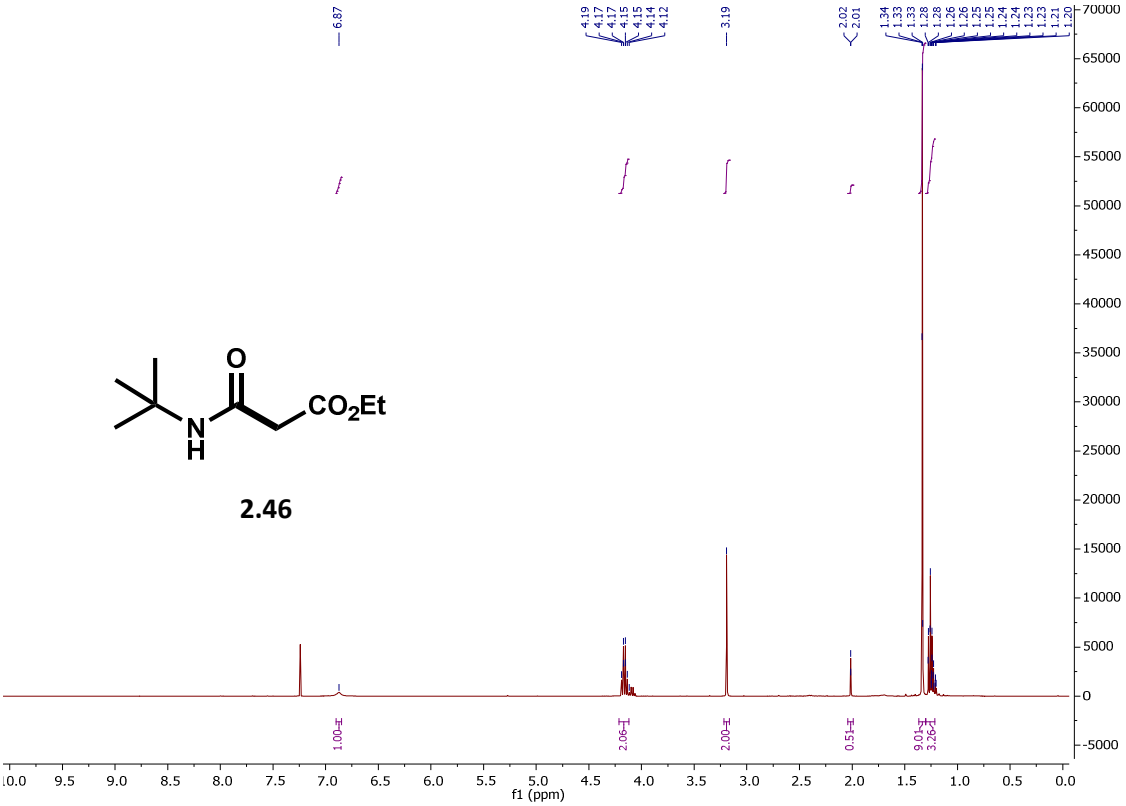
6.87
4.19
4.17
4.17
4.15
4.15
4.14
4.12
3.19
2.02
2.01
1.34
1.33
1.33
1.28
1.28
1.26
1.26
1.25
1.25
1.24
1.24
1.23
1.23
1.21
1.20
1.00
2.06
2.00
0.51
9.01
3.26
f1 (ppm)

O
N
H
CO2Et

2.46

169.82
163.82
61.31
51.20
42.06
28.53
13.93
f1 (ppm)

O
N
H
CO2Et

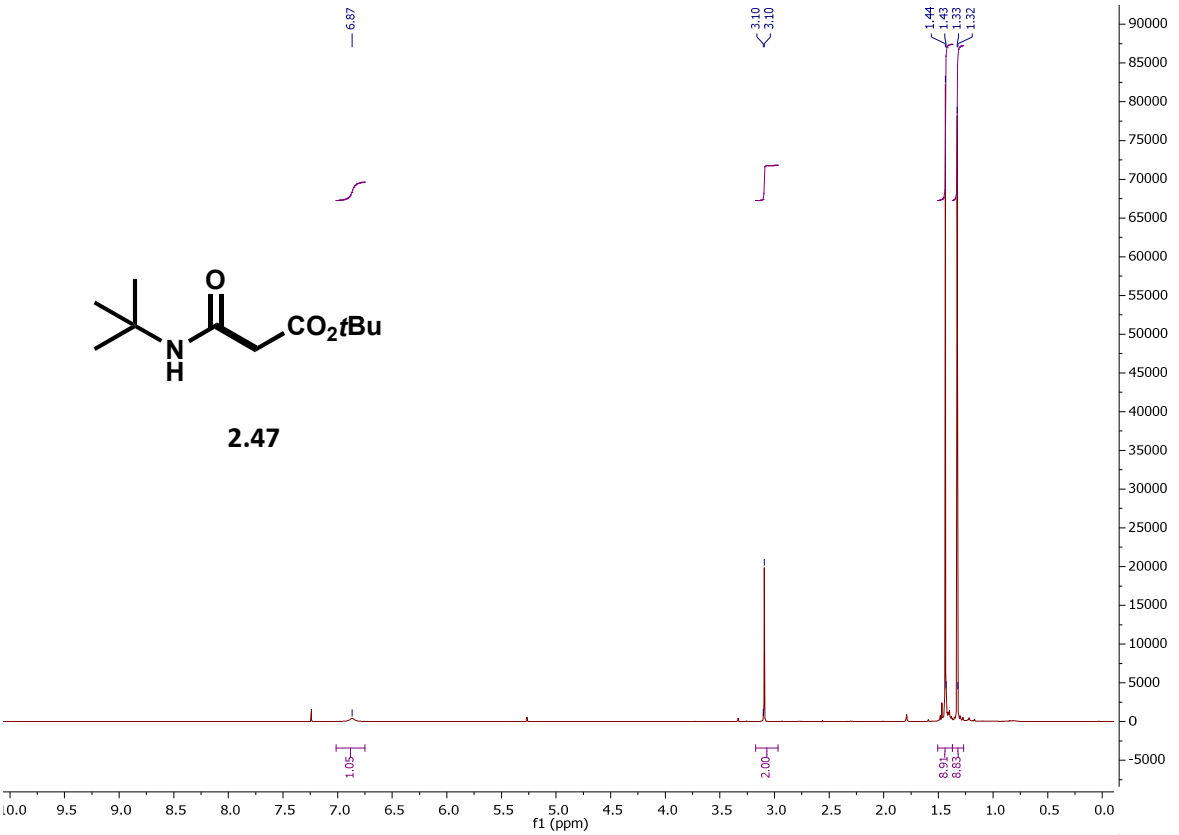
6.87
3.10
3.10
1.44
1.43
1.33
1.32
O
N
H
CO2tBu
1.05
2.00
8.91
8.83
f1 (ppm)

2.47

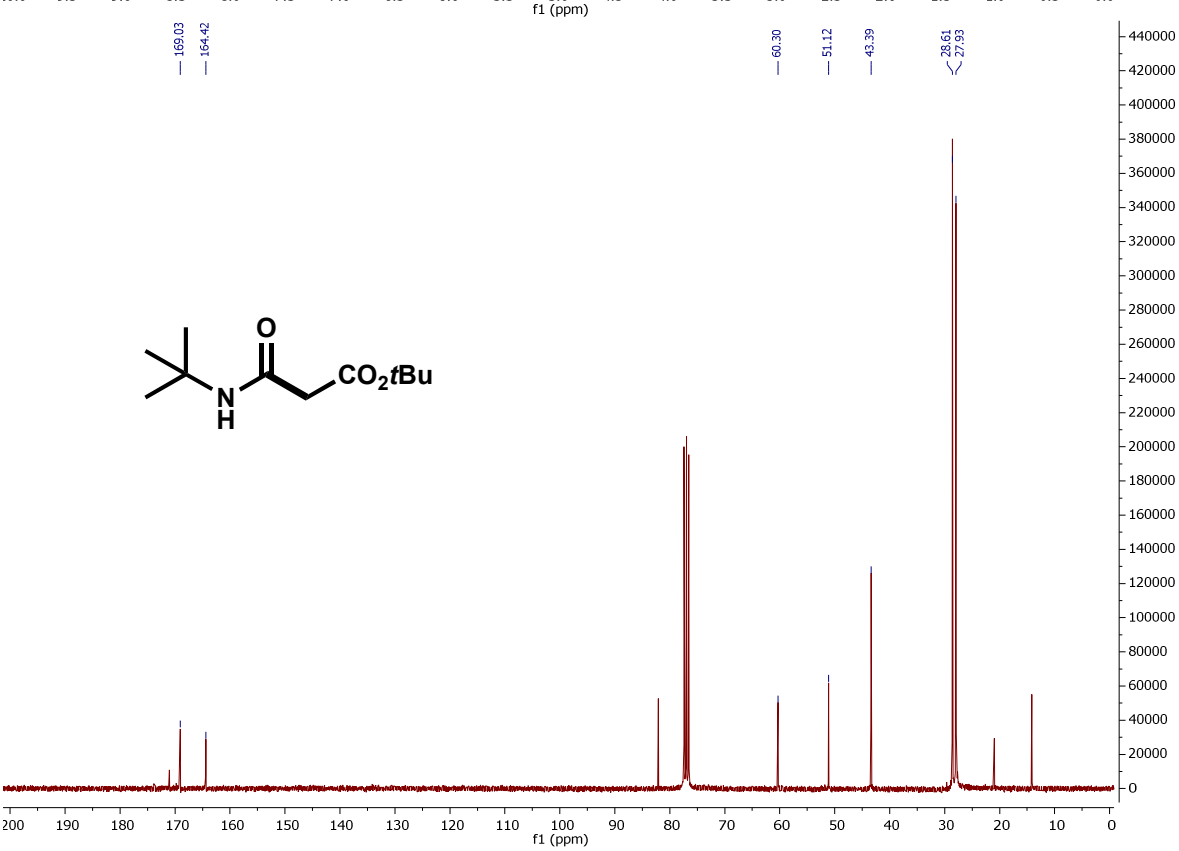
169.03
164.42
60.30
51.12
43.39
28.61
27.93
O
N
H
CO2tBu
f1 (ppm)

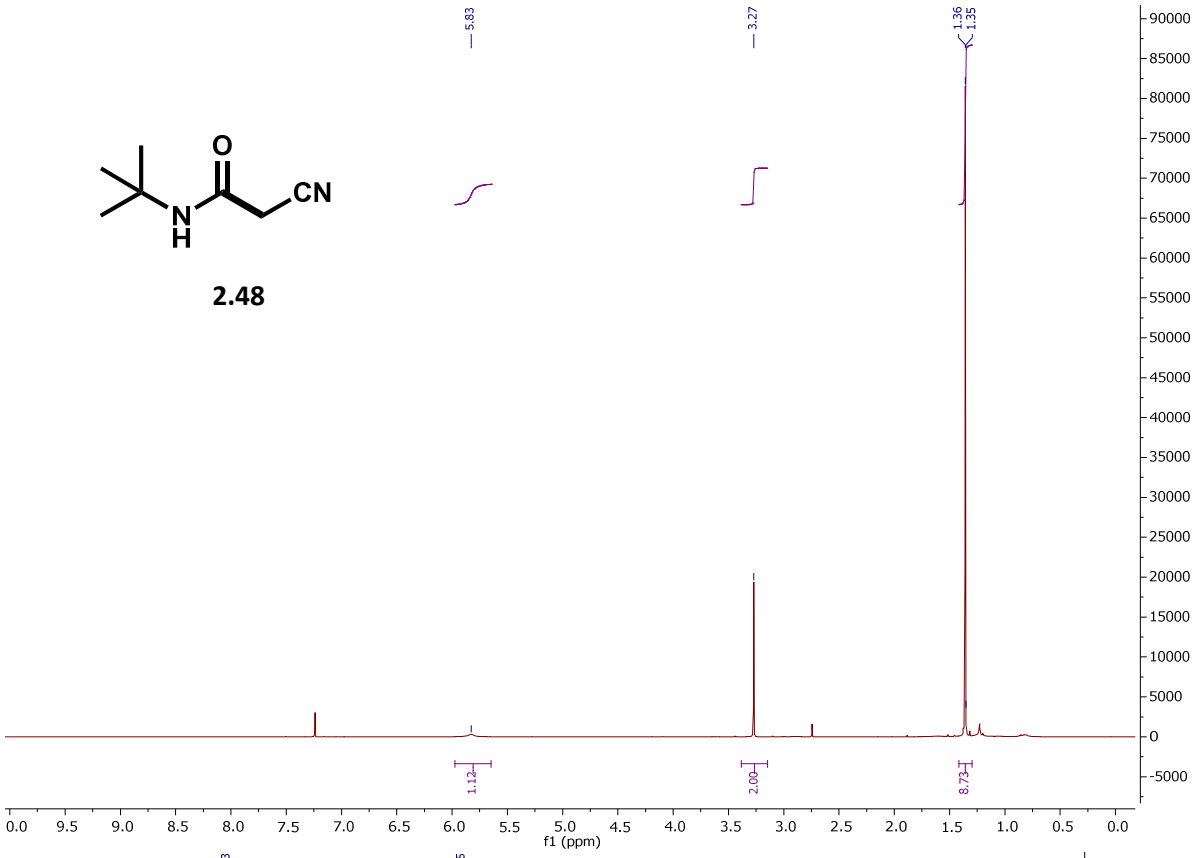
5.83
3.27
1.36
1.35
1.12
2.00
8.73
f1 (ppm)

2.48

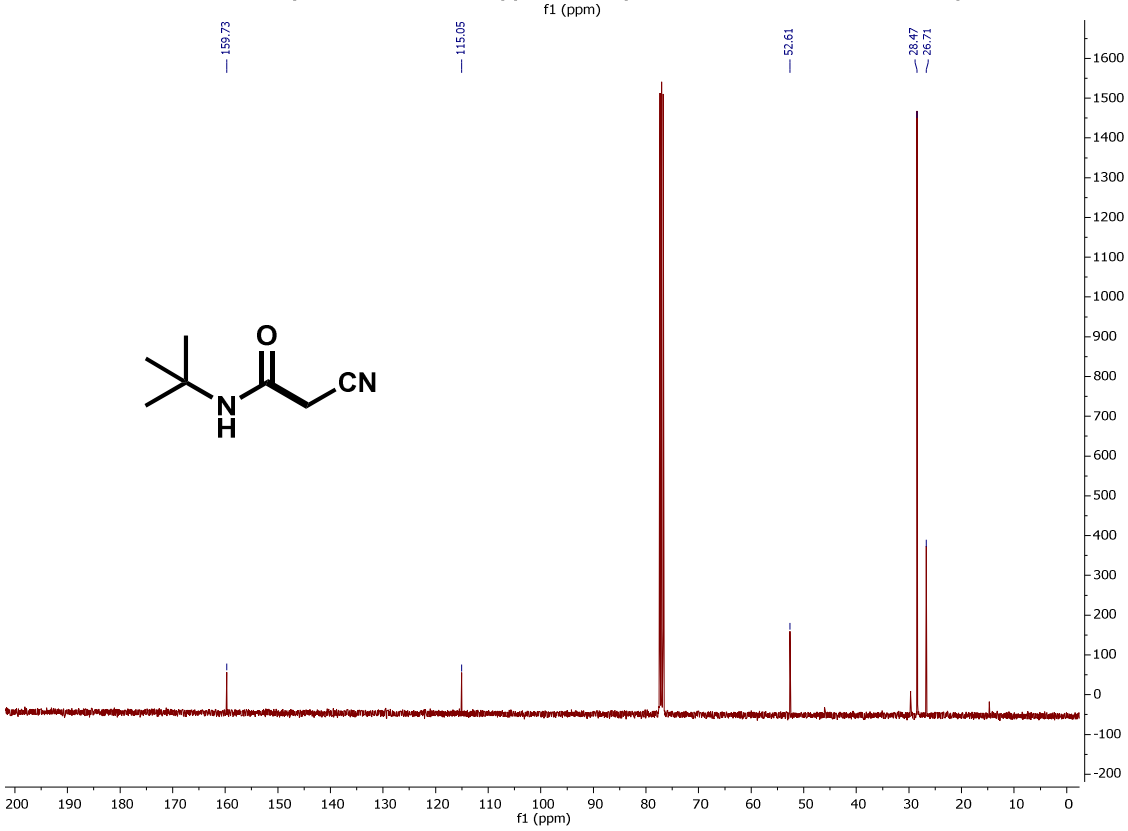
159.73
115.05
52.61
28.47
26.71
f1 (ppm)

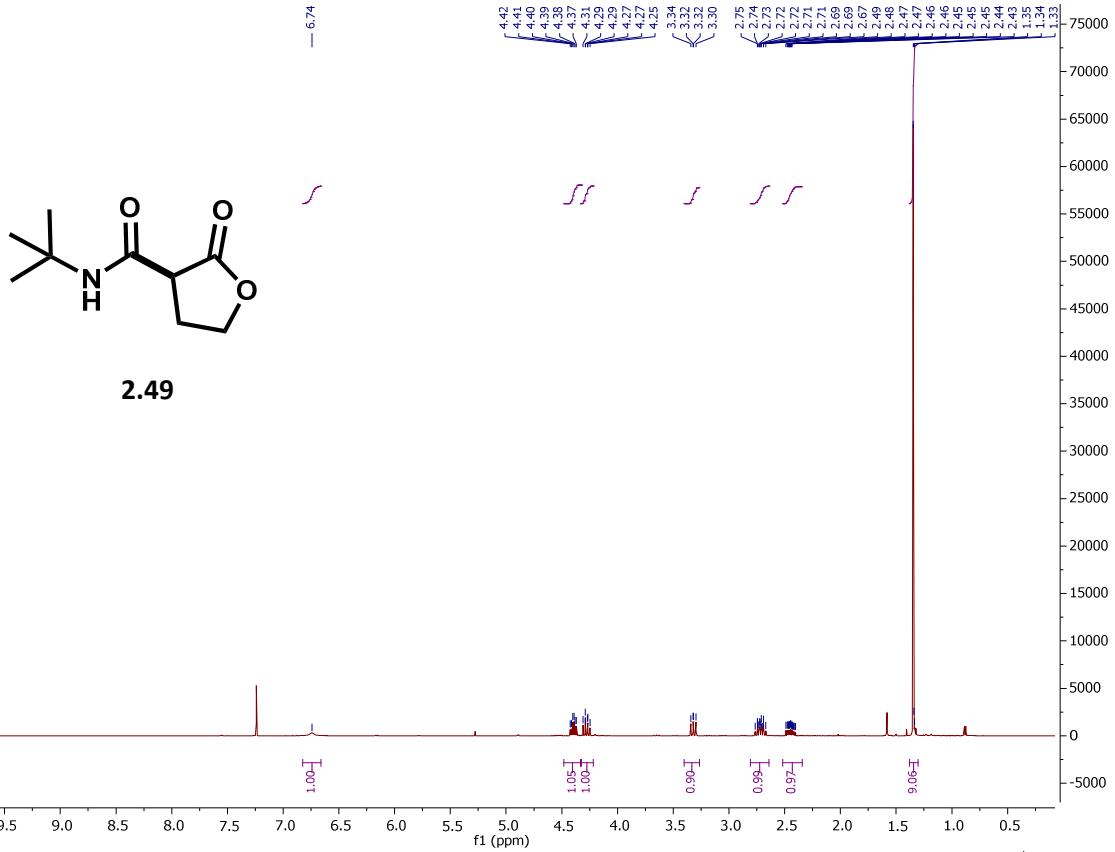
6.74
4.42
4.41
4.40
4.39
4.38
4.37
4.31
4.29
4.29
4.27
4.27
4.25
3.34
3.32
3.32
3.30
2.75
2.74
2.73
2.72
2.72
2.71
2.71
2.69
2.69
2.67
2.49
2.48
2.47
2.47
2.46
2.46
2.45
2.45
2.45
2.44
2.43
1.35
1.34
1.33
1.00
1.05
1.00
0.90
0.99
0.97
9.06
f1 (ppm)

2.49

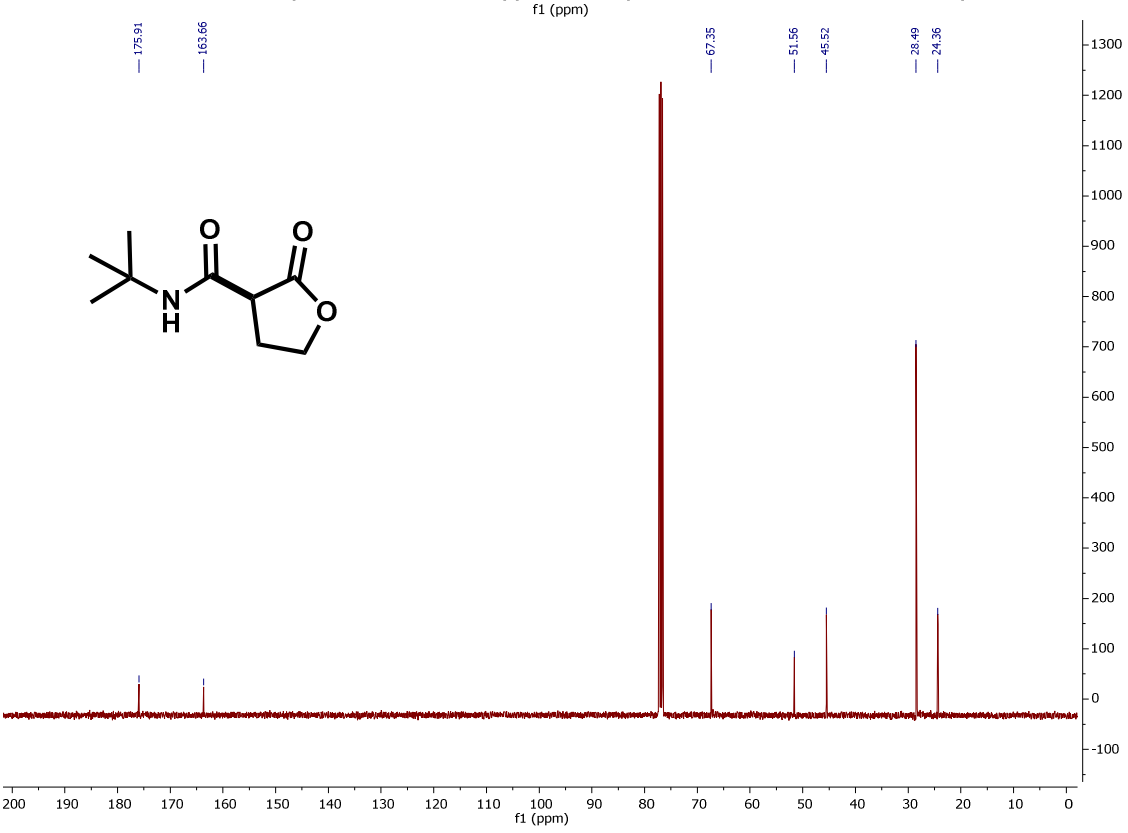
175.91
163.66
67.35
51.56
45.52
28.49
24.36
f1 (ppm)

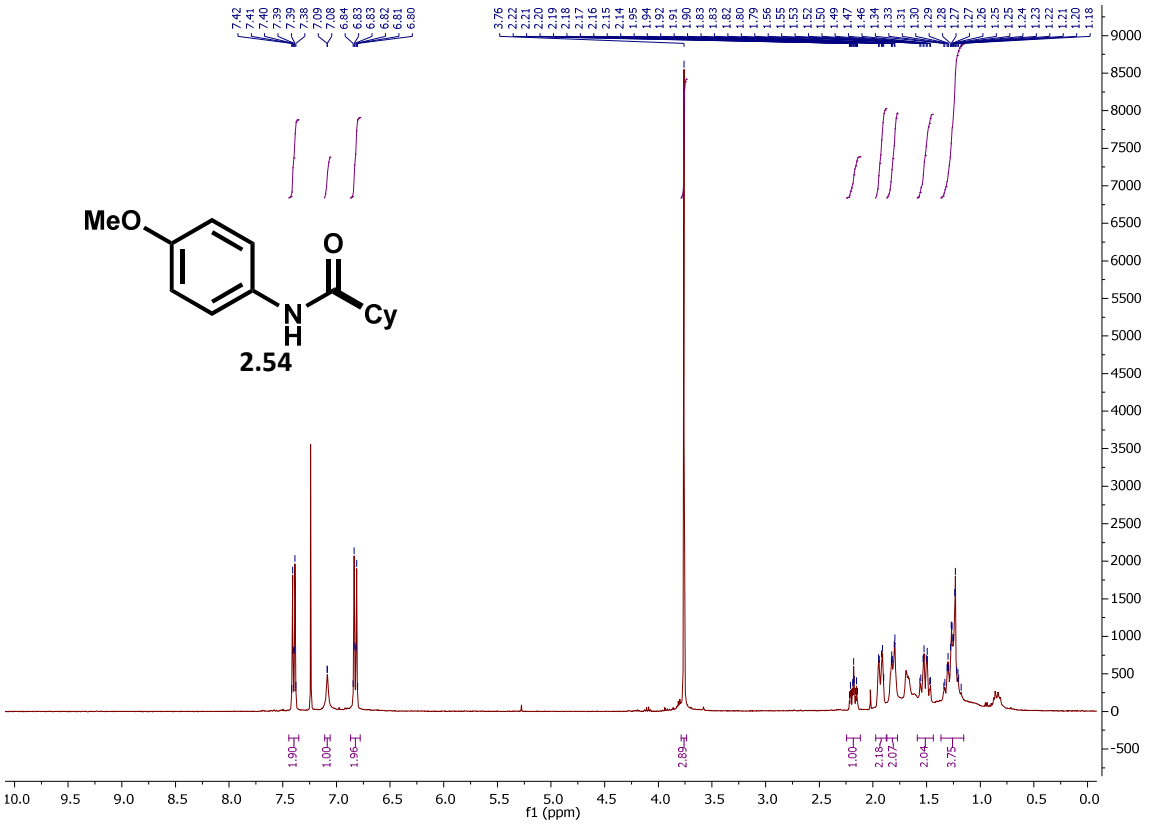
MeO
O
N
H
Cy
2.54
f1 (ppm)

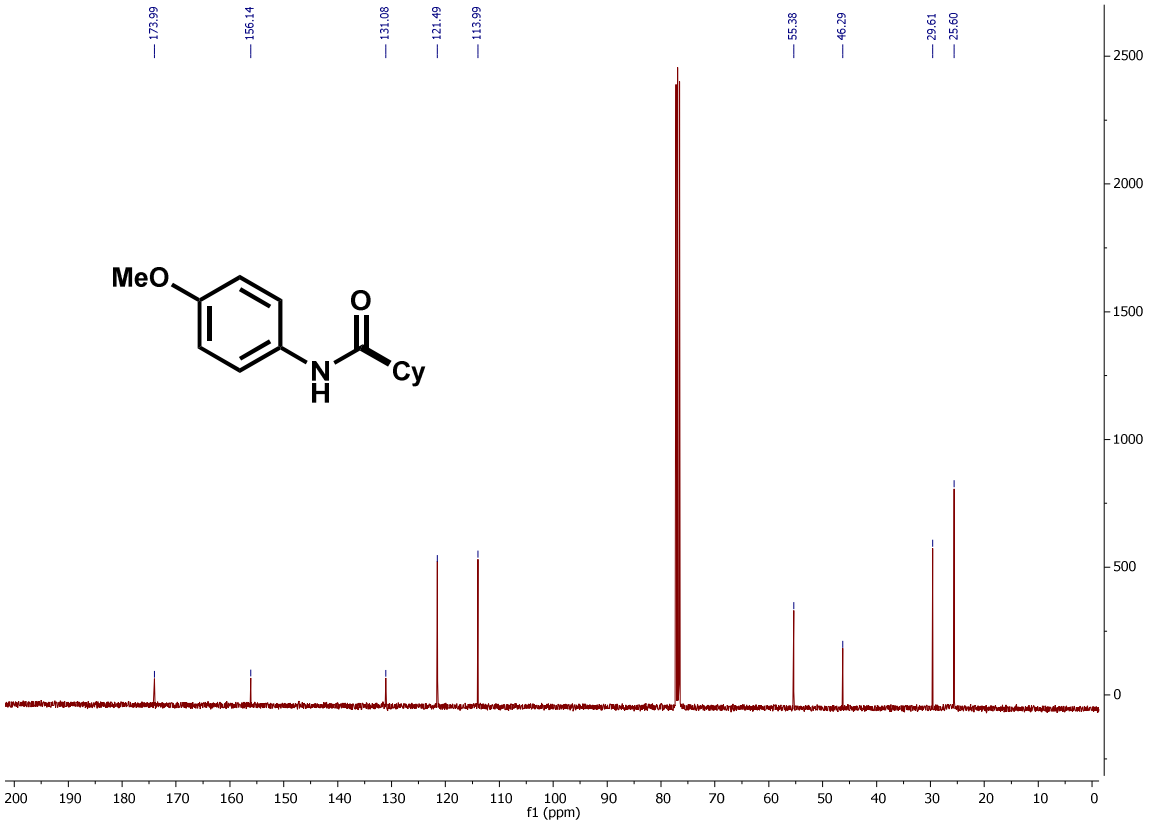
MeO
O
N
H
Cy
f1 (ppm)

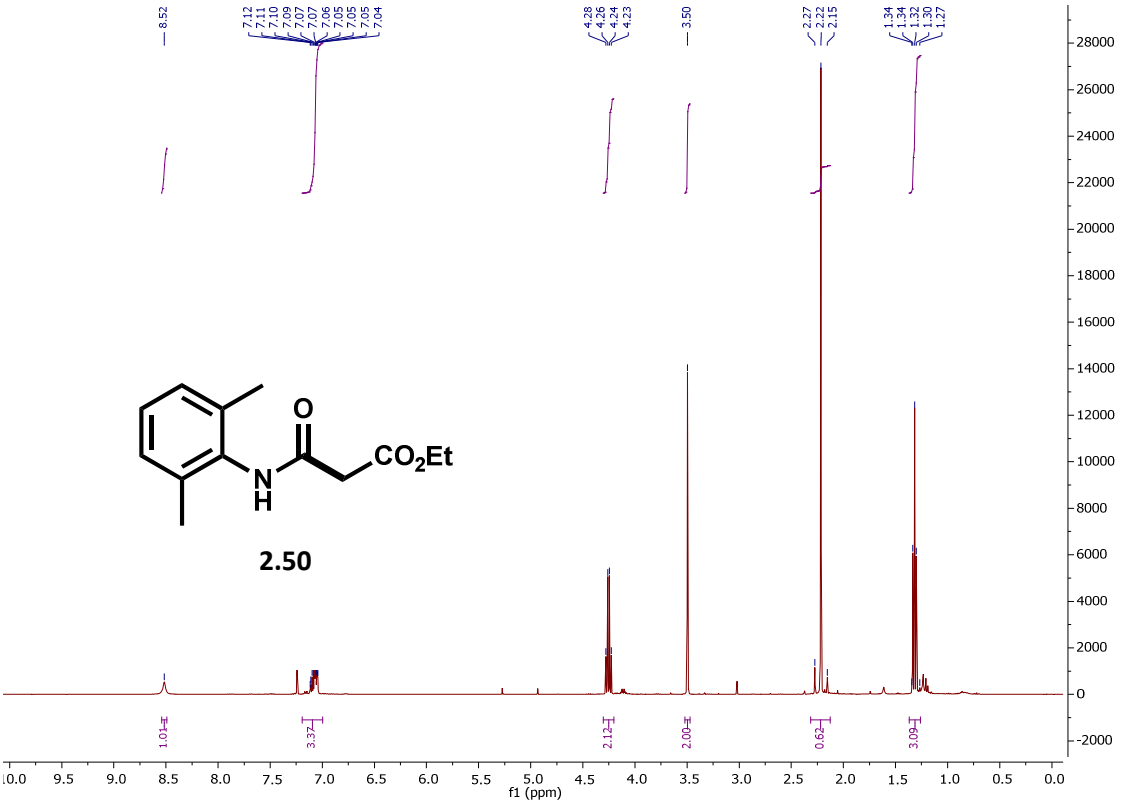
8.52
7.12
7.11
7.10
7.09
7.07
7.07
7.06
7.05
7.05
7.05
7.04
4.28
4.26
4.24
4.23
3.50
2.27
2.22
2.15
1.34
1.34
1.32
1.30
1.27
O
CO2Et
N
H
2.50
1.01
3.37
2.12
2.00
0.62
3.09
f1 (ppm)

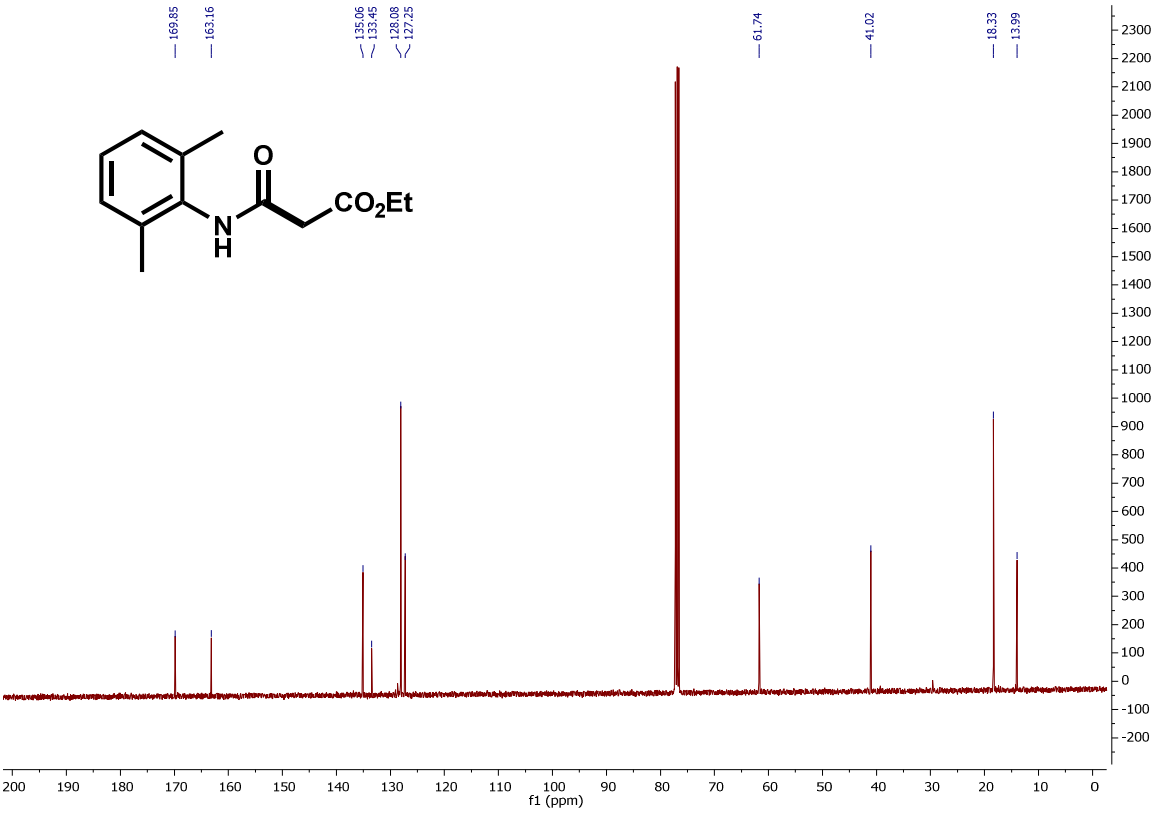
169.85
163.16
135.06
133.45
128.08
127.25
61.74
41.02
18.33
13.99
O
CO2Et
N
H
f1 (ppm)

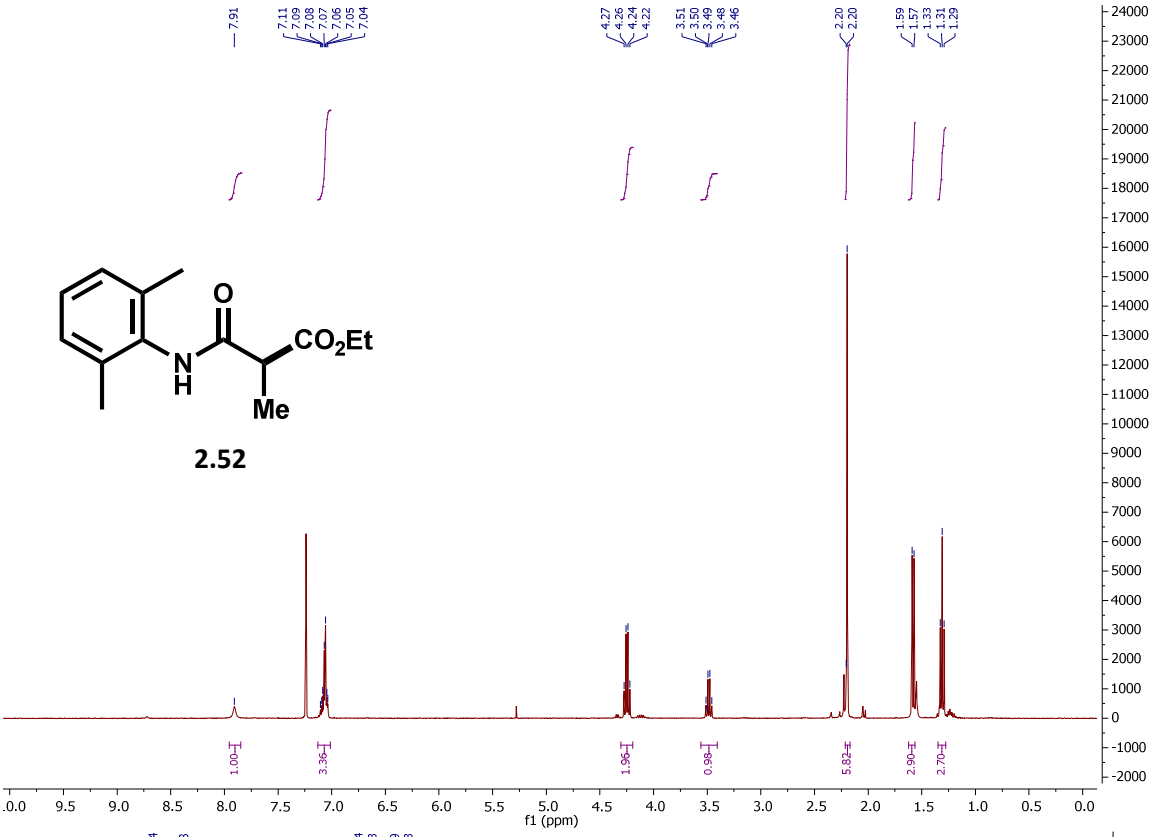
7.91
7.11
7.09
7.08
7.07
7.06
7.05
7.04
4.27
4.26
4.24
4.22
3.51
3.50
3.49
3.48
3.46
2.20
2.20
1.59
1.57
1.33
1.31
1.29
1.00
3.36
1.96
0.98
5.82
2.90
2.70
f1 (ppm)

O
N
H
CO2Et
Me

2.52

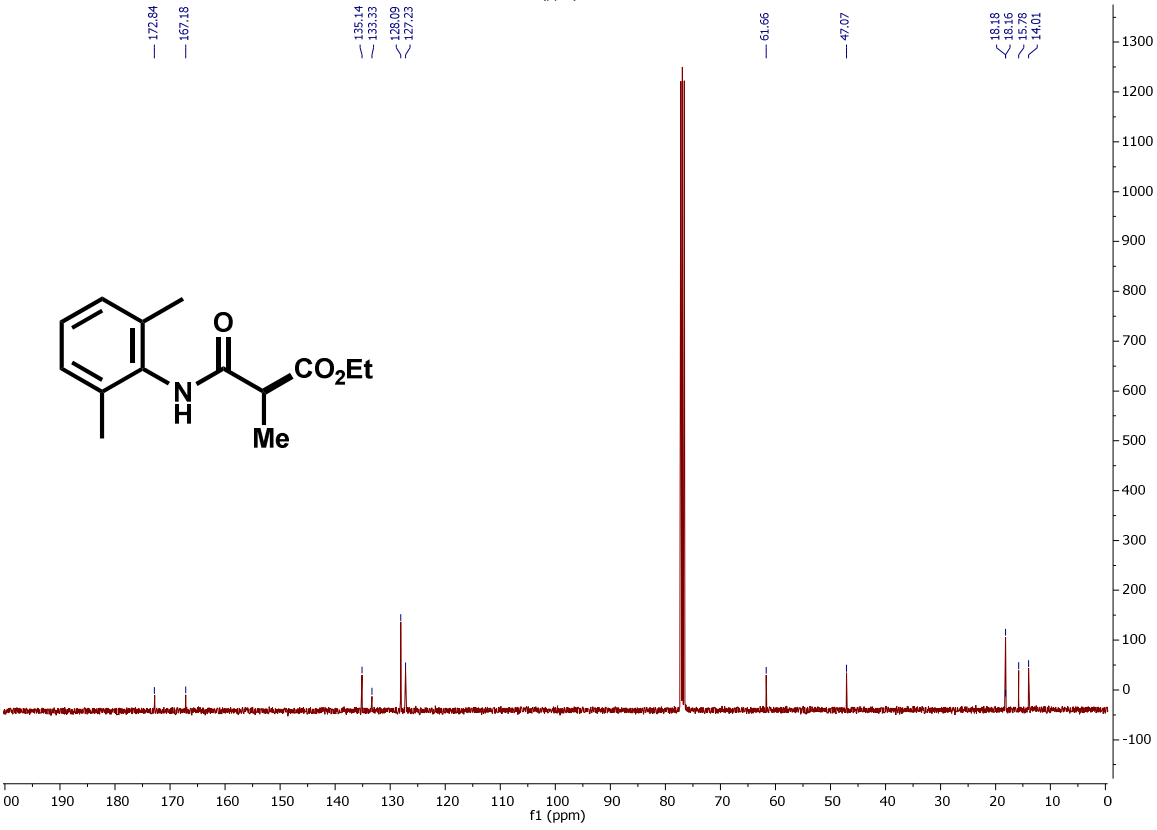
172.84
167.18
135.14
133.33
128.09
127.23
61.66
47.07
18.18
18.16
15.78
14.01
f1 (ppm)

O
N
H
CO2Et
Me

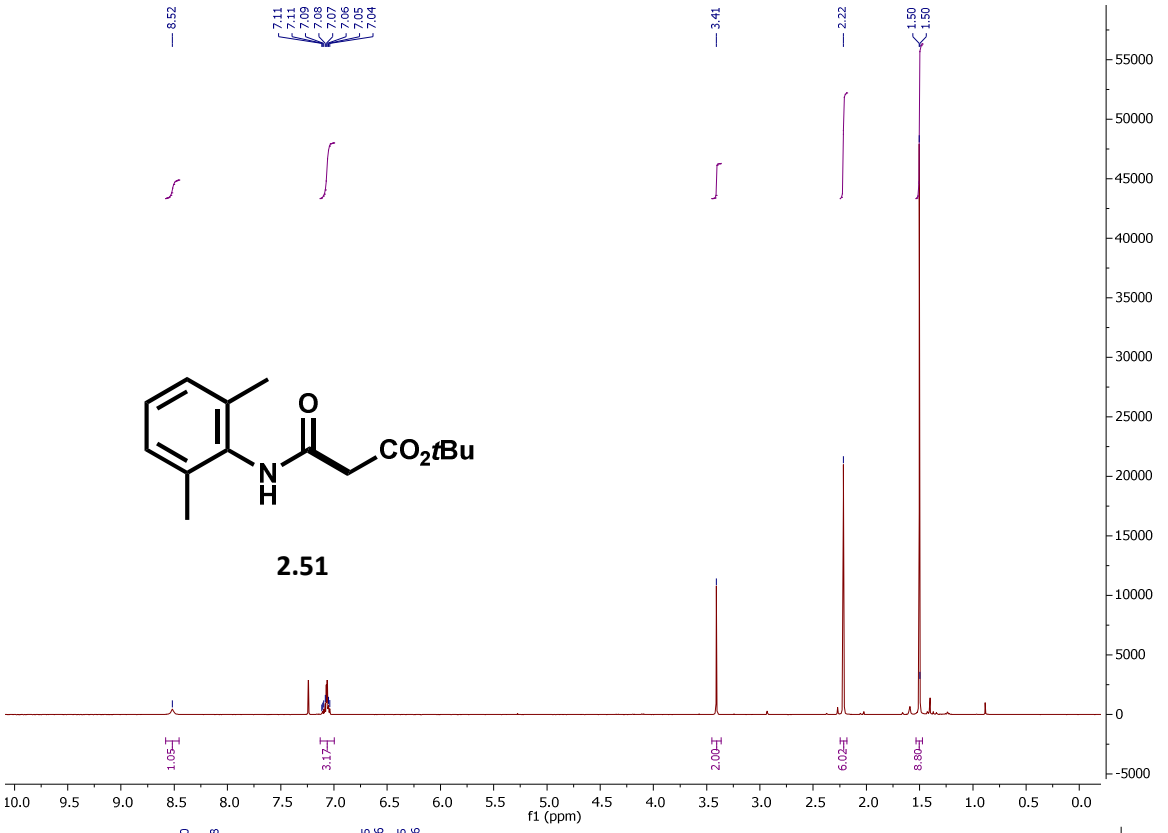
8.52
7.11
7.11
7.09
7.08
7.07
7.06
7.05
7.04
3.41
2.22
1.50
1.50
O
N
H
CO2tBu
1.05
3.17
2.00
6.02
8.80
f1 (ppm)

2.51

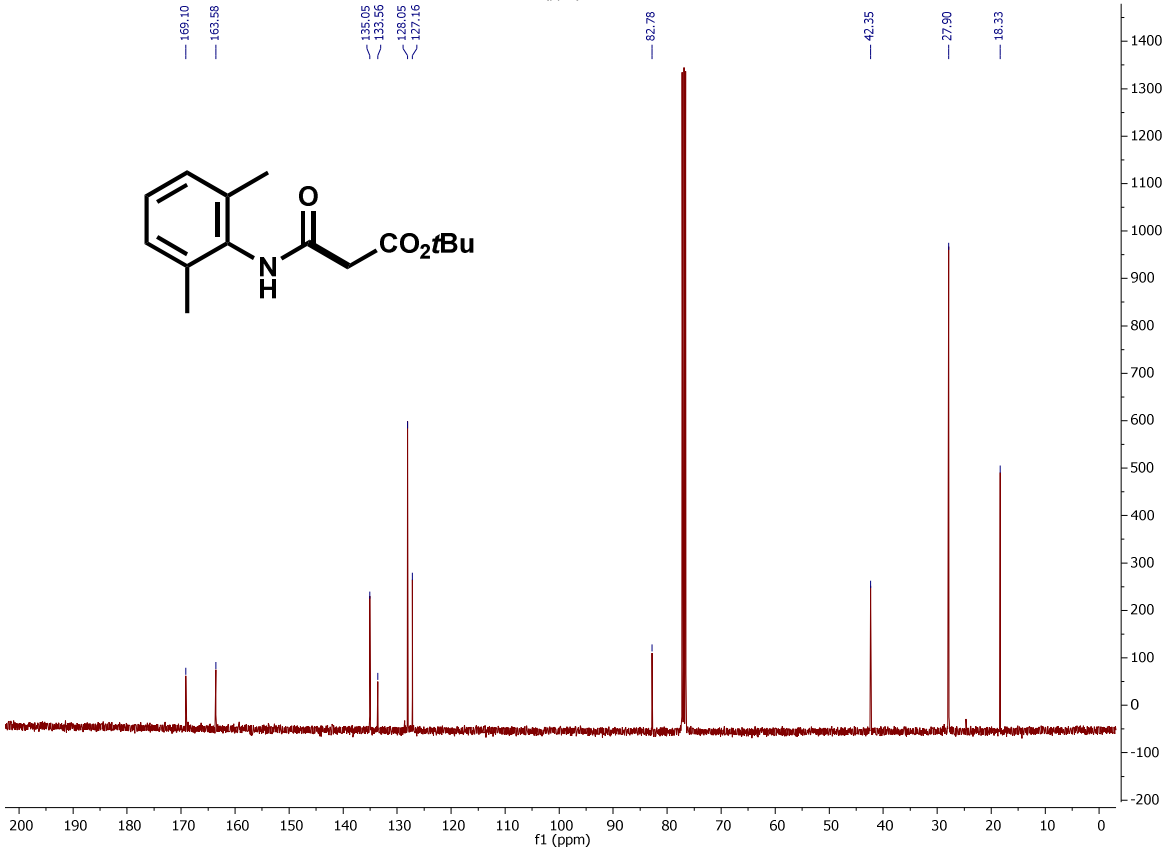
169.10
163.58
135.05
133.56
128.05
127.16
82.78
42.35
27.90
18.33
O
N
H
CO2tBu
f1 (ppm)

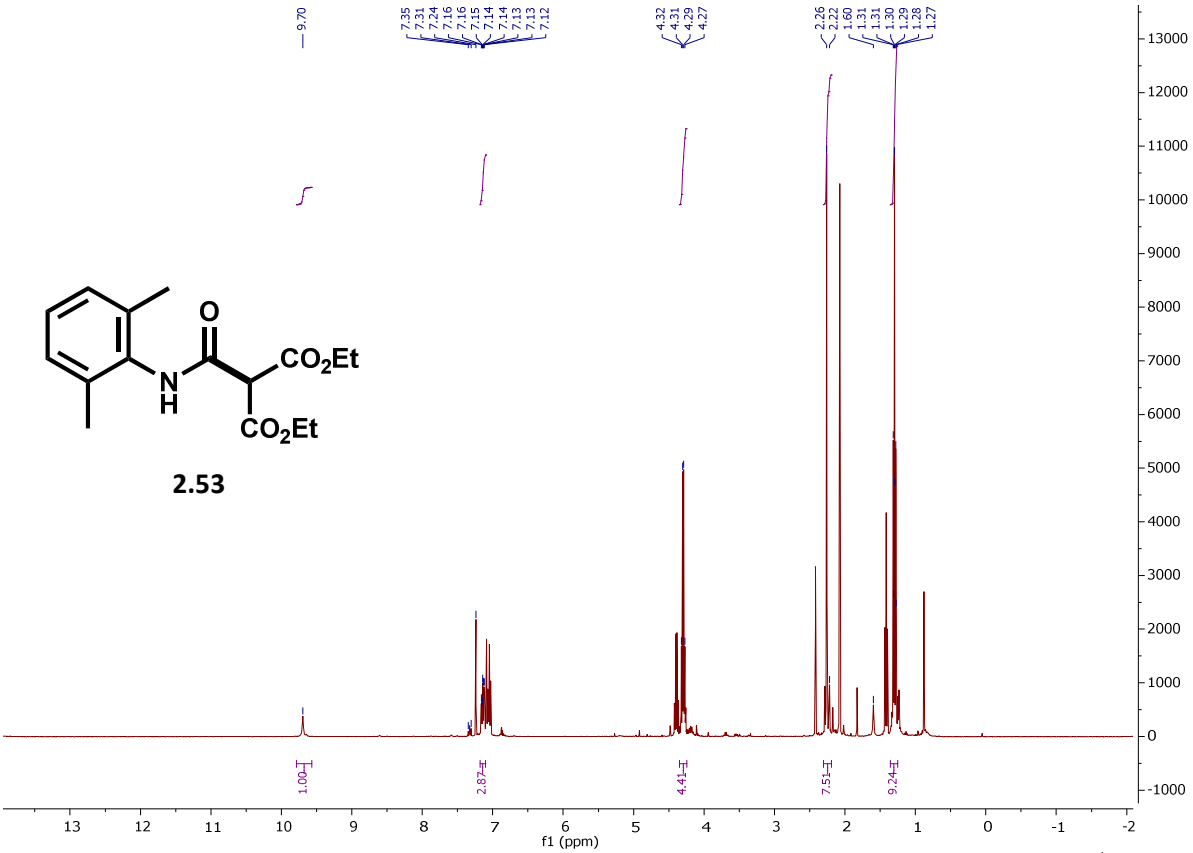
9.70
7.35
7.31
7.24
7.16
7.16
7.15
7.14
7.14
7.13
7.13
7.12
4.32
4.31
4.29
4.27
2.26
2.22
1.60
1.31
1.31
1.30
1.29
1.28
1.27
1.00
2.87
4.41
7.51
9.24
f1 (ppm)

O
N
H
CO2Et
CO2Et

2.53

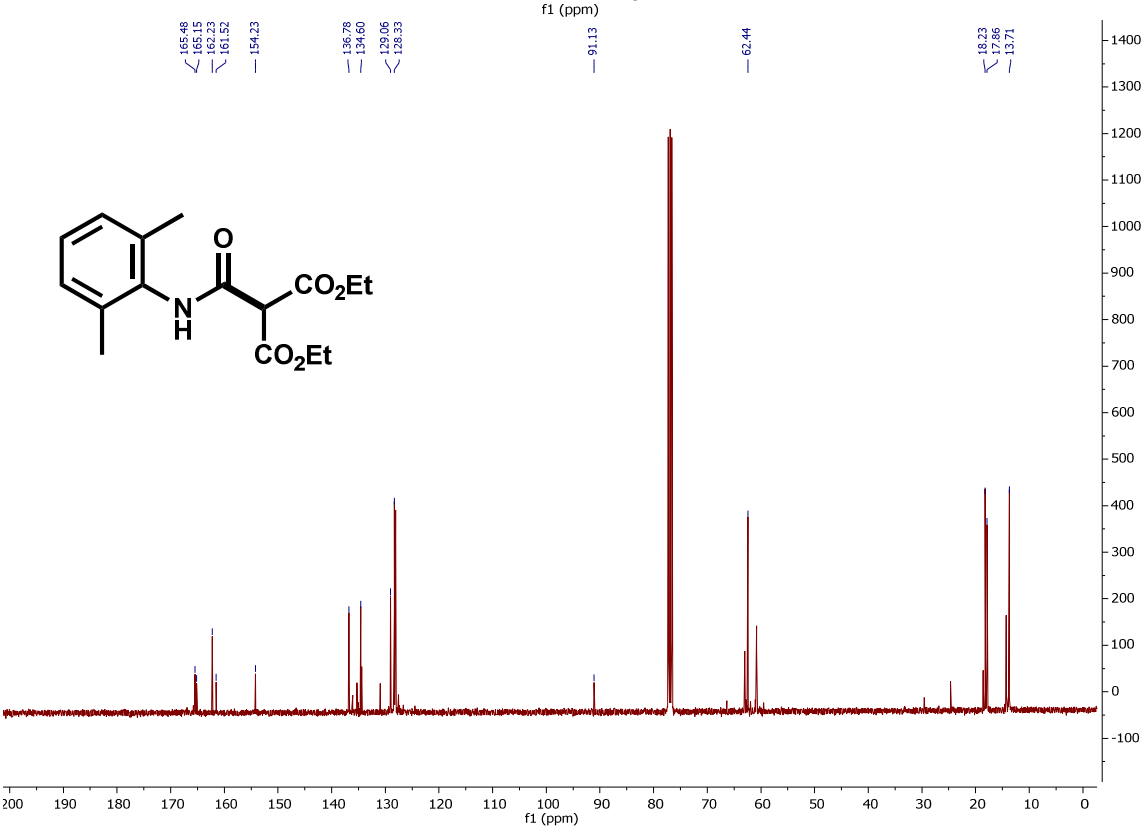
165.48
165.15
162.23
161.52
154.23
136.78
134.60
129.06
128.33
91.13
62.44
18.23
17.86
13.71
f1 (ppm)

O
N
H
CO2Et
CO2Et

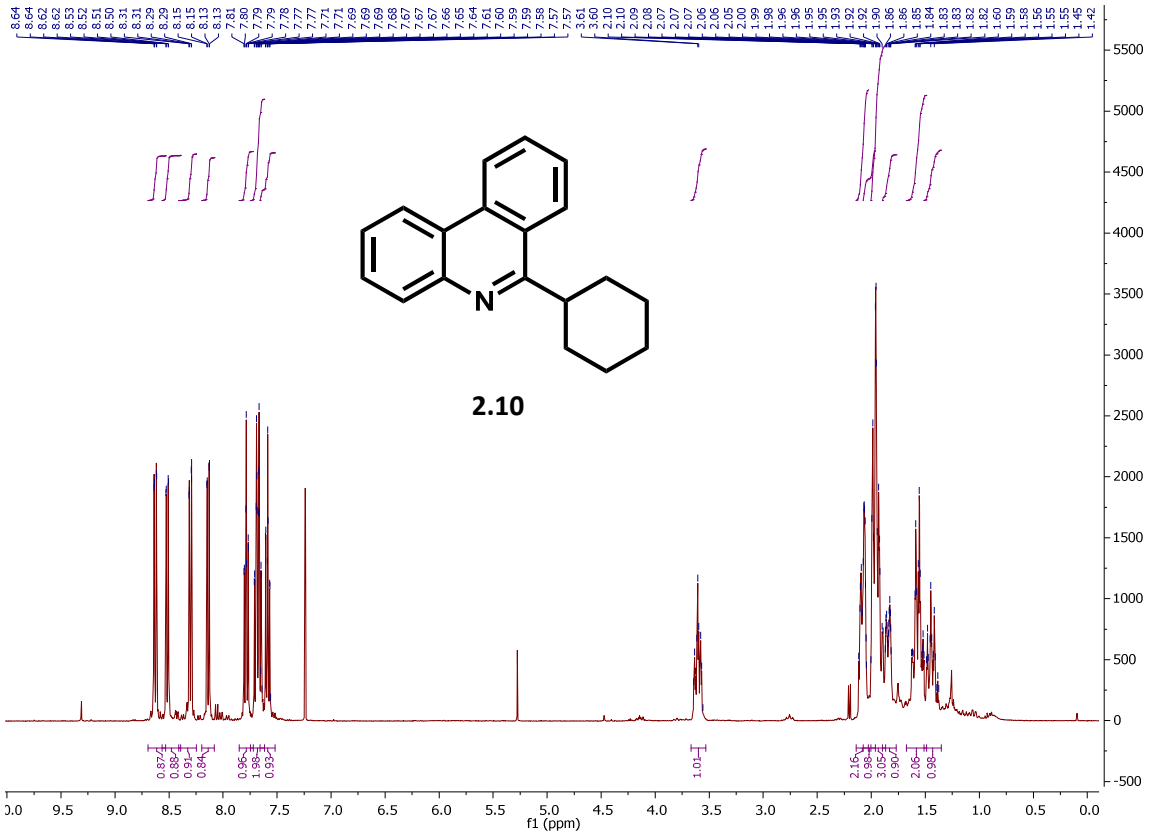
N
2.10
f1 (ppm)

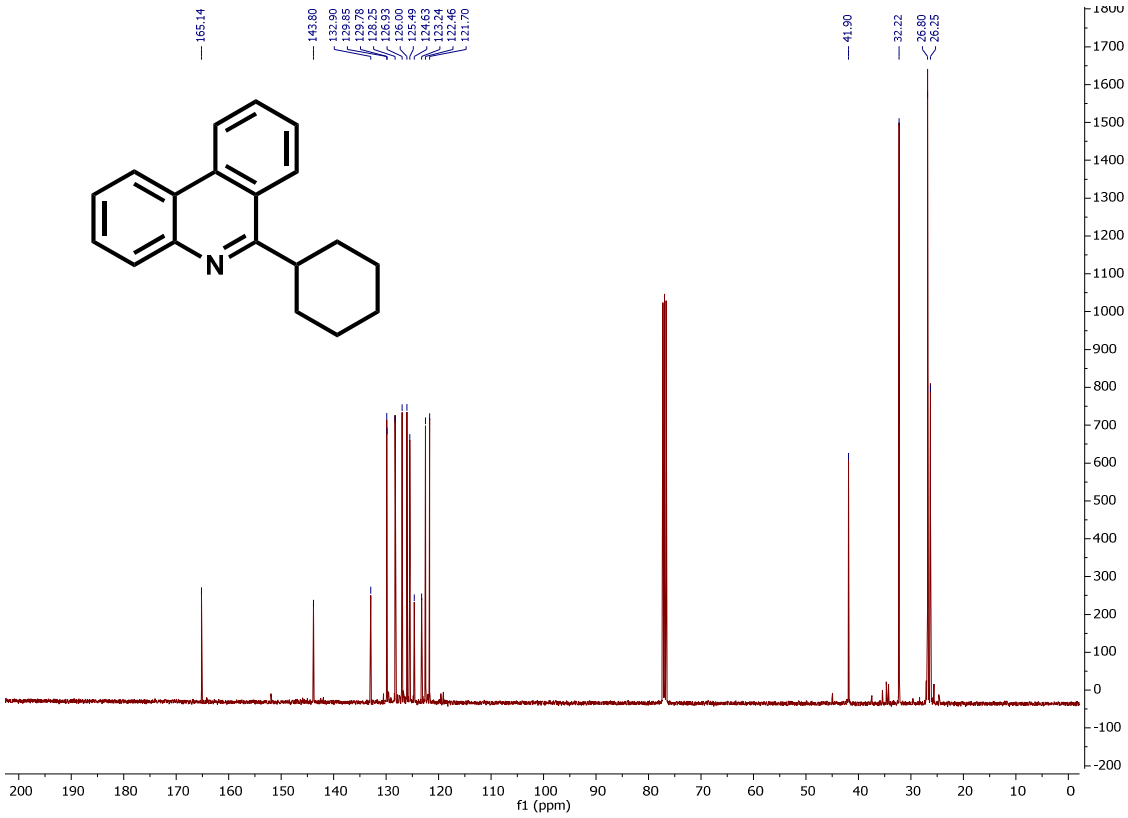
N
f1 (ppm)

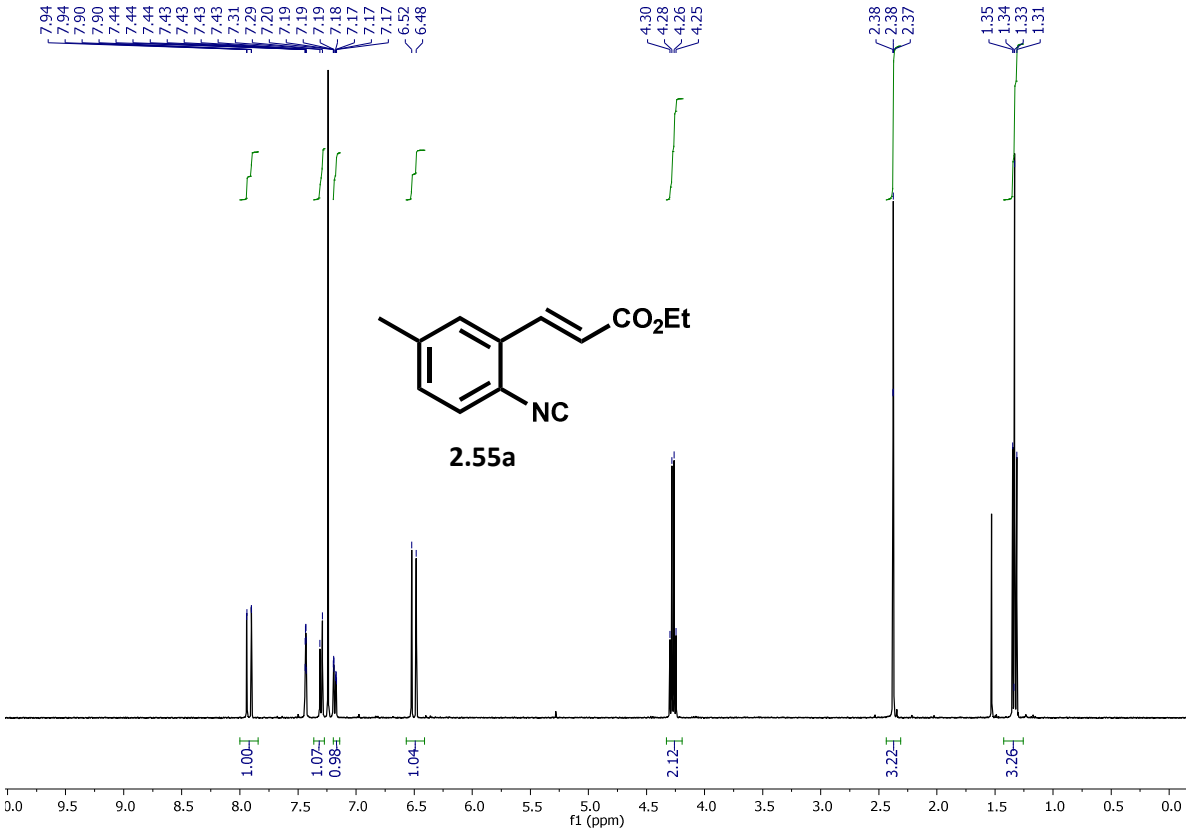
7.94
7.94
7.90
7.90
7.44
7.44
7.44
7.43
7.43
7.43
7.43
7.31
7.29
7.20
7.19
7.19
7.19
7.18
7.17
7.17
7.17
6.52
6.48
4.30
4.28
4.26
4.25
2.38
2.38
2.37
1.35
1.34
1.33
1.31
CO2Et
NC
2.55a
1.00
1.07
0.98
1.04
2.12
3.22
3.26
f1 (ppm)

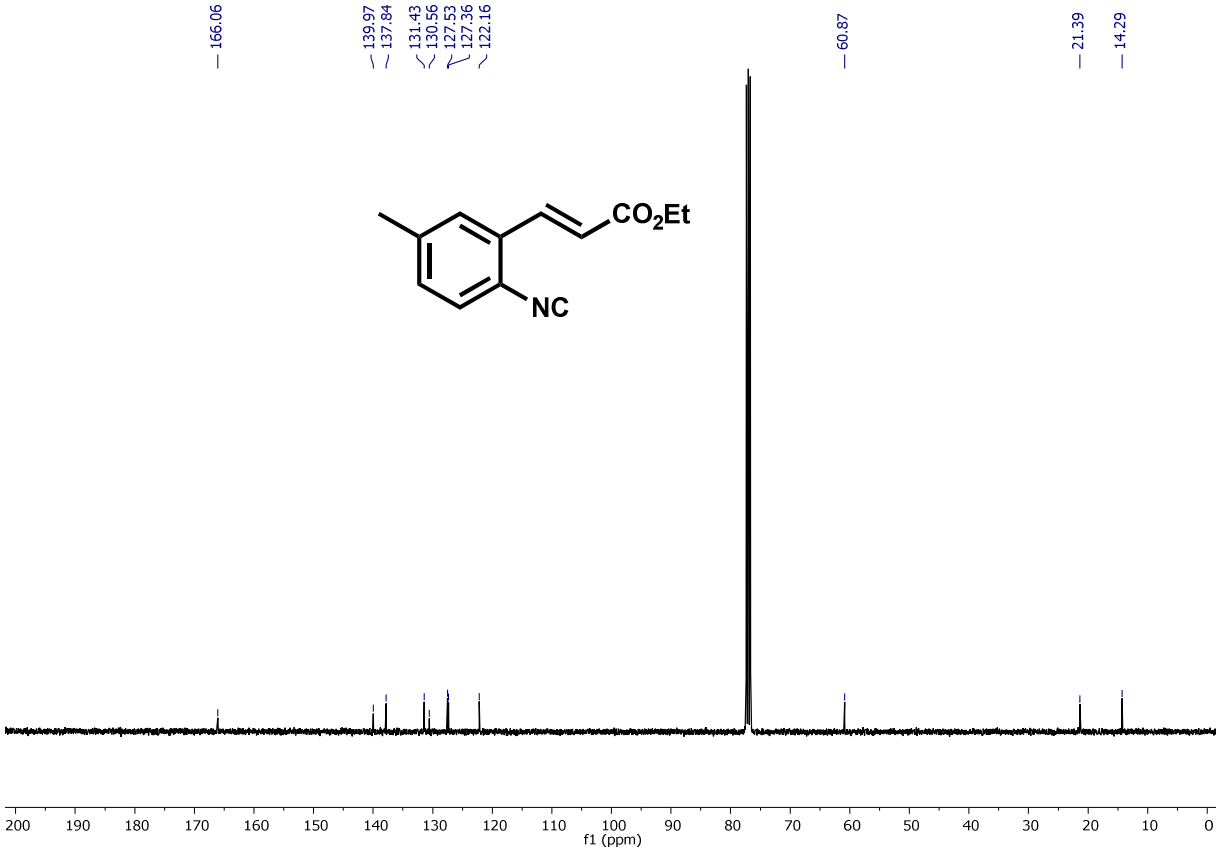
166.06
139.97
137.84
131.43
130.56
127.53
127.36
122.16
60.87
21.39
14.29
CO2Et
NC
f1 (ppm)

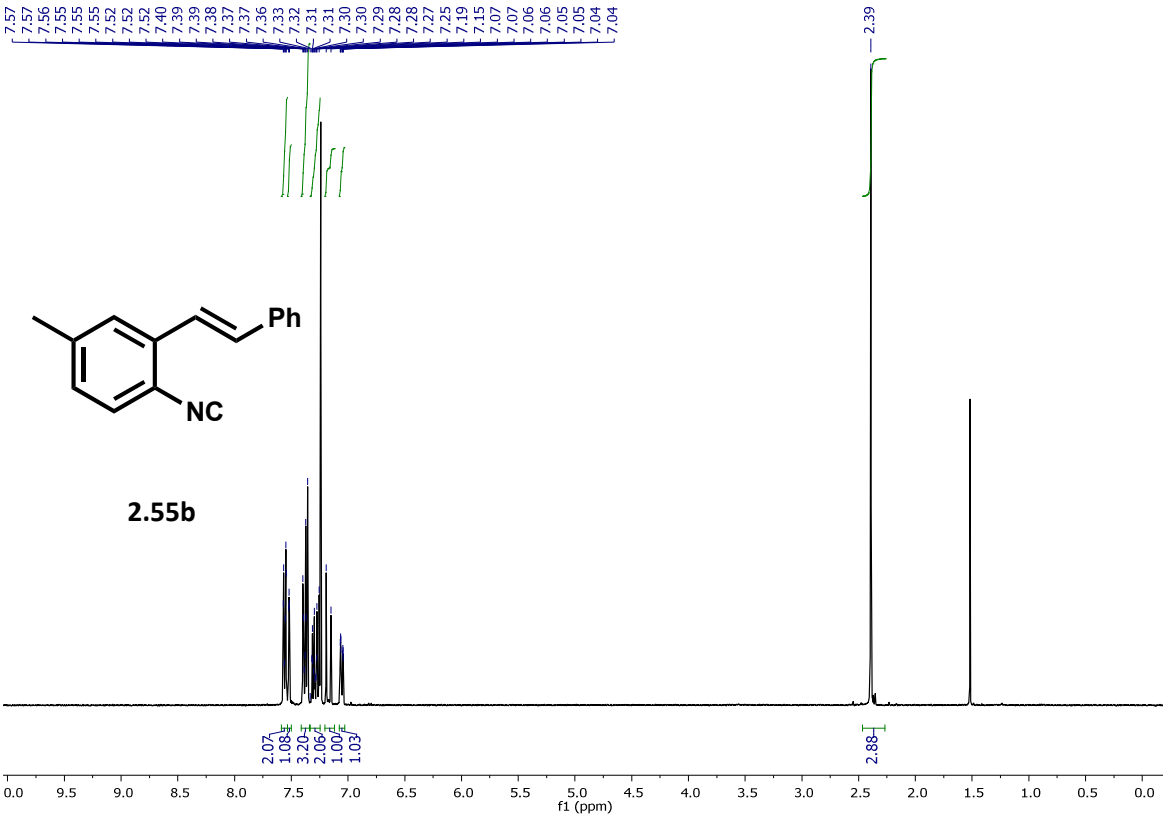
Ph
NC
2.55b
2.39
2.88
2.07
1.08
3.20
2.06
1.00
1.03
f1 (ppm)

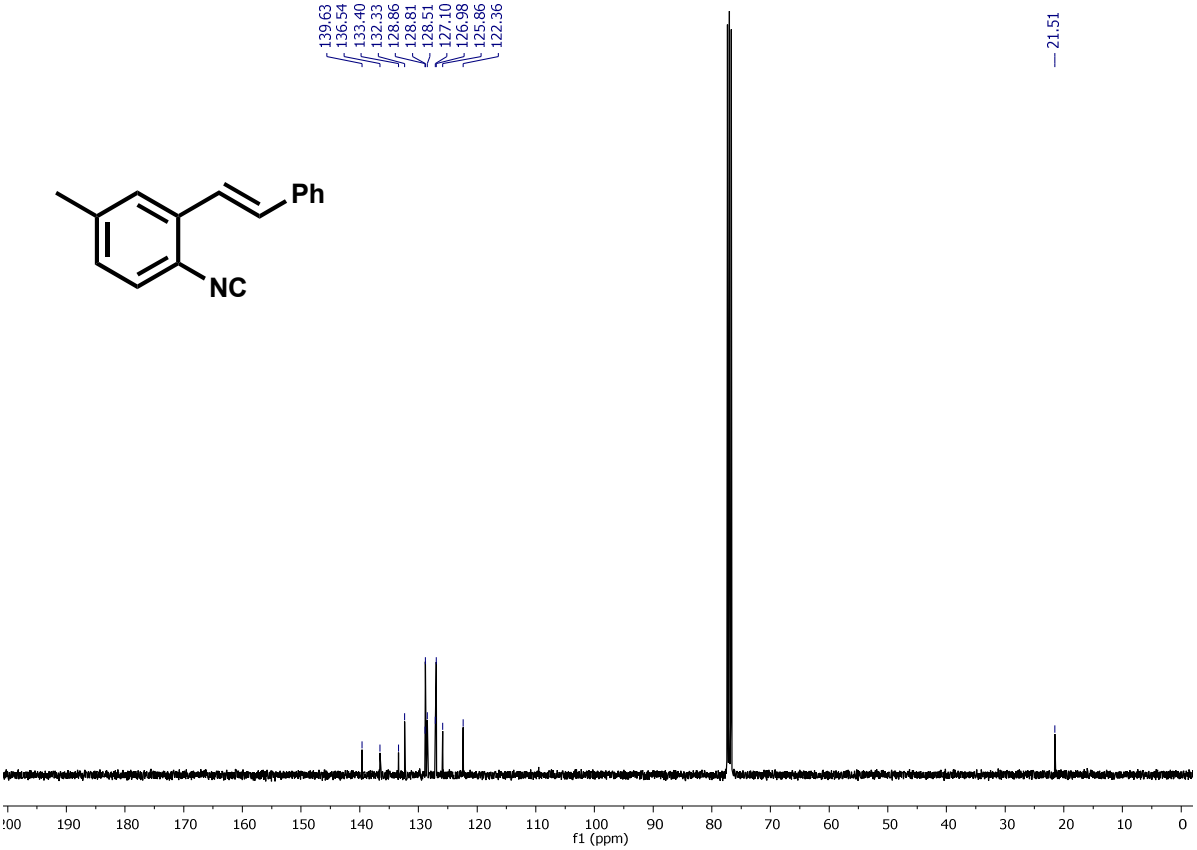
Ph
NC
139.63
136.54
133.40
132.33
128.86
128.81
128.51
127.10
126.98
125.86
122.36
21.51
f1 (ppm)

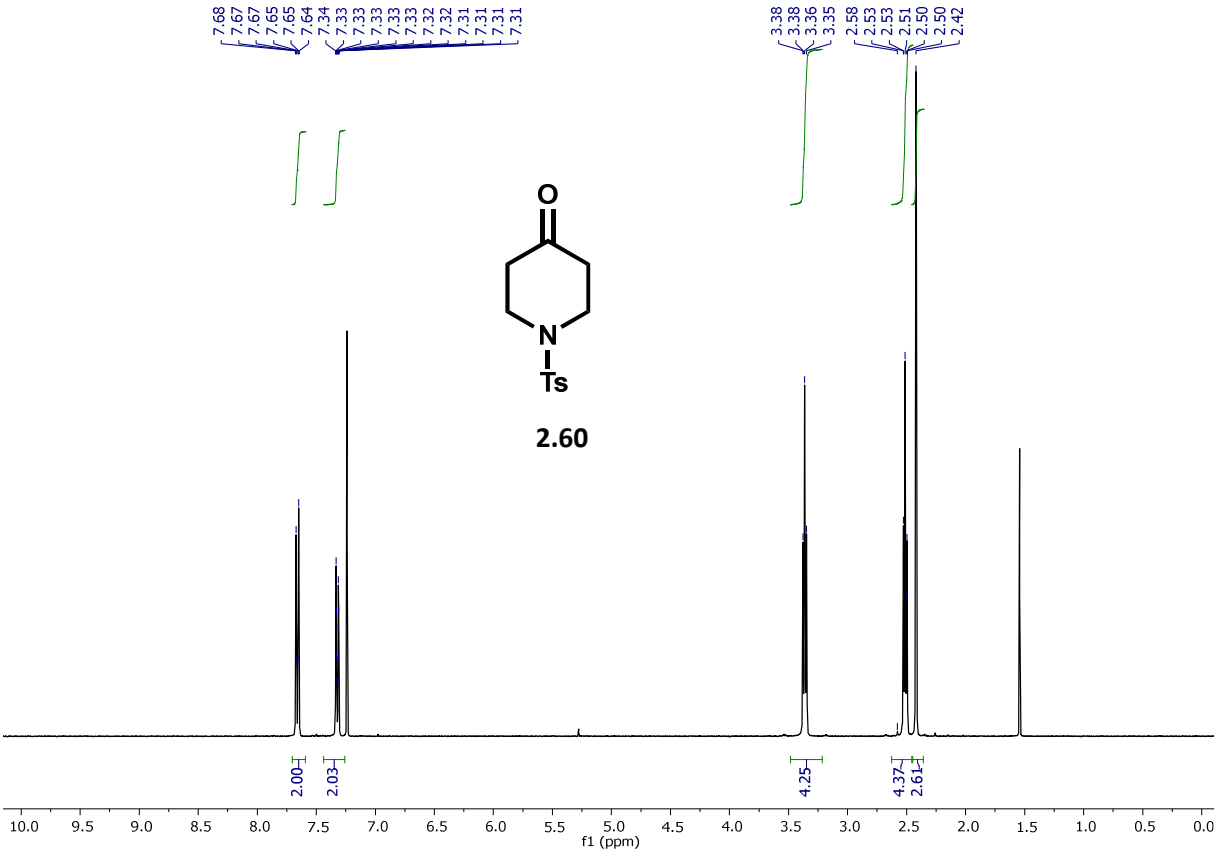
7.68
7.67
7.67
7.65
7.65
7.64
7.34
7.33
7.33
7.33
7.33
7.33
7.32
7.32
7.31
7.31
7.31
7.31
3.38
3.38
3.36
3.35
2.58
2.53
2.53
2.51
2.50
2.50
2.42
O
N
Ts
2.60
2.00
2.03
4.25
4.37
2.61
10.0
9.5
9.0
8.5
8.0
7.5
7.0
6.5
6.0
5.5
5.0
4.5
4.0
3.5
3.0
2.5
2.0
1.5
1.0
0.5
0.0
f1 (ppm)

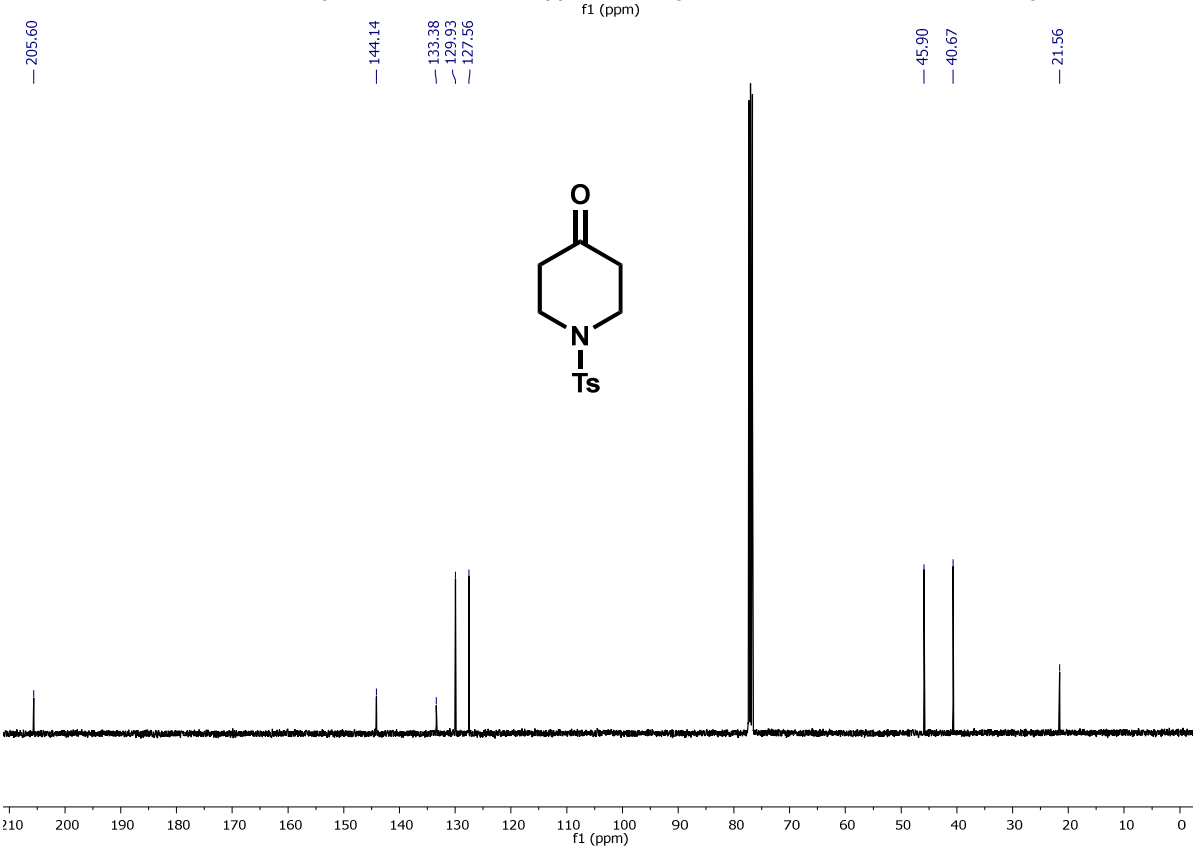
205.60
144.14
133.38
129.93
127.56
45.90
40.67
21.56
O
N
Ts
210
200
190
180
170
160
150
140
130
120
110
100
90
80
70
60
50
40
30
20
10
0
f1 (ppm)

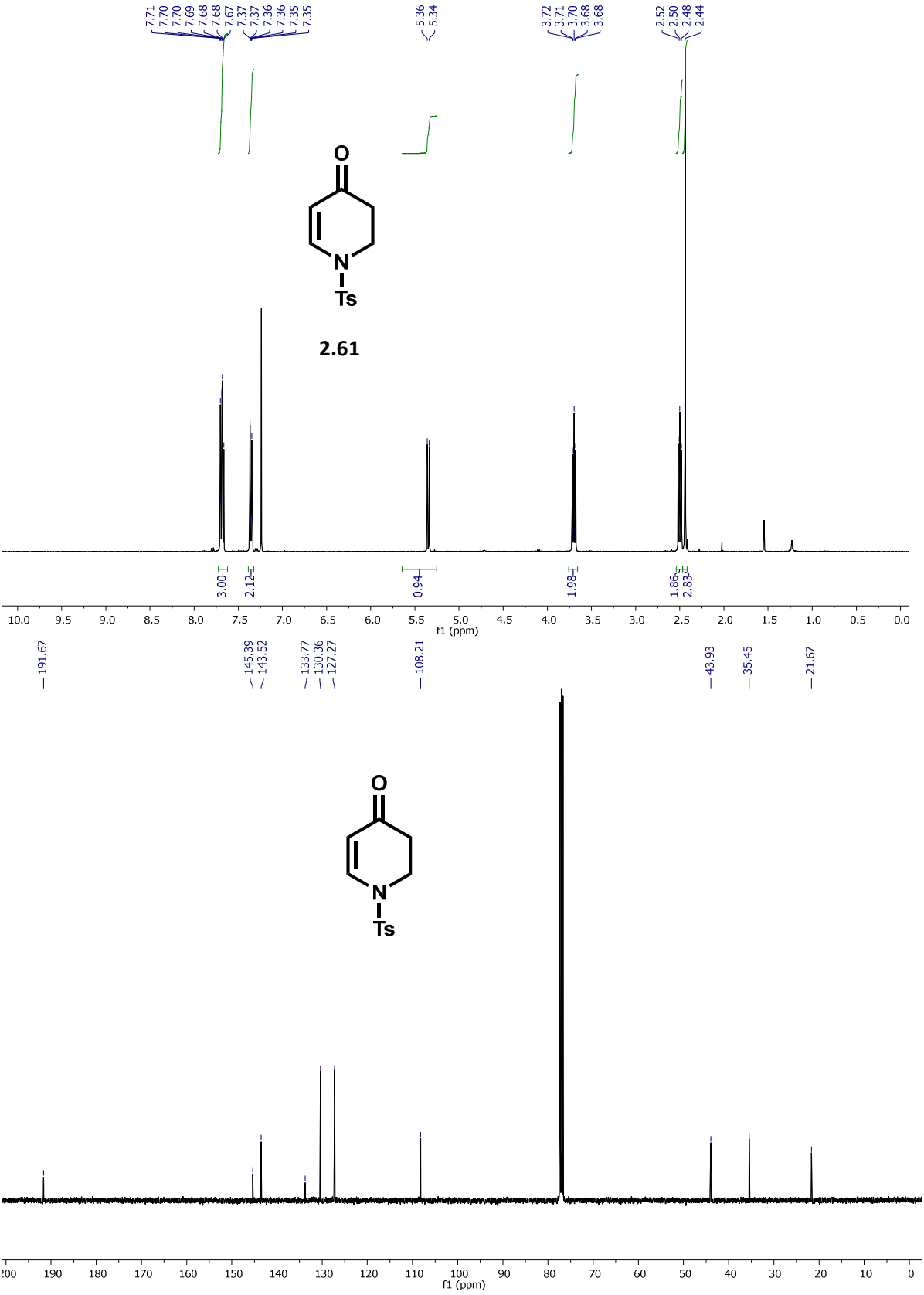
7.71
7.70
7.70
7.69
7.68
7.68
7.67
7.37
7.37
7.36
7.36
7.35
7.35
5.36
5.34
3.72
3.71
3.70
3.68
3.68
2.52
2.50
2.48
2.44
O
N
Ts
2.61
3.00
2.12
0.94
1.98
1.86
2.83
f1 (ppm)
191.67
145.39
143.52
133.77
130.36
127.27
108.21
43.93
35.45
21.67
O
N
Ts
f1 (ppm)

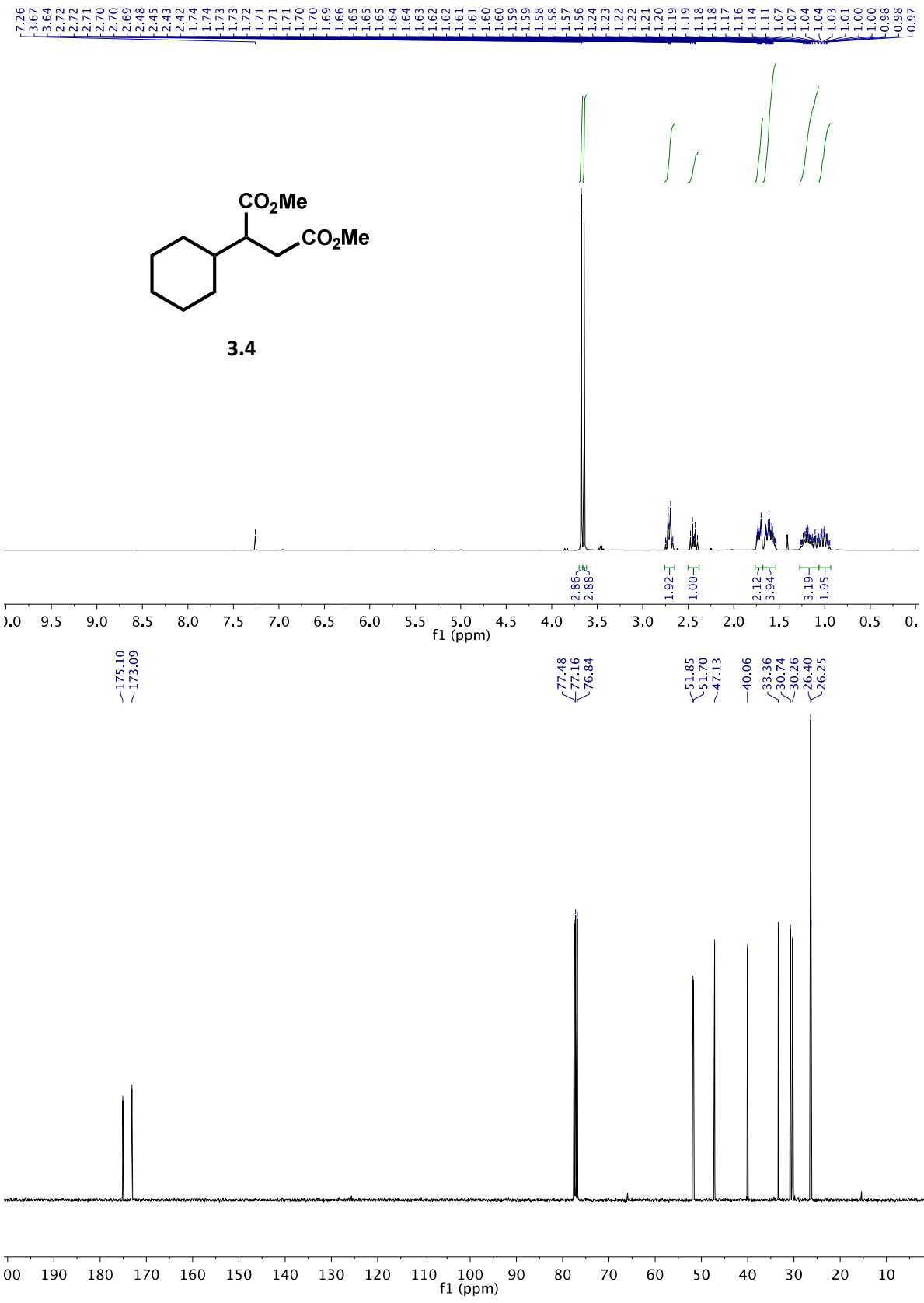
CO2Me
CO2Me
3.4
f1 (ppm)
f1 (ppm)

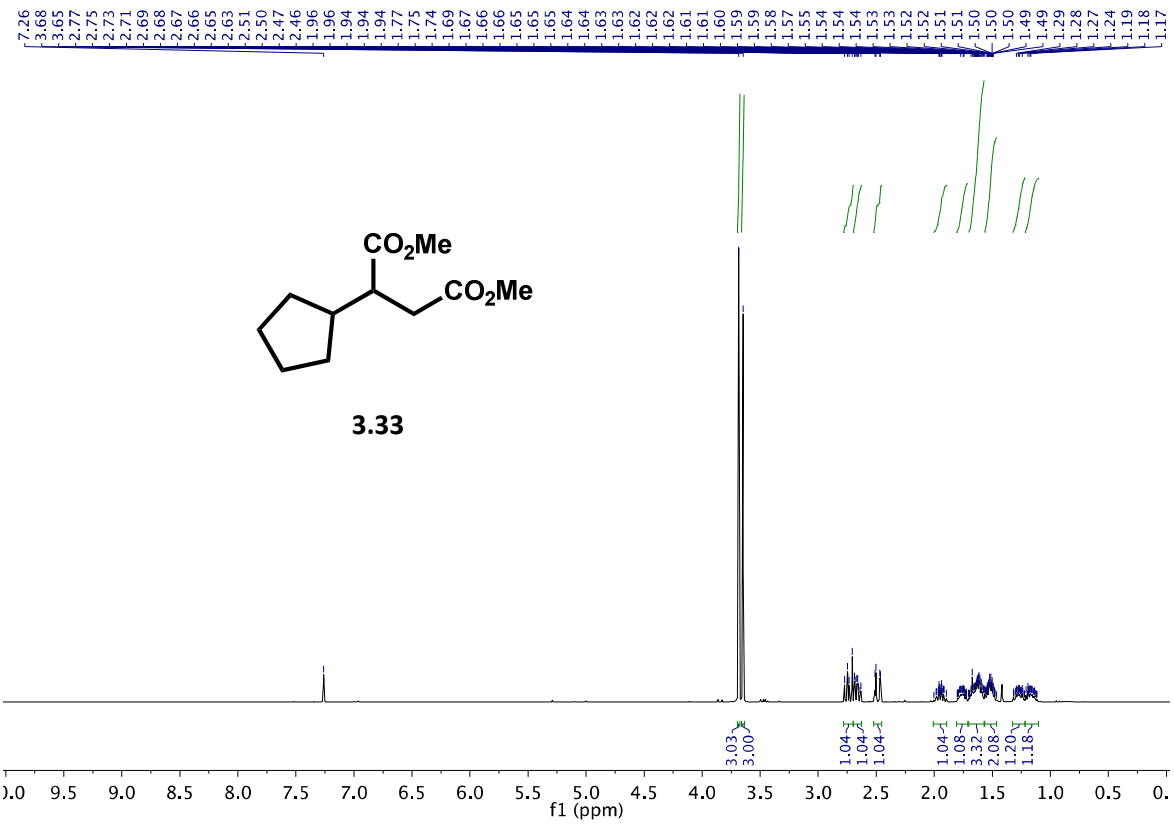

3.33

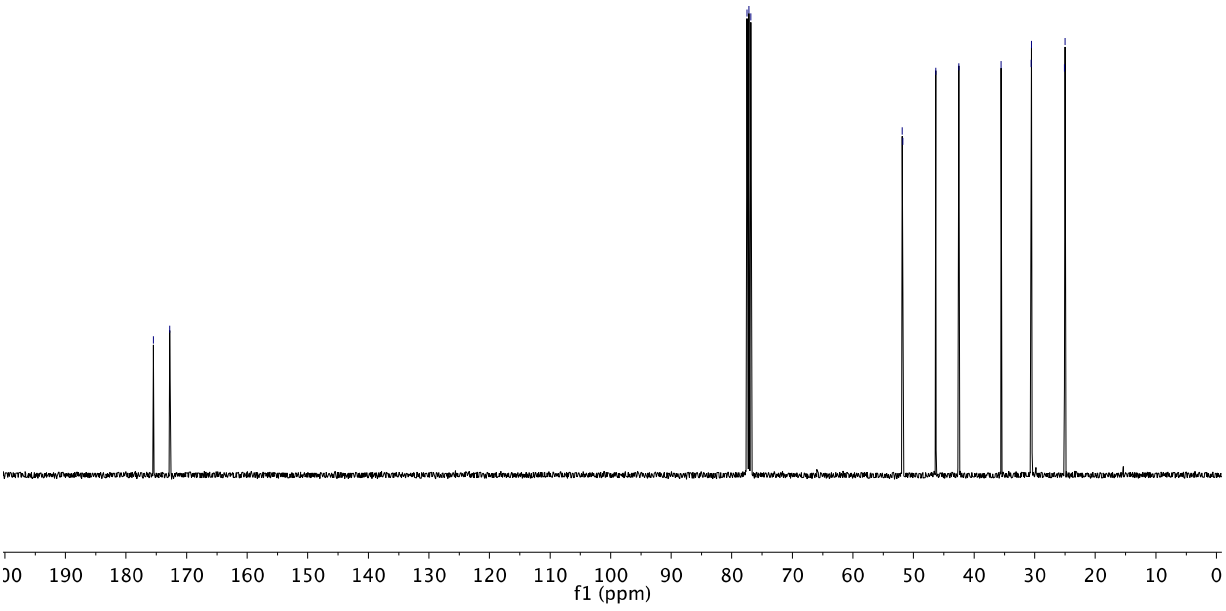

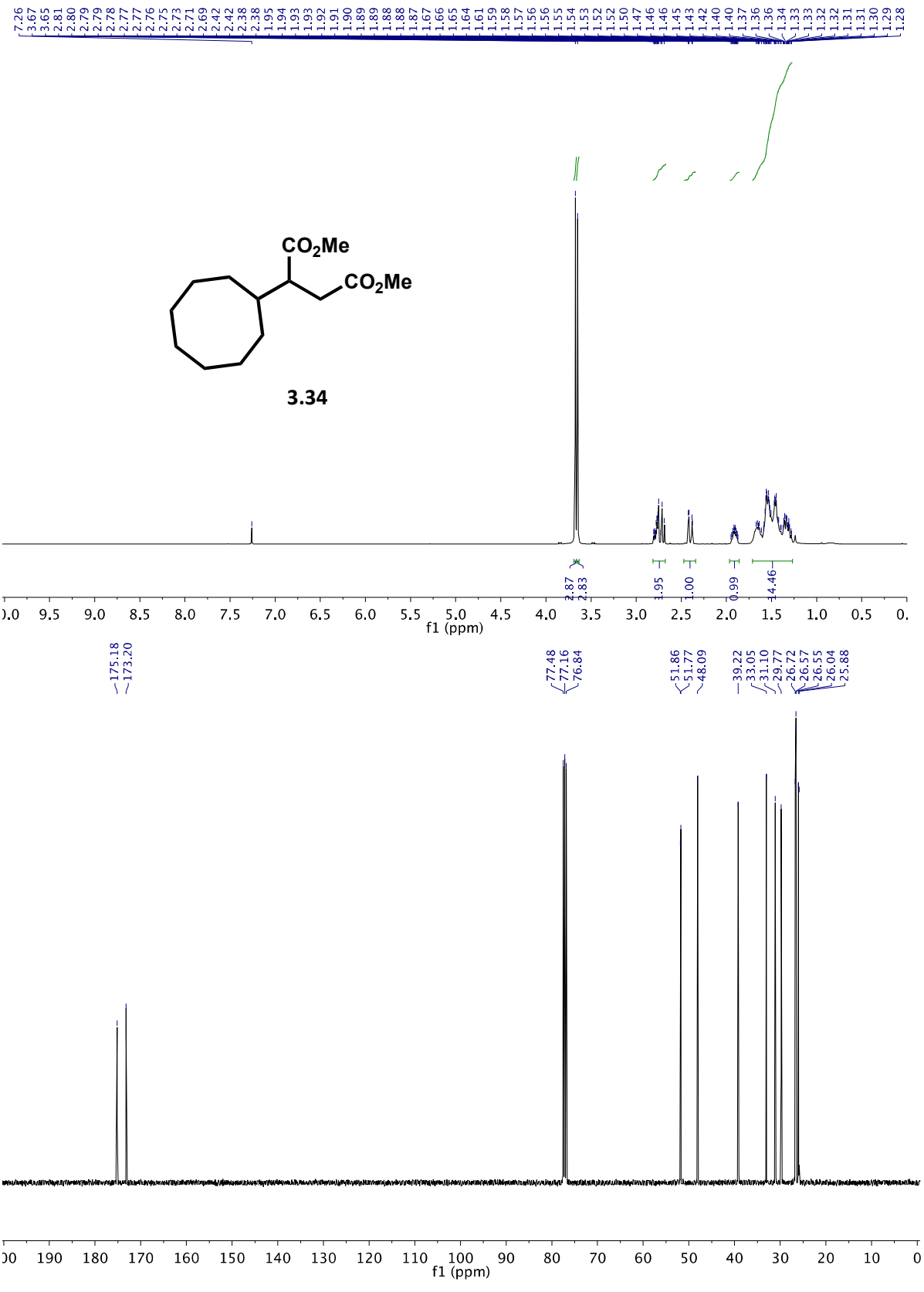
CO2Me
CO2Me
3.34
f1 (ppm)
f1 (ppm)

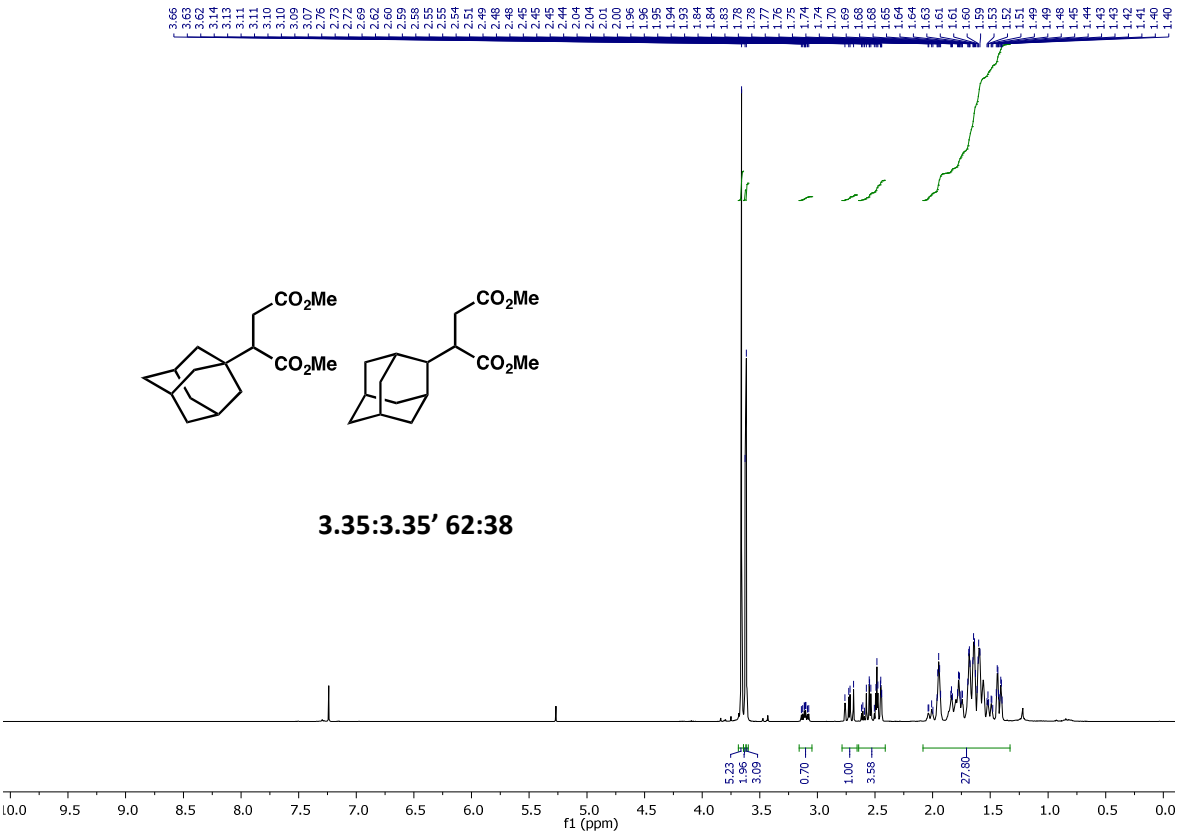
CO2Me
CO2Me
CO2Me
CO2Me
3.35:3.35’ 62:38
f1 (ppm)

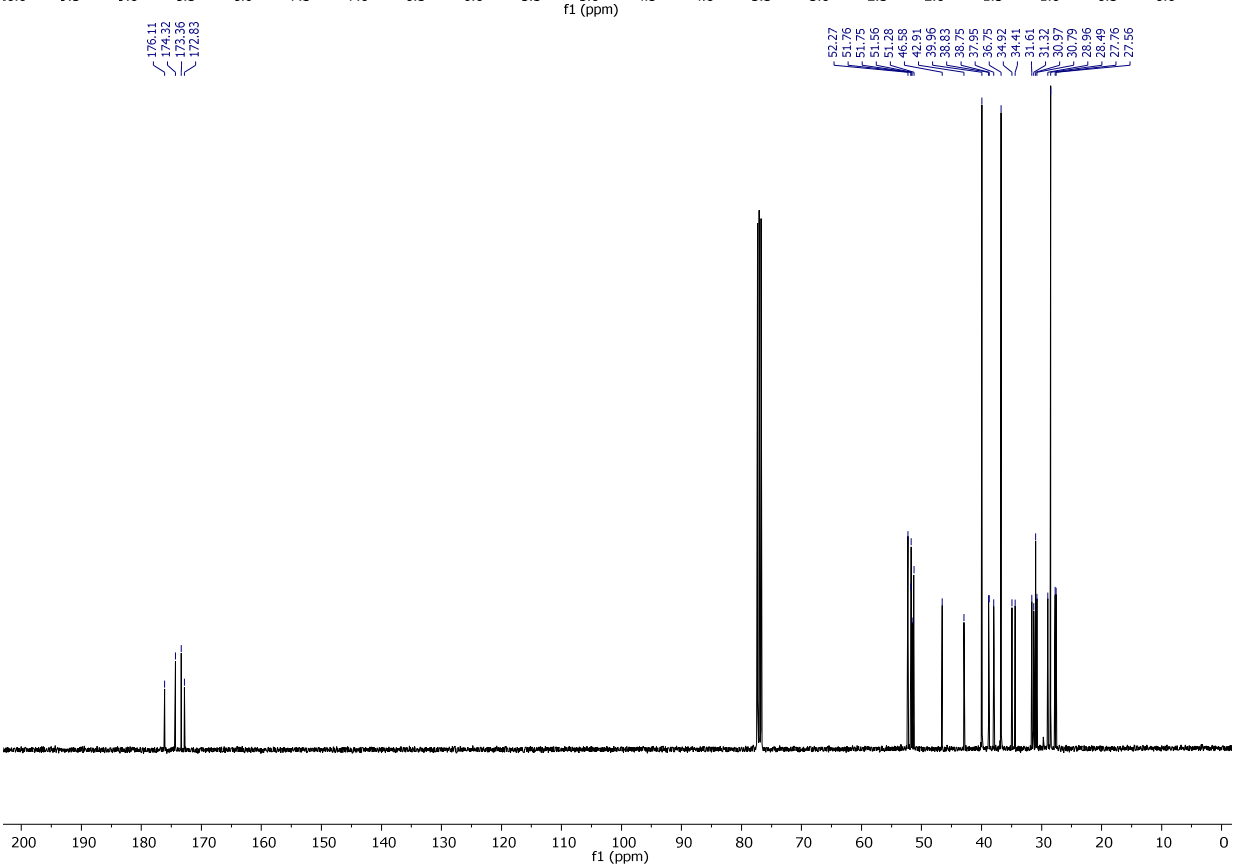
f1 (ppm)

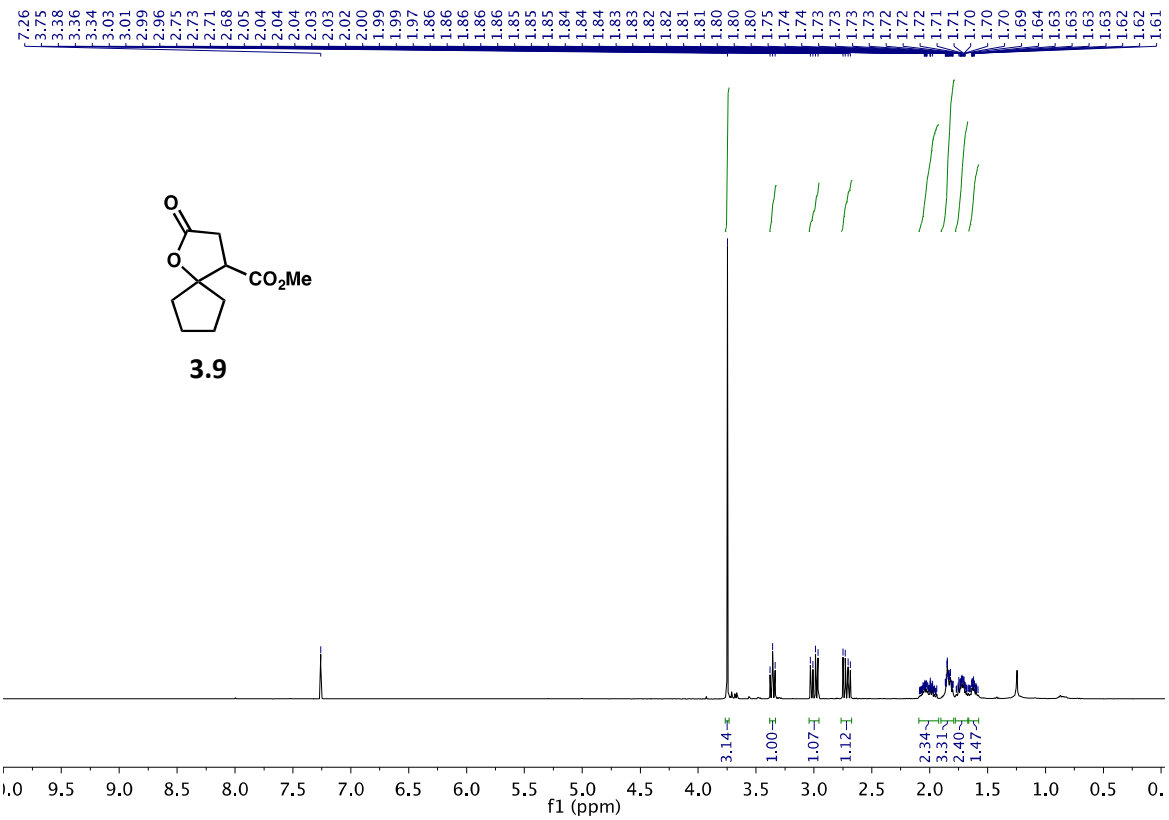
7.26
3.75
3.38
3.36
3.34
3.03
3.01
2.99
2.96
2.75
2.73
2.71
2.68
2.05
2.04
2.04
2.04
2.03
2.03
2.02
2.00
1.99
1.99
1.97
1.86
1.86
1.86
1.86
1.86
1.85
1.85
1.85
1.84
1.84
1.84
1.83
1.83
1.82
1.82
1.81
1.81
1.80
1.80
1.80
1.80
1.75
1.74
1.74
1.73
1.73
1.73
1.73
1.72
1.72
1.72
1.71
1.71
1.71
1.70
1.70
1.70
1.69
1.64
1.63
1.63
1.63
1.62
1.62
1.61
O
O
CO2Me
3.14
1.00
1.07
1.12
2.34
3.31
2.40
1.47
f1 (ppm)

3.9

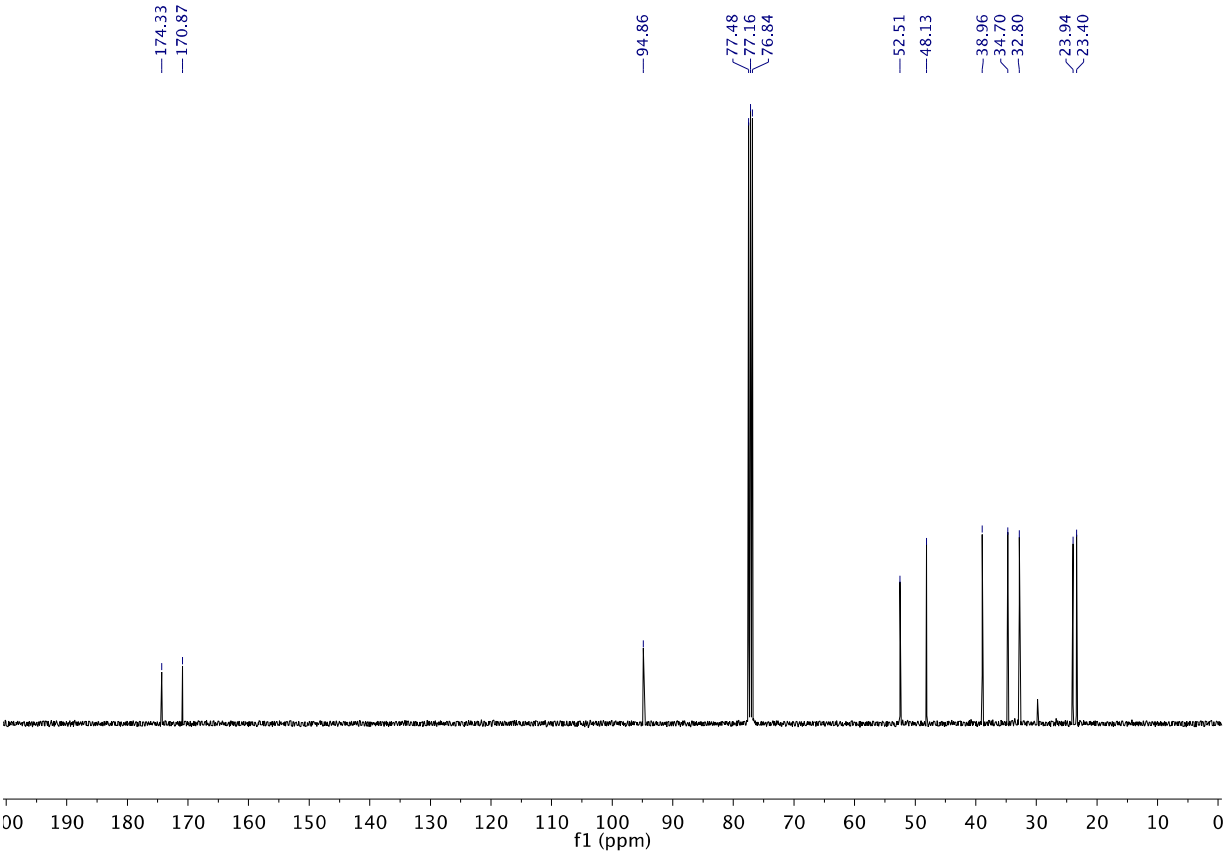
174.33
170.87
94.86
77.48
77.16
76.84
52.51
48.13
38.96
34.70
32.80
23.94
23.40
f1 (ppm)

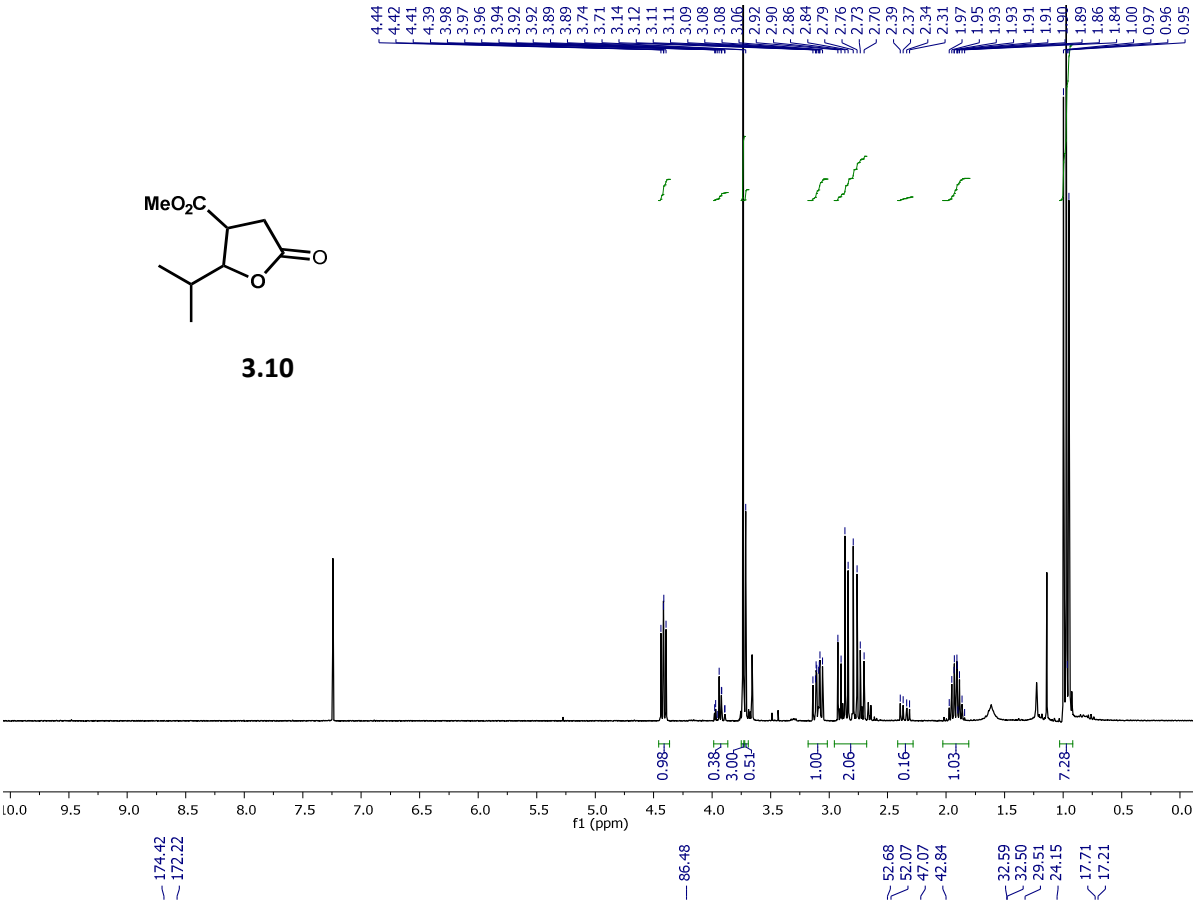
MeO2C
O
O
4.44 4.42 4.41 4.39 3.98 3.97 3.96 3.94 3.92 3.92 3.89 3.89 3.74 3.71 3.14 3.12 3.11 3.11 3.09 3.08 3.08 3.06 2.92 2.90 2.86 2.84 2.79 2.76 2.73 2.70 2.39 2.37 2.34 2.31 1.97 1.95 1.93 1.93 1.91 1.91 1.90 1.89 1.86 1.84 1.00 0.97 0.96 0.95
0.98 0.38 3.00 0.51 1.00 2.06 0.16 1.03 7.28
f1 (ppm)

3.10

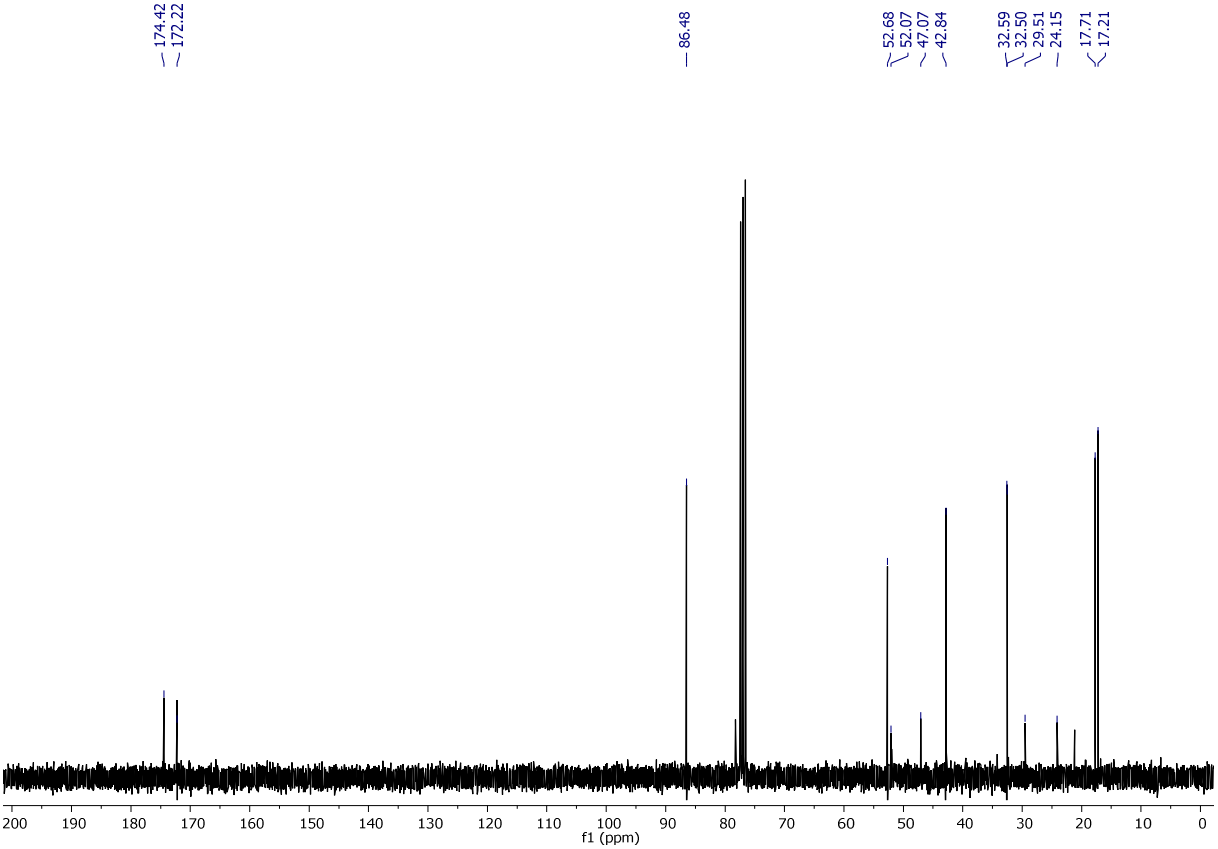
174.42 172.22 86.48 52.68 52.07 47.07 42.84 32.59 32.50 29.51 24.15 17.71 17.21
f1 (ppm)

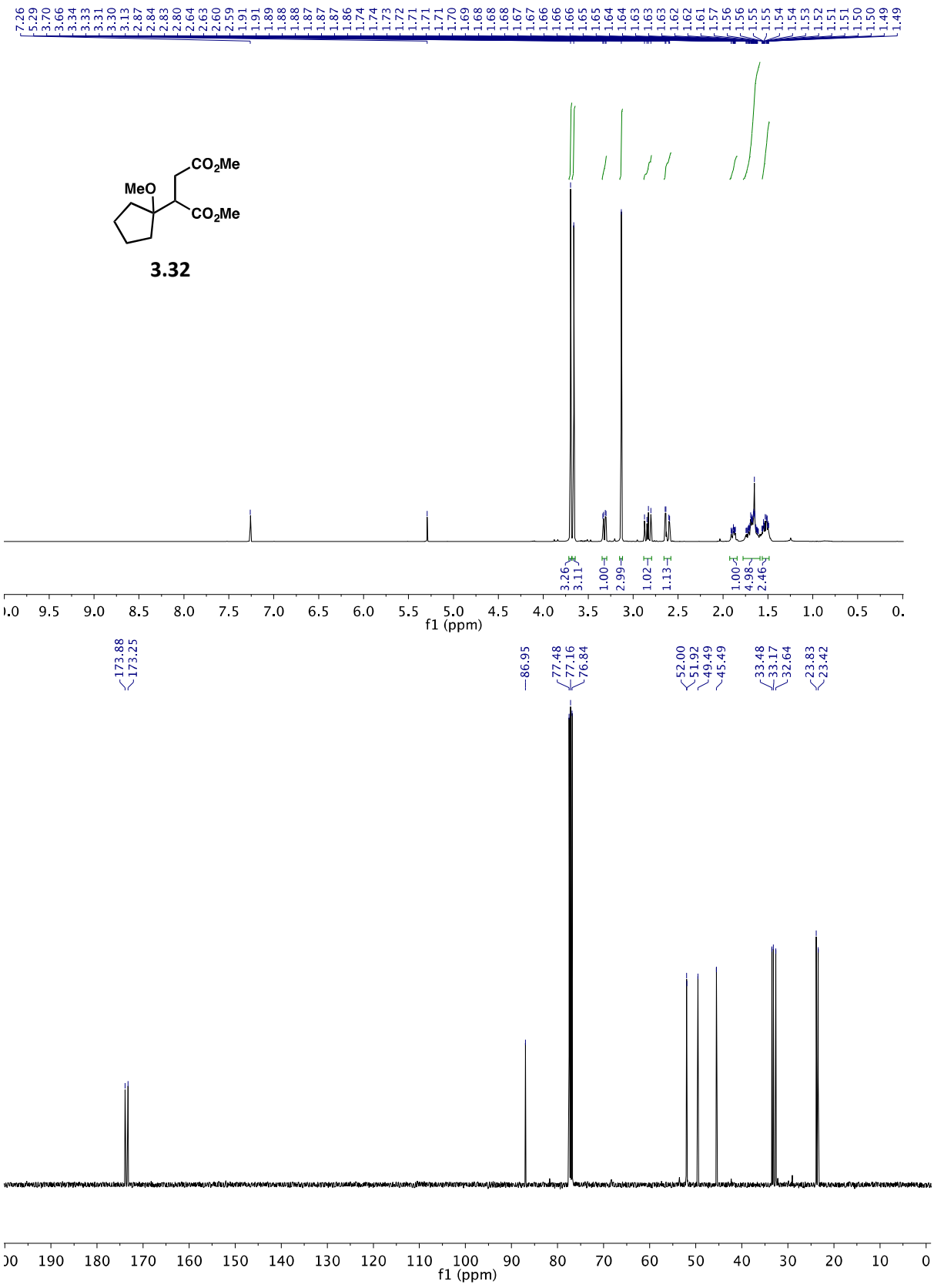
MeO
CO2Me
CO2Me
3.32
f1 (ppm)
f1 (ppm)

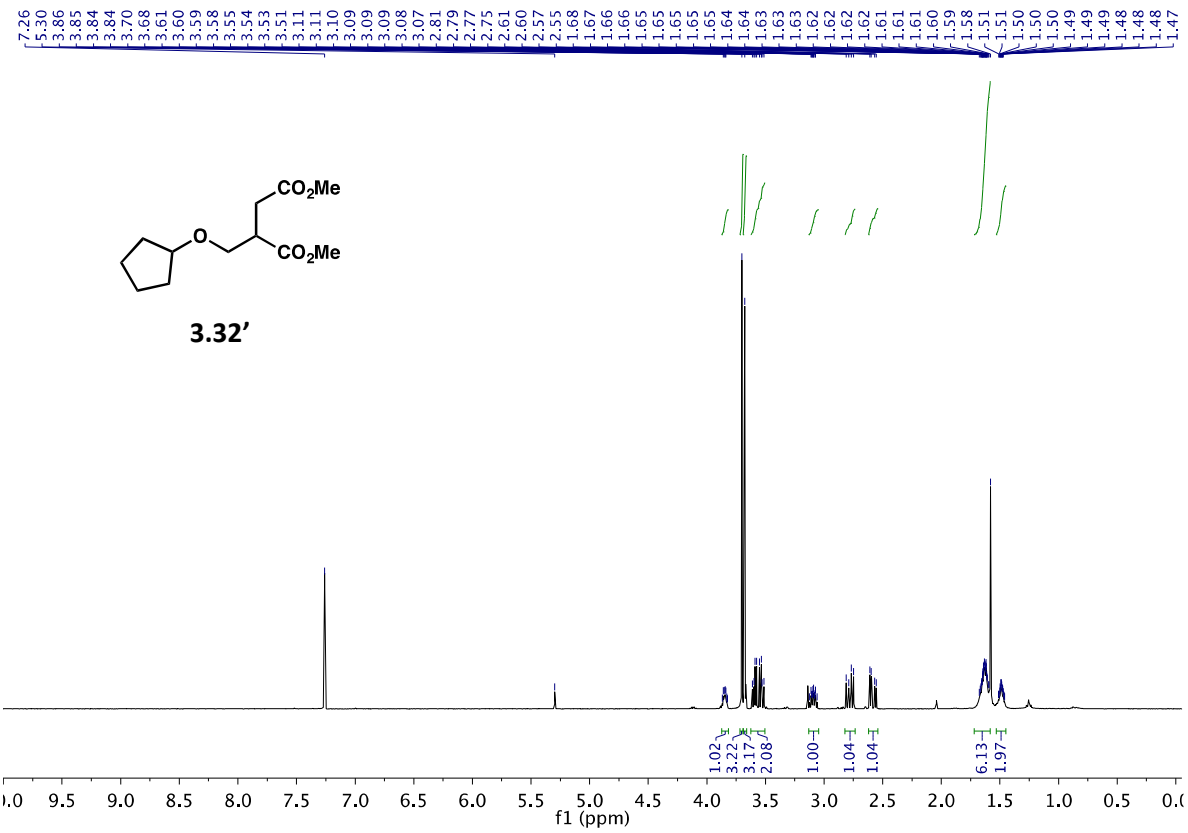

3.32'

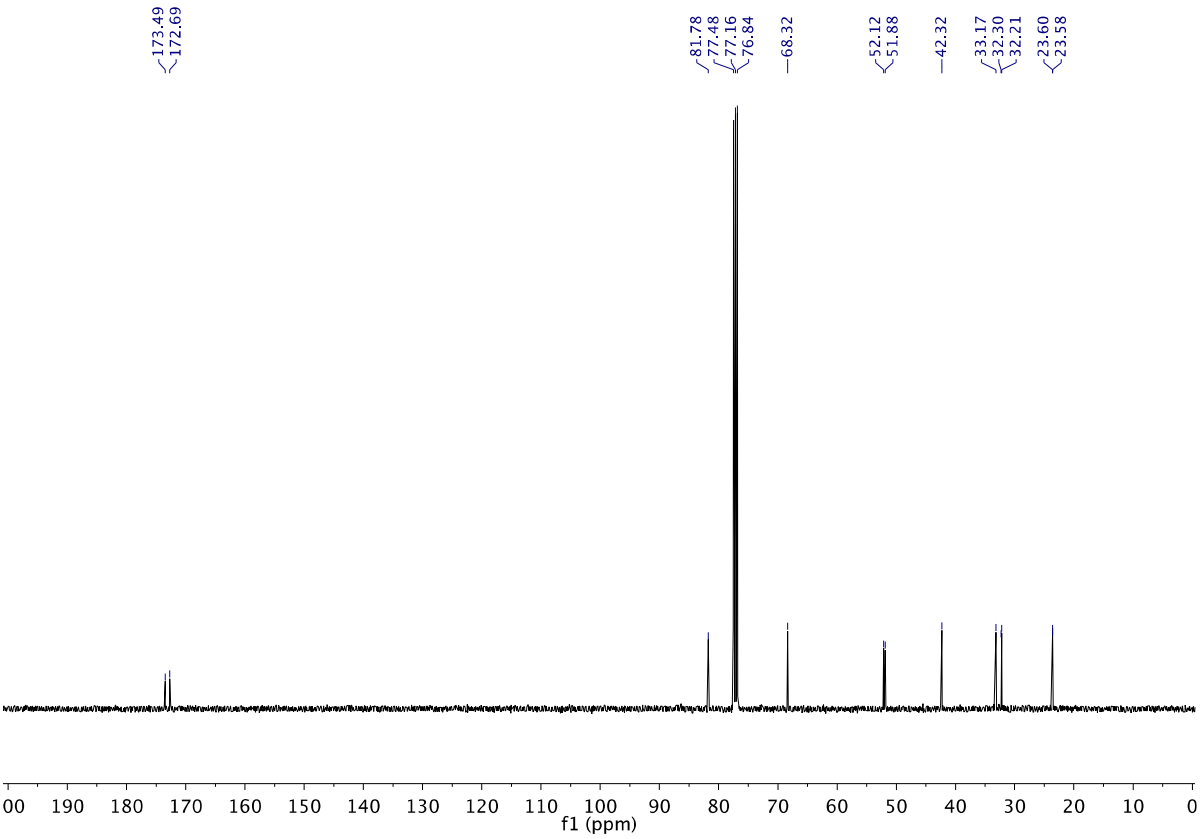

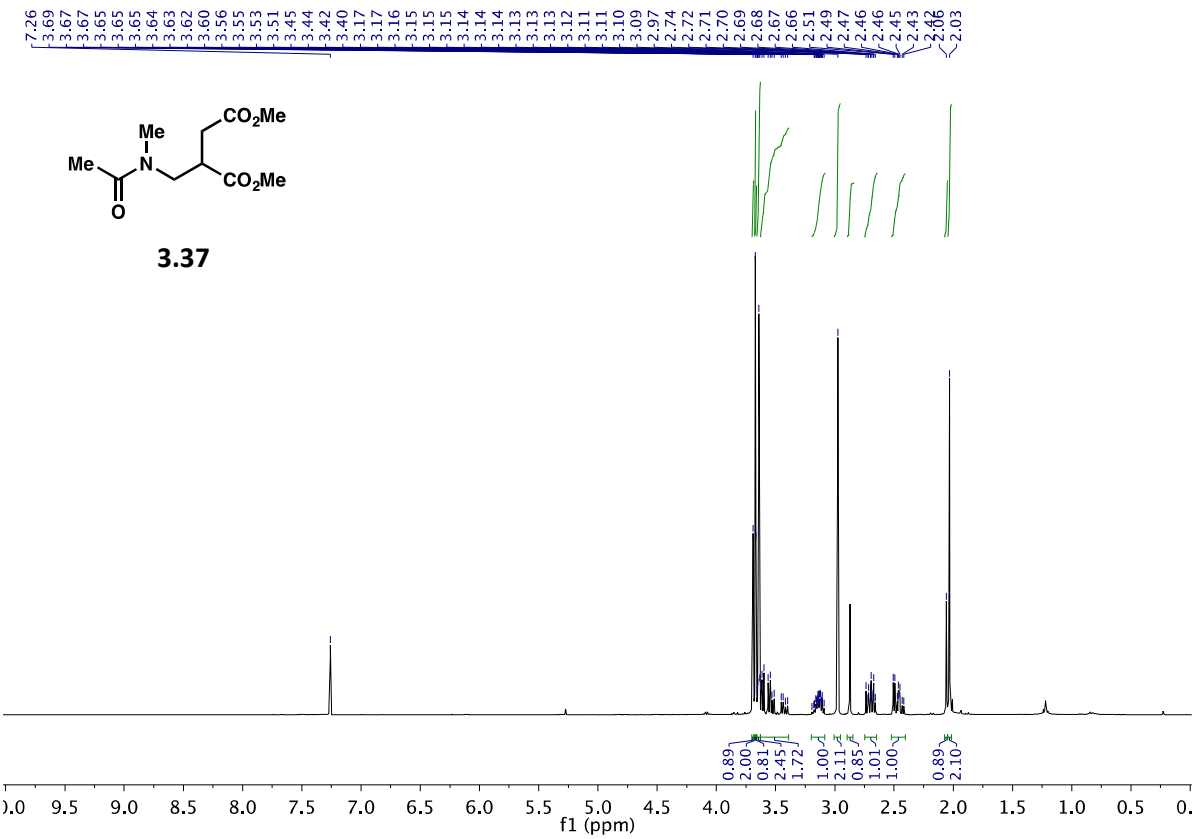

3.37

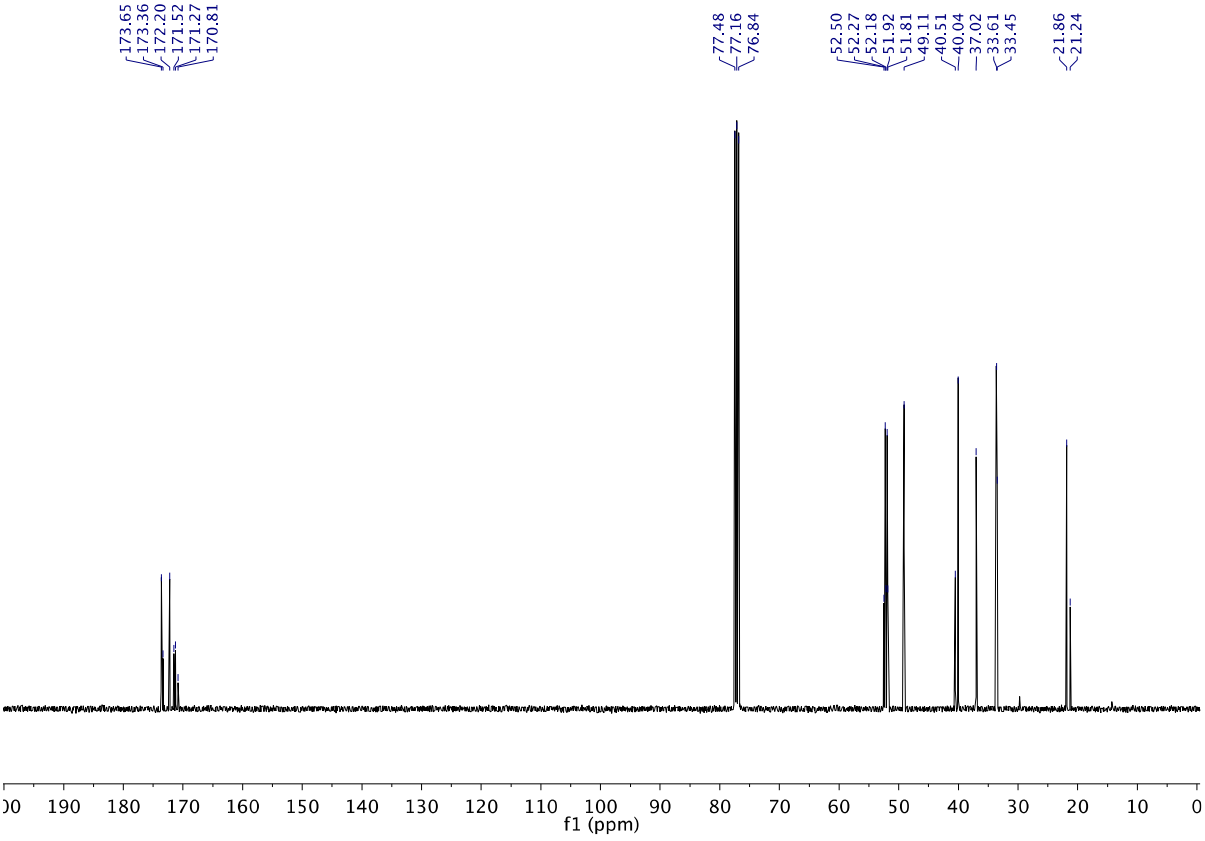

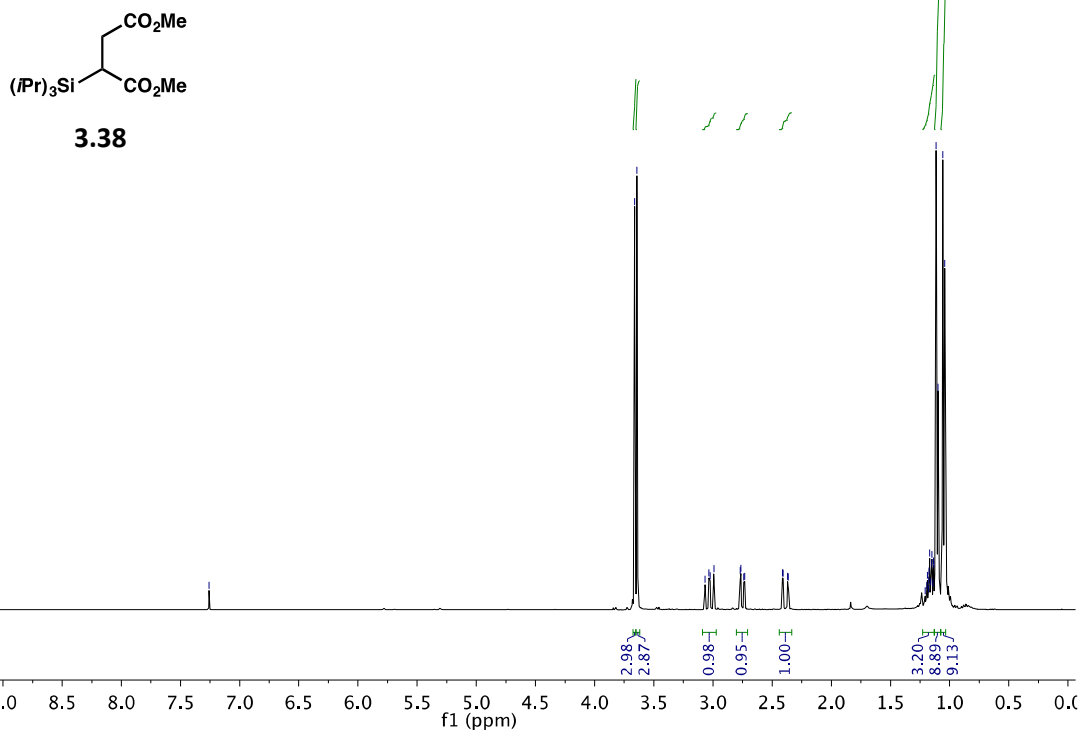

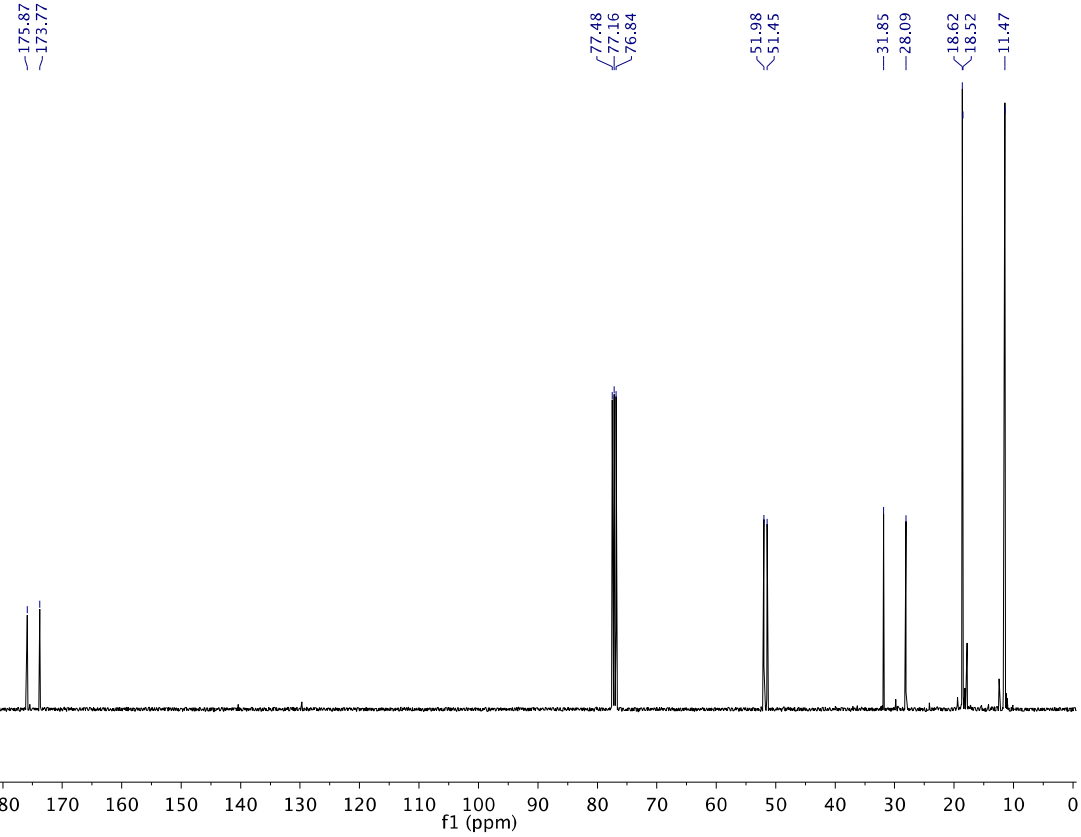

$(i\text{Pr})_3\text{Si}$, CO_2Me, CO_2Me

3.38

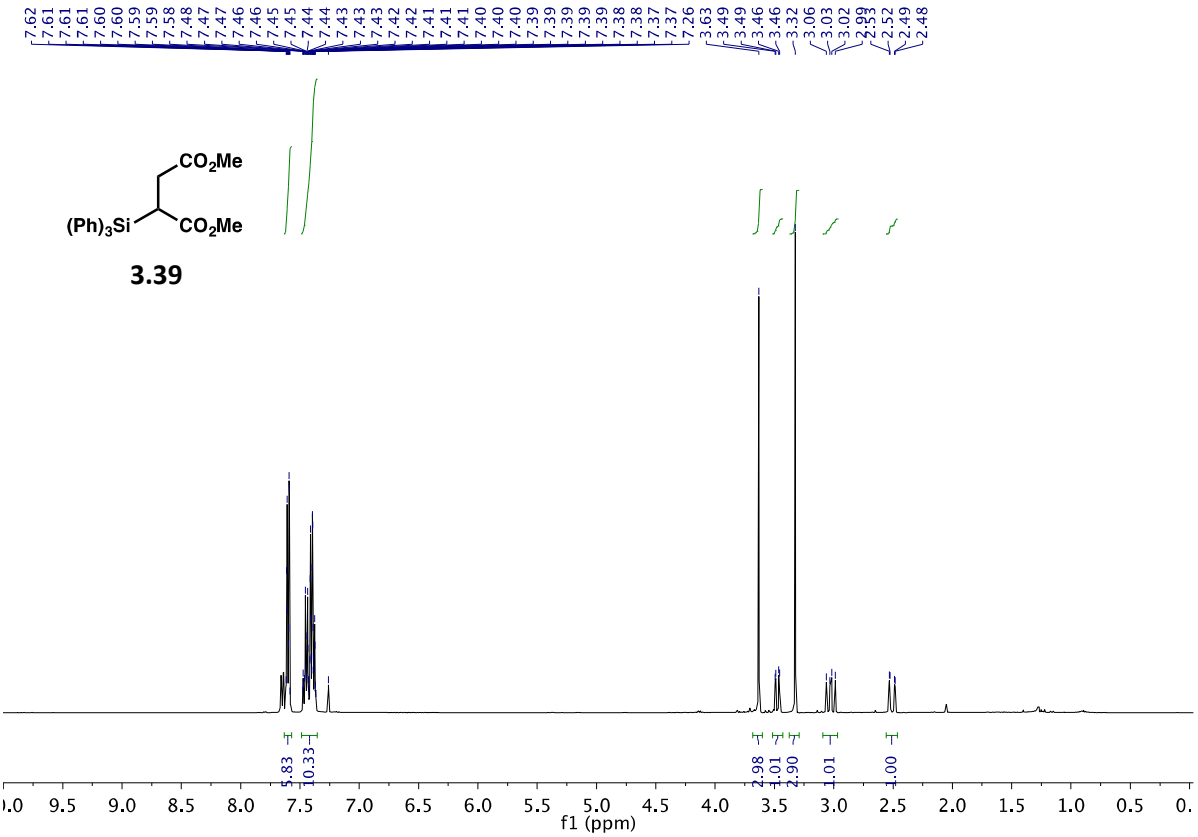
7.62 7.61 7.61 7.61 7.60 7.60 7.59 7.59 7.58 7.48 7.47 7.47 7.46 7.46 7.45 7.45 7.44 7.44 7.43 7.43 7.43 7.42 7.42 7.41 7.41 7.41 7.40 7.40 7.40 7.39 7.39 7.39 7.39 7.38 7.38 7.37 7.37 7.26 3.63 3.49 3.49 3.46 3.46 3.32 3.06 3.03 3.02 2.99 2.53 2.52 2.49 2.48
CO2Me
(Ph)3Si
CO2Me
3.39
5.83
10.33
2.98
1.01
2.90
1.01
1.00
f1 (ppm)

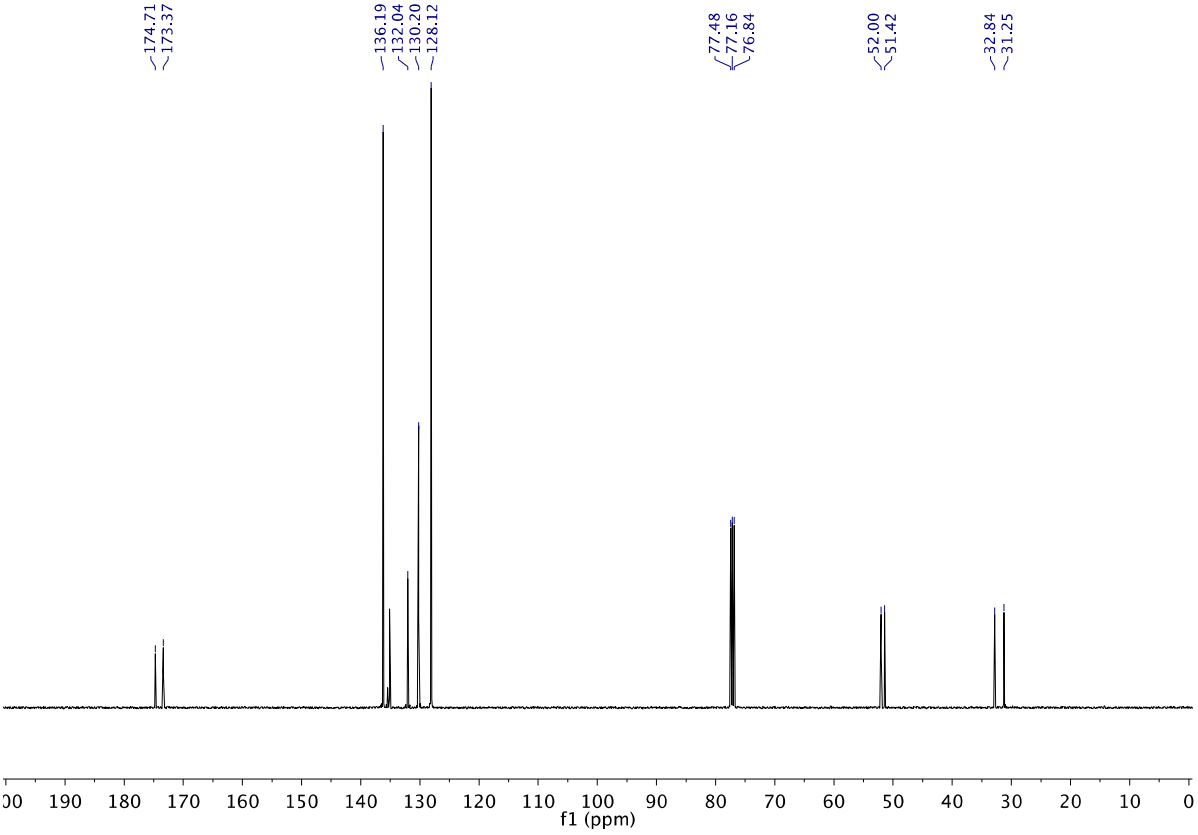
174.71 173.37 136.19 132.04 130.20 128.12 77.48 77.16 76.84 52.00 51.42 32.84 31.25
f1 (ppm)

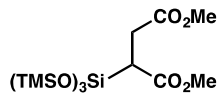
CO2Me
(TMSO)3Si
CO2Me

3.40

7.26
3.67
3.65
2.88
2.85
2.84
2.81
2.51
2.50
2.48
2.47
2.43
2.42
2.38
2.37
1.57
0.11
2.94
2.92
1.00
1.98
27.23
f1 (ppm)

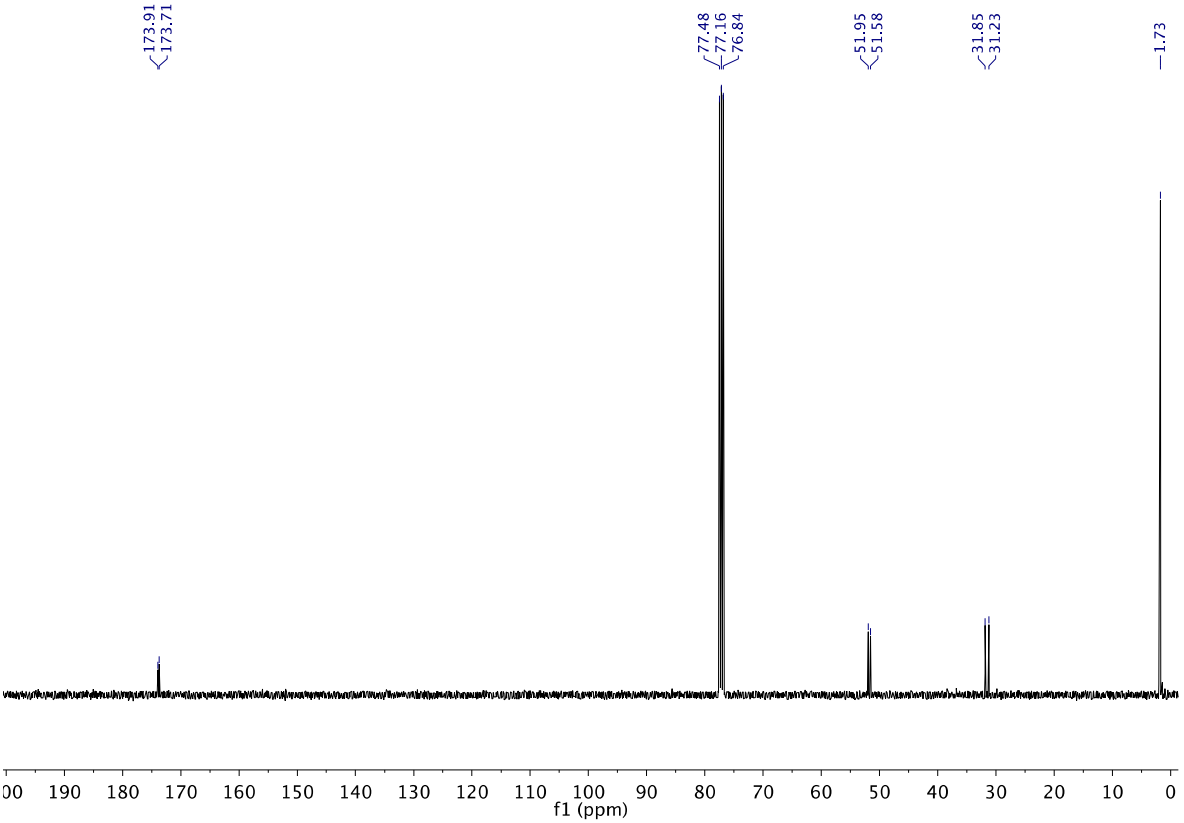
173.91
173.71
77.48
77.16
76.84
51.95
51.58
31.85
31.23
1.73
f1 (ppm)

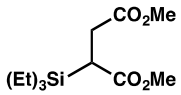
CO2Me
(Et)3Si
CO2Me

3.41

3.65
3.64
2.91
2.88
2.87
2.84
2.58
2.58
2.55
2.55
2.34
2.33
2.29
2.29
0.96
0.94
0.92
0.63
0.62
0.61
0.61
0.60
0.60
0.59
0.59
0.58
0.58
0.57
0.56
6.30
1.06
1.00
1.07
8.96
5.98
f1 (ppm)

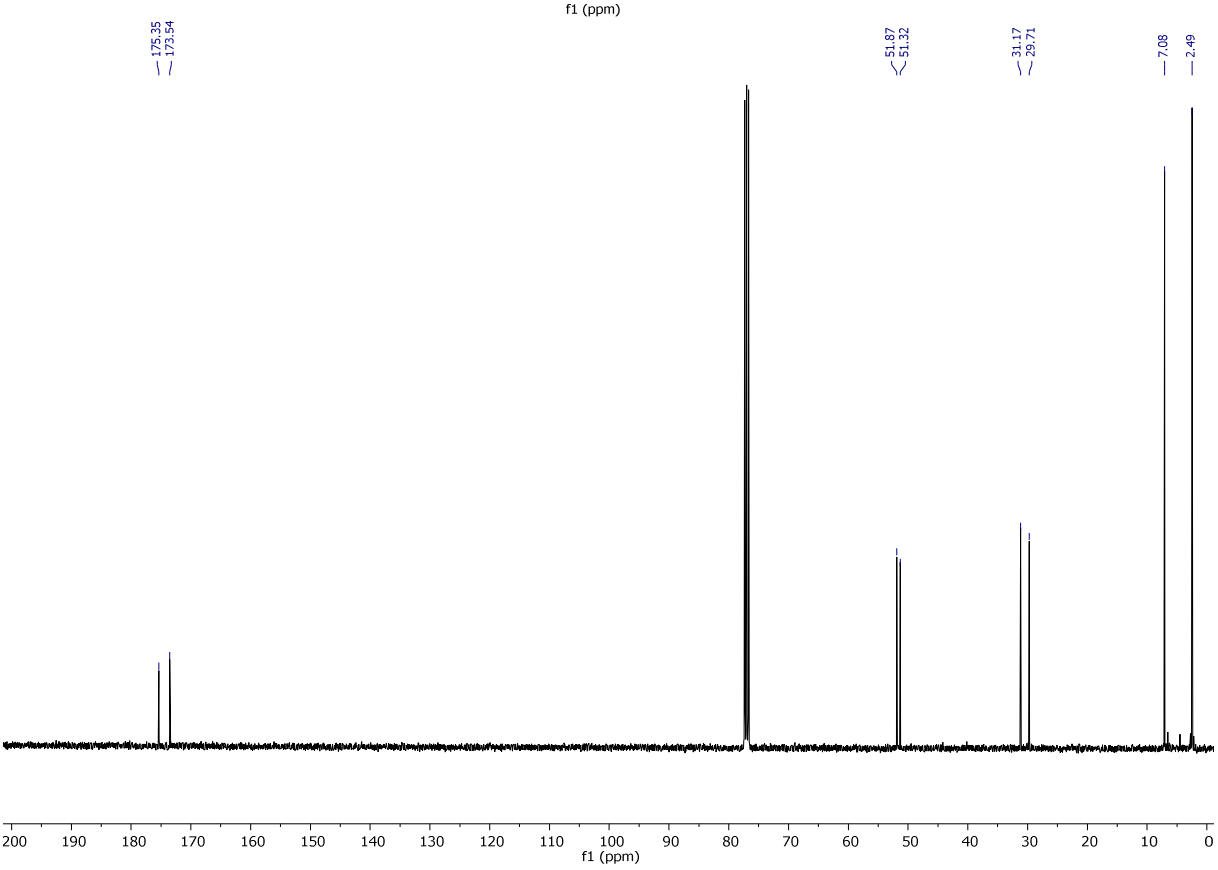
175.35
173.54
51.87
51.32
31.17
29.71
7.08
2.49
f1 (ppm)

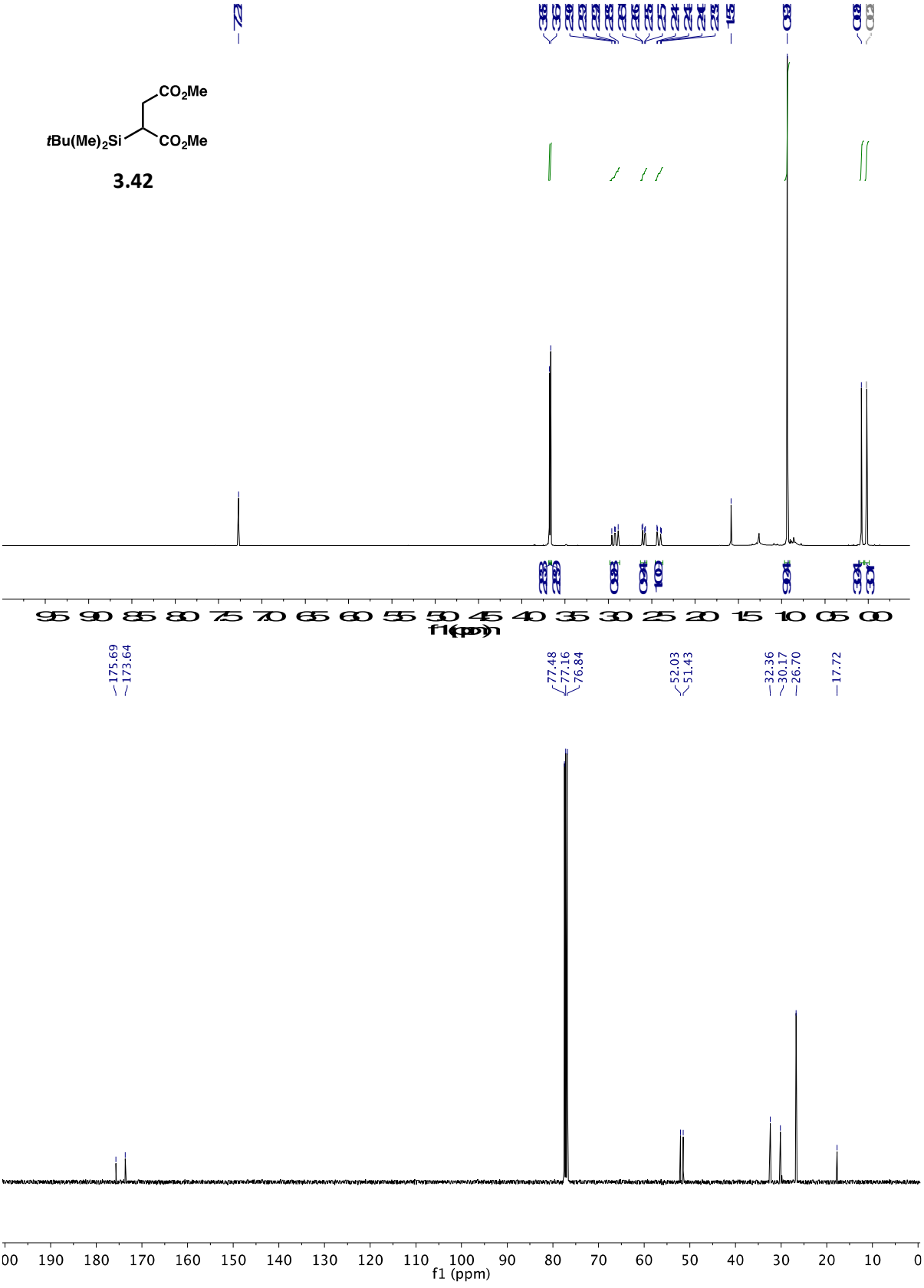
CO2Me
tBu(Me)2Si
CO2Me
3.42
f1 (ppm)
175.69
173.64
77.48
77.16
76.84
52.03
51.43
32.36
30.17
26.70
17.72
f1 (ppm)

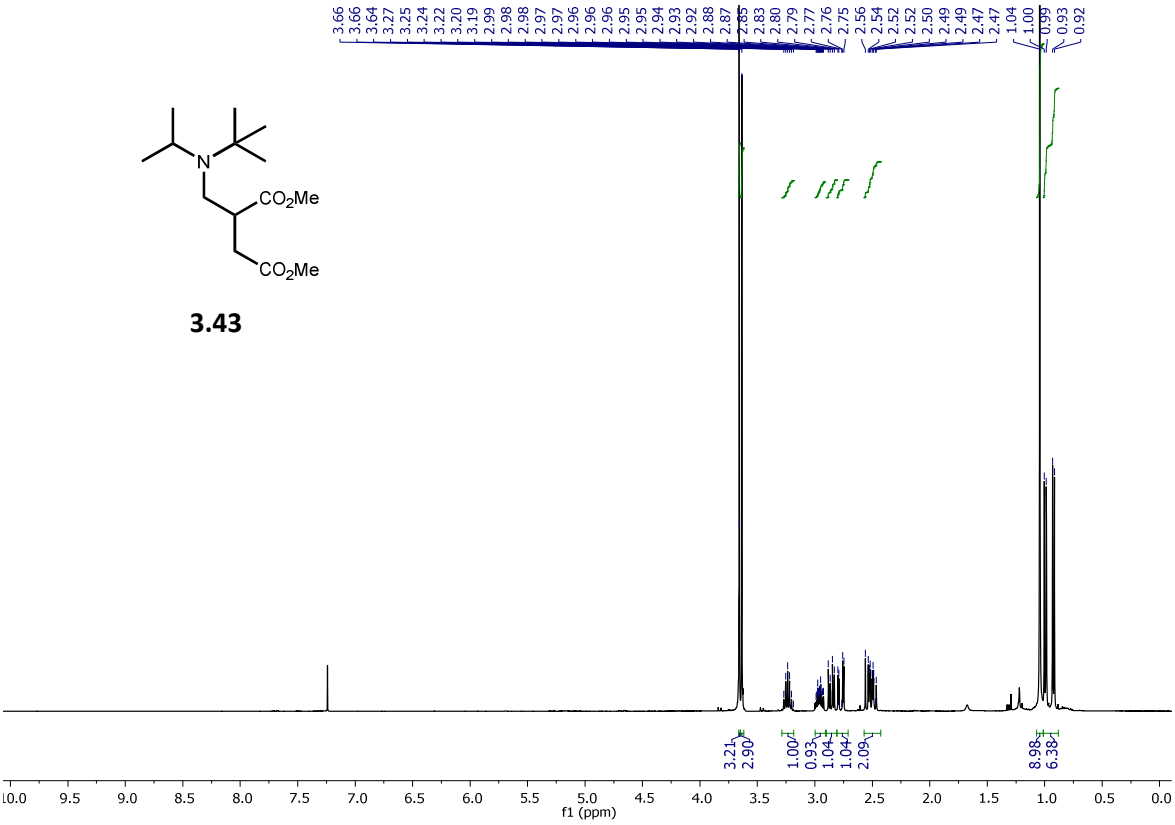
3.66
3.66
3.64
3.27
3.25
3.24
3.22
3.20
3.19
2.99
2.98
2.98
2.97
2.97
2.96
2.96
2.96
2.95
2.95
2.94
2.93
2.92
2.88
2.87
2.85
2.83
2.80
2.79
2.77
2.76
2.75
2.56
2.54
2.52
2.52
2.50
2.49
2.49
2.47
2.47
1.04
1.00
0.99
0.93
0.92
N
CO2Me
CO2Me
3.21
2.90
1.00
0.93
1.04
1.04
2.09
8.98
6.38
f1 (ppm)

3.43

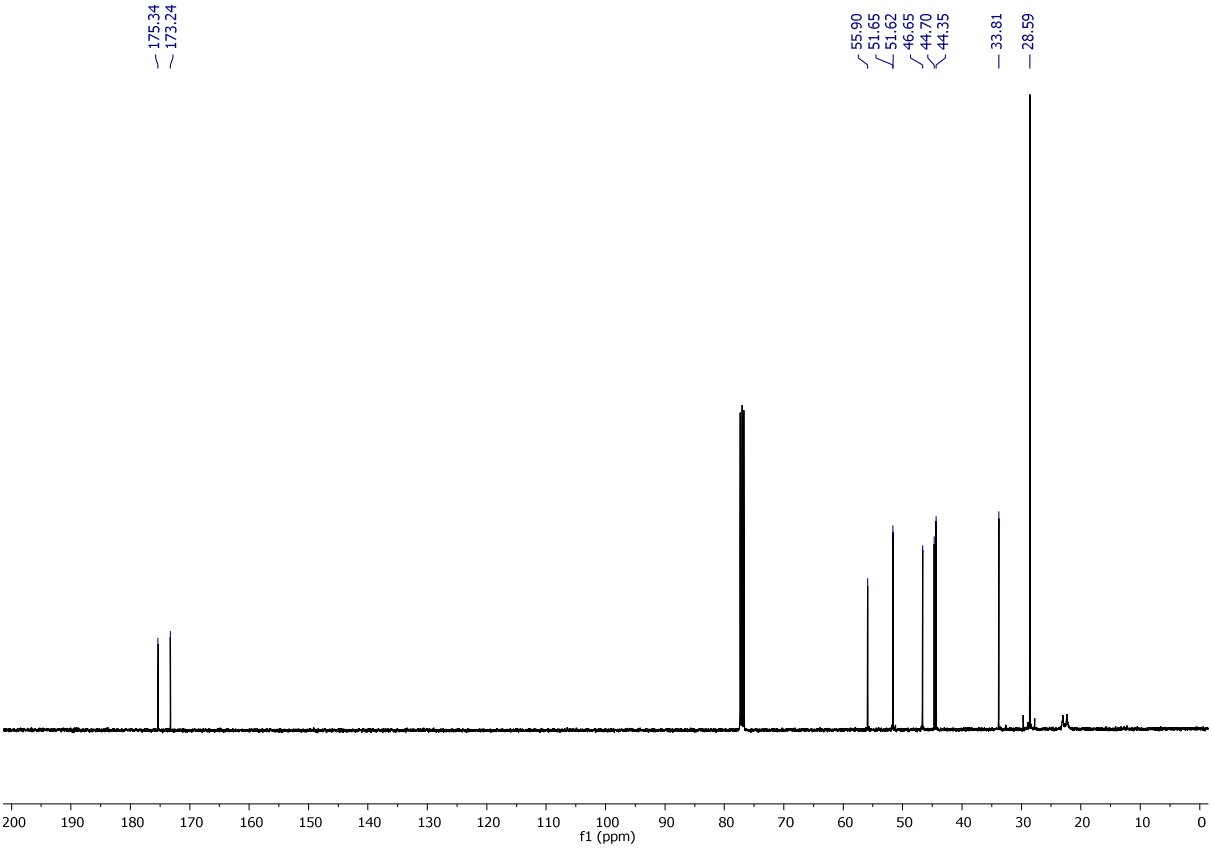
175.34
173.24
55.90
51.65
51.62
46.65
44.70
44.35
33.81
28.59
f1 (ppm)

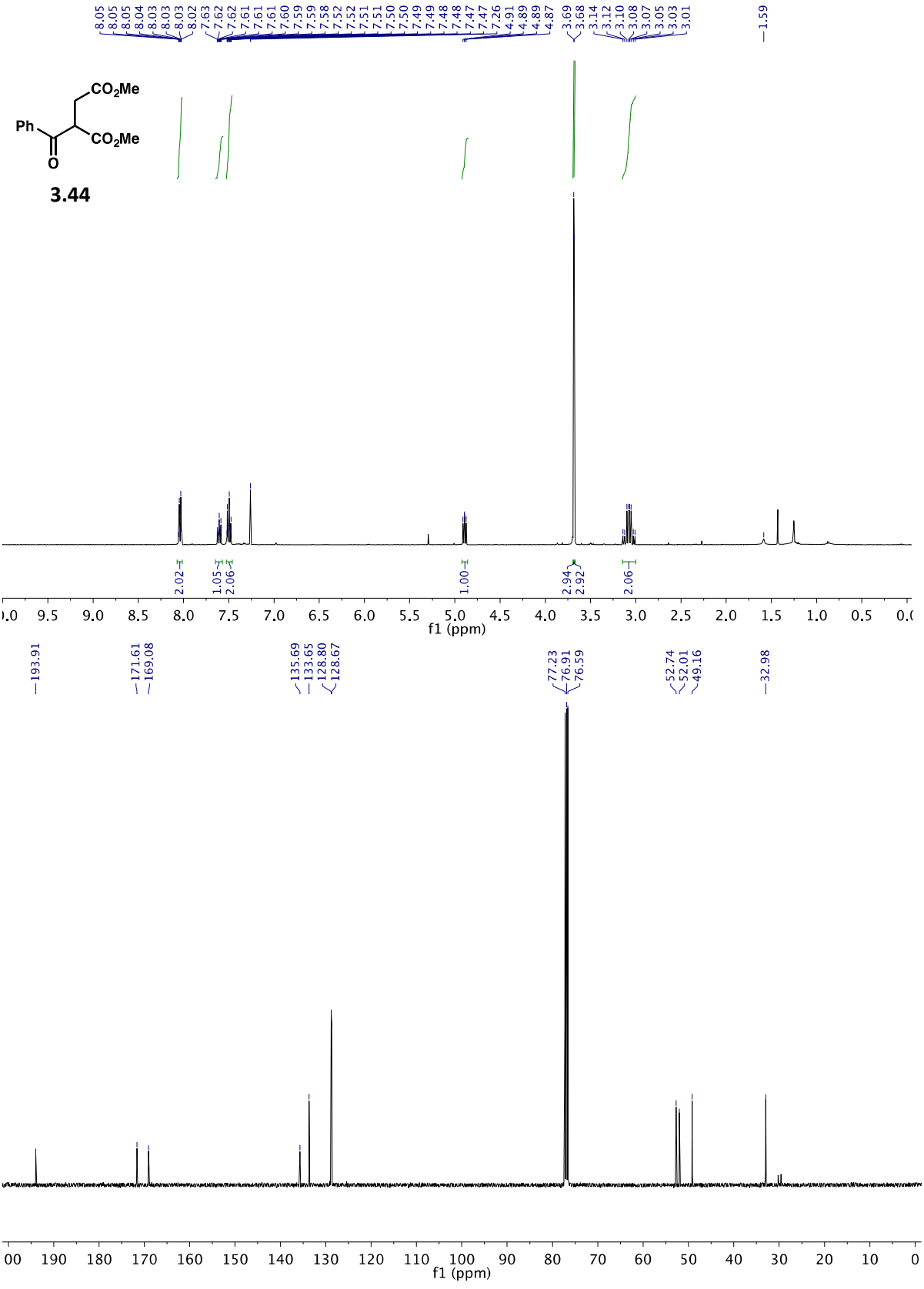
8.05
8.05
8.05
8.04
8.03
8.03
8.03
8.02
7.63
7.62
7.62
7.61
7.61
7.61
7.60
7.59
7.59
7.58
7.52
7.51
7.51
7.50
7.50
7.49
7.49
7.48
7.48
7.47
7.47
7.26
4.91
4.89
4.89
4.87
3.69
3.68
3.14
3.12
3.10
3.08
3.07
3.05
3.03
3.01
1.59
CO2Me
Ph
CO2Me
O
3.44
2.02
1.05
2.06
1.00
2.94
2.92
2.06
f1 (ppm)
193.91
171.61
169.08
135.69
133.65
128.80
128.67
77.23
76.91
76.59
52.74
52.01
49.16
32.98
f1 (ppm)

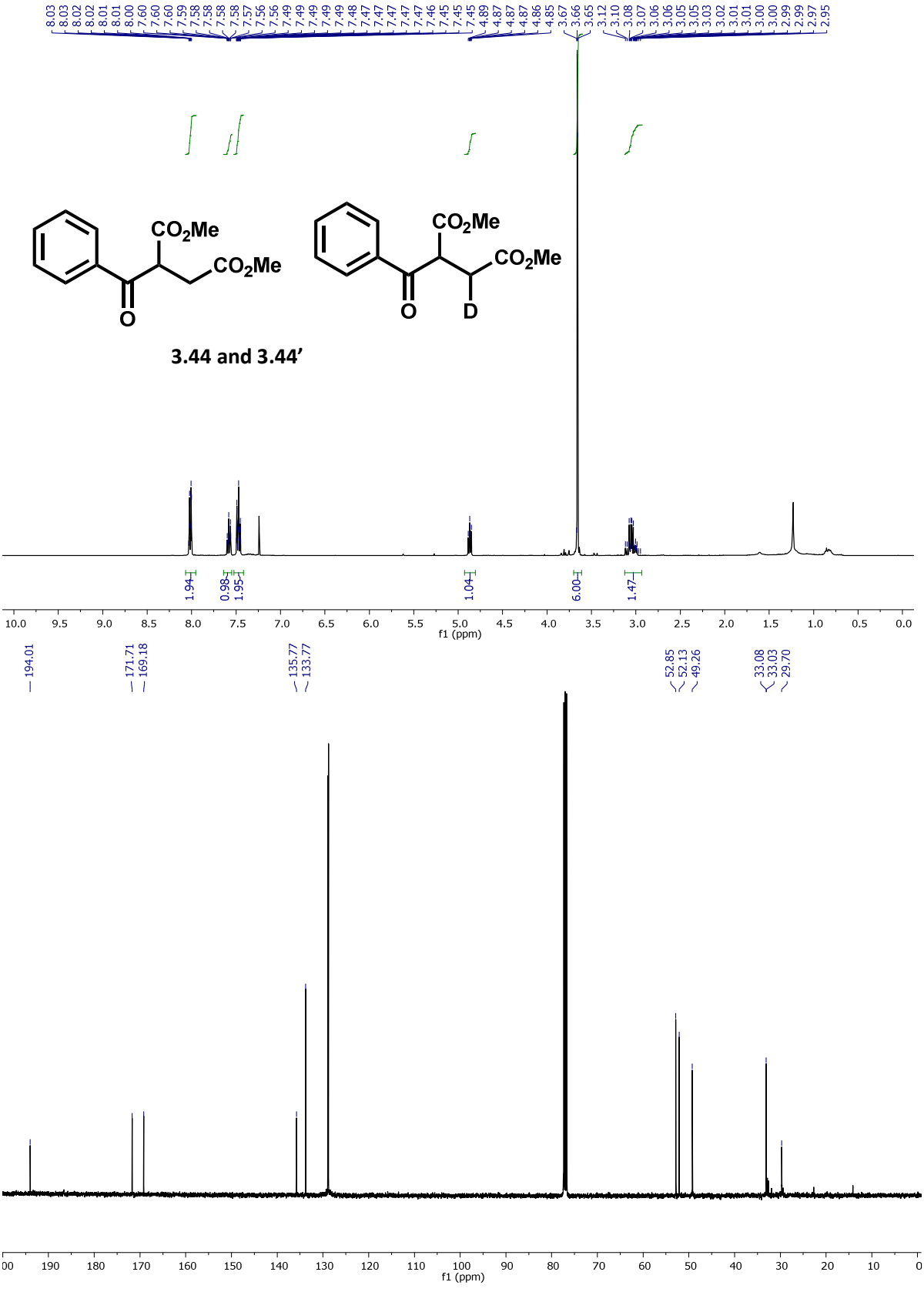
8.03 8.03 8.02 8.02 8.01 8.01 8.00 7.60 7.60 7.60 7.59 7.58 7.58 7.58 7.58 7.57 7.56 7.56 7.49 7.49 7.49 7.49 7.49 7.48 7.47 7.47 7.47 7.47 7.47 7.46 7.45 7.45 7.45 4.89 4.87 4.87 4.87 4.86 4.85 3.67 3.66 3.65 3.12 3.10 3.08 3.07 3.06 3.06 3.05 3.05 3.03 3.02 3.01 3.01 3.00 3.00 2.99 2.99 2.97 2.95
CO2Me
CO2Me
O
CO2Me
CO2Me
O
D
3.44 and 3.44'
1.94 0.98 1.95 1.04 6.00 1.47
10.0 9.5 9.0 8.5 8.0 7.5 7.0 6.5 6.0 5.5 5.0 4.5 4.0 3.5 3.0 2.5 2.0 1.5 1.0 0.5 0.0
f1 (ppm)
194.01
171.71
169.18
135.77
133.77
52.85
52.13
49.26
33.08
33.03
29.70
190 180 170 160 150 140 130 120 110 100 90 80 70 60 50 40 30 20 10 0
f1 (ppm)

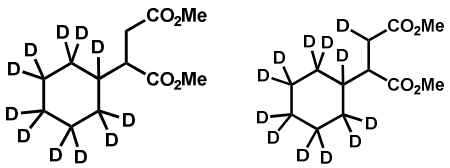
CO2Me
CO2Me
D
CO2Me
CO2Me

3.45 and 3.45’

3.67
3.66
3.64
3.63
2.73
2.71
2.70
2.69
2.68
2.68
2.66
2.65
2.45
2.44
2.43
2.42
2.41
2.40
2.38
2.99
2.62
1.95
1.00
f1 (ppm)

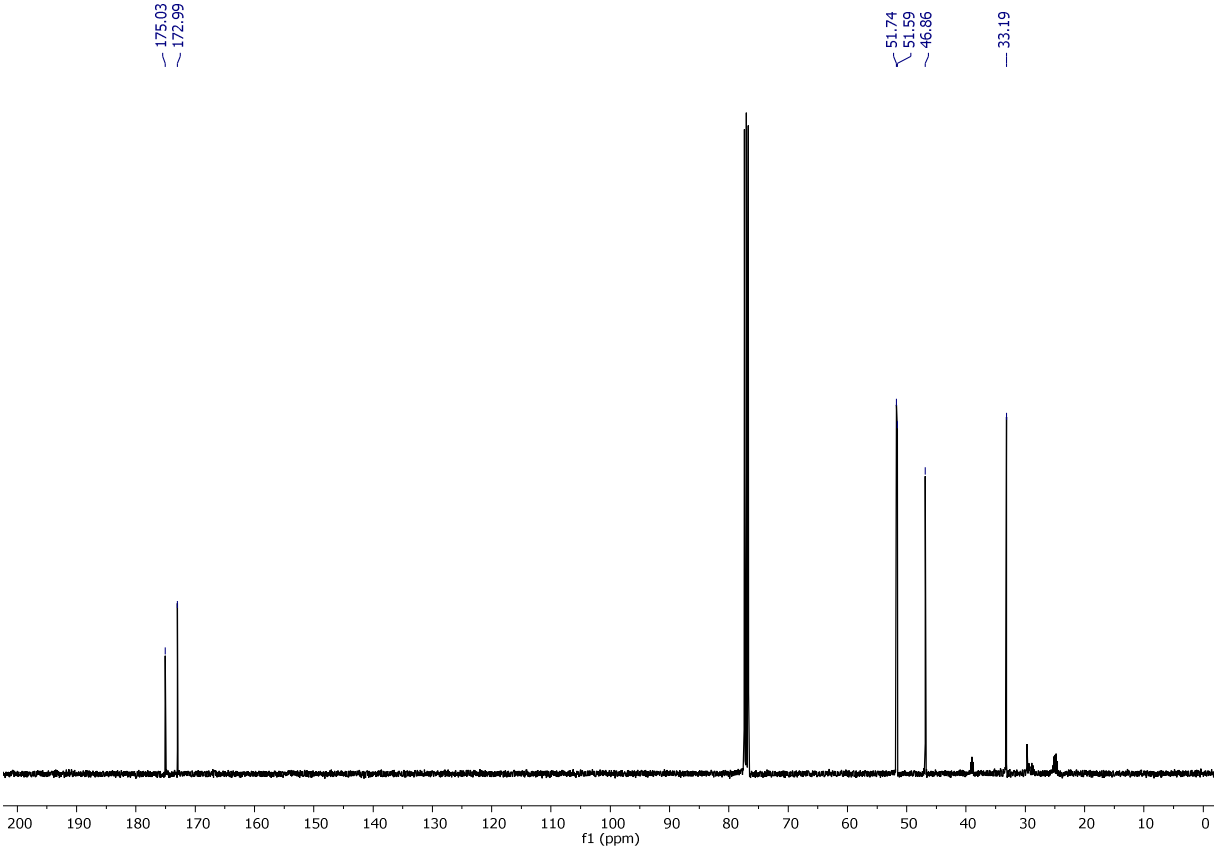
175.03
172.99
51.74
51.59
46.86
33.19
f1 (ppm)

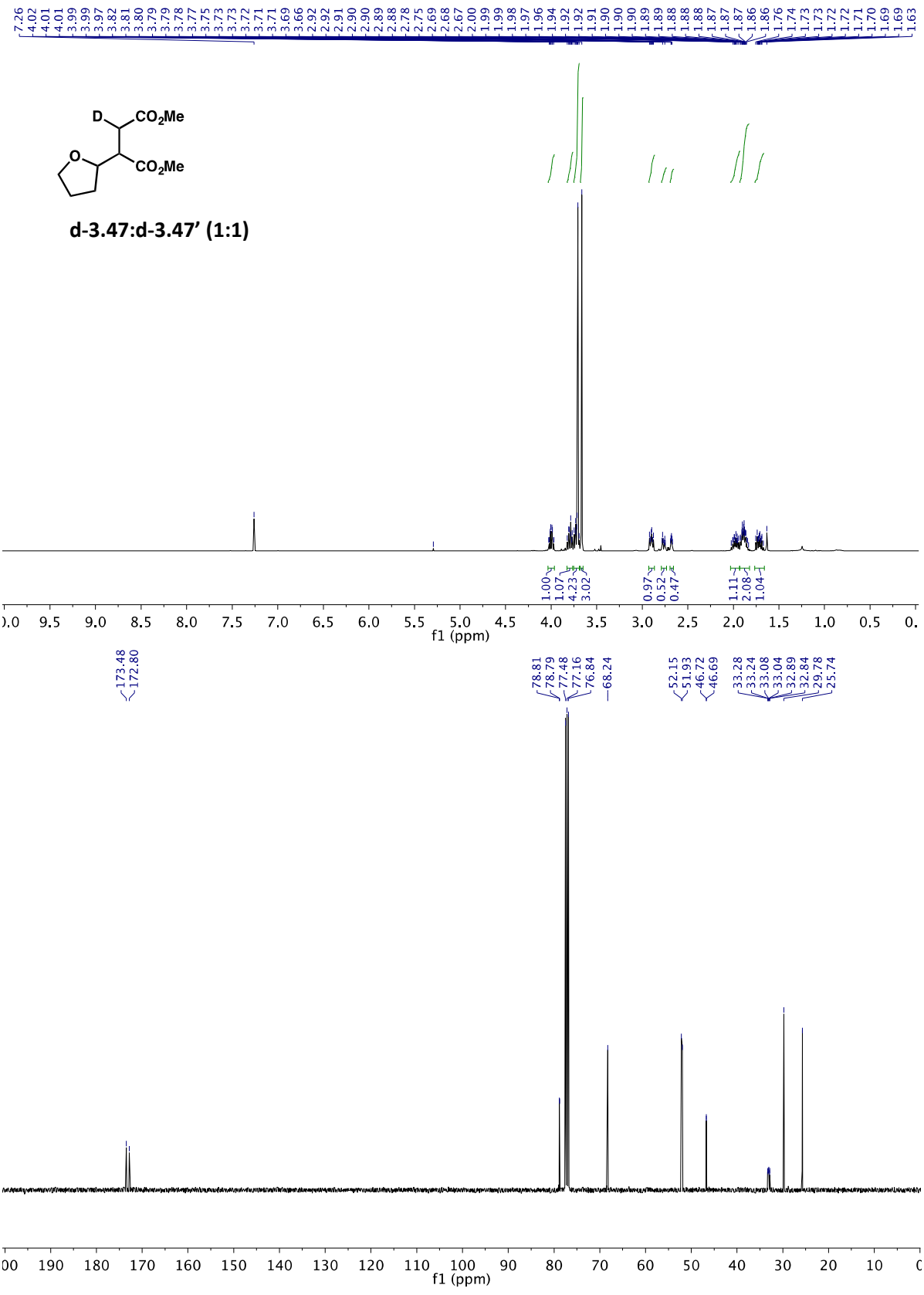
D
CO2Me
O
CO2Me
d-3.47:d-3.47' (1:1)
f1 (ppm)
f1 (ppm)

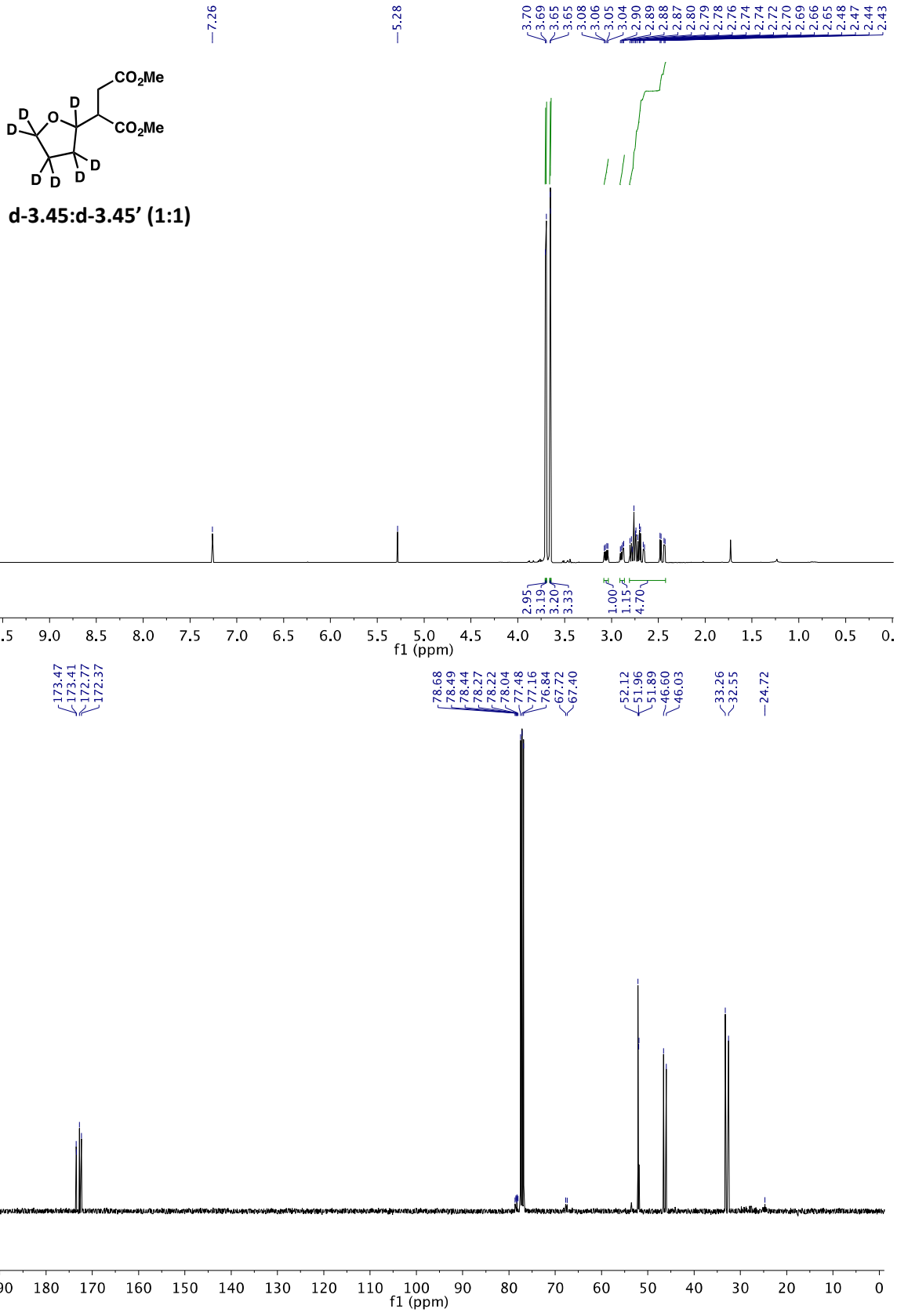
CO2Me
CO2Me
D
O
d-3.45:d-3.45' (1:1)
f1 (ppm)
f1 (ppm)

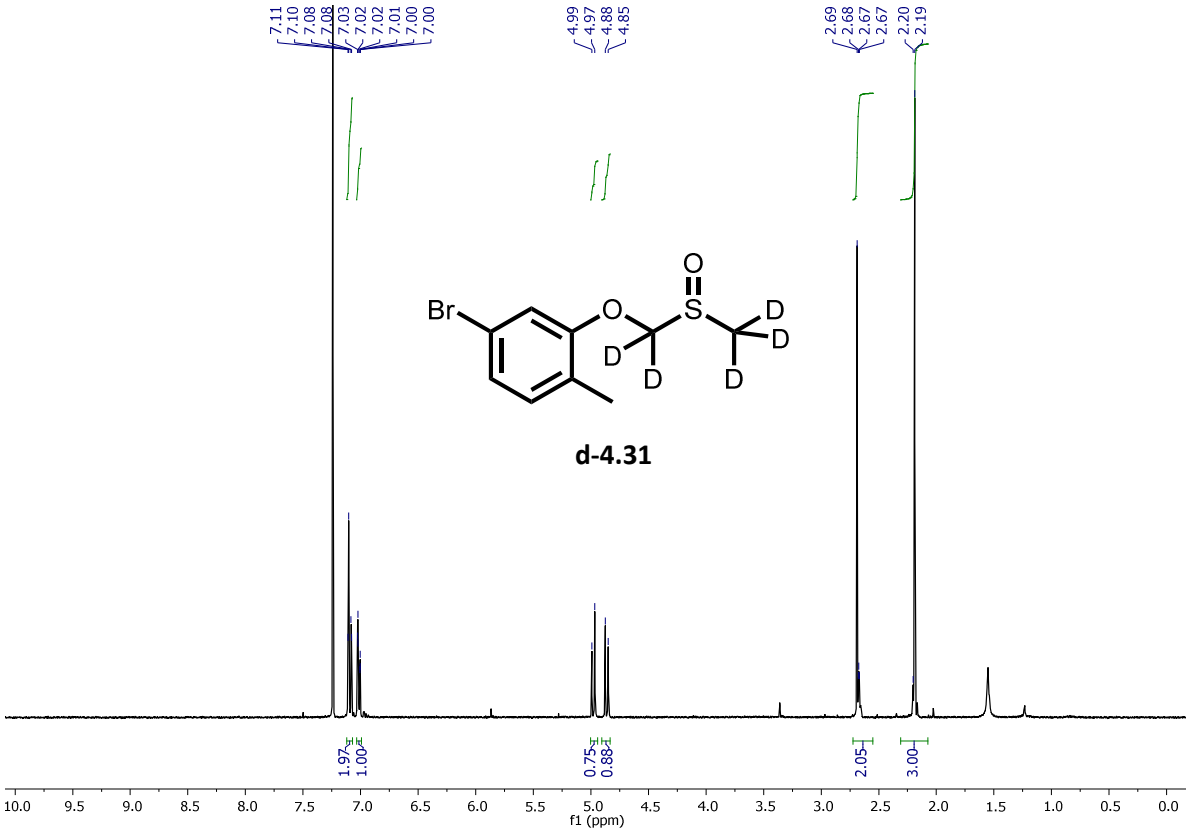
7.11
7.10
7.08
7.08
7.03
7.02
7.02
7.01
7.00
7.00
4.99
4.97
4.88
4.85
2.69
2.68
2.67
2.67
2.20
2.19
Br
O
S
O
D
D
D
D
D
1.97
1.00
0.75
0.88
2.05
3.00
f1 (ppm)

d-4.31

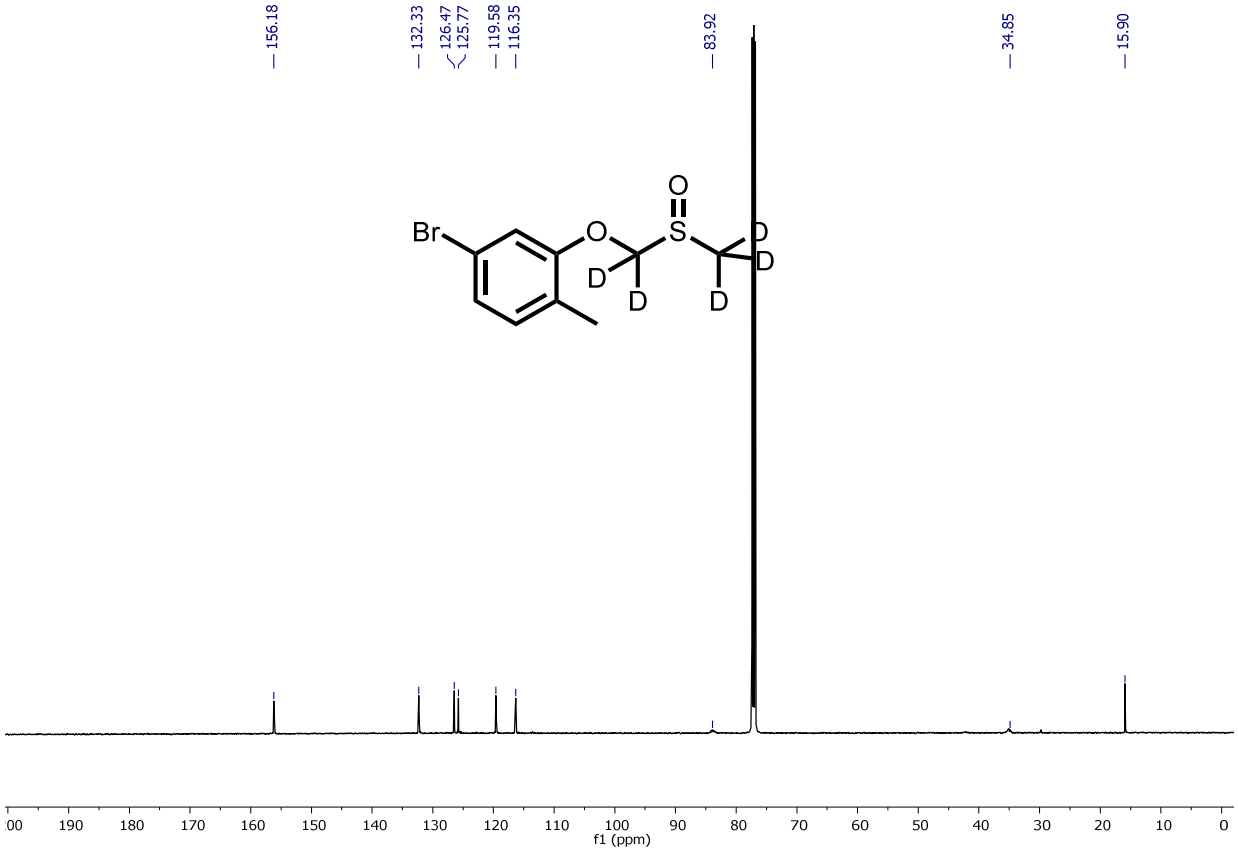
156.18
132.33
126.47
125.77
119.58
116.35
83.92
34.85
15.90
Br
O
S
O
D
D
D
D
D
f1 (ppm)

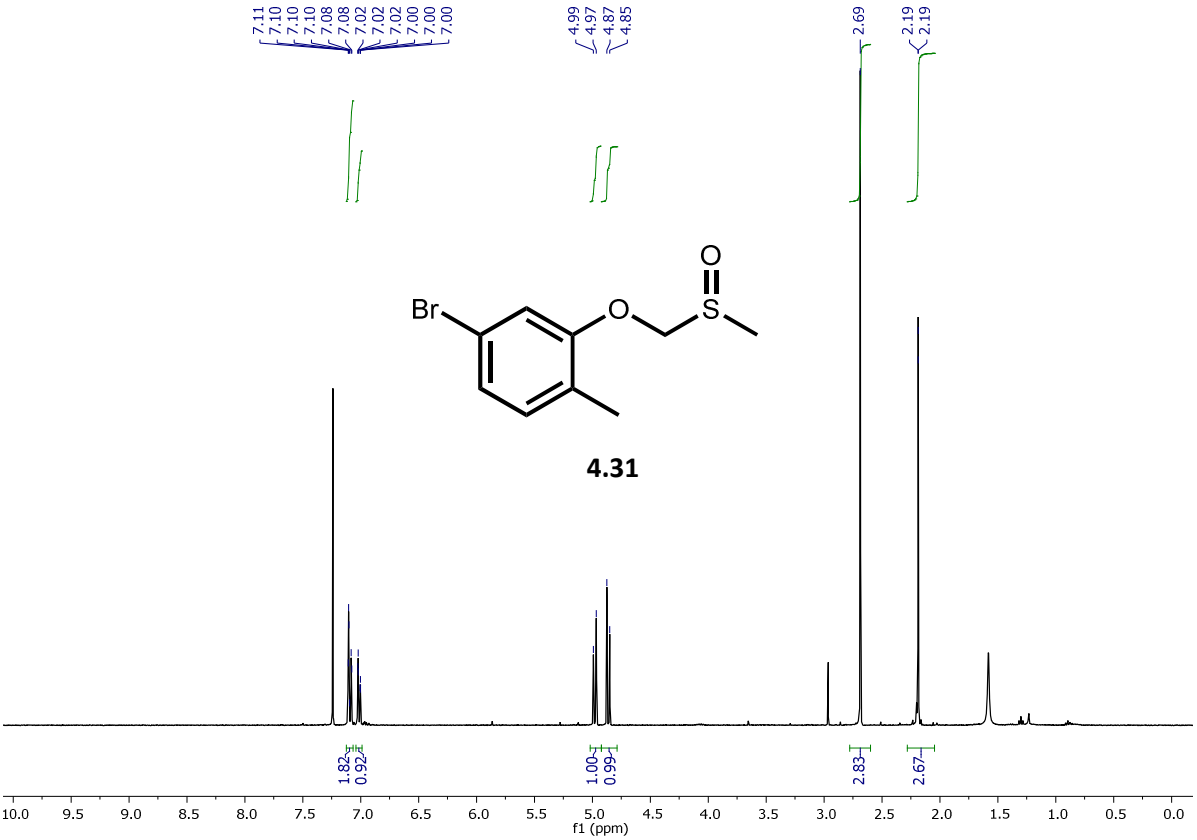
7.11
7.10
7.10
7.10
7.08
7.08
7.02
7.02
7.02
7.00
7.00
7.00
4.99
4.97
4.87
4.85
2.69
2.19
2.19
Br
O
O
S
1.82
0.92
1.00
0.99
2.83
2.67
f1 (ppm)

4.31

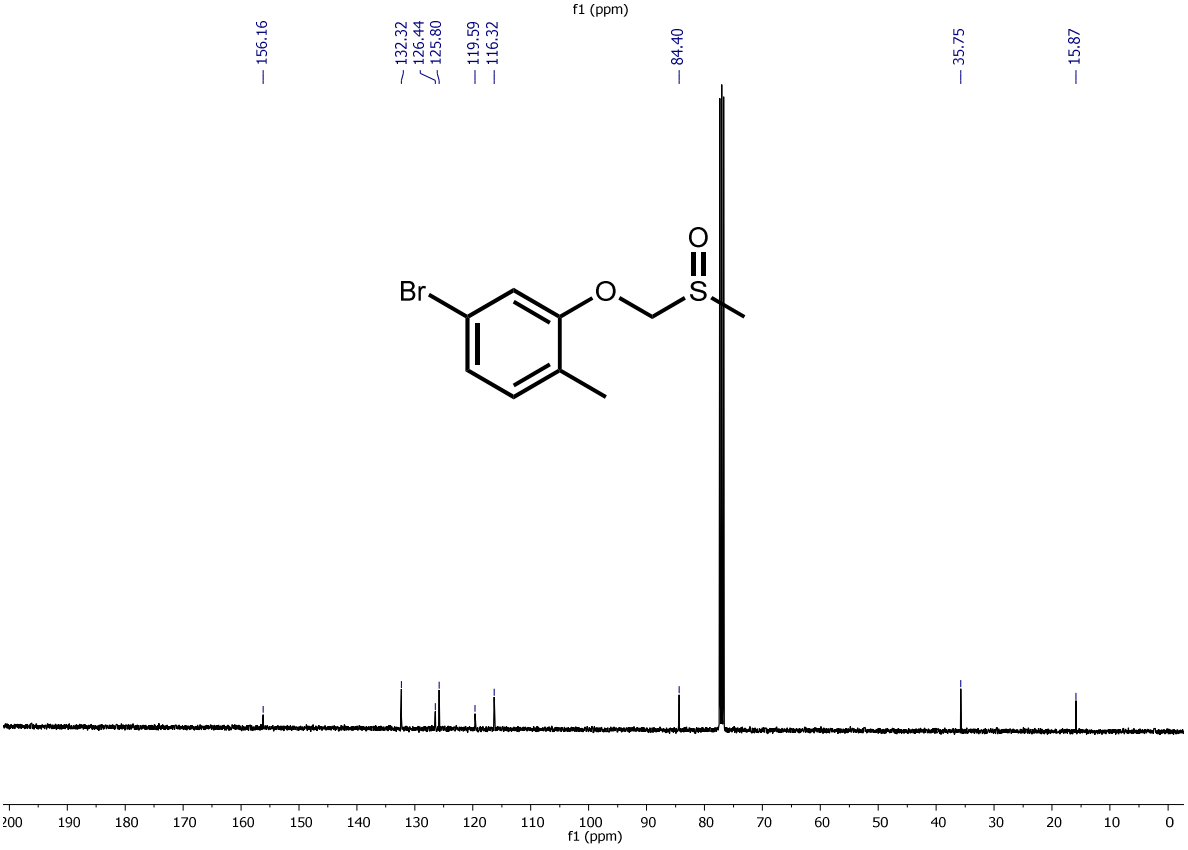
156.16
132.32
126.44
125.80
119.59
116.32
84.40
35.75
15.87
Br
O
O
S
f1 (ppm)

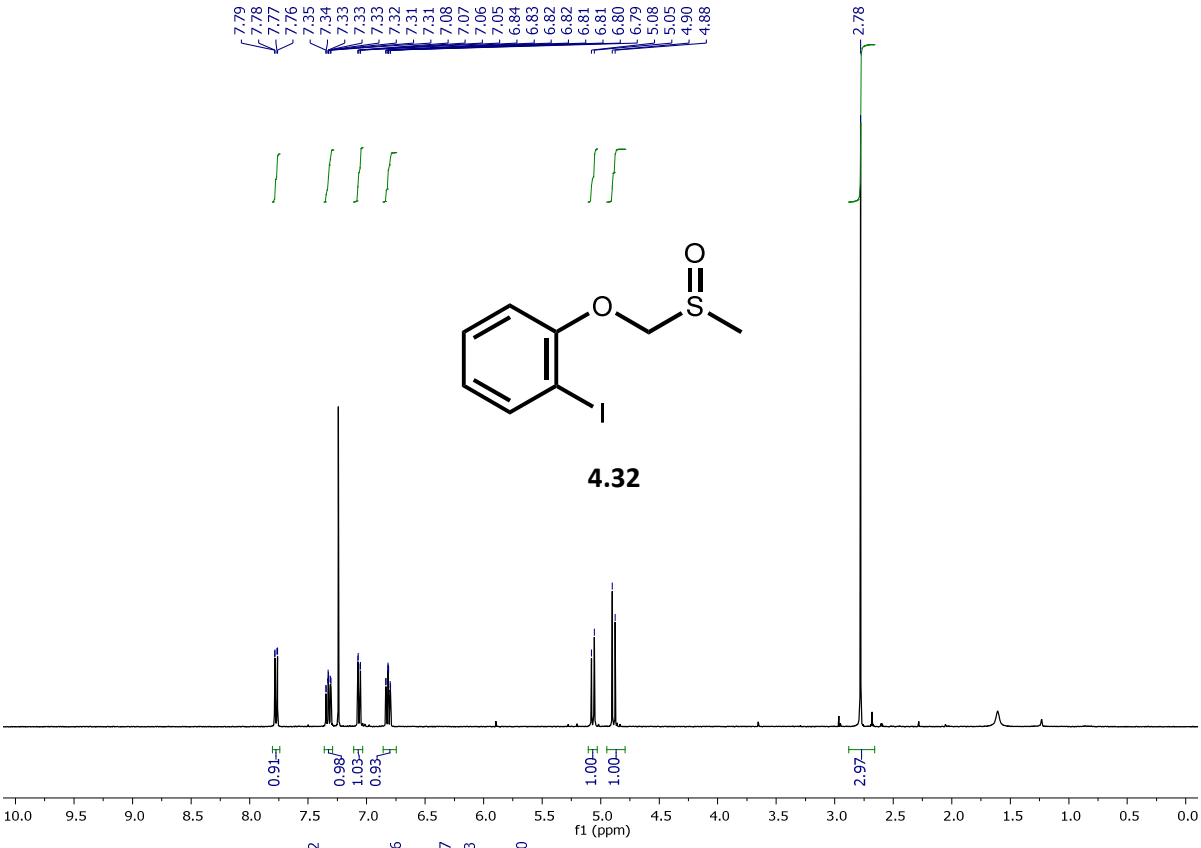
7.79
7.78
7.77
7.76
7.35
7.34
7.33
7.33
7.33
7.32
7.31
7.31
7.08
7.07
7.06
7.05
6.84
6.83
6.82
6.82
6.81
6.81
6.80
6.79
5.08
5.05
4.90
4.88
2.78
O
O
S
I
0.91
0.98
1.03
0.93
1.00
1.00
2.97
10.0 9.5 9.0 8.5 8.0 7.5 7.0 6.5 6.0 5.5 5.0 4.5 4.0 3.5 3.0 2.5 2.0 1.5 1.0 0.5 0.0
f1 (ppm)

4.32

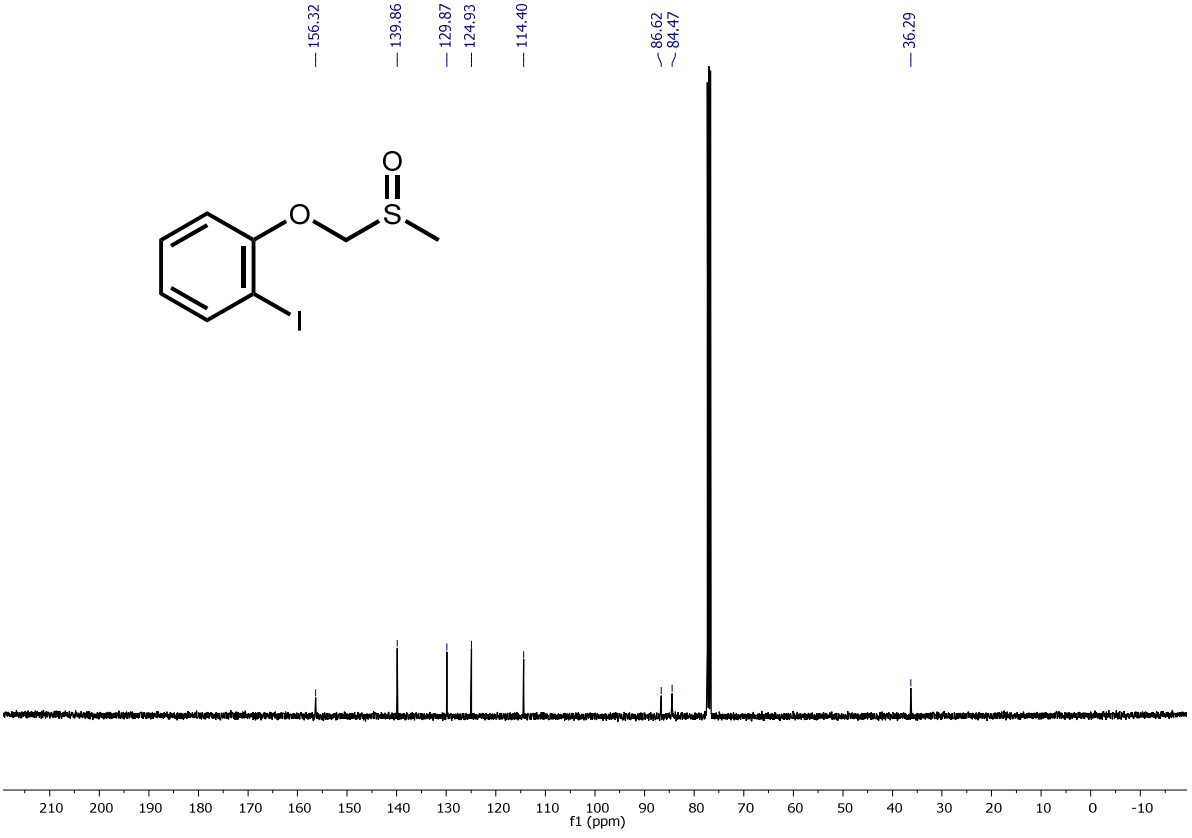
156.32
139.86
129.87
124.93
114.40
86.62
84.47
36.29
O
O
S
I
210 200 190 180 170 160 150 140 130 120 110 100 90 80 70 60 50 40 30 20 10 0 -10
f1 (ppm)

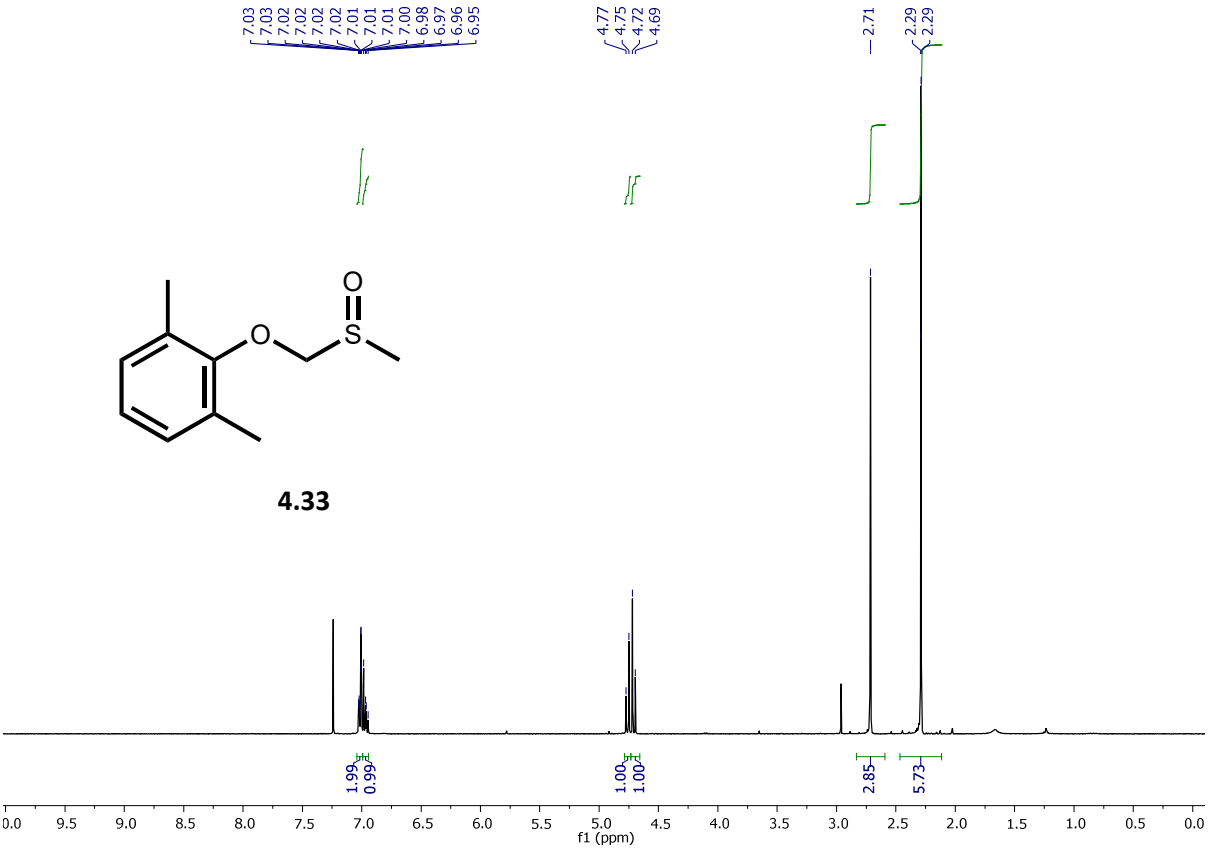
7.03
7.03
7.02
7.02
7.02
7.02
7.01
7.01
7.01
7.00
6.98
6.97
6.96
6.95
4.77
4.75
4.72
4.69
2.71
2.29
2.29
O
O
S
1.99
0.99
1.00
1.00
2.85
5.73
f1 (ppm)

4.33

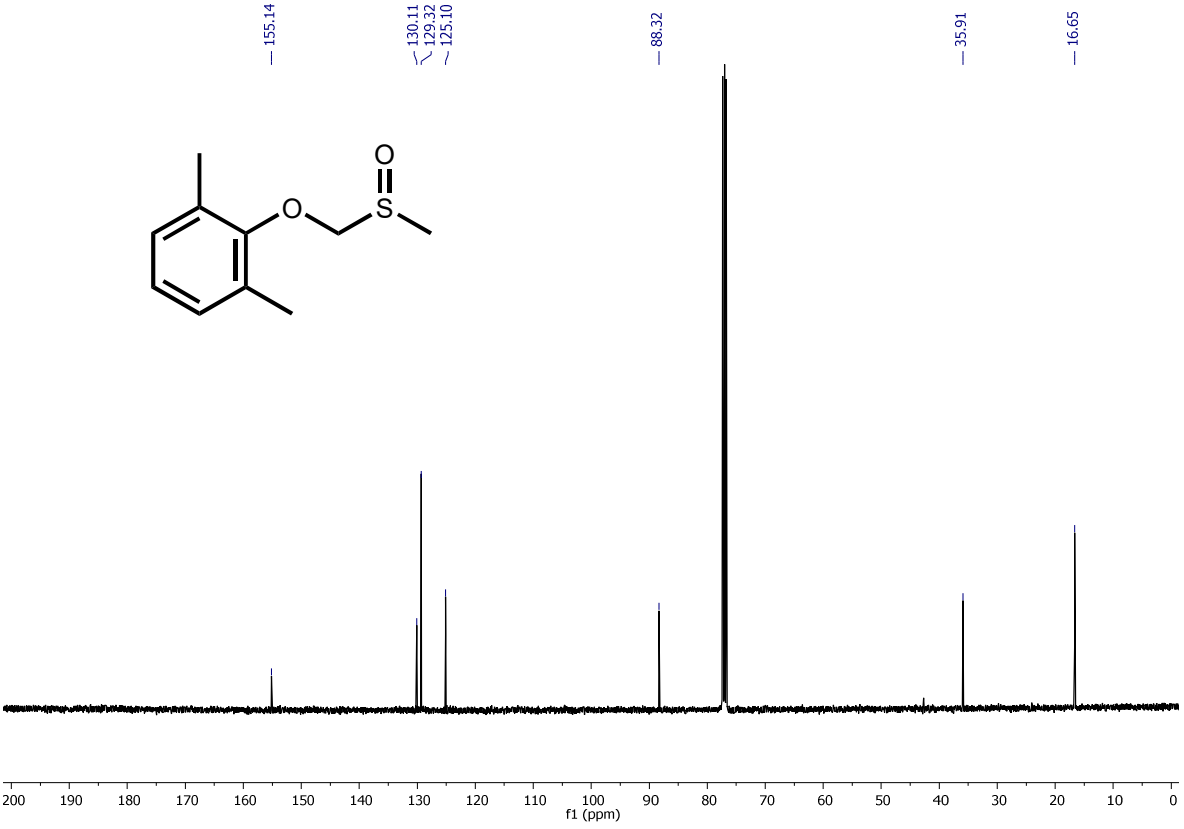
155.14
130.11
129.32
125.10
88.32
35.91
16.65
O
O
S
f1 (ppm)

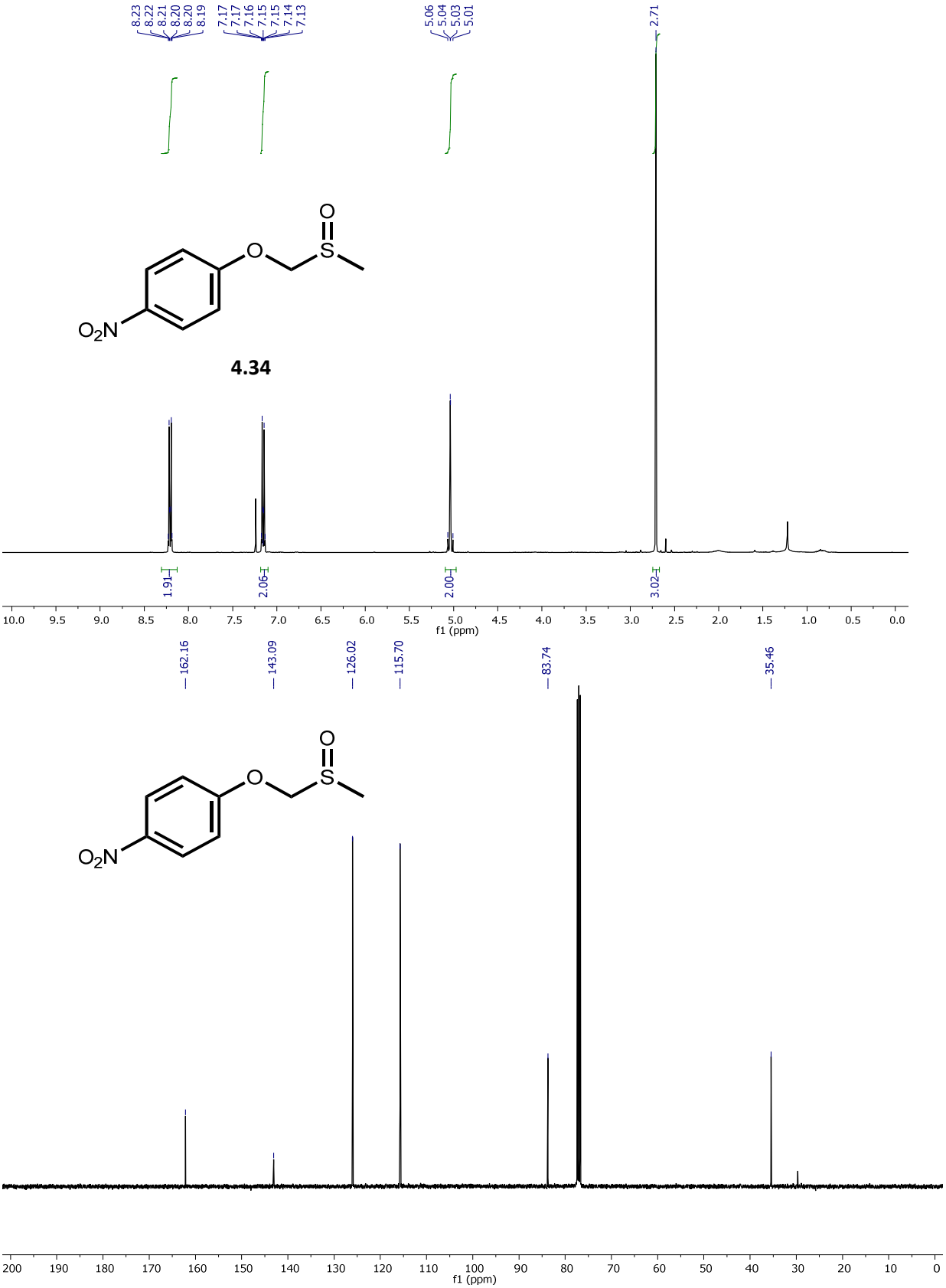
8.23
8.22
8.21
8.20
8.20
8.19
7.17
7.17
7.16
7.15
7.15
7.14
7.13
5.06
5.04
5.03
5.01
2.71
O
O
S
O2N
4.34
1.91
2.06
2.00
3.02
f1 (ppm)
162.16
143.09
126.02
115.70
83.74
35.46
O
O
S
O2N
f1 (ppm)

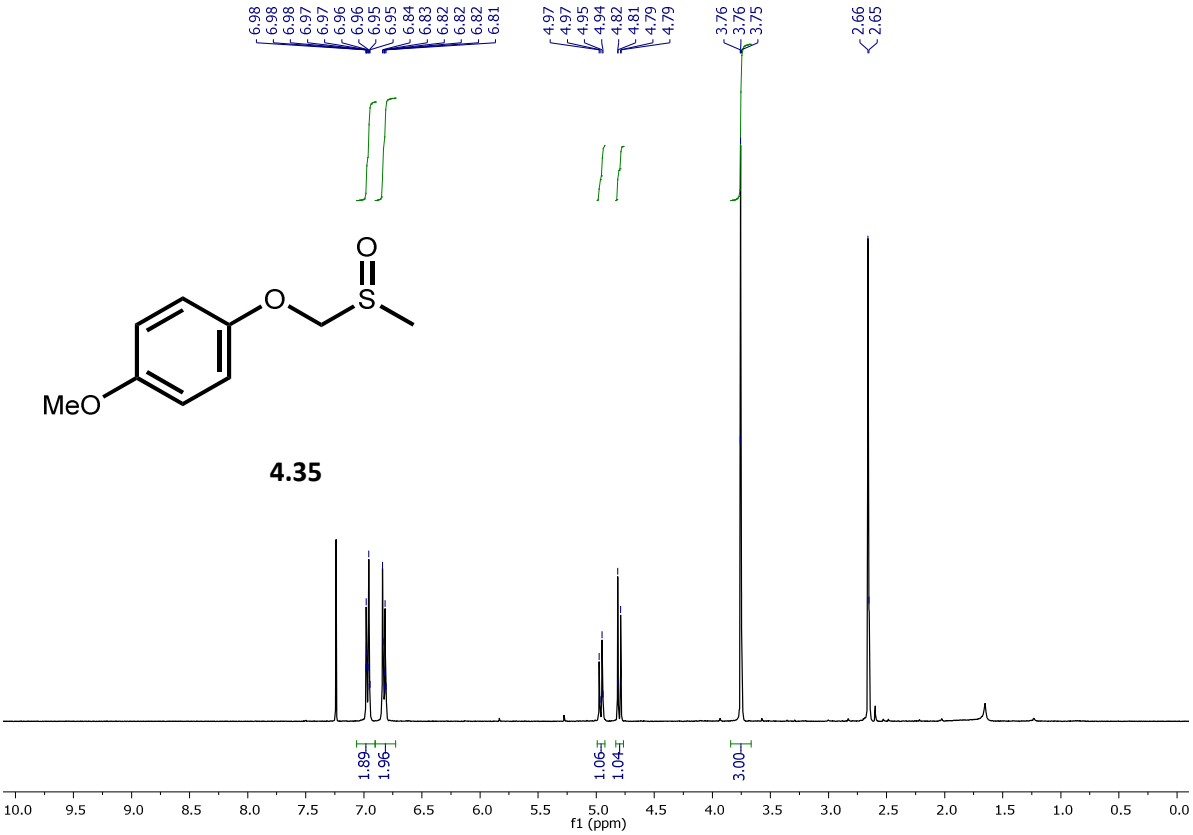
6.98
6.98
6.98
6.97
6.97
6.96
6.96
6.96
6.95
6.95
6.84
6.83
6.82
6.82
6.82
6.81
4.97
4.97
4.95
4.94
4.82
4.81
4.79
4.79
3.76
3.76
3.75
2.66
2.65
O
S
O
MeO
1.89
1.96
1.06
1.04
3.00
10.0
9.5
9.0
8.5
8.0
7.5
7.0
6.5
6.0
5.5
5.0
4.5
4.0
3.5
3.0
2.5
2.0
1.5
1.0
0.5
0.0
f1 (ppm)

4.35

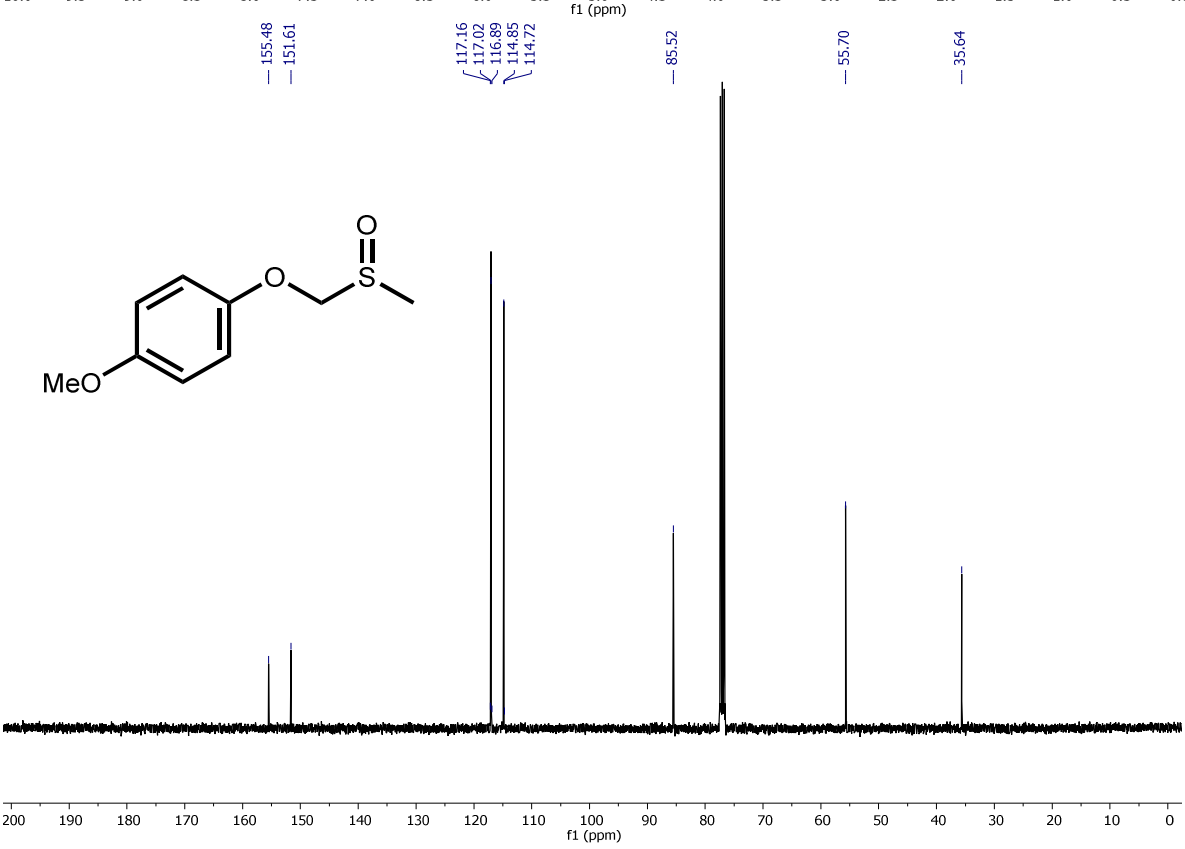
155.48
151.61
117.16
117.02
116.89
114.85
114.72
85.52
55.70
35.64
O
S
O
MeO
200
190
180
170
160
150
140
130
120
110
100
90
80
70
60
50
40
30
20
10
0
f1 (ppm)

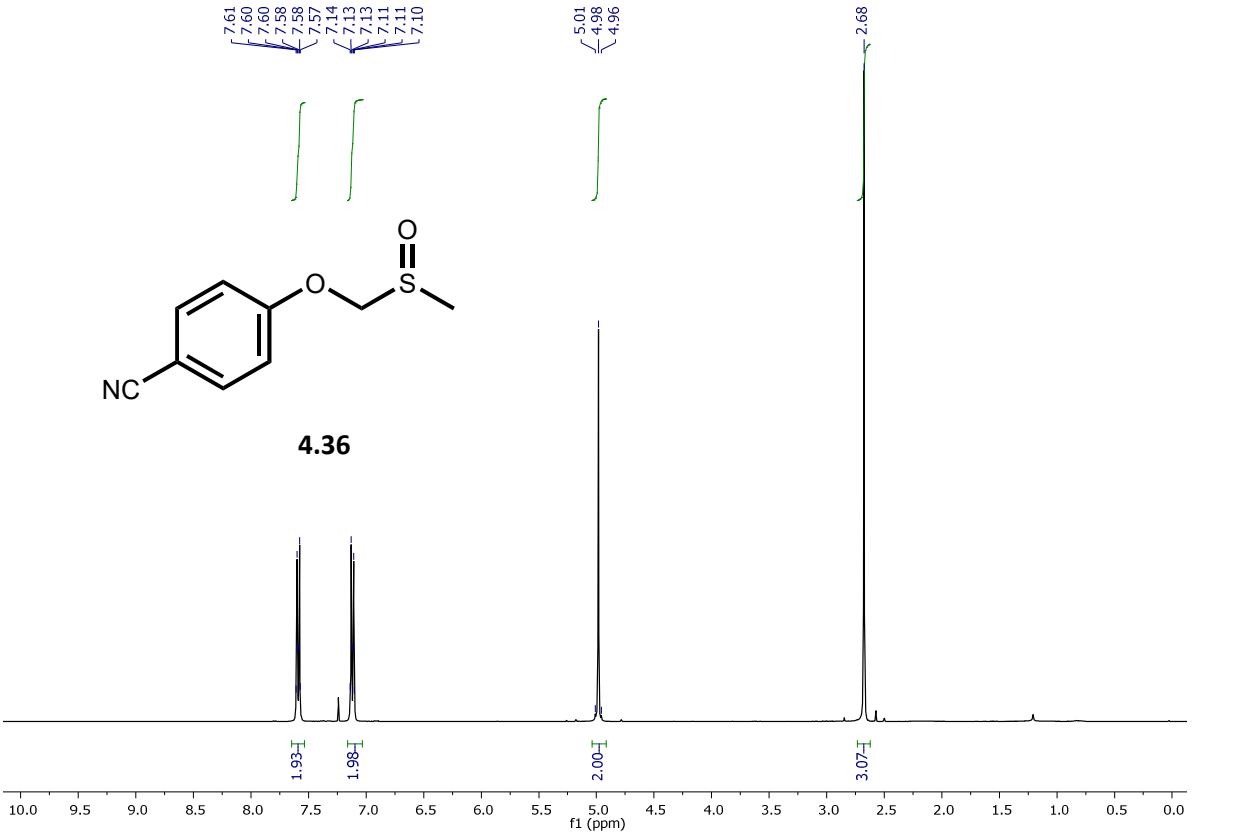
7.61
7.60
7.60
7.58
7.58
7.57
7.14
7.13
7.13
7.11
7.11
7.10
5.01
4.98
4.96
2.68
O
O
S
NC
1.93
1.98
2.00
3.07
10.0
9.5
9.0
8.5
8.0
7.5
7.0
6.5
6.0
5.5
5.0
4.5
4.0
3.5
3.0
2.5
2.0
1.5
1.0
0.5
0.0
f1 (ppm)

4.36

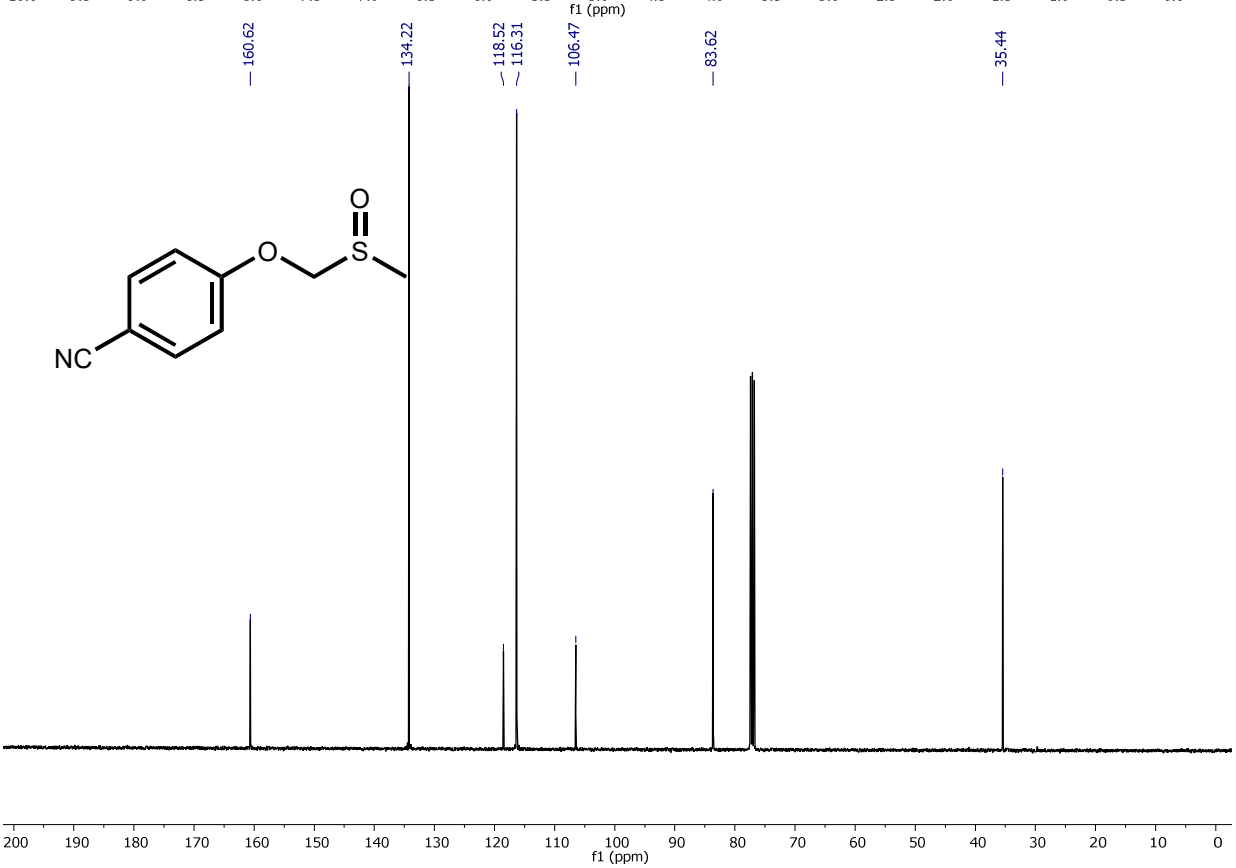
160.62
134.22
118.52
116.31
106.47
83.62
35.44
O
O
S
NC
200
190
180
170
160
150
140
130
120
110
100
90
80
70
60
50
40
30
20
10
0
f1 (ppm)

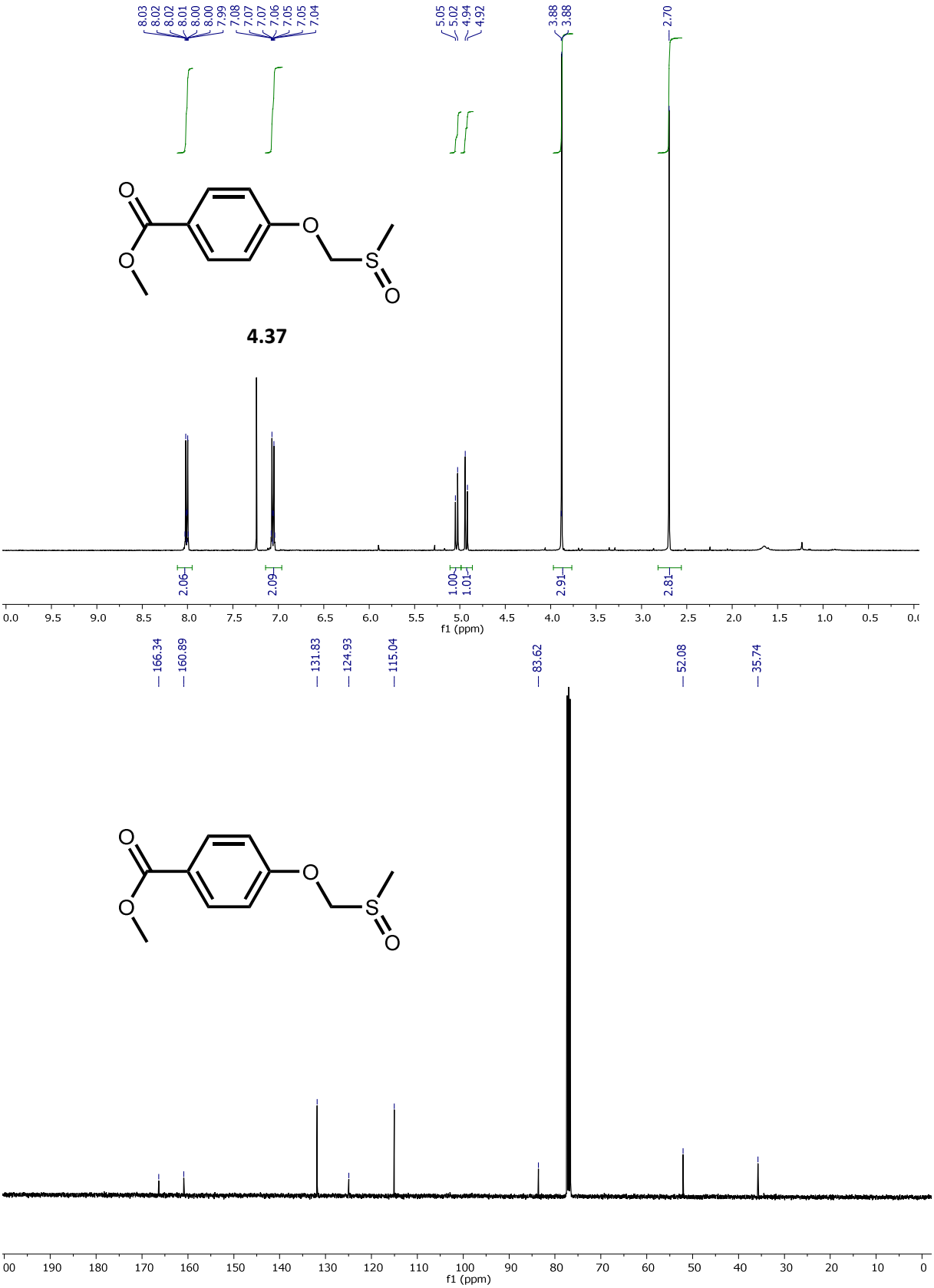
8.03
8.02
8.02
8.01
8.00
8.00
7.99
7.08
7.07
7.07
7.06
7.05
7.05
7.04
5.05
5.02
4.94
4.92
3.88
3.88
2.70
O
O
O
S
O
4.37
2.06
2.09
1.00
1.01
2.91
2.81
f1 (ppm)
166.34
160.89
131.83
124.93
115.04
83.62
52.08
35.74
f1 (ppm)

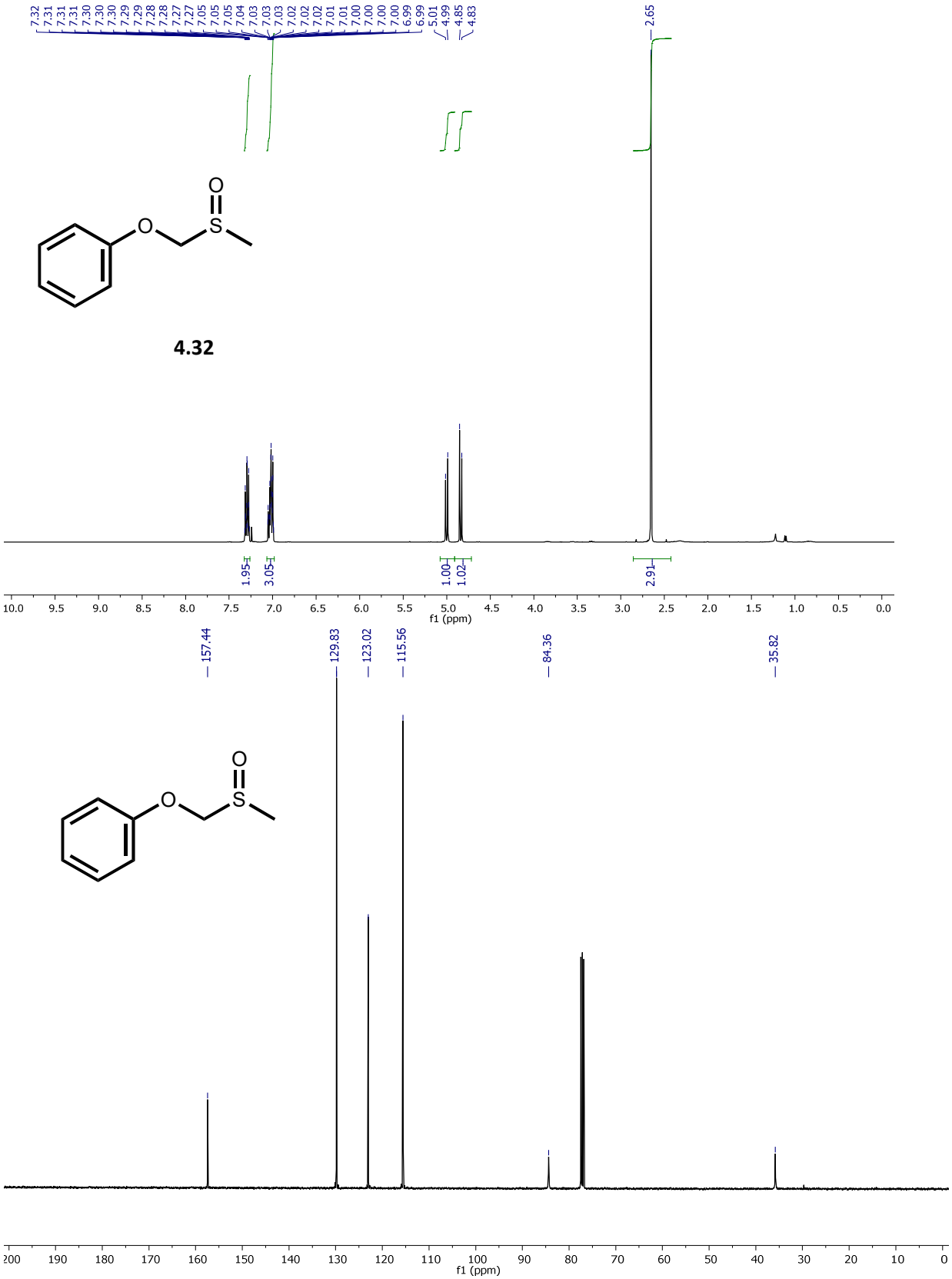
7.32
7.31
7.31
7.31
7.30
7.30
7.30
7.29
7.29
7.28
7.28
7.27
7.27
7.05
7.05
7.05
7.04
7.03
7.03
7.03
7.02
7.02
7.02
7.01
7.01
7.00
7.00
7.00
7.00
6.99
6.99
5.01
4.99
4.85
4.83
2.65
O
O
S
4.32
1.95
3.05
1.00
1.02
2.91
10.0
9.5
9.0
8.5
8.0
7.5
7.0
6.5
6.0
5.5
5.0
4.5
4.0
3.5
3.0
2.5
2.0
1.5
1.0
0.5
0.0
f1 (ppm)
157.44
129.83
123.02
115.56
84.36
35.82
O
O
S
200
190
180
170
160
150
140
130
120
110
100
90
80
70
60
50
40
30
20
10
0
f1 (ppm)

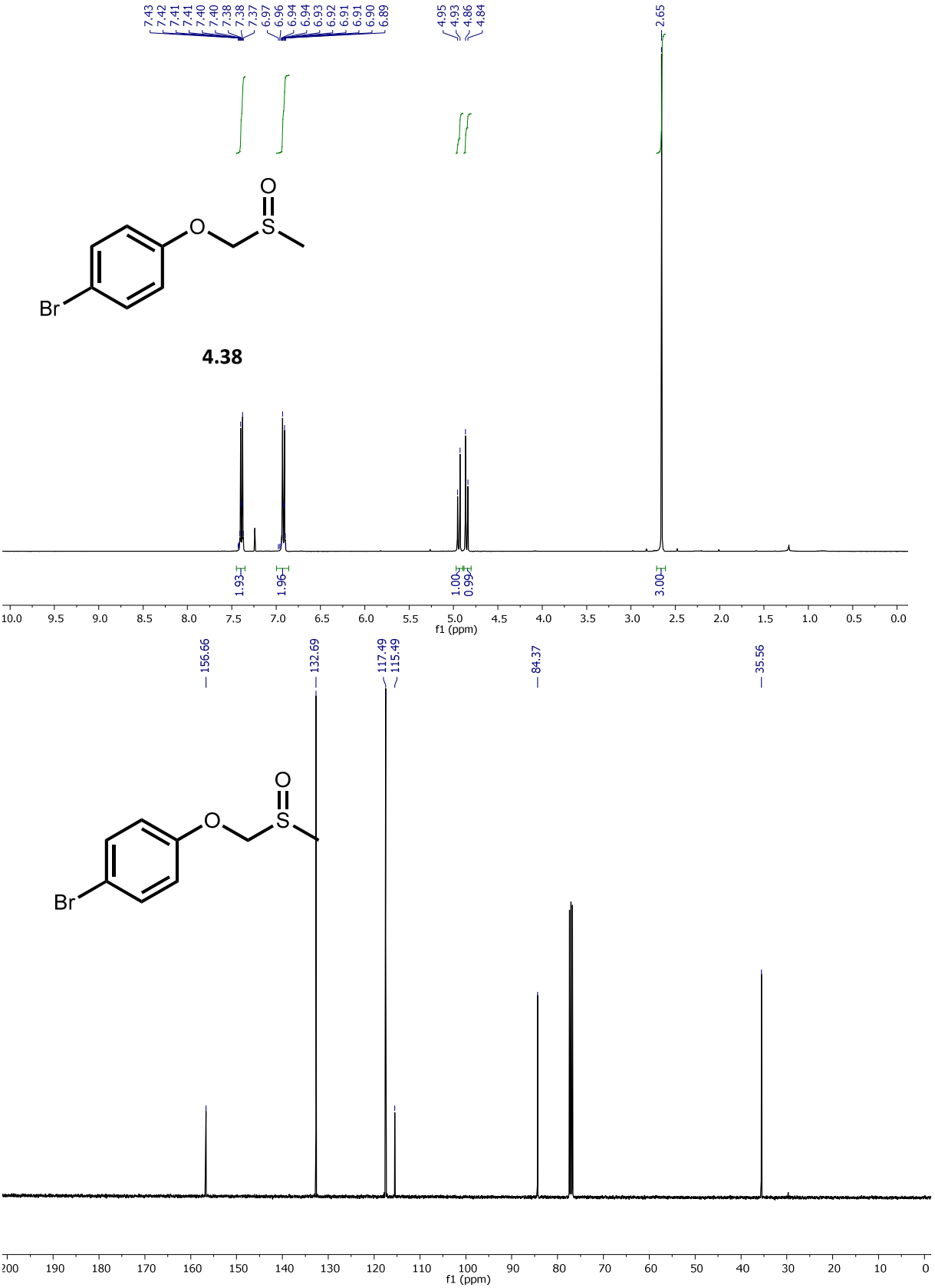
7.43
7.42
7.41
7.41
7.40
7.40
7.38
7.38
7.37
6.97
6.96
6.94
6.94
6.93
6.92
6.91
6.91
6.90
6.89
4.95
4.93
4.86
4.84
2.65
O
O
S
Br
4.38
1.93
1.96
1.00
0.99
3.00
f1 (ppm)
156.66
132.69
117.49
115.49
84.37
35.56
O
O
S
Br
f1 (ppm)

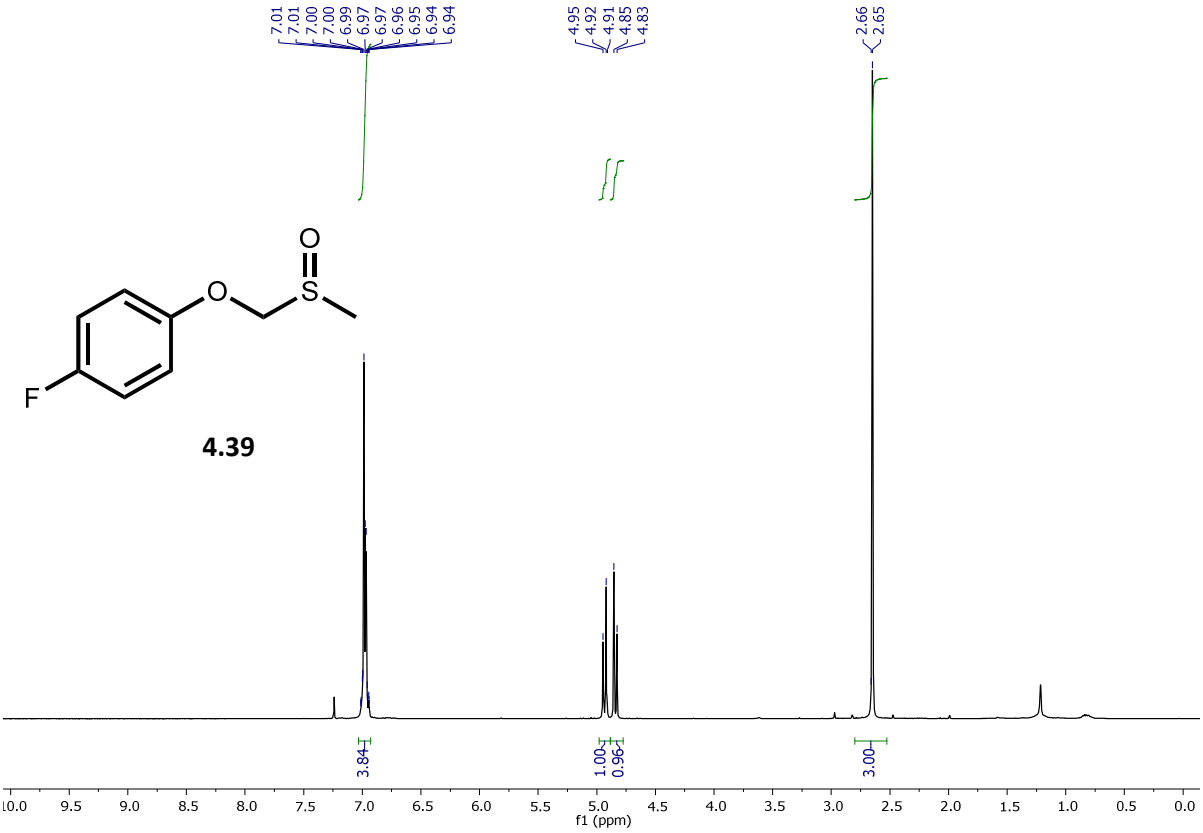
7.01
7.01
7.00
7.00
7.00
6.99
6.97
6.97
6.96
6.95
6.94
6.94
4.95
4.92
4.91
4.85
4.83
2.66
2.65
O
O
S
F
4.39
3.84
1.00
0.96
3.00
f1 (ppm)

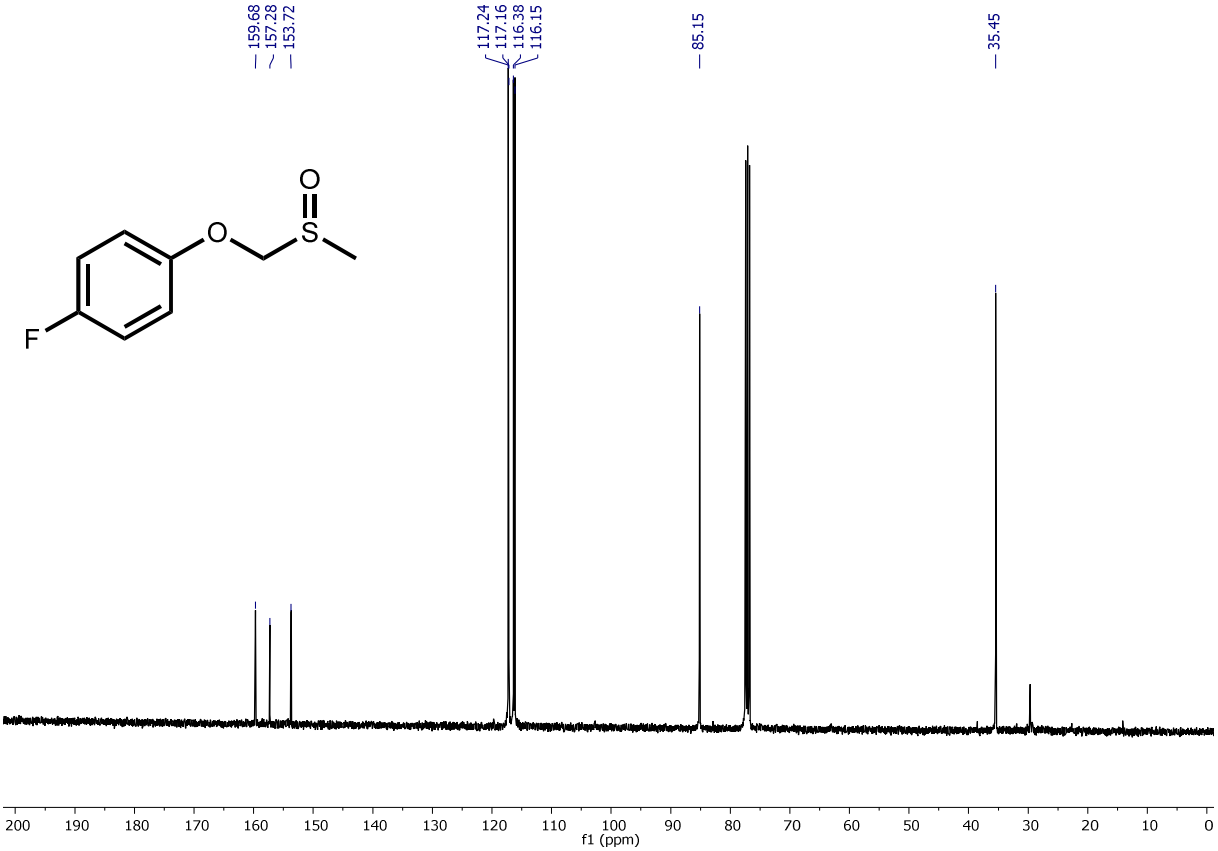
159.68
157.28
153.72
117.24
117.16
116.38
116.15
85.15
35.45
O
O
S
F
f1 (ppm)

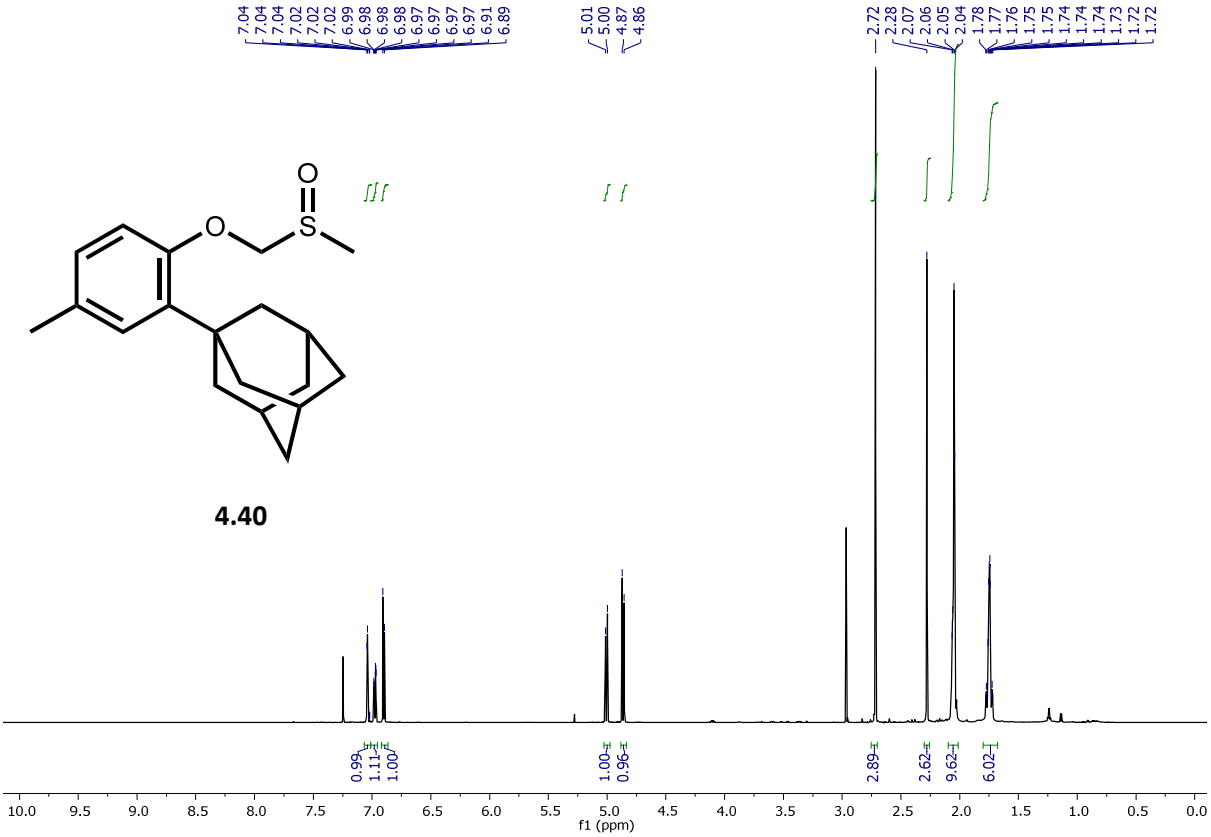
7.04
7.04
7.04
7.02
7.02
7.02
6.99
6.98
6.98
6.98
6.97
6.97
6.97
6.97
6.91
6.89
5.01
5.00
4.87
4.86
2.72
2.28
2.07
2.06
2.05
2.04
1.78
1.77
1.76
1.75
1.75
1.74
1.74
1.74
1.73
1.72
1.72
O
O
S
4.40
0.99
1.11
1.00
1.00
0.96
2.89
2.62
9.62
6.02
10.0 9.5 9.0 8.5 8.0 7.5 7.0 6.5 6.0 5.5 5.0 4.5 4.0 3.5 3.0 2.5 2.0 1.5 1.0 0.5 0.0
f1 (ppm)

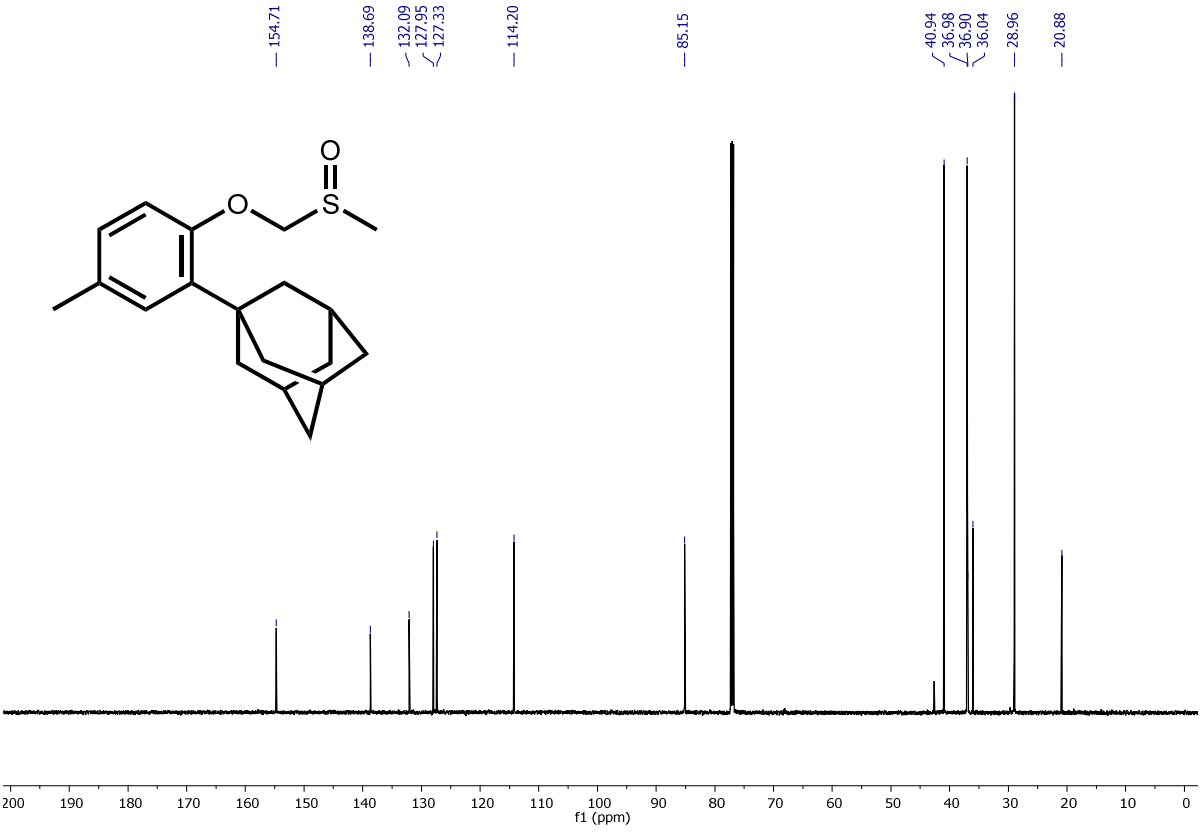
154.71
138.69
132.09
127.95
127.33
114.20
85.15
40.94
36.98
36.90
36.04
28.96
20.88
O
O
S
200 190 180 170 160 150 140 130 120 110 100 90 80 70 60 50 40 30 20 10 0
f1 (ppm)

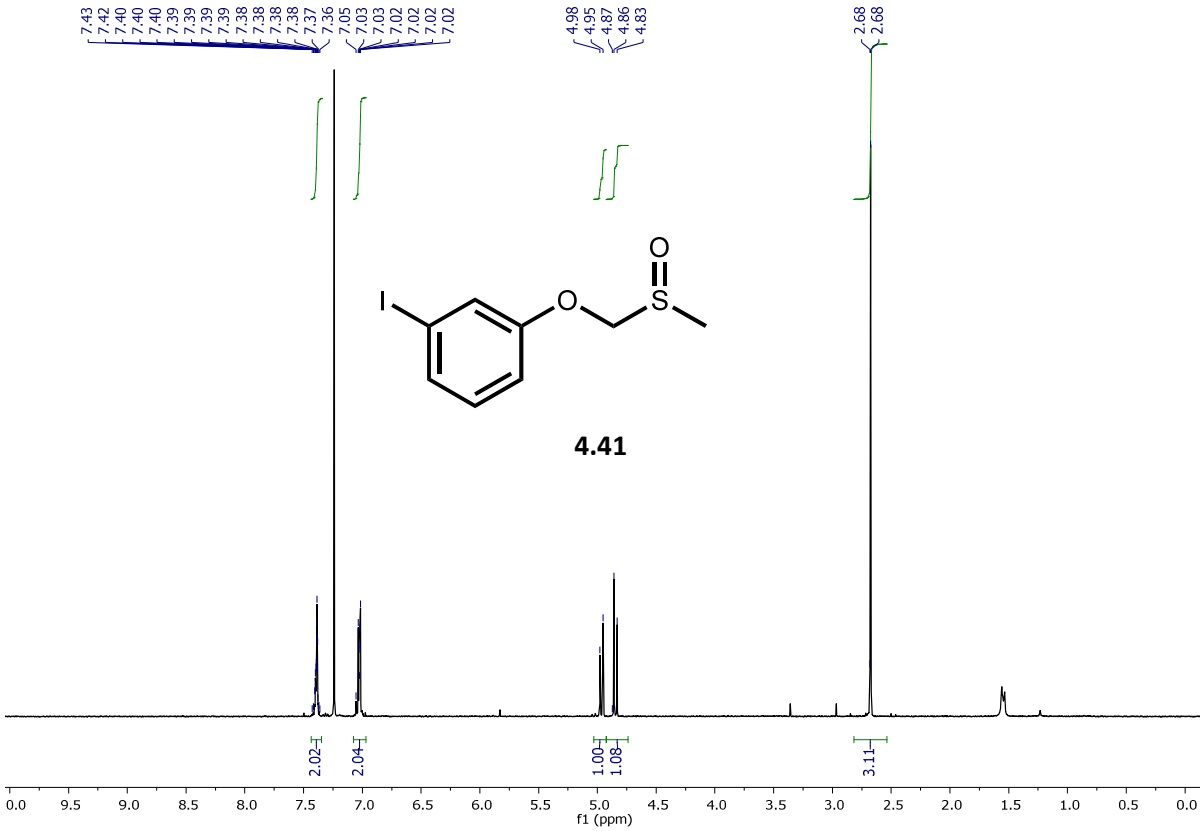
7.43
7.42
7.40
7.40
7.40
7.39
7.39
7.39
7.39
7.38
7.38
7.38
7.37
7.36
7.05
7.03
7.03
7.02
7.02
7.02
7.02
4.98
4.95
4.87
4.86
4.83
2.68
2.68
O
I
O
S
2.02
2.04
1.00
1.08
3.11
0.0
9.5
9.0
8.5
8.0
7.5
7.0
6.5
6.0
5.5
5.0
4.5
4.0
3.5
3.0
2.5
2.0
1.5
1.0
0.5
0.0
f1 (ppm)

4.41

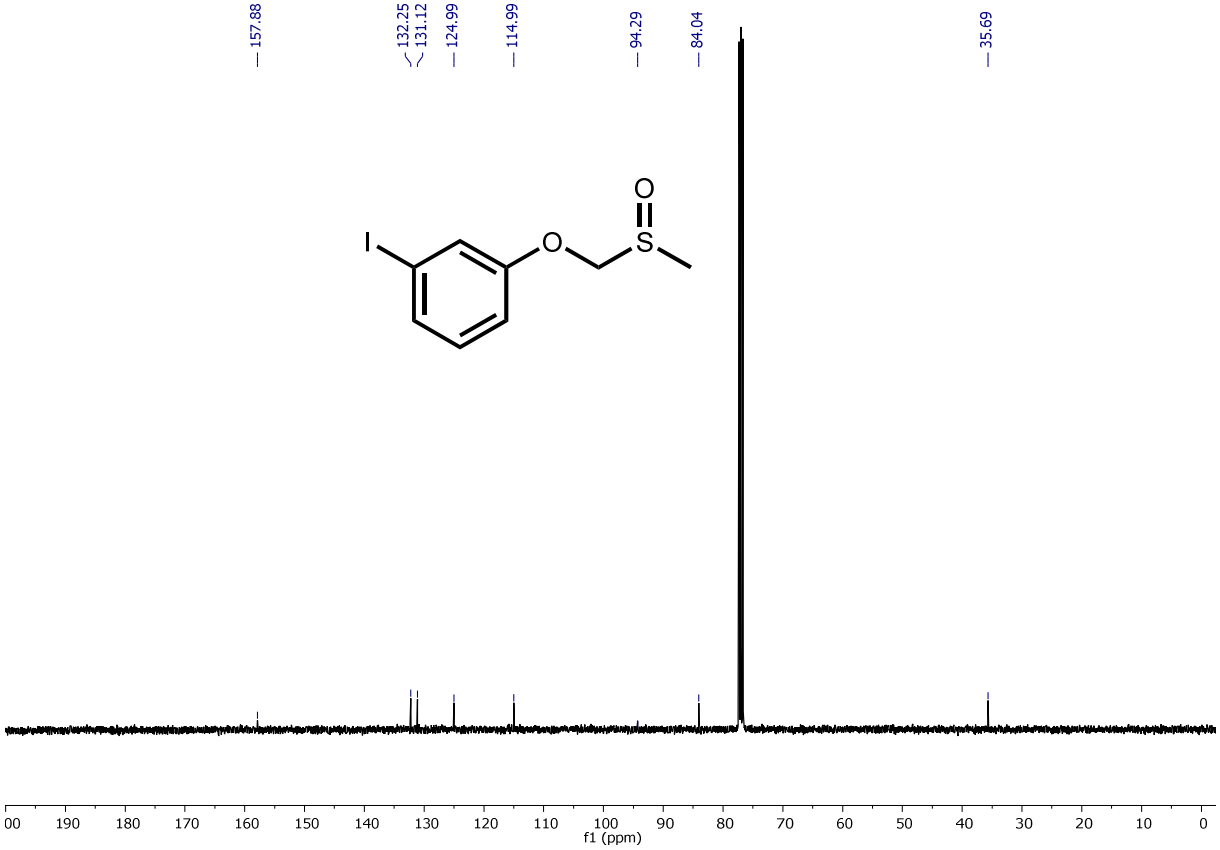
157.88
132.25
131.12
124.99
114.99
94.29
84.04
35.69
O
I
O
S
190
180
170
160
150
140
130
120
110
100
90
80
70
60
50
40
30
20
10
0
f1 (ppm)

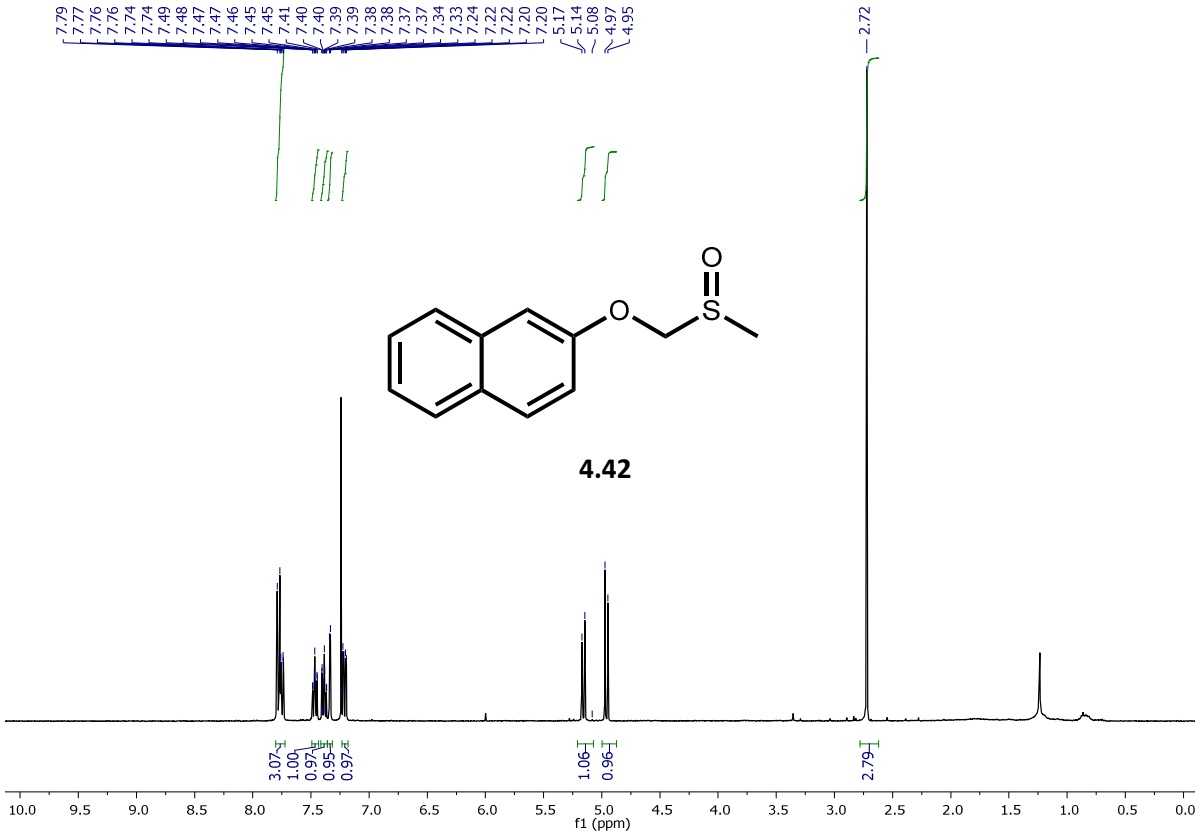
7.79
7.77
7.76
7.76
7.74
7.74
7.49
7.48
7.47
7.47
7.46
7.45
7.45
7.41
7.40
7.40
7.39
7.39
7.38
7.38
7.37
7.37
7.34
7.33
7.24
7.22
7.22
7.20
7.20
5.17
5.14
5.08
4.97
4.95
2.72
O
O
S
4.42
3.07
1.00
0.97
0.95
0.97
1.06
0.96
2.79
10.0
9.5
9.0
8.5
8.0
7.5
7.0
6.5
6.0
5.5
5.0
4.5
4.0
3.5
3.0
2.5
2.0
1.5
1.0
0.5
0.0
f1 (ppm)

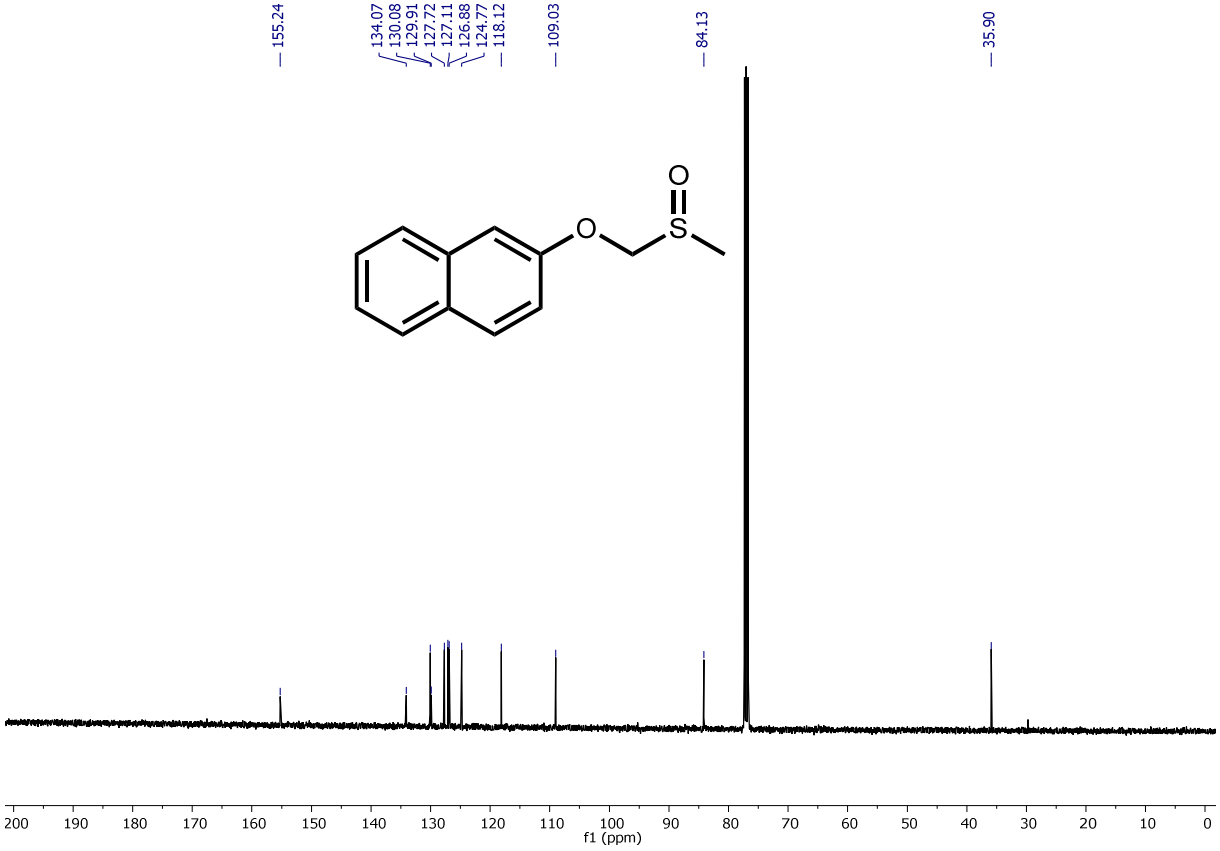
155.24
134.07
130.08
129.91
127.72
127.11
126.88
124.77
118.12
109.03
84.13
35.90
O
O
S
200
190
180
170
160
150
140
130
120
110
100
90
80
70
60
50
40
30
20
10
0
f1 (ppm)

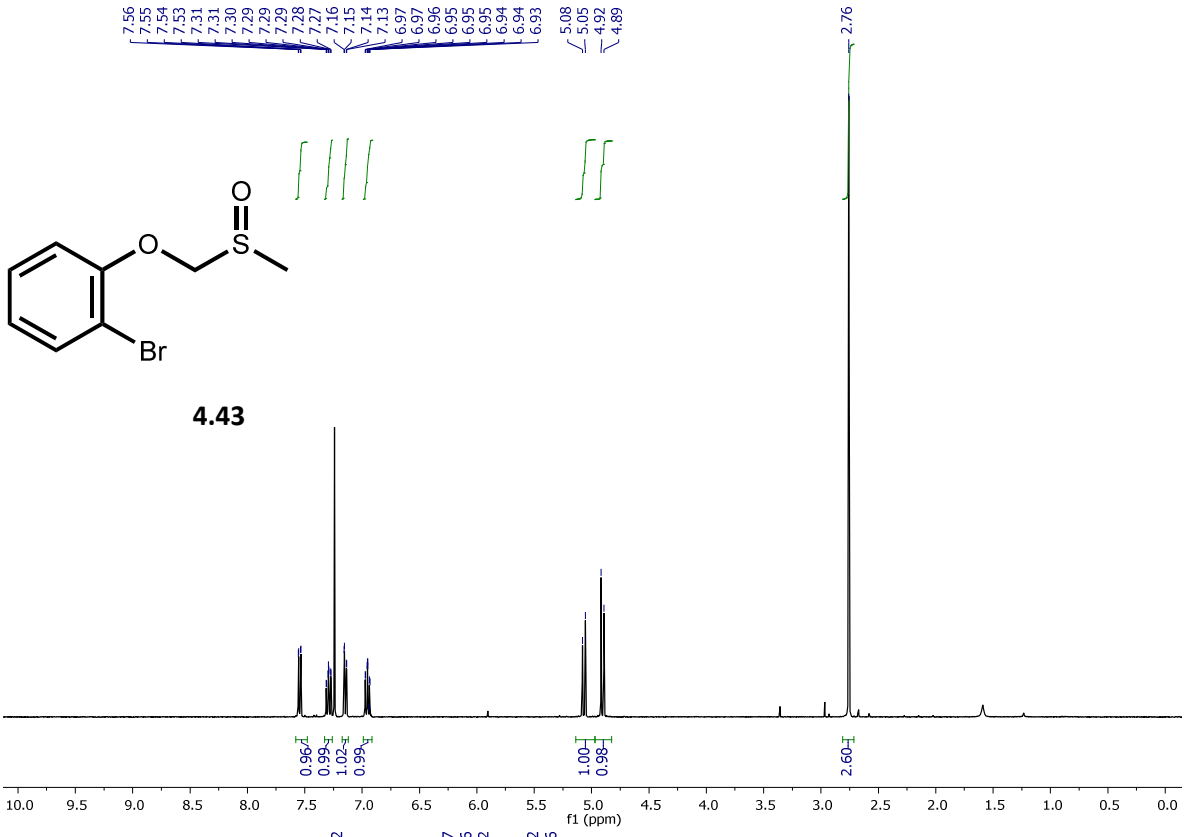
7.56
7.55
7.54
7.53
7.31
7.31
7.30
7.29
7.29
7.29
7.28
7.27
7.16
7.15
7.14
7.13
6.97
6.97
6.96
6.95
6.95
6.95
6.94
6.94
6.93
5.08
5.05
4.92
4.89
2.76
O
O
S
Br
0.96
0.99
1.02
0.99
1.00
0.98
2.60
10.0
9.5
9.0
8.5
8.0
7.5
7.0
6.5
6.0
5.5
5.0
4.5
4.0
3.5
3.0
2.5
2.0
1.5
1.0
0.5
0.0
f1 (ppm)

4.43

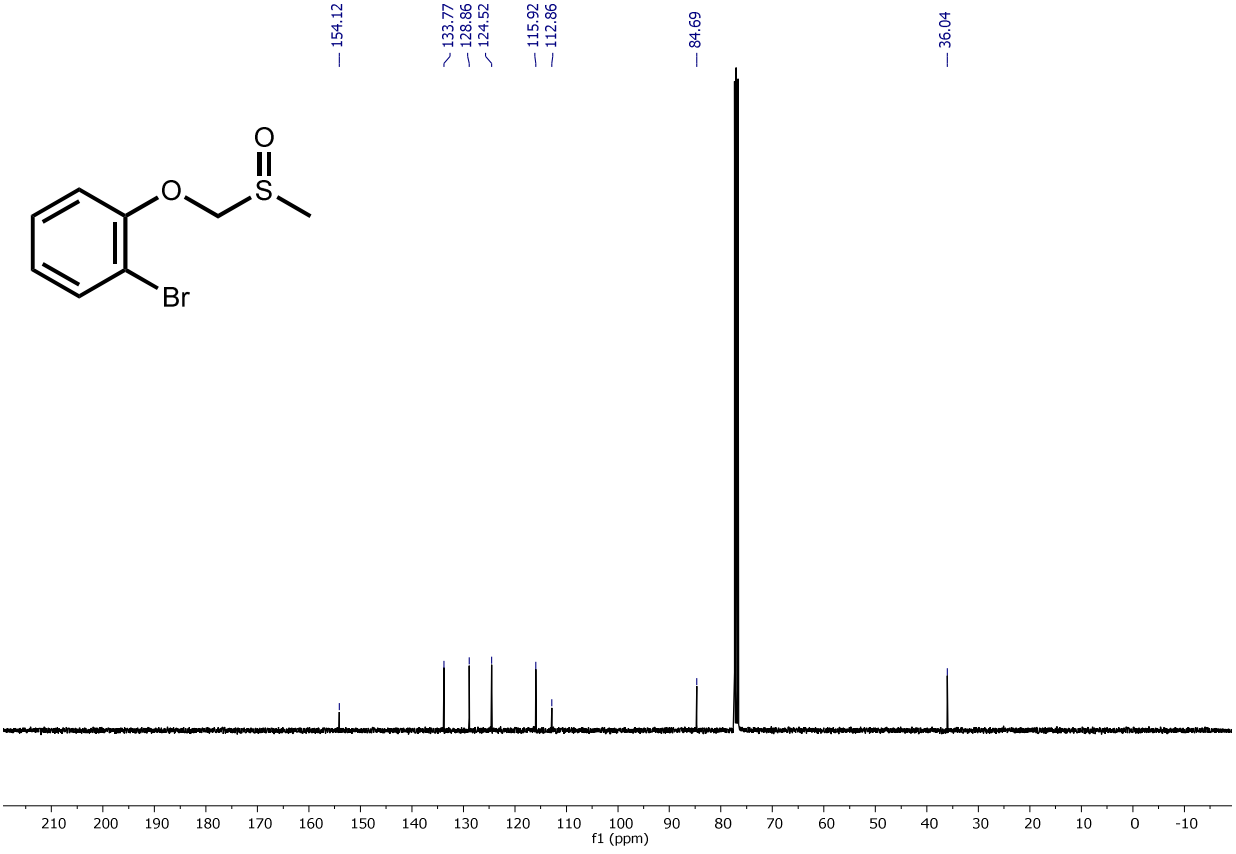
154.12
133.77
128.86
124.52
115.92
112.86
84.69
36.04
O
O
S
Br
210
200
190
180
170
160
150
140
130
120
110
100
90
80
70
60
50
40
30
20
10
0
-10
f1 (ppm)

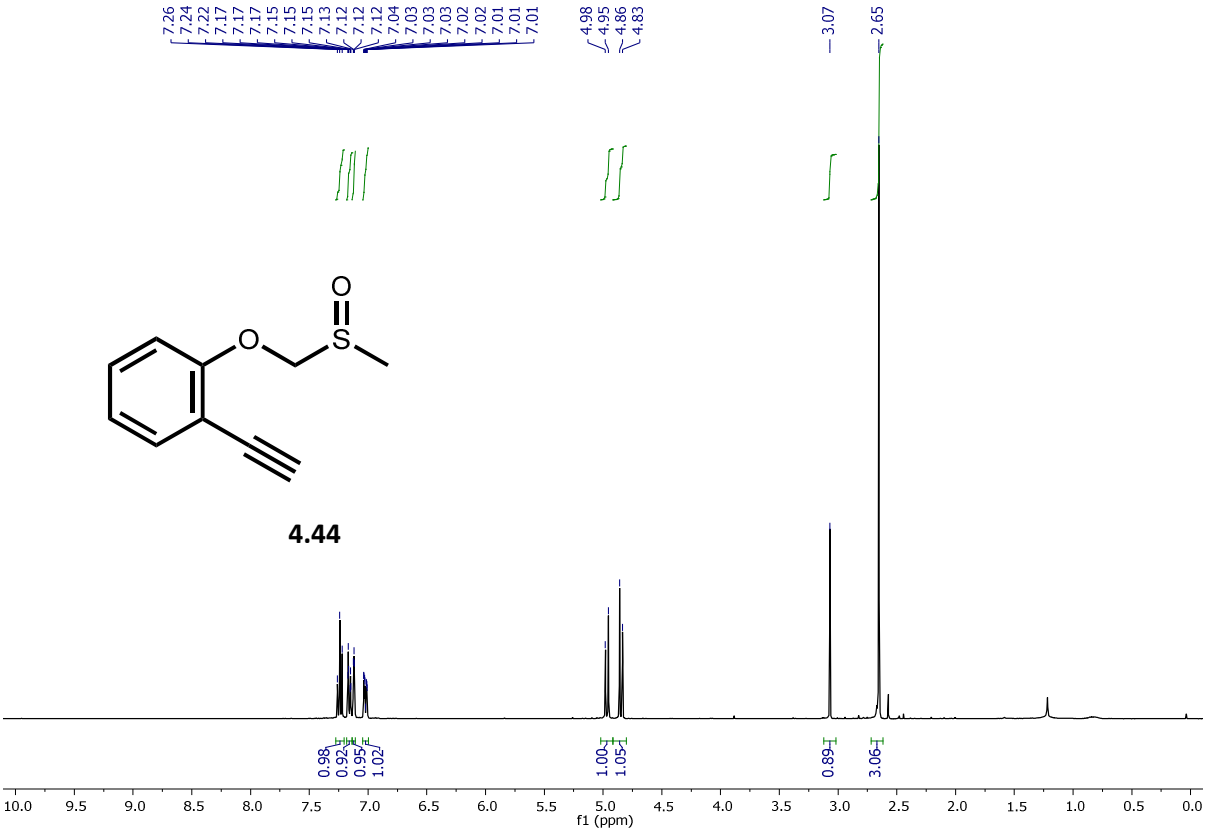
7.26
7.24
7.22
7.17
7.17
7.17
7.15
7.15
7.15
7.13
7.12
7.12
7.12
7.04
7.03
7.03
7.03
7.02
7.02
7.01
7.01
7.01
4.98
4.95
4.86
4.83
3.07
2.65
O
O
S
0.98
0.92
0.95
1.02
1.00
1.05
0.89
3.06
10.0
9.5
9.0
8.5
8.0
7.5
7.0
6.5
6.0
5.5
5.0
4.5
4.0
3.5
3.0
2.5
2.0
1.5
1.0
0.5
0.0
f1 (ppm)

4.44

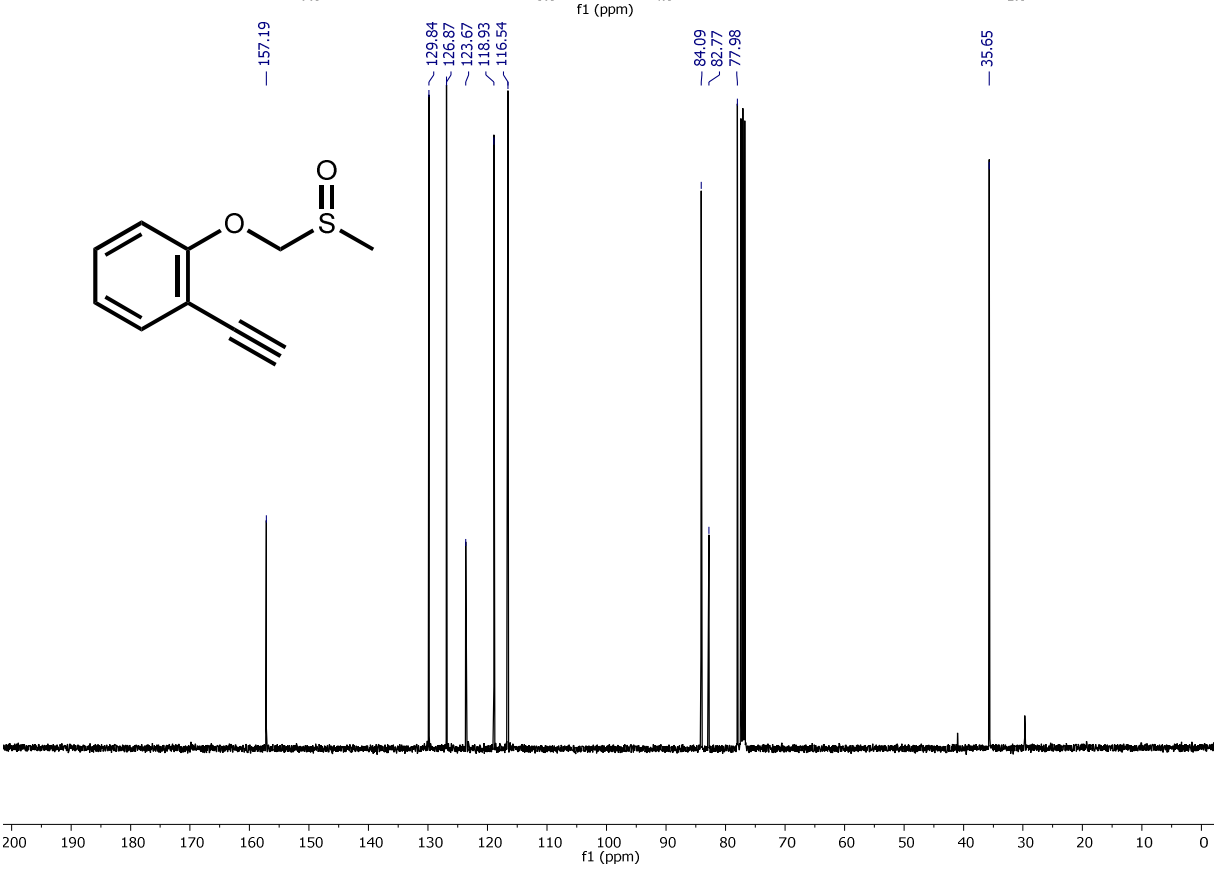
157.19
129.84
126.87
123.67
118.93
116.54
84.09
82.77
77.98
35.65
O
O
S
200
190
180
170
160
150
140
130
120
110
100
90
80
70
60
50
40
30
20
10
0
f1 (ppm)

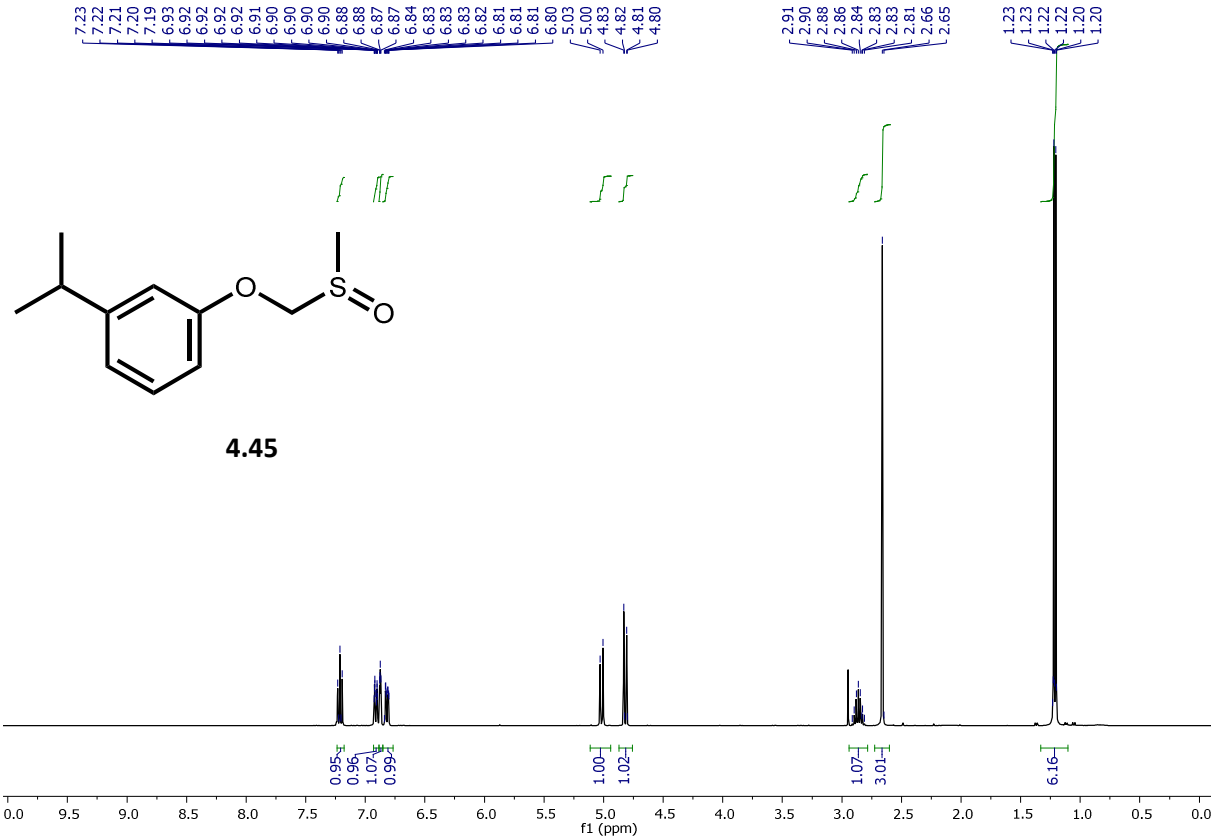
7.23 7.22 7.21 7.20 7.19 6.93 6.92 6.92 6.92 6.92 6.91 6.90 6.90 6.90 6.90 6.88 6.88 6.87 6.87 6.84 6.83 6.83 6.83 6.82 6.81 6.81 6.81 6.80 5.03 5.00 4.83 4.82 4.81 4.80 2.91 2.90 2.88 2.86 2.84 2.83 2.83 2.81 2.66 2.65 1.23 1.23 1.22 1.22 1.20 1.20
O
S
O
0.95 0.96 1.07 0.99 1.00 1.02 1.07 3.01 6.16
f1 (ppm)

4.45

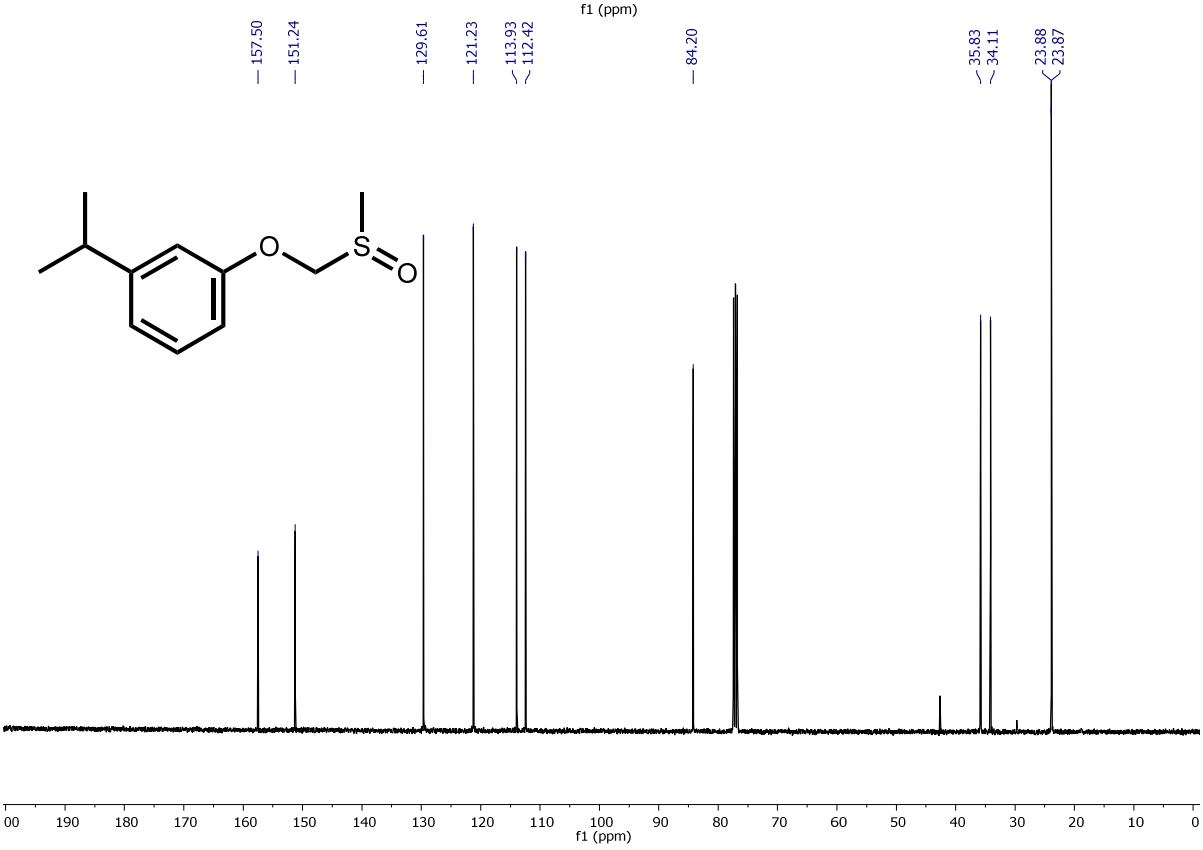
157.50 151.24 129.61 121.23 113.93 112.42 84.20 35.83 34.11 23.88 23.87
O
S
O
f1 (ppm)

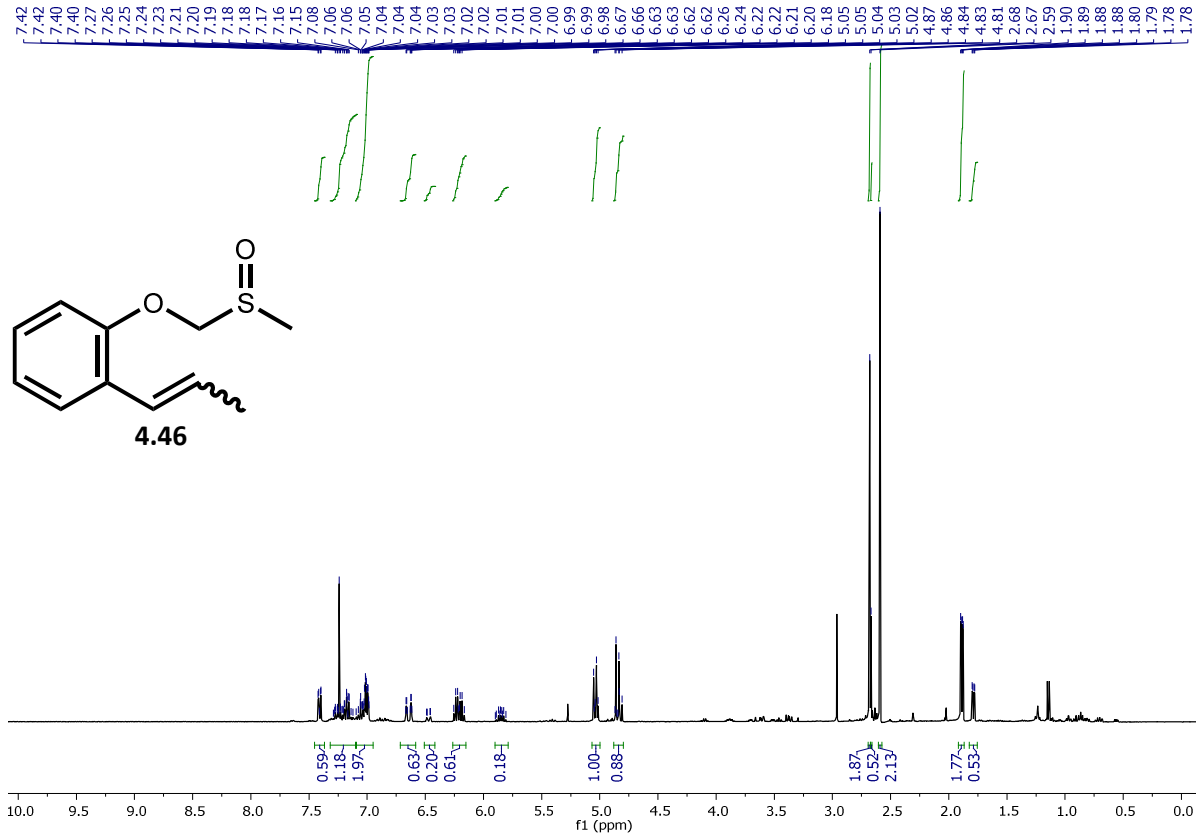
7.42 7.42 7.40 7.40 7.27 7.26 7.25 7.24 7.23 7.21 7.20 7.19 7.18 7.18 7.17 7.16 7.15 7.08 7.06 7.06 7.05 7.04 7.04 7.04 7.03 7.03 7.02 7.02 7.01 7.01 7.00 7.00 6.99 6.99 6.98 6.67 6.66 6.63 6.63 6.62 6.62 6.26 6.24 6.22 6.22 6.21 6.20 6.18 5.05 5.05 5.04 5.03 5.02 4.87 4.86 4.84 4.83 4.81 2.68 2.67 2.59 1.90 1.89 1.88 1.88 1.80 1.79 1.78 1.78
O
S
O
4.46
0.59 1.18 1.97 0.63 0.20 0.61 0.18 1.00 0.88 1.87 0.52 2.13 1.77 0.53
10.0 9.5 9.0 8.5 8.0 7.5 7.0 6.5 6.0 5.5 5.0 4.5 4.0 3.5 3.0 2.5 2.0 1.5 1.0 0.5 0.0
f1 (ppm)

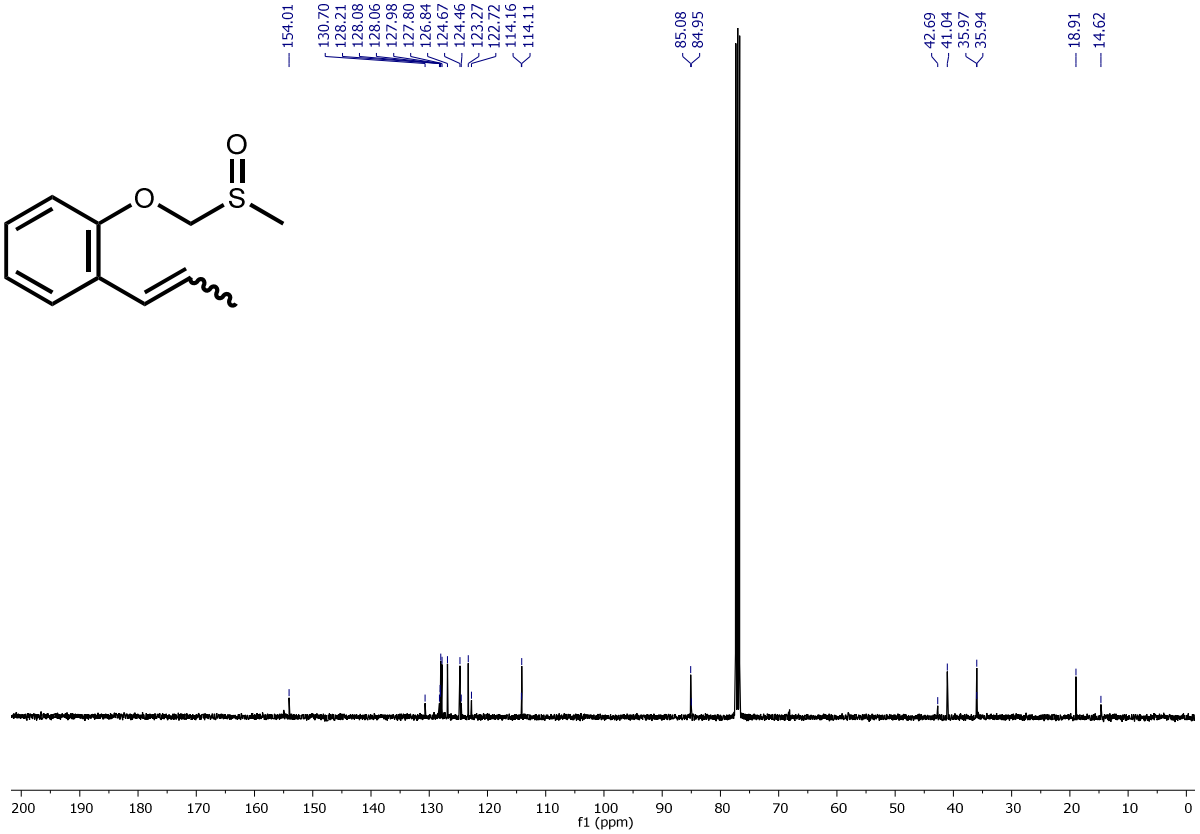
154.01 130.70 128.21 128.08 128.06 127.98 127.80 126.84 124.67 124.46 123.27 122.72 114.16 114.11 85.08 84.95 42.69 41.04 35.97 35.94 18.91 14.62
O
S
O
200 190 180 170 160 150 140 130 120 110 100 90 80 70 60 50 40 30 20 10 0
f1 (ppm)

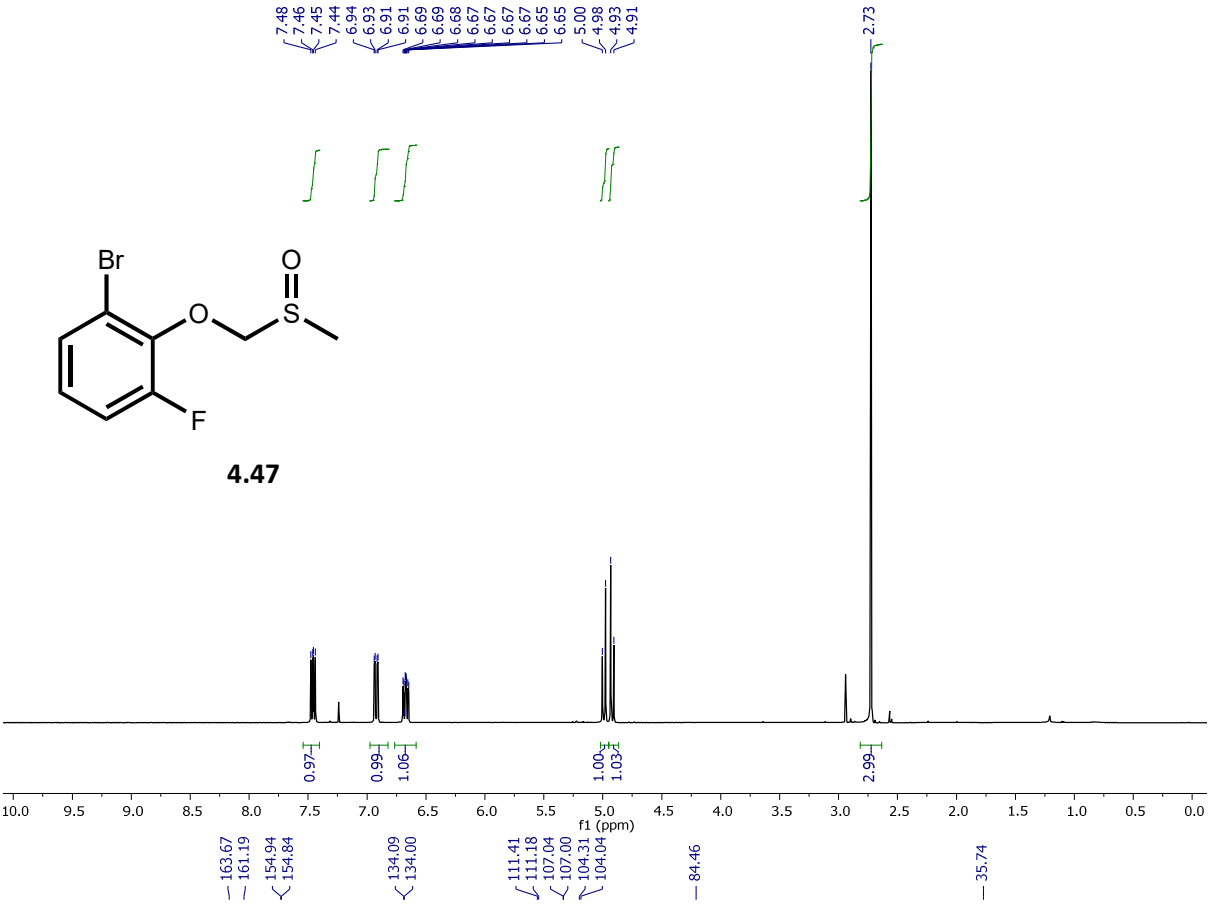
7.48
7.46
7.45
7.44
6.94
6.93
6.91
6.91
6.69
6.69
6.68
6.67
6.67
6.67
6.67
6.65
6.65
5.00
4.98
4.93
4.91
2.73
Br
O
O
S
F
0.97
0.99
1.06
1.00
1.03
2.99
f1 (ppm)

4.47

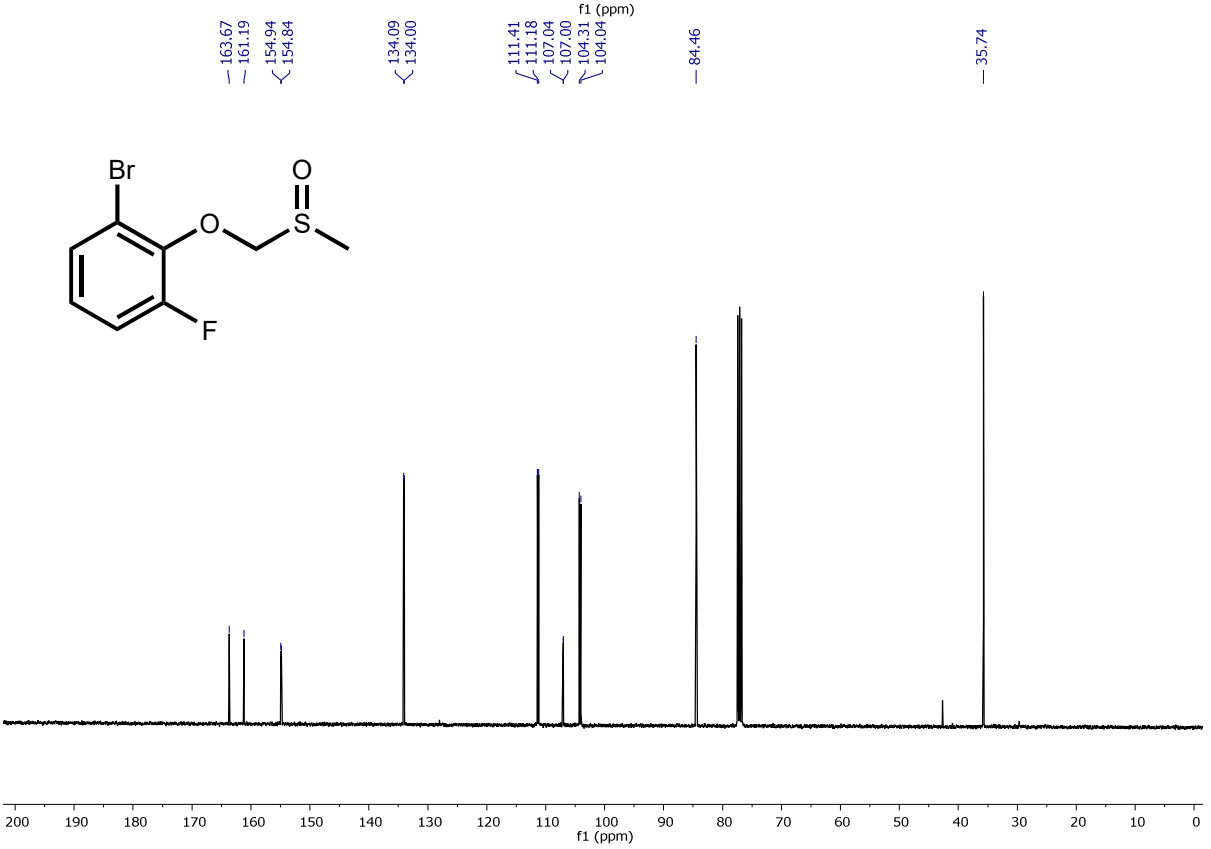
163.67
161.19
154.94
154.84
134.09
134.00
111.41
111.18
107.04
107.00
104.31
104.04
84.46
35.74
Br
O
O
S
F
f1 (ppm)

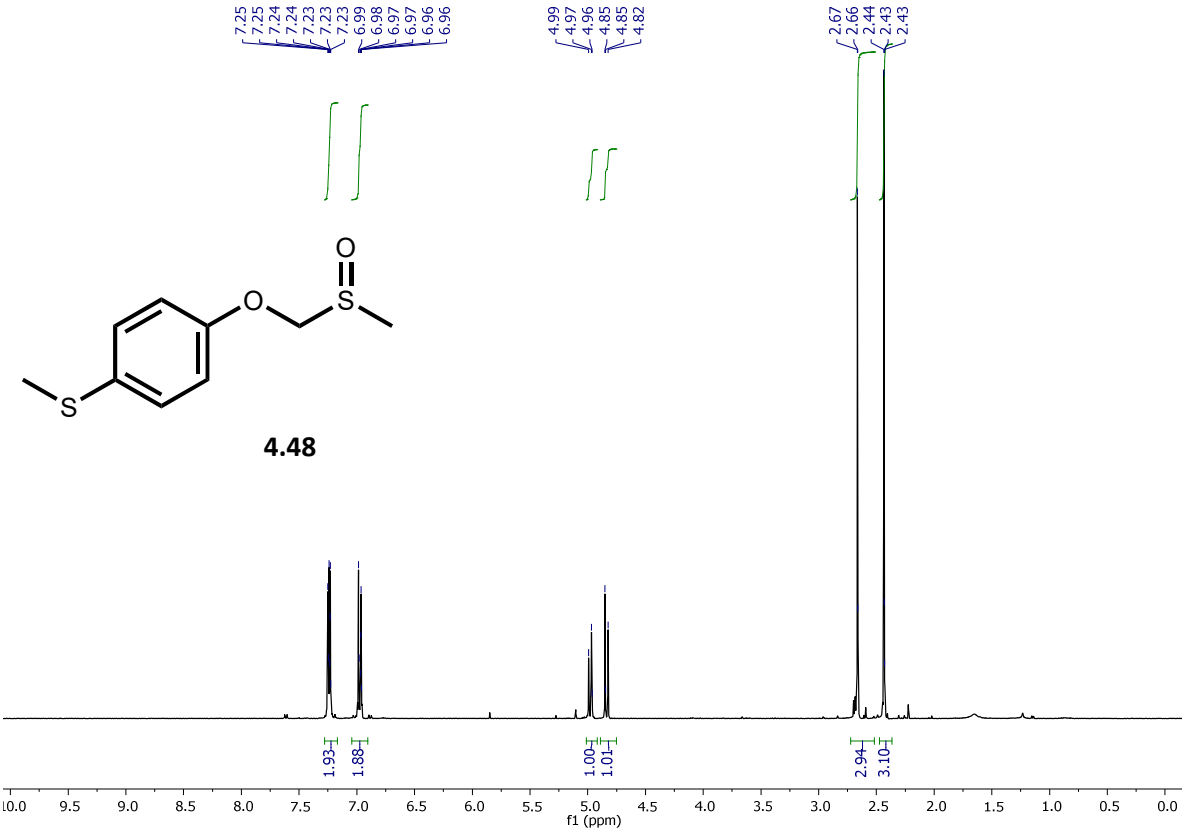
7.25
7.25
7.24
7.24
7.23
7.23
7.23
6.99
6.98
6.97
6.97
6.96
6.96
4.99
4.97
4.96
4.85
4.85
4.82
2.67
2.66
2.44
2.43
2.43
O
O
S
S
1.93
1.88
1.00
1.01
2.94
3.10
f1 (ppm)

4.48

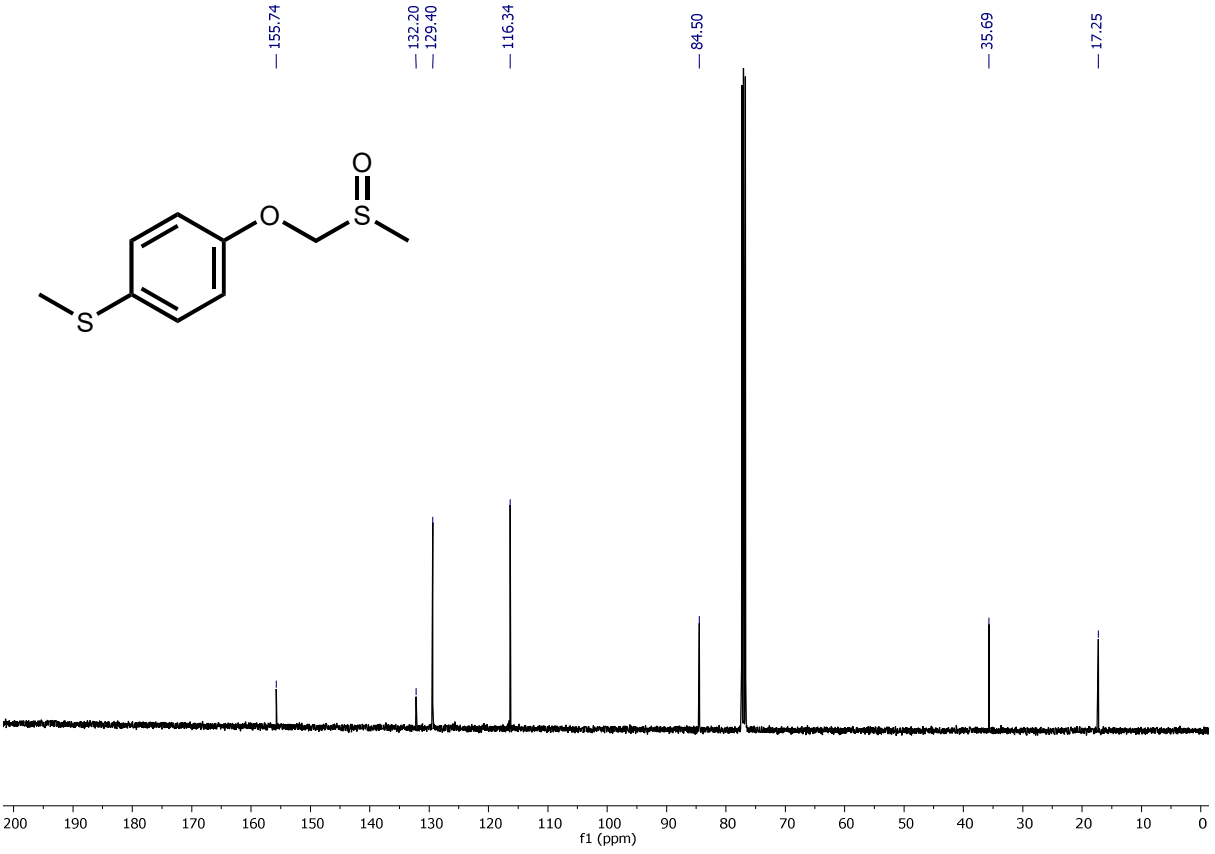
155.74
132.20
129.40
116.34
84.50
35.69
17.25
O
O
S
S
f1 (ppm)

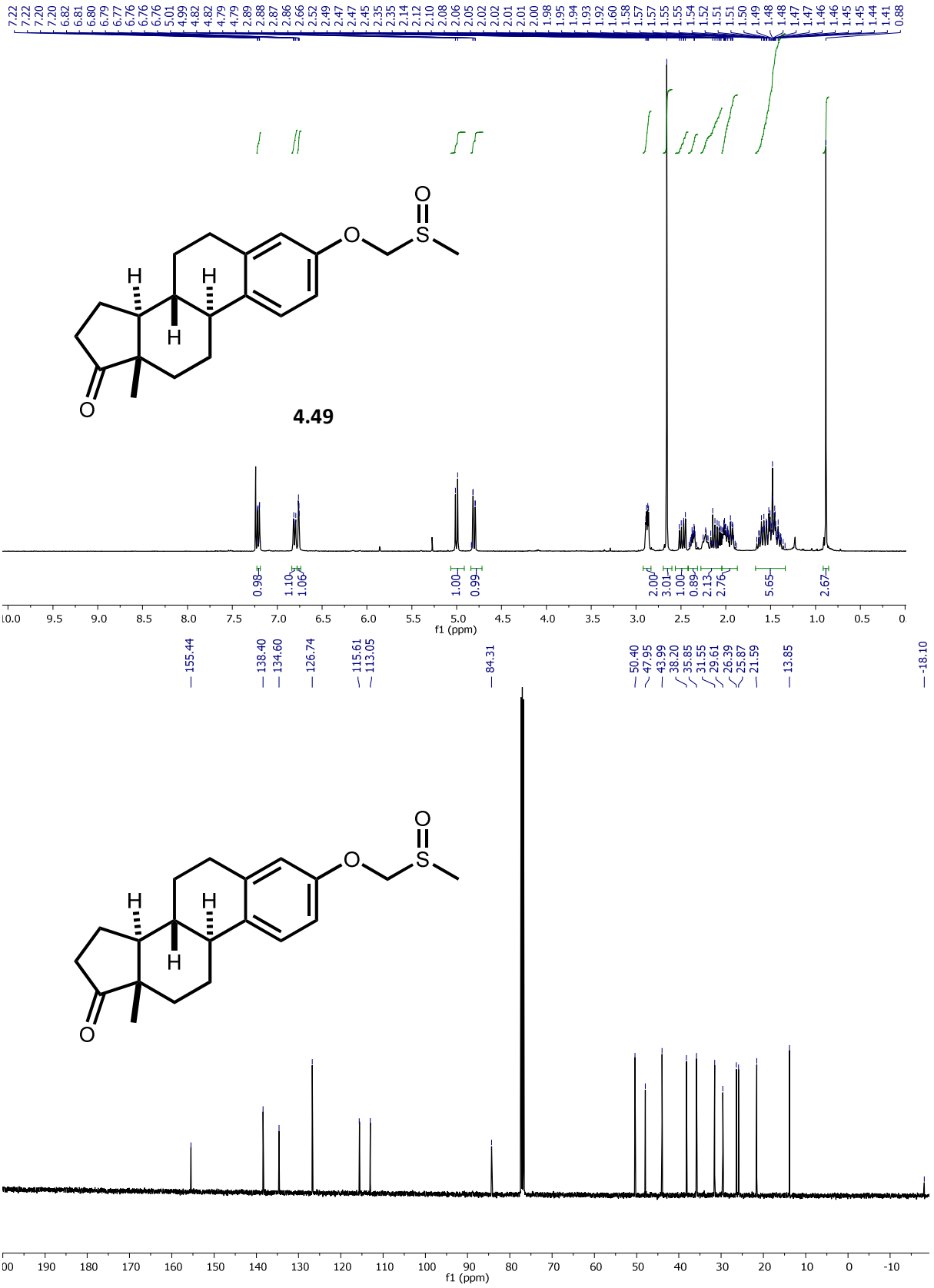
4.49
f1 (ppm)
f1 (ppm)


4.50
f1 (ppm)
f1 (ppm)